

Λ -Shaped Photo-Switches Designed by Employing the Tröger's Base Scaffold

Masoud Kazem-Rostami

*Bachelor of Pure Chemistry
Imam Khomeini International University, Iran
Masters of Organic Chemistry
Bu-Ali Sina University, Iran*

A thesis submitted in partial fulfilment of the requirements for the degree of

Doctor of Philosophy



MACQUARIE
University

**Department of Molecular Sciences
Macquarie University
Sydney Australia**

April 2018

Table of Contents

Table of Contents	i
Table of Figures.....	v
List of Tables	viii
Statement of Originality.....	ix
Acknowledgements.....	x
Justification of Thesis by Publication.....	xi
List of Original Publications (Thesis Map)	xi
Thesis Summary.....	xiii
Thesis Chapters Overview	xiv
Research Chapter One Synopsis (Incorporates Paper I)	xiv
Research Chapter Two Synopsis (Incorporates Paper II)	xiv
Research Chapter Three Synopsis (Incorporates Paper III)	xv
Thesis Objectives and Achievements	xvi
Research Chapter One (Incorporates Paper I)	xvi
Research Chapter Two (Incorporates Paper II)	xviii
Research Chapter Three (Incorporates Paper III).....	xix
List of Abbreviations	xxiii
INTRODUCTION.....	1
1. Introduction to display technology.....	1
1.1 Liquid crystal displays	1

1.2	Liquid crystals	2
2.	LCDs evolution towards the design of smart displays	6
2.1	Alignment and orientation of LC molecules.....	6
2.1.1	Mechanical alignment.....	6
2.1.2	Orientating LC molecules by surfactants	10
2.1.3	Orientating LC molecules by electric field.....	11
2.1.4	Photo-alignment and design of smarter LCDs	12
2.2	Introduction of chirality.....	18
2.3	Introduction of photo-tunable properties	18
2.4	Structure-function relationships of liquid crystals	22
3.	Tröger's base (TB) overview.....	23
3.1	TB special features.....	23
3.1.1	Chirality and racemisation	23
3.1.2	Chiral resolution of TBAs	27
3.1.3	Unique shape of TB scaffolds.....	28
3.1.4	Unique spectral properties of TBAs	29
3.2	TB common applications	30
3.2.1	Chiral discriminator in molecular recognition.....	30
3.2.2	Building blocks/monomers.....	31
3.2.3	Molecular design	32
3.3	Former studies in this field.....	33
3.4	TBAs drawbacks	34

3.4.1	Diazocine bridge clipping	34
3.4.2	Undesired couplings and side-reactions	34
3.4.3	Racemisation.....	35
3.5	Availability of the desired TBA	36
4.	Aims and existing gaps.....	38
5.	Current challenges of LCD design	40
THESIS OUTCOMES.....		41
Paper I (Main Article).....		41
Paper I (Supporting Information).....		52
Paper II (Main Article)		99
Paper II (Supporting Information).....		105
Paper III (Main Article)		154
Paper III (Supporting Information).....		160
SIGNIFICANCE AND FUTURE DIRECTIONS		213
Photo-alignment agents.....		213
Photo-responsive elastomers		215
Design of light-driven machines		217
Design of light-driven molecular machines.....		219
Smart drug delivery systems.....		220
Molecular recognition.....		223
Design of membranes and polymers.....		224
Fluorescent and pH sensing analogues		227

Magnetic and photochromism studies	229
Crystallography and aggregation studies.....	229
The design of sensing surfaces	231
LC dopants: contribution in the design of smart LCDs	232
CONCLUSION	235
REFERENCES AND NOTES.....	236
APPENDICES.....	245
Appendix 1: The DSC results	245
Appendix 2: 3D presentation of the Λ -shaped void	287
Appendix 3: The X-ray crystallography results.....	294
Appendix 4: Photo-isomerisation studies by NMR	319
Appendix 5: The author's biography	324

Table of Figures

Figure 1 Multi-layered structure of one LCD unit (RGB pixel)	2
Figure 2 Helical LC structure and pitch length	4
Figure 3 Marbled texture of an unaligned LC phase	4
Figure 4 Classification of LCs	5
Figure 5 Pulled polymer becomes transparent ⁵⁴	7
Figure 6 Brushing method for mechanical alignments	8
Figure 7 The chemical structure of 7CB	10
Figure 8 The schematic- (top) and optical-views (bottom) of LC layers.....	10
Figure 9 Classification of polar LCs	11
Figure 10 An example of a flexible LCD (a) and image quality (b)	13
Figure 11 Proportionality of light absorption	14
Figure 12 A typical synthetic azo dye	15
Figure 13 Comparing the angular view	16
Figure 14 A bisazo compound used in the design of ultrathin LCDs ^{64, 65}	17
Figure 15 Introduction of chirality by chiral centre addition	18
Figure 16 Typical examples of photoswitchable functional groups.....	19
Figure 17 Absorption spectra of an azo compound.....	21
Figure 18 Photo-isomerisation of an azo molecule ^{115, 117}	21
Figure 19 Introduction of chirality and photo-tunable properties.....	22
Figure 20 Introduction of chirality and photo-tunable properties.....	22

Figure 21 Inversion of configuration	23
Figure 22 Racemisation of Tröger's base.....	24
Figure 23 TB enantiomers.....	27
Figure 24 Functionalised TBA binds to dicarboxylic acids	30
Figure 25 Three examples of TBAs carrying polyimides:.....	31
Figure 26 TBA carrying polyhydrazide	32
Figure 27 TB based molecular tweezers ¹⁴⁵	32
Figure 28 Two examples of TBA carrying ligands	33
Figure 29 Typical TBAs investigated as thermotropic LCs	33
Figure 30 Tröger's base after clipping the diazocine bridge	34
Figure 31 Two examples of the azo-carrying TBAs	34
Figure 32 Diazocine bridge modification prevents TBAs racemisation	35
Figure 33 Typical structure of the desired products	39
Figure 34 A typical example of the Λ -shaped products.....	214
Figure 35 A schematic view of the crossed oscillators.....	214
Figure 36 Light-driven deformation.....	216
Figure 37 Suggested compounds.....	217
Figure 38 A light-driven liquid-crystalline elastomer	218
Figure 39 Copolymerisation of azo-carrying TBAs	219
Figure 40 A typical bis-azo molecular hinge ¹⁸⁴	219
Figure 41 Hinge-like feature of azo-carrying TBAs	220
Figure 42 A photo-switchable ion-channel ^{185, 186}	221

Figure 43 The assembly of light-triggered gates	222
Figure 44 Light-triggered gates in action	222
Figure 45 The <i>cis</i> photo-isomer provides a grip.....	223
Figure 46 The chemical structure of a triazene-based ligand.....	224
Figure 47 2D and simplified 3D presentation	225
Figure 48 Triazene-based polymers	225
Figure 49 Proposed copolymerisation of TBAs.....	226
Figure 50 Absorption spectra and the appearance	227
Figure 51 Absorption, emission and excitation spectra	228
Figure 52 Images of the crystallised azo-carrying TBAs	229
Figure 53 Images of the produced crystals of TBAs	230
Figure 54 SEM images of the produced TBAs spherical aggregates	231
Figure 55 Proposed surface modification by TBAs	232
Figure 56 Visualisation of image on photo-tunable LC phase	233
Figure 57 RGB colour cells.....	234
Figure 58 Colours created by manipulation of the RGB ratio	234

List of Tables

Table 1. The position of LCs	2
Table 2. Different arrangement of molecules.....	3
Table 3. The relationship between pitch length and observed colour	5
Table 4. Comparing the optical activity.....	26
Table 5. Dihedral angle between aromatic moieties of the TB scaffold.....	29
Table 6. Synthesis of TB and its di-amino analogues	37
Table 7 Non-ITO versus ITO conductors.....	40

Statement of Originality

I, Masoud Kazem-Rostami, certify that this thesis entitled " *Λ -Shaped photo-switches designed by employing the Tröger's base scaffold*" does not contain any material that has been submitted for the award of any other academic degree or diploma in other educational institutions. I also certify that all the materials in this thesis, including original research articles, have been designed, conducted, written and published by me, and to the best of my knowledge, this thesis does not contain any material previously published by other individuals, except where due references have been clearly made.

Masoud Kazem-Rostami

April 2018

Date

Acknowledgements

I gratefully acknowledge the Australian Government and Macquarie University for providing me with a Research Training Program Scholarship (IPRS-2014004), stipend, PGRF2016R2-1672525 fund, and HDR43010477 budget.

I would like to thank Dr Andrew Piggott, Dr Jennifer Rowland, Prof. Barbara Messerle, Prof. Peter Karuso, A/Prof. Joanne Jamie, Prof. Alison Rodger, Dr Ian Jamie, A/Prof. Paul Wormell, Ms Suzanne Lindsay, Dr Novruz Akhmedov, Prof. Yves De Deene, Ms Jennifer Minard, Ms Catherine Wong, Dr Jason R. Smith, Mr Mark Tran, Mr Tony Wang, Dr Arthur Chien, Dr Kavita Ragini, Ms Lesley Nearn-Cavanagh, Dr Sophia Goodchild, Dr Wendy L. Loa-Kum-Cheung, Dr Yuling Wang, Dr Fei Liu, Dr Soo Jean Park and Dr Christopher McRae for their support, technical assistance and provision of access to facilities. Thanks to all my dear friends especially Sadegh, Renee, Morgan, Donald, Ben, Shahnaz, Ketan, Ardeshir, Nirmal, Nazma, Sviatoslav, Kalpa, Ehsan, and Tahnim for their company and all the happy moments we have shared.

I thank all my former teachers who deserve my sincerest acknowledgment for their invaluable lectures and guidance during my BSc and MSc courses in Iran, especially Prof. Ardeshir Khazaei, A/Prof. Mohammad Bayat, A/Prof. Ahmad Reza Moosavi-Zare, and Prof. Abdolkarim Zare for building my independence in chemical research by teaching me the skill set for laboratory work.

Last but not least, I dedicate this work to my dear family who sacrificed everything they could without any hesitation to let me study for twenty-five years free of emotional and financial concerns. No words can express my gratitude for my dear parent's kindness.

Dedicated to my beloved mother and father...

پیشکش به مادر و پدر مهربانم

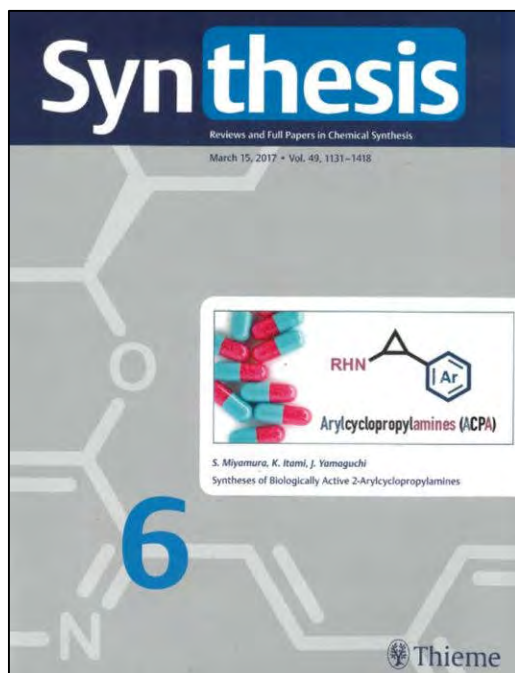
Justification of Thesis by Publication

This thesis is based on the following original research articles, which are numbered here and referred to throughout the thesis, by Roman numbers I–III. These original research publications have been reproduced following obtaining permission from each of the corresponding copyright holders/publishers. I, Masoud Kazem-Rostami, declare that Dr Amirhossein Moghanian is my only co-author in Paper II owing to his invaluable assistance with the final preparation of the corresponding paper, performing all the micro-elemental analysis and HPLC tests and covering the expenses from his grants. Those who have not had sufficient contribution to be considered as a co-author, are appropriately acknowledged in the related journal articles.

List of Original Publications (Thesis Map)

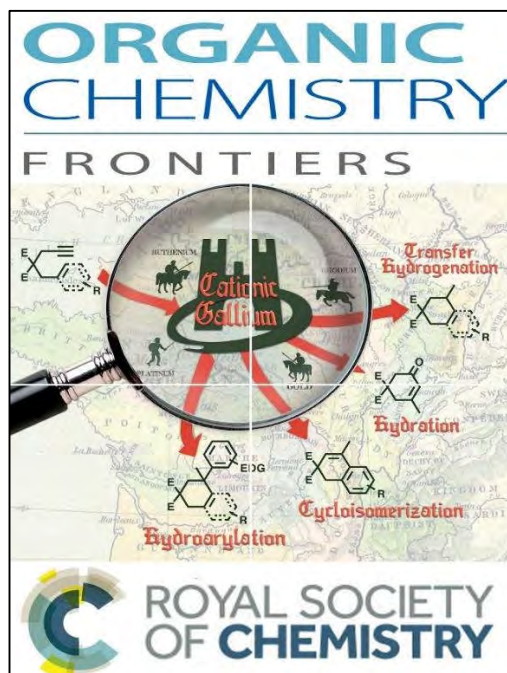
- I. Kazem-Rostami, M., Design and synthesis of Λ -shaped photo-switchable compounds employing Tröger's base scaffold. *Synthesis* **2017**, 49, 1214–1222.
- II. Kazem-Rostami, M.; Moghanian, A., Hünlich's base derivatives as photo-responsive Λ -shaped hinges. *Organic Chemistry Frontiers* **2017**, 4, 224–228.
- III. Kazem-Rostami, M., Facile preparation of Λ -shaped building blocks: Hünlich's base derivatization. *Synlett* **2017**, 28, 1641–1645.

Paper I



Journal Impact Factor: 2.689

Paper II



Journal Impact Factor: 4.955

Paper III



Journal Impact Factor: 2.419

Thesis Summary

This thesis introduces the first family of photo-responsive analogues of Tröger's base within three chapters, each incorporating one journal article. First, the availability of amino-carrying Tröger's base analogues was assessed following a review of the chemical literature and the most affordable one was chosen as the main building block in this thesis. Second, the syntheses were achieved by utilising standard diazotisation and azo-coupling procedures, which were optimised to improve the quality and quantity of the products. Therefore, various phenols were selected and coupled with a freshly produced bis-diazonium-carrying Tröger's base analogue to establish a new family of Λ -shaped molecular switches. The derivatisation of the selected compounds by Williamson's etherification reaction was also performed. Afterwards, the photo-isomerisation of the selected alkylated product was compared with the non-alkylated precursor to prove the photo-responsive nature of the obtained products. At the end, some issues including the racemisation of methano-strapped analogues, and the problematic production of the hydroxyl carrying ones, and various limitations imposed by the conventional synthesis procedures for Tröger's base analogues, were addressed.

Furthermore, this thesis elaborates on the high yielding and economically viable preparation of various ethano-strapped Tröger's base analogues as versatile Λ -shaped building blocks. The introduced building blocks that carry triazenyl, sulfhydryl, hydroxyl, carbamate and amino groups are the first of their kind. These smooth the way towards the formation of various novel molecules including non-racemisable and photo-switchable compounds. Based on the collected experimental results and comparing them with similar examples found in the literature, it can be concluded that these products have opened a new chapter into the design of molecular photo-switches, chiral liquid crystal dopants, photo-switchable molecular-recognition hosts, and chiral photo-alignment agents. The possible applications of the produced products are also elaborated on in the future directions section of the thesis.

Thesis Chapters Overview

This thesis employs Tröger's base analogues (TBAs) in the design of the first family of photo-switchable compounds with Λ -shaped scaffolds. This is described within three research chapters as follows:

Research Chapter One Synopsis (Incorporates Paper I)

Chapter One introduces the synthesis of the first family of bis-azo TBAs and elaborates on their molecular structure and properties. The syntheses were achieved by utilising standard diazotisation and azo-coupling procedures, which were optimised to improve the quality and quantity of the products in this work. The first bis-azo carrying TBA (Compd **1**, Paper I) was found to display an appropriate response to an applied electromagnetic stimulant, the ultraviolet wavelength of 365 nm, which encouraged using this product as a photo-isomerisable Λ -shaped core in the preparation of various derivatives. Therefore, this photo-switchable core was modified by Williamson's etherification reaction and a series of alkyl- and benzyl-group carrying derivatives were obtained in good yields. This series of products includes 17 novel compounds introduced in Paper I.

Research Chapter Two Synopsis (Incorporates Paper II)

Based on the experiences gained from the work described in the first research chapter, the design of bis-azo TBAs was further developed by manipulating their structures in this chapter (Paper II). First, the availability of amino-carrying TBAs was assessed following a review of the literature and the most affordable one was chosen as the main building block. Second, various phenols were selected and coupled with a freshly produced bis-diazonium-TBA to establish a new family of Λ -shaped molecular switches. The

derivatisation of the selected compounds by etherification reaction was also performed. Afterwards, the photo-isomerisation of an alkylated product was compared with its non-alkylated precursor. At the end, some issues including the racemisation of methano-strapped TBAs, and the problematic purification of the poly-hydroxyl carrying TBAs (Compounds **6–7**, Paper II) were discussed.

Research Chapter Three Synopsis (Incorporates Paper III)

Due to various limitations imposed by the conventional synthesis procedures of TBAs, the previous chapters only included racemisable products. The issues earlier discussed in Research Chapter Two, such as the racemisation and the problematic preparation of the desired TBAs, are addressed in this chapter. This chapter elaborates on obstacles in the production of non-racemisable and photo-responsive TBAs, and introduces the first non-racemisable and photo-switchable TBA.

This chapter fulfils the ultimate goal of this thesis by presenting optimised methodologies to provide the desired products in faster, cheaper and safer ways in larger scales with good yields. It also elaborates on the possible applications of the products. Therefore, these products have opened a new chapter into the design of chiral liquid crystal dopants, photo-switchable molecular-recognition hosts, and chiral photo-alignment agents. Furthermore, this chapter elaborates on the high yielding and economically viable preparation of various ethano-strapped TBAs as versatile Λ -shaped building blocks. The introduced building blocks carry triazenyl, sulfhydryl, hydroxyl, carbamate and amino groups that can facilitate the production of various novel TBAs. This smoothes the way towards the formation of chiral TBAs including the non-racemisable photo-switchable analogues.

Thesis Objectives and Achievements

Research Chapter One (Incorporates Paper I)

The main fulfilled goals of this chapter can be summarised in four aspects, as follows:

1. Synthetic aspect

The Tröger's base scaffold includes two tertiary amine groups that flank a diazocine bridge. This bridge plays a vital role in the preservation of the unique Λ -shaped structure of the TBAs. According to the literature,¹ treating TBAs with HCl/NaNO₂ aqueous solution leads to the removal of the diazocine bridge. Therefore, applying traditional diazotisation reagents (HCl/NaNO₂) was initially deemed to be inappropriate in the production of azo-carrying TBAs. Furthermore, the diazocine bridge amine groups are known to readily undergo side reactions including alkylation,^{2, 3} formation of quaternary amine salts,^{3, 4} or even ring-opening and rearrangement reactions.² These two pessimistic predictions were put to the test in this chapter. First, the diazotisation reaction was carefully optimised. Afterwards, various alkylation reactions were performed to evaluate the reactivity of the diazocine bridge amine groups and the chance of obtaining the desired alkylated derivatives. Delightfully, with slight changes in the reactions conditions, the desired products were obtained except for the benzyl-carrying or methylated ones (Paper I, compounds **16** and **2**; respectively), as explained within the corresponding journal article.

2. Photo-switching aspect

The Λ -shaped structure of the produced bis-azo TBAs, and the existing spatial hindrance around their bent scaffold, make the switchability of the azo groups questionable. Therefore, this uncertainty encouraged the study of how such molecules may respond to

the photonic stimuli. Tracking the UV/Vis absorption spectra of the major building block in this work (Paper I, Compd **1**) proved the isomerisation of the azo units occurred in a reversible fashion. Studying the isomerisation with NMR (Appendix 4) not only proved the photo-stability of the tested compound (Paper I, Compd **7**), but also determined its thermal back-relaxation rate.

3. Liquid crystal display (LCD) application aspect

LCD-related applications were the major aim of this project; and hence, the products were designed carrying various alkyl and benzyl groups to enhance their miscibility and dispersion in host LCs. Furthermore, it was found that within a certain range of the alkyl chains length, *e.g.* hexyl to octadecyl, these products showed multiple phase transitions, as seen by differential scanning calorimetry (DSC). This encouraged investigating them as LCs (Appendix 1). Appendix 1 includes all the related results collected from the thermal analysis of the selected compounds. The DSC along with observations of the heated samples determined the thermal stability of the products.

4. Molecular assembly aspect

The TBAs introduced in Paper I (*e.g.* compounds **1** and **13 – 15**) are equipped with reactive extremities to facilitate their application in the design of molecular hinges. These products can be readily attached to other hydroxyl, amine, acid or sulfhydryl group(s)-carrying molecules to develop their structures and confer photo-responsive properties to them. Further information and various futuristic applications are elaborated in the Thesis Significance Section.

Research Chapter Two (Incorporates Paper II)

The major achievements of this chapter can be summarised in four sections as follow:

1. Changing the void size

As discussed earlier, the Λ -shaped structure of TBAs is one of their most important features. The Λ -shaped scaffold possesses a void that can host smaller molecules inside and has been used in molecular recognition studies.⁵⁻¹² In this chapter, various substituted phenols were coupled with a bis-diazonium TBA to obtain a set of molecular switches with different void sizes and differently positioned substituents in or around the void. Therefore, these products may selectively host and respond to different molecules. The second paper and Appendix 2 display the corresponding products in more details.

2. Modification of the photonic properties

Azo compounds typically photo-isomerise following the absorption of a wavelength of light equal to their maximum wavelength of absorption. Substituents can affect the wavelength of absorption of the azo compounds. Hence, in this work the phenols were chosen in a way to cover most regions of the UV-Vis spectra. These structural modifications have provided a set of molecular photo-switches with selective responses to certain wavelengths of light. This enables applying two or more of these products simultaneously, and selectively exciting a desired one at a time by a certain wavelength of light. This provides a handy tool-kit, including a set of photo-switches to be used in molecular machines design.

Biologists and LCD manufacturers prefer use of longer wavelengths of light due to their less damaging nature towards skin and eyes. Therefore, this chapter offers a wide-range working set of photo-switches to satisfy such requirements (Paper II, Figure 1).

Furthermore, this chapter studies the substituent effects on the Λ -shaped void geometry based on the gleaned experimental data and the computational modelling (Appendices 2 and 3).

3. Synthesis, purification and characterisation challenges

This chapter is a fruitful exercise to a better understating of the chemistry of such large photo-switchable molecules. Condensation reactions, azo coupling and etherification reactions may initially look simple but the unique features of the TBAs give extra dimensions to the work and raise various challenges, which are discussed within the second journal article. This chapter also briefly reviews the earlier synthetic work, suggesting appropriate building blocks that can be transformed to bis azo TBAs. Furthermore, the obstacles in obtaining chiral-resolved products are discussed in Paper II.

4. The photo-switchability and kinetic aspects

As expected, modification of the chromophore structures influenced the response of these products to the external stimulant and they displayed various rates of back-isomerisation. This can be of interest in time-sensitive applications; for instance, in the design of smart drug delivery systems or optically activated shutters.¹³ Therefore, the photo-isomerisation of an alkylated product was compared with its non-alkylated precursor as a proof of concept.

Research Chapter Three (Incorporates Paper III)

The first two chapters included methano-strapped and racemisable TBAs, and all the synthetic work started with a methano-strapped diamino TBA. The third chapter introduces some superior synthesis strategies with numerous advantages over the applied methodologies within the first two chapters, as follows:

1. Sustainable optical activity

This chapter elaborates on some obstacles in the production of non-racemisable and photo-responsive TBAs. Various strategies are elaborated in detail in Paper III as well as being compared with other tested methods found in the literature. These have provided a better understanding of TBA chemistry as well as improving the efficiency of the applied methods. Methano-strapped TBAs racemise¹⁴ under the acidic condition of the conventional diazotization reaction. Therefore, chiral resolution has to be performed afterward to obtain the corresponding chiral azo-carrying TBAs. The chiral resolution of each racemisable product may require specific conditions, reagents and methods; therefore, finding an acid-resistant¹⁵ building block could be strategically superior to Paper I and Paper II methods. The handedness of ethano-strapped TBAs is not influenced by pH; and hence, they can be suitable chiral starting materials for the diazotisation reaction (elaborated in Figure 32).¹⁵ This chapter introduces the first ethano-strapped diamino-TBA, which can be used as an enhanced building block. Furthermore, this chapter elaborates every practical strap-change operation that can be performed on an affordable TB building block, called Hünlich's base, as well as a selected compound from the first two research chapters. The strap-change operation or modification of the diazocine bridge resulted in the TBAs being resistant to racemisation under acidic conditions. This may facilitate the production of the desired LC dopants out of these products.

The synthetic methods, optimised within the first two chapters, were accordingly used in this chapter to obtain the first non-racemisable and photo-switchable TBA out of the modified building blocks. This can be considered as the ultimate accomplishment of the entire project.

2. Simplified and enhanced chemistry

In this chapter, the production of TBAs is simplified and the yields are improved through optimising the reaction conditions and the purification methods. The reaction times and the production costs are significantly reduced. The novel TB building blocks introduced in this chapter provide more approaches toward formation of azo-carrying TBAs. For instance, phenoxy-carrying TBAs (compounds **3**, **11**, and **13**, Paper III) can be coupled with inexpensive diazonium salts to form new azo-carrying TBAs.

3. Novel TBAs

In addition to the required TBAs for this project, some innovative TBAs carrying triazene or sulfhydryl groups are introduced for the first time in this chapter. Although numerous methods have reported the production of TBAs including azide or triazole-carrying analogues;^{16, 17} to date, no TBA has been produced carrying triazene or sulfhydryl functional groups. These would be useful in coordination,¹⁸⁻²¹ polymer,^{22, 23} surface,²⁴⁻²⁷ and organometallic/heterocyclic²⁸ chemistries. The triazene group can be converted to functionalised lactams,²⁹ triazoles,³⁰ dibenzopyranones and coumarins,^{31, 32} or be utilised as a substrate for perfluoroalkylation reactions³³ or design of prodrugs.³⁴ Furthermore, the triazene group can be replaced with many other functional groups³⁵⁻³⁷ by being consumed as a diazonium source in organic solutions³⁶ or ionic liquids.^{38, 39} This enabled the *in situ* replacement of diazonium (leaving group) by hydrogen sulfide (nucleophile),³⁶ and the production of the first bithiophenol-carrying TBA (Paper III, Compd **2**) in this chapter, which might be useful in the design of disulfide-based networks.⁴⁰

4. New strategies

The protection of the diamino-TBAs is also reported in this chapter. This has significantly extended the shelf life of the sensitive starting materials. The *in situ* deprotection of the

Boc-protected TBAs (Paper III, Compd **4** and **5**) is fast and easy⁴¹ and releases the corresponding diamino-TBAs, which can be easily converted to the other desired compounds, as is described within the corresponding journal article (Paper III).

To overcome the obstacles in the preparation of chiral and photo-switchable TBAs, and passing through the limitations of the traditional synthesis procedures, new strategies were introduced and applied in this chapter; such as unconventional^{42, 43} azo coupling reactions starting with carbamates. Furthermore, an azo coupling reaction can be performed between a hydroxyl-carrying TBA with diazonium salts to generate new switchable TBAs. This means that the role of TBAs in azo coupling reaction can be changed from a bis-diazonium salt to the phenolic substrates, which can be more productive than the previous methods. Therefore, the preparation of various hydroxyl-carrying TBAs are reported in Paper III.

5. Photo-responsivity and related applications

As discussed earlier, the Λ -shaped structure of TBAs is one of their most important features. The TBAs Λ -shaped scaffold possesses a void that can host smaller molecules inside and has been used in molecular recognition studies.⁵⁻¹² In this chapter, the diazocine bridge was modified to obtain ethano-strapped TBAs as molecular hosts with different void shapes. Therefore, these products may selectively host and respond to different molecules. The photo-isomerisation of the modified products were also tested and compared with their methano-strapped counterparts. This comparison revealed that the photo-isomerisation yield, thermal-relaxation rate, back-isomerisation period, maximum wavelength of absorption, and $\log \epsilon$ values are almost identical. Therefore, no matter whether an ethano- or methano- strapped TBA is made, the azo groups can freely isomerise, and then undergo the thermal relaxation. These observations proved that the TB scaffold does not interfere with the photo-switching mechanism and can be employed in the design of novel chiral photo-responsive liquid crystal dopants.

List of Abbreviations

The applied abbreviations throughout the thesis and the journal articles are listed as follows:

1D	One dimensional
2D	Two dimensional
6CB	4'-Hexyl-4-biphenylcarbonitrile
7CB	4'-Heptyl-4-biphenylcarbonitrile
AB	Azobenzene
ACN	Acetonitrile
Aq	Aqueous
BINAP	2,2'-Bis(diphenylphosphino)-1,1'-binaphthyl
Calcd	Calculated
CDCl₃	Deuterated chloroform
CD₃CN	Deuterated acetonitrile
CD₃OD	Deuterated methanol
COSY	(Proton-proton) correlation spectroscopy
CPRLCDs	Chiral and photo-responsive liquid crystal dopants
CPSTBAs	Chiral and photo-switchable Tröger's base analogue
DB	Diazocine bridge

DBTA	2,3-Dibenzoyltartaric acid
(+)DBTA	(+)-2,3-Dibenzoyl-D-tartaric acid
(-)DBTA	(-)-2,3-Dibenzoyl-L-tartaric acid
DGA	Diglycolic acid
DMSO	Dimethyl sulfoxide
DMSO-<i>d</i>₆	Deuterated dimethyl sulfoxide
<i>E</i>	<i>Trans</i> isomer (from German: “entgegen” meaning opposite)
EtOAc	Ethyl acetate
Equiv	Mole equivalent
ESI	Electrospray ionisation
ESI-MS	Electrospray ionisation mass spectrometry
Fig.	Figure
HB	Hünlich's base
HDR	Higher degree by research
HCl	Hydrochloric acid
HMBC	Heteronuclear multiple-bond correlation
HPLC	High performance liquid chromatography
H₂SO₄	Sulfuric acid
HSQC	Heteronuclear single-quantum correlation spectroscopy

HTP	Helical twisting power
IPRS	International postgraduate research scholarship
IR	Infrared
ITO	Indium tin oxide
LC	Liquid crystal
LCD	Liquid crystal display
LCMS	Liquid chromatography mass spectrometry
MeOH	Methanol
N/A	Not applicable / not available
nm	Nanometre
NMR	Nuclear magnetic resonance
NOE	Nuclear Overhauser enhancement
PFA	Paraformaldehyde
PGRF	Postgraduate research fund
PL	Pitch length
POM	Polarised optical microscope
PPA	polyphosphoric acid
Py	Pyridine
Py-<i>d</i>₅	Deuterated pyridine

ROESY	Rotating-frame Overhauser effect spectroscopy
SEM	Scanning electron microscope
SG	Silica gel
SI	Supplementary information
TB	Tröger's base
TBA	Tröger's base analogue
TCAA	Trichloroacetic acid
TEM	Transmission electron microscopy
TFA	Trifluoroacetic acid
TLC	Thin layer chromatography
TMS	Tetramethylsilane
UV	Ultraviolet
Vis	Visible
Z	<i>Cis</i> isomer (from German: "zusammen" meaning together)

Introduction

1. Introduction to display technology

1.1 Liquid crystal displays

Liquid crystal display (LCD) technology has contributed to human life to the extent that nowadays imagining the world without it is impossible. LCDs are being widely used for educational, recreational and commercial purposes every day worldwide. This technology has not only replaced the old and bulky cathode-ray vacuum tube televisions, but has also significantly contributed to the reduction of our reliance on paper-based tasks.

Displaying information on electronic panels, like LCDs, instead of printing hard copies helps the protection and preservation of natural resources. The commercialised applications of LCDs have strengthened its industrial production and hence has driven their non-stop development to feed this global sky-rocketing demand. LCDs are the major components of electronic devices from simple boogie boards, calculators or digital clocks, to computers, smartphones and even sophisticated spacecraft control panels. In fact, LCDs are an interface through which humans and machines communicate.

LCDs are multi-layer sandwiched structures that contain at least one layer of liquid crystals (LCs), two glass or plastic substrates, a pair of transparent electrodes made of Indium Tin Oxide (ITO), colour filters and a pair of polariser-analyser films (Figure 1).

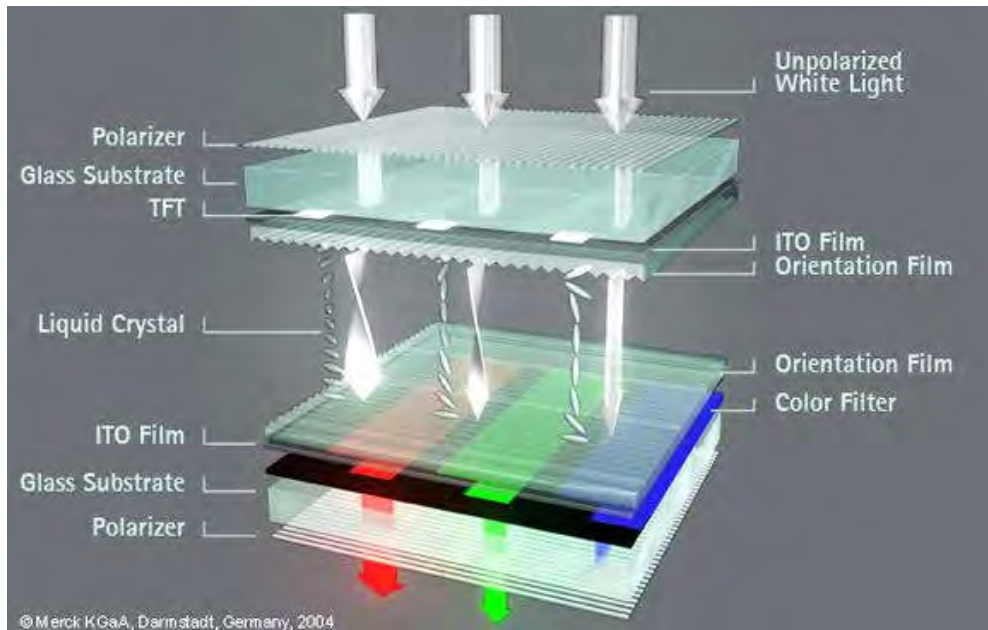


Figure 1 Multi-layered structure of one LCD unit (RGB pixel)
Reproduced figure by permission from Merck⁴⁴

1.2 Liquid crystals


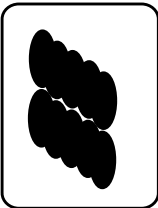
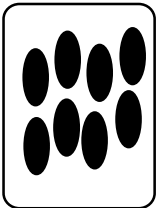
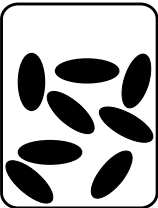
Liquid crystals (LCs), which function as the key component of LCDs, are mesophase(s) laid between the solid state and isotropic liquid. Pursuant to the definition of states of matter, an LC phase may be considered as the intermediate between solid and liquid; however, it technically is classified as one of the non-classical states of matter (Table 1). The non-classical states of matter represent special features and properties which strictly belong to this category of materials. Accordingly, due to the special physical and optical properties of LCs, they have been utilised in the design of LCDs.

Table 1. The position of LCs
amongst various states of matter^{45, 46}

Fundamental	Non-classical	Low-temperature	High-energy	Others
Gas	Glass	Bose–Einstein condensate	Colour-glass condensate	Dark matter
Liquid	<u>Liquid crystal</u>	Fermionic condensate	Degenerate matter	String-net liquid
Plasma	Magnetically ordered	Rydberg molecule	Quark–gluon plasma	Superglass
Solid	Microphase	Super-fluid	Very high energy states	Super-solid

In the LC phase, the molecules not only have some extent of freedom in movement, like those sliding over each other in liquids, but are also ordered in a specific orientation (*i.e.* the same direction), making a pseudo-solid lattice (Table 2). Based on this definition, many of the molecules that play significant roles in nature, such as proteins and cell membranes, can also be classified as LCs. Bio-liquid crystals were discovered by observing biomaterials such as cell membranes and some biological fluids such as lecithin⁴⁷ (obtained from the egg yolk) or myelin⁴⁸ (existing isolator in nerve tissues) under polarised-optical microscopes.⁴⁹

Table 2. Different arrangement of molecules in solid, LC, and liquid state

Phase	Solid	LC	Liquid
 : A molecule			
Molecules order			
Orientational	Yes	Yes	No
Positional	Yes	No	No

Several layers of orientated LC molecules may generate a helical twisted structure (Figure 2) that is capable of rotating polarised light. This helical twisting power (HTP) is the basis of how LCDs work. This means that the LC layer can twist the beam of polarised light, permitting it to pass through the crossed polarisers (Figure 1). Any interruption to the helix prevents the light beam from passing through the crossed polarisers. These features allow LCs to be used to make a screen shiny or ON when the light passes through and dark or OFF when the light cannot pass through.⁵⁰

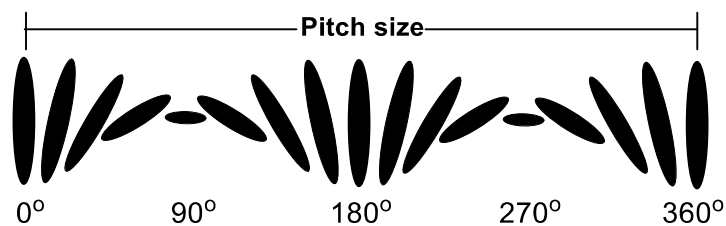


Figure 2 Helical LC structure and pitch length

The distance through the twists in which LC molecules experience a full turn is defined as pitch length (Figure 2). A wavelength of light equal to the pitch size can be reflected by LCs. The pitch size varies at different temperatures. This means a rise of temperature can expand the pitch size and shifts the reflected light to the red and lowering the temperature contracts the pitch size and shifts the reflected light to the blue. This phenomenon elaborates the LC thermometers mechanism. Similarly, due to the proportionality of pitch size and the length of reflected light, LC layers with a random surface or tackiness are seen as a marbled⁴⁹ texture (Figure 3) under a polarised optical microscope.

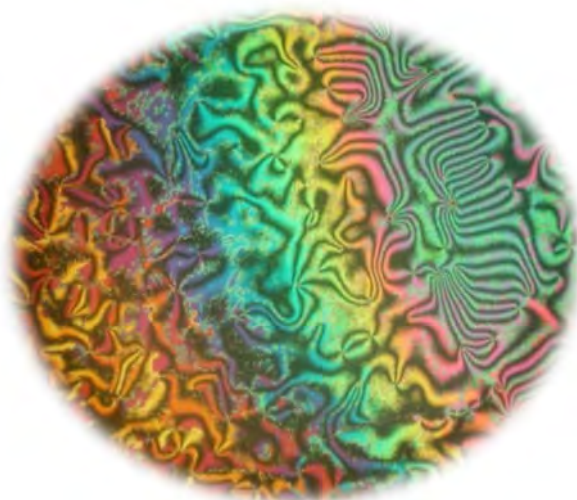
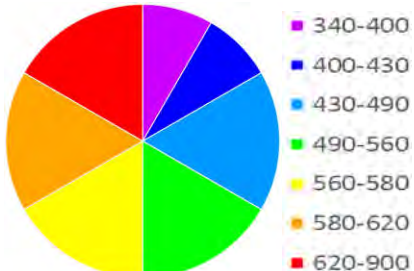


Figure 3 Marbled texture of an unaligned LC phase
This figure is adapted from Dr Ji-Hoon Lee's website⁵¹

In Figure 3, a poly-domain LC phase is shown in which the boundary of the domains is continuous. Therefore, the domains appear as threads, which are called *nema* in Greek; and hence, such a phase is called *nematic*. The pitch lengths that correspond to the observed colours, are listed in Table 3.

Table 3. The relationship between pitch length and observed colour

Observed colour	Reflected wavelength (nm)	Approx. Pitch length (nm)	Colour and wavelength wheel
<i>Violet</i>	400–430	400–430	
<i>Blue</i>	430–490	430–490	
<i>Green</i>	490–560	480–560	
<i>Yellow</i>	560–580	560–580	
<i>Orange</i>	580–620	580–620	
<i>Red</i>	620–700	620–700	

LCs are typically divided into three major groups of thermotropic,⁵² lyotropic and metallotropic, based on the factors that limit the LC characteristics of these materials (Figure 4).⁵³ LCs having both organic and inorganic composition are classified as metallotropic. LCs of organic origin that exhibit LC properties at a certain range of temperature or concentration are known as thermotropic and lyotropic, respectively (Figure 4). Thermotropic LCs^{50, 53} are further classified as bowlic, discotic, sanidic and calamitic by their shape.⁵² Thermotropic LCs are the focus of this dissertation.

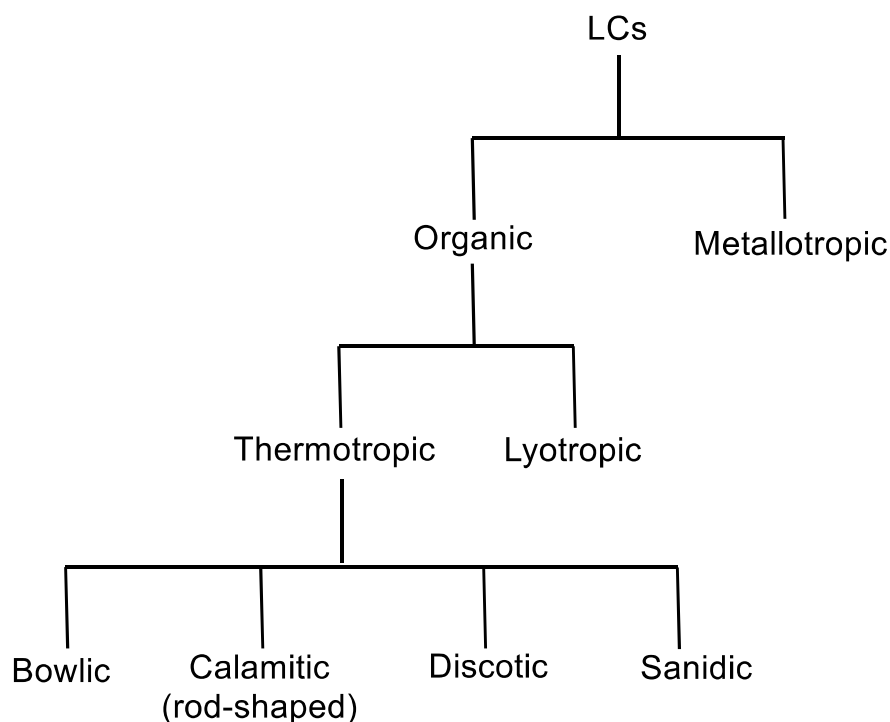


Figure 4 Classification of LCs

2. LCDs evolution towards the design of smart displays

The performance of LCs has been continuously improved during the last two decades by introducing new properties to them such as the addition of polar groups, chiral centres, and isomerisable units and by improving the LC layer preparation techniques. Advances in the performance of LCs are briefly discussed in the following subsections.

2.1 Alignment and orientation of LC molecules

LC molecules in defined conditions are capable of sliding over each other to generate self-orientated microscopic domains. Extending a uniform alignment of LC molecules in a specific and desired direction has been a challenge in the manufacture of LCDs. An ideal alignment of the LC molecules results in the appearance of the highest brightness on the display. Any failure in the alignment leads to serious optical defects on the screen, which can be easily detected by the human eye. The structures of LCs and the applied techniques in the alignment of LCs have evolved significantly. These are both briefly reviewed in the following subsections.

2.1.1 Mechanical alignment

Uniform alignment of molecules by imposing mechanical forces is called mechanical alignment. Mechanical alignment can influence how materials interact with light. For instance, stretching a thin layer of an elastic polymer can uniformly align the pulled polymer chains and enhance the transparency of the film. To illustrate the basis of this phenomenon a simple analogy can be made by imagining many trees and a straight-moving vehicle. In this analogy, when the trees are randomly grown in a dense jungle traveling through them by a straight-moving vehicle is impossible; while, this vehicle can easily travel through an aligned forest in the specific direction(s). In fact, in this example, light, just like the vehicle,

is blocked by the trees and that is why our vision in a dense jungle is limited to a couple of metres; while in an aligned forest our vision covers hundreds of metres ahead. Similarly, when a beam of light meets a film consisting of polymer chains entangled with each other, it interacts with every polymer chain and may become scattered, reflected or absorbed over the film (Figure 5, left). This random positioning of the chains blocks the path of light travelling in a straight line. Therefore, light has a very low chance of penetrating deep into the film and passing through it. In contrast, when the film is stretched under a mechanical force, the polymer chains gradually align and the light beam will pass through the film more easily, and hence the film becomes translucent. If the pulling is continued, the film reaches a stage in which the chains are perfectly aligned and the beam of light can easily pass through the film, making the film appear transparent (Figure 5, right). Switching between these transparent and non-transparent states of liquid crystalline elastomers is a desirable optical property that has been imitated in the design of smart LC windows.⁵⁴⁻⁵⁶

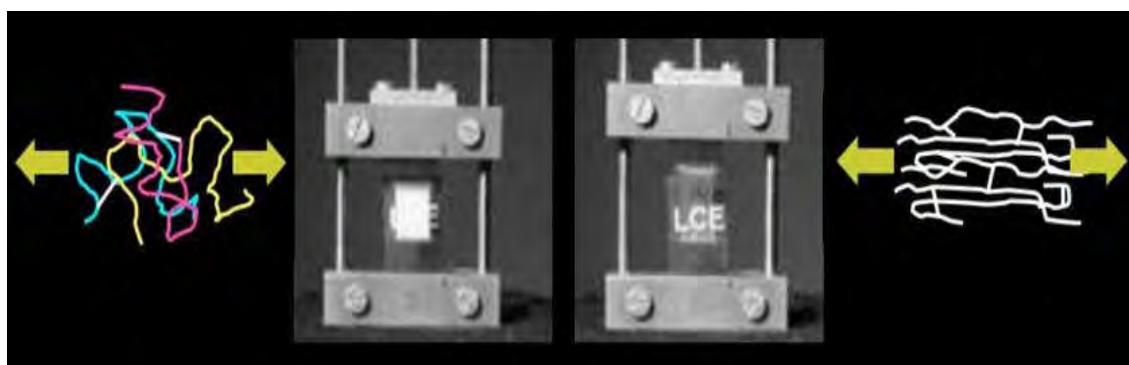


Figure 5 Pulled polymer becomes transparent⁵⁴

In Figure 5 (left) the unstretched polymer film having a random structure is not transparent, however when it is stretched it becomes aligned and nearly mono-domain, which is transparent (Figure 5, right).⁵⁴ The pulled polymer can return to its initial state if the polymer-chains are properly crosslinked; otherwise, it will become loose and remain mono-domain and transparent. Liquid-crystal elastomers may contain LC components as the main part of their elastomeric backbone, or as pendent moieties assembled on it.^{55, 56}

Mechanical alignment is the oldest⁵⁷ method for alignment of LC molecules. This process starts by coating the LCDs glass-made substrates with a very thin and transparent layer of polymer (mainly polyimides). Then, these soft linings are brushed to generate surface scratches that can facilitate alignment of LC molecules (Figure 6). This thin layer of polymer is called orientation film (shown in Figure 1).



Figure 6 Brushing method for mechanical alignments

Unfortunately, this macroscopic process due to its high sensitivity has significant disadvantages such as being limited to a single-direction and superficial patterning, unwanted generation of electrostatic charges and interference of dust, topological randomness, and physical damage. The presence of any external object such as dust particles in the LC layer interferes with the arrangement of LC molecules and may induce physical changes such as crystallization or solidification. These disable the screen and no image would be produced. Unwanted dust particles and topological randomness may change the thickness of the LC layer that is precisely controlled by the addition of glass bead spacers (often in size ranges of 27–30, 37–40, or 50–53 micron in diameter). The topological randomness generates unwanted colour gradients or wavy images on the screen. Moreover, any impurity introduced by these particles may chemically react with the LC molecules and cause permanent damage leading to dead or stuck pixels. The consequences of these abnormalities are often called optical defects as they are not caused by the LCDs electronic components and they always lower the image quality and optical efficiency of LCDs. Nonetheless, mechanical alignment is currently the most

common method in the conventional LCs alignment. Figure 7 presents the chemical structure of a typical member of commercially available conventional LCs, namely alkyl-biphenylcarbonitriles. The commercial name of such LCs is an abbreviation including a number indicating the length of the alkyl group and a “CB” suffix representing cyanobiphenyl carrying LCs; for example, 6CB and 7CB stand for 4'-hexyl-4-biphenylcarbonitrile and 4'-heptyl-4-biphenyl carbonitrile, respectively.⁵⁸ Such conventional LCs have a polar head and a rigid body that facilitate the alignment by dipole-dipole and π -stacking intermolecular interactions. These noncovalent interactions can create some degree of initial orientation in the absence of an electric field. Therefore, LC molecules stack up in column-like structures (Table 2). The extremities of these columns reach and anchor to the orientation films (Figure 1). This phenomenon creates a uniform helical twist in LC columns due to the fact that the orientation films are crossed and hold the columns extremities perpendicular to one another. This state can be called ON (bright) mode when the pixels are equipped with crossed polarizer films (Red subpixel, Figure 1). When an electric field is introduced the LCs dipoles contribute to a new alignment that hold the LC molecules in the direction of the electric field regardless of the orientation films or the intermolecular interactions. This state can be called OFF (dark) mode in which the polarization plane of light cannot be rotated and light does not pass through the crossed polarizers (Blue subpixel, Figure 1). Therefore, the brightness of each subpixel can be adjusted by tuning the applied voltage on its ITO electrodes (Green subpixel, Figure 1). In this particular example (Figure 1), due to the produced RGB ratio, the pixel may appear orangish-yellow. When the ITOs voltage is cut, the electric field becomes absent and the LC molecules will again become orientated by their intermolecular interactions and the orientation film. The structure of conventional LCs (Figure 7) also includes a non-polar flexible alkyl chain that lowers the phase transition onset(s) and the risk of solidification. Furthermore, the latter lowers the viscosity of the monomeric LCs as well as influencing the elasticity of the LC elastomers.

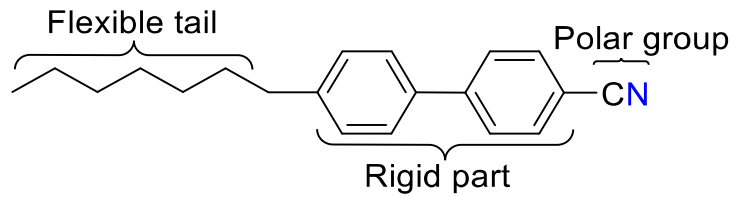


Figure 7 The chemical structure of 7CB
(4'-heptyl-4-biphenylcarbonitrile)

2.1.2 Orientating LC molecules by surfactants

Immersing an LC layer in water and applying surfactants such as phospholipids can dynamically modify the LC molecules' orientation. This alignment occurs when the existing interface between the LC and aqueous layer hosts the surfactant (Figure 8). In fact, the hydrophobic tail of the surfactant aligns the LC molecules by digging into the mesophase and anchoring itself at the interface (Figure 8, right). This simple method results in an excellent LC alignment; however, this method suffers from disadvantages such as impossible removal of the surfactant, LC phase solidification and mono-domain orientation.⁵⁹

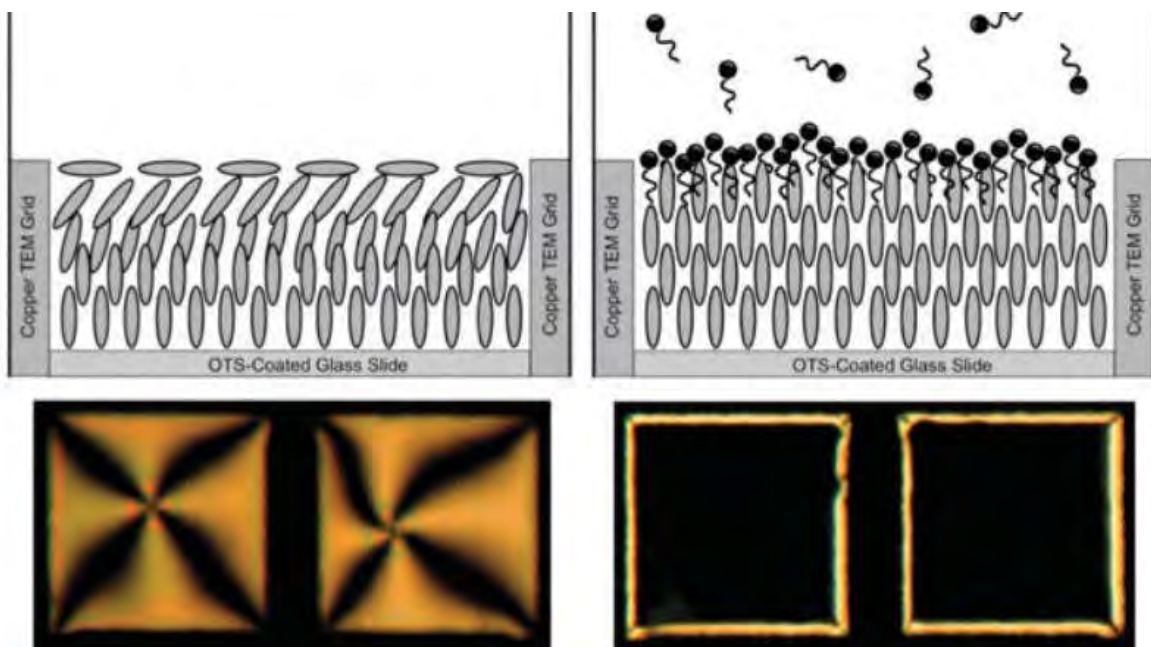


Figure 8 The schematic- (top) and optical-views (bottom) of LC layers in contact with brine (left), and an aqueous solution containing a surfactant (right)⁵⁹

2.1.3 Orientating LC molecules by electric field

Application of an electric field, accompanying the methods already explained, can give an extra dimension to the LC alignment. Basically, in most of the LCDs, LC molecules are aligned by the orientation films and their helical twisting power (HTP) enables the light beam to pass through the crossed polarisers (Figure 1). When an electric field is imposed, LC molecules change their arrangement to align with the electric field. When the electric current is cut, the molecules again get aligned as the orientation films dictate. Therefore, these switching states can make the screen ON or OFF depending on what angles exist among the polarisers, the orientation films, and the electric field. Substituting one alignment method by another requires modifying the chemical structures of the LC, and vice versa. Therefore, the alignment of LC molecules under electric fields requires redesigning the LCs structures and LCDs. The addition of polar groups, *e.g.* cyano or methoxy substituents (Figure 9, bottom)⁶⁰ and π -systems, enables the alignment of LC molecules under electric fields.⁶¹ This idea has led to the classification of the polar LCs⁶² into ferroelectric, antiferroelectric, banana-shaped, and columnar subgroups, based on their shape and response to electric fields (Figure 9).⁶² Although polar LCs have been classified as discussed, the members of each class may not necessarily exhibit a similar morphology or surface chemistry.⁶²

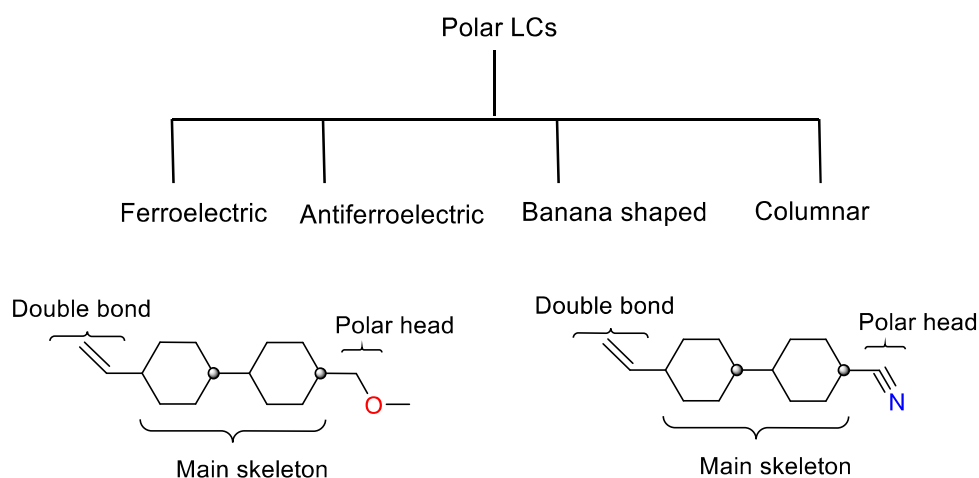


Figure 9 Classification of polar LCs with two typical ferroelectric LC examples⁶²

The required electric field is obtained by introducing a voltage to a pair of transparent indium tin oxide (ITO) electrodes sandwiched into the multi-layered structure of the LCD (Figure 1). The inclusion of ITO electrodes makes the screens thick, rigid and costly. The latter is due to the fact that indium is not found in the form of a known ore in nature and is only obtained as the byproduct of other metals refinement. Therefore, indium is very expensive and limited in its availability. A current state of art in this field is the replacement of ITO electrodes with silver nanowires or organic transparent conductive films having carbon nanotubes and graphene. To date, the replacement of ITO with these alternatives has been an industrial challenge and hence new horizons are being explored in this field like using photo-alignment methods as an ultimate solution.

2.1.4 Photo-alignment and design of smarter LCDs

The evolution of LCDs has been rapid, in part spurred on by their fascinating and wide-range applications. The most recent development of LCDs has led to them being thin, flexible and smart (Figure 10).⁶³⁻⁶⁶ This has enabled LCDs to work without being connected to external power supplies, or bulky or costly electronic circuits. This type of LCD can even be produced with no internal conductive ITO layers or thick glassy substrates.⁶⁷ Such displays can be considered as optically rewriteable⁶⁸ screens with a temporary graphical memory.⁶³ This type of LCD also has a noticeable stability, a long lifespan and a fairly high contrast (Figure 10).⁶⁹ Therefore, this rapid development of LCDs has led to a tremendous demand for designing new LCs and materials that can be combined with LCs to enhance their properties; namely dopants. As already explained, substituting an alignment method by another imposes a requirement of modifying the chemical structure of the LCs, and *vice versa*. These major evolutions of the LCs have become feasible by the introduction of chirality and photo-tunable properties as well as by applying much more developed alignment techniques; the latter of which are briefly reviewed below.

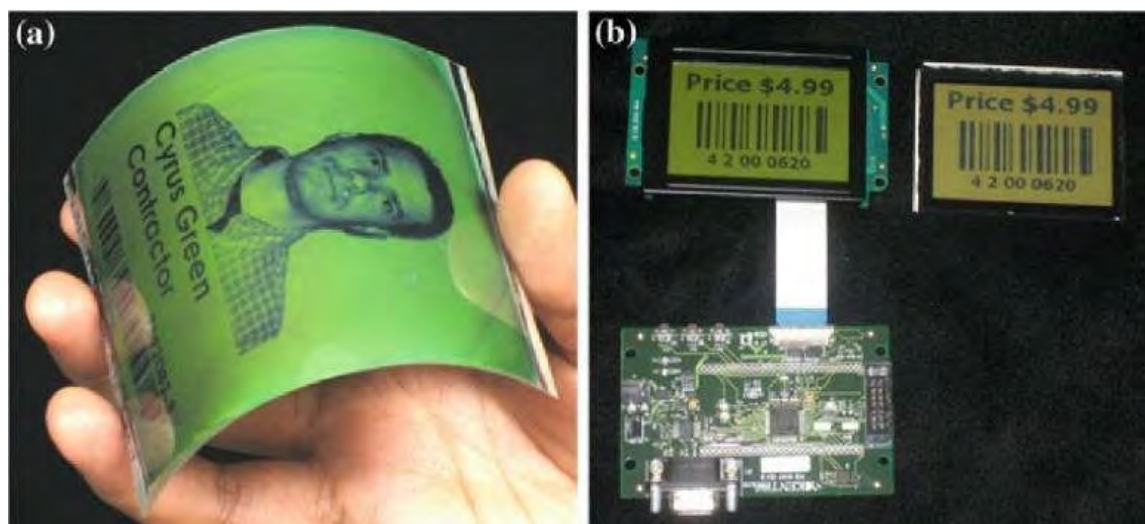


Figure 10 An example of a flexible LCD (a) and image quality (b) produced by a conventional LCD (b, left) versus a self-powered reflective LCD⁶⁶ (b, right)

LC photo-alignment was first discovered in 1988 by embedding and illuminating a molecular layer of azo materials in LCDs in which the azo groups functioned as a photo-responsive mechanism.⁷⁰ Although photo-alignment is regarded as the best method of LC alignment, it could not easily occupy a foothold in mass production of LCDs until its recent revolutionary contribution in the evolution of LCDs; *e.g.*, utilised by *Apple*[®] in the design of the *iPhone-6*[®] screen.

LC photo-alignment is based on how its chromophores interact with light. For example, when a linear polarised light source illuminates azo dyes, the light interacts with the azo chromophores. This interaction involves the absorption of light, which photo-excites the molecule. According to the literature,⁷¹⁻⁷³ the absorption of light is minimised when the dye molecule is positioned at a specific angle. In that specific angle the molecule's transition dipole moment is perpendicular to the direction of the polarised light and hence has the lowest probability to absorb the electromagnetic energy (Figure 11). Hence, those molecules positioned parallel or even semi-angled to the polarisation vector, will absorb the light and become photo-excited. The elevated energy level of these excited molecules causes greater vibrational and rotational motions and facilitates positioning of the

molecules in the desired perpendicular angle, in which molecules can relax and contribute to the photo-alignment (Figure 11).

This photo-induced-ordering phenomenon results in a uniform alignment of the azo molecules.⁷⁴ Photo-alignment depends on radiant exposure of light, which is the irradiance of a surface integrated over time of irradiation, measured by the joule per square metre ($J.m^{-2}$). Therefore, the higher intensity and the longer exposure time to the light, the faster and the better the alignment will be. When the lined-up molecules stack perfectly, their intermolecular interactions, e.g. π -stacking, stabilise the alignment. Such aligned structures are sustainable even after switching off the light source and raising the temperature by a few degrees for annealing the aligned layer.⁷³ The photo-aligned layers have better optoelectrical properties than the mechanically rubbed polyimide substrates.⁷⁴
⁷⁵ Also, the photo-alignment technique includes none of the mechanical alignment disadvantages discussed earlier (Section 2.1.1).⁷²

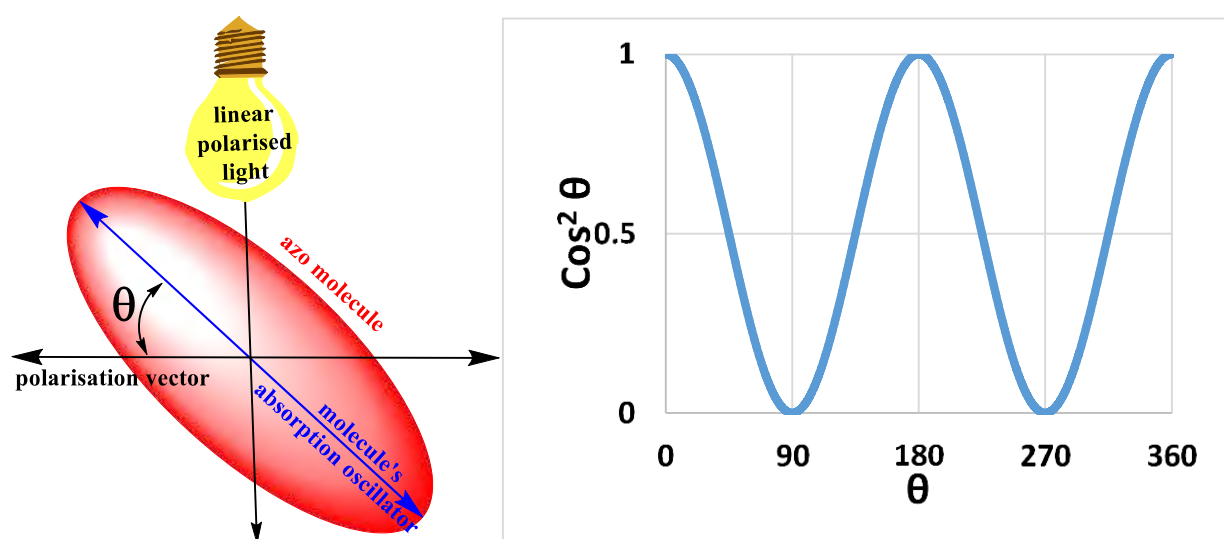


Figure 11 Proportionality of light absorption and the angle of polarised light

Azo-assisted LC photo-alignment is based on the negative phototropism of azo materials. This means that azo chromophores position their oscillators perpendicular to the direction of the electric polarisation vector to escape the electromagnetic radiation.⁷⁶ As shown in Figure 11, the absorption of light is proportional to $\propto \cos^2 \theta$, where θ is the angle between the polarised light electric vector and the chromophore's oscillator.^{71, 77} The chemical structure of a typical azo photo-aligner is shown in Figure 12.

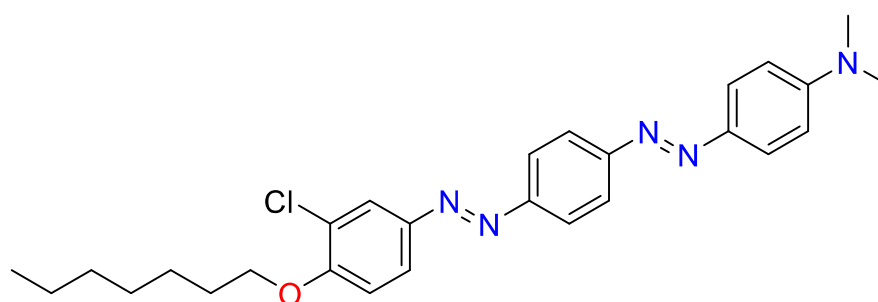


Figure 12 A typical synthetic azo dye used in photo-alignment of LCs⁷⁸

The photo-alignment technique, unlike the older methods discussed in Sections 2.1.1 – 2.1.3, can easily provide dual- or multi-domain alignments, which provides an excellent angular view of the screen (Figure 13). As is shown in Figure 13, mono-domain LC alignment fails to display true colours to the viewers who are in an angled position to the screen (viewers at $\pm 45^\circ$);⁷⁹ while, dual- or multi-domain alignments result in an angle-independent display. Therefore, all the viewers have equal colour vision on the dual-domain screen. The angle-independent view of a dual-domain LCD is shown at the bottom of Figure 13 for making a comparison to the angle-dependent view of a single domain LCD shown at the top.^{75, 80, 81} This technology also improves the stability of the LCDs to heat and light exposure as well as providing stronger anchoring energy and a more controllable LC tilting angle.^{71, 82-84}

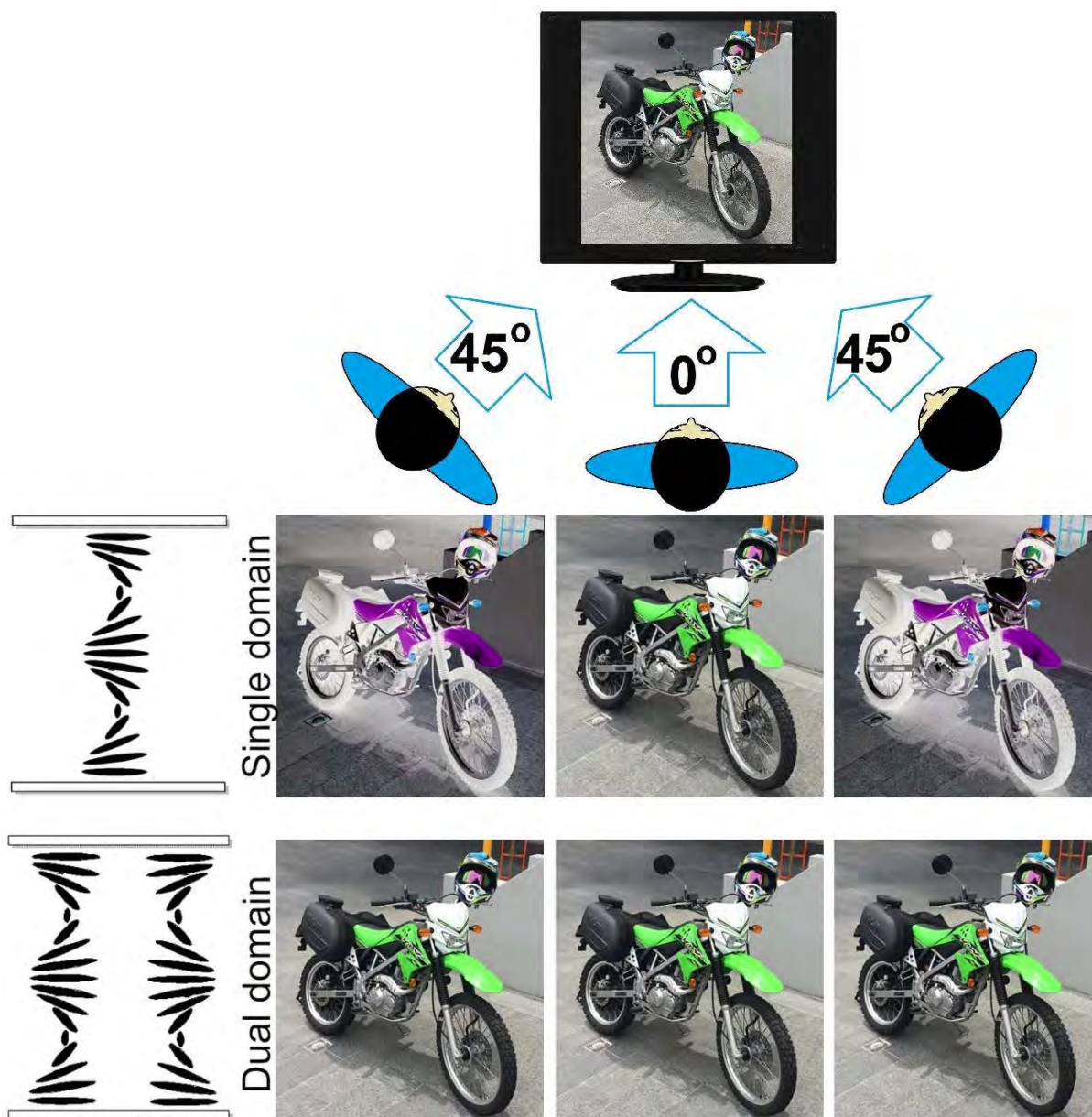


Figure 13 Comparing the angular view of a dual-domain display versus single-domain

Furthermore, the versatile family of azo materials can be used as molecular solvates, namely “azo dopants” in LC hosts; as well as monomeric or copolymerised photo-responsive layers that can be used in the design of super-thin alignment substrates^{64, 65} (Figure 14) or photovoltaic films.⁸⁵ A wide range of photo-alignment techniques have been developed by utilisation of different materials and methods such as polyimide photo-degradation^{86, 87} and cinnamoyl derivative polymerisation,^{78, 88} however none have been as successful as azo materials.

Azo compounds function as reversible photo-isomerisable units that undergo no chemical change; however, the two other aforementioned techniques, using polyimides and cinnamoyl derivatives, involve chemical reactions that may influence the other LCD components and may lower the resolution. Therefore, azo compounds stand on the top in this category of materials for the following advantages in the photo-alignment of LCs:

- 1) Minimising surface–LC interaction to anisotropic Van-der-Waals-forces (namely contact-free)
- 2) Achieving a multi-domain and patterned alignment⁸⁹
- 3) Higher resolution with none of the tilted-angles issues
- 4) Making the LCD down to 0.2 mm thin (Figure 14)
- 5) Controlled fixation of the alignment
- 6) Obtaining more stability to heat
- 7) Reduction of LCD weight

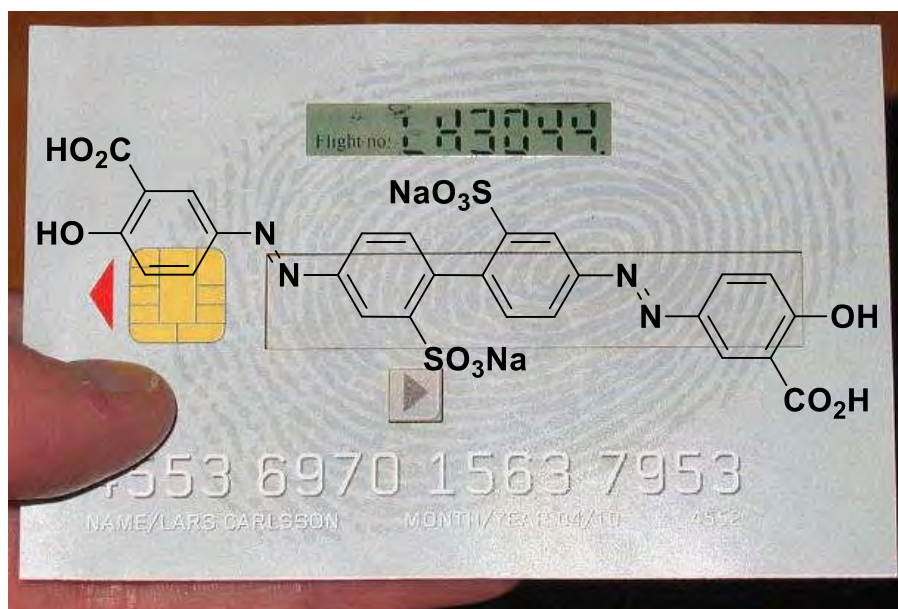


Figure 14 A bisazo compound used in the design of ultrathin LCDs^{64, 65}

2.2 Introduction of chirality

Combining a chiral dopant and an achiral LC induces chirality throughout the mesophase and empowers the helical twisting power (HTP). Interestingly, the handedness of the LC obeys the handedness of the added chiral dopant.⁹⁰ Unfortunately, dopant addition is limited by dispersion and miscibility factors and may impose inevitable changes to the physical characteristics of the host LC, like phase transition onsets. In addition, non-chiral photo-switchable additives provide a narrow tuning-range of mostly less than 100 nm.⁹⁰ Therefore, LCs have been developed by addition of chiral and photo-switchable units in their main structure, namely photo-responsive chiral LCs. This family of LCs has received much recent attention due to their valuable thermal and optoelectrical properties.⁹¹ Various chiral cores have been utilised in the design of photo-responsive and/or chiral LCs, as well as the synthesis of LC dopants, such as bicyclics (e.g. spiro, Figure 15),⁹²⁻⁹⁷ helices like biphenyls^{94, 96, 97} or binaphthyls (Figure 20),^{13, 98-101} and others (Figure 19).¹⁰²⁻¹⁰⁵

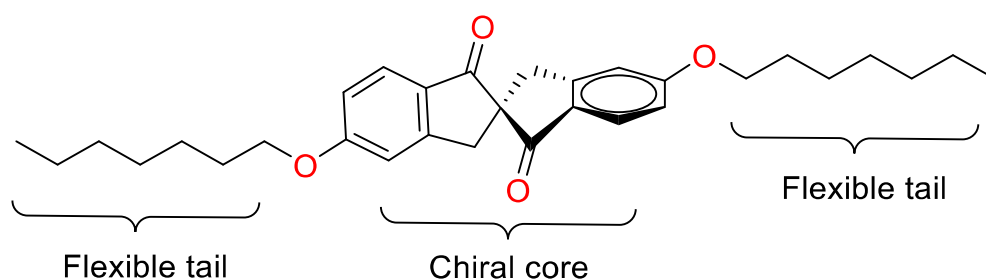


Figure 15 Introduction of chirality by chiral centre addition

2.3 Introduction of photo-tunable properties

Photoswitchable molecules have a functional group (Figure 16) that can be selectively switched from one configuration to another in a reversible manner by irradiation with a specific wavelength of light. Such configurations must have distinguishable geometries and exhibit different properties, for instance, stilbenes or azo groups can perform $E \leftrightarrow Z$ photo-isomerism upon irradiation with a particular wavelength of UV-Vis light.

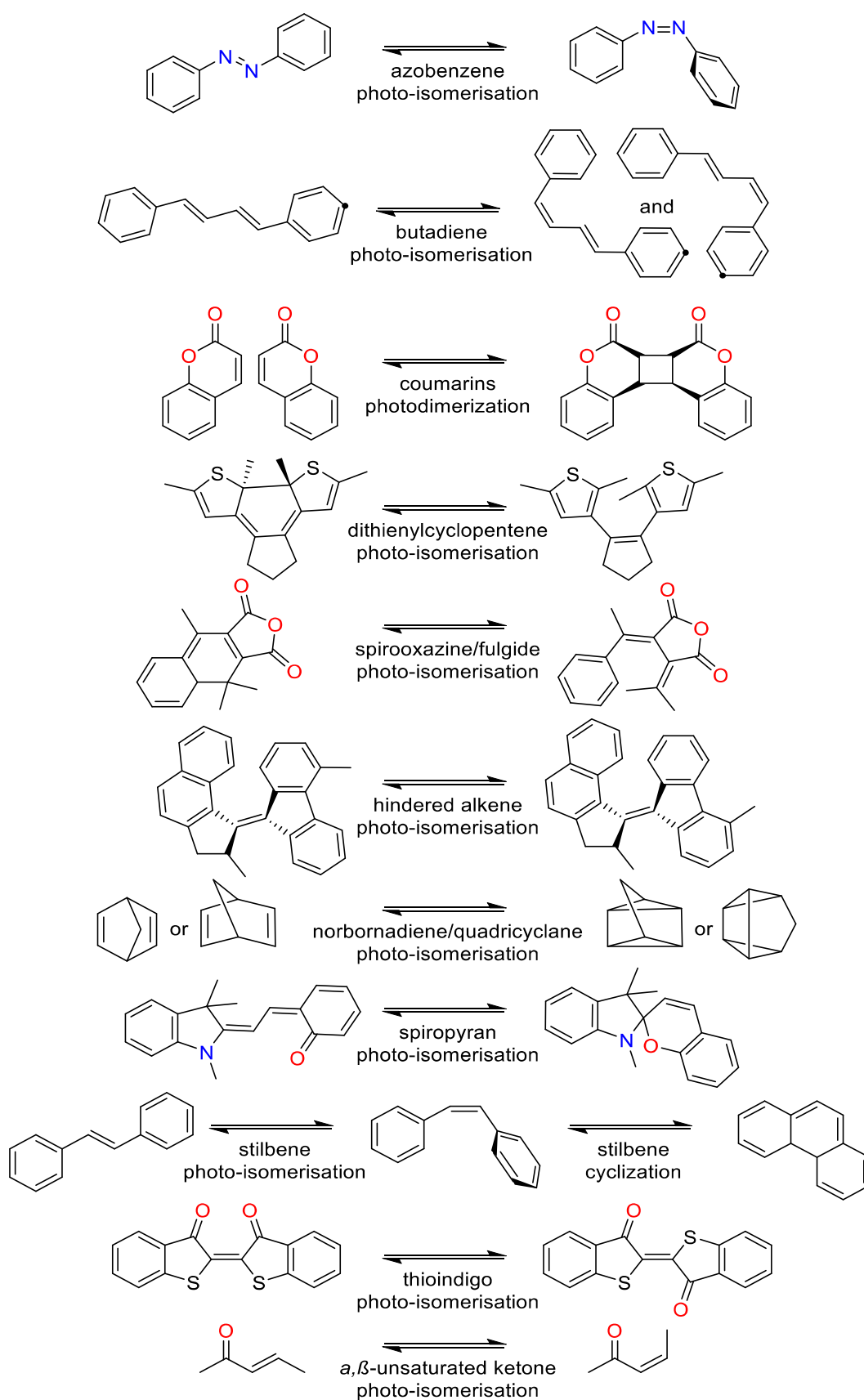


Figure 16 Typical examples of photoswitchable functional groups

Although these switching groups (Figure 16) have displayed fascinating properties in numerous applications most of them suffer a few disadvantages. For instance, spirooxazine-fulgide,^{106, 107} and arylated diene¹⁰⁸ systems have four¹⁰⁹ and multiple¹⁰⁸ photo-isomerised states, respectively, which complicate the studies. Moreover, some of these systems are UV-activated only and particularly function under short-wave UV such as dienes,¹⁰⁸ stilbenes,¹¹⁰ and unsaturated ketones. The use of short-wave UV is restricted in the design of devices to avoid the health-related hazards it causes to the skin and eyes. In addition, the challenging synthesis, low switching durability and significant spatial hindrance of overcrowded alkene, thioindigo,^{111, 112} spiropyran,^{113, 114} and dithienylcyclopentene systems are problematic and have to be taken into the account.

Among these photoswitchable functional groups (Figure 16), the azo group was selected in this project due to its simplicity of production (through azo coupling reaction), its desirable activity within long-wave UVA (360–400 nm) or visible regions (400–700 nm), ease of modification and high compatibility with other functional groups, predictable $E \leftrightarrow Z$ photoisomer geometry, remarkable photostability, and high endurance.

To induce the photoexcitation of azo compounds, and consequently photoisomerize the *trans* to the *cis*, a specific wavelength of light (Figure 17, λ_1) is required. This specific wavelength triggers an allowed electron transition from π to π^* . To reverse the photoisomerization, from the *cis* to the *trans*, a longer wavelength of light (Figure 17, λ_2) is required. The last is often indicated as a minor peak in the absorption spectra, which stands for a non-allowed transition of n to π^* .¹¹⁵ Due to the instability of the *cis* isomer, it slowly undergoes the back-isomerisation through thermal-relaxation even in the absence of λ_2 (Figure 17).

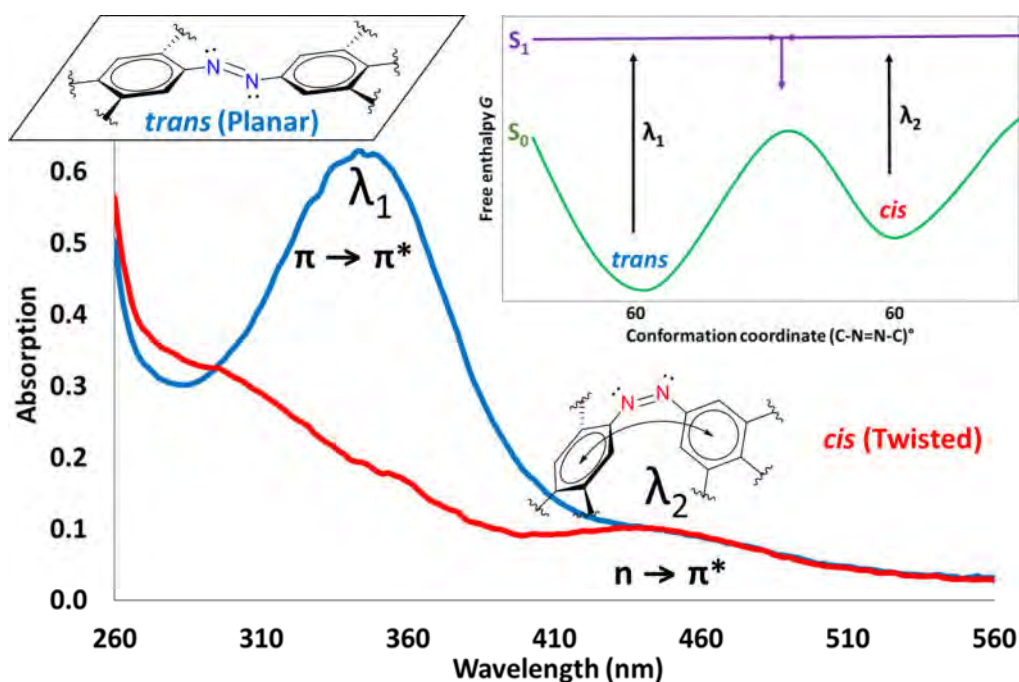


Figure 17 Absorption spectra of an azo compound photoisomers, *E* in blue and *Z* in red

The addition of photo-responsive dopants, for instance, an azo compound (Figure 18 and Figure 19), to LCs results in photo-tunable properties. This is due to the fact that reversible photo-isomerisation of the dopant influences its molecular geometry and order parameters in the surrounding liquid crystalline phase, which consequently varies the pitch size.⁹⁰ Azo photoisomers are distinguished by their molecular geometries,¹¹⁵⁻¹¹⁷ namely *cis* and *trans* (Figure 18), and exhibit different physical properties such as dipole moment, wettability, viscosity, and aggregation behavior.¹¹⁸

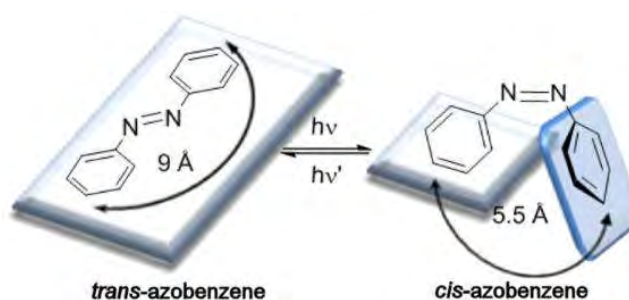


Figure 18 Photo-isomerisation of an azo molecule^{115, 117}

Azo dopant photo-isomerisation often decreases the helical twisting power (HTP), *i.e.* pitch-length expansion, and therefore the reflected wavelength shifts to red. These changes are temporary due to the fact that back isomerisation of azo groups eventually occurs as a completely reversible process. Figure 19^{92, 119} and Figure 20⁹⁹ display the chemical structure of two common examples of azo-carrying chiral compounds that have been employed in LCD design.

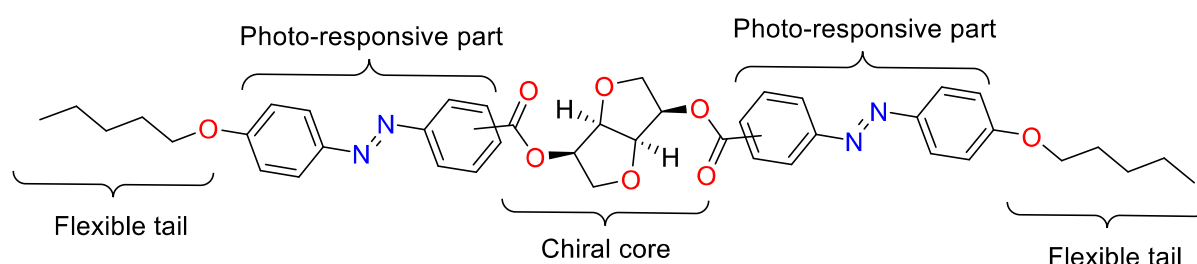


Figure 19 Introduction of chirality and photo-tunable properties by addition of chiral cores and photo-responsive units^{92, 119}

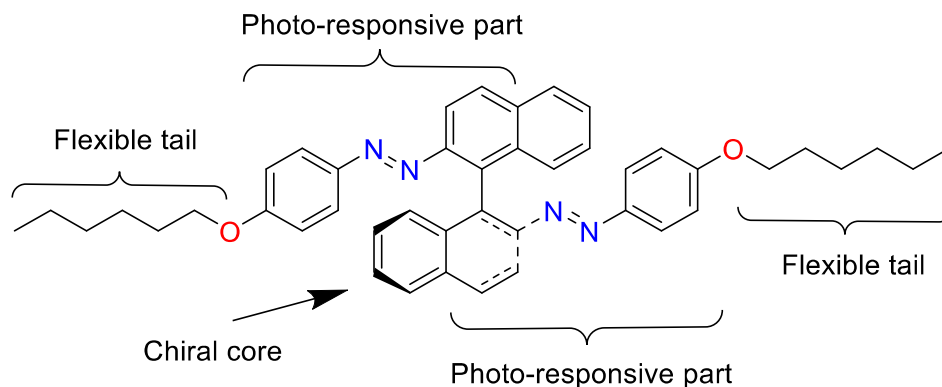


Figure 20 Introduction of chirality and photo-tunable properties by addition of azo groups to optically active binaphthyls^{99, 101}

2.4 Structure-function relationships of liquid crystals

Based on the reviewed examples throughout the introduction section it is apparent that the chemical structure of liquid crystals can determine their physical properties and accordingly their potential applications. For instance, alkyl chains can lower the phase transition onset(s), viscosity and the risk of solidification. This is particularly important in

the design of thermotropic and thermochromic LCs like those that have been utilised in LC displays and thermometers. Aromatic rings, polar and photo-responsive groups can facilitate LCs alignment by intermolecular π -stacking or dipole-dipole interactions and their response to external electric or photonic stimuli. These functions play vital roles in LC display technology. Research Chapter I will further describe how these structure-function relationships have been employed in the design of the products of this thesis.

3. Tröger's base (TB) overview

In this project, Tröger's base analogues (TBAs) have been utilised as the major building blocks throughout all the synthetic work. The logic behind this selection is presented below.

3.1 TB special features

3.1.1 Chirality and racemisation

Due to a quick inversion of configuration, substituted nitrogen atoms cannot generally be chiral centres (Figure 21).

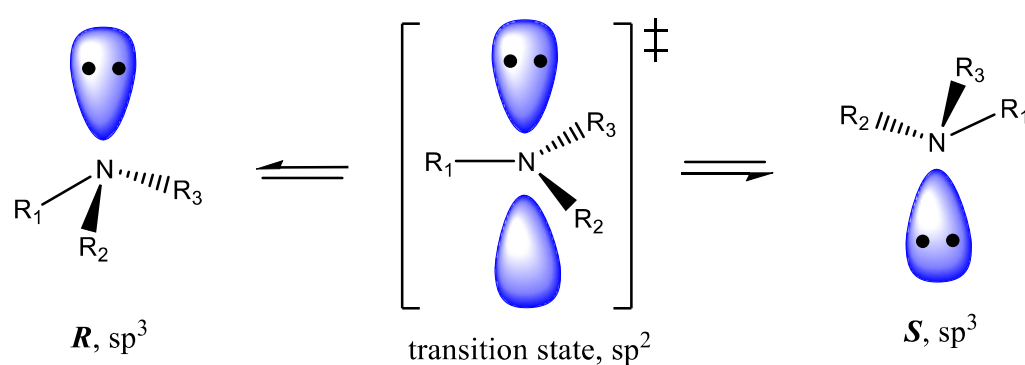


Figure 21 Inversion of configuration of nitrogen centres at room temperature

The nitrogen atoms in the Tröger's base (TB) scaffold flank a diazocine bridge (indicated as the opening/reclosing part of the ring in Figure 22), which prevents the inversion of configuration in neutral or basic conditions. In acidic environments, the formation of an iminium intermediate enables TBAs to undergo racemisation by the inversion of the nitrogen centre (Figure 22).^{120, 121}

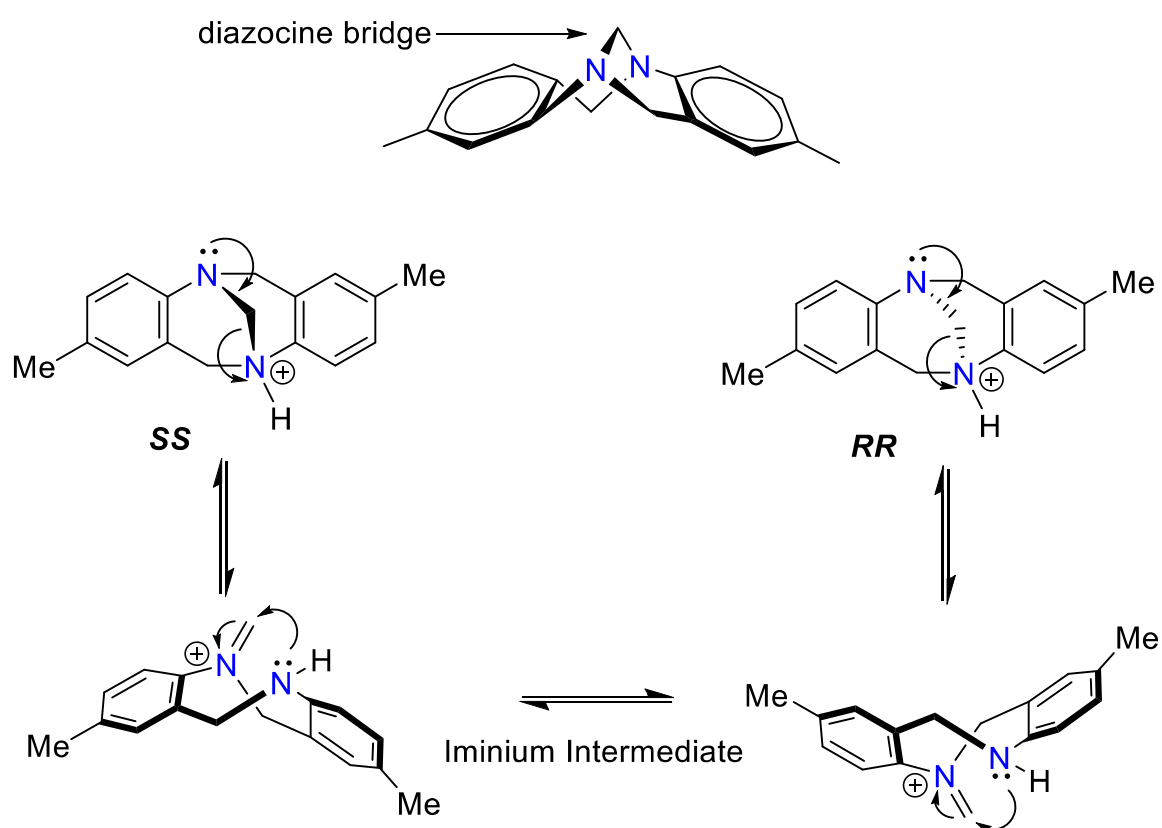


Figure 22 Racemisation of Tröger's base in an acidic environment through an iminium intermediate¹⁴

The unusual nitrogen-centred chirality of TBAs is generated by a pair of adjacent tertiary amine groups. Their optical resolution has been performed by various methods,¹²² and surprisingly the optical activity of these materials is found to be very large.¹²³⁻¹²⁸ The optical activity of TB analogues is in many instances greater than other chiral molecules (Table 4). It is postulated that the rigid Λ -shape structure of this valuable family of chiral building blocks extends the chirality of the stereogenic amine groups throughout the entire scaffold,

and hence amplifies the optical activity. These special features of TBAs encouraged the idea of employing them in the design of the first non-racemisable and photo-responsive liquid crystal dopant in this project, which is discussed in the third research chapter.

Although various TBAs have been resolved, it is not feasible to directly compare the applied resolution methods as different methods have been used for the chiral resolution of different TBAs in the literature. For instance, chiral HPLC is not easily scalable, but it often provides excellent resolution. On the other hand, diastereomeric salt formation is scalable but resolution is not as efficient as chiral HPLC. Moreover, methano strapped TBAs are transformed into a single enantiomer, while ethano strapped TBAs are resolved to two enantiomers. On the other hand, active TBA (e.g. amine- or methoxy-carrying analogues) degrade during and after chiral resolution, while nitro- or halogen-carrying TBAs generally do not undergo the degradation. Furthermore, very few chiral TBAs are fully assigned (by X-ray crystallography) and the rest are unknown to date. These differences make the comparison nearly impossible and do not suggest a general resolution method for TBAs.

While other chiral compounds such as the helicenes exhibit a much greater optical activity than TBAs, they are not as ideal as TBAs. For example, helicenes are synthetically far more challenging to make than the TBAs.¹²⁹ As polycyclic aromatics they are also photo-reactive, photo-degradable, sensitive to oxygen, and very often carcinogenic. In addition, polycyclic aromatics may fluoresce or phosphoresce which can interfere with the function of fast response optical devices such as LCDs. Moreover, the dispersion and miscibility of large helicene molecules in LC hosts may not be as desirable as smaller chiral cores like TBAs. The convenient production (Table 6) and obtained properties of the introduced TBAs (Papers I-III) in this thesis include none of the aforementioned drawbacks.

Table 4. Comparing the optical activity of TBAs to other types of chiral centres

En.	Compound name	Chemical structure	$[\alpha]_D^{22\pm3^\circ} \pm 1^\circ$	Ref.
1	D-(-)-tartaric acid		-12° C=20, H ₂ O	130
2	dianhydro-D-glucitol		$+45^\circ$ C=3, H ₂ O	130
3	dibenzoyl-L-tartaric acid		-116° C=9, EtOH	130
4	(R)-(+)-1,1'-binaphthyl-2,2'-diamine		$+157^\circ$ C=1, Py	130
5	(5S,11S)-2,8-dimethyl-6H,12H-5,11-methanodibenzo[b,f][1,5]diazocine		$+282$ C=0.112, CHCl ₃	131
6	(5S,11S)-2,8-dimethoxy-6H,12H-5,11-methanodibenzo[b,f][1,5]diazocine		$+236$ C=0.110, CHCl ₃	131
7	(5S,11S)-2,8-dibromo-6H,12H-5,11-methanodibenzo[b,f][1,5]diazocine		$+379$ C=0.114, CHCl ₃	131

En: entry; C: concentration (g.L⁻¹), D: sodium line; $[\alpha]$: specific rotation

The racemisation of TBAs can be disadvantageous; however, it can also be an advantage to allow preparation of single enantiomers of TBAs out of racemates by crystallisation-induced asymmetric enantiomer transformation^{126, 131} in the presence of an acidic resolving agents. This is explained within the next subsections.

As described above, this unusual family of chiral compounds exhibit greater values of optical activity than many other chiral cores (Table 4). The chirality of tetracyclic TBAs arises from the stereogenic nitrogens located on the diazocine bridge and perhaps the rigid nanometre-long body of these building blocks amplify the optical activity. Comparison of phenylethanol to its ether derivatives or tartaric acid to its ester derivatives (Table 4, **1** and **3** entries), which all exhibit enhanced values of optical activity after enlargement of the molecule, supports this postulation.

3.1.2 Chiral resolution of TBAs

TB was first resolved by Vladimir Prelog in 1944 by chiral chromatography (Figure 23).¹³² The chiral resolution of TBAs has been performed by various techniques, such as chiral HPLC,¹²⁵ diastereomeric covalent bond formation¹⁷ or salt precipitation,¹³³ and crystallisation-induced asymmetric enantiomer transformation in the absence¹³⁴ or presence of resolving agents¹³¹ through iminium intermediate formation (Figure 22), as previously described by Wilen *et al.*¹²⁰

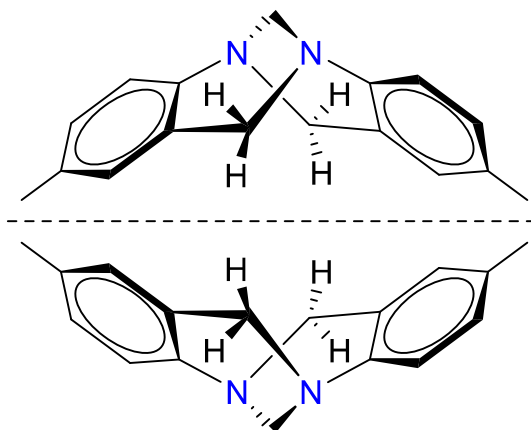


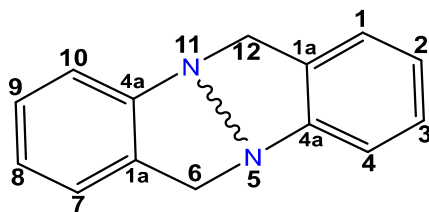
Figure 23 TB enantiomers

Although various TBAs have been resolved, it is not feasible to compare the applied resolution methods to one another due to the fact that different methods have been used for the chiral resolution of different TBAs in the literature. These methods and materials are fundamentally different and are not comparable. For instance, chiral HPLC is not scalable in large quantities however provides a great precision. On the other hand salt transformation method is scalable but not as accurate as chiral HPLC. Moreover, methano strapped TBAs are transformed into a single enantiomer at a time, while ethano strapped TBAs are resolved to two enantiomers. On the other hand, active TBA (e.g. amine or methoxy carrying ones) degrade during and after chiral resolution, while nitro or halogen carrying TBAs mainly do not suffer the degradation. Furthermore, very few chiral TBAs are fully assigned (by X-ray crystallography) and the rest are unknown to date. These differences make the comparison nearly impossible and does not allow suggesting a general resolution method for TBAs.

3.1.3 Unique shape of TB scaffolds

The TB scaffold is a bent structure which due to a roughly perpendicular dihedral angle (Table 5) existing between its aromatic moieties is described as a V-shaped or Λ -shaped scaffold. Replacement of the methylene group of the diazocine group with ethylene or longer alkene groups influences the angular strain and rigidity of the TB scaffold. Accordingly, ethano-strapped TBAs mostly show smaller dihedral angles (7–13° less) than their methano-strapped analogues. Surprisingly, propano-strapped TBAs are flat and look asymmetrical.¹³⁵ The formation of longer diazocine bridges may not be possible due to the unfavourable size of the rings. Furthermore, long diazocine bridges loosen the scaffold and hence a rigid Λ -shaped structure cannot be obtained. Therefore, ethano-strapped TBAs were regarded as the best candidates for being used as the rigid Λ -shaped building blocks in this project due to their superior properties and the desired shape.

Table 5. Dihedral angle between aromatic moieties of the TB scaffold



Substitutions	Bridge type and the dihedral angle ^{133, 135}	
	NCH ₂ N	NCH ₂ CH ₂ N
R (2,8)		
H	95.4°	75.9°
Cl	95.6°	87.0°
Br	94.5°	87.0°
Me	102.2°	89.0°

This remarkable family of nano-scale chiral cores all have a Λ -shaped scaffold and the TB itself has an approximate distance of ca. 1 nm between the two extremities.¹³³

3.1.4 Unique spectral properties of TBAs

According to the chemical literature,¹³⁶ a single chromophore or its fused duplicates linked *via* the diazocine ring have almost identical electronic/spectral properties; however, the oscillator strength of the bischromophore is almost double. In fact, the diazocine ring detaches the delocalised electrons of the TB aromatic moieties by holding the rings apart in a roughly perpendicular dihedral angle, binding them with bridgehead methylene isolators. These resonance barriers provide an easier determination of spectral properties of abreast chromophores on a TB scaffold, appearing as single chromophores. Therefore, the maximum wavelength of absorption of the bisazo-carrying TBAs should appear like the common range of single azo chromophores (around 350 nm), which gives these molecules a distinct advantage compared to any other fused chromophores sharing electrons and resonance together. Nonetheless, having two independent photo-switching groups on each TB molecule confers a more intense response to the external stimuli and

this may enhance photo-tuning properties of LCs with a lower concentration of applied dopant (Figure 11).

3.2 TB common applications

TBAs have played a substantial role as versatile building blocks employed in the design of Λ -shaped photo-switchable molecular hinges,^{14, 122} chiral ligands,¹³⁷ catalysts,¹³⁸ receptors,^{5, 7, 139-142} supramolecules,^{9, 143} sensors,^{6, 8, 10-12, 139, 144, 145} polymers,^{146, 147} molecular tweezers,¹⁴⁸ leashes,¹⁴⁸⁻¹⁵⁰ and can functionalise fullerenes.¹⁵¹⁻¹⁵⁸ Furthermore, owing to the remarkable properties of the TB scaffold, its analogues have been utilised in membrane design,¹⁵⁹ molecule recognition,^{6, 11, 12, 139, 144, 145} assembly,¹⁴³ and others.¹⁴⁸⁻¹⁵⁰

3.2.1 Chiral discriminator in molecular recognition

TBAs have been utilised in the design of artificial fluorescent receptors to examine how the TB scaffold can selectively generate hydrogen-bonding^{160, 161} interactions (Figure 24) with various acids, e.g. camphoric acid.^{144, 162} A survey of the chemical literature has proven the effectiveness of TBAs in recognition of organic molecules.⁵⁻

12, 139, 144, 145, 162

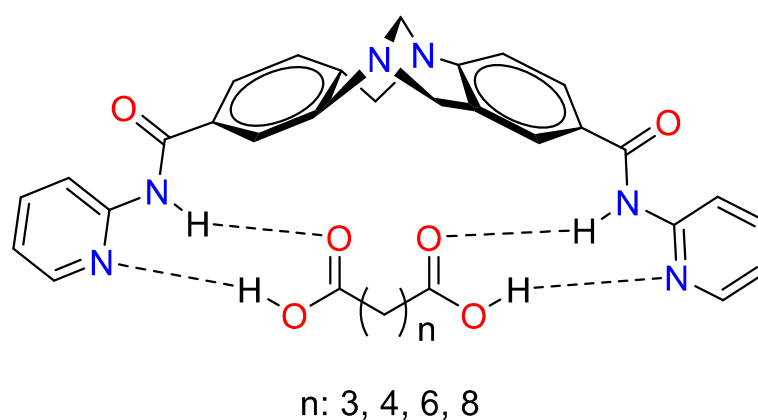


Figure 24 Functionalised TBA binds to dicarboxylic acids
Adapted from professor Shyamaprosad Goswami's work^{144, 162}

3.2.2 Building blocks/monomers

TBAs have been used as Λ -shaped building blocks¹⁵ or monomers in polymerisation reactions.^{146, 159} The TB scaffold enhances the stiffness and porosity of the obtained polymeric products (Figure 25), owing to its rigid Λ -shaped structure. For instance, TBA-carrying polyimides^{159, 163, 164} have shown a satisfactory permeability, microporosity, and high selectivity, which enables them to be applied as permeable membranes in high-performance gas chromatography (Figure 25).

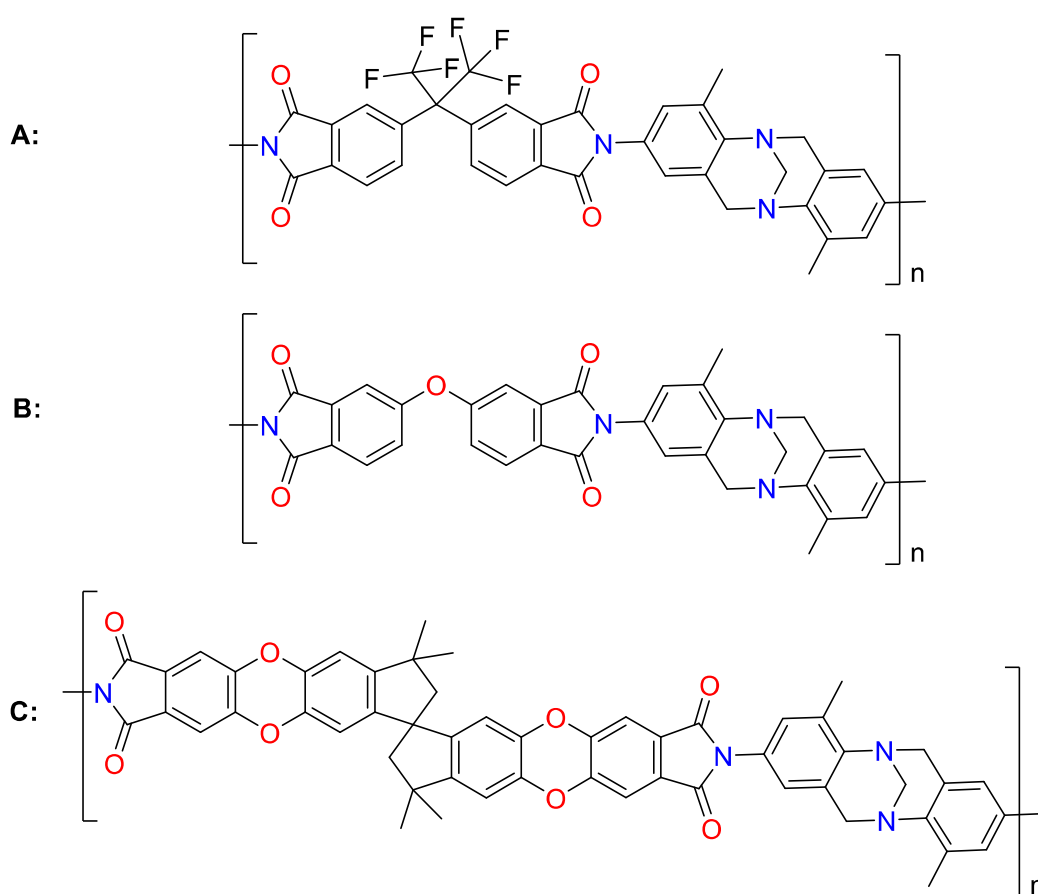


Figure 25 Three examples of TBAs carrying polyimides:
A,^{159, 163} B,¹⁵⁹ and C¹⁶⁴

TBA-carrying polyhydrazides¹⁴⁶ are also found to be conveniently solution-casted to form polymeric films (Figure 26). The obtained transparent films showed an appropriate

combination of flexibility and toughness.¹⁴⁶ These have desired mechanical properties for material science and related applications.

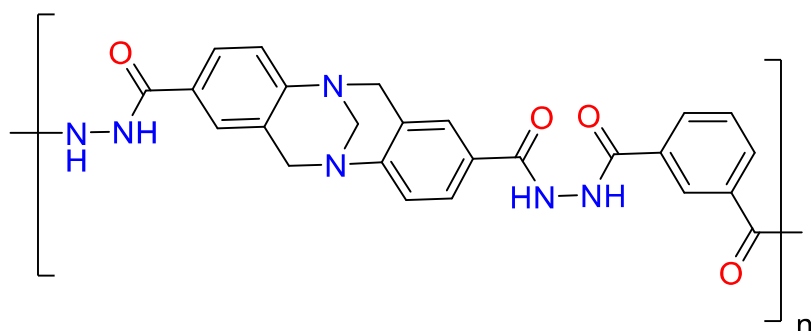


Figure 26 TBA carrying polyhydrazone

3.2.3 Molecular design

TBAs have been employed in the design of various molecular structures, *e.g.* tweezers.^{145, 148, 165} The obtained molecular tweezers exhibit different binding properties depending on how the diazocine bridges are positioned to one another (Figure 27).

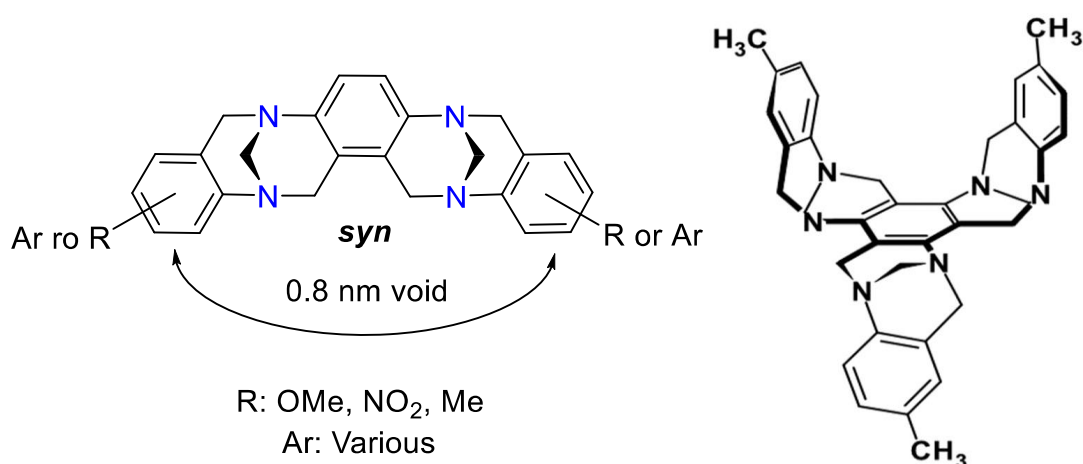


Figure 27 TB based molecular tweezers¹⁴⁵

TBAs have also been utilised in the design of ligands and self-assembled structures. For example, TBAs carrying 2,2'-bipyridine^{143, 166} and 2-pyridylmethanimine¹⁶⁶ moieties are two brilliant examples for diastereoselective self-assembly of dinuclear complexes (Figure 28).^{143, 148-150, 166}

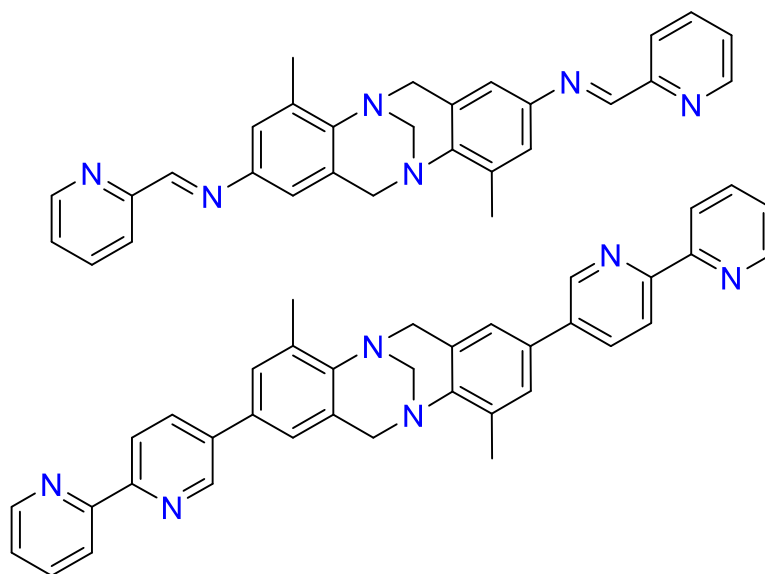


Figure 28 Two examples of TBA carrying ligands

3.3 Former studies in this field

A previous study on the alkylated TBA properties (Figure 29) showed limited interesting clues. Those clues were not enough to prove a new concept, but taken as the motivation for further investigations. In that study,¹⁶⁷ it was found that the longer the alkoxy chain, the lower the melting point, and indeed the higher the chance of obtaining mesophase(s). The latter occurred within a certain range of the chain length, *e.g.* from hexyl to octadecyl.¹⁶⁷

Considering the recent advances in the design of LCs, mentioned earlier in Sections 2.1 – 2.3, and the properties TBAs provide, inspired the idea of introducing a new family of TBAs in this project with a focus on their possible LCD related applications.

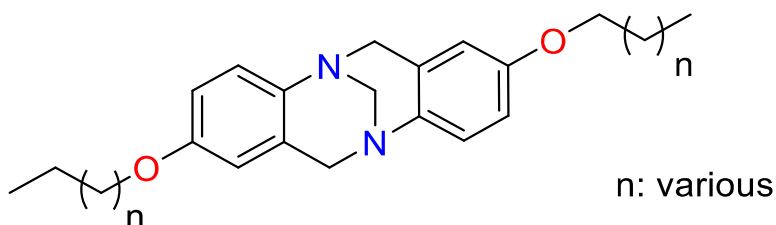


Figure 29 Typical TBAs investigated as thermotropic LCs

3.4 TBAs drawbacks

3.4.1 Diazocine bridge clipping

The aqueous solution of NaNO_2 /mineral acid, which is used for the diazotisation reaction, was reported as a method for the removal of the diazocine bridge.¹⁶⁸ This reaction resulted in clipping the diazocine bridge and converting the amino groups from tertiary to secondary type (Figure 30). Therefore, the conversion of amine-carrying TBAs to the corresponding azo-carrying TBAs was deemed to be impossible.

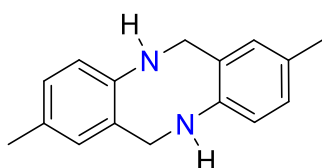


Figure 30 Tröger's base after clipping the diazocine bridge

3.4.2 Undesired couplings and side-reactions

Previous studies¹⁶⁹ on the diazotisation and coupling reaction of TBAs to form bis-azo-carrying derivatives (**A** and **B**, Figure 31) showed numerous spots on the crude TLC. Owing to the untidy reaction profiles, further examinations and characterisations were not pursued.¹⁶⁹ Therefore, the production of azo-carrying TBAs remained unachieved for almost a decade and their syntheses were not further investigated. The innovative methodologies developed by professor Paul Watts,^{42, 43} and the non-traditional approaches used in this thesis, could have provided the desired molecules.

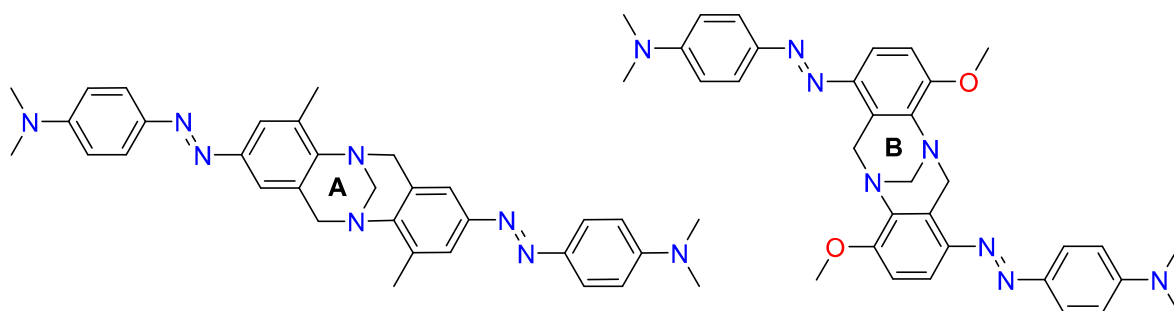


Figure 31 Two examples of the azo-carrying TBAs that were unable to be synthesised¹⁶⁹

3.4.3 Racemisation

As described earlier, chiral methano-strapped TBAs undergo racemisation in acidic conditions.¹²¹ Based on the racemisation mechanism (Figure 32), modification of the diazocine bridge could provide an acid resistant chirality for TBAs. The ethano-strapped TBAs (Figure 32) would have to racemise *via* the formation of a primary carbocation, which is very unlikely to occur. Even if such an unstable carbocationic intermediate was formed, it would not be expected to tumble from one face of the molecule to the other. This carbocation, owing to its steric hindrance, could create a large energy barrier (Figure 32). Therefore, TBAs elongated diazocine bridges would not be expected to swing back and forth through the eight-membered ring and the chirality should remain the same.

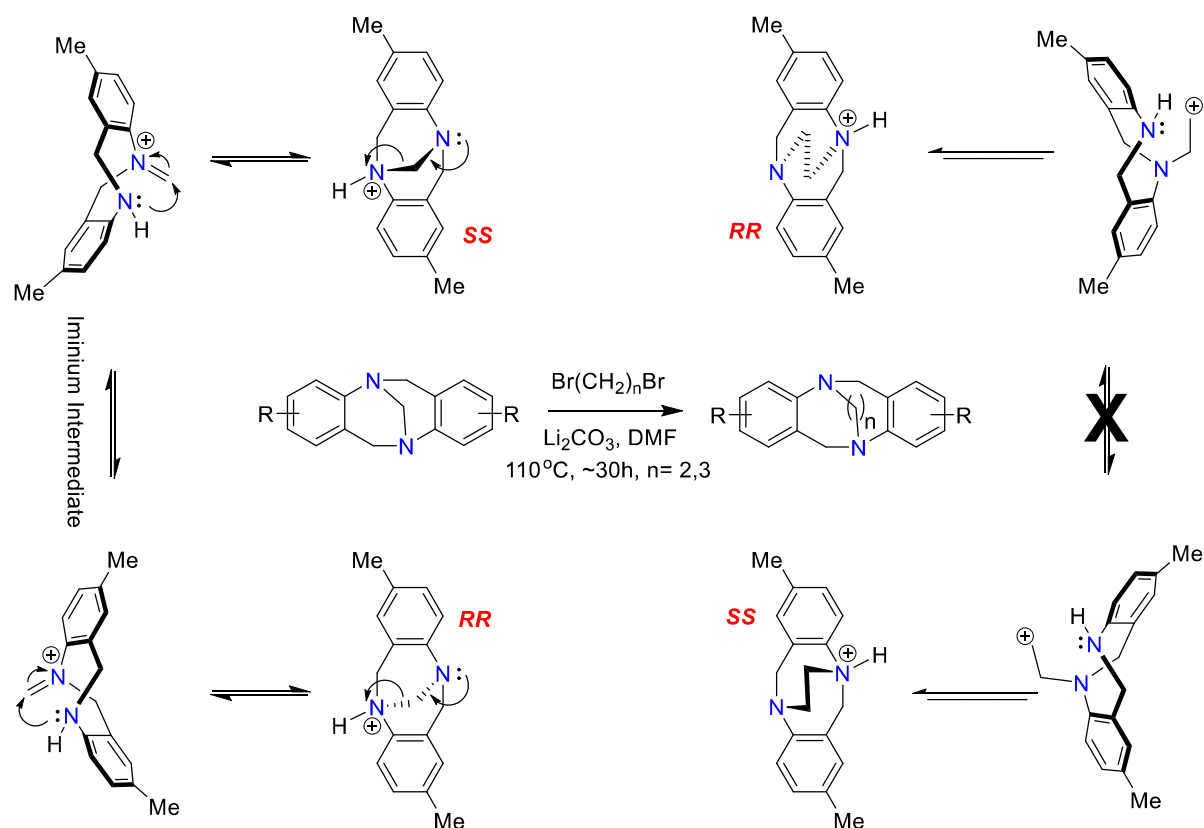


Figure 32 Diazocine bridge modification prevents TBAs racemisation

3.5 Availability of the desired TBA

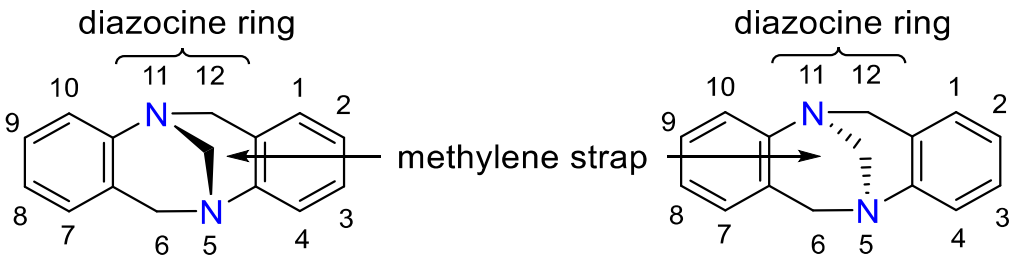
As described, the main goal of this project was the production of azo-carrying TBAs and the easiest way to obtain azo compounds is *via* the diazotisation reaction, which converts amino groups to the corresponding diazonium salts. Then the obtained diazonium salts, as electrophiles, can react with activated aromatic rings, with noticeable electron density *e.g.* phenoxides, to produce the desired azo materials. Therefore, amine-carrying TBAs were required as the starting material for this project (Table 6).

The production of amine-carrying TBAs was reviewed and it was deduced that the most recent reported one — Hünlich's base (HB) — would be an appropriate building block (Table 6, entry 9). As explained in Paper II,¹⁴ HB (Table 6, entry 9) represents a readily available building block from inexpensive and relatively safe starting materials. Therefore, HB was selected as the major building block in this project.

Converting a diamino compound to its azo derivative results in having two photo-switchable units on the final product. These photo-switches change the shape of the molecule significantly upon receiving an external stimulant. This intense response is advantageous, *e.g.* in the case of applying such materials as LCs dopant, a lower concentration of them would be required to photo-tune the host LC. This helps to maintain the desirable physical properties of the host LC.

In addition, such symmetrical bisazo-compounds would be more useful for molecular recognition purposes or light-driven machines design. Therefore, the preparation of diamino analogues of TB was reviewed to assess the availability of these valuable precursors.

Table 6. Synthesis of TB and its di-amino analogues

			
Entry	Author Ref.	Substituents *	Step(s) and Condition(s)
1	Tröger ¹⁷⁰	2,8:CH ₃	i. CH ₂ O/ HCl
2	Cibulka ¹⁷¹	1,7:NH ₂	i. (a); ii. (d); iii. Pd/H ₂
3	Cibulka ¹⁷¹	1,7:NH ₂ ; 2,8:Br; 4,10:Cl	i. (a); ii. (d); iii. Zn/AcOH
4	Try ¹⁷²	1,7:NH ₂ ; 2,4,8,10:CH ₃	i. (a); ii. SnCl ₂ /EtOH
5	Try ¹⁷²	2,8:NH ₂	i. DGA/PPA; ii. Pd/C, H ₂
6	Sergeyev ¹⁷³	2,8:NH ₂	i. (a); ii. (b); iii. (c)
7	Lützen ^{143, 166}	2,8:NH ₂ ; 4,10:CH ₃	i. (a); ii. Fe/AcOH
8	Lützen ¹⁶⁶	3,9:NH ₂ ; 4,10:CH ₃	i. (a); ii. Fe/AcOH
9	Giannis ¹⁷	3,9:NH ₂ ; 2,8:CH ₃	i. CH ₂ O/ H ₂ SO ₄
10	Sergeyev ¹⁷³	4,10:NH ₂	i. (a); ii. (b); iii. (c)
11	Cibulka ¹⁷¹	4,10:NH ₂	i. (a); ii. (d); iii. Pd/H ₂
12	Cibulka ¹⁷¹	4,10:NH ₂ ; 2,8:Br	i. (a); ii. (d); iii. SnCl ₂ /HCl
13	Lützen ¹²⁴	4,10:NH ₂ ; 2,8:CH ₃	i. (a); <i>n</i> BuLi/TsN ₃ ; ii. NaBH ₄ /THF

* Except protons. (a) Paraformaldehyde in trifluoroacetic acid, (b) Ph₂C=NH, *t*-BuONa, Pd₂(dba)₃ and BINAP. (c) HCl (aq), (d) KNO₃/H₂SO₄. DGA: diglycolic acid, PPA: polyphosphoric acid.

Formation of a diazocine bridge “Trögeration reaction”, as defined by Dolenský,¹⁷⁴ is interrupted by the presence of amino groups in addition to those considered to flank the bridge. HB synthesis is the only exception, where no interference occurs. Therefore, other TB di-amino analogues have been produced *via* the synthesis of nitro-¹⁷² or halogen-containing¹⁷³ analogues, which successfully accomplish the Trögeration reaction. Afterwards, the nitro or halogen groups of these precursors can be reduced to or replaced by amino groups, respectively, to generate the desired di-amino TB analogues, as listed in Table 6.

The product Walter Hünlich's had obtained in 1914 through condensation of 2,4-diaminotoluene and formaldehyde was reinvestigated after almost a century and its exact structure was finally revealed in 2013.¹⁷ The reported methodology has provided a one-step synthesis of a diamino analogue of TB at multigram scale, which can be readily prepared from inexpensive materials (Table 6). Hünlich's base (HB) has also been resolved by preparation and separation of amino acid-carrying diastereomers¹⁷ and their alkaline hydrolysis. These separated enantiomers racemise¹²⁰ in acidic conditions which incapacitates them to be applied as the starting materials of this work. Nonetheless, it was anticipated that every HB analogue might be resolvable by the aforementioned methods, which have been successful in the case of TB analogues.

4. Aims and existing gaps

Although various chiral cores have been employed in the design of LC systems (listed in Sections 2.2, 2.3 and Paper I), the potentials of many others in LC science are yet unexplored. The growing high-tech and commercial applications of LCs have driven their non-stop development motivating further exploration in this new field of material sciences. This thesis, for the first time, employs the TB scaffold in the design of a new group of photoswitchable materials that can be used as LC dopants. These products should provide a specific response to photonic stimuli due to their unique Λ -shape structure that holds two identical photoswitching groups at a perpendicular angle to one another (Figure 34 and Figure 35). This not only should provide a controlled response to the light (Figure 1 in Papers I and II), but also may improve LCs photo-alignment (Figure 35). Moreover, the molar absorption coefficient of these new products is found to be almost double of ordinary azo compounds.¹²² In addition, these products are expected to exhibit a significant optical activity (Table 4) that would be at least two times greater than the currently available LC dopants (Figure 19 and Figure 20). These properties are highly desired in LCDs design as explained in the introductory Sections 2.2 and 2.3.

All the aforementioned points encouraged the production of azo-carrying TBAs as the major aim of this project. The proposed structures (Figure 33) would be the first family of azo-carrying TBAs reported. Therefore, the first aim of the project was to evaluate the availability of the required building blocks. Afterward, the possibility of the formation of the desired products would need to be assessed and, if successful, be increased through optimisation of the reaction conditions. These studies should result in a straightforward syntheses with inexpensive materials and in good to high yield (Figure 33).

Therefore, this project was expected to confirm the possibility of obtaining the desired azo-carrying TBAs with an appropriate response to photonic stimuli. The final and futuristic aim was the design of azo-carrying TBAs that can be resolved and modified with other functional groups to improve their properties. These products are expected to improve optical properties of the available LCs by introducing to them photo-tunable properties, chirality, and enabling their multi-domain photo-alignment.

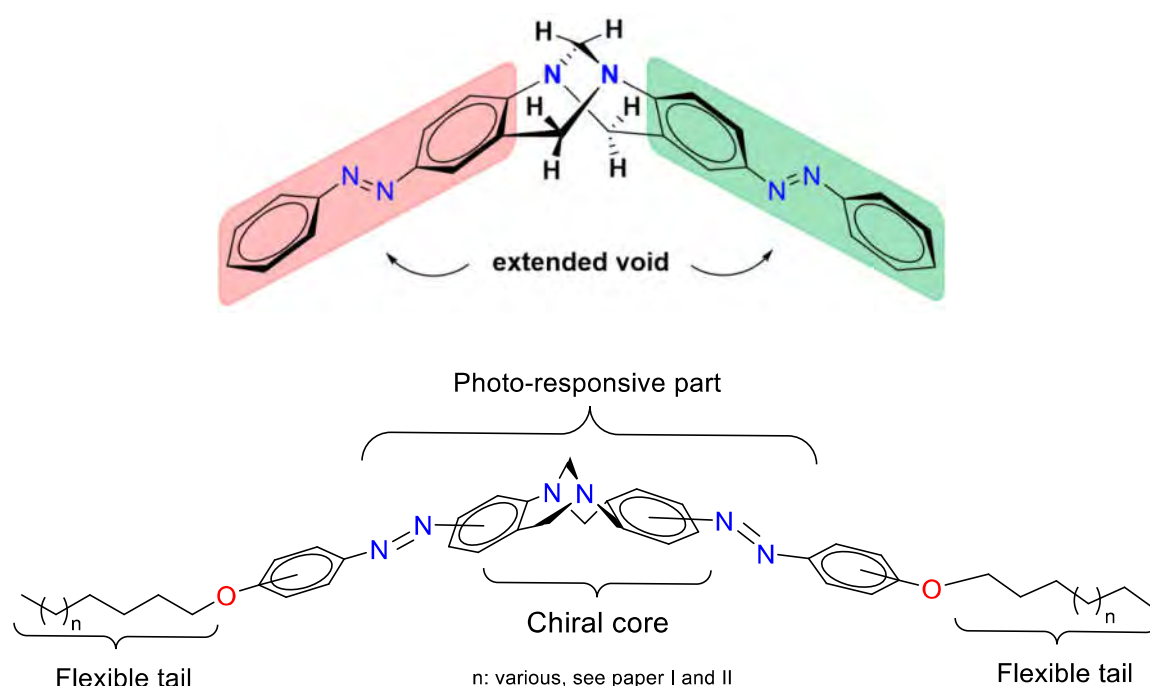
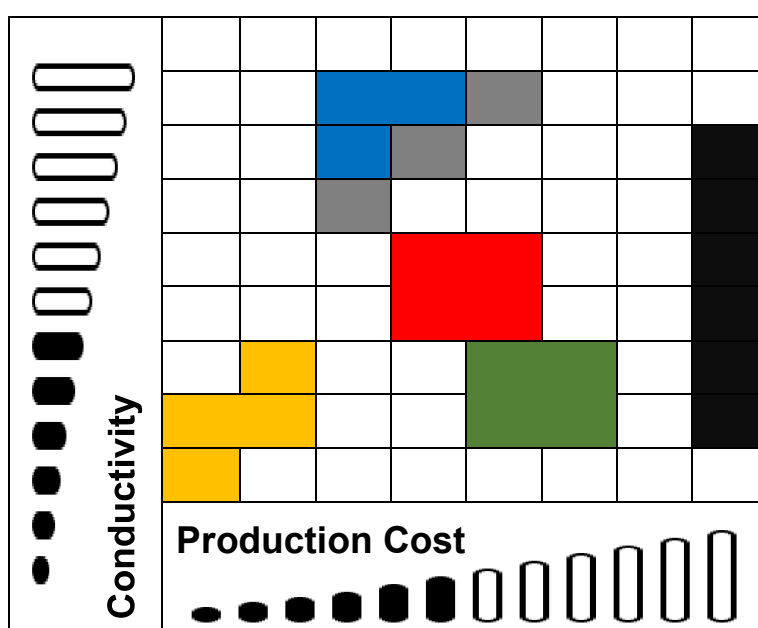


Figure 33 Typical structure of the desired products

5. Current challenges of LCD design

As discussed previously in the Introduction Section 2, currently used LCDs mainly function on the basis of how LC molecules align under an applied electric field. The required electric field is obtained by introducing a voltage to a pair of transparent indium tin oxide (ITO) electrodes sandwiched into the multi-layered structure of the LCD (Figure 1). The inclusion of ITO electrodes makes the screens thick, rigid and costly. The latter is due to the fact that indium is not found in the form of a known ore in nature and is only obtained as the byproduct of other metals refinement. Therefore, indium has limited availability in the global market at a considerable and increasing price. The current state of the art in this field is the replacement of ITO electrodes (Table 7, Shown in Red) with silver nanowire (Table 7, Grey), metal mesh (Table 7, Blue), organic films or transparent conductive polymers (Table 7, Orange), carbon nanotubes (Table 7, Green) and graphene (Table 7, Black). To date, the replacement of ITO with these alternatives has been an industrial challenge and hence new horizons are being explored in this field such as using photo-alignment methods as an ultimate solution. The following chapters will explain how the molecules presented in this thesis can contribute to the LC photo-alignment methods.

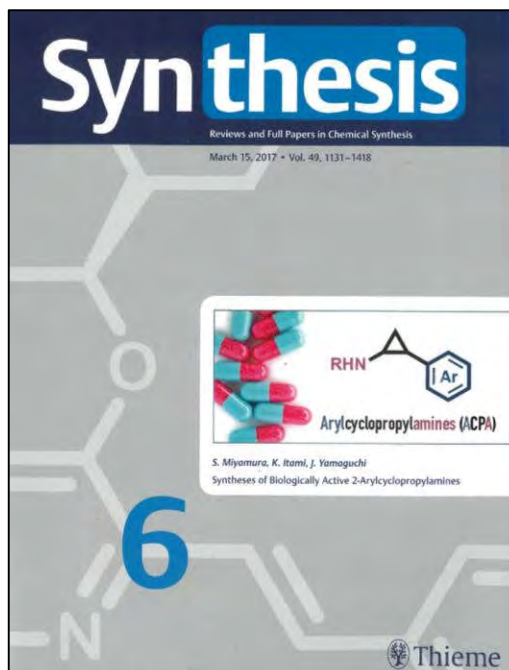
Table 7 Non-ITO versus ITO conductors



Thesis Outcomes

RESEARCH CHAPTER ONE

Paper I (Main Article)



Journal Impact Factor: 2.689

Disclaimer Notification

The following copyrighted materials are reproduced with a license, numbered 4119030834308, obtained from *Thieme publisher* on May 30, 2017. In accordance with an agreement between the author and the publisher, the accepted version of the publication is restrictedly allowed to be presented in this copy of the thesis only. Any other use of the following material has to be explicitly authorised by the copyright holder of *Synthesis* © 2017 Georg Thieme Verlag KG.

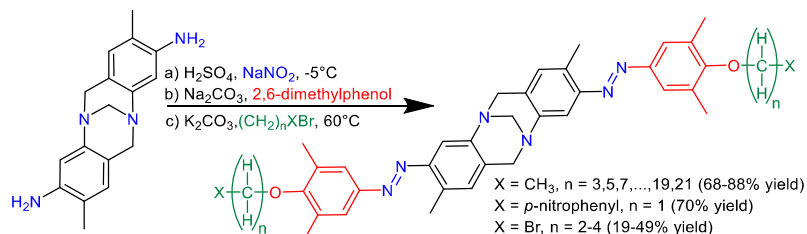
Λ-Shaped Photo-Switchable Compounds Design Employing Tröger's Base Scaffold

Masoud Kazem-Rostami*

Department of Chemistry and Biomolecular Sciences,
Macquarie University, North Ryde, NSW 2109, Australia

masoud.kazem-rostami@hdr.mq.edu.au,
masoud.kr@gmail.com

Dedicated to the memory of Dr. Walter Hünlich



Received:
Accepted:
Published online:
DOI:

Abstract The production of azo derivatives of a di-amino analogue of Tröger's base (*Hünlich's base*), by employing the standard procedures of diazotisation, azo-coupling and Williamson etherification is described here. These versatile molecules possess a Λ-shaped core, photo-switchable groups and some carry two modifiable extremities to enable further synthesis or molecular assembly. The synthesis is straightforward and requires inexpensive starting-materials, which facilitates their application to different fields of research such as light-driven molecular machine design.

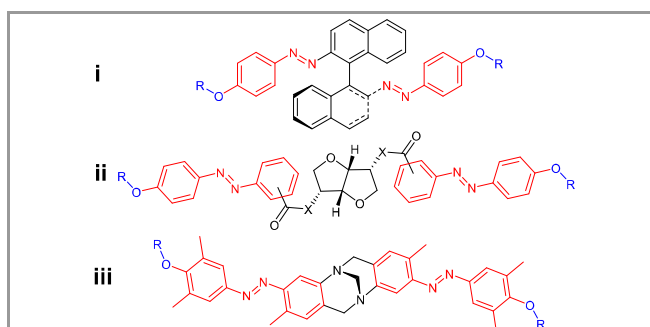
Key words alkylation, azo compounds, chromophores, diazo compounds, isomerization

The mesophase(s) laid between the solid state and isotropic liquid is called liquid crystalline phase. In liquid crystal (LC), the molecules not only have some extent of freedom in movement, like those sliding on each other in liquids, but are also ordered in a specific orientation by being pointed in the same direction and making a pseudo-solid lattice. Several layers of orientated LC molecules may generate a helical twisted structure which is capable of rotating polarized light. This helical twisting power (HTP) is the basis of how liquid crystal displays (LCDs) work. The distance through the twists in which LC molecules experience a full turn is defined as pitch length. A wavelength of light equal to the pitch size can be reflected by LC and pitch size varies at different temperatures which elaborates the LC thermometers mechanism.

Addition of photo-responsive dopants, for instance an azo compound, to LC results in photo-tunable properties. This is due to the fact that reversible photo-isomerization of the dopant influences its molecular geometry and order parameters in the surrounding liquid crystalline phase, which consequently varies the pitch size.¹ Azo photo-isomers distinguished by their molecular geometries, named *cis* and *trans*, exhibit different physical properties such as dipole moment, wettability, viscosity, and aggregation behavior.² Often, the photo-isomerization of azo

dopants decreases the HTP by extending the pitch-length, and thus leading to a redshift in the reflected wavelength. These changes are temporary because back-isomerization of azo groups eventually occurs as a completely reversible process.

Combining a non-chiral LC and chiral dopant induces chirality and empowers the HTP. Interestingly the handedness of the LC obeys the handedness of the added chiral dopant.¹ Unfortunately, dopant addition is limited by dispersion and miscibility factors and may impose inevitable changes to the physical characteristics of LC, like phase transition onsets. In addition, non-chiral photo-switchable additives provide a narrow tuning range of mostly less than 100 nm;¹ Therefore, LCs have been developed by addition of chiral and photo-switchable units in their main structure, namely photo-responsive chiral LCs. This family of LCs has been developed dramatically recently due to their valuable thermal and optoelectrical properties.³ Various chiral cores have been utilized in the design of photo-responsive and/or chiral LCs, as well as the synthesis of LC dopants, such as bicyclic compounds *e.g.* spiro,^{4, 5} helixes like biphenyls⁵ or binaphthyls,^{6, 7, 8} and others.⁹



Scheme 1 Typical examples of chiral cores in black, photo-switchable units in red, and miscibility adjusters in blue; R: H or (CH₂)_nCH₃, n: Various, X: CH₂ or O

Scheme 1 compares two examples of these typical chiral photo-switchable compounds **i**⁷ and **ii**¹⁰ to the novel structures represented in this work **iii**, designed by employing a Tröger's base (TB) analogue as a core functionalized by two abreast photo-switchable units. The resemblance among **i-iii** encourages the hypothesis of introducing a new family of chiral photo-responsive LC dopants.

Table 1 Tröger's and Hünlich's Bases Synthesis

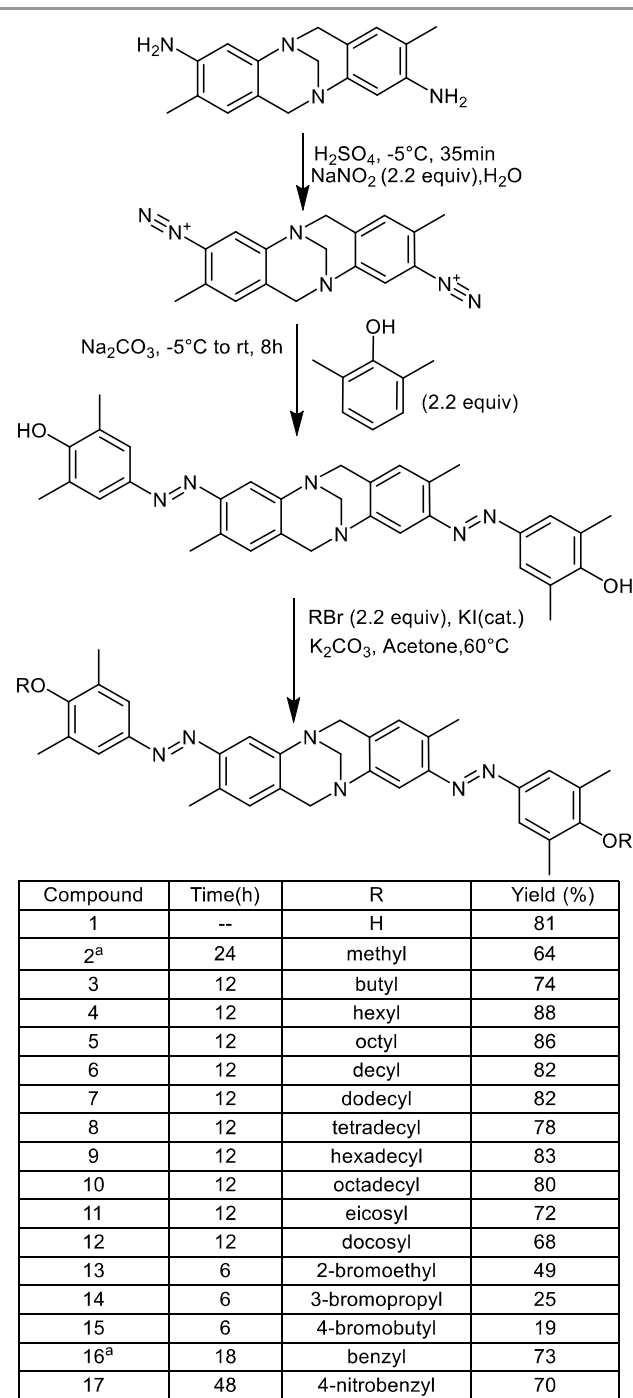
compound Ref.	R'	R''	reagent and solvent
Tröger's base ¹¹	H	CH ₃	CH ₂ O, HCl (aq)
Hünlich's base ¹²	NH ₂	CH ₃	CH ₂ O, H ₂ SO ₄ (aq)

The product Walter Hünlich had obtained in 1914 through condensation of 2,4-diaminotoluene and formaldehyde, was reinvestigated after almost a century and its exact structure was finally revealed in 2013.¹² The reported methodology has provided one-step synthesis of a diamino analogue of TB at multigram scale, which can be readily prepared from inexpensive materials (Table 1). This remarkable family of nano-scale chiral cores all have a Λ -shaped scaffold and the TB itself has an approximate distance of ca.1 nm between the two extremities;¹³ hence, they have attracted a lot of interest in molecular assembling,¹⁴ recognition,¹⁵ and design.¹⁶ With these purposes in mind, compounds **1** and **13-15** are introduced (Scheme 2), which have interactive/modifiable extremities. The **1**st compound is also capable of hydrogen-bond interactions to achieve more interesting properties like full-range tuning.⁸

Due to a quick inversion of configuration, ordinary substituted nitrogen atoms cannot be generally considered to be chiral centres, but the nitrogen atoms in the TB scaffold flank a diazocine bridge (Indicated in Table 1), which prevents the inversion of configuration unless in an acidic environment by formation of an iminium intermediate which undertakes racemization.¹⁷ Chiral resolution of TB analogues has been performed by various techniques, such as chiral HPLC,¹⁸ diastereomeric covalent bond formation¹² or salt precipitation,¹³ and crystallization-induced asymmetric enantiomer transformation in the absence¹⁹ or presence of resolving agents²⁰ through iminium intermediate formation previously described by Wilen et al.¹⁷ Hünlich's base (HB) has also been resolved by preparation and separation of amino acid carrying diastereomers¹² and their alkaline hydrolysis. These separated enantiomers racemise¹⁷ in acidic conditions which incapacitates them to be applied as the starting materials of this work. Nonetheless, every HB analogue might be resolvable by the aforementioned methods which have been successful in the case of TB analogues.

Although this report is focused on the synthesis and characterization of the compounds **1-17**, some basic experiments were also performed to evaluate the possibility of their chiral resolution; for instance, exposing the **4**th entry (Scheme 2) to (R)-(-)-1,1'-Binaphthyl-2,2'-diyl hydrogenphosphate or (S)-(+)-1,1'-Binaphthyl-2,2'-diyl hydrogenphosphate simply gave partially

resolved material showing optical rotation after removal of the acid residue by alkaline work up.



^a Please check their exceptional structures elucidated in scheme 3.

Scheme 2 Stepwise synthesis of 1-17

HB was chosen for this study as the initial racemic building block possessing two amino groups, and then by diazotizing and coupling them with a substituted phenol (Scheme 2), its azo derivative was obtained.

Preparation of diazonium salts as an exothermic reaction is more productive at lower temperature and higher concentration of mineral acid. In fact, these factors prevent decomposition of the thermally unstable diazonium salt and minimize generation of

the unwanted phenol produced by hydrolysis of diazonium salt in aqueous solution. Therefore, this step was optimized by performing it at -5°C and using the appropriate ratio of acid:water to prevent freezing the reaction mixture²¹ and keeping the diazonium intermediate as intact as possible. Meanwhile the coupling reaction gradually progresses by mixing the diazonium salt and desired phenol solution. The reaction mixture pH must not be suddenly changed as it causes an uncontrolled rise in temperature during acid neutralization and consequently leads to diazonium decomposition. It is also essential to start with fresh and highly-pure HB to obtain a clean reaction profile.

In the next step, the phenoxy groups at the elongated molecule extremities were reacted with a variety of alkyl or aryl halides to obtain the rest of the derivatives as briefly shown in (Scheme 2) and clarified in the supplementary data sheets. The length of these alkyl chains influences the phase transition onsets and miscibility of the products in host LCs.

It needs to be mentioned that the phenol (Scheme 2) was chosen substituted on both of the ortho positions to prevent the electron-donating phenoxy group leading the electrophile (Diazonium cation) on the ortho positions and to avoid triggering any side-product formation.

According to the existing literature,²² a single chromophore or its fused duplicates *via* diazocine ring has almost identical electronic/spectral properties, however the oscillator strength of bischromophoric is almost double. In fact, the diazocine ring (Shown in Table 1) detaches the delocalized electrons of the TB aromatic moieties by holding the rings apart in a roughly perpendicular dihedral angle binding them with bridgehead methylene isolators.

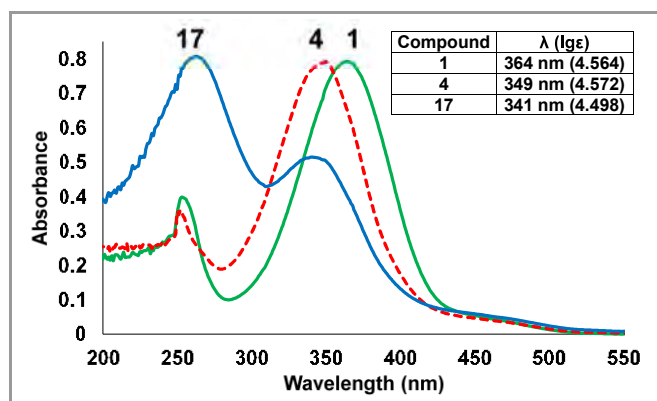


Figure 1 The normalised UV-Vis spectra of compounds **1**, **4**, and **17** in EtOAc.

These resonance barriers provide an easier determination of spectral properties of abreast chromophores on a TB scaffold, appearing as single chromophores, comparing to any other fused chromophores sharing electrons and resonance together. Therefore the maximum wavelength of absorption of compounds **1-17** appears to be around the common range of simple azo chromophores around 360 nm (Figure 1). Nonetheless, having two independent photo-switching groups on each molecule of **1-17** confers a more intense response to the external stimuli and this may enhance photo-tuning properties of LCs with a lower concentration of applied dopant (Figure 2).

In molecular recognition experiments, azo compounds are often used in their *cis* form to tighten their grip on the targeted molecules²³ and obviously the unstable *cis* form has to undergo back-isomerization. This relaxation may cause complexity of the studies and less efficiency due to fact that the major population of the molecules is normally in the *trans* form. The presented products in this work obviously provide a unique grip as the TB scaffold dictates their spatial Λ -Shape.

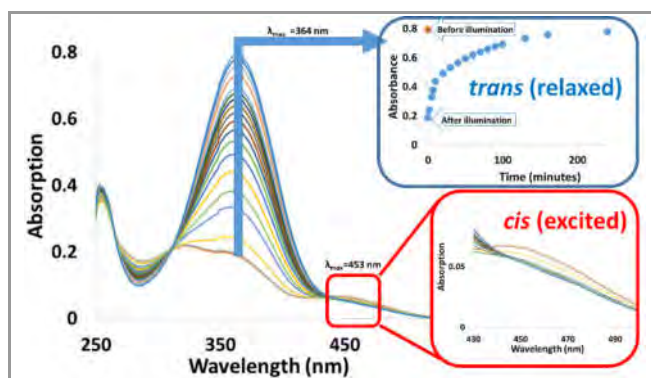
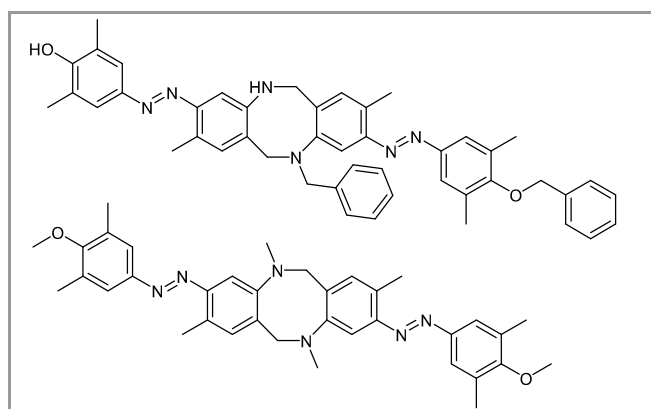


Figure 2 Tracking the photo-isomerization of **1** by UV-Vis spectra, 25°C , EtOAc.

Contrary to common perception, reacting **1** and 1,2 dibromo ethane successfully gives **13** instead of reacting with the bridge's nitrogen atoms and changing the methano strap to ethano or committing undesired ring opening or oligomerization reactions;²⁴ however yield noticeably decreases on making **14** and **15** which could have been caused by the aforementioned side reactions. Compounds **1** and **13-15** are nano scale Λ -shaped photo-responsive units, which can be easily attached to other nano structures, such as functionalized carbon nanotubes, fullerenes, porphyrins, peptides,²⁵ or even polymers to act as photo-switchable hinges. In addition, **1**'s compound phenoxy groups or **13-15**'s brominated extremities can be subjected to a variety of reactions and be readily converted to other functional groups to facilitate every assembly process. Length and flexibility of the hinges can also be modified by using different alkyl/aryl halides, which is, for instance, an ethylene in the case of the **13**th entry or a butylene in the **15**th.



Scheme 3 Compounds **2** (bottom) and **16** (top) structures

Methylation of **1**, and also its reaction with benzyl bromide, fails to give the expected products: **2**nd and **16**th entries respectively

(Scheme 2). This may be due to the uncontrolled reactivity of iodomethane and the SN1 pathway, which might be preferred by benzyl bromide. These two reagents, clip the diazocine strap by targeting a bridge-head nitrogen. In agreement with the available literature, reacting benzyl bromide on **1** gives major demethylenated product.²⁶ It is postulated that benzyl bromide initially strikes the bridge head nitrogen and the other remaining equivalent of it has to react with one of the phenoxy groups which leads to asymmetric product **16**. In case of the **2nd** entry, detection of the reaction completion is not as simple as it seems; hence, an excess amount of iodomethane was applied to finalize the reaction with a single over-methylated product (Scheme 3).

Although azo compounds are known as ultimate photo-responsive materials, most have negligible quantum yield and consequently show no fluorescence. More substituted analogues, in some circumstances, are self-assembled and form fluorescent spherical aggregates. This is proven by observing deviation of isosbestic points and the fluorescent aggregates can be large enough to be seen by SEM.²⁷ Aggregation behavior of the products is beyond the focus of this report, however will be investigated in the future following chiral resolution, photo-isomerization, and LC-related studies.

To conclude, seventeen derivatives of HB carrying photo-switchable units are introduced. These products can act as Λ -shape photo-switchable hinges, and they encourage a plethora of novel ideas in the field of light-driven molecular machine engineering, nano-technology, photo-responsive polymer or adlayer design. The author reckons that these materials after chiral resolution might be used, as photo-responsive chiral LC dopants, in design of optically-activated shutters or photo-tunable displays, as well as light-responsive discriminator hosts in molecular recognition studies.

Synthesis of Hünlich's base:

Hünlich's base was produced and purified according to an existing procedure¹² with minor modifications as described below:

2,4-diaminotoluene (36.6 g, 300 mmol, 2.05 eq.) was dissolved in an aqueous solution of sulfuric acid (5 %, 1000 ml). Then, formaldehyde (37 % in H₂O, 10.9 ml, 11.9 g, 146 mmol, 1.00 eq.) was slowly added to the solution and stirred for 48 hours at room temperature in a sealed container kept away from light. After checking the completion of the reaction by TLC, ice (300 g) and ammonia (25 %, 300 ml) were added and the precipitated crude product was filtrated. The crude was dissolved in boiling methanol (200 ml) and gradually cooled down to -20°C. Filtration yielded Hünlich's base (14.2 g, 50.8 mmol, 34.7 %) as an off-white solid. Chemical Formula: C₁₇H₂₀N₄, Molecular Weight: 280.38, R_f: 0.5 (MeOH/ DCM = 10% v/v) silica gel.

¹H-NMR (400 MHz, DMSO-*d*₆) δ [ppm] : 6.24 (s, 2H, CH) , 6.29 (s, 2H, CH), 4.57 (b, 4H, NH), 4.35-4.39 (d, *J* = 16.2 Hz, 2H, H-6b, H-12b), 4.03 (s, 2H, -N-CH₂-N-), 3.77-3.81 (d, *J* = 16.3 Hz, 2H, H-6a, H-12a) , 1.91 (s, 6H, 2 \times -CH₃).

IR: (Neat) ν_{\max} [cm⁻¹] = 3402, 3335, 3236, 2986, 2887, 2844, 1620, 1573, 1498, 1441, 1183, 1085, 913, 870.

MS (EtOH): (ESI positive) calc. for [C₁₇H₂₁N₄]⁺: [M+H]⁺ 281.17, found 281.2.

Synthesis and characterization of compound (\pm)-1:

Hünlich's base (0.56 g, 2.0 mmol, 1.0 eq.) was dissolved in an aqueous solution of H₂SO₄ (6.5% v/v, 30 mL), and cooled down to -5°C. A NaNO₂ solution (0.30 g, 4.4 mmol, 2.2 eq. in 5 mL of water) was dropped into the reaction flask and stirred for 35 min. The resulting yellowish diazonium solution was poured into a solution of 2,6-dimethylphenol (0.51 g, 4.2 mmol, 2.1 eq.) and Na₂CO₃ (2.0 g, 19 mmol) in 100 mL of cold water. Then, two more grams of Na₂CO₃ was added to the mixture and stirred for 8 hours. Afterwards, an orange precipitate was filtered off, washed with water and desiccated to obtain the product (0.88 g, 1.6 mmol, 81%). Chemical Formula: C₃₃H₃₄N₆O₂, Molecular Weight: 546.68, R_f: 0.33 (EtOAc/ n-Hexane = 40% v/v) silica gel.

¹H-NMR (400 MHz, DMSO-*d*₆) δ [ppm]: 9.07 (br, 2H, OH) , 7.53 (s, 4H, 4 \times CH), 7.26 (s, 2H, H-4, H-10), 6.92 (s, 2H, H-1, H-7), 4.61-4.65 (d, *J* = 17.2 Hz, 2H, H-6b, H-12b), 4.25 (s, 2H, -N-CH₂-N-), 4.12-4.16 (d, *J* = 17.3 Hz, 2H, H-6a, H-12a) , 2.47 (s, 6H, 2 \times -CH₃), 2.26 (s, 12H, 4 \times -CH₃).

¹³C-NMR (100 MHz, DMSO-*d*₆) δ [ppm]: 156.7, 149.2, 146.5, 145.3, 131.9, 130.6, 129.2, 124.8, 123.3, 110.4, 66.2, 58.4, 16.7, 16.5.

IR: (Neat) ν_{\max} [cm⁻¹] = 3563, 2946, 2914, 2843, 1592, 1480, 1417, 1298, 1182, 1111, 913, 728.

MS (Acetonitrile 90%, EtOAc 5%, H₂O 5%): (ESI positive) calc. for [C₃₃H₃₅N₆O₂]⁺: [M+H]⁺ 547.2, found 547.4. (ESI negative) calc. for [C₃₃H₃₃N₆O₂]⁻: [M-H]⁻ 545.2, found 545.5.

UV-Vis: (EtOAc) λ (lg ϵ) = 364nm (4.598).

Anal. calcd: C, 72.50; H, 6.27; N, 15.37. found: C, 72.63; H, 6.08; N, 14.98.

General Procedure for Synthesis of compounds 2-16:

Appropriate amounts of **1**, KI and K₂CO₃ were mixed in 10 ml of acetone, then an alkyl or aryl halide was injected into the mixture and refluxed in darkness. The reaction was monitored by TLC until showed a single spot at the conclusion (Indicated in Scheme 2). Afterwards, 50 ml of water was added and the crude was extracted with EtOAc (3 \times 30ml). The collected organic layers were combined and dried over MgSO₄ and filtered off. After removing the solvent, the residue was chromatographed to obtain the orange sticky solids **2-16** (Scheme 2).

Characterization of compound 2:

Starting with **1** (0.55 g, 1.0 mmol, 1.0 eq.), K₂CO₃ (0.69 g, 5.0 mmol) and methyl iodide (1.0 g, 7.0 mmol, 2.3 eq.) to obtain **2** (0.38 g, 0.64 mmol, 64%) Chemical Formula: C₃₆H₄₂N₆O₂, Molecular Weight: 590.7. R_f: 0.9 (MeOH/ DCM = 4% v/v) silica gel.

¹H-NMR (400 MHz, CDCl₃) δ [ppm]: 7.62 (s, 4H, H), 7.18 (b, 2H, H-4,10), 7.09 (s, 2H, H-1,7), 4.34 (b, 4H, H-6,12), 3.78 (s, 6H, OCH₃), 2.94 (b, 6H, NCH₃), 2.64 (s, 6H, CH₃-2,8), 2.39 (s, 12H, CH₃).

¹³C-NMR (100 MHz, CDCl₃) δ [ppm]: 159.4, 150.6, 149.2, 133.9, 131.7, 130.3, 123.6, 101.8, 59.9, 58.5, 39.6, 16.6, 16.4.

IR: (Neat) ν_{\max} [cm⁻¹] = 2921, 2856, 1606, 1476, 1411, 1337, 1286, 1220, 1112, 1004, 885, 662.

MS (EtOH 50%, 1-Propanol 50%): (ESI positive) calc. for $[C_{36}H_{43}N_6O_2]^+$: $[M+H]^+$ 591.34, found 591.4.

UV: (EtOAc) λ (lg ϵ) = 342 nm (4.625).

Anal. calcd: C, 73.19; H, 7.17; N, 14.23. found: C, 73.44; H, 7.33; N, 14.15.

Characterization of compound (\pm)-3:

Starting with **1** (2.2 g, 4.0 mmol, 1.0 eq.), K_2CO_3 (1.4 g, 10 mmol), some extra acetone (20 ml) and 1-iodobutane (1.7 g, 9.0 mmol, 2.3 eq.) to obtain **3** (2.0 g, 3.0 mmol, 74%) Chemical Formula: $C_{41}H_{50}N_6O_2$, Molecular Weight: 658.89, R_f: 0.77 (EtOAc/ n-hexane = 40% v/v) silica gel.

1H -NMR (400 MHz, $CDCl_3$) δ [ppm]: 7.62 (s, 4H, CH), 7.45 (s, 2H, H-4, H-10), 6.86 (s, 2H, H-1, H-7), 4.69-4.74 (d, J = 17.1 Hz, 2H, H-6b, H-12b), 4.35 (s, 2H, -N-CH₂-N-), 4.27-4.31 (d, J = 17.2 Hz, 2H, H-6a, H-12a), 3.83-3.86 (t, J = 8.1 Hz, 4H, CH₂), 2.59 (s, 6H, CH₃), 2.39 (s, 12H, CH₃), 1.81-1.84 (m, 4H, CH₂), 1.54-1.64 (m, 4H, CH₂), 1.02-1.06 (t, J = 8.1 Hz, 6H, CH₃).

^{13}C -NMR (100 MHz, $CDCl_3$) δ [ppm]: 158.7, 150.3, 149.0, 146.5, 133.6, 131.8, 130.7, 129.3, 123.6, 111.5, 72.3, 67.2, 59.0, 32.6, 19.4, 17.1, 16.6, 14.1.

IR: (Neat) ν_{max} [cm^{-1}] = 2932, 2826, 1584, 1472, 1379, 1307, 1205, 1112, 1083, 997, 918, 899, 758, 610.

MS (ACN 90%, EtOAc 5%, H₂O 5%): (ESI positive) calc. for $[C_{41}H_{51}N_6O_2]^+$: $[M+H]^+$ 659.40, found 659.2.

UV-Vis: (EtOAc) λ (lg ϵ) = 349 nm (4.587).

Anal. calcd: C, 74.74; H, 7.65; N, 12.76. found: C, 74.37; H, 7.71; N, 12.59.

Characterization of compound (\pm)-4:

Starting with **1** (0.55 g, 1.0 mmol, 1.0 eq.), K_2CO_3 (0.69 g, 5.0 mmol), 1-bromohexane (0.50 g, 3.0 mmol, 1.5 eq.) and a catalytic amount of KI (0.01 g, 0.06 mmol) to obtain **4** (0.63 g, 0.88 mmol, 88%) Chemical Formula: $C_{45}H_{58}N_6O_2$, Molecular Weight: 715.00, R_f: 0.63 (EtOAc/ n-hexane = 30% v/v) silica gel.

1H -NMR (400 MHz, $CDCl_3$) δ [ppm]: 7.60 (s, 4H, CH), 7.45 (s, 2H, H-4, H-10), 6.82 (s, 2H, H-1, H-7), 4.71-4.75 (d, J = 16.8 Hz, 2H, H-6b, H-12b), 4.37 (s, 2H, -N-CH₂-N-), 4.27-4.31 (d, J = 16.7 Hz, 2H, H-6a, H-12a), 3.81-3.84 (t, J = 6.6 Hz, 4H, CH₂), 2.58 (s, 6H, CH₃), 2.38 (s, 12H, CH₃), 1.81-1.88 (m, 4H, CH₂), 1.50-1.58 (m, 4H, CH₂), 1.36-1.41 (m, 8H, CH₂), 0.93-0.96 (t, J = 7.1 Hz, 6H, CH₃).

^{13}C -NMR (100 MHz, $CDCl_3$) δ [ppm]: 158.8, 150.3, 148.9, 146.0, 133.8, 131.8, 130.4, 129.4, 123.6, 111.5, 72.6, 67.2, 58.9, 31.8, 30.5, 25.9, 22.7, 17.1, 16.6, 14.1.

IR: (Neat) ν_{max} [cm^{-1}] = 2926, 2858, 1586, 1474, 1375, 1302, 1208, 1111, 1086, 999, 920, 898, 748, 609.

MS (ACN 90%, EtOAc 5%, H₂O 5%): (ESI positive) calc. for $[C_{45}H_{59}N_6O_2]^+$: $[M+H]^+$ 715.4, found 715.7.

UV-Vis: (EtOAc) λ (lg ϵ) = 349 nm (4.572).

Anal. calcd: C, 75.59; H, 8.18; N, 11.75. found: C, 75.83; H, 7.94; N, 11.60

Characterization of compound (\pm)-5:

Starting with **1** (0.55 g, 1.0 mmol, 1.0 eq.), K_2CO_3 (0.69 g, 5.0 mmol), 1-bromooctane (0.45 g, 2.3 mmol, 1.2 eq.) and a catalytic amount of KI (0.01 g, 0.06 mmol) to obtain **5** (0.66 g, 0.86 mmol, 86%) Chemical Formula: $C_{49}H_{66}N_6O_2$, Molecular Weight: 771.11, R_f: 0.43 (EtOAc/ n-hexane = 20% v/v) silica gel.

1H -NMR (400 MHz, $CDCl_3$) δ [ppm]: 7.59 (s, 2H, H-4, H-10), 7.42 (s, 4H, CH), 6.86 (s, 2H, H-1, H-7), 4.69-4.73 (d, J = 17.0 Hz, 2H, H-6b, H-12b), 4.34 (s, 2H, -N-CH₂-N-), 4.26-4.30 (d, J = 16.9 Hz, 2H, H-6a, H-12a), 3.80-3.84 (t, J = 8.1 Hz, 4H, CH₂), 2.57 (s, 6H, CH₃), 2.37 (s, 12H, CH₃), 1.80-1.86 (m, 4H, CH₂), 1.51-1.55 (m, 4H, CH₂), 1.32-1.37 (m, 16H, CH₂), 0.89-0.93 (t, J = 8.0 Hz, 6H, CH₃).

^{13}C -NMR (100 MHz, $CDCl_3$) δ [ppm]: 158.7, 150.3, 149.0, 146.5, 133.6, 131.8, 130.7, 129.3, 123.6, 111.5, 72.7, 67.2, 59.0, 31.9, 30.5, 29.6, 29.4, 26.2, 22.7, 17.1, 16.7, 14.2.

IR: (Neat) ν_{max} [cm^{-1}] = 2923, 2859, 1585, 1468, 1371, 1308, 1212, 1113, 1087, 997, 921, 899 and 613.

MS (ACN 90%, EtOAc 5%, H₂O 5%): (ESI positive) calc. for $[C_{49}H_{67}N_6O_2]^+$: $[M+H]^+$ 771.52, found 771.0.

UV-Vis: (EtOAc) λ (lg ϵ) = 349 nm (4.558).

Anal. calcd: C, 76.32; H, 8.63; N, 10.90. found: C, 76.61; H, 8.39; N, 10.77

Characterization of compound (\pm)-6:

Starting with **1** (0.55 g, 1.0 mmol, 1.0 eq.), K_2CO_3 (0.69 g, 5.0 mmol), a catalytic amount of KI (0.01 g, 0.06 mmol) and 1-bromodecane (0.51 g, 2.3 mmol, 1.2 eq.) to obtain **6** (0.68 g, 0.82 mmol, 82%) Chemical Formula: $C_{53}H_{74}N_6O_2$, Molecular Weight: 827.22, R_f: 0.45 (EtOAc/ n-hexane = 20% v/v) silica gel.

1H -NMR (400 MHz, $CDCl_3$) δ [ppm]: 7.60 (s, 2H, H-4, H-10), 7.43 (s, 4H, CH), 6.86 (s, 2H, H-1, H-7), 4.69-4.73 (d, J = 17.0 Hz, 2H, H-6b, H-12b), 4.34 (s, 2H, -N-CH₂-N-), 4.26-4.30 (d, J = 17.1 Hz, 2H, H-6a, H-12a), 3.81-3.84 (t, J = 7.3 Hz, 4H, CH₂), 2.57 (s, 6H, CH₃), 2.38 (s, 12H, CH₃), 1.82-1.86 (m, 4H, CH₂), 1.51-1.55 (m, 4H, CH₂), 1.30-1.38 (m, 24H, CH₂), 0.89-0.92 (t, J = 8.1 Hz, 6H, CH₃).

^{13}C -NMR (100 MHz, $CDCl_3$) δ [ppm]: 158.8, 150.3, 149.0, 146.5, 133.6, 131.8, 130.7, 129.4, 123.6, 111.6, 72.7, 67.3, 59.0, 32.0, 30.6, 29.8, 29.7, 29.6, 29.4, 26.2, 22.8, 17.1, 16.6, 14.2.

IR: (Neat) ν_{max} [cm^{-1}] = 2920, 2853, 2358, 1586, 1478, 1304, 1207, 1114, 1083, 920, 897, 719 and 612.

MS (ACN 90%, EtOAc 5%, H₂O 5%): (ESI positive) calc. for $[C_{53}H_{75}N_6O_2]^+$: $[M+H]^+$ 827.59, found 828.1.

UV-Vis: (EtOAc) λ (lg ϵ) = 349 nm (4.570).

Anal. calcd: C, 76.95; H, 9.02; N, 10.16. found: C, 76.85; H, 9.31; N, 10.51.

Characterization of compound (\pm)-7:

Starting with **1** (0.55 g, 1.0 mmol, 1.0 eq.), K_2CO_3 (0.69 g, 5.0 mmol), a catalytic amount of KI (0.01 g, 0.06 mmol) and 1-bromododecane (0.75 g, 3.0 mmol, 1.5 eq.) to obtain **7** (0.73 g, 0.82 mmol, 82%) Chemical Formula: $C_{57}H_{82}N_6O_2$, Molecular Weight: 883.32, R_f: 0.44 (ethyl acetate/ n-hexane = 20% v/v) silica gel.

¹H-NMR (400 MHz, CDCl₃) δ [ppm]: 7.64 (s, 4H, CH), 7.50 (s, 2H, H-4, H-10), 6.85 (s, 2H, H-1, H-7), 4.70–4.74 (d, *J* = 17.0 Hz, 2H, H-6b, H-12b), 4.35 (s, 2H, -N-CH₂-N-), 4.28–4.32 (d, *J* = 17.3 Hz, 2H, H-6a, H-12a), 3.83–3.86 (t, *J* = 7.2 Hz, 4H, CH₂), 2.60 (s, 6H, CH₃), 2.40 (s, 12H, CH₃), 1.85–1.88 (m, 4H, CH₂), 1.55–1.58 (m, 4H, CH₂), 1.27–1.47 (m, 32H, CH₂), 0.93–0.97 (t, *J* = 8.1 Hz, 6H, CH₃).

¹³C-NMR (100 MHz, CDCl₃) δ [ppm]: 158.6, 150.1, 148.9, 146.3, 133.5, 131.6, 130.5, 129.3, 123.5, 111.4, 72.5, 67.1, 58.9, 31.9, 30.5, 29.7, 29.7, 29.6, 29.6, 29.6, 29.4, 26.2, 22.7, 17.0, 16.5, 14.1.

IR: (Neat) ν_{\max} [cm⁻¹] = 2921, 2851, 2359, 1589, 1479, 1304, 1208, 1112, 1085, 921, 897, 749, 719, 610.

MS (1-Propanol 50%, Ethanol 50%): (ESI positive) calc. for [C₅₇H₈₃N₆O₂]⁺: [M+H]⁺ 883.6, found 884.1.

UV: (EtOAc) λ (lgε) = 349 nm (4.612).

Anal. calcd: C, 77.51; H, 9.36; N, 9.51. found: C, 77.75; H, 9.55; N, 9.33.

Characterization of compound (±)-8:

Starting with **1** (0.55 g, 1.0 mmol, 1.0 eq.), K₂CO₃ (0.69 g, 5.0 mmol), a catalytic amount of KI (0.01 g, 0.06 mmol) and 1-bromotetradecane (0.64 g, 2.3 mmol, 1.2 eq.) to obtain **8** (0.73 g, 0.78 mmol, 78%) Chemical Formula: C₆₁H₉₀N₆O₂, Molecular Weight: 939.43, R_f: 0.48 (EtOAc/ n-hexane = 20% v/v) silica gel.

¹H-NMR (400 MHz, CDCl₃) δ [ppm]: 7.62 (s, 2H, H-4, H-10), 7.46 (s, 4H, CH), 6.86 (s, 2H, H-1, H-7), 4.70–4.74 (d, *J* = 17.1 Hz, 2H, H-6b, H-12b), 4.35 (s, 2H, -N-CH₂-N-), 4.27–4.31 (d, *J* = 17.1 Hz, 2H, H-6a, H-12a), 3.82–3.85 (t, *J* = 7.9 Hz, 4H, CH₂), 2.59 (s, 6H, CH₃), 2.39 (s, 12H, CH₃), 1.84–1.87 (m, 4H, CH₂), 1.53–1.57 (m, 4H, CH₂), 1.31–1.43 (m, 40H, CH₂), 0.90–0.94 (t, *J* = 8.1 Hz, 6H, CH₃).

¹³C-NMR (100 MHz, CDCl₃) δ [ppm]: 158.7, 150.2, 149.0, 146.5, 133.5, 131.7, 130.7, 129.3, 123.6, 111.5, 72.6, 67.2, 59.0, 32.0, 30.5, 29.8, 29.8, 29.7, 29.6, 29.5, 26.2, 22.8, 17.1, 16.6, 14.2.

IR: (Neat) ν_{\max} [cm⁻¹] = 2923, 2850, 2357, 1588, 1478, 1305, 1207, 1110, 1083, 899, 749, 721 and 610.

MS (Isopropyl alcohol 50%, EtOH 50%): (ESI positive) calc. for [C₆₁H₉₁N₆O₂]⁺: [M+H]⁺ 939.71, found 939.6.

UV-Vis: (EtOAc) λ (lgε) = 349 nm (4.564).

Anal. calcd: C, 77.99; H, 9.66; N, 8.95. found: C, 77.86; H, 9.45; N, 8.67.

Characterization of compound (±)-9:

Starting with **1** (0.55 g, 1.0 mmol, 1.0 eq.), K₂CO₃ (0.69 g, 5.0 mmol), a catalytic amount of KI (0.01 g, 0.06 mmol) and 1-bromohexadecane (0.64 g, 2.3 mmol, 1.2 eq.) to obtain **9** (0.83 g, 0.83 mmol, 83%) Chemical Formula: C₆₅H₉₈N₆O₂, Molecular Weight: 995.54, R_f: 0.48 (EtOAc/ n-hexane = 20% v/v) silica gel.

¹H-NMR (400 MHz, CDCl₃) δ [ppm]: 7.59 (s, 2H, H-4, H-10), 7.41 (s, 4H, CH), 6.85 (s, 2H, H-1, H-7), 4.69–4.73 (d, *J* = 16.9 Hz, 2H, H-6b, H-12b), 4.34 (s, 2H, -N-CH₂-N-), 4.25–4.30 (d, *J* = 16.9 Hz, 2H, H-6a, H-12a), 3.80–3.84 (t, *J* = 7.9 Hz, 4H, CH₂), 2.57 (s, 6H, CH₃), 2.37 (s, 12H, CH₃), 1.80–1.86 (m, 4H, CH₂), 1.49–1.54 (m, 4H, CH₂), 1.28–1.42 (m, 48H, CH₂), 0.87–0.91 (t, *J* = 7.8 Hz, 6H, CH₃).

¹³C-NMR (100 MHz, CDCl₃) δ [ppm]: 158.7, 150.3, 149.0, 146.5, 133.6, 131.8, 130.7, 129.4, 123.6, 111.5, 72.7, 67.2, 59.0, 32.0, 30.6, 29.8, 29.8, 29.7, 29.7, 29.5, 26.3, 22.8, 17.1, 16.7, 14.2.

IR: (Neat) ν_{\max} [cm⁻¹] = 2921, 2851, 1588, 1466, 1375, 1304, 1207, 1083, 1046, 907, 773, 722, 688.

MS (Isopropyl alcohol 50%, EtOH 50%): (ESI positive) calc. for [C₆₅H₉₉N₆O₂]⁺: [M+H]⁺ 995.78, found 996.3.

UV-Vis: (EtOAc) λ (lgε) = 349 nm (4.559).

Anal. calcd: C, 78.42; H, 9.92; N, 8.44. found: C, 78.56; H, 9.88; N, 8.36.

Characterization of compound (±)-10:

Starting with **1** (0.55 g, 1.0 mmol, 1.0 eq.), K₂CO₃ (0.69 g, 5.0 mmol), a catalytic amount of KI (0.01 g, 0.06 mmol) and 1-bromooctadecane (1.0 g, 3.0 mmol, 1.5 eq.) to obtain **10** (0.69 g, 0.66 mmol, 66 %) Chemical Formula: C₆₉H₁₀₆N₆O₂, Molecular Weight: 1051.65, R_f: 0.55 (ethyl acetate/ n-hexane = 20% v/v) silica gel.

¹H-NMR (400 MHz, CDCl₃) δ [ppm]: 7.60 (s, 4H, CH), 7.45 (s, 2H, H-4, H-10), 6.87 (s, 2H, H-1, H-7), 4.71–4.76 (d, *J* = 17.2 Hz, 2H, H-6b, H-12b), 4.38 (s, 2H, -N-CH₂-N-), 4.27–4.31 (d, *J* = 17.2 Hz, 2H, H-6a, H-12a), 3.81–3.84 (t, *J* = 7.8 Hz, 4H, CH₂), 2.58 (s, 6H, CH₃), 2.38 (s, 12H, CH₃), 1.81–1.88 (m, 4H, CH₂), 1.49–1.57 (m, 4H, CH₂), 1.24–1.42 (m, 56H, CH₂), 0.88–0.91 (t, *J* = 7.9 Hz, 6H, CH₃).

¹³C-NMR (100 MHz, CDCl₃) δ [ppm]: 158.8, 150.3, 148.9, 145.8, 133.9, 131.8, 130.2, 129.4, 123.6, 111.5, 72.6, 67.2, 58.8, 32.0, 30.5, 29.8, 29.8, 29.7, 29.7, 29.6, 29.5, 26.2, 22.8, 17.1, 16.7, 14.2.

IR: (Neat) ν_{\max} [cm⁻¹] = 2919, 2850, 1589, 1467, 1376, 1305, 1208, 1084, 1044, 921, 901, 774, 720, 692.

MS (1-Propanol 50%, Ethanol 50%): (ESI positive) calc. for [C₆₉H₁₀₇N₆O₂]⁺: [M+H]⁺ 1051.84, found 1052.0.

UV: (EtOAc) λ (lgε) = 349 nm (4.590).

Anal. calcd: C, 78.81; H, 10.16; N, 7.99. found: C, 78.93; H, 10.25; N, 7.77.

Characterization of compound (±)-11:

Starting with **1** (0.55 g, 1.0 mmol, 1.0 eq.), K₂CO₃ (0.69 g, 5.0 mmol), a catalytic amount of KI (0.01 g, 0.06 mmol) and 1-bromoeicosane (0.83 g, 2.3 mmol, 1.2 eq.) to obtain **11** (0.80 g, 0.72 mmol, 72%) Chemical Formula: C₇₃H₁₁₄N₆O₂, Molecular Weight: 1107.76, R_f: 0.60 (EtOAc/ n-hexane = 20% v/v) silica gel.

¹H-NMR (400 MHz, CDCl₃) δ [ppm]: 7.61 (s, 2H, H-4, H-10), 7.45 (s, 4H, CH), 6.86 (s, 2H, H-1, H-7), 4.69–4.74 (d, *J* = 17.2 Hz, 2H, H-6b, H-12b), 4.35 (s, 2H, -N-CH₂-N-), 4.27–4.31 (d, *J* = 17.1 Hz, 2H, H-6a, H-12a), 3.82–3.85 (t, *J* = 7.2 Hz, 4H, CH₂), 2.58 (s, 6H, CH₃), 2.39 (s, 12H, CH₃), 1.82–1.87 (m, 4H, CH₂), 1.51–1.54 (m, 4H, CH₂), 1.29 (m, 64H, CH₂), 0.89–0.92 (t, *J* = 7.9 Hz, 6H, CH₃).

¹³C-NMR (100 MHz, CDCl₃) δ [ppm]: 158.7, 150.2, 149.0, 146.5, 133.6, 131.8, 130.7, 129.3, 123.6, 111.5, 72.6, 67.2, 59.0, 32.0, 30.5, 29.8, 29.7, 29.7, 29.5, 26.2, 22.8, 17.1, 16.6, 14.2.

IR: (Neat) ν_{\max} [cm⁻¹] = 2920, 2851, 1588, 1466, 1376, 1304, 1209, 1082, 1043, 920, 720, 697.

MS (isopropyl alcohol 60%, EtOAc 40%): (ESI positive) calc. for $[C_{73}H_{115}N_6O_2]^+$: $[M+H]^+$ 1107.90, found 1107.2.

UV-Vis: (EtOAc) λ (lg ϵ) = 349 nm (4.563).

Anal. calcd: C, 79.15; H, 10.37; N, 7.59. found: C, 79.25; H, 10.24; N, 7.78.

Characterization of compound (\pm)-12:

Starting with **1** (0.55 g, 1.0 mmol, 1.0 eq.), K_2CO_3 (0.69 g, 5.0 mmol), a catalytic amount of KI (0.01 g, 0.06 mmol) and 1-bromodocosane (0.90 g, 2.3 mmol, 1.2 eq.) to obtain **12** (0.79 g, 0.68 mmol, 68%) Chemical Formula: $C_{77}H_{122}N_6O_2$, Molecular Weight: 1163.86, R_f: 0.63 (EtOAc/ n-hexane = 20% v/v) silica gel.

1H -NMR (400 MHz, $CDCl_3$) δ [ppm]: 7.60 (s, 2H, H-4, H-10), 7.43 (s, 4H, CH), 6.86 (s, 2H, H-1, H-7), 4.69–4.73 (d, J = 16.9 Hz, 2H, H-6b, H-12b), 4.34 (s, 2H, -N-CH₂-N-), 4.26–4.30 (d, J = 17.1 Hz, 2H, H-6a, H-12a), 3.81–3.84 (t, J = 7.8 Hz, 4H, CH₂), 2.57 (s, 6H, CH₃), 2.38 (s, 12H, CH₃), 1.81–1.84 (m, 4H, CH₂), 1.49–1.54 (m, 4H, CH₂), 1.23–1.46 (m, 72H, CH₂), 0.88–0.91 (t, J = 7.1 Hz, 6H, CH₃).

^{13}C -NMR (100 MHz, $CDCl_3$) δ [ppm]: 158.8, 150.3, 149.0, 146.5, 133.6, 131.8, 130.7, 129.4, 123.6, 111.5, 72.7, 67.3, 59.0, 32.0, 30.6, 29.8, 29.7, 29.7, 29.5, 26.3, 22.8, 17.1, 16.7, 14.2.

IR: (Neat) ν_{max} [cm^{-1}] = 2922, 2850, 1586, 1469, 1379, 1304, 1207, 1083, 1042, 921, 909, 771 and 692.

MS (Isopropyl alcohol 60%, EtOAc 40%): (ESI positive) calc. for $[C_{77}H_{123}N_6O_2]^+$: $[M+H]^+$ 1163.96, found 1163.2 and 1164.3.

UV-Vis: (EtOAc) λ (lg ϵ) = 349 nm (4.588).

Anal. calcd: C, 79.46; H, 10.57; N, 7.22. found: C, 79.55; H, 10.69; N, 7.40.

Characterization of compound (\pm)-13:

Starting with **1** (0.55 g, 1.0 mmol, 1.0 eq.), K_2CO_3 (0.69 g, 5.0 mmol) and 1,2-dibromoethane (0.50 g, 2.7 mmol, 1.3 eq.) to obtain **13** (0.37 g, 0.49 mmol, 49%) Chemical Formula: $C_{37}H_{40}Br_2N_6O_2$, Molecular Weight: 760.58. R_f: 0.55 (ethyl acetate/ n-hexane = 40% v/v) silica gel.

1H -NMR (400 MHz, $CDCl_3$) δ [ppm]: 7.60 (s, 4H, CH), 7.50 (s, 2H, H-4, H-10), 6.90 (s, 2H, H-1, H-7), 4.76–4.81 (d, J = 17.04 Hz, 2H, H-6b, H-12b), 4.45 (s, 2H, -N-CH₂-N-), 4.28–4.33 (d, J = 17.16 Hz, 2H, H-6a, H-12a), 4.14–4.17 (t, J = 7.3 Hz, 4H, CH₂), 3.68–3.71 (t, J = 7.4 Hz, 4H, CH₂), 2.58 (s, 6H, CH₃), 2.40 (s, 12H, CH₃).

^{13}C -NMR (100 MHz, $CDCl_3$) δ [ppm]: 157.7, 150.4, 149.3, 134.8, 131.8, 129.5, 123.9, 123.8, 111.5, 71.8, 67.2, 58.6, 30.1, 17.2, 16.8.

IR: (Neat) ν_{max} [cm^{-1}] = 2949, 2916, 2849, 1732, 1588, 1477, 1395, 1375, 1278, 1201, 1111, 1084, 1000, 893, 745, 688.

MS (Acetonitrile 90%, EtOAc 5%, H₂O 5%) (ESI positive) calc. for $[C_{37}H_{41}Br_2N_6O_2]^+$: $[M+H]^+$ 759.16, found 759.45 and 761.40.

UV: (EtOAc) λ (lg ϵ) = 345nm (4.596).

Anal. calcd: C, 58.43; H, 5.30; Br, 21.01; N, 11.05. found: C, 58.66; H, 5.21; N, 11.24.

Characterization of compound (\pm)-14:

Starting with **1** (1.1 g, 2.0 mmol, 1.0 eq.), K_2CO_3 (1.4 g, 10 mmol) and 1,3-dibromopropane (0.93 g, 4.6 mmol, 2.3 eq.) to obtain **14** (0.39 g, 0.50 mmol, 25%) Chemical Formula: $C_{39}H_{44}Br_2N_6O_2$,

Molecular Weight: 788.63. R_f: 0.60 (ethyl acetate/ n-hexane = 40% v/v) silica gel.

1H -NMR (400 MHz, $CDCl_3$) δ [ppm]: 7.60 (s, 4H, CH), 7.44 (s, 2H, H-4, H-10), 6.86 (s, 2H, H-1, H-7), 4.69–4.73 (d, J = 17.0 Hz, 2H, H-6b, H-12b), 4.34 (s, 2H, -N-CH₂-N-), 4.26–4.31 (d, J = 17.1 Hz, 2H, H-6a, H-12a), 3.95–3.97 (t, J = 5.9 Hz, 4H, CH₂), 3.71–3.74 (t, J = 6.2 Hz, 4H, CH₂), 2.58 (s, 6H, CH₃), 2.39 (s, 12H, CH₃), 2.34–2.38 (m, 4H, CH₂).

^{13}C -NMR (100 MHz, $CDCl_3$) δ [ppm]: 158.0, 150.2, 149.2, 146.5, 133.6, 131.7, 130.8, 129.4, 123.6, 111.5, 69.3, 67.2, 59.0, 33.5, 30.2, 17.1, 16.6.

IR: (Neat) ν_{max} [cm^{-1}] = 2948, 2917, 2849, 1733, 1587, 1475, 1395, 1375, 1276, 1203, 1112, 1084, 1001, 893, 744, 679.

MS (Isopropyl alcohol 50%, Acetonitrile 40%, EtOAc 10%) (ESI positive) calc. for $[C_{39}H_{45}Br_2N_6O_2]^+$: $[M+H]^+$ 787.19, found 786.8, 789.2 and 792.1.

UV: (EtOAc) λ (lg ϵ) = 345nm (4.577).

Anal. calcd: C, 59.40; H, 5.62; N, 10.66. found: C, 59.51; H, 5.48; N, 10.38.

Characterization of compound (\pm)-15:

Starting with **1** (1.1 g, 2.0 mmol, 1.0 eq.), K_2CO_3 (1.4 g, 10 mmol) and 1,4-dibromobutane (1.0 g, 4.6 mmol, 2.3 eq.) to obtain **15** (0.31 g, 0.38 mmol, 19%) Chemical Formula: $C_{41}H_{48}Br_2N_6O_2$, Molecular Weight: 816.68. R_f: 0.65 (ethyl acetate/ n-hexane = 40% v/v) silica gel.

1H -NMR (400 MHz, $CDCl_3$) δ [ppm]: 7.59 (s, 4H, CH), 7.42 (s, 2H, H-4, H-10), 6.86 (s, 2H, H-1, H-7), 4.69–4.73 (d, J = 17.1 Hz, 2H, H-6b, H-12b), 4.34 (s, 2H, -N-CH₂-N-), 4.26–4.30 (d, J = 17.3 Hz, 2H, H-6a, H-12a), 3.84–3.87 (t, J = 6.4 Hz, 4H, CH₂), 3.52–3.55 (t, J = 6.9 Hz, 4H, CH₂), 2.57 (s, 6H, CH₃), 2.37 (s, 12H, CH₃), 2.11–2.19 (m, 4H, CH₂), 1.94–2.08 (m, 4H, CH₂).

^{13}C -NMR (100 MHz, $CDCl_3$) δ [ppm]: 158.4, 150.2, 149.1, 146.5, 133.6, 131.7, 130.8, 129.4, 123.6, 111.5, 71.4, 67.2, 59.0, 33.6, 29.7, 29.2, 17.1, 16.6.

IR: (Neat) ν_{max} [cm^{-1}] = 2950, 2919, 2848, 1743, 1586, 1479, 1395, 1376, 1278, 1203, 1109, 1084, 999, 894, 746, 678.

MS (Isopropyl alcohol 50%, Acetonitrile 40%, EtOAc 10%) (ESI positive) calc. for $[C_{41}H_{49}Br_2N_6O_2]^+$: $[M+H]^+$ 815.22, found 815.8, 818.9 and 820.3.

UV: (EtOAc) λ (lg ϵ) = 345nm (4.581).

Anal. calcd: C, 60.30; H, 5.92; N, 10.29. found: C, 60.21; H, 5.74; N, 10.58.

Characterization of compound 16:

Starting with **1** (0.55 g, 1.0 mmol, 1.0 eq.), K_2CO_3 (0.69 g, 5.0 mmol), a catalytic amount of KI (0.01 g, 0.06 mmol) and benzyl bromide (0.38 g, 2.2 mmol, 1.1 eq.) to obtain **16** (0.29 g, 0.36 mmol, 73%) Chemical Formula: $C_{46}H_{46}N_6O_2$, Molecular Weight: 714.914, R_f: 0.44 (EtOAc/ n-Hex = 20% v/v) silica gel.

1H -NMR (400 MHz, DMSO- d_6) δ [ppm]: 7.56 (s, 2H, CH), 7.46–7.54 (m, 5H, CH), 7.32–7.46 (m, 5H, CH), 7.22–7.24 (m, 3H, CH), 7.12 (s, 1H, CH), 6.99 (s, 1H, CH), 6.97 (s, 1H, CH), 6.94 (s, 1H, CH), 6.16–6.20 (t, J = 7.8 Hz, 1H, NH), 4.88 (s, 2H, CH₂), 4.86 (s, 2H,

CH₂), 4.43 (b, 4H, CH₂), 2.52 (s, 3H, CH₃), 2.48 (s, 3H, CH₃), 2.34 (s, 6H, CH₃), 2.31 (s, 6H, CH₃).

¹³C-NMR (100 MHz, DMSO-*d*₆) δ [ppm]: 157.7, 157.7, 149.4, 148.9, 148.5, 148.3, 147.4, 147.3, 138.8, 137.2, 134.3, 133.7, 133.3, 131.9, 131.8, 128.4, 128.2, 128.1, 128.0, 127.5, 127.3, 127.2, 126.7, 126.2, 122.9, 102.4, 101.8, 73.6, 55.3, 54.9, 49.0, 16.4, 16.3, 16.1.

IR: (Neat) ν_{\max} [cm⁻¹] = 3408, 2916, 1608, 1497, 1451, 1368, 1306, 1291, 1200, 1110, 1016, 980, 887, 755, 690.

MS (Ethanol 50%, Isopropyl Alcohol 50%) (ESI positive) calc. for [C₄₆H₄₇N₆O₂]⁺: calc. 715.37, found 715.2.

UV-Vis: (EtOAc) λ [lgε] = 345nm (4.605).

Anal. calcd: C, 77.28; H, 6.49; N, 11.76. found: C, 77.37; H, 6.35; N, 11.91.

Synthesis and Characterization of compound (±)-17:

1 (0.55 g, 1.0 mmol, 1.0 eq.), K₂CO₃ (0.69 g, 5.0 mmol), a catalytic amount of KI (0.01 g, 0.06 mmol) and 4-nitrobenzyl bromide (0.43 g, 2.2 mmol, 2.2 eq.) were refluxed in acetone (10ml) for 48h. Then, ice (50 g) and EtOAc (5 ml) were added to the reaction mixture and mixed for 30 minutes. The desired product **17** was obtained, by filtration of the mixture and desiccation under high-vacuum (0.57 g, 0.70 mmol, 70%) Chemical Formula: C₄₇H₄₄N₈O₆, Molecular Weight: 816.92. R_f: 0.8 (MeOH/ DCM = 4% v/v) silica gel.

¹H-NMR (600 MHz, CDCl₃) δ [ppm]: 8.27-8.29 (d, 4H, *J* = 8.7 Hz), 7.67-7.68 (d, 4H, *J* = 8.8 Hz), 7.63 (s, 4H, CH), 7.44 (s, 2H, H-4, H-10), 6.88 (s, 2H, H-1, H-7), 4.98 (s, 4H, C-CH₂-C), 4.71-4.74 (d, *J* = 17.1 Hz, 2H, H-6b, H-12b), 4.35 (s, 2H, -N-CH₂-N-), 4.27-4.30 (d, *J* = 17.1 Hz, 2H, H-6a, H-12a), 2.58 (s, 6H, CH₃), 2.38 (s, 12H, CH₃).

¹³C-NMR (150 MHz, CDCl₃) δ [ppm]: 157.7, 150.2, 149.5, 147.7, 146.5, 144.8, 133.8, 131.8, 131.0, 129.4, 127.8, 123.9, 123.8, 111.5, 72.6, 67.3, 59.0, 17.1, 16.7.

IR: (Neat) ν_{\max} (cm⁻¹) = 2921, 2851, 1712, 1603, 1515, 1341, 1198, 1108, 1013, 853, 735, 697.

MS (Acetonitrile 50%, EtOAc 50%) (ESI positive) calc. for [C₄₇H₄₅N₈O₆]⁺: [M+H]⁺ 817.34, found 817.1.

UV(EtOAc): λ [lgε] = 341nm (4.498).

Anal. calcd: C, 69.10; H, 5.43; N, 13.72. found: C, 69.27; H, 5.15; N, 13.95.

Photo-isomerization of (±)1:

A tightly sealed quartz cuvette containing a solution of compound **1** (2x10⁻⁵ mol.L⁻¹, EtOAc, r.t.) was scanned to obtain the UV-Vis absorption spectra of the *trans* isomer. Afterwards, it was exposed to a 365 nm UV light-source (Spectroline® ENF-260C/FE [230V, 50Hz, 0.17A], Spectronics Corporation, Westbury, New York, USA) installed on a standard fluorescence cabinet (Spectroline® CM10) for 5 minutes and then instantly scanned to obtain the UV-Vis spectra at the most enriched population of the *cis* isomer. Then, the sample was incubated in absolute darkness at the room temperature and periodically rescanned to track its thermal back-isomerization until the peaks reached to their initial values. This cycle was quite repeatable and

reversible; however, for simplification only one isomerization /relaxation cycle is shown (Figure 2).

Acknowledgment

The author appreciates Macquarie University for awarding him with PGRF and IMQRES/IPRS, valued Dr Jennifer Rowland (Dean-HDR office, Macquarie University, Australia) for revising this paper and Mr Amirhossein Moghanian (Harvard-MIT Division of Health Sciences and Technology, Harvard Medical School, USA) for the elemental analysis.

Supporting Information

Detailed synthesis procedures and the NMR spectra including ¹H, ¹³C, COSY, HSQC, HMBC, and NOESY accompanied with Mass Spectroscopy, Infrared, and UV-Vis results are available *via* the Internet at (links)

Primary Data

NO (this text will be deleted prior to publication)

References

- (1) White, T. J.; McConney, M. E.; Bunning, T. J. *J. Mater. Chem.* **2010**, 20, 9832-9847.
- (2) Wang, D.; Wang, X. *Prog. Polym. Sci.* **2013**, 38, 271-301.
- (3) Mathews, M.; Zola, R. S.; Yang, D.-k.; Li, Q. *J. Mater. Chem.* **2011**, 21, 2098-2103.
- (4) Zahangir Alam, M.; Yoshioka, T.; Ogata, T.; Nonaka, T.; Kurihara, S. *Liq. Cryst.* **2007**, 34, 1215-1219; Finden, J. G.; Yuh, E.; Huntley, C.; Lemieux, R. P. *Liq. Cryst.* **2007**, 34, 1095-1106; Cui, Q.; Huntley, C. M.; Lemieux, R. P. *J. Mater. Chem.* **2009**, 19, 5188-5192.
- (5) Cui, Q.; Lemieux, R. P. *J. Mater. Chem. C* **2013**, 1, 1011-1017; Boulton, C. J.; Sutherland, J. J.; Lemieux, R. P. *J. Mater. Chem.* **2003**, 13, 644-646; Boulton, C. J.; Finden, J. G.; Yuh, E.; Sutherland, J. J.; Wand, M. D.; Wu, G.; Lemieux, R. P. *J. Am. Chem. Soc.* **2005**, 127, 13656-13665.
- (6) Morris, S. M.; Qasim, M. M.; Cheng, K. T.; Castles, F.; Ko, D. H.; Gardiner, D. J.; Nosheen, S.; Wilkinson, T. D.; Coles, H. J.; Burgess, C.; Hill, L. *Appl. Phys. Lett.* **2013**, 103, 101105; Kwon, H.-K.; Lee, K.-T.; Hur, K.; Moon, S. H.; Qasim, M. M.; Wilkinson, T. D.; Han, J.-Y.; Ko, H.; Han, I.-K.; Park, B.; Min, B. K.; Ju, B.-K.; Morris, S. M.; Friend, R. H.; Ko, D.-H. *Adv. Energy Mater.* **2015**, 5, 1-6.
- (7) Li, Q.; Green, L.; Venkataraman, N.; Shiyonovskaya, I.; Khan, A.; Urbas, A.; Doane, J. W. *J. Am. Chem. Soc.* **2007**, 129, 12908-12909.
- (8) Jin, O.; Fu, D.; Ge, Y.; Wei, J.; Guo, J. *New J. Chem.* **2015**, 39, 254-261.
- (9) Li, Q., *Nanoscience with Liquid Crystals*, ed.; Springer: Ohio, USA, 2014; Zhao, Y.; Ikeda, T., *Smart light-responsive materials: azobenzene-containing polymers and liquid crystals*, ed.; John Wiley & Sons Inc.: New Jersey, USA, 2009; Vol. 1; Eelkema, R. *Liq. Cryst.* **2011**, 38, 1641-1652; Kim, D.-Y.; Lee, S.-A.; Choi, Y.-J.; Hwang, S.-H.; Kuo, S.-W.; Nah, C.; Lee, M.-H.; Jeong, K.-U. *Chem. - Eur. J.* **2014**, 20, 5689-5695.
- (10) Yoshioka, T.; Ogata, T.; Nonaka, T.; Moritsugu, M.; Kim, S.-N.; Kurihara, S. *Adv. Mater. (Weinheim, Ger.)* **2005**, 17, 1226-1229; Kurihara, S.; Yoshioka, T.; Moritsugu, M.; Ogata, T.; Nonaka, T. *Mol. Cryst. Liq. Cryst.* **2005**, 443, 69-78.
- (11) Tröger, J. *J. Prakt. Chem.* **1887**, 36, 225-245.
- (12) Rigol, S.; Beyer, L.; Hennig, L.; Sieler, J.; Giannis, A. *Org. Lett.* **2013**, 15, 1418-1420.
- (13) Sergeyev, S. *Helv. Chim. Acta* **2009**, 92, 415-444.
- (14) Kiehne, U.; Weilandt, T.; Lützen, A. *Org. Lett.* **2007**, 9, 1283-1286.
- (15) Satishkumar, S.; Periasamy, M. *Tetrahedron: Asymmetry* **2009**, 20, 2257-2262; Goswami, S.; Ghosh, K.; Dasgupta, S. *J. Org. Chem.* **2000**, 65, 1907-1914; Adrian, J.; Wilcox, C. *J. Am. Chem. Soc.* **1989**, 111, 8055-8057; Adrian, J.; Wilcox,

C. *J. Am. Chem. Soc.* **1992**, 114, 1398-1403; Boyle, E. M.; Comby, S.; Molloy, J. K.; Gunnlaugsson, T. *J. Org. Chem.* **2013**, 78, 8312-9; Valík, M.; Strongin, R. M.; Král, V. *Supramol. Chem.* **2005**, 17, 347-367.

(16) Tatar, A.; Cejka, J.; Kral, V.; Dolensky, B. *Org. Lett.* **2010**, 12, 1872-1875; Sergeyev, S.; Diederich, F. *Angew. Chem. Int. Ed.* **2004**, 43, 1738-1740; Havlik, M.; Kral, V.; Kaplanek, R.; Dolensky, B. *Org. Lett.* **2008**, 10, 4767-4769.

(17) Wilen, S. H.; Qi, J. Z.; Williard, P. G. *J. Org. Chem.* **1991**, 56, 485-487.

(18) Sergeyev, S.; Diederich, F. *Chirality* **2006**, 18, 707-712.

(19) Valík, M.; Dolenský, B.; Herdtweck, E.; Král, V. *Tetrahedron: Asymmetry* **2005**, 16, 1969-1974.

(20) Jameson, D. L.; Field, T.; Schmidt, M. R.; DeStefano, A. K.; Stiteler, C. J.; Venditto, V. J.; Krovic, B.; Hoffman, C. M.; Ondisco, M. T.; Belowich, M. E. *J. Org. Chem.* **2013**, 78, 11590-11596.

(21) Ohtake, T. *Tellus B* **1993**, 45, 138-144.

(22) Sergeyev, S.; Didier, D.; Boitsov, V.; Teshome, A.; Asselberghs, I.; Clays, K.; Vande Velde, C. M. L.; Plaquet, A.; Champagne, B. *Chem. Eur. J.* **2010**, 16, 8181-8190.

(23) Goswami, S.; Ghosh, K.; Halder, M. *Tetrahedron Lett.* **1999**, 40, 1735-1738.

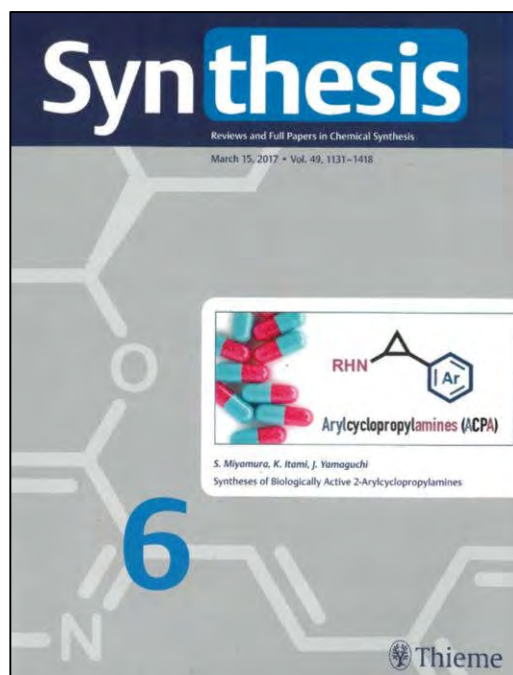
(24) Hamada, Y.; Mukai, S. *Tetrahedron: Asymmetry* **1996**, 7, 2671-2674.

(25) Rück-Braun, K.; Kempa, S.; Priewisch, B.; Richter, A.; Seedorff, S.; Wallach, L. *Synthesis* **2009**, 2009, 4256-4267; Kitzig, S.; Thilemann, M.; Cordes, T.; Rück-Braun, K. *ChemPhysChem* **2016**, 17, 1252-1263.

(26) Michon, C.; Sharma, A.; Bernardinelli, G.; Francotte, E.; Lacour, J. *Chem. Commun.* **2010**, 46, 2206-2208; Häring, M. *Helv. Chim. Acta* **1963**, 46, 2970-2982; Cooper, F.; Partridge, M. *J. Chem. Soc.* **1957**, 2888-2893.

(27) Han, M. R.; Hara, M. *New J. Chem.* **2006**, 30, 22

Paper I (Supporting Information)



Journal Impact Factor: 2.689

Notification

The following materials are *open access* and are available online free of charges *via* the Internet at: <http://dx.doi.org/10.1055/s-0036-1588913>. Every use of the following material is permitted, however has to be referred to the corresponding publication: *Synthesis* **2017**, 49, 1214–1222.

Supporting Information for DOI:
10.1055/s-0036-1588913
© Georg Thieme Verlag KG Stuttgart · New York 2016

Supporting Information

Design and Synthesis of Λ -Shaped Photoswitchable Compounds Employing Tröger's Base Scaffold

Masoud Kazem-Rostami*

Department of Chemistry and Biomolecular Sciences, Macquarie University, North Ryde, NSW 2109, Australia

masoud.kazem-rostami@hdr.mq.edu.au, masoud.kr@gmail.com

Table of Contents

General Remarks and Procedures	2
1. Starting Materials	2
2. Instrumentation	3
Synthesis and Characterization	4
1. Synthesis and Characterization of 1	4
2. Synthesis and Characterization of 2	6
3. Synthesis and Characterization of 3	7
4. Synthesis and Characterization of 4	9
5. Synthesis and Characterization of 5	11
6. Synthesis and Characterization of 6	12
7. Synthesis and Characterization of 7	14
8. Synthesis and Characterization of 8	16
9. Synthesis and Characterization of 9	17
10. Synthesis and Characterization of 10	19
11. Synthesis and Characterization of 11	21
12. Synthesis and Characterization of 12	22
13. Synthesis and Characterization of 13	24
14. Synthesis and Characterization of 14	25
15. Synthesis and Characterization of 15	27
16. Synthesis and Characterization of 16	28
17. Synthesis and Characterization of 17	30
2D NMR Results	32
Comparative Infrared and NMR Spectra	45
Reference	45

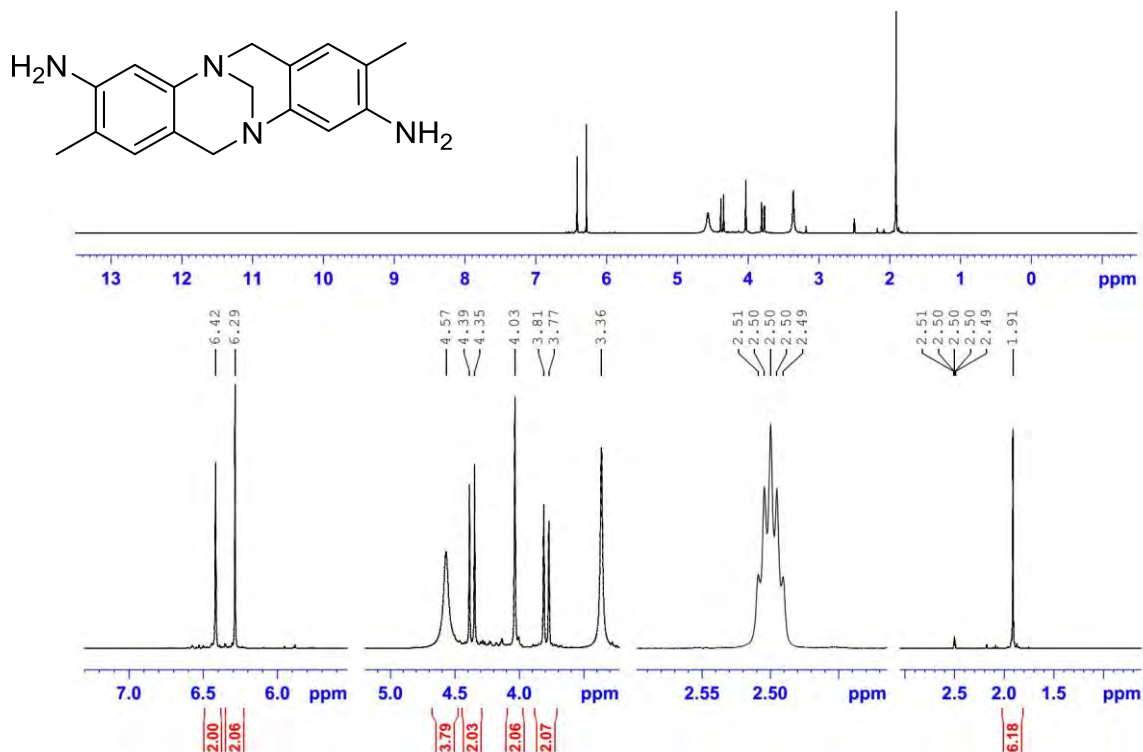
General Remarks and Procedures

1. Starting Materials: All the starting materials and solvents were purchased from Sigma-Aldrich commercial chemical suppliers and used without any further purification except chloroform and acetone which were respectively deacidified and dried over anhydrous K_2CO_3 prior to use.

Synthesis of Hünlich's base:

Hünlich's base was produced and purified according to an existing procedure¹ with minor modifications as described below:

2,4-diaminotoluene (36.6 g, 300 mmol, 2.05 eq.) was dissolved in an aqueous solution of sulfuric acid (5 %, 1000 ml). Then, formaldehyde (37 % in H_2O , 10.9 ml, 11.9 g, 146 mmol, 1.00 eq.) was slowly added to the solution and stirred for 48 hours at room temperature in a sealed container kept away from light. After checking the completion of the reaction by TLC, ice (300 g) and ammonia (25 %, 300 ml) were added and the precipitated crude product was filtrated. The crude was dissolved in boiling methanol (200 ml) and gradually cooled down to $-20^\circ C$. Filtration yielded Hünlich's base (14.2 g, 50.8 mmol, 34.7 %) as an off-white solid. Chemical Formula: $C_{17}H_{20}N_4$, Molecular Weight: 280.38, R_f : 0.5 (MeOH/ DCM = 10% v/v) silica gel. 1H -NMR (400 MHz, $DMSO-d_6$) δ [ppm] : 6.24 (s, 2H, CH), 6.29 (s, 2H, CH), 4.57 (b, 4H, NH), 4.35-4.39 (d, $J = 16.2$ Hz, 2H, H-6b, H-12b), 4.03 (s, 2H, -N-CH₂-N-), 3.77-3.81 (d, $J = 16.3$ Hz, 2H, H-6a, H-12a), 1.91 (s, 6H, $2 \times -CH_3$). IR: (Neat) ν_{max} [cm^{-1}] = 3402, 3335, 3236, 2986, 2887, 2844, 1620, 1573, 1498, 1441, 1183, 1085, 913, 870. MS (EtOH): (ESI positive) calc. for $[C_{17}H_{21}N_4]^+$: $[M+H]^+$ 281.17, found 281.2.

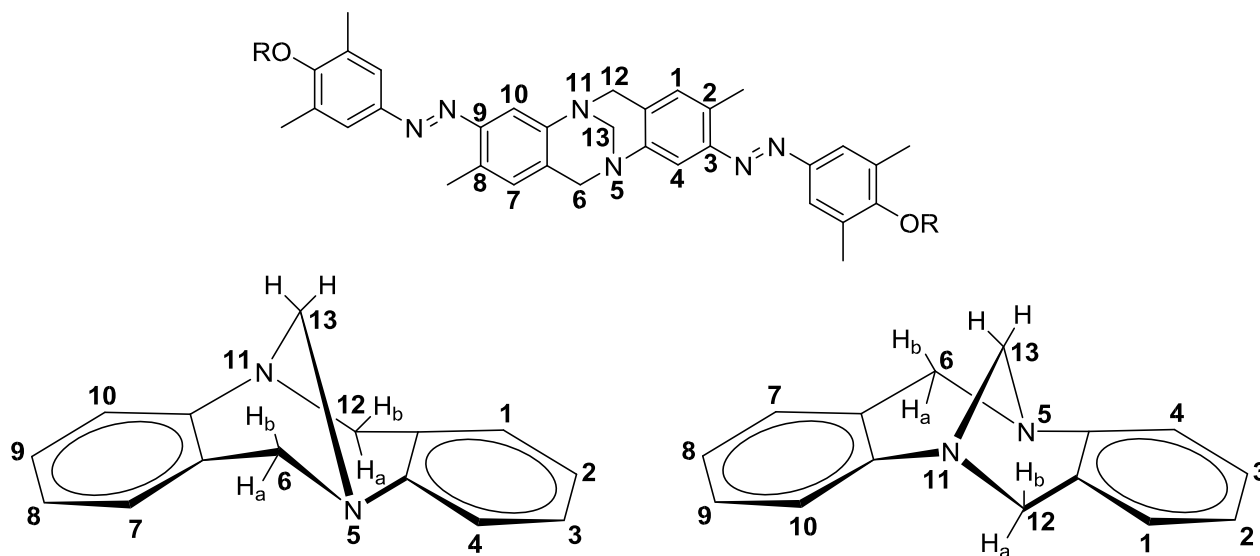


Hünlich's base, 1H -NMR (400 MHz, $DMSO-d_6$)

2. Instrumentation: Reaction profiles were monitored by Thin Layer Chromatography (TLC) on silica gel plates and colourless spots were visualized by UV lamps of 254 and 365nm. Column chromatography was performed using 40-63 micron silica gel as the stationary phase and applied mobile phases are described by a retention factor R_f for each compound. Mass spectra were obtained from direct sample injections to a Shimadzu LCMS-2010EV or Agilent 6130LCMS both set on ElectroSpray Ionization (ESI) and using the described solvents combination for each compound. The organic elemental analysis was performed by using a Vario EL-Elementar or Perkin Elmer-2400 series II CHSNO elemental analysers. The NMR spectra were recorded by running Topspin 3.2 on Bruker AVANCE DRX400 or 600MHz NMR spectrometers at 298.15 K (^1H : 400 or 600 MHz, ^{13}C : 100.6 or 150.9 MHz). ^1H NMR and ^{13}C NMR chemical shifts were corrected relative to the chemical shifts of the peaks of the applied NMR solvents as written follow in ppm:

APPLIED SOLVENT	¹ H-NMR	¹³ C-NMR
DMSO- <i>d</i> ₆	2.50	39.52
CDCl ₃	7.26	77.16

Splitting patterns are abbreviated in the reports as follow: **s** for Singlet, **d** for doublet, **t** for triplet, **q** for quartet; **b** for broad, **m** for multiplet; and coupling constants *J* in Hertz rounded into one decimal and the integrals are calibrated to the expected value for the most recognizable peak. UV-Vis and IR spectra were recorded by serving Thermo Scientific Nicolet iS5/ATR10 and Varian Cary 1 spectrophotometers respectively.

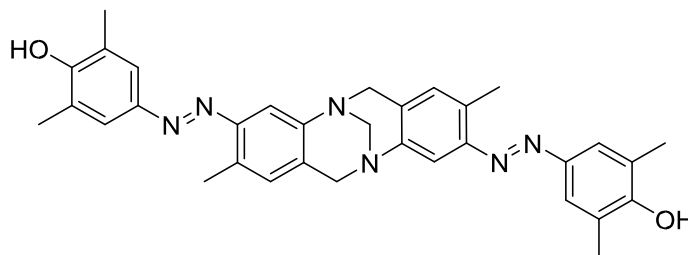


Numbering system used in the NMR interpretation

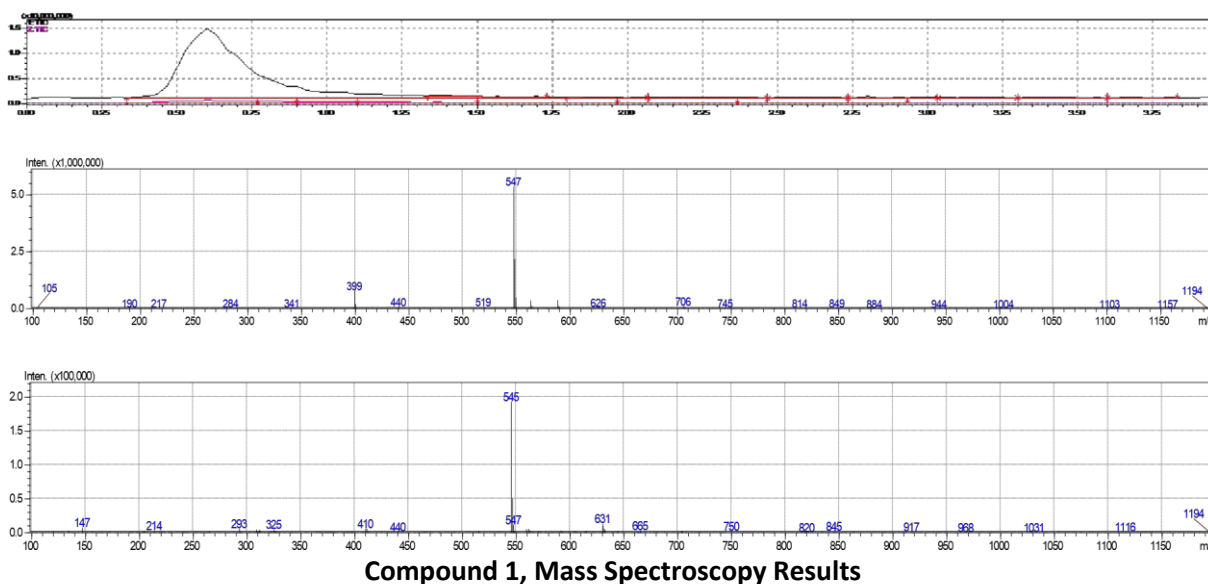
Synthesis and Characterization

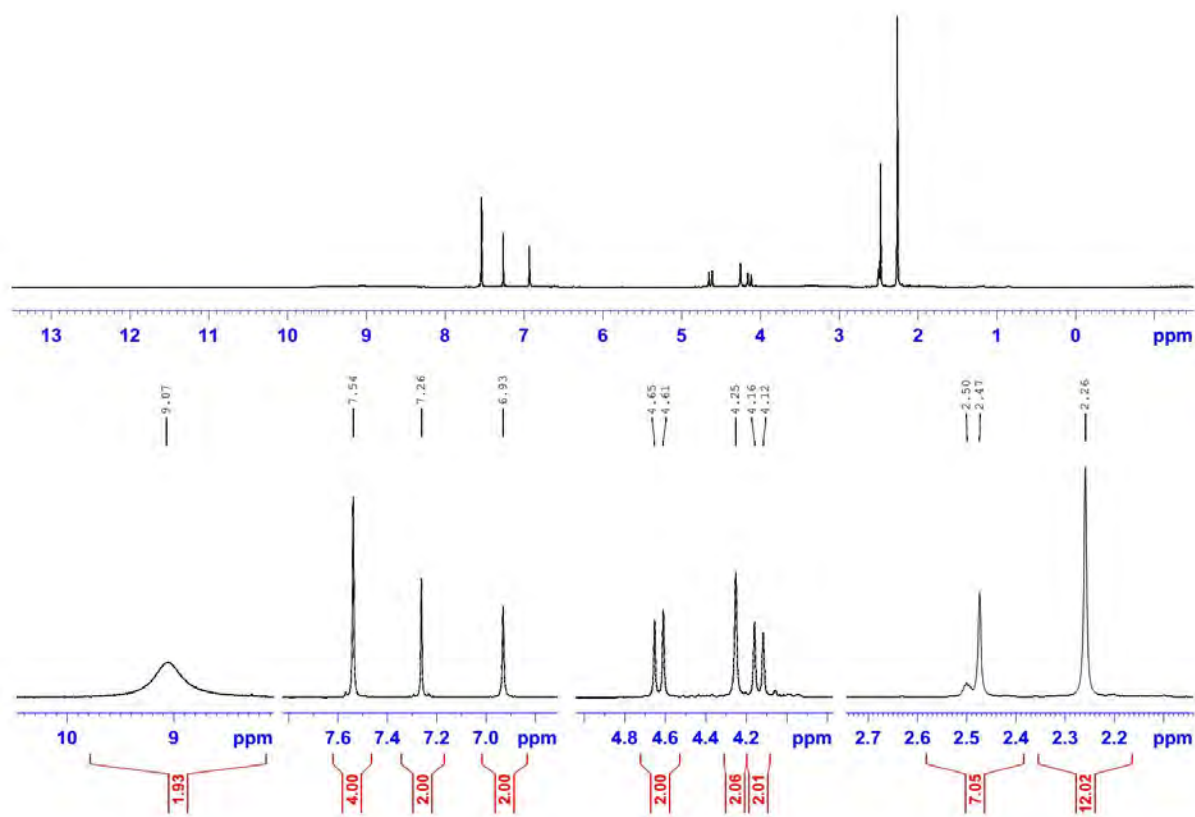
1. Synthesis and Characterization of (\pm 1)

4,4'-((2,8-dimethyl-6H,12H-5,11-methanodibenzo[b,f][1,5]diazocine-3,9-diyl)bis(diazeno-2,1-diyl))bis(2,6-dimethylphenol)

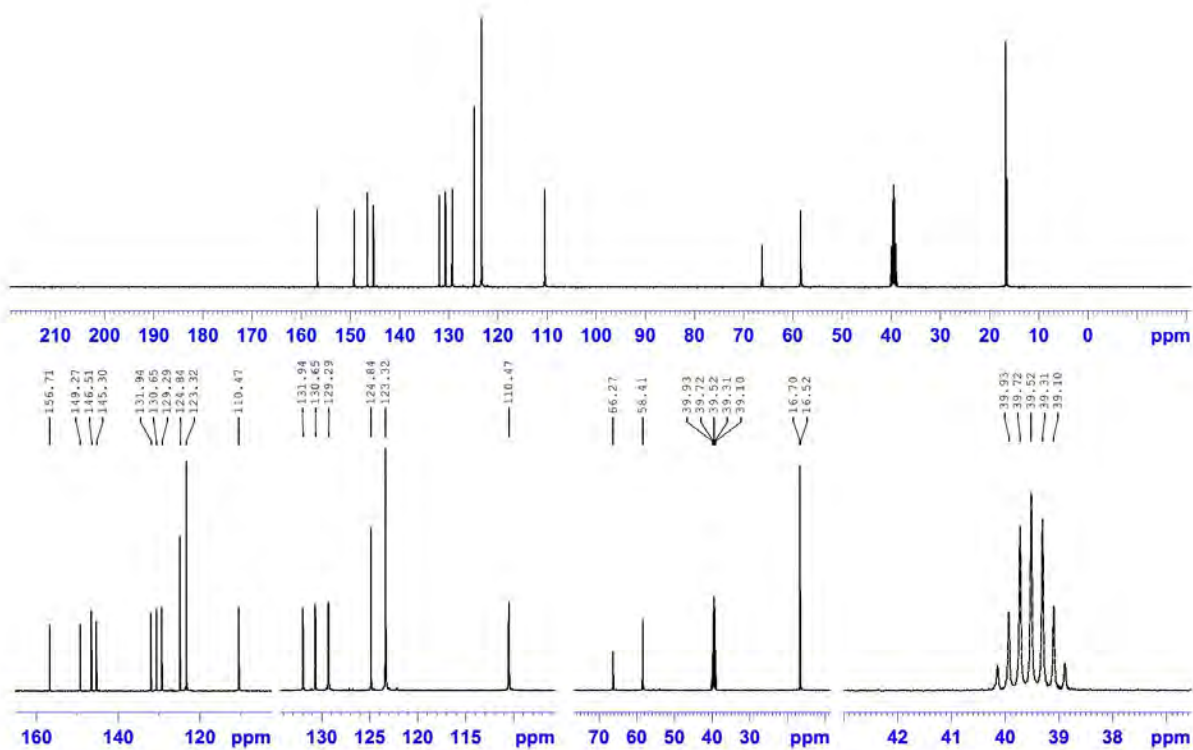


Hünlich's base (0.56 g, 2.0 mmol, 1.0 eq.) was dissolved in an aqueous solution of H_2SO_4 (6.5% v/v, 30 mL), and cooled down to -5°C . A NaNO_2 solution (0.30 g, 4.4 mmol, 2.2 eq. in 5 mL of water) was dropped into the reaction flask and stirred for 35 min. The resulting yellowish diazonium solution was poured into a solution of 2,6-dimethylphenol (0.51 g, 4.2 mmol, 2.1 eq.) and Na_2CO_3 (2.0 g, 19 mmol) in 100 mL of cold water. Then, two more grams of Na_2CO_3 was added to the mixture and stirred for 8 hours. Afterwards, an orange precipitate was filtered off, washed with water and desiccated to obtain the product (0.88 g, 1.6 mmol, 81%). Chemical Formula: $\text{C}_{33}\text{H}_{34}\text{N}_6\text{O}_2$, Molecular Weight: 546.68, R_f : 0.33 (EtOAc/ n-Hexane = 40% v/v) silica gel. $^1\text{H-NMR}$ (400 MHz, $\text{DMSO-}d_6$) δ [ppm]: 9.07 (br, 2H, OH), 7.53 (s, 4H, 4 \times CH), 7.26 (s, 2H, H-4, H-10), 6.92 (s, 2H, H-1, H-7), 4.61-4.65 (d, J = 17.2 Hz, 2H, H-6b, H-12b), 4.25 (s, 2H, -N-CH₂-N-), 4.12-4.16 (d, J = 17.3 Hz, 2H, H-6a, H-12a), 2.47 (s, 6H, 2 \times -CH₃), 2.26 (s, 12H, 4 \times -CH₃). $^{13}\text{C-NMR}$ (100 MHz, $\text{DMSO-}d_6$) δ [ppm]: 156.7, 149.2, 146.5, 145.3, 131.9, 130.6, 129.2, 124.8, 123.3, 110.4, 66.2, 58.4, 16.7, 16.5. IR: (Neat) ν_{max} [cm^{-1}] = 3563, 2946, 2914, 2843, 1592, 1480, 1417, 1298, 1182, 1111, 913, 728. MS (Acetonitrile 90%, EtOAc 5%, H_2O 5%): (ESI positive) calc. for $[\text{C}_{33}\text{H}_{35}\text{N}_6\text{O}_2]^+$: $[\text{M}+\text{H}]^+$ 547.2, found 547.4. (ESI negative) calc. for $[\text{C}_{33}\text{H}_{33}\text{N}_6\text{O}_2]^-$: $[\text{M}-\text{H}]^-$ 545.2, found 545.5. UV-Vis: (EtOAc) λ (lg ϵ) = 364nm (4.598). Anal. calcd: C, 72.50; H, 6.27; N, 15.37. found: C, 72.63; H, 6.08; N, 14.98.





Compound 1, ¹H-NMR (400 MHz, DMSO-*d*₆)



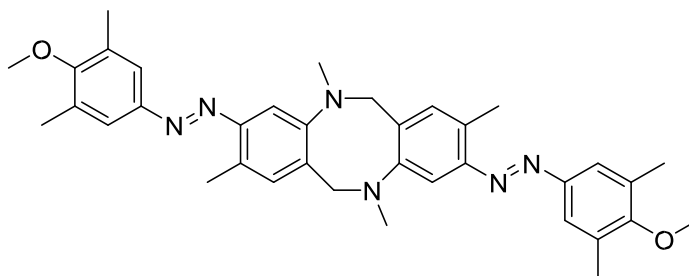
Compound 1, ¹³C-NMR (100 MHz, DMSO-*d*₆)

General Procedure for Synthesis of compounds 2-16:

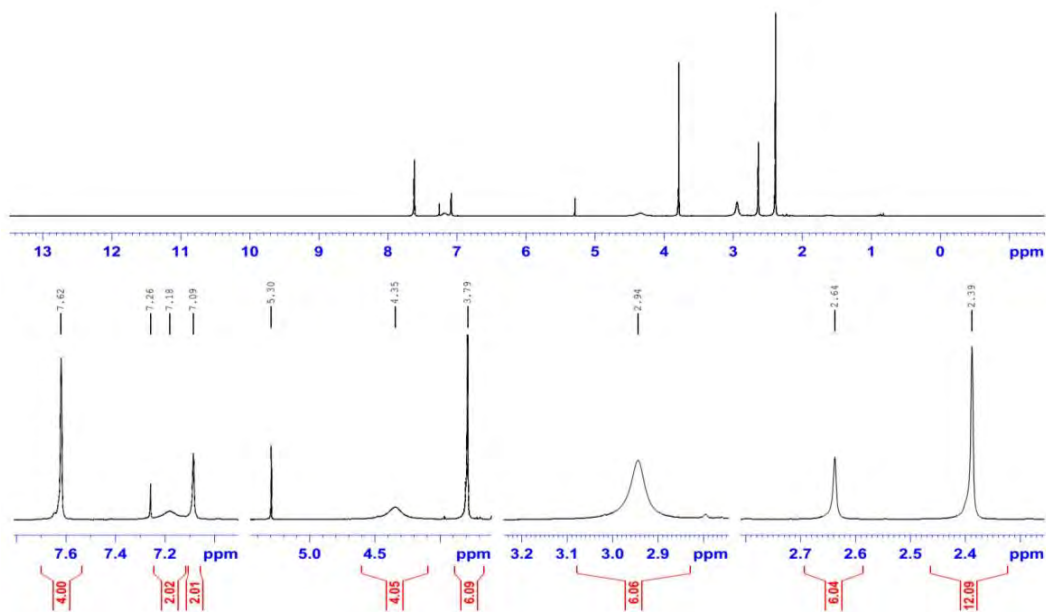
Appropriate amounts of **1**, KI and K₂CO₃ were mixed in 10 ml of acetone, then an alkyl or aryl halide was injected into the mixture and refluxed in darkness. The reaction was monitored by TLC until showed a single spot at the conclusion (Indicated in Scheme 2). Afterwards, 50 ml of water was added and the crude was extracted with EtOAc (3×30ml). The collected organic layers were combined and dried over MgSO₄ and filtered off. After removing the solvent, the residue was chromatographed to obtain the orange sticky solids **2-16** (Scheme 2).

2. Synthesis and Characterization of (2)

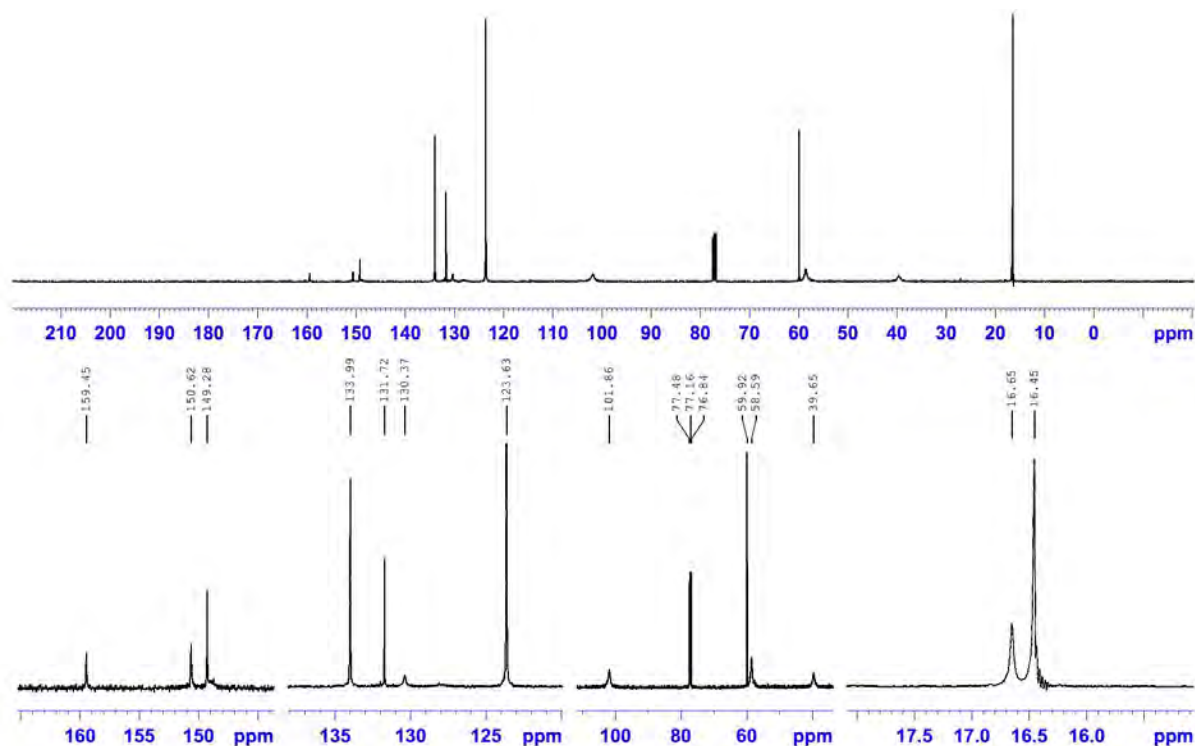
3,9-bis((E)-(4-methoxy-3,5-dimethylphenyl)diazenyl)-2,5,8,11-tetramethyl-5,6,11,12-tetrahydrodibenzo[b,f][1,5]diazocine



Starting with **1** (0.55 g, 1.0 mmol, 1.0 eq.), K₂CO₃ (0.69 g, 5.0 mmol) and methyl iodide (1.0 g, 7.0 mmol, 2.3 eq.) to obtain **2** (0.38 g, 0.64 mmol, 64%) Chemical Formula: C₃₆H₄₂N₆O₂, Molecular Weight: 590.7. R_f: 0.9 (MeOH/ DCM = 4% v/v) silica gel. ¹H-NMR (400 MHz, CDCl₃) δ [ppm]: 7.62 (s, 4H, H), 7.18 (b, 2H, H-4,10), 7.09 (s, 2H, H1,7), 4.34 (b, 4H, H-6,12), 3.78 (s, 6H, OCH₃), 2.94 (b, 6H, NCH₃), 2.64 (s, 6H, CH₃-2,8), 2.39 (s, 12H, CH₃). ¹³C-NMR (100 MHz, CDCl₃) δ [ppm]: 159.4, 150.6, 149.2, 133.9, 131.7, 130.3, 123.6, 101.8, 59.9, 58.5, 39.6, 16.6, 16.4. IR: (Neat) ν_{max} [cm⁻¹] = 2921, 2856, 1606, 1476, 1411, 1337, 1286, 1220, 1112, 1004, 885, 662. MS (EtOH 50%, 1Propanol 50%): (ESI positive) calc. for [C₃₆H₄₃N₆O₂]⁺: [M+H]⁺ 591.34, found 591.4. UV: (EtOAc) λ (lgε) = 342 nm (4.625). Anal. calcd: C, 73.19; H, 7.17; N, 14.23. found: C, 73.44; H, 7.33; N, 14.15.



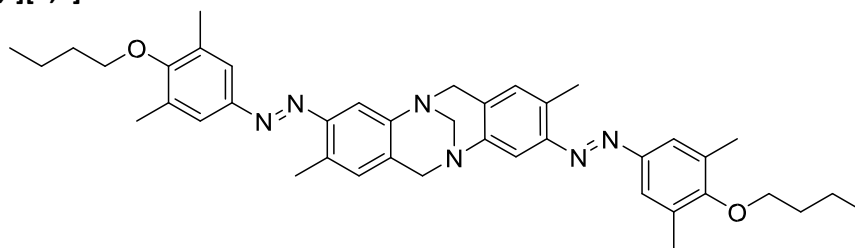
Compound **2**, ¹H-NMR (400 MHz, CDCl₃)



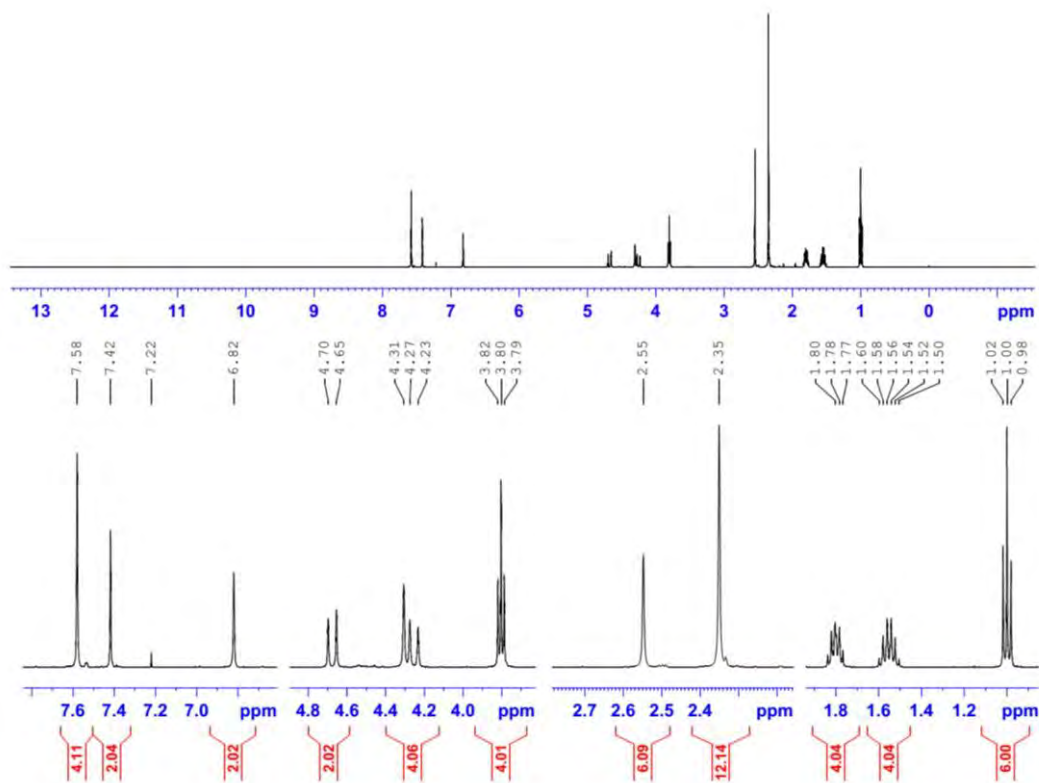
Compound 2, ^{13}C -NMR (100 MHz, CDCl_3)

3. Synthesis and Characterization of (\pm)

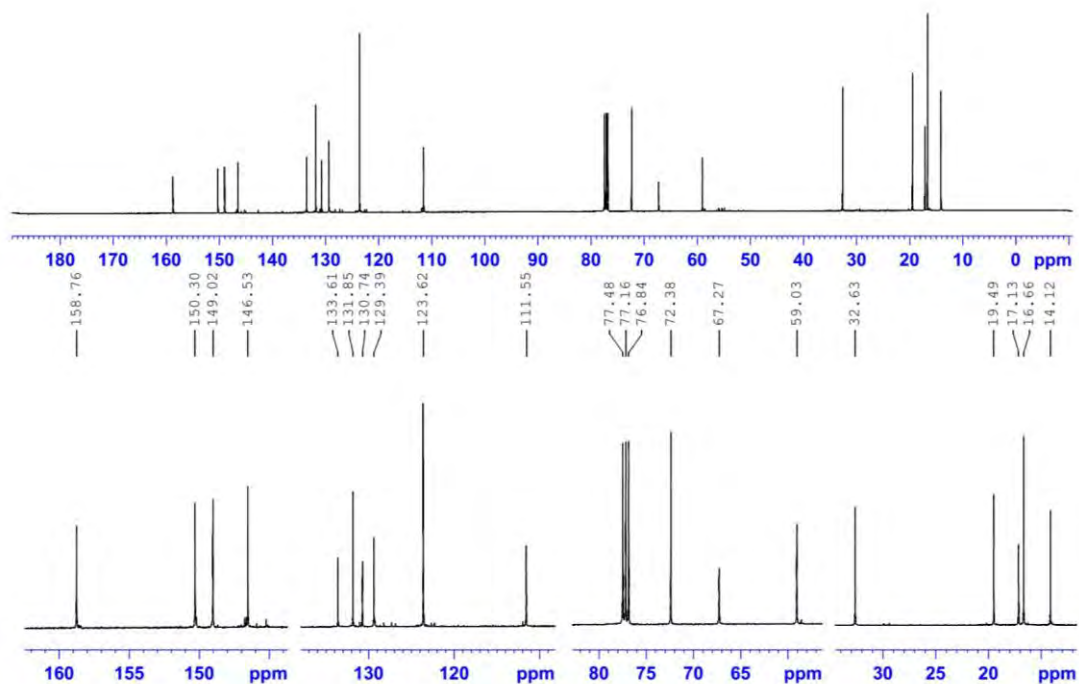
3,9-bis((E)-(4-butoxy-3,5-dimethylphenyl)diazenyl)-2,8-dimethyl-6H,12H-5,11-methanodibenzo[b,f][1,5]diazocine



Starting with **1** (2.2 g, 4.0 mmol, 1.0 eq.), K_2CO_3 (1.4 g, 10 mmol), some extra acetone (20 ml) and 1-iodobutane (1.7 g, 9.0 mmol, 2.3 eq.) to obtain **3** (2.0 g, 3.0 mmol, 74%) Chemical Formula: $\text{C}_{41}\text{H}_{50}\text{N}_6\text{O}_2$, Molecular Weight: 658.89, R_f : 0.77 (EtOAc/ n-hexane = 40% v/v) silica gel. ^1H -NMR (400 MHz, CDCl_3) δ [ppm] : 7.62 (s, 4H, CH) , 7.45 (s, 2H, H-4, H-10) , 6.86 (s, 2H, H-1, H-7) , 4.69-4.74 (d, J = 17.1 Hz, 2H, H-6b, H-12b) , 4.35 (s, 2H, -N-CH₂-N-) , 4.274.31 (d, J = 17.2 Hz, 2H, H-6a, H-12a) , 3.83-3.86 (t, J = 8.1 Hz, 4H, CH₂) , 2.59 (s, 6H, CH₃) , 2.39 (s, 12H, CH₃) , 1.811.84 (m, 4H, CH₂) , 1.54-1.64 (m, 4H, CH₂) , 1.02-1.06 (t, J = 8.1 Hz, 6H, CH₃). ^{13}C -NMR (100 MHz, CDCl_3) δ [ppm]: 158.7, 150.3, 149.0, 146.5, 133.6, 131.8, 130.7, 129.3, 123.6, 111.5, 72.3, 67.2, 59.0, 32.6, 19.4, 17.1, 16.6, 14.1. IR: (Neat) ν_{max} [cm^{-1}] = 2932, 2826, 1584, 1472, 1379, 1307, 1205, 1112, 1083, 997, 918, 899, 758, 610. MS (ACN 90%, EtOAc 5%, H₂O 5%): (ESI positive) calc. for $[\text{C}_{41}\text{H}_{51}\text{N}_6\text{O}_2]^+$: $[\text{M}+\text{H}]^+$ 659.40, found 659.2. UV-Vis: (EtOAc) λ (lg ϵ) = 349 nm (4.587). Anal. calcd: C, 74.74; H, 7.65; N, 12.76. found: C, 74.37; H, 7.71; N, 12.59.



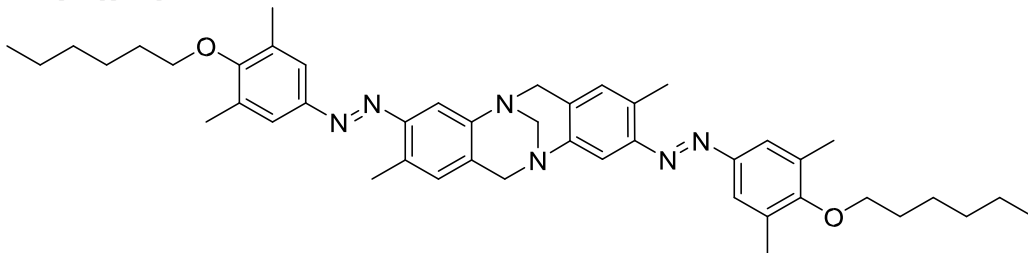
Compound 3, ¹H-NMR (400 MHz, CDCl₃)



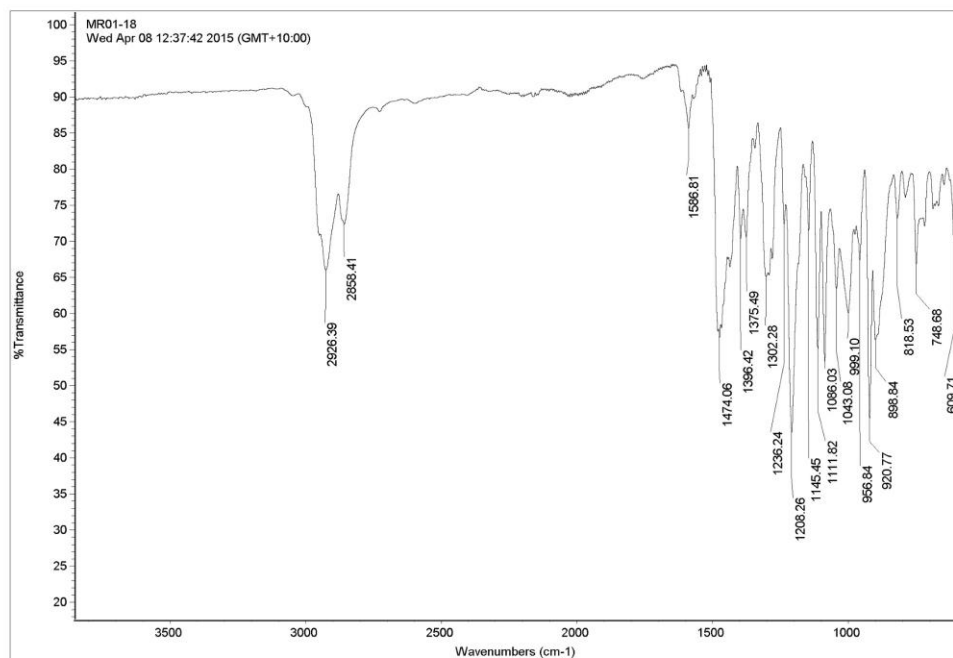
Compound 3, ¹³C-NMR (100 MHz, CDCl₃)

4. Synthesis and Characterization of (\pm 4)

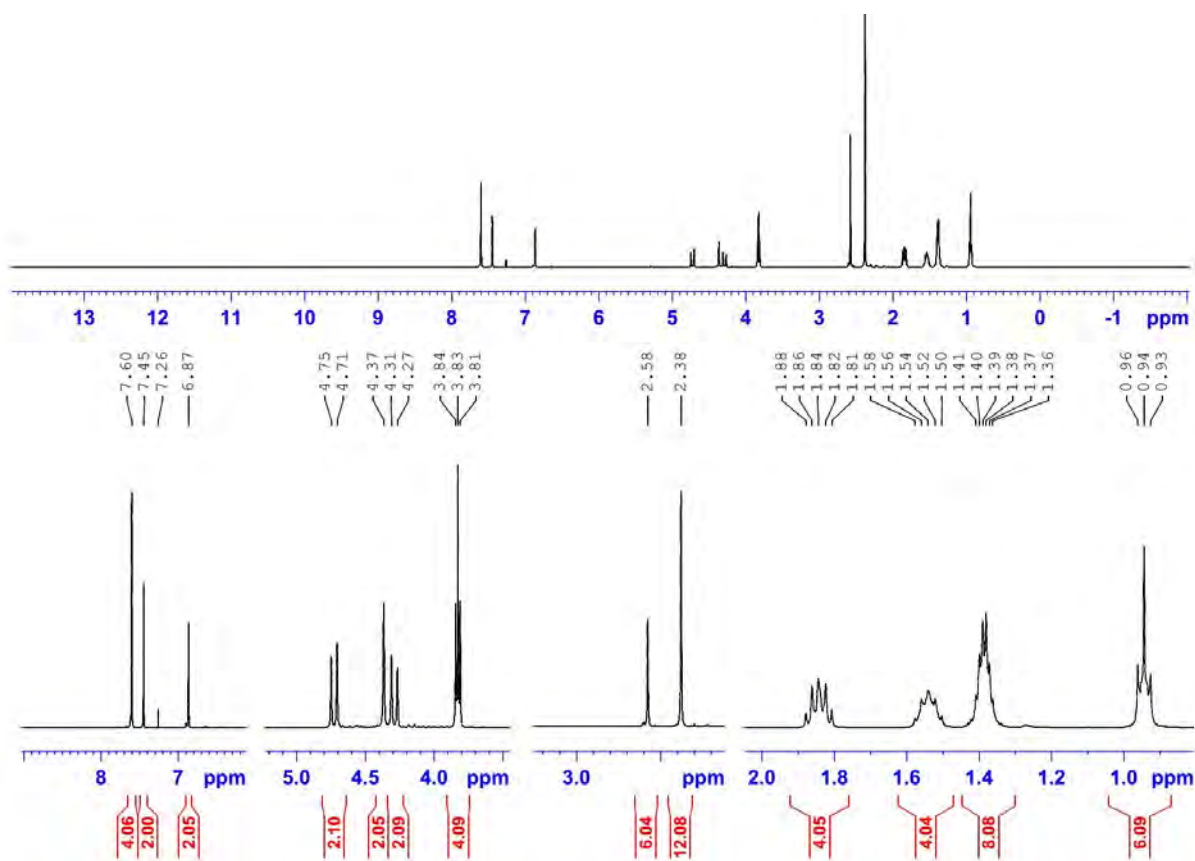
3,9-bis((E)-(4-(hexyloxy)-3,5-dimethylphenyl)diazenyl)-2,8-dimethyl-6H,12H-5,11-methanodibenzo[b,f][1,5]diazocine



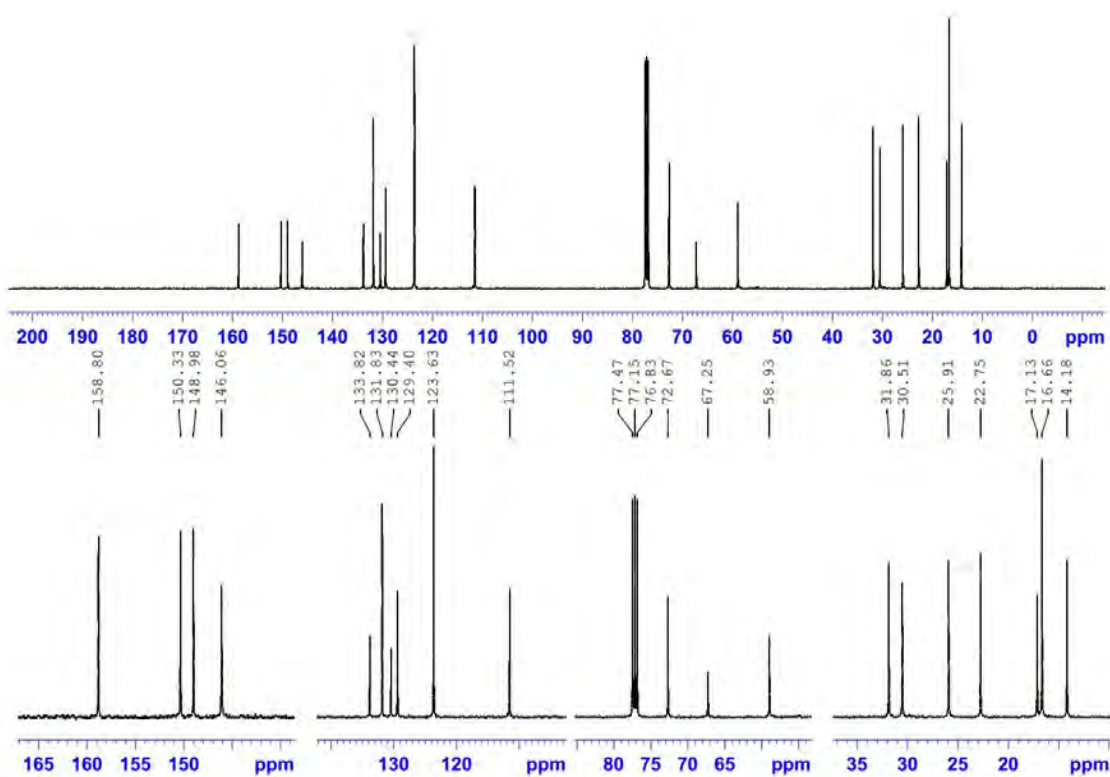
Starting with **1** (0.55 g, 1.0 mmol, 1.0 eq.), K_2CO_3 (0.69 g, 5.0 mmol), 1-bromohexane (0.50 g, 3.0 mmol, 1.5 eq.) and a catalytic amount of KI (0.01 g, 0.06 mmol) to obtain **4** (0.63 g, 0.88 mmol, 88%) Chemical Formula: $C_{45}H_{58}N_6O_2$, Molecular Weight: 715.00, R_f : 0.63 (EtOAc/ n-hexane = 30% v/v) silica gel. 1H -NMR (400 MHz, $CDCl_3$) δ [ppm]: 7.60 (s, 4H, CH), 7.45 (s, 2H, H-4, H-10), 6.82 (s, 2H, H-1, H-7), 4.71-4.75 (d, J = 16.8 Hz, 2H, H-6b, H12b), 4.37 (s, 2H, -N-CH₂-N-), 4.27-4.31 (d, J = 16.7 Hz, 2H, H-6a, H-12a), 3.81-3.84 (t, J = 6.6 Hz, 4H, CH₂), 2.58 (s, 6H, CH₃), 2.38 (s, 12H, CH₃), 1.81-1.88 (m, 4H, CH₂), 1.50-1.58 (m, 4H, CH₂), 1.36-1.41 (m, 8H, CH₂), 0.93-0.96 (t, J = 7.1 Hz, 6H, CH₃). ^{13}C -NMR (100 MHz, $CDCl_3$) δ [ppm]: 158.8, 150.3, 148.9, 146.0, 133.8, 131.8, 130.4, 129.4, 123.6, 111.5, 72.6, 67.2, 58.9, 31.8, 30.5, 25.9, 22.7, 17.1, 16.6, 14.1. IR: (Neat) ν_{max} [cm^{-1}] = 2926, 2858, 1586, 1474, 1375, 1302, 1208, 1111, 1086, 999, 920, 898, 748, 609. MS (ACN 90%, EtOAc 5%, H₂O 5%): (ESI positive) calc. for $[C_{45}H_{58}N_6O_2]^+$: $[M+H]^+$ 715.4, found 715.7. UV-Vis: (EtOAc) λ (lg ϵ) = 349 nm (4.572). Anal. calcd: C, 75.59; H, 8.18; N, 11.75. found: C, 75.83; H, 7.94; N, 11.60



Compound 4, Infrared Transmittance (neat)



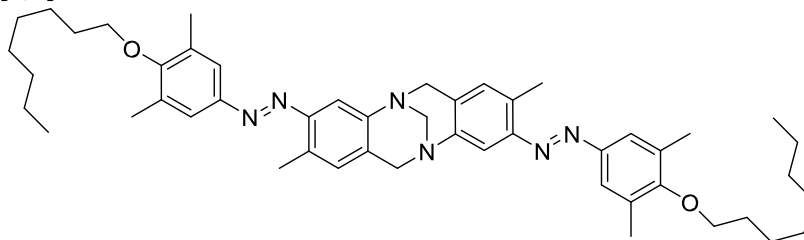
Compound 4, ¹H-NMR (600 MHz, CDCl₃)



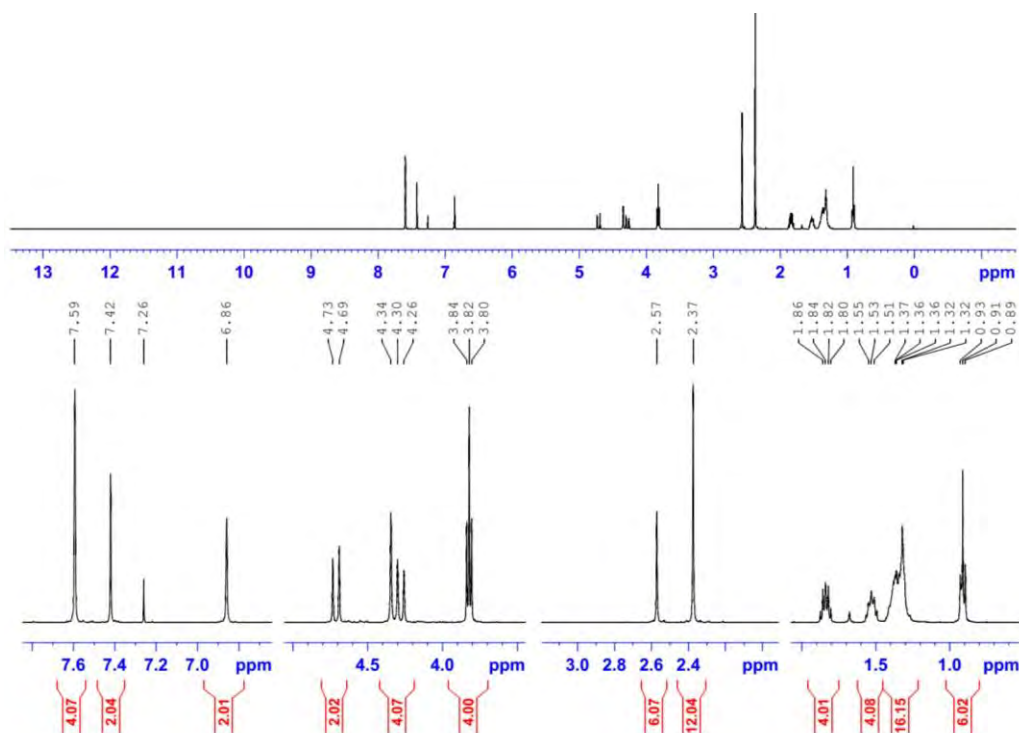
Compound 4, ¹³C-NMR (150 MHz, CDCl₃)

5. Synthesis and Characterization of (\pm 5)

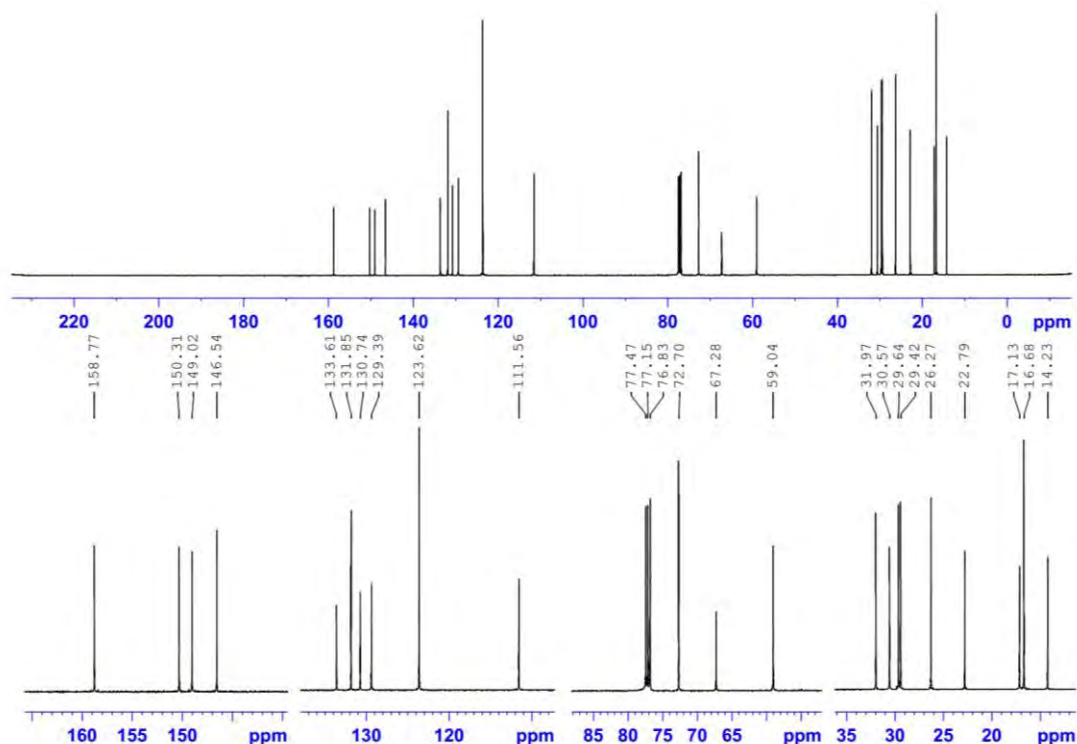
3,9-bis((E)-(3,5-dimethyl-4-(octyloxy)phenyl)diazenyl)-2,8-dimethyl-6H,12H-5,11-methanodibenzo[b,f][1,5]diazocine



Starting with **1** (0.55 g, 1.0 mmol, 1.0 eq.), K_2CO_3 (0.69 g, 5.0 mmol), 1-bromooctane (0.45 g, 2.3 mmol, 1.2 eq.) and a catalytic amount of KI (0.01 g, 0.06 mmol) to obtain **5** (0.66 g, 0.86 mmol, 86%) Chemical Formula: $C_{49}H_{66}N_6O_2$, Molecular Weight: 771.11, R_f : 0.43 (EtOAc/ n-hexane = 20% v/v) silica gel. 1H -NMR (400 MHz, $CDCl_3$) δ [ppm] : 7.59 (s, 2H, H-4, H-10) , 7.42 (s, 4H, CH) , 6.86 (s, 2H, H-1, H-7) , 4.69-4.73 (d, J = 17.0 Hz, 2H, H-6b, H-12b) , 4.34 (s, 2H, -N-CH₂-N-), 4.26-4.30 (d, J = 16.9 Hz, 2H, H-6a, H-12a) , 3.80-3.84 (t, J = 8.1 Hz, 4H, CH₂) , 2.57 (s, 6H, CH₃) , 2.37 (s, 12H, CH₃) , 1.80-1.86 (m, 4H, CH₂) , 1.51-1.55 (m, 4H, CH₂) , 1.32-1.37 (m, 16H, CH₂), 0.89-0.93 (t, J = 8.0 Hz, 6H, CH₃). ^{13}C -NMR (100 MHz, $CDCl_3$) δ [ppm]: 158.7, 150.3, 149.0, 146.5, 133.6, 131.8, 130.7, 129.3, 123.6, 111.5, 72.7, 67.2, 59.0, 31.9, 30.5, 29.6, 29.4, 26.2, 22.7, 17.1, 16.7, 14.2. IR: (Neat) ν_{max} [cm^{-1}] = 2923, 2859, 1585, 1468, 1371, 1308, 1212, 1113, 1087, 997, 921, 899 and 613. MS (ACN 90%, EtOAc 5%, H₂O 5%): (ESI positive) calc. for $[C_{49}H_{67}N_6O_2]^+$: $[M+H]^+$ 771.52, found 771.0. UV-Vis: (EtOAc) λ (lge) = 349 nm (4.558). Anal. calcd: C, 76.32; H, 8.63; N, 10.90. found: C, 76.61; H, 8.39; N, 10.77.



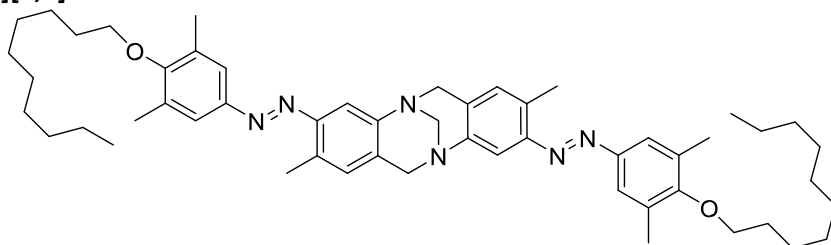
Compound **5**, 1H -NMR (400 MHz, $CDCl_3$)



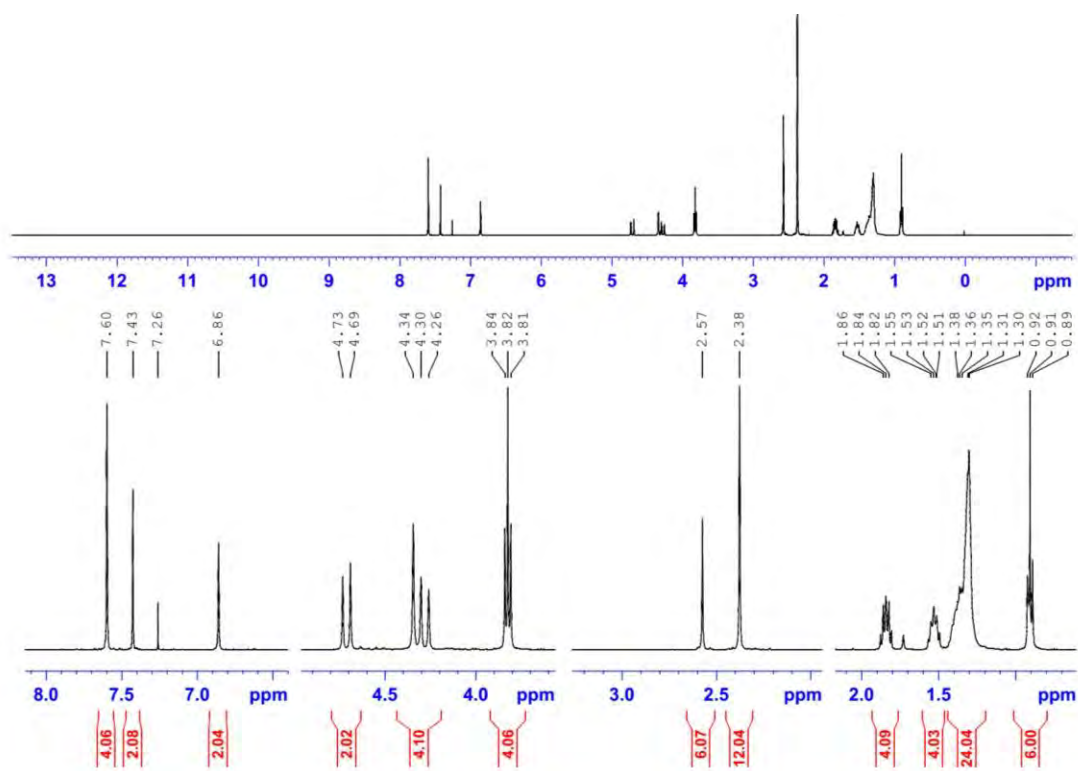
Compound 5, ^{13}C -NMR (100 MHz, CDCl_3)

6. Synthesis and Characterization of (\pm 6)

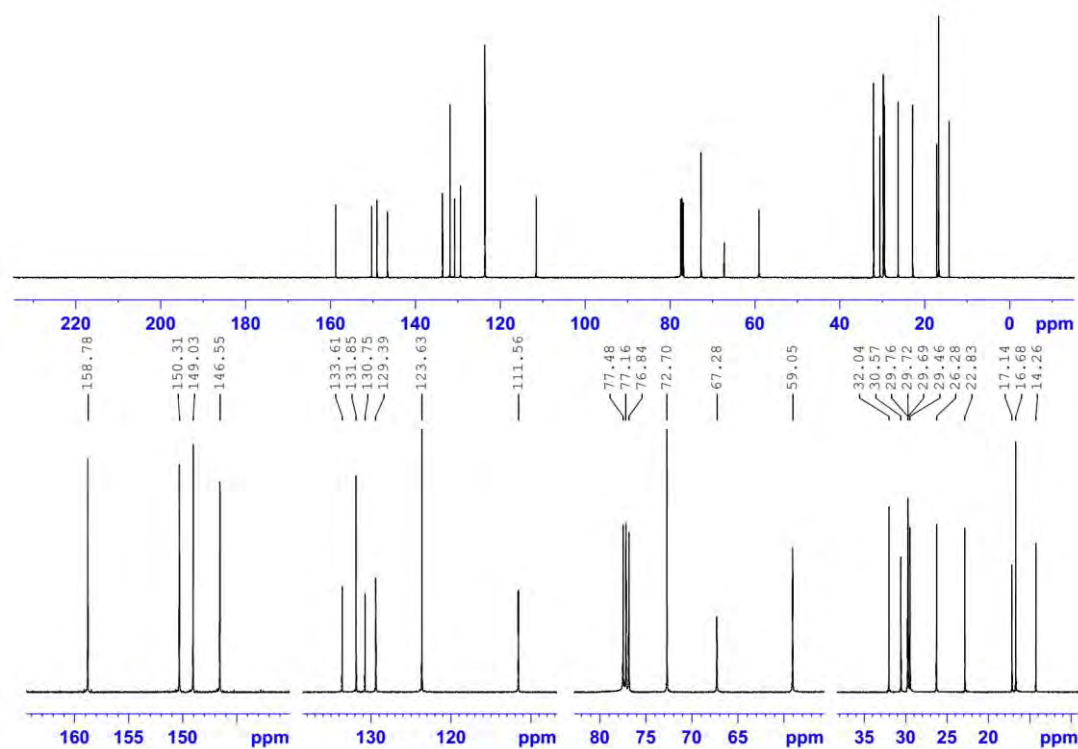
3,9-bis((E)-(4-(decyloxy)-3,5-dimethylphenyl)diazenyl)-2,8-dimethyl-6H,12H-5,11-methanodibenzo[b,f][1,5]diazocine



Starting with **1** (0.55 g, 1.0 mmol, 1.0 eq.), K_2CO_3 (0.69 g, 5.0 mmol), a catalytic amount of KI (0.01 g, 0.06 mmol) and 1-bromodecane (0.51 g, 2.3 mmol, 1.2 eq.) to obtain **6** (0.68 g, 0.82 mmol, 82%) Chemical Formula: $\text{C}_{53}\text{H}_{74}\text{N}_6\text{O}_2$, Molecular Weight: 827.22, R_f : 0.45 (EtOAc/ n-hexane = 20% v/v) silica gel. ^1H -NMR (400 MHz, CDCl_3) δ [ppm] : 7.60 (s, 2H, H-4, H-10) , 7.43 (s, 4H, CH) , 6.86 (s, 2H, H-1, H-7) , 4.69-4.73 (d, J = 17.0 Hz, 2H, H-6b, H12b) , 4.34 (s, 2H, -N-CH₂-N-), 4.26-4.30 (d, J = 17.1 Hz, 2H, H-6a, H-12a) , 3.81-3.84 (t, J = 7.3 Hz, 4H, CH₂) , 2.57 (s, 6H, CH₃) , 2.38 (s, 12H, CH₃) , 1.82-1.86 (m, 4H, CH₂) , 1.51-1.55 (m, 4H, CH₂) , 1.30-1.38 (m, 24H, CH₂) , 0.890.92 (t, J = 8.1 Hz, 6H, CH₃). ^{13}C -NMR (100 MHz, CDCl_3) δ [ppm]: 158.8, 150.3, 149.0, 146.5, 133.6, 131.8, 130.7, 129.4, 123.6, 111.6, 72.7, 67.3, 59.0, 32.0, 30.6, 29.8, 29.7, 29.6, 29.4, 26.2, 22.8, 17.1, 16.6, 14.2. IR: (Neat) ν_{max} [cm^{-1}] = 2920, 2853, 2358, 1586, 1478, 1304, 1207, 1114, 1083, 920, 897, 719 and 612. MS (ACN 90%, EtOAc 5%, H₂O 5%): (ESI positive) calc. for $[\text{C}_{53}\text{H}_{75}\text{N}_6\text{O}_2]^+$: $[\text{M}+\text{H}]^+$ 827.59, found 828.1. UV-Vis: (EtOAc) λ (lge) = 349 nm (4.570). Anal. calcd: C, 76.95; H, 9.02; N, 10.16. found: C, 76.85; H, 9.31; N, 10.51.



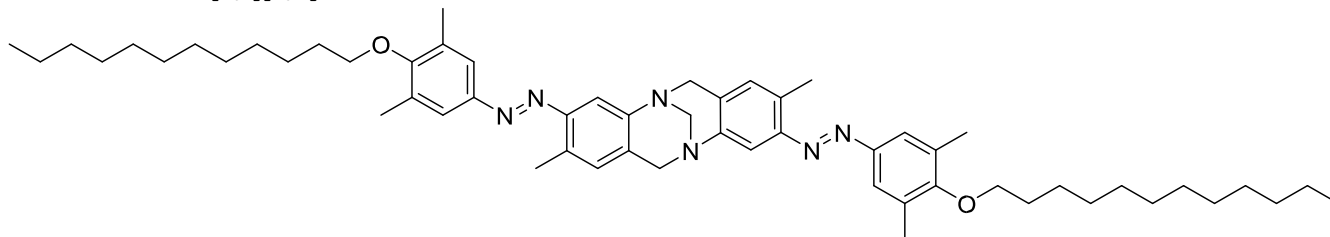
Compound 6, ¹H-NMR (400 MHz, CDCl₃)



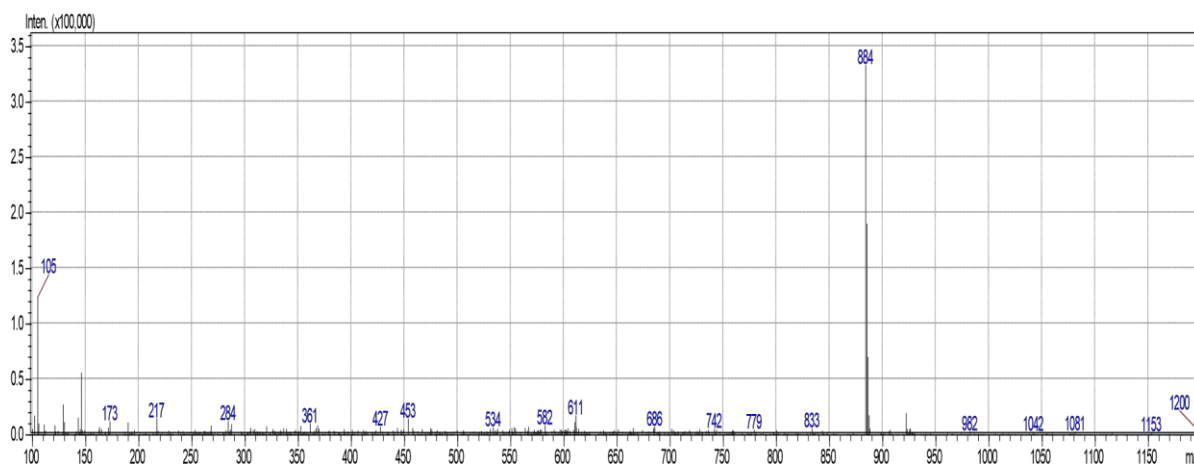
Compound 6, ¹³C-NMR (100 MHz, CDCl₃)

7. Synthesis and Characterization of (\pm)7

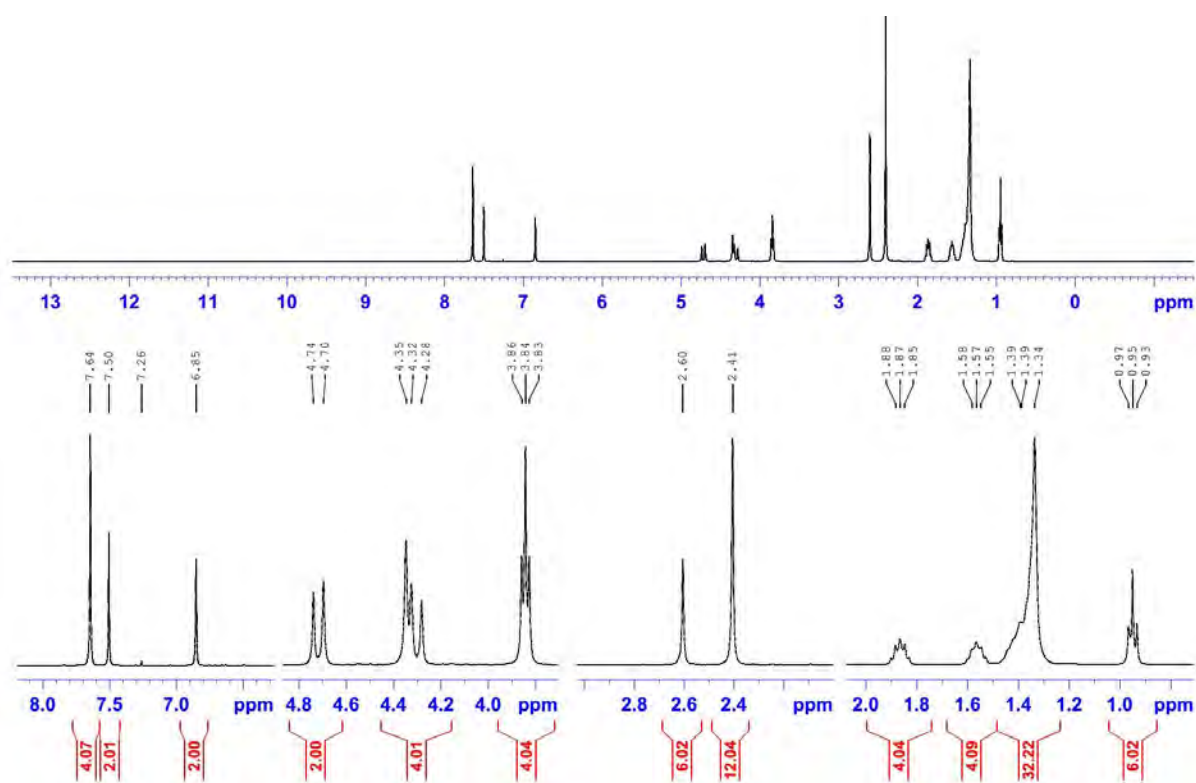
3,9-bis((E)-(4-(dodecyloxy)-3,5-dimethylphenyl)diazenyl)-2,8-dimethyl-6H,12H-5,11-methanodibenzo[b,f][1,5]diazocine



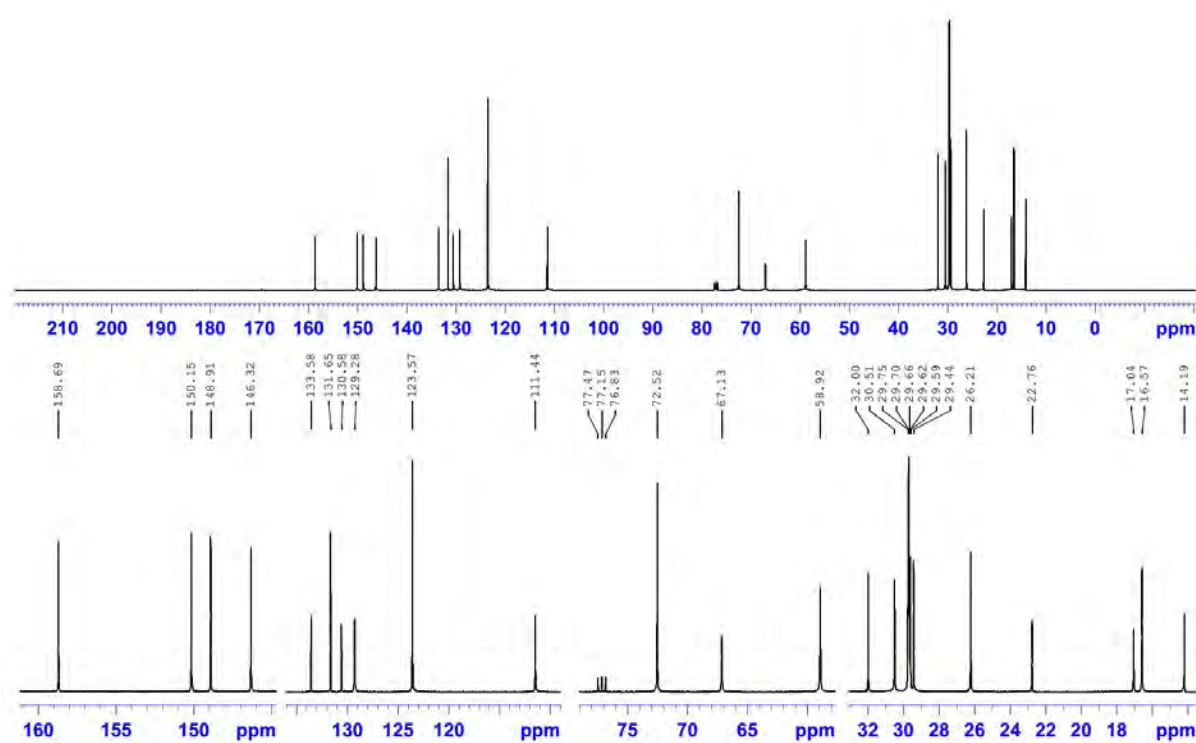
Starting with **1** (0.55 g, 1.0 mmol, 1.0 eq.), K_2CO_3 (0.69 g, 5.0 mmol), a catalytic amount of KI (0.01 g, 0.06 mmol) and 1-bromododecane (0.75 g, 3.0 mmol, 1.5 eq.) to obtain **7** (0.73 g, 0.82 mmol, 82%) Chemical Formula: $C_{57}H_{82}N_6O_2$, Molecular Weight: 883.32. R_f : 0.44 (ethyl acetate/ n-hexane = 20% v/v) silica gel. 1H -NMR (400 MHz, $CDCl_3$) δ [ppm] : 7.64 (s, 4H, CH) , 7.50 (s, 2H, H-4, H-10) , 6.85 (s, 2H, H-1, H-7) , 4.70-4.74 (d, J = 17.0 Hz, 2H, H6b, H-12b) , 4.35 (s, 2H, -N-CH₂-N-), 4.28-4.32 (d, J = 17.3 Hz, 2H, H-6a, H-12a) , 3.83-3.86 (t, J = 7.2 Hz, 4H, CH₂) , 2.60 (s, 6H, CH₃) , 2.40 (s, 12H, CH₃) , 1.85-1.88 (m, 4H, CH₂) , 1.55-1.58 (m, 4H, CH₂) , 1.27-1.47 (m, 32H, CH₂) , 0.93-0.97 (t, J = 8.1 Hz, 6H, CH₃). ^{13}C -NMR (100 MHz, $CDCl_3$) δ [ppm] : 158.6, 150.1, 148.9, 146.3, 133.5, 131.6, 130.5, 129.3, 123.5, 111.4, 72.5, 67.1, 58.9, 31.9, 30.5, 29.7, 29.7, 29.6, 29.6, 29.6, 29.4, 26.2, 22.7, 17.0, 16.5, 14.1. IR: (Neat) ν_{max} [cm^{-1}] = 2921, 2851, 2359, 1589, 1479, 1304, 1208, 1112, 1085, 921, 897, 749, 719, 610. MS (1-Propanol 50%, Ethanol 50%): (ESI positive) calc. for $[C_{57}H_{83}N_6O_2]^+$: $[M+H]^+$ 883.6, found 884.1. UV: (EtOAc) λ (lg ϵ) = 349nm (4.612). Anal. calcd: C, 77.51; H, 9.36; N, 9.51. found: C, 77.75; H, 9.55; N, 9.33.



Compound 7, Mass Spectra (ESI positive)



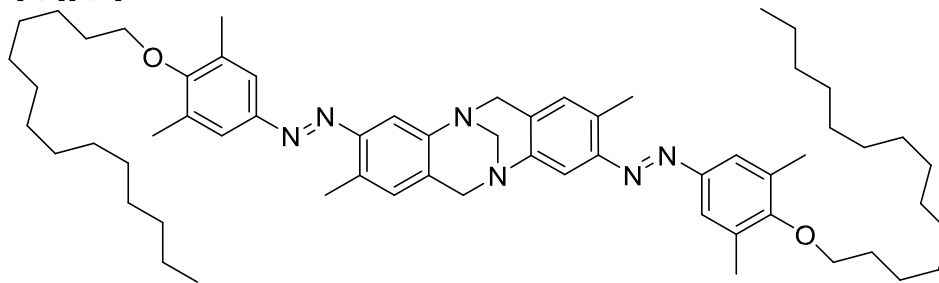
Compound 7, ¹H-NMR (400 MHz, CDCl₃)



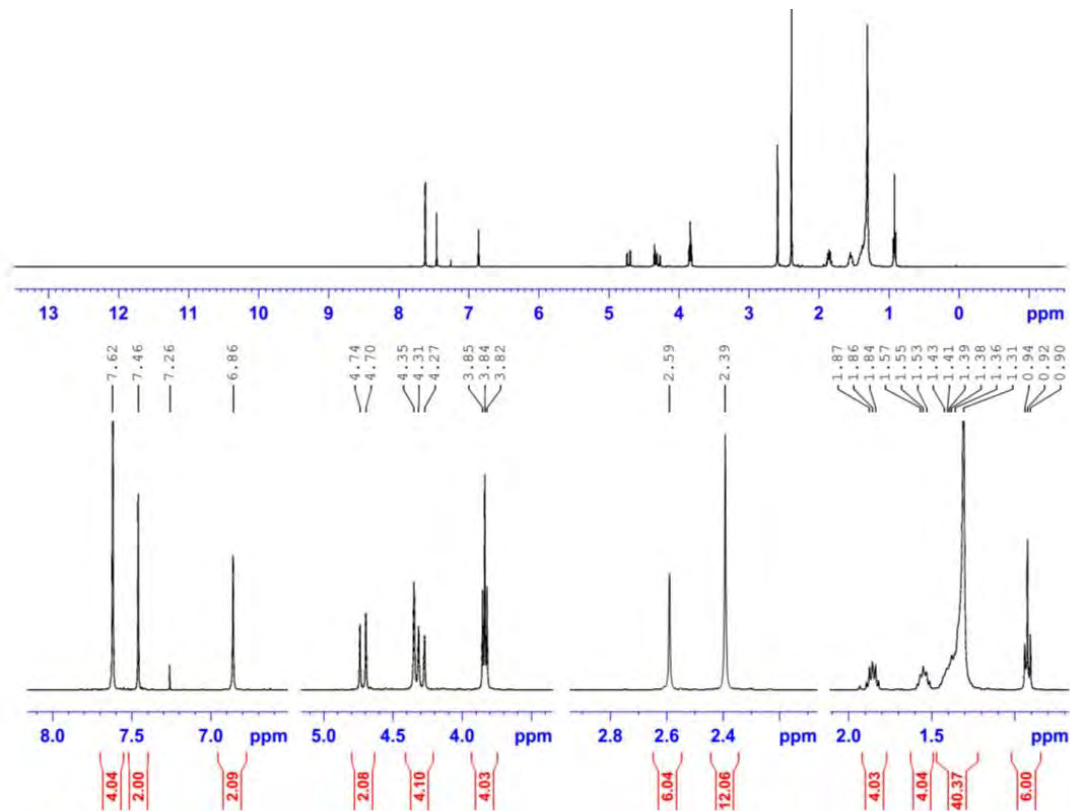
Compound 7, ¹³C-NMR (100 MHz, CDCl₃)

8. Synthesis and Characterization of (\pm 8)

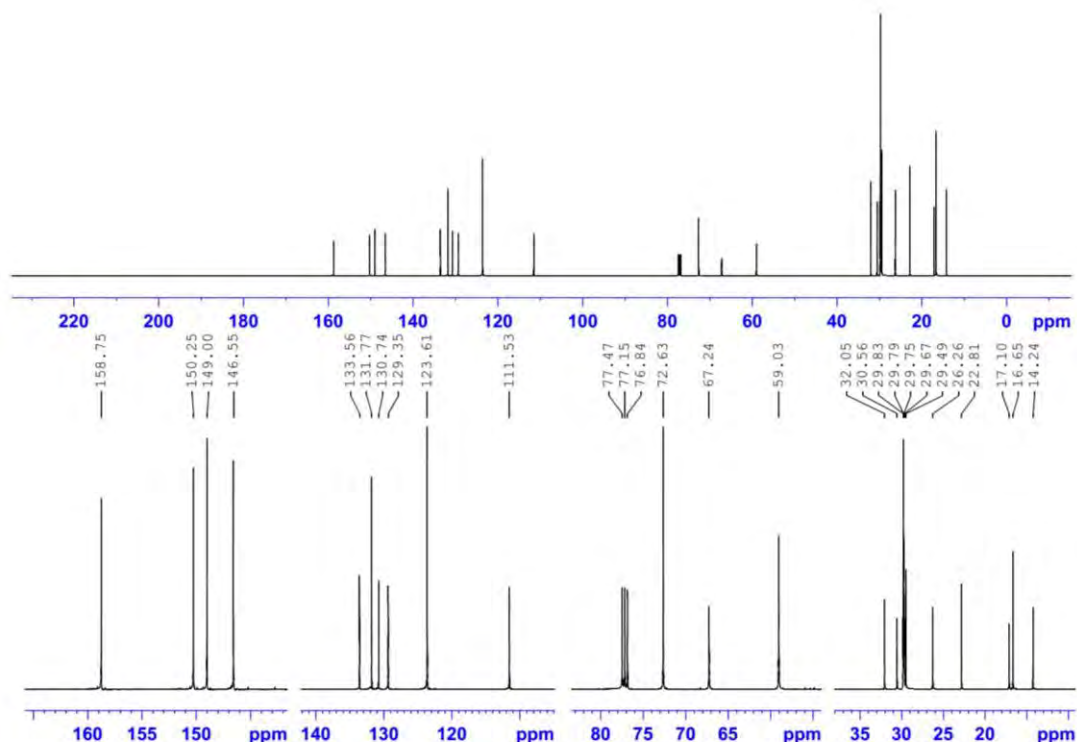
3,9-bis((E)-(3,5-dimethyl-4-(tetradecyloxy)phenyl)diazenyl)-2,8-dimethyl-6H,12H-5,11-methanodibenzo[b,f][1,5]diazocine



Starting with **1** (0.55 g, 1.0 mmol, 1.0 eq.), K_2CO_3 (0.69 g, 5.0 mmol), a catalytic amount of KI (0.01 g, 0.06 mmol) and 1-bromotetradecane (0.64 g, 2.3 mmol, 1.2 eq.) to obtain **8** (0.73 g, 0.78 mmol, 78%) Chemical Formula: $C_{61}H_{90}N_6O_2$, Molecular Weight: 939.43, R_f : 0.48 (EtOAc/ n-hexane = 20% v/v) silica gel. 1H -NMR (400 MHz, $CDCl_3$) δ [ppm] : 7.62 (s, 2H, H-4, H-10) , 7.46 (s, 4H, CH) , 6.86 (s, 2H, H-1, H-7) , 4.70-4.74 (d, J = 17.1 Hz, 2H, H-6b, H12b) , 4.35 (s, 2H, -N-CH₂-N-), 4.27-4.31 (d, J = 17.1 Hz, 2H, H-6a, H-12a) , 3.82-3.85 (t, J = 7.9 Hz, 4H, CH₂) , 2.59 (s, 6H, CH₃) , 2.39 (s, 12H, CH₃) , 1.84-1.87 (m, 4H, CH₂) , 1.53-1.57 (m, 4H, CH₂) , 1.31-1.43 (m, 40H, CH₂) , 0.900.94 (t, J = 8.1 Hz, 6H, CH₃). ^{13}C -NMR (100 MHz, $CDCl_3$) δ [ppm]: 158.7, 150.2, 149.0, 146.5, 133.5, 131.7, 130.7, 129.3, 123.6, 111.5, 72.6, 67.2, 59.0, 32.0, 30.5, 29.8, 29.8, 29.7, 29.6, 29.5, 26.2, 22.8, 17.1, 16.6, 14.2. IR: (Neat) ν_{max} [cm^{-1}] = 2923, 2850, 2357, 1588, 1478, 1305, 1207, 1110, 1083, 899, 749, 721 and 610. MS (Isopropyl alcohol 50%, EtOH 50%): (ESI positive) calc. for $[C_{61}H_{91}N_6O_2]^+$: $[M+H]^+$ 939.71, found 939.6. UV-Vis: (EtOAc) λ (Ige) = 349 nm (4.564). Anal. calcd: C, 77.99; H, 9.66; N, 8.95. found: C, 77.86; H, 9.45; N, 8.67.



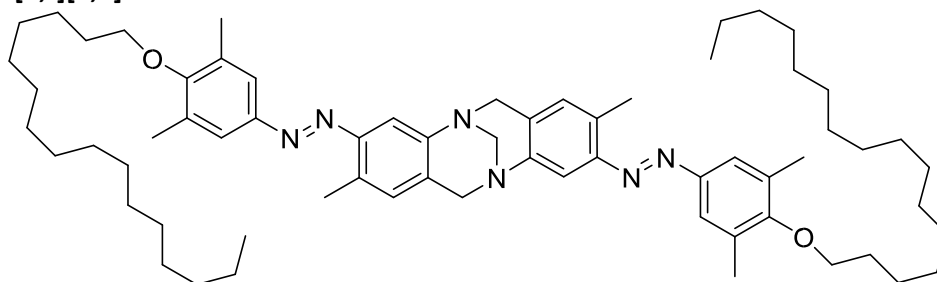
Compound **8**, 1H -NMR (400 MHz, $CDCl_3$)



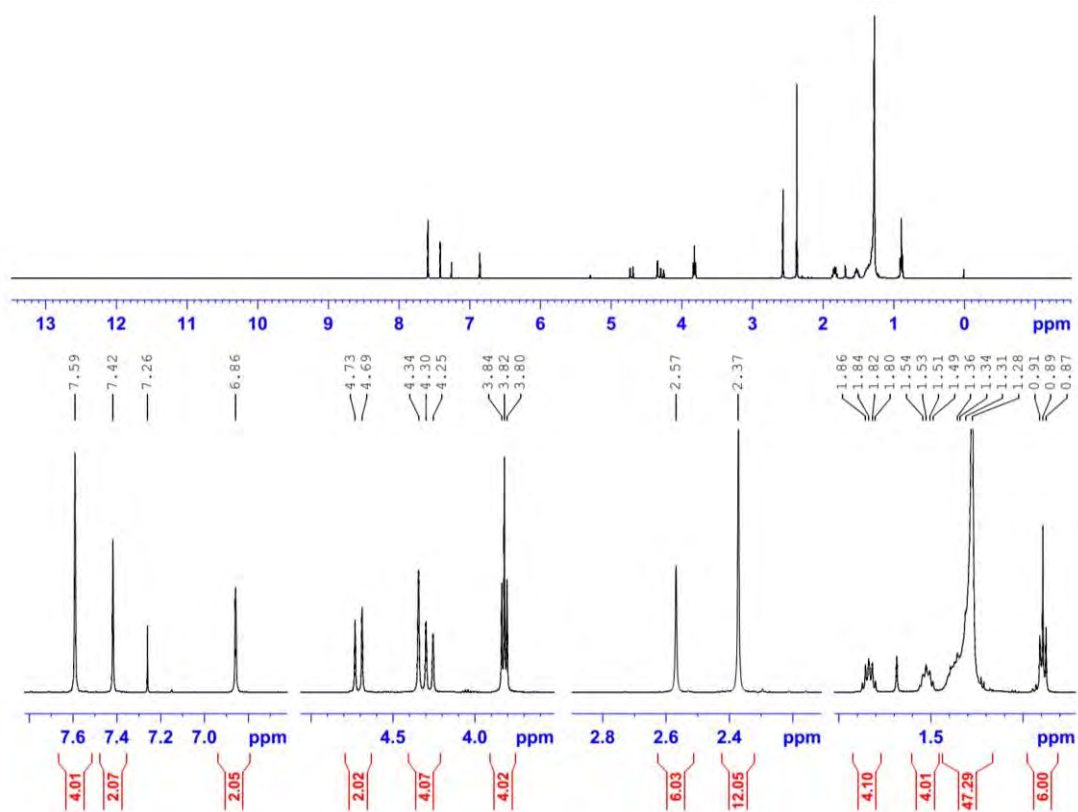
Compound 8, ^{13}C -NMR (100 MHz, CDCl_3)

9. Synthesis and Characterization of (\pm 9)

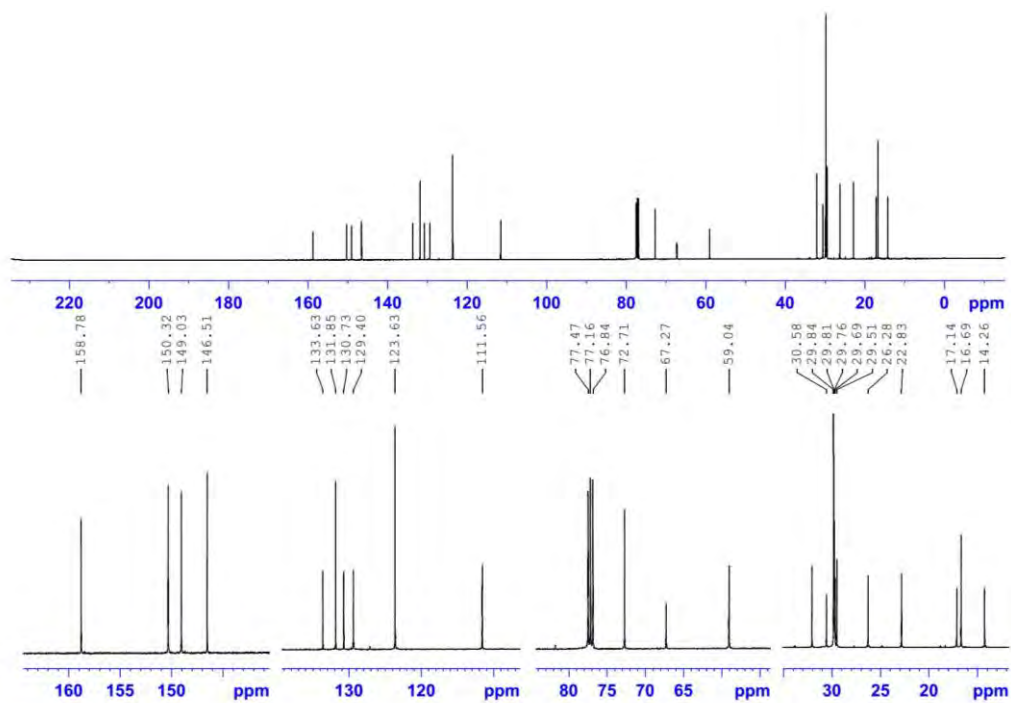
3,9-bis((E)-(4-(hexadecyloxy)-3,5-dimethylphenyl)diazenyl)-2,8-dimethyl-6H,12H-5,11-methanodibenzo[b,f][1,5]diazocine



Starting with **1** (0.55 g, 1.0 mmol, 1.0 eq.), K_2CO_3 (0.69 g, 5.0 mmol), a catalytic amount of KI (0.01 g, 0.06 mmol) and 1-bromohexadecane (0.64 g, 2.3 mmol, 1.2 eq.) to obtain **9** (0.83 g, 0.83 mmol, 83%) Chemical Formula: $\text{C}_{65}\text{H}_{98}\text{N}_6\text{O}_2$, Molecular Weight: 995.54, R_f : 0.48 (EtOAc/ n-hexane = 20% v/v) silica gel. ^1H -NMR (400 MHz, CDCl_3) δ [ppm] : 7.59 (s, 2H, H-4, H-10) , 7.41 (s, 4H, CH) , 6.85 (s, 2H, H-1, H-7) , 4.69-4.73 (d, J = 16.9 Hz, 2H, H-6b, H12b) , 4.34 (s, 2H, -N-CH₂-N-), 4.25-4.30 (d, J = 16.9 Hz, 2H, H-6a, H-12a) , 3.80-3.84 (t, J = 7.9 Hz, 4H, CH₂) , 2.57 (s, 6H, CH₃) , 2.37 (s, 12H, CH₃) , 1.80-1.86 (m, 4H, CH₂) , 1.49-1.54 (m, 4H, CH₂) , 1.28-1.42 (m, 48H, CH₂) , 0.870.91 (t, J = 7.8 Hz, 6H, CH₃). ^{13}C -NMR (100 MHz, CDCl_3) δ [ppm]: 158.7, 150.3, 149.0, 146.5, 133.6, 131.8, 130.7, 129.4, 123.6, 111.5, 72.7, 67.2, 59.0, 32.0, 30.6, 29.8, 29.8, 29.7, 29.7, 29.5, 26.3, 22.8, 17.1, 16.7, 14.2. IR: (Neat) ν_{max} [cm^{-1}] = 2921, 2851, 1588, 1466, 1375, 1304, 1207, 1083, 1046, 907, 773, 722, 688. MS (Isopropyl alcohol 50%, EtOH 50%): (ESI positive) calc. for $[\text{C}_{65}\text{H}_{99}\text{N}_6\text{O}_2]^+$: $[\text{M}+\text{H}]^+$ 995.78, found 996.3. UV-Vis: (EtOAc) λ (lge) = 349 nm (4.559). Anal. calcd: C, 78.42; H, 9.92; N, 8.44. found: C, 78.56; H, 9.88; N, 8.36.



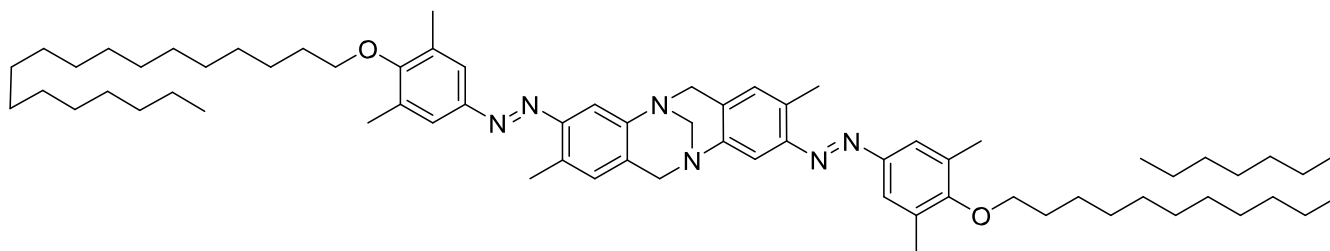
Compound 9, ¹H-NMR (400 MHz, CDCl₃)



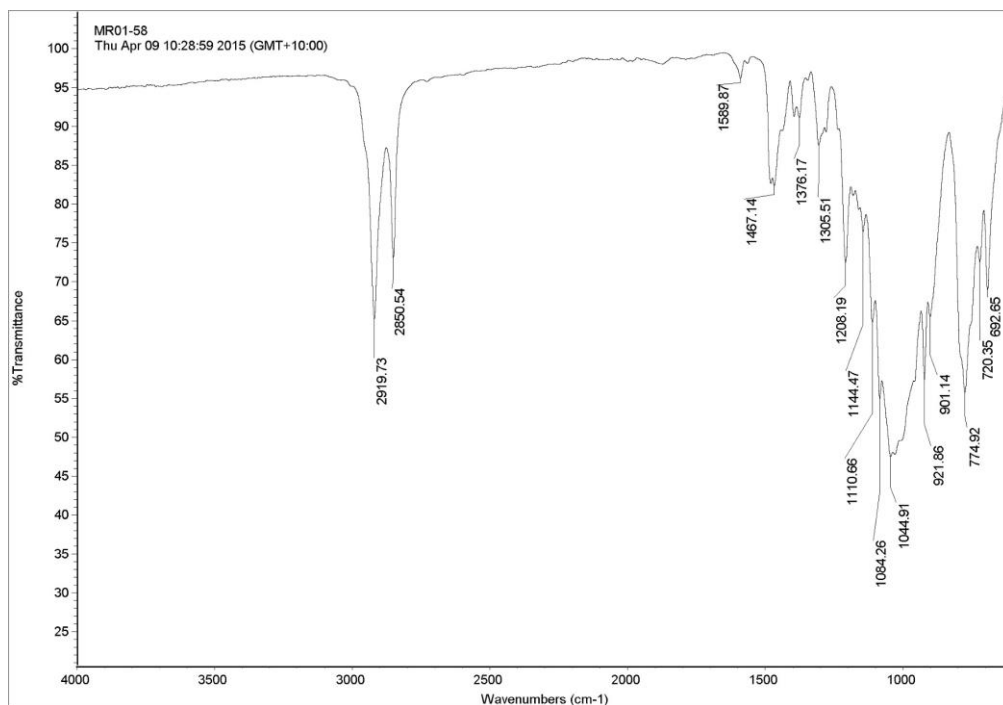
Compound 9, ¹³C-NMR (100 MHz, CDCl₃)

10. Synthesis and Characterization of (\pm 10)

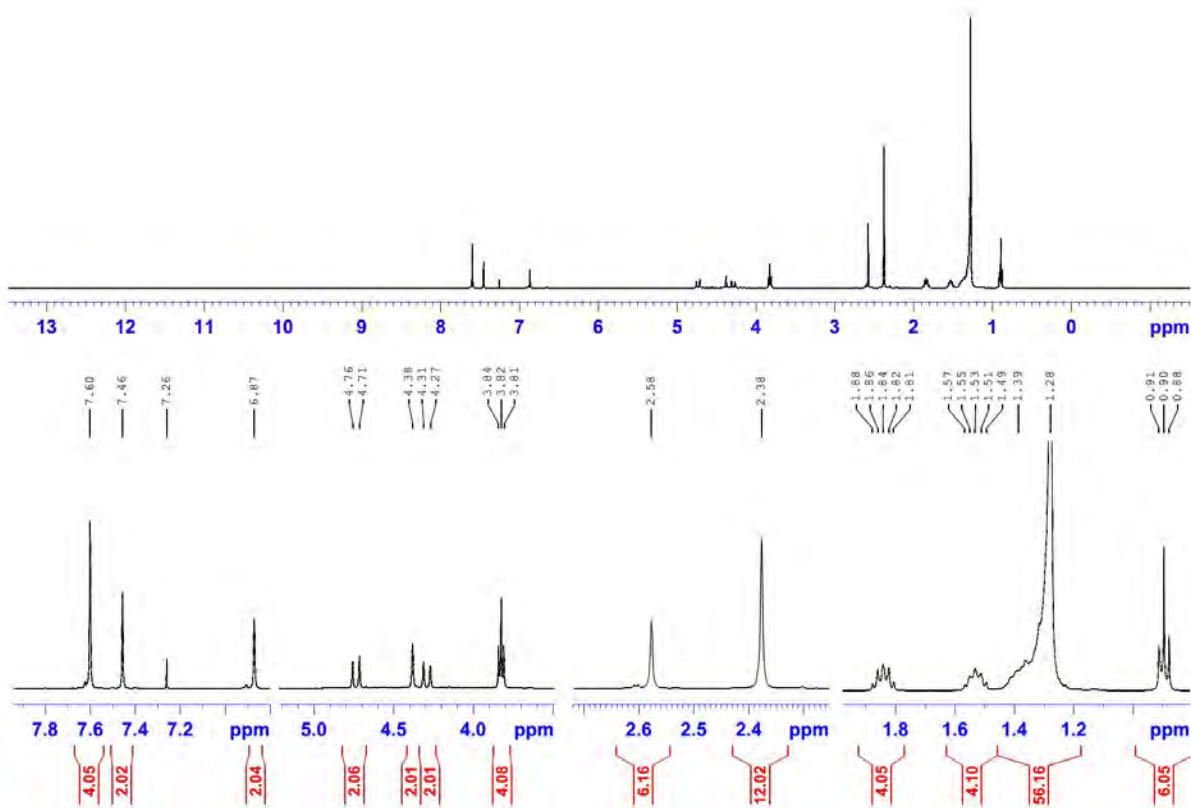
3,9-bis((E)-(3,5-dimethyl-4-(octadecyloxy)phenyl)diazenyl)-2,8-dimethyl-6H,12H-5,11-methanodibenzo[b,f][1,5]diazocine



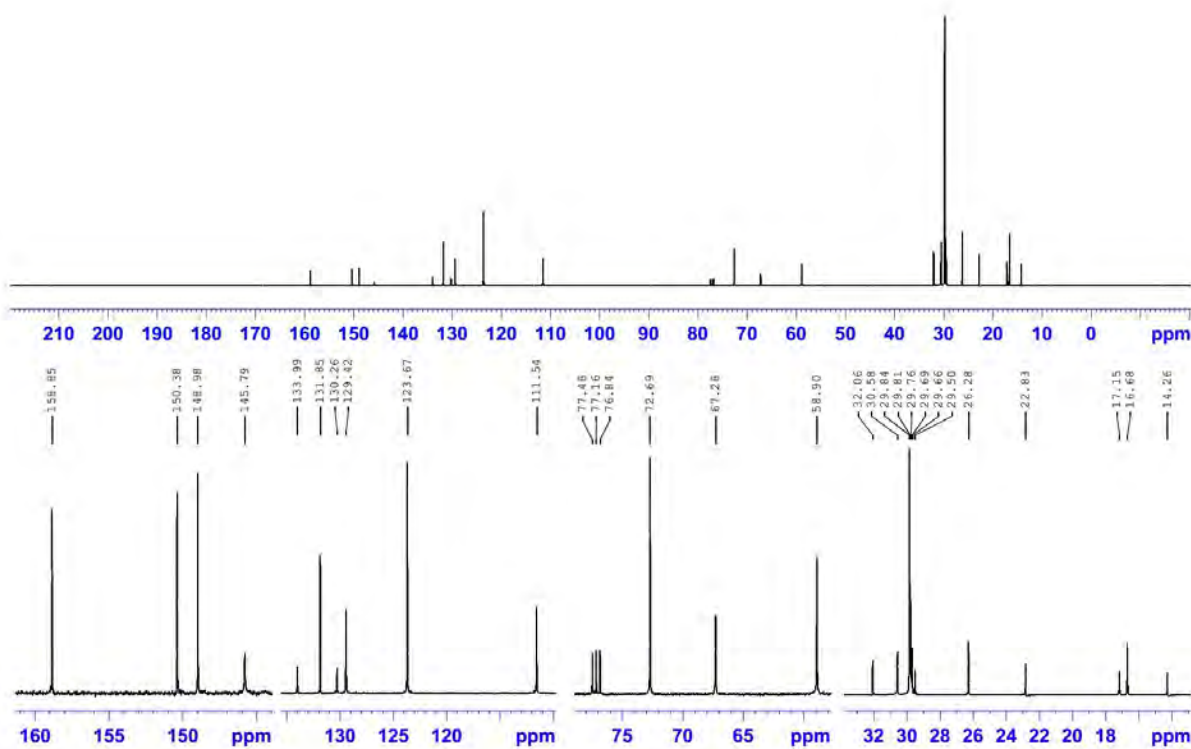
Starting with **1** (0.55 g, 1.0 mmol, 1.0 eq.), K_2CO_3 (0.69 g, 5.0 mmol), a catalytic amount of KI (0.01 g, 0.06 mmol) and 1-bromooctadecane (1.0 g, 3.0 mmol, 1.5 eq.) to obtain **10** (0.69 g, 0.66 mmol, 66 %) Chemical Formula: $C_{69}H_{106}N_6O_2$, Molecular Weight: 1051.65. R_f : 0.55 (ethyl acetate/ n-hexane = 20% v/v) silica gel. 1H -NMR (400 MHz, $CDCl_3$) δ [ppm] : 7.60 (s, 4H, CH) , 7.45 (s, 2H, H-4, H-10) , 6.87 (s, 2H, H-1, H-7) , 4.71-4.76 (d, J = 17.2 Hz, 2H, H6b, H-12b) , 4.38 (s, 2H, -N-CH₂-N-), 4.27-4.31 (d, J = 17.2 Hz, 2H, H-6a, H-12a) , 3.81-3.84 (t, J = 7.8 Hz, 4H, CH₂) , 2.58 (s, 6H, CH₃) , 2.38 (s, 12H, CH₃) , 1.81-1.88 (m, 4H, CH₂) , 1.49-1.57 (m, 4H, CH₂) , 1.24-1.42 (m, 56H, CH₂) , 0.88-0.91 (t, J = 7.9 Hz, 6H, CH₃). ^{13}C -NMR (100 MHz, $CDCl_3$) δ [ppm] : 158.8, 150.3, 148.9, 145.8, 133.9, 131.8, 130.2, 129.4, 123.6, 111.5, 72.6, 67.2, 58.8, 32.0, 30.5, 29.8, 29.8, 29.7, 29.7, 29.6, 29.5, 26.2, 22.8, 17.1, 16.7, 14.2. IR: (Neat) ν_{max} [cm^{-1}] = 2919, 2850, 1589, 1467, 1376, 1305, 1208, 1084, 1044, 921, 901, 774, 720, 692. MS (1-Propanol 50%, Ethanol 50%): (ESI positive) calc. for $[C_{69}H_{107}N_6O_2]^+$: $[M+H]^+$ 1051.84, found 1052.0. UV: (EtOAc) λ (lg ϵ) = 349nm (4.590). Anal. calcd: C, 78.81; H, 10.16; N, 7.99. found: C, 78.93; H, 10.25; N, 7.77.



Compound 10, Infrared Transmittance (neat)



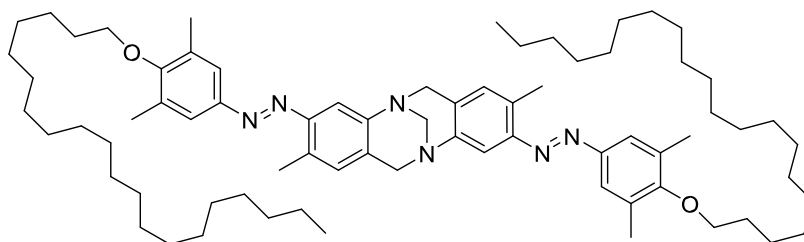
Compound 10, ¹H-NMR (400 MHz, CDCl₃)



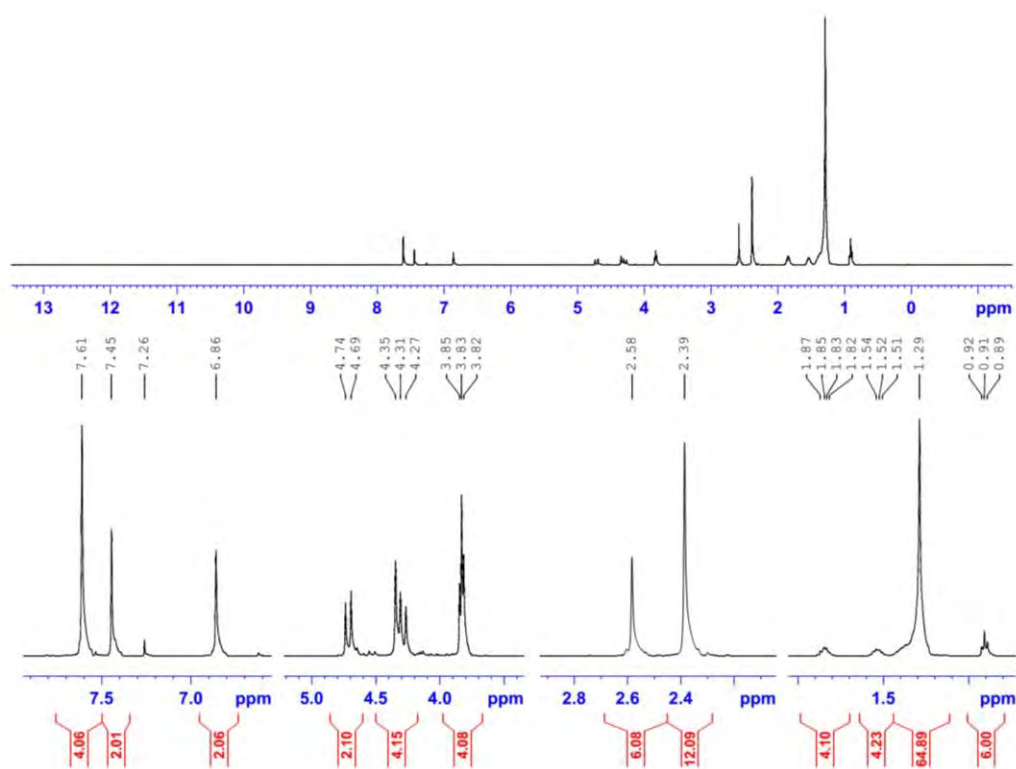
Compound 10, ¹³C-NMR (100 MHz, CDCl₃)

11. Synthesis and Characterization of (\pm 11)

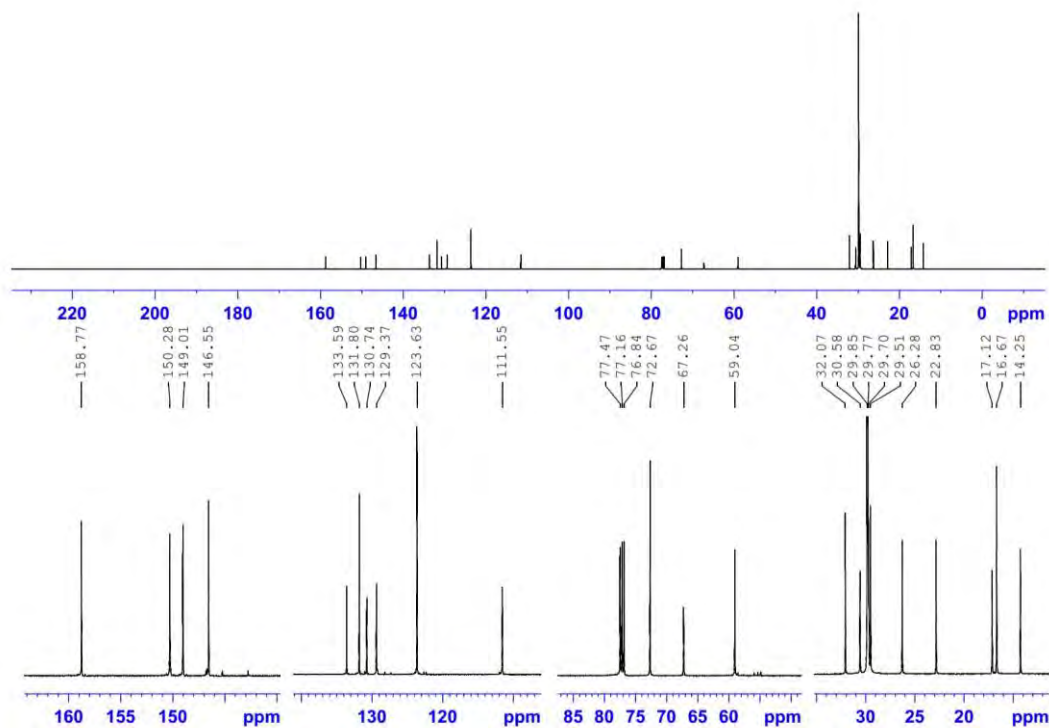
3,9-bis((E)-4-(icosyloxy)-3,5-dimethylphenyl)diazenyl)-2,8-dimethyl-6H,12H-5,11-methanodibenzo[b,f][1,5]diazocine



Starting with **1** (0.55 g, 1.0 mmol, 1.0 eq.), K_2CO_3 (0.69 g, 5.0 mmol), a catalytic amount of KI (0.01 g, 0.06 mmol) and 1-bromoeicosane (0.83 g, 2.3 mmol, 1.2 eq.) to obtain **11** (0.80 g, 0.72 mmol, 72%) Chemical Formula: $C_{73}H_{114}N_6O_2$, Molecular Weight: 1107.76, R_f : 0.60 (EtOAc/ n-hexane = 20% v/v) silica gel. 1H -NMR (400 MHz, $CDCl_3$) δ [ppm] : 7.61 (s, 2H, H-4, H-10) , 7.45 (s, 4H, CH) , 6.86 (s, 2H, H-1, H-7) , 4.69-4.74 (d, J = 17.2 Hz, 2H, H-6b, H12b) , 4.35 (s, 2H, -N-CH₂-N-), 4.27-4.31 (d, J = 17.1 Hz, 2H, H-6a, H-12a) , 3.82-3.85 (t, J = 7.2 Hz, 4H, CH₂) , 2.58 (s, 6H, CH₃) , 2.39 (s, 12H, CH₃) , 1.82-1.87 (m, 4H, CH₂) , 1.51-1.54 (m, 4H, CH₂) , 1.29 (m, 64H, CH₂), 0.89-0.92 (t, J = 7.9 Hz, 6H, CH₃). ^{13}C -NMR (100 MHz, $CDCl_3$) δ [ppm]: 158.7, 150.2, 149.0, 146.5, 133.6, 131.8, 130.7, 129.3, 123.6, 111.5, 72.6, 67.2, 59.0, 32.0, 30.5, 29.8, 29.7, 29.7, 29.5, 26.2, 22.8, 17.1, 16.6, 14.2. IR: (Neat) ν_{max} [cm^{-1}] = 2920, 2851, 1588, 1466, 1376, 1304, 1209, 1082, 1043, 920, 720, 697. MS (isopropyl alcohol 60%, EtOAc 40%): (ESI positive) calc. for $[C_{73}H_{115}N_6O_2]^+$: $[M+H]^+$ 1107.90, found 1107.2. UV-Vis: (EtOAc) λ (lg ϵ) = 349 nm (4.563). Anal. calcd: C, 79.15; H, 10.37; N, 7.59. found: C, 79.25; H, 10.24; N, 7.78.



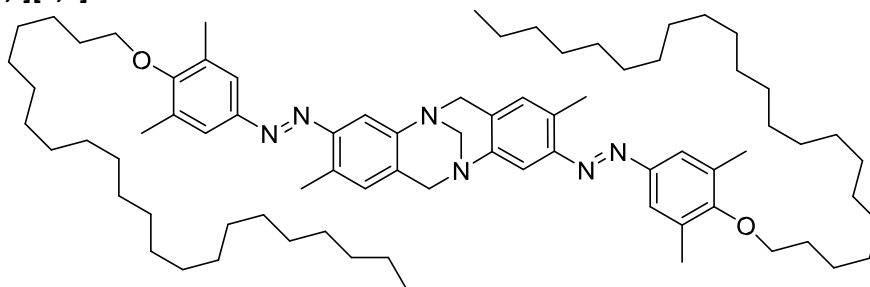
Compound **11**, 1H -NMR (400 MHz, $CDCl_3$)



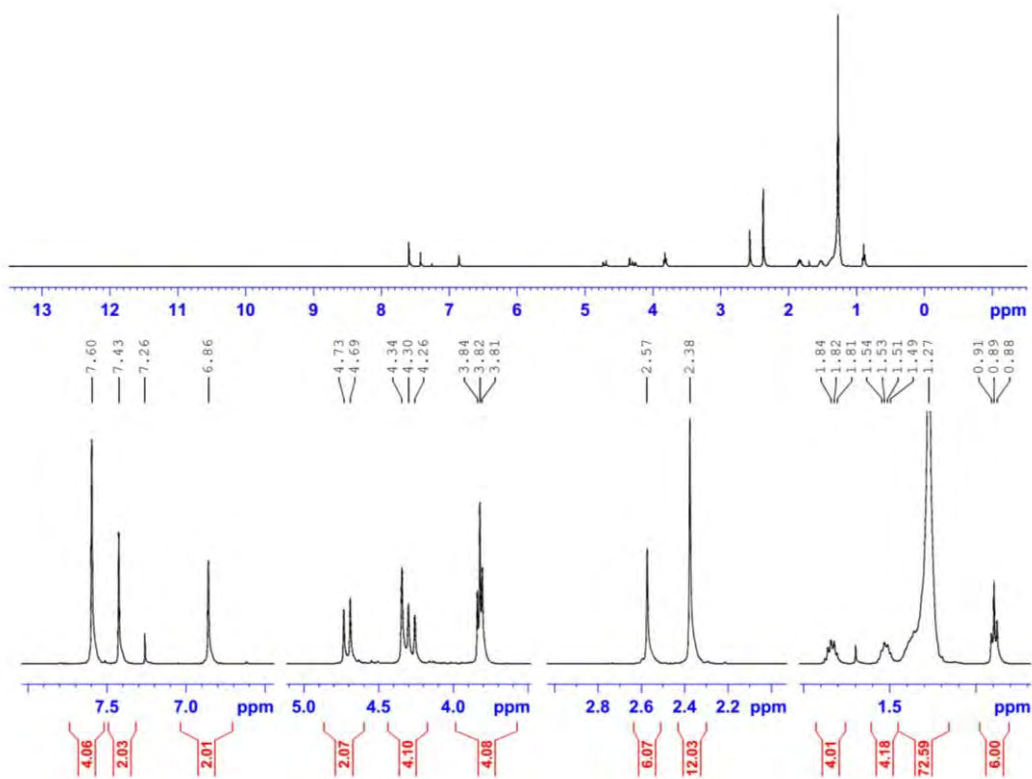
Compound 11, ^{13}C -NMR (100 MHz, CDCl_3)

12. Synthesis and Characterization of (\pm 12)

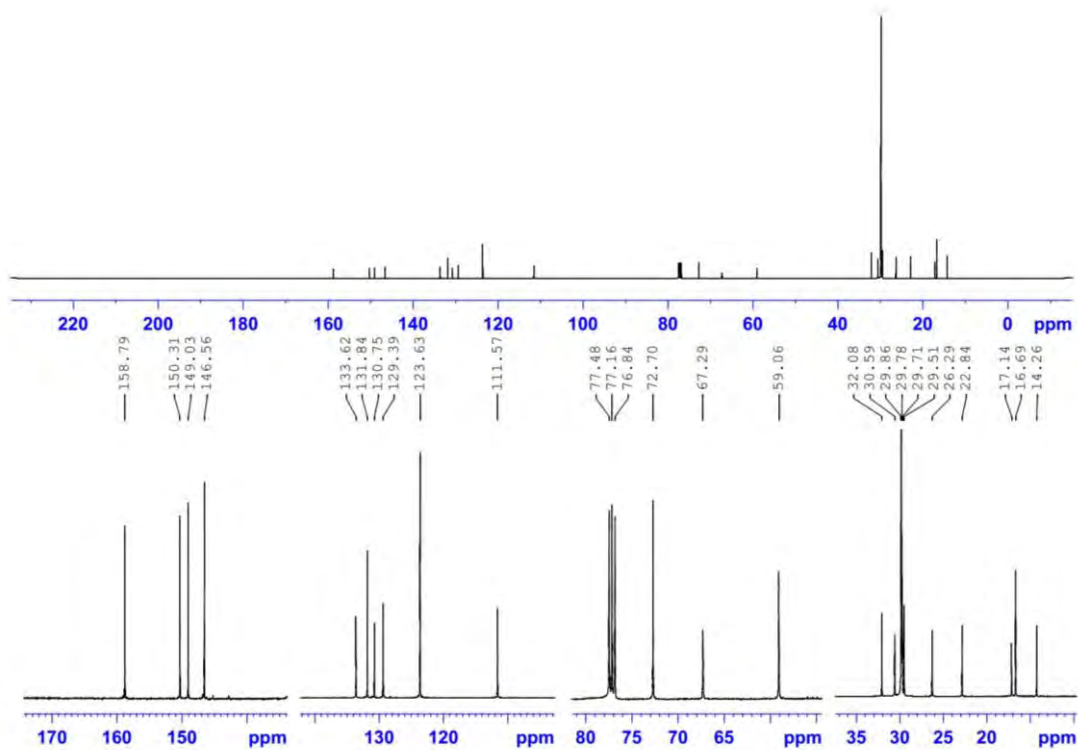
3,9-bis((E)-(4-(docosyloxy)-3,5-dimethylphenyl)diazenyl)-2,8-dimethyl-6H,12H-5,11-methanodibenzo[b,f][1,5]diazocine



Starting with **1** (0.55 g, 1.0 mmol, 1.0 eq.), K_2CO_3 (0.69 g, 5.0 mmol), a catalytic amount of KI (0.01 g, 0.06 mmol) and 1-bromodocosane (0.90 g, 2.3 mmol, 1.2 eq.) to obtain **12** (0.79 g, 0.68 mmol, 68%) Chemical Formula: $\text{C}_{77}\text{H}_{122}\text{N}_6\text{O}_2$, Molecular Weight: 1163.86, R_f : 0.63 (EtOAc/ n-hexane = 20% v/v) silica gel. ^1H -NMR (400 MHz, CDCl_3) δ [ppm] : 7.60 (s, 2H, H-4, H-10) , 7.43 (s, 4H, CH) , 6.86 (s, 2H, H-1, H-7) , 4.69-4.73 (d, J = 16.9 Hz, 2H, H-6b, H12b) , 4.34 (s, 2H, -N-CH₂-N-), 4.26-4.30 (d, J = 17.1 Hz, 2H, H-6a, H-12a) , 3.81-3.84 (t, J = 7.8 Hz, 4H, CH₂) , 2.57 (s, 6H, CH₃) , 2.38 (s, 12H, CH₃) , 1.81-1.84 (m, 4H, CH₂) , 1.49-1.54 (m, 4H, CH₂) , 1.23-1.46 (m, 72H, CH₂), 0.880.91 (t, J = 7.1 Hz, 6H, CH₃). ^{13}C -NMR (100 MHz, CDCl_3) δ [ppm]: 158.8, 150.3, 149.0, 146.5, 133.6, 131.8, 130.7, 129.4, 123.6, 111.5, 72.7, 67.3, 59.0, 32.0, 30.6, 29.8, 29.7, 29.7, 29.5, 26.3, 22.8, 17.1, 16.7, 14.2. IR: (Neat) ν_{max} [cm^{-1}] = 2922, 2850, 1586, 1469, 1379, 1304, 1207, 1083, 1042, 921, 909, 771 and 692. MS (Isopropyl alcohol 60%, EtOAc 40%): (ESI positive) calc. for $[\text{C}_{77}\text{H}_{123}\text{N}_6\text{O}_2]^+$: $[\text{M}+\text{H}]^+$ 1163.96, found 1163.2 and 1164.3. UV-Vis: (EtOAc) λ (lg ϵ) = 349 nm (4.588). Anal. calcd: C, 79.46; H, 10.57; N, 7.22. found: C, 79.55; H, 10.69; N, 7.40.



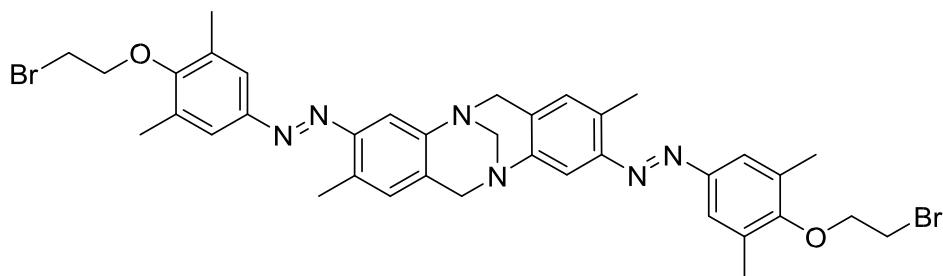
Compound 12, ¹H-NMR (400 MHz, CDCl₃)



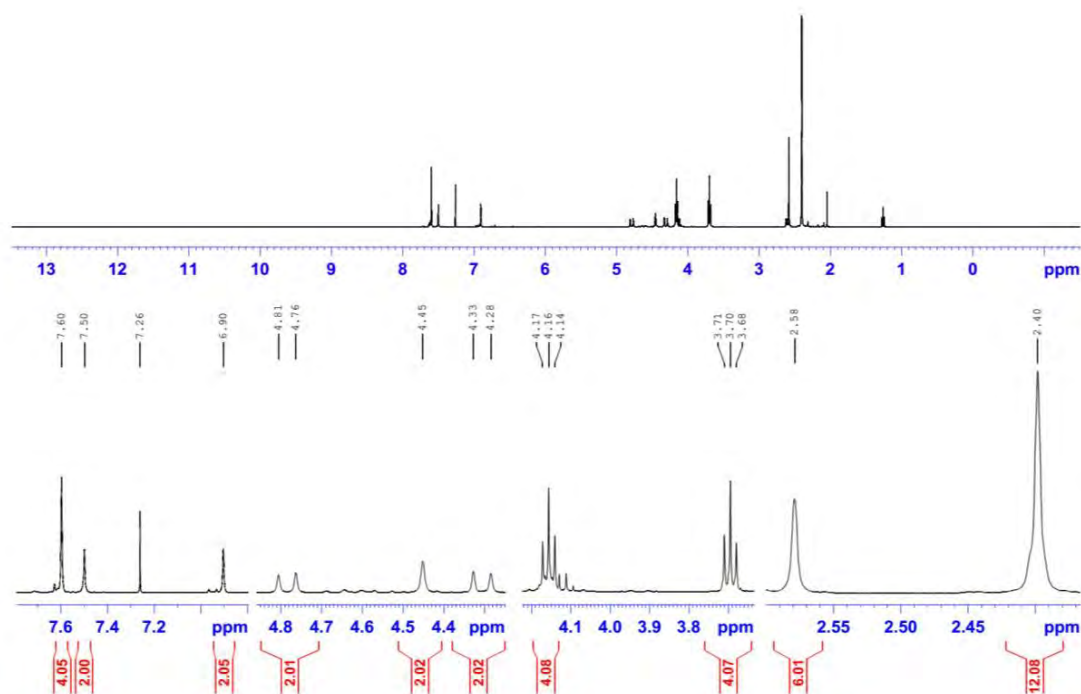
Compound 12, ¹³C-NMR (100 MHz, CDCl₃)

13. Synthesis and Characterization of (\pm 13)

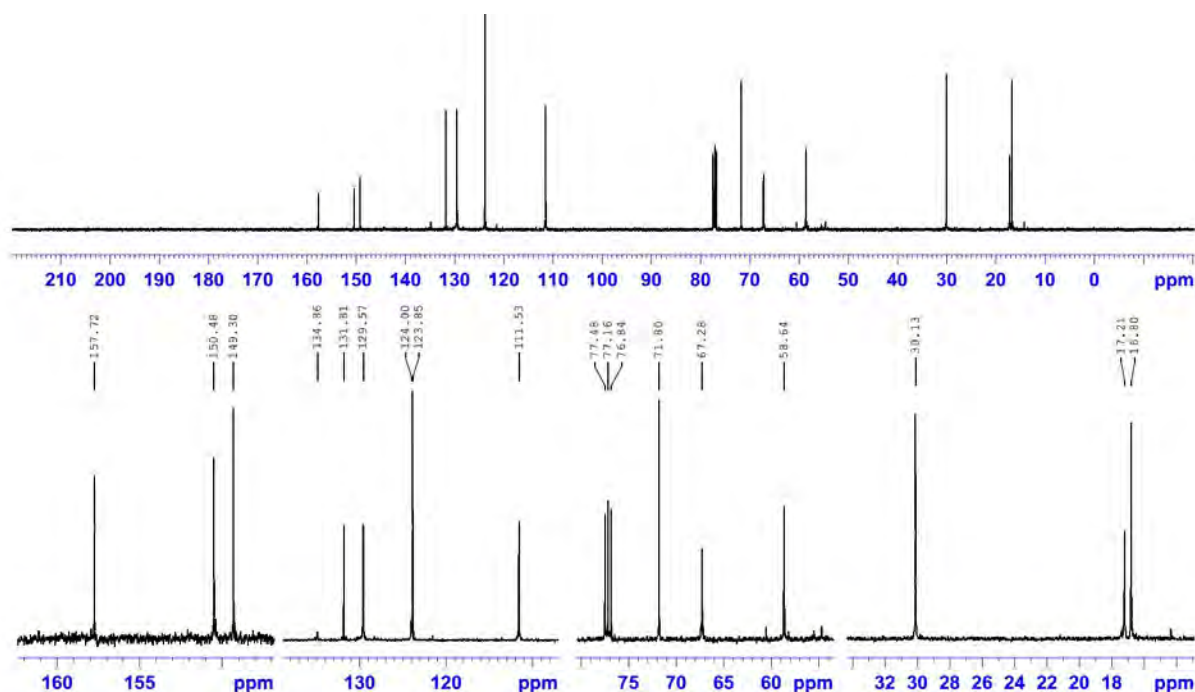
3,9-bis((E)-(4-(2-bromoethoxy)-3,5-dimethylphenyl)diazenyl)-2,8-dimethyl-6H,12H-5,11-methanodibenzo[b,f][1,5]diazocine



Starting with **1** (0.55 g, 1.0 mmol, 1.0 eq.), K_2CO_3 (0.69 g, 5.0 mmol) and 1,2-dibromoethane (0.50 g, 2.7 mmol, 1.3 eq.) to obtain **13** (0.37 g, 0.49 mmol, 49%) Chemical Formula: $C_{37}H_{40}Br_2N_6O_2$, Molecular Weight: 760.58. R_f: 0.55 (ethyl acetate/ n-hexane = 40% v/v) silica gel. 1H -NMR (400 MHz, $CDCl_3$) δ [ppm] : 7.60 (s, 4H, CH) , 7.50 (s, 2H, H-4, H-10) , 6.90 (s, 2H, H-1, H-7) , 4.76-4.81 (d, J = 17.04 Hz, 2H, H-6b, H-12b) , 4.45 (s, 2H, -N-CH₂-N-), 4.284.33 (d, J = 17.16 Hz, 2H, H-6a, H-12a) , 4.14-4.17 (t, J = 7.3 Hz, 4H, CH₂) , 3.68-3.71 (t, J = 7.4 Hz, 4H, CH₂) , 2.58 (s, 6H, CH₃), 2.40 (s, 12H, CH₃). ^{13}C -NMR (100 MHz, $CDCl_3$) δ [ppm]: 157.7, 150.4, 149.3, 134.8, 131.8, 129.5, 123.9, 123.8, 111.5, 71.8, 67.2, 58.6, 30.1, 17.2, 16.8. IR: (Neat) ν_{max} [cm^{-1}] = 2949, 2916, 2849, 1732, 1588, 1477, 1395, 1375, 1278, 1201, 1111, 1084, 1000, 893, 745, 688. MS (Acetonitrile 90%, EtOAc 5%, H₂O 5%) (ESI positive) calc. for $[C_{37}H_{41}Br_2N_6O_2]^+$: $[M+H]^+$ 759.16, found 759.45 and 761.40. UV: (EtOAc) λ (lg ϵ) = 345nm (4.596). Anal. calcd: C, 58.43; H, 5.30; Br, 21.01; N, 11.05. found: C, 58.66; H, 5.21; N, 11.24.



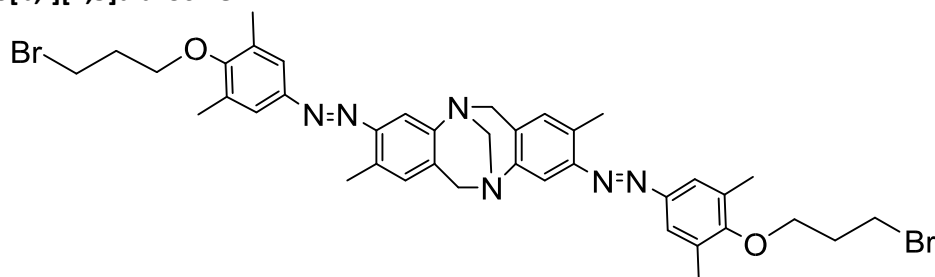
Compound 13, 1H -NMR (400 MHz, $CDCl_3$)



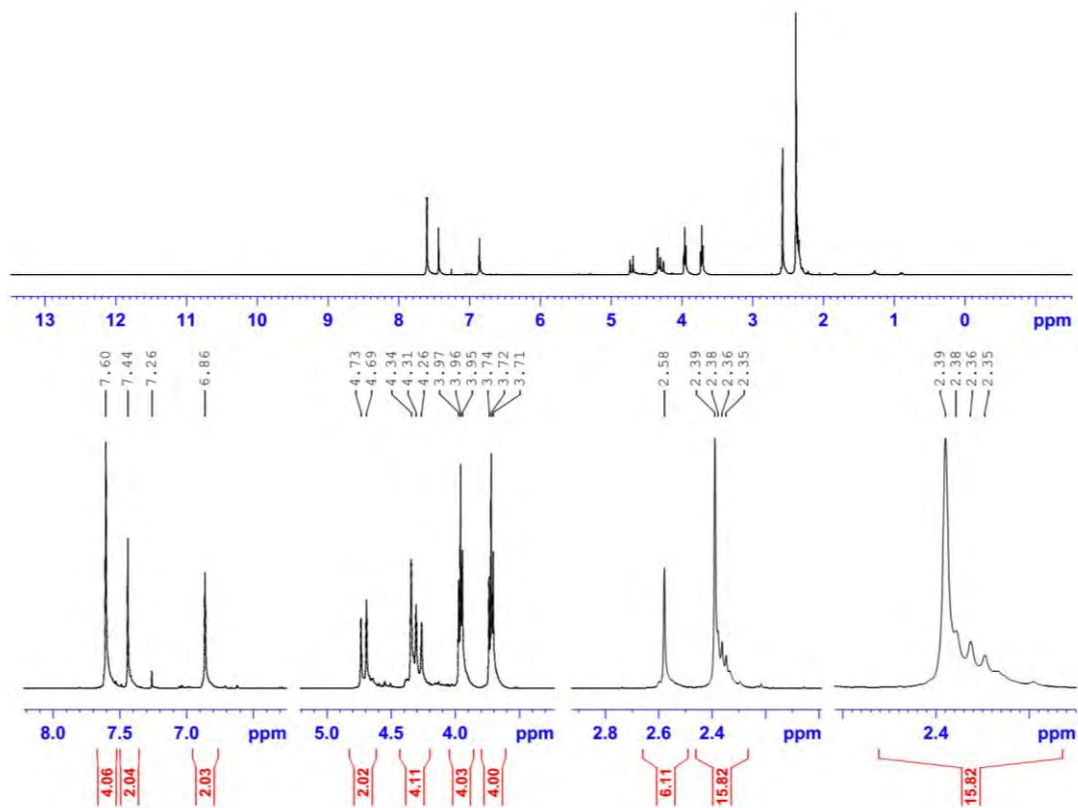
Compound 13, ^{13}C -NMR (100 MHz, CDCl_3)

14. Synthesis and Characterization of (\pm 14)

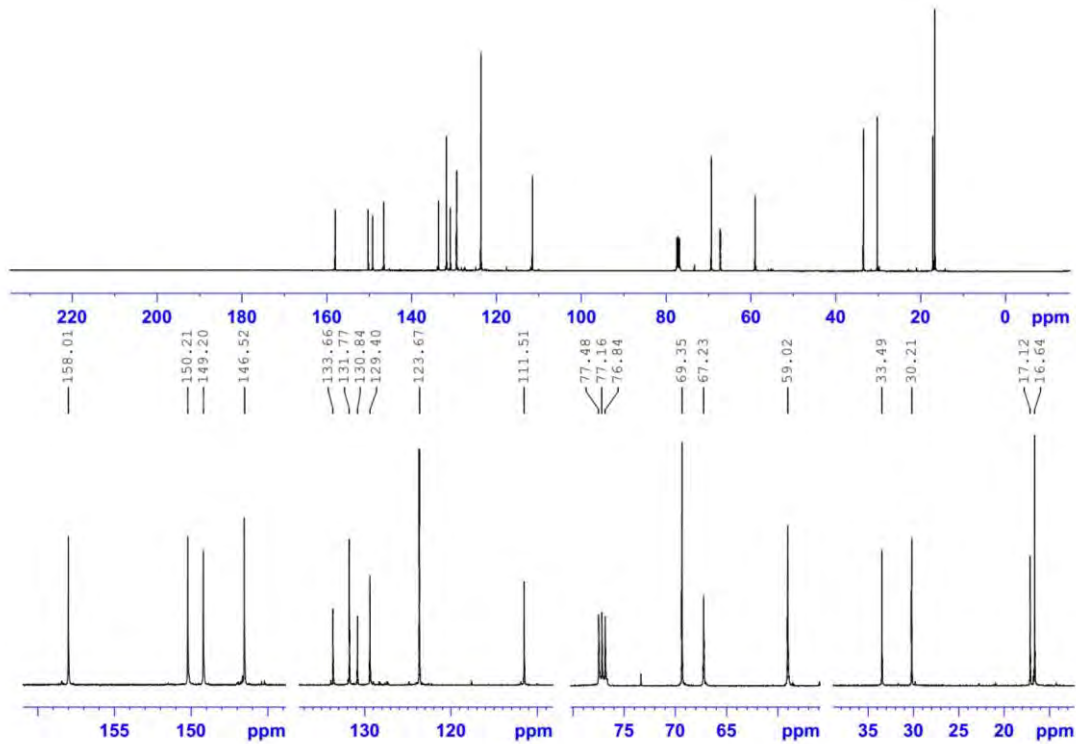
3,9-bis((E)-(4-(3-bromopropoxy)-3,5-dimethylphenyl)diazenyl)-2,8-dimethyl-6H,12H-5,11-methanodibenzo[b,f][1,5]diazocine



Starting with **1** (1.1 g, 2.0 mmol, 1.0 eq.), K_2CO_3 (1.4 g, 10 mmol) and 1,3-dibromopropane (0.93 g, 4.6 mmol, 2.3 eq.) to obtain **14** (0.39 g, 0.50 mmol, 25%) Chemical Formula: $\text{C}_{39}\text{H}_{44}\text{Br}_2\text{N}_6\text{O}_2$, Molecular Weight: 788.63. R_f : 0.60 (ethyl acetate/ n-hexane = 40% v/v) silica gel. ^1H -NMR (400 MHz, CDCl_3) δ [ppm] : 7.60 (s, 4H, CH) , 7.44 (s, 2H, H4, H-10) , 6.86 (s, 2H, H-1, H-7) , 4.69-4.73 (d, J = 17.0 Hz, 2H, H-6b, H-12b) , 4.34 (s, 2H, -N-CH₂-N-) , 4.26-4.31 (d, J = 17.1 Hz, 2H, H-6a, H-12a) , 3.95-3.97 (t, J = 5.9 Hz, 4H, CH₂) , 3.71-3.74 (t, J = 6.2 Hz, 4H, CH₂) , 2.58 (s, 6H, CH₃) , 2.39 (s, 12H, CH₃) , 2.34-2.38 (m, 4H, CH₂). ^{13}C -NMR (100 MHz, CDCl_3) δ [ppm]: 158.0, 150.2, 149.2, 146.5, 133.6, 131.7, 130.8, 129.4, 123.6, 111.5, 69.3, 67.2, 59.0, 33.5, 30.2, 17.1, 16.6. IR: (Neat) ν_{max} [cm^{-1}] = 2948, 2917, 2849, 1733, 1587, 1475, 1395, 1375, 1276, 1203, 1112, 1084, 1001, 893, 744, 679. MS (Isopropyl alcohol 50%, Acetonitrile 40%, EtOAc 10%) (ESI positive) calc. for $[\text{C}_{39}\text{H}_{45}\text{Br}_2\text{N}_6\text{O}_2]^+$: $[\text{M}+\text{H}]^+$ 787.19, found 786.8, 789.2 and 792.1. UV: (EtOAc) λ (lge) = 345nm (4.577). Anal. calcd: C, 59.40; H, 5.62; N, 10.66. found: C, 59.51; H, 5.48; N, 10.38.



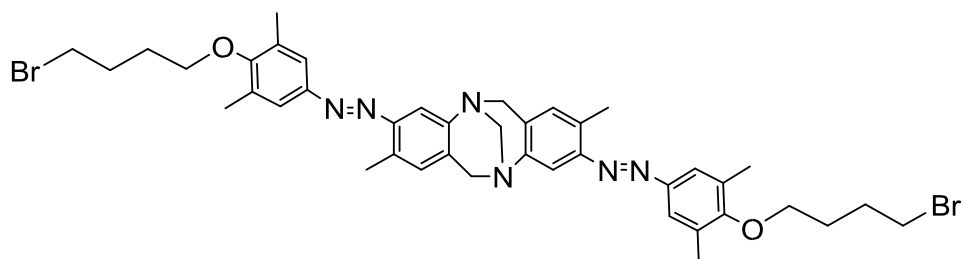
Compound 14, ¹H-NMR (400 MHz, CDCl₃)



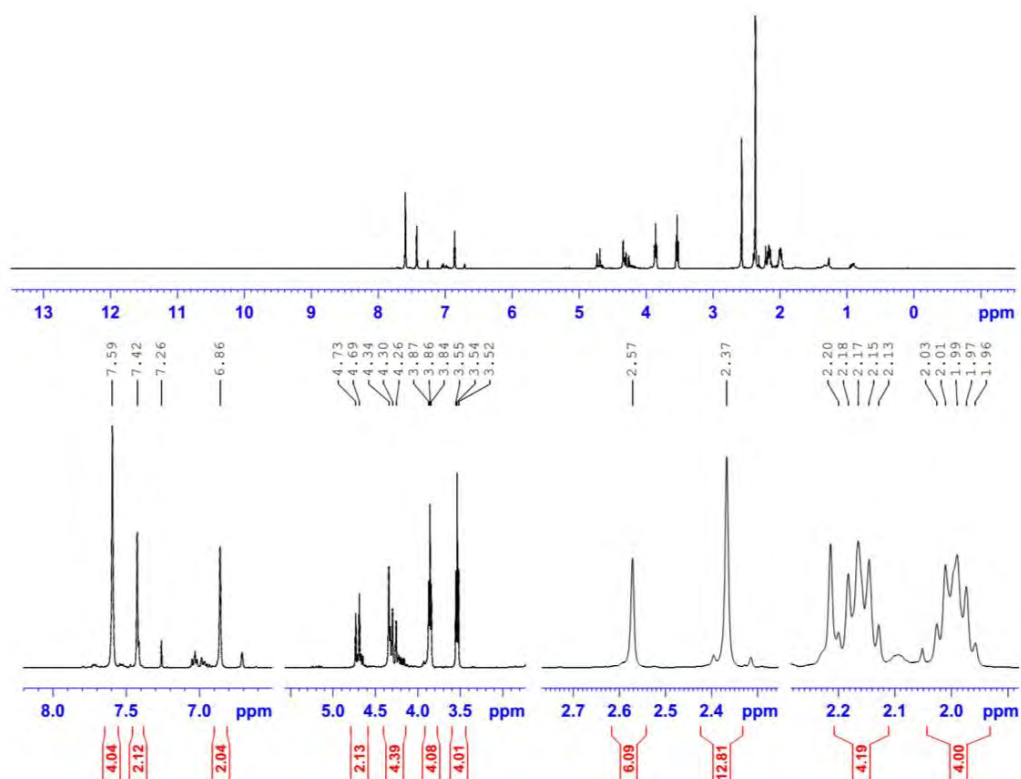
Compound 14, ¹³C-NMR (100 MHz, CDCl₃)

15. Synthesis and Characterization of (\pm 15)

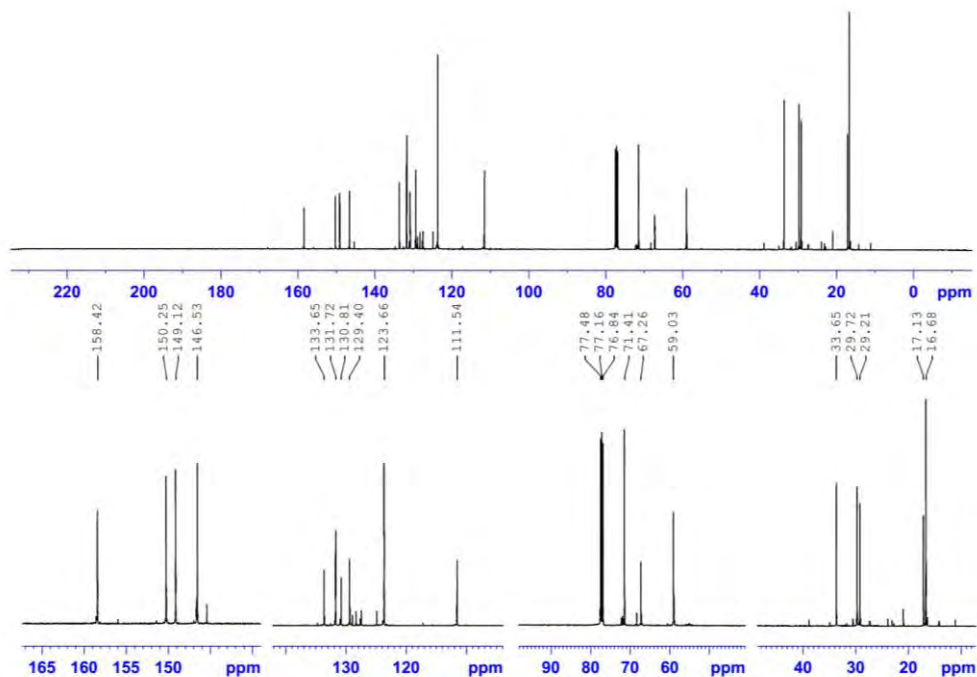
3,9-bis((E)-4-(4-bromobutoxy)-3,5-dimethylphenyl)diazenyl)-2,8-dimethyl-6H,12H-5,11-methanodibenzo[b,f][1,5]diazocine



Starting with **1** (1.1 g, 2.0 mmol, 1.0 eq.), K_2CO_3 (1.4 g, 10 mmol) and 1,4-dibromobutane (1.0 g, 4.6 mmol, 2.3 eq.) to obtain **15** (0.31 g, 0.38 mmol, 19%) Chemical Formula: $C_{41}H_{48}Br_2N_6O_2$, Molecular Weight: 816.68. R_f : 0.65 (ethyl acetate/ n-hexane = 40% v/v) silica gel. 1H -NMR (400 MHz, $CDCl_3$) δ [ppm] : 7.59 (s, 4H, CH) , 7.42 (s, 2H, H-4, H10) , 6.86 (s, 2H, H-1, H-7) , 4.69-4.73 (d, J = 17.1 Hz, 2H, H-6b, H-12b) , 4.34 (s, 2H, -N-CH₂-N-), 4.26-4.30 (d, J = 17.3 Hz, 2H, H-6a, H-12a) , 3.84-3.87 (t, J = 6.4 Hz, 4H, CH₂) , 3.52-3.55 (t, J = 6.9 Hz, 4H, CH₂) , 2.57 (s, 6H, CH₃) , 2.37 (s, 12H, CH₃) , 2.11-2.19 (m, 4H, CH₂) , 1.94-2.08(m, 4H, CH₂). ^{13}C -NMR (100 MHz, $CDCl_3$) δ [ppm]: 158.4, 150.2, 149.1, 146.5, 133.6, 131.7, 130.8, 129.4, 123.6, 111.5, 71.4, 67.2, 59.0, 33.6, 29.7, 29.2, 17.1, 16.6. IR: (Neat) ν_{max} [cm^{-1}] =2950, 2919, 2848, 1743, 1586, 1479, 1395, 1376, 1278, 1203, 1109, 1084, 999, 894, 746, 678. MS (Isopropyl alcohol 50%, Acetonitrile 40%, EtOAc 10%) (ESI positive) calc. for $[C_{41}H_{49}Br_2N_6O_2]^+$: $[M+H]^+$ 815.22, found 815.8, 818.9 and 820.3. UV: (EtOAc) λ (lg ϵ) = 345nm (4.581). Anal. calcd: C, 60.30; H, 5.92; N, 10.29. found: C, 60.21; H, 5.74; N, 10.58.



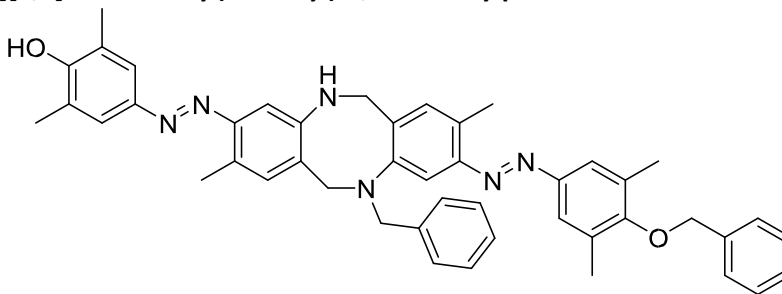
Compound 15, 1H -NMR (400 MHz, $CDCl_3$)



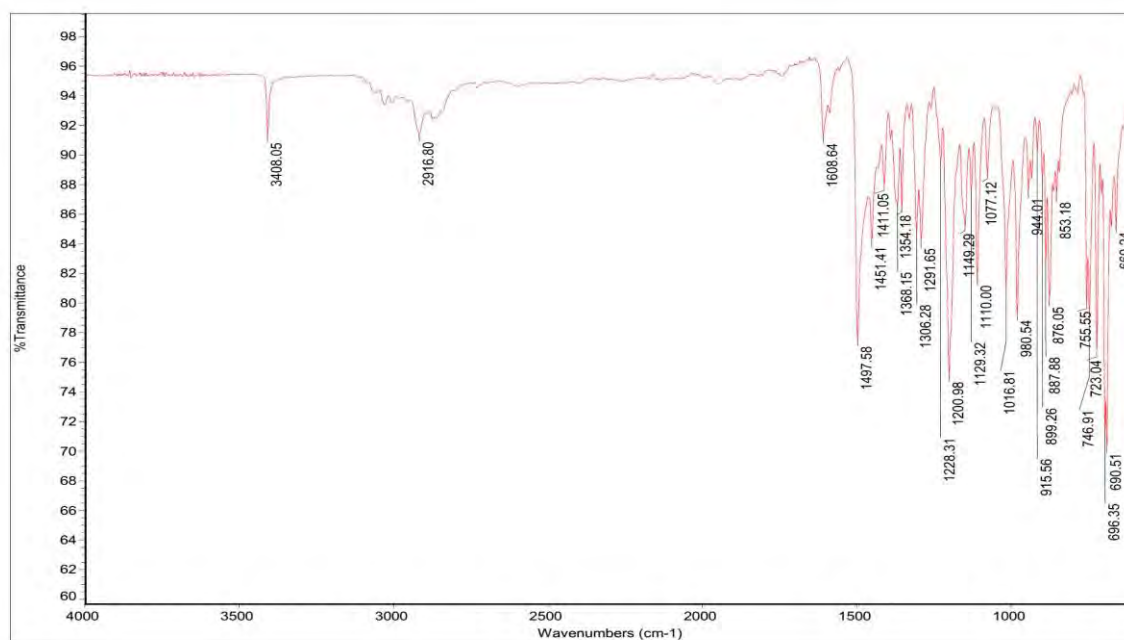
Compound 15, ^{13}C -NMR (100 MHz, CDCl_3)

16. Synthesis and Characterization of (16)

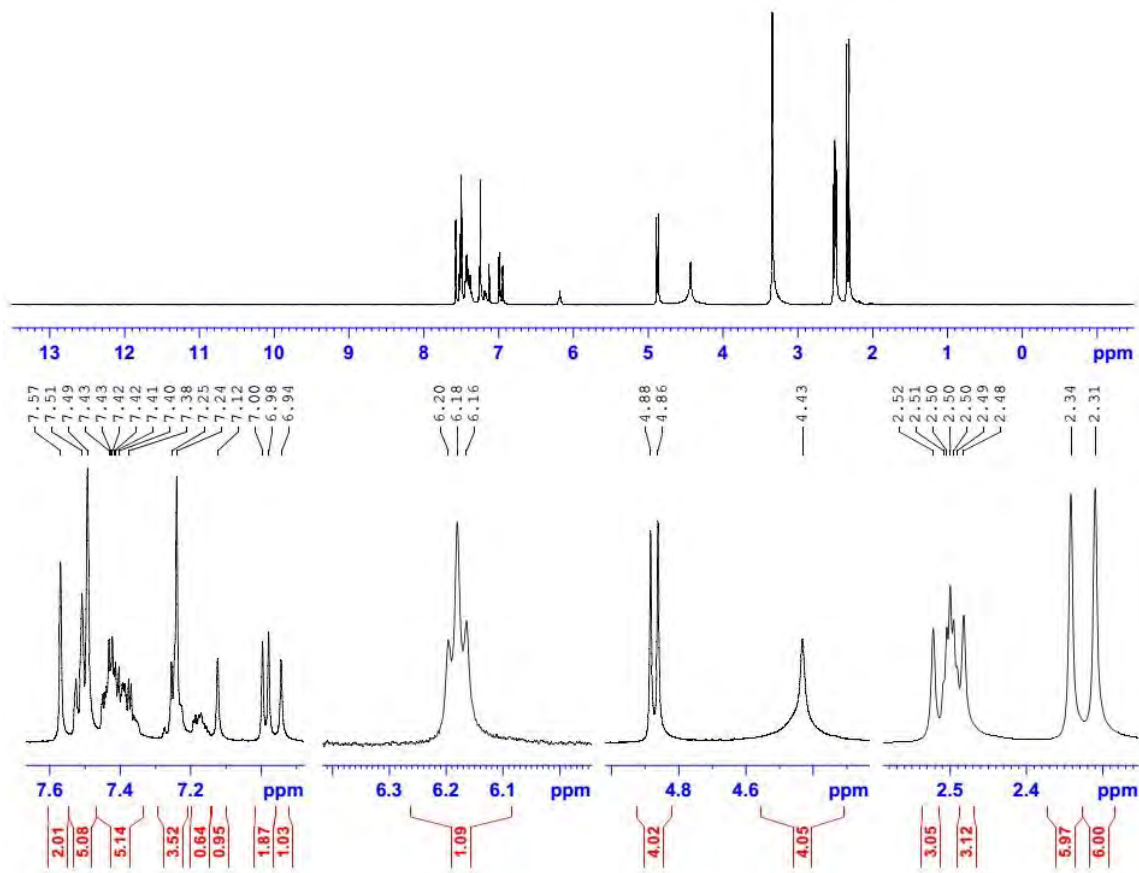
4-((E)-(11-benzyl-9-((E)-(4-(benzyloxy)-3,5-dimethylphenyl)diazenyl)-2,8-dimethyl-5,6,11,12-tetrahydrodibenzo[b,f][1,5]diazocin-3-yl)diazenyl)-2,6-dimethylphenol



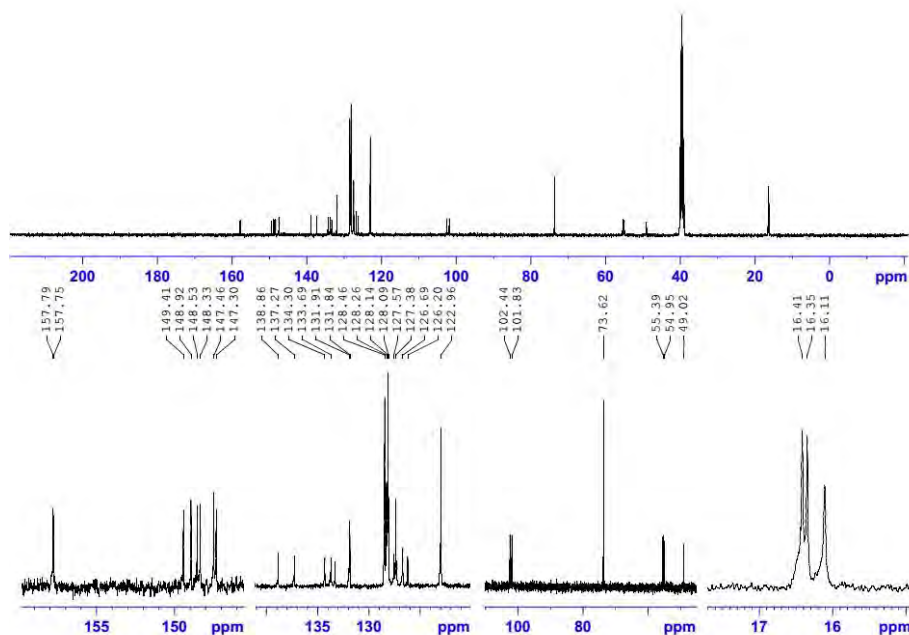
Starting with **1** (0.55 g, 1.0 mmol, 1.0 eq.), K_2CO_3 (0.69 g, 5.0 mmol), a catalytic amount of KI (0.01 g, 0.06 mmol) and benzyl bromide (0.38 g, 2.2 mmol, 1.1 eq.) to obtain **16** (0.29 g, 0.36 mmol, 73%) Chemical Formula: $\text{C}_{46}\text{H}_{46}\text{N}_6\text{O}_2$, Molecular Weight: 714.914, R_f : 0.44 (EtOAc/ n-Hex = 20% v/v) silica gel. ^1H -NMR(400 MHz, $\text{DMSO}-d_6$) δ [ppm] : 7.56 (s, 2H, CH) , 7.46-7.54 (m, 5H, CH) , 7.32-7.46 (m, 5H, CH) , 7.22-7.24 (m, 3H, CH) , 7.12 (s, 1H, CH) , 6.99 (s, 1H, CH) , 6.97 (s, 1H, CH) , 6.94 (s, 1H, CH) , 6.16-6.20 (t, $J = 7.8$ Hz, 1H, NH) , 4.88 (s, 2H, CH_2) , 4.86 (s, 2H, CH_2) , 4.43 (b, 4H, CH_2) , 2.52 (s, 3H, CH_3) , 2.48 (s, 3H, CH_3) , 2.34 (s, 6H, CH_3) , 2.31 (s, 6H, CH_3). ^{13}C -NMR(100 MHz, $\text{DMSO}-d_6$) δ [ppm]: 157.7, 157.7, 149.4, 148.9, 148.5, 148.3, 147.4, 147.3, 138.8, 137.2, 134.3, 133.7, 133.3, 131.9, 131.8, 128.4, 128.2, 128.1, 128.0, 127.5, 127.3, 127.2, 126.7, 126.2, 122.9, 102.4, 101.8, 73.6, 55.3, 54.9, 49.0, 16.4, 16.3, 16.1. IR: (Neat) ν_{max} [cm^{-1}] = 3408, 2916, 1608, 1497, 1451, 1368, 1306, 1291, 1200, 1110, 1016, 980, 887, 755, 690. MS (Ethanol 50%, Isopropyl Alcohol 50%) (ESI positive) calc. for $[\text{C}_{46}\text{H}_{45}\text{N}_6\text{O}_2]^+$: calc. 713.37, found 713.2. UV-Vis: (EtOAc) λ (lg ϵ) = 345nm (4.605). Anal. calcd: C, 77.28; H, 6.49; N, 11.76. found: C, 77.37; H, 6.35; N, 11.91.



Compound 16, Infrared Transmittance (neat)



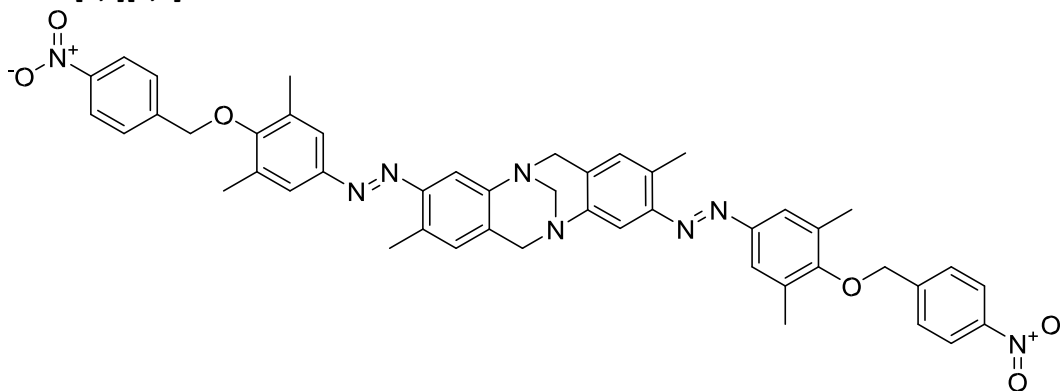
Compound 16, ¹H-NMR (400 MHz, DMSO-*d*₆)



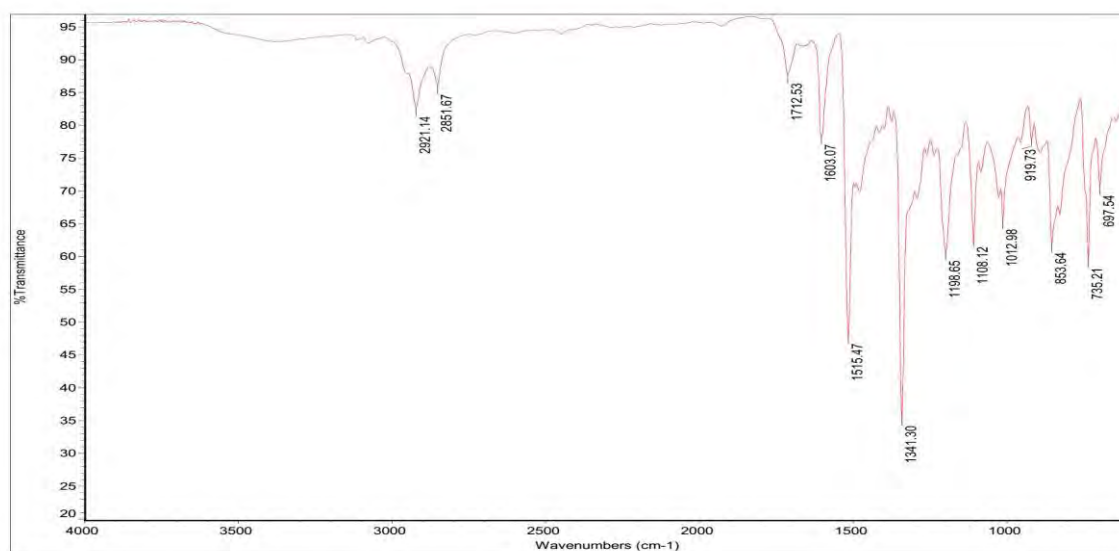
Compound 16, ^{13}C -NMR (100 MHz, $\text{DMSO}-d_6$)

17. Synthesis and Characterization of (± 17)

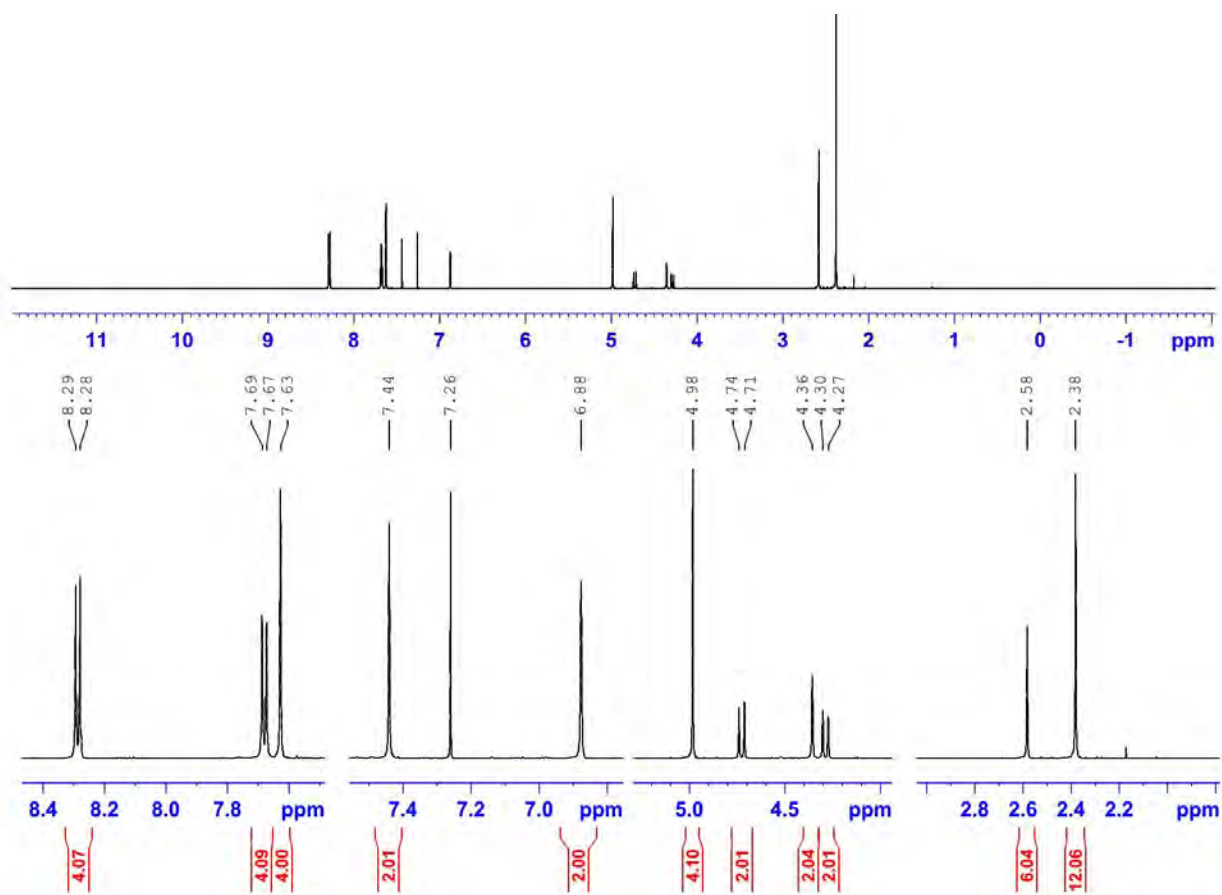
3,9-bis((E)-(3,5-dimethyl-4-((4-nitrobenzyl)oxy)phenyl)diazenyl)-2,8-dimethyl-6H,12H-5,11-methanodibenzo[b,f][1,5]diazocine



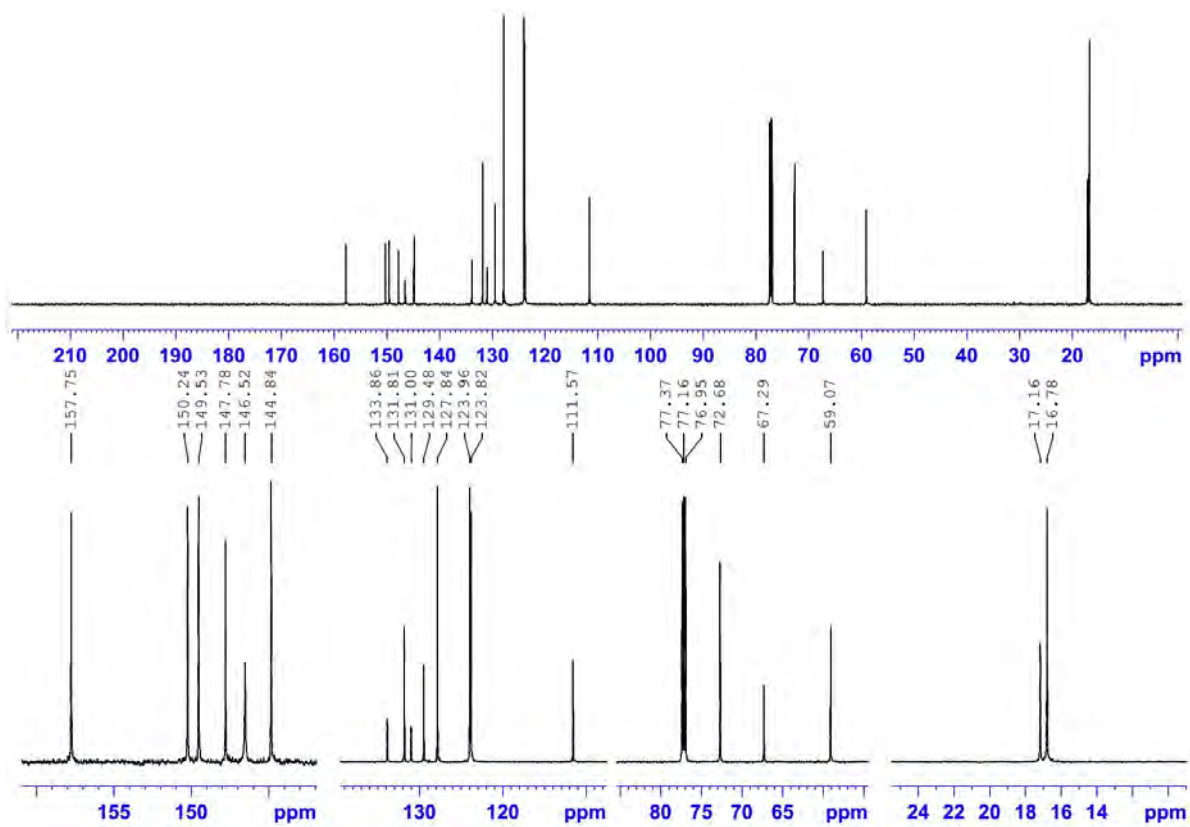
1 (0.55 g, 1.0 mmol, 1.0 eq.), K_2CO_3 (0.69 g, 5.0 mmol), a catalytic amount of KI (0.01 g, 0.06 mmol) and 4-nitrobenzyl bromide (0.43 g, 2.2 mmol, 2.2 eq.) were refluxed in acetone (10ml) for 48h. Then, ice (50 g) and EtOAc (5 ml) were added to the reaction mixture and mixed for 30 minutes. The desired product **17** was obtained, by filtration of the mixture and desiccation under high-vacuum (0.57 g, 0.70 mmol, 70%) Chemical Formula: $\text{C}_{47}\text{H}_{44}\text{N}_8\text{O}_6$, Molecular Weight: 816.92. R_f : 0.8 (MeOH/ DCM = 4% v/v) silica gel. ^1H -NMR (600 MHz, CDCl_3) δ [ppm] : 8.27-8.29 (d, 4H, J = 8.7 Hz) , 7.67-7.68 (d, 4H, J = 8.8 Hz) , 7.63 (s, 4H, CH), 7.44 (s, 2H, H-4, H-10), 6.88 (s, 2H, H1, H-7), 4.98 (s, 4H, C- CH_2 -C), 4.71-4.74 (d, J = 17.1 Hz, 2H, H-6b, H-12b) , 4.35 (s, 2H, -N- CH_2 -N-), 4.27-4.30 (d, J = 17.1 Hz, 2H, H-6a, H-12a), 2.58 (s, 6H, CH_3), 2.38 (s, 12H, CH_3). ^{13}C -NMR (150 MHz, CDCl_3) δ [ppm]: 157.7, 150.2, 149.5, 147.7, 146.5, 144.8, 133.8, 131.8, 131.0, 129.4, 127.8, 123.9, 123.8, 111.5, 72.6, 67.3, 59.0, 17.1, 16.7. IR: (Neat) ν_{max} (cm^{-1}) = 2921, 2851, 1712, 1603, 1515, 1341, 1198, 1108, 1013, 853, 735, 697. MS (Acetonitrile 50%, EtOAc 50%) (ESI positive) calc. for $[\text{C}_{47}\text{H}_{45}\text{N}_8\text{O}_6]^+$: $[\text{M}+\text{H}]^+$ 817.34, found 817.1. UV(EtOAc): λ (Ige) = 341nm (4.498). Anal. calcd: C, 69.10; H, 5.43; N, 13.72. found: C, 69.27; H, 5.15; N, 13.95.



Compound 17, Infrared Transmittance (neat)

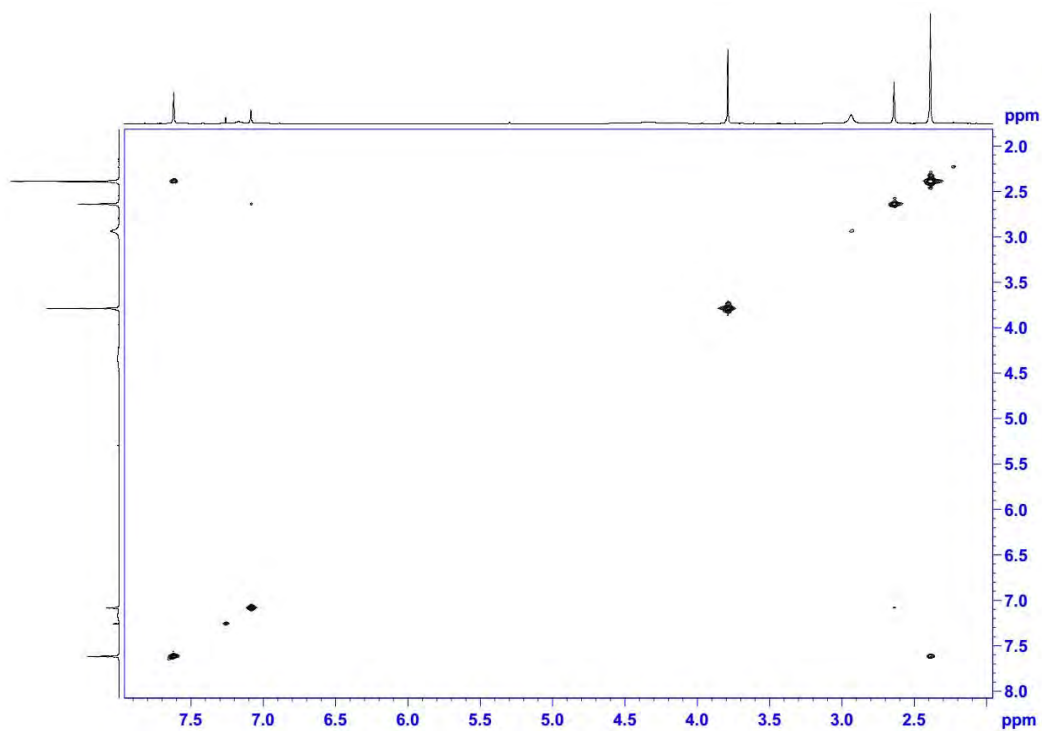


Compound 17, ¹H-NMR (600 MHz, CDCl₃)

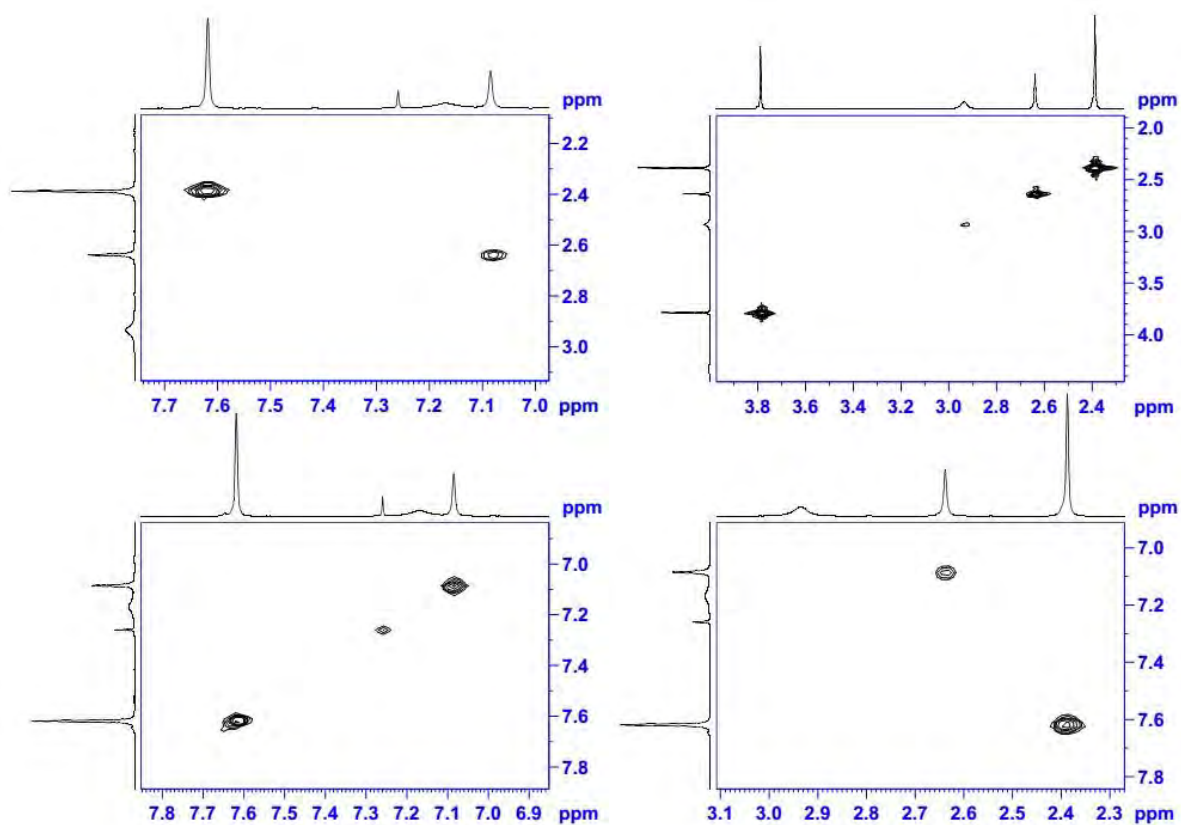


Compound 17, ¹³C-NMR (150 MHz, CDCl₃)

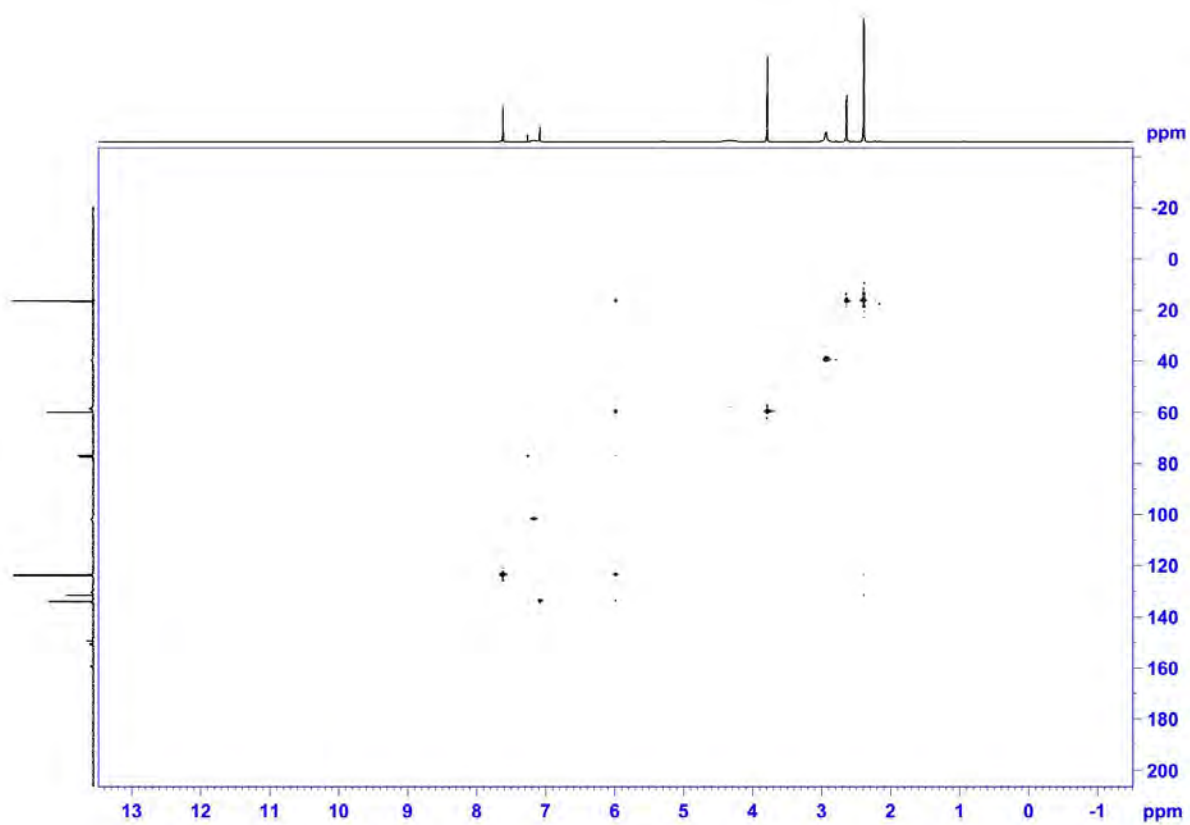
2D NMR Results



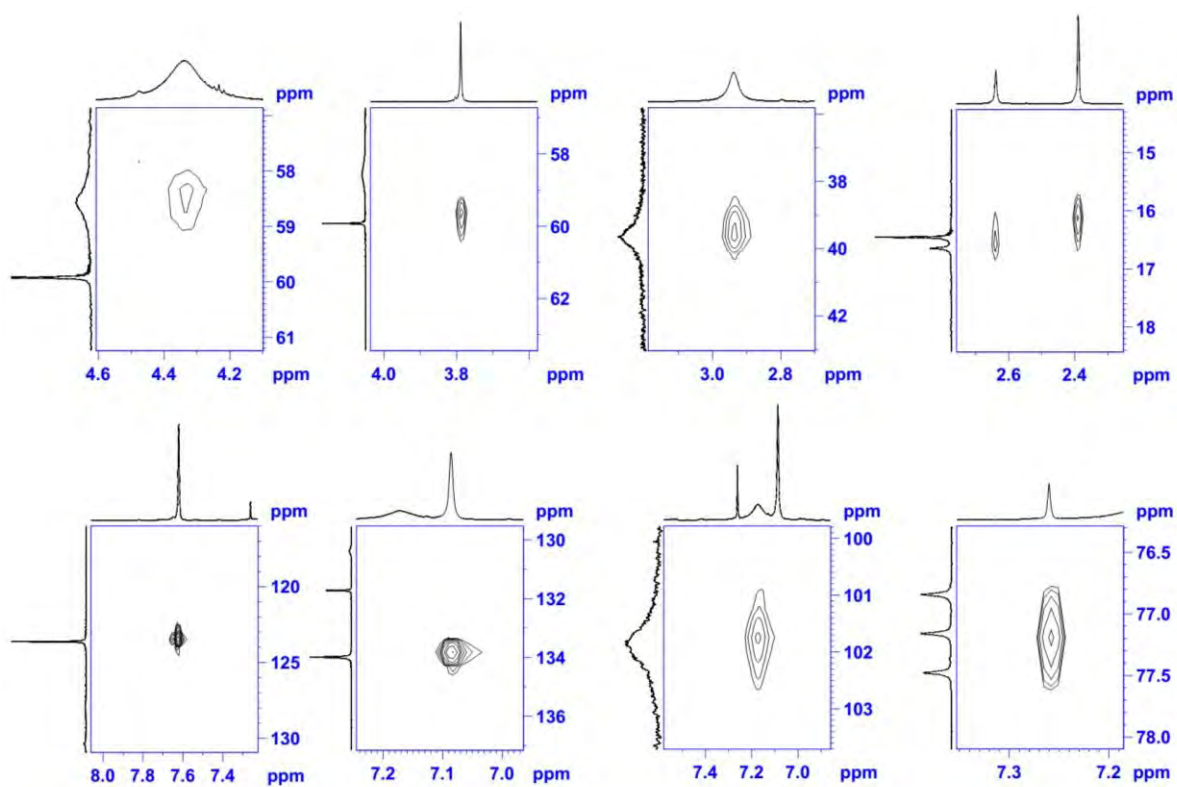
Compound 2, COSY (400 MHz, CDCl₃)



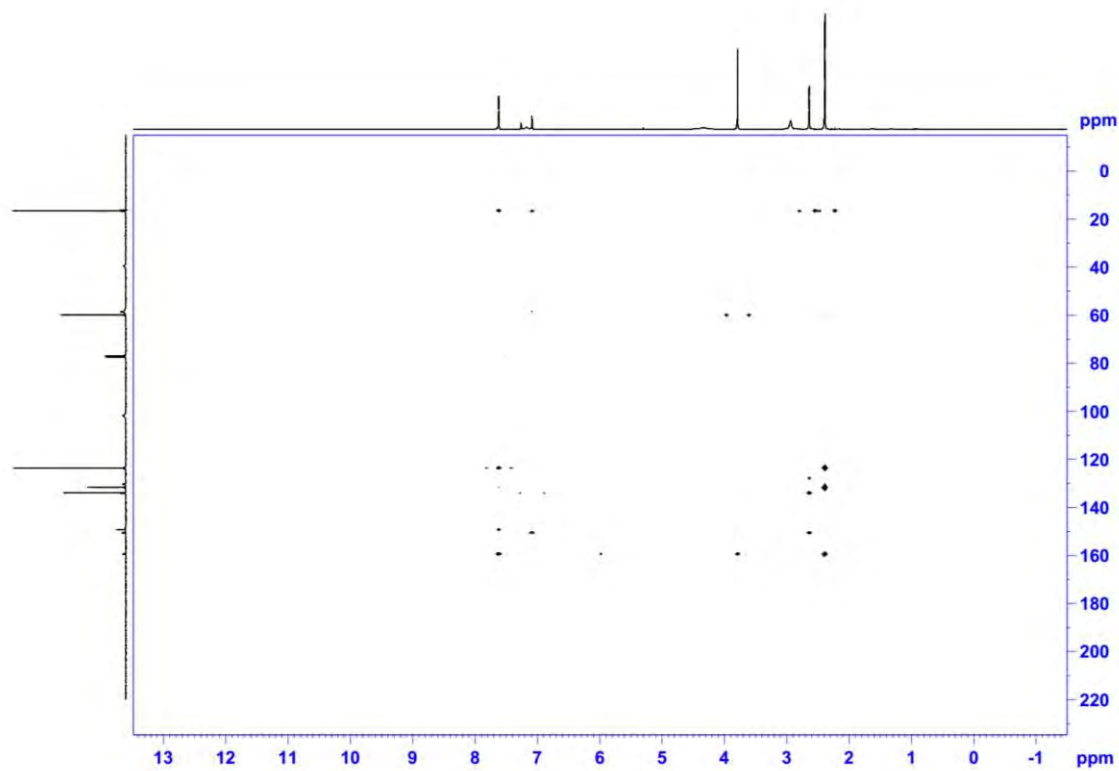
Compound 2, COSY (400 MHz, CDCl₃)



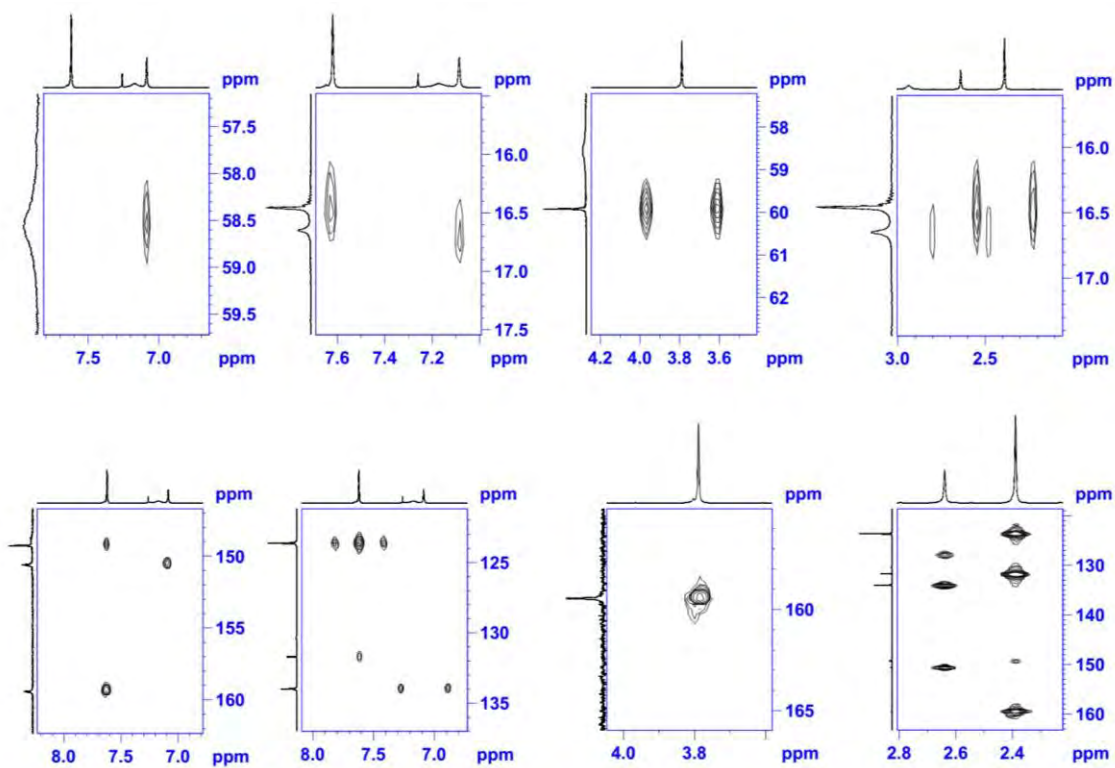
Compound 2, HSQC (400 MHz, CDCl₃)



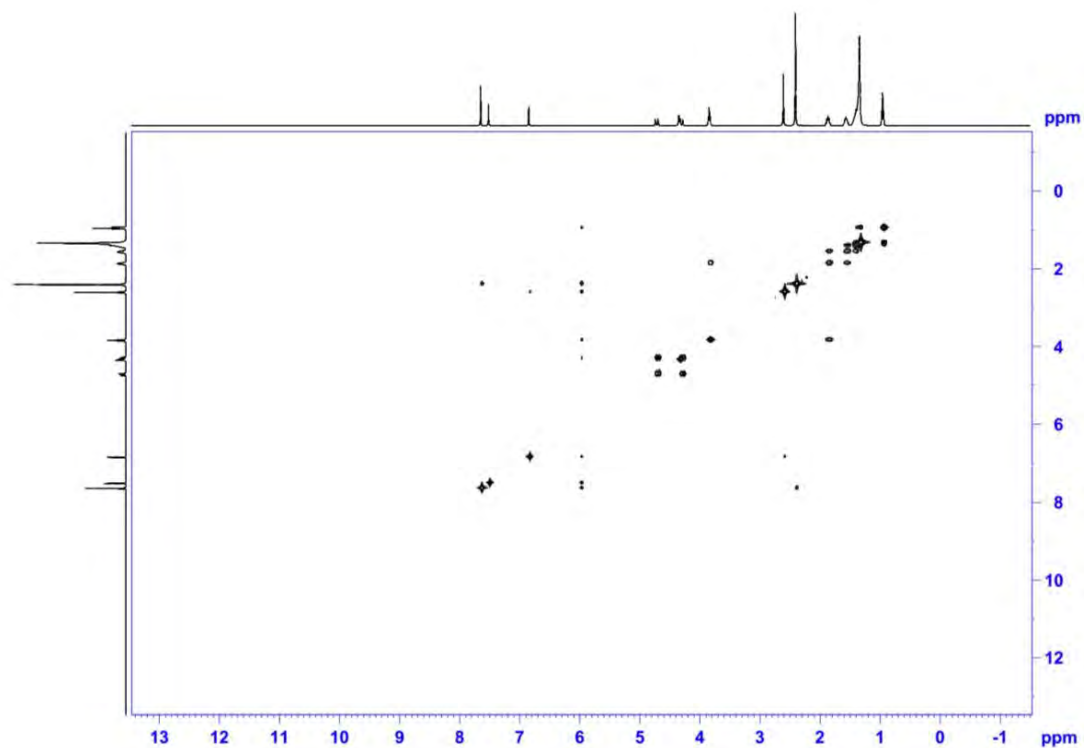
Compound 2, HSQC (400 MHz, CDCl_3)



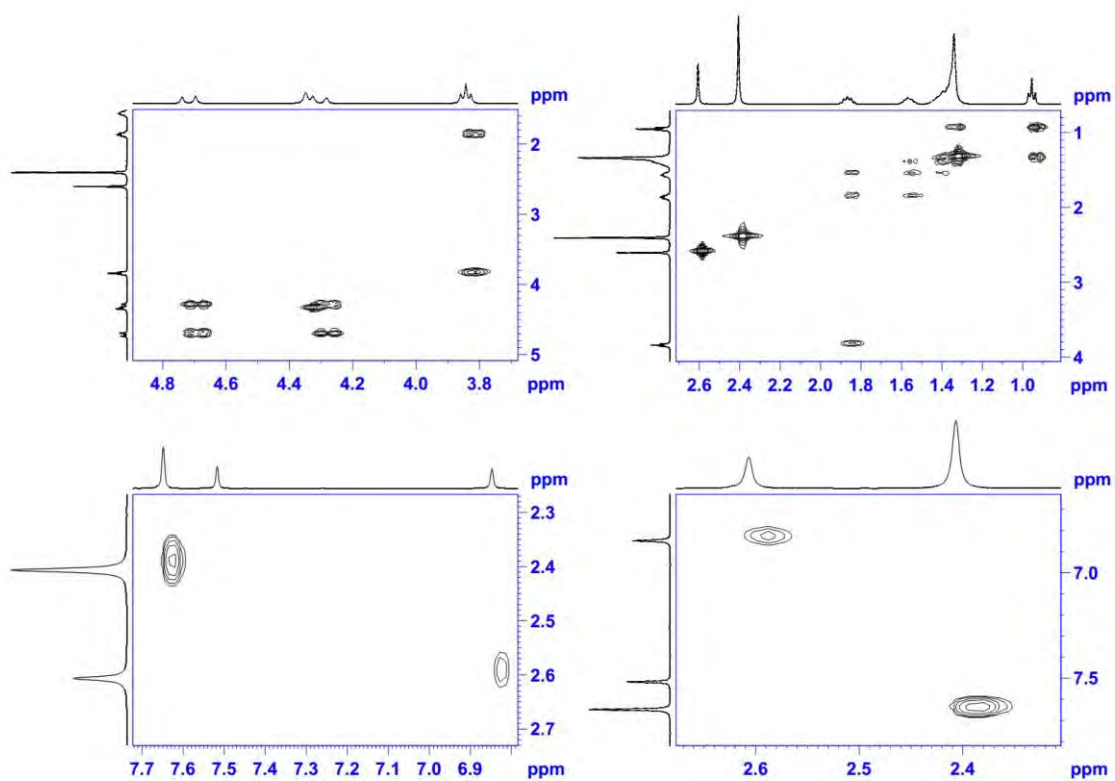
Compound 2, HMBC (400 MHz, CDCl_3)



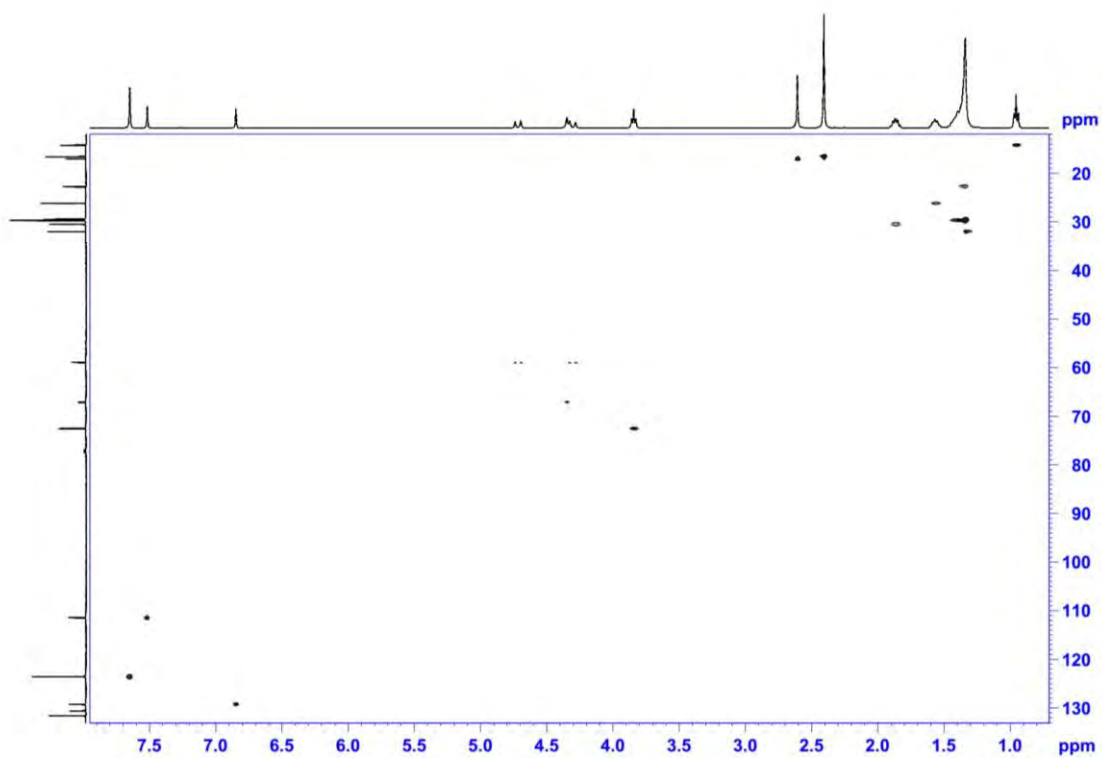
Compound 2, HMBC (400 MHz, CDCl_3)



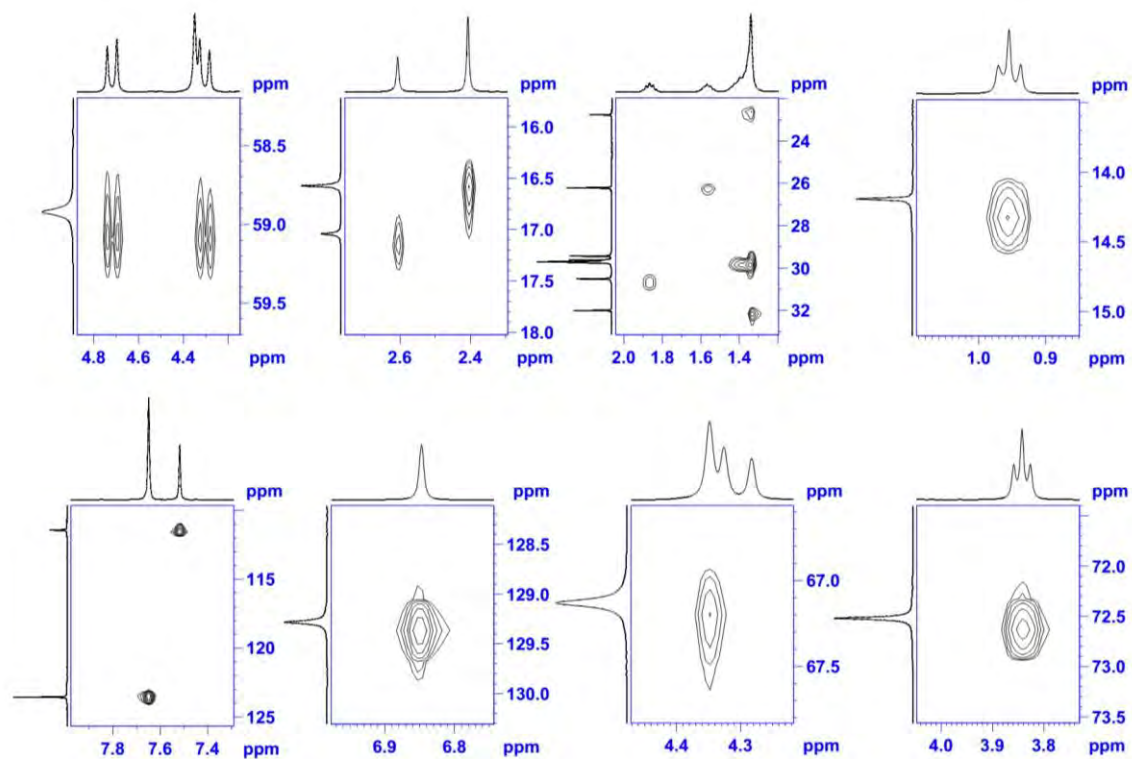
Compound 7, COSY (400 MHz, CDCl_3)



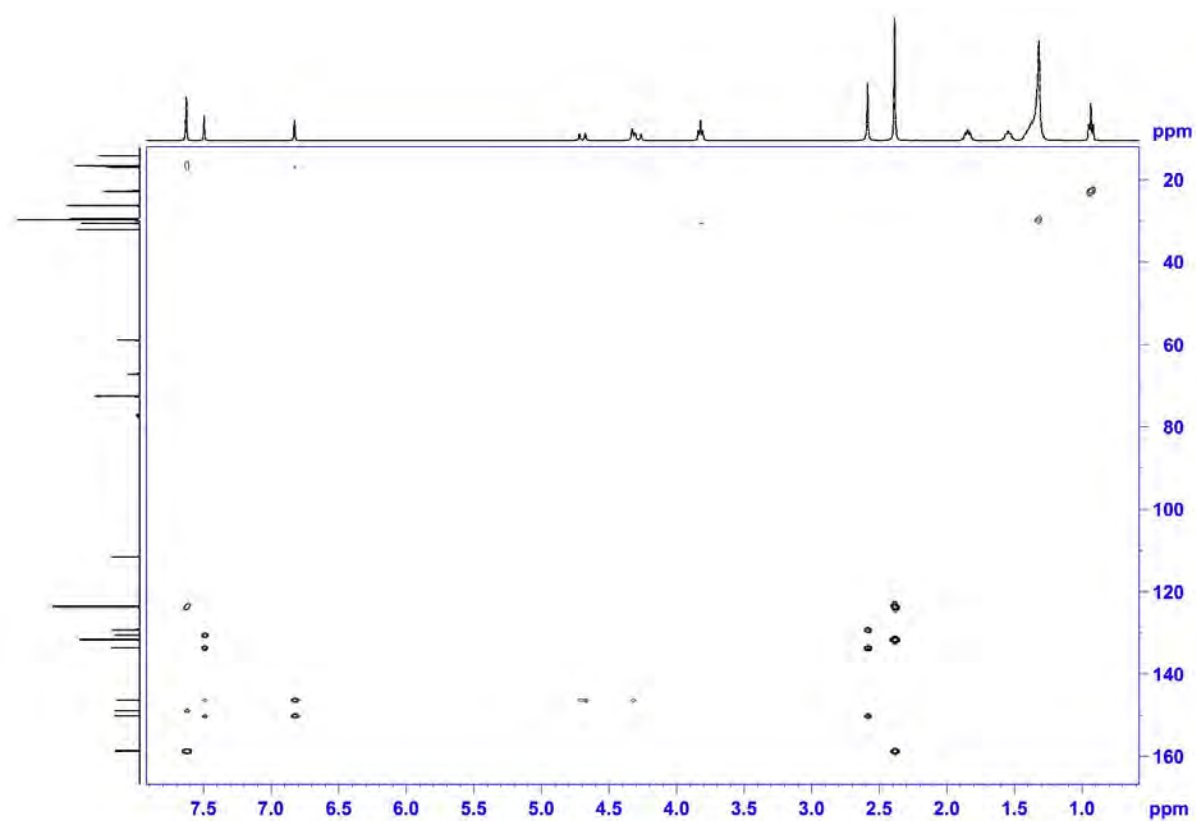
Compound 7, COSY (400 MHz, CDCl_3)



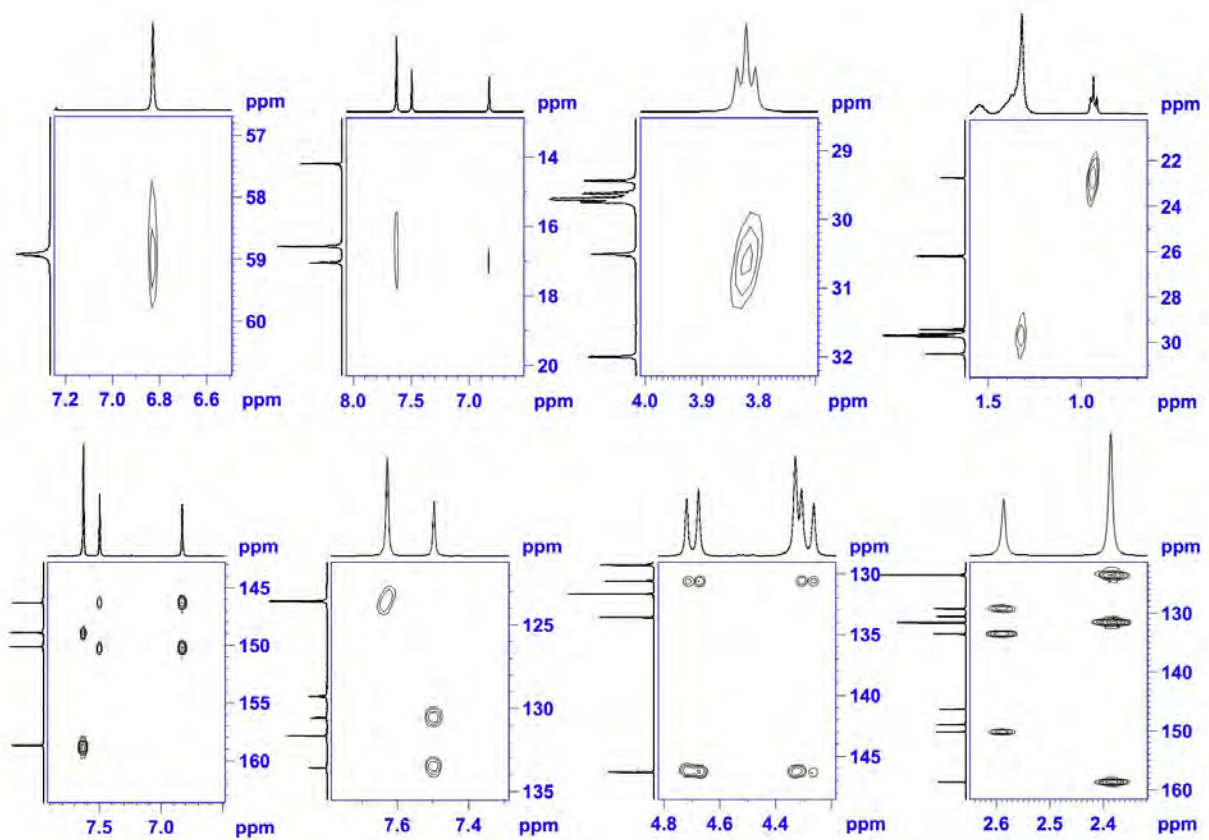
Compound 7, HSQC (400 MHz, CDCl_3)



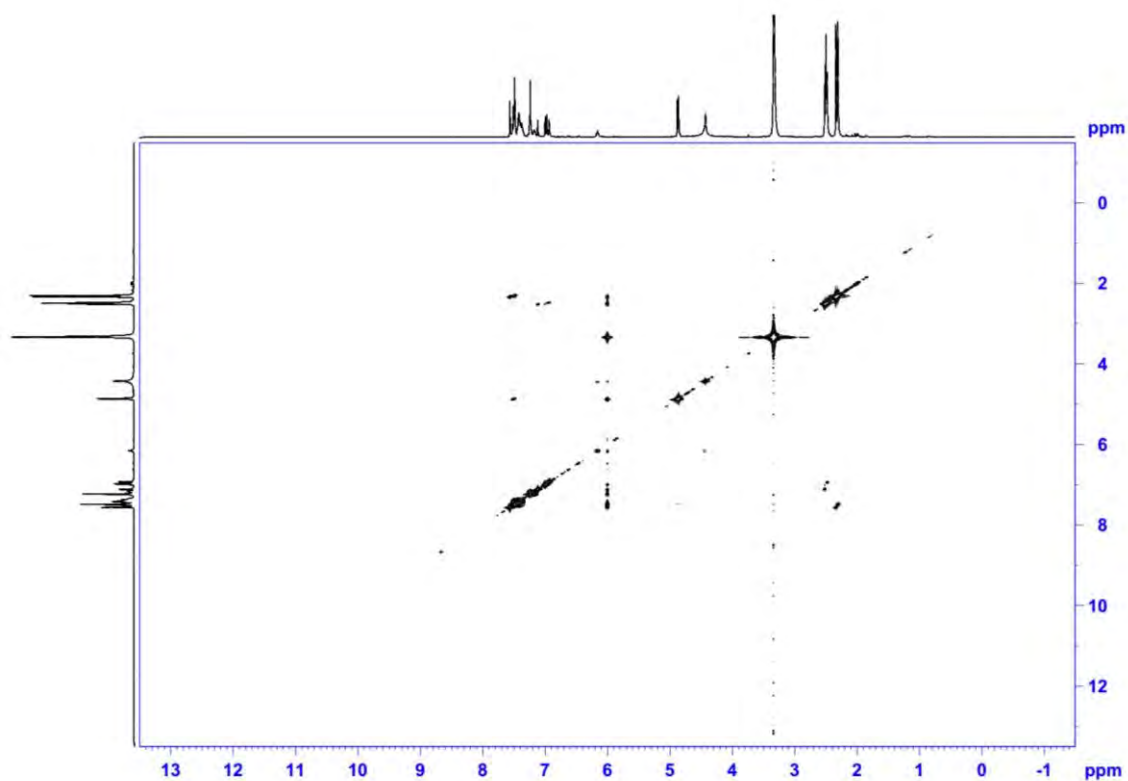
Compound 7, HSQC (400 MHz, CDCl_3)



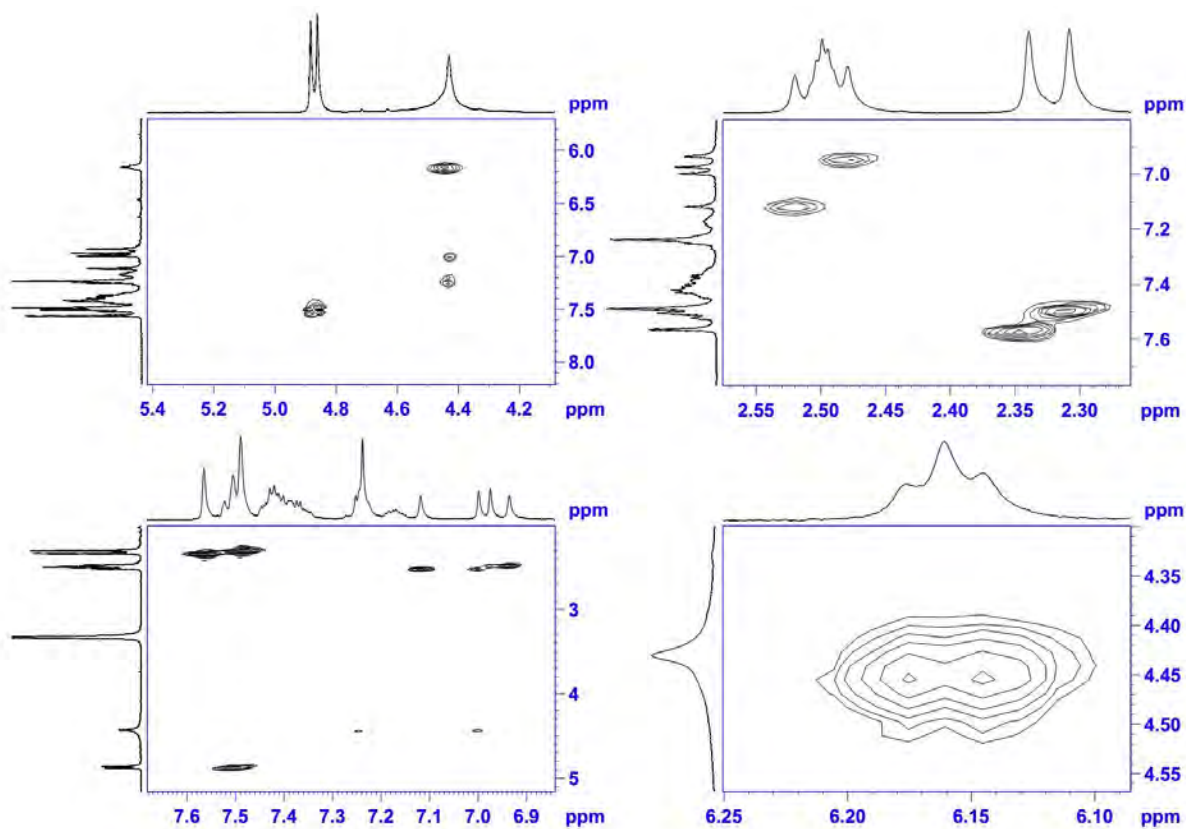
Compound 7, HMBC (400 MHz, CDCl_3)



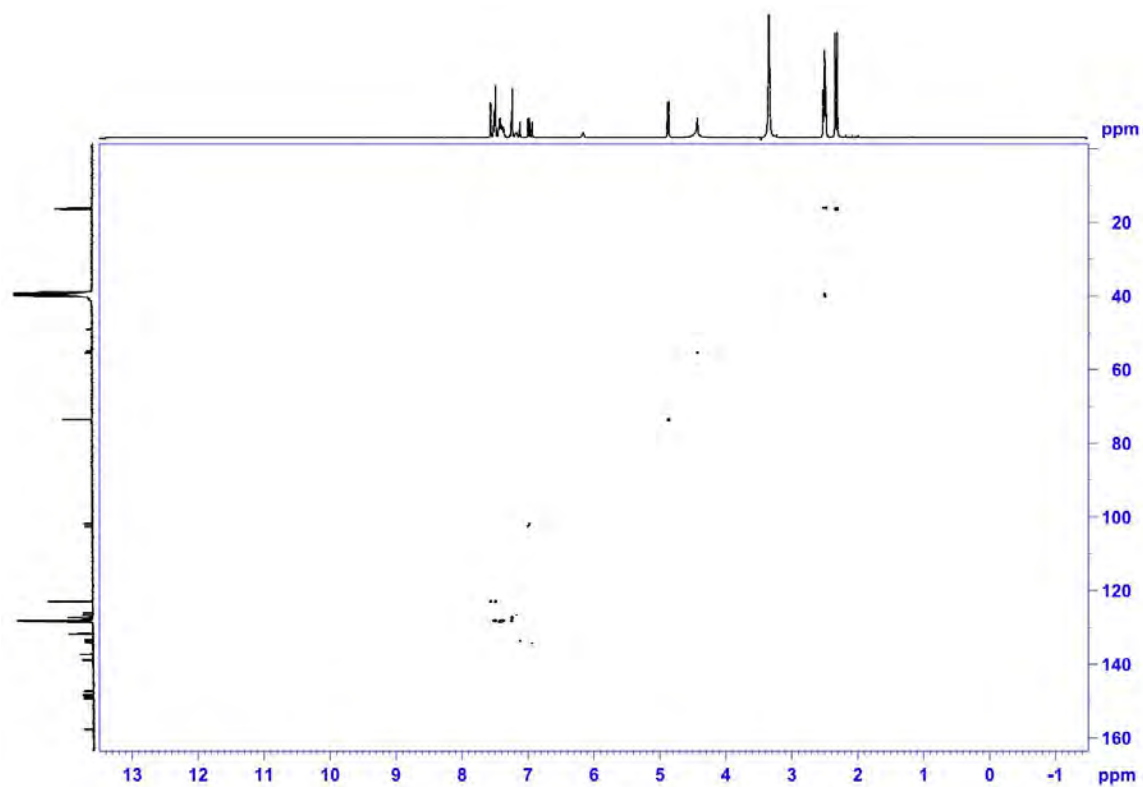
Compound 7, HMBC (400 MHz, CDCl₃)



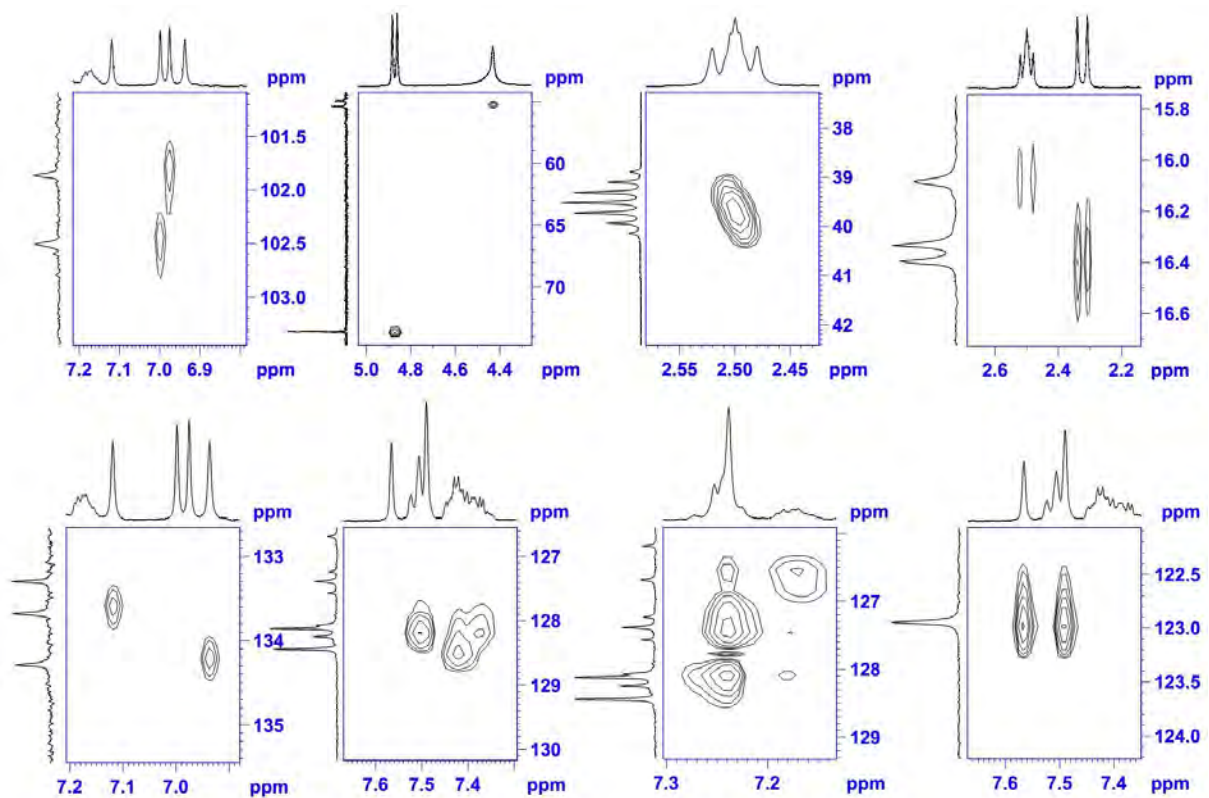
Compound 16, COSY (400 MHz, DMSO-*d*₆)



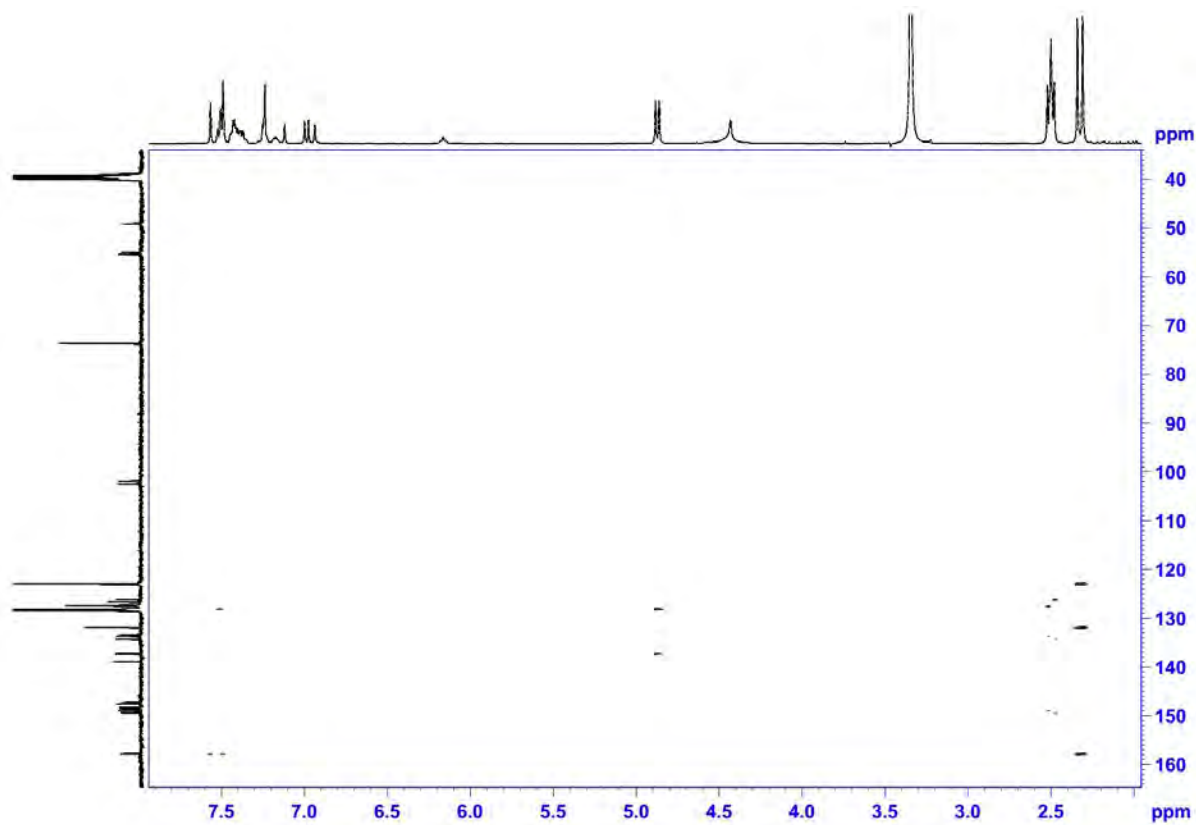
Compound 16, COSY (400 MHz, DMSO-*d*₆)



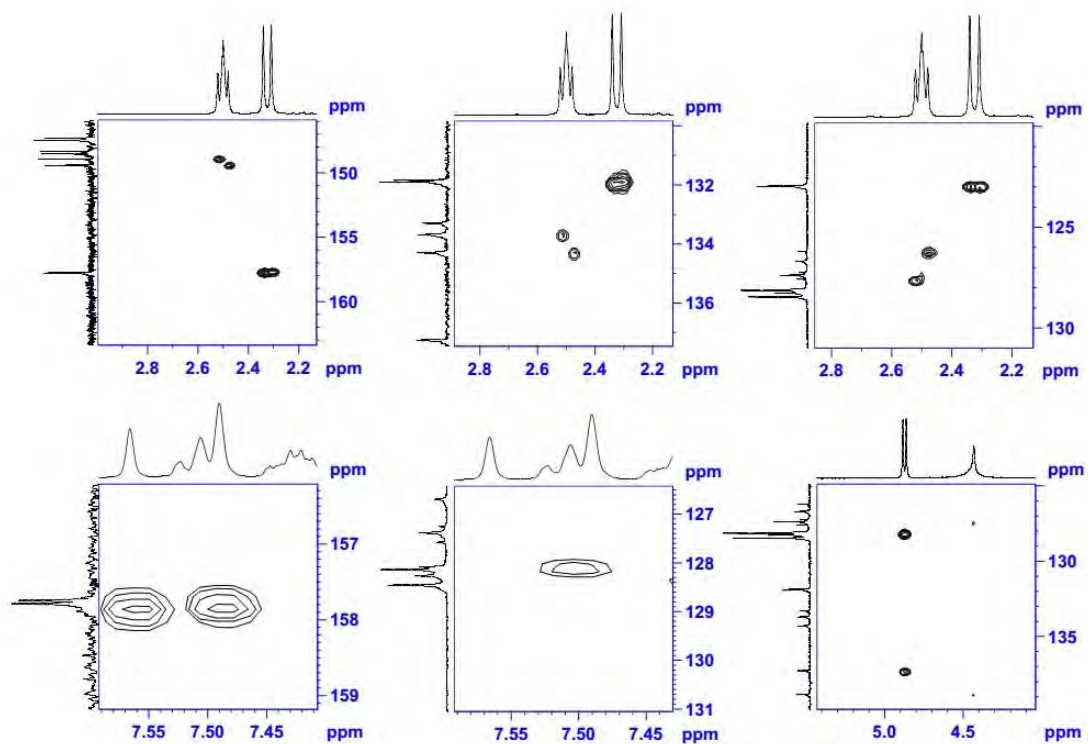
Compound 16, HSQC (400 MHz, DMSO-*d*₆)



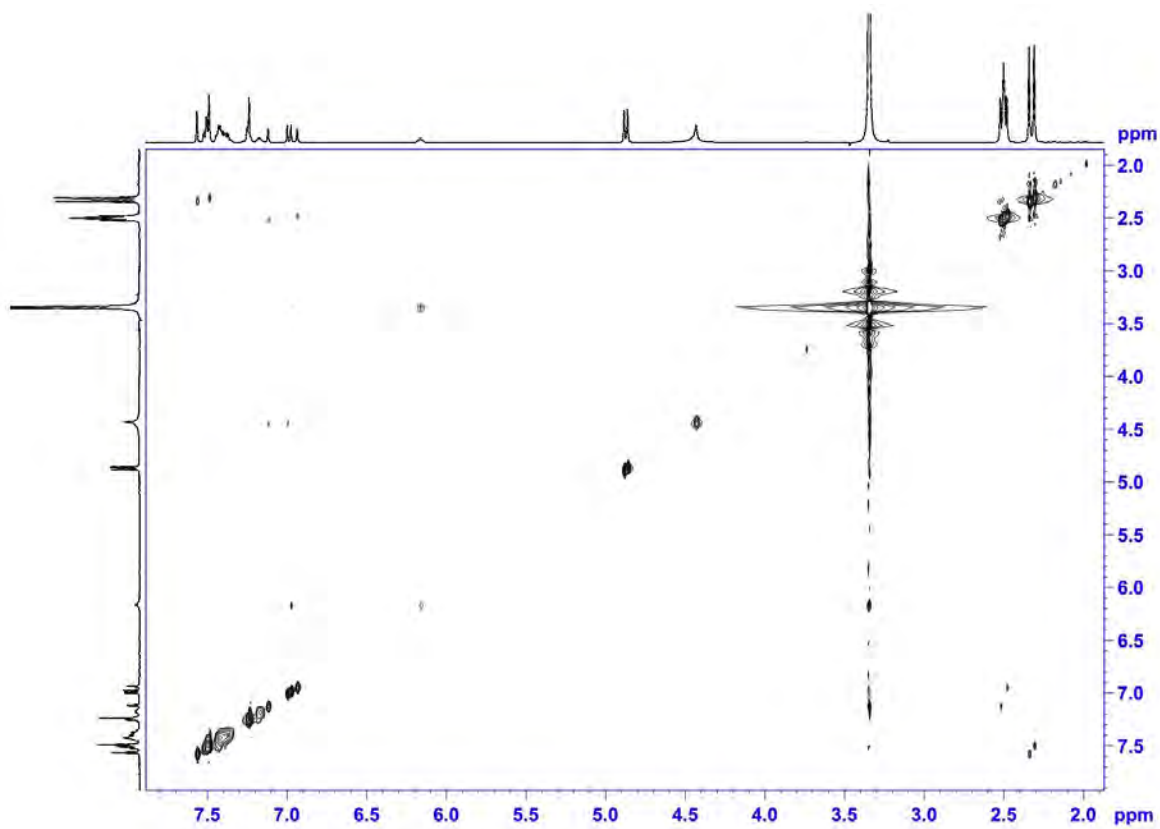
Compound 16, HSQC (400 MHz, DMSO-*d*₆)



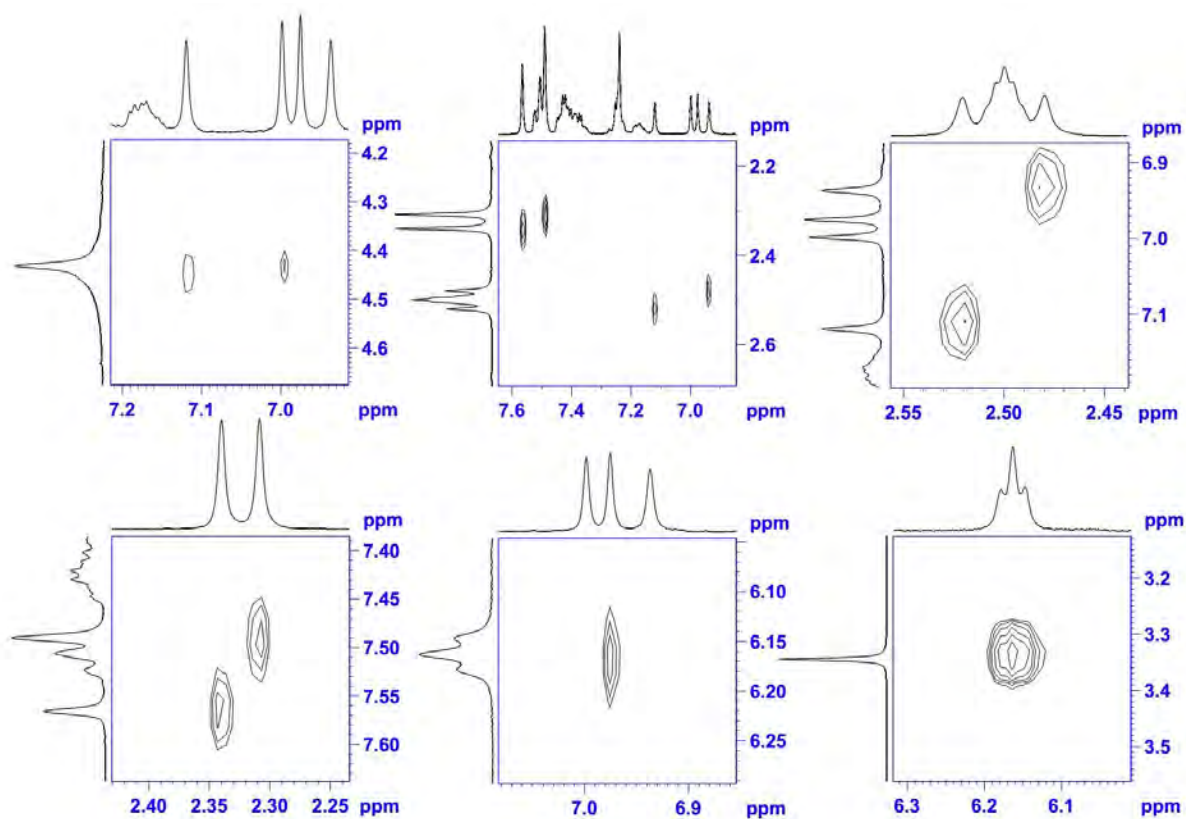
Compound 16, HMBC (400 MHz, DMSO-*d*₆)



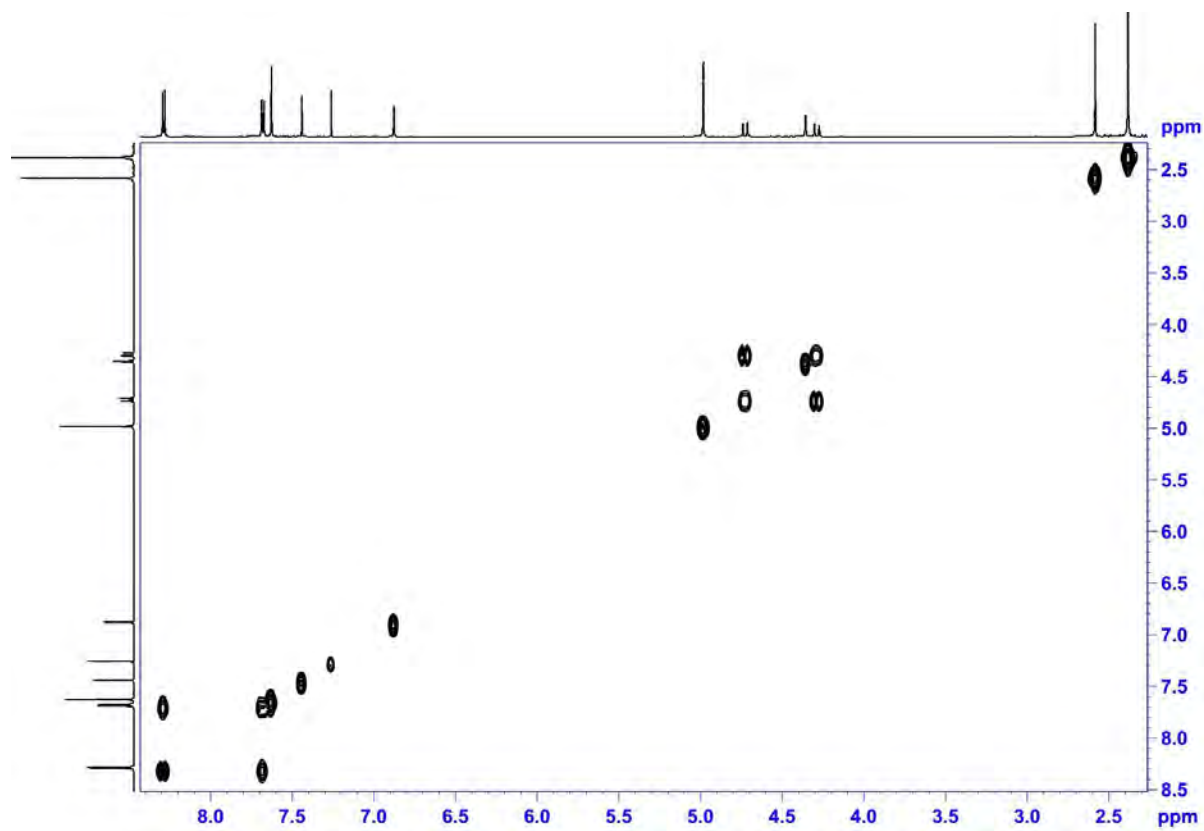
Compound 16, HMBC (400 MHz, DMSO-*d*₆)



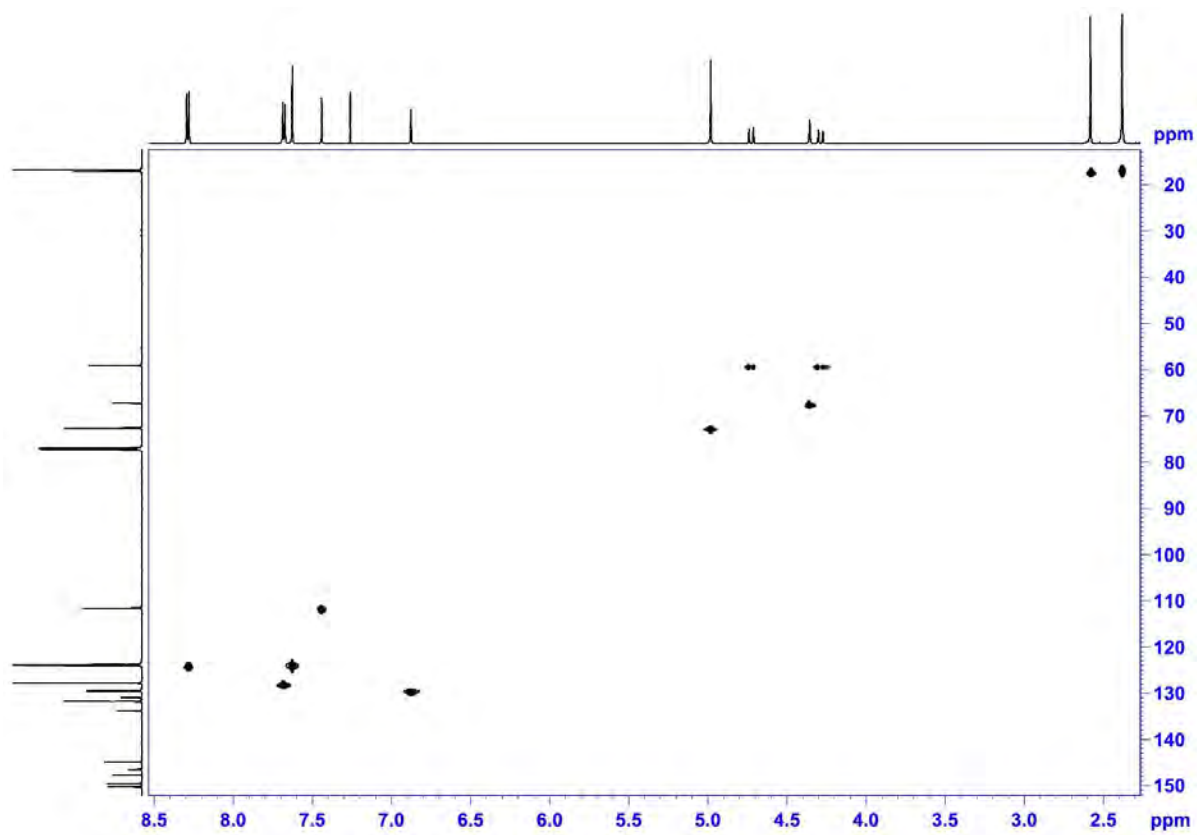
Compound 16, NOESY (400 MHz, DMSO-*d*₆)



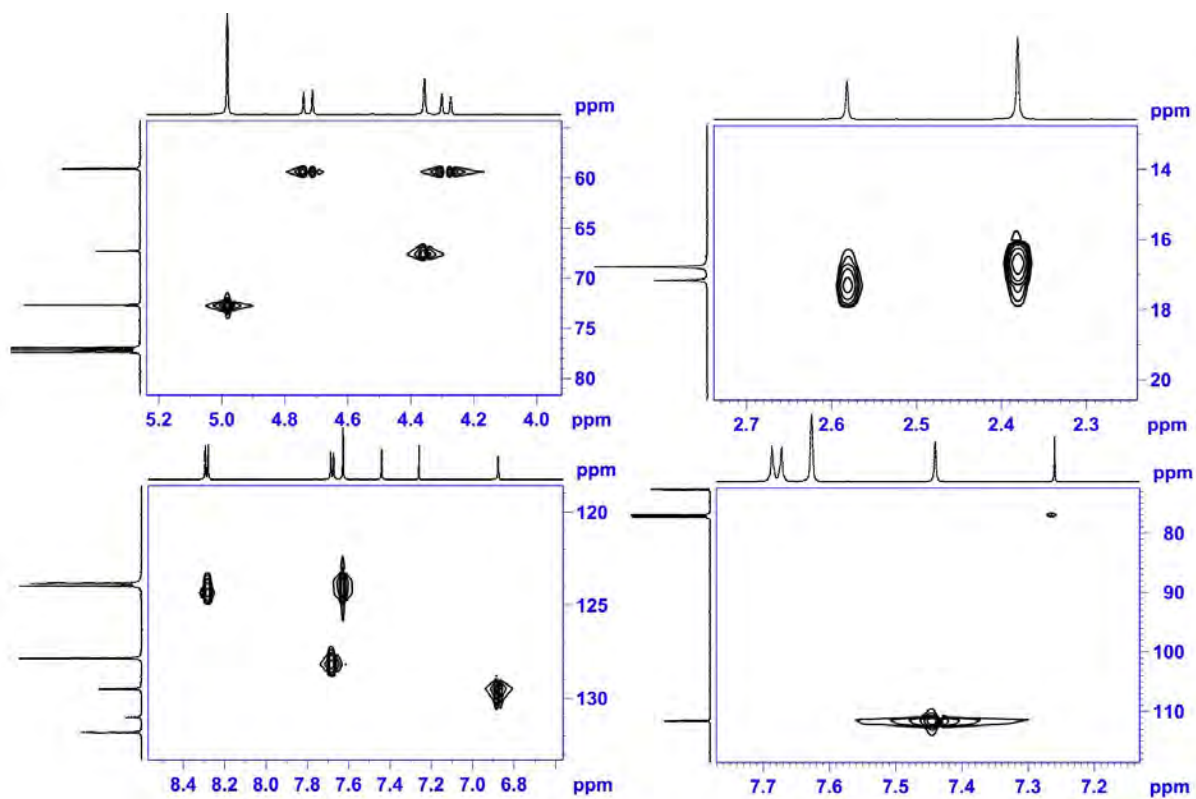
Compound 16, NOESY (400 MHz, DMSO- d_6)



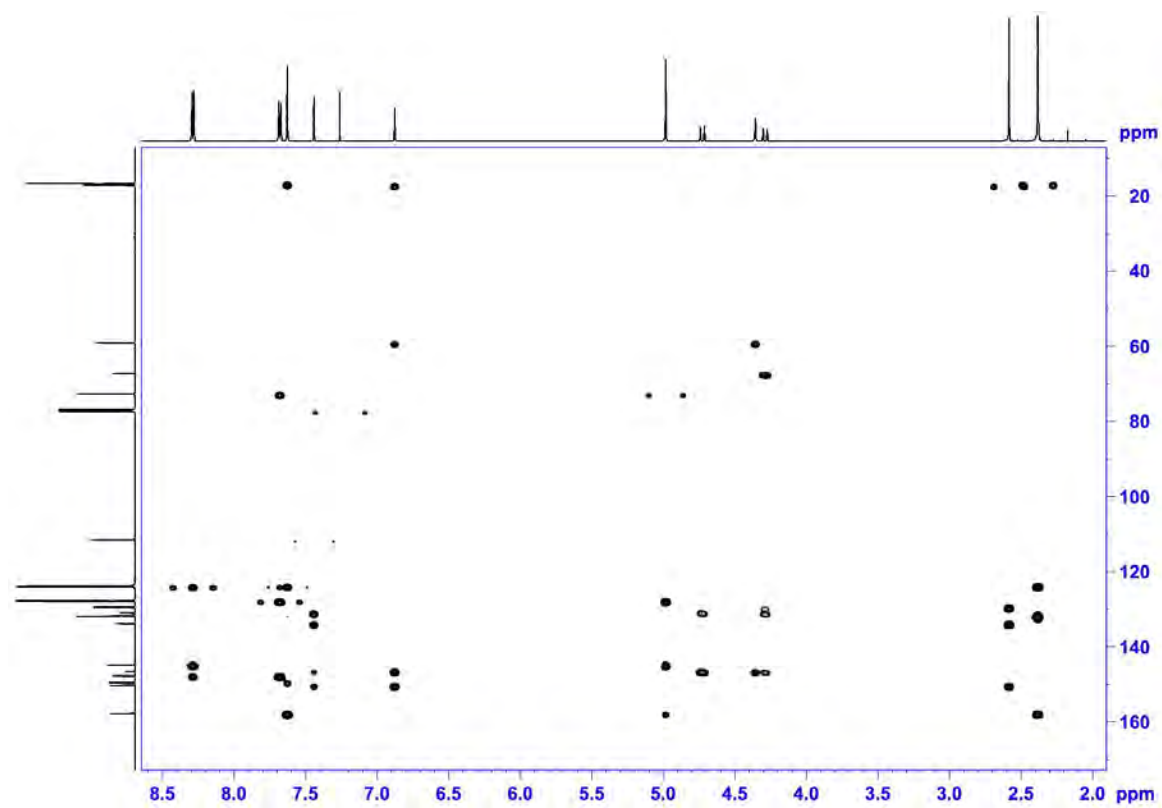
Compound 17, COSY (600 MHz, CDCl_3)



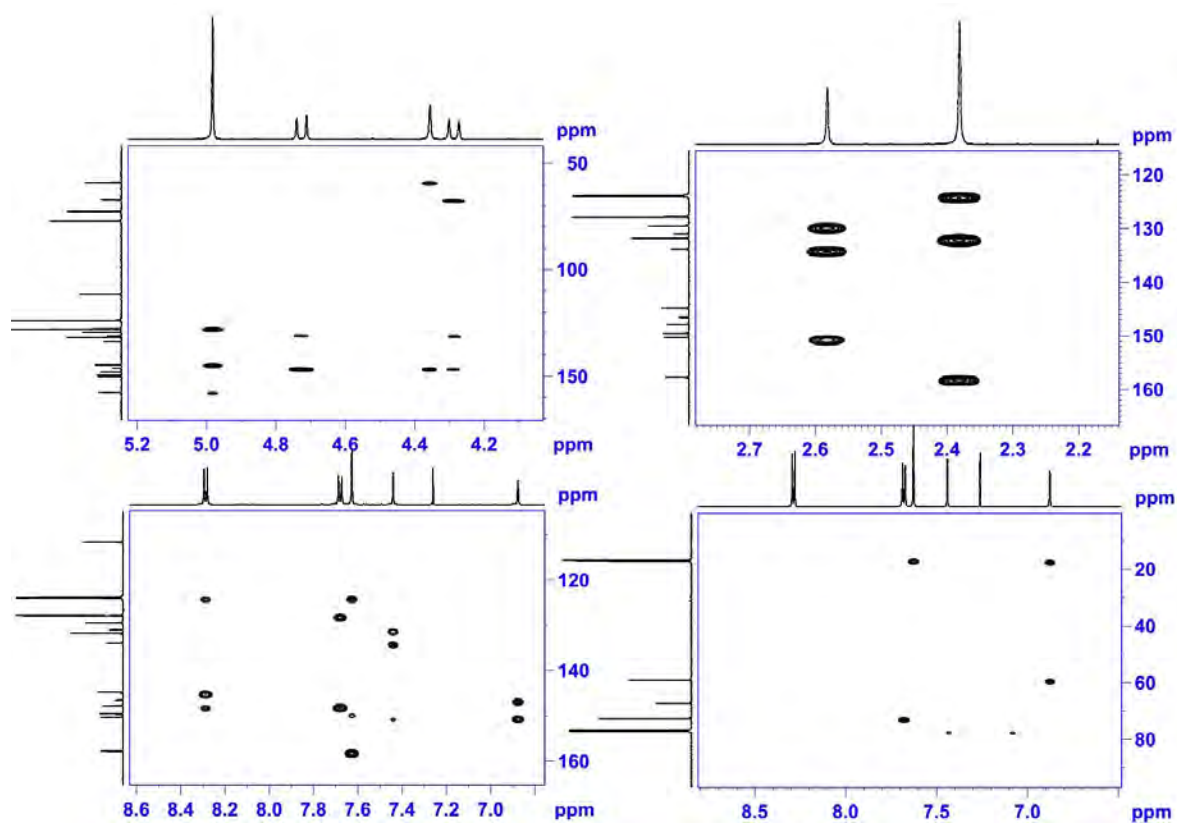
Compound 17, HSQC (600 MHz, CDCl_3)



Compound 17, HSQC (600 MHz, CDCl_3)

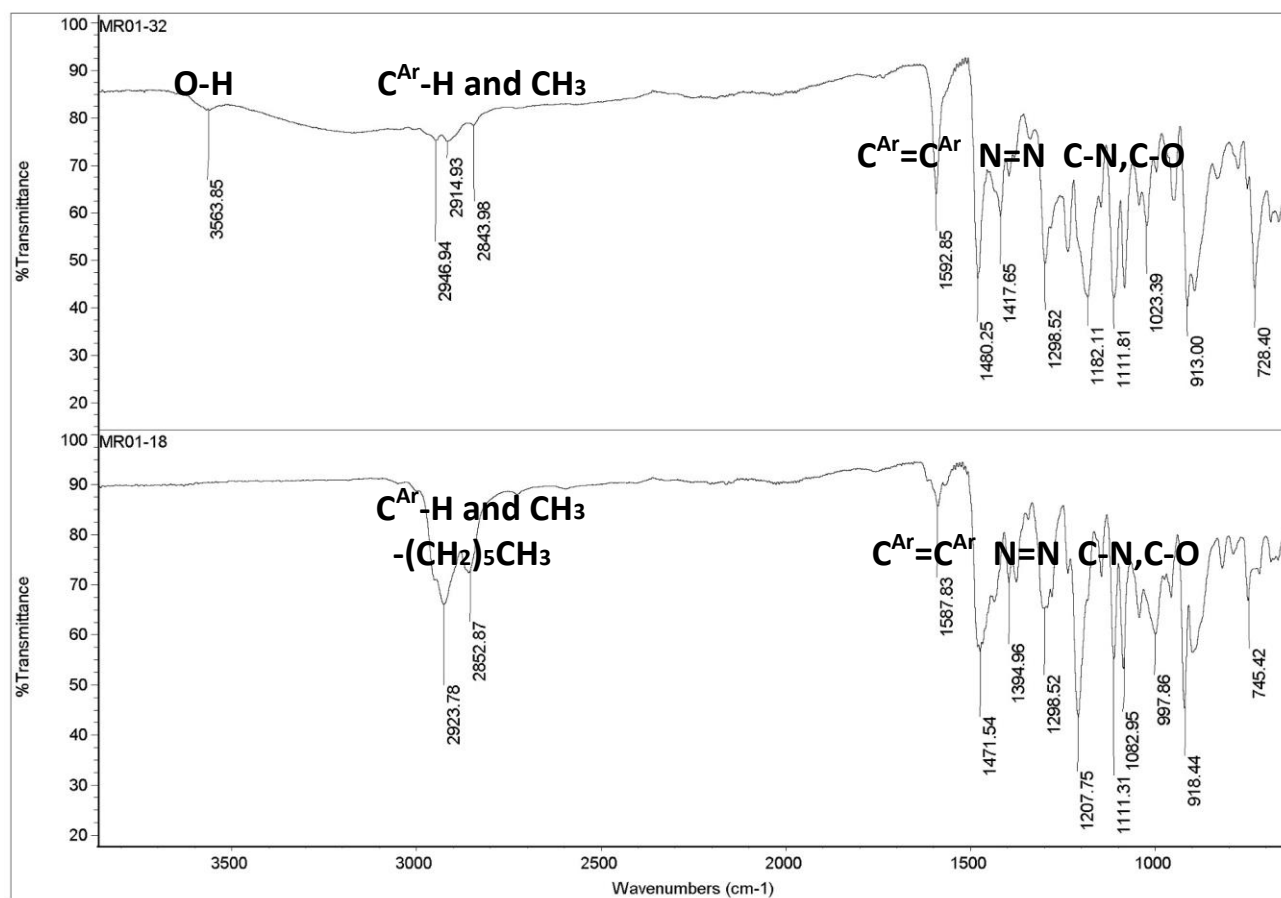


Compound 17, HMBC (600 MHz, CDCl₃)

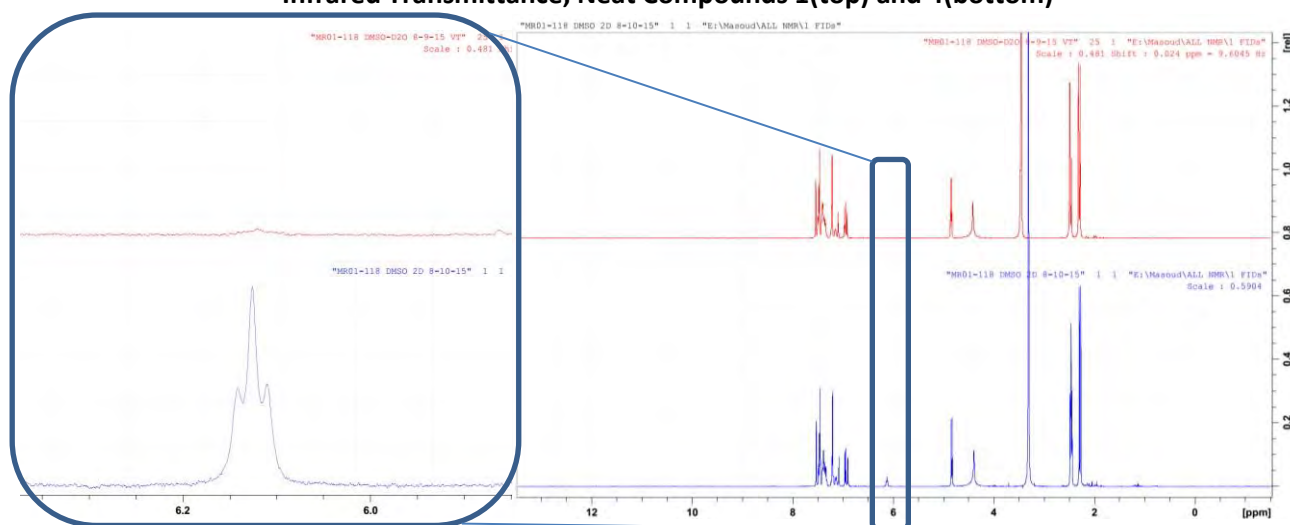


Compound 17, HMBC (600 MHz, CDCl₃)

Comparative Infrared and NMR Spectra



Infrared Transmittance, Neat Compounds 1(top) and 4(bottom)



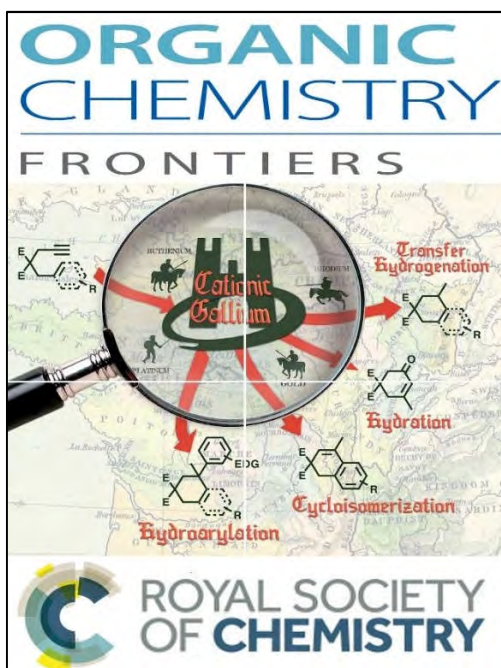
400 MHz ¹H NMR Spectra Compound 16 in, (DMSO-d₆ in blue and DMSO-d₆+D₂O in red)

Reference:

- (1) Rigol, S.; Beyer, L.; Hennig, L.; Sieler, J.; Giannis, A. *Org. Lett.* **2013**, 15, 1418-1420.

RESEARCH CHAPTER TWO

Paper II (Main Article)



Journal Impact Factor: 4.955

Disclaimer Notification

The following copyrighted material¹⁴ is reproduced by permission of the PCCP Owner Societies, on 7 June 2017, in accordance with the given rights to the authors by *The Royal Society of Chemistry* (RSC) on behalf of the editorial board of *Organic Chemistry Frontiers*. Any other use of the following material has to be explicitly authorised by the copyright holder of *Organic Chemistry Frontiers* © 2017 RSC.

Contact RSC for further information: Contracts-Copyright@rsc.org

Link to the original publication: <https://doi.org/10.1039/c6qo00653a>

RESEARCH ARTICLE



Cite this: *Org. Chem. Front.*, 2017, 4, 224

Received 23rd October 2016,
Accepted 14th November 2016

DOI: 10.1039/c6qo00653a

rs.c.li/frontiers-organic

Hünlich base derivatives as photo-responsive Λ -shaped hinges†

Masoud Kazem-Rostami*^a and Amirhossein Moghanian^{b,c,d}

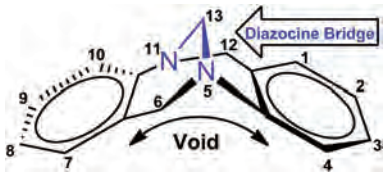
This article describes the synthesis and characterization of azo derivatives of the Hünlich base. The possession of modifiable extremities, a Λ -shaped core, and photo-responsive groups are features of these novel products. Such materials may provide a handy tool-kit including a set of photoswitches with a specific response to external stimuli.

Introduction

The bizarre arrangement of atoms in the tetracyclic scaffold of Tröger's Base¹ (TB) has resulted in the emergence of various interesting properties and enabled a plethora of applications. For instance, stereogenic nitrogen atoms located on the diazocine bridge (Table 1) generate chirality and the unique Λ -shaped void of these nano-sized² building-blocks. Due to the remarkable properties of the TB scaffold, its analogues have been utilized in membrane design,³ molecule recognition,^{4–9} assembly,¹⁰ and other applications.^{11–13} The unique shape of the TB scaffold has encouraged the idea of producing its azo analogues and introducing them as nano-sized photoswitchable hinges in this work.

A century ago, W. Hünlich had condensed formalin with an acidic solution of 4-methylbenzene-1,3-diamine and obtained an unknown product. His struggle with the elaboration of its structure remained futile due to the obsolete characterization methods of that era and his early death during WWI.¹⁴ In 2013, A. Giannis *et al.* not only uncovered the exact molecular structure of Hünlich's product, but also named it after him—"the Hünlich Base" (HB).¹⁴ Accordingly, a simple multigram-scale procedure, which effortlessly provides HB as an amine analogue of TB, has been reported. HB synthesis may not overtake previous reports on TB di-amino analogue pre-

Table 1 Synthesis of TB and its di-amino analogues



Author ^{Ref.}	Substituents ^a	Step(s) and condition(s)
Tröger ¹	2,8:CH ₃	i. CH ₂ O/HCl
Cibulka ¹⁸	1,7:NH ₂	i. (a); ii. (d); iii. Pd/H ₂
Cibulka ¹⁸	1,7:NH ₂ ; 2,8:Br; 4,10:Cl	i. (a); ii. (d); iii. Zn/AcOH
Try ¹⁶	1,7:NH ₂ ; 2,4,8,10:CH ₃	i. (a); ii. SnCl ₂ /EtOH
Try ¹⁶	2,8:NH ₂	i. DGA/PPA; ii. Pd/C, H ₂
Sergeyev ¹⁷	2,8:NH ₂	i. (a); ii. (b); iii. (c)
Lützen ^{10,19}	2,8:NH ₂ ; 4,10:CH ₃	i. (a); ii. Fe/AcOH
Lützen ¹⁹	3,9:NH ₂ ; 4,10:CH ₃	i. (a); ii. Fe/AcOH
Giannis ¹⁴	3,9:NH ₂ ; 2,8:CH ₃	i. CH ₂ O/H ₂ SO ₄
Sergeyev ¹⁷	4,10:NH ₂ ; 2,8:CH ₃	i. (a); ii. (b); iii. (c)
Cibulka ¹⁸	4,10:NH ₂	i. (a); ii. (d); iii. Pd/H ₂
Cibulka ¹⁸	4,10:NH ₂ ; 2,8:Br	i. (a); ii. (d); iii. SnCl ₂ /HCl
Lützen ²⁰	4,10:NH ₂ ; 2,8:CH ₃	i. (a); ii. nBuLi/TsN ₃ ; ii. NaBH ₄ /THF

^a Except protons. (a) Paraformaldehyde in trifluoroacetic acid, (b) Ph₂C=NH, *t*-BuONa, Pd₂(dba)₃ and BINAP, (c) HCl (aq) and (d) KNO₃/H₂SO₄. DGA: diglycolic acid and PPA: polyphosphoric acid.

paration due to the fact that in each report the amine groups are differently positioned on the main scaffold (Table 1). Nonetheless, considering the utilization of an inexpensive acid, the mild and less hazardous reaction conditions, and its single-step procedure, HB represents a valuable building block.

Formation of a diazocine bridge (trögeration reaction), as defined by Dolenský,¹⁵ is interrupted by the presence of additional amine groups to those considered to flank the bridge. HB synthesis is the only exception, where no interference occurs. Therefore, other TB di-amino analogues have been produced *via* the synthesis of nitro-¹⁶ or halogen-containing¹⁷ analogues,

^aDepartment of Chemistry and Biomolecular Sciences, Macquarie University, North Ryde, NSW 2109, Australia. E-mail: masoud.kazem-rostami@hdr.mq.edu.au, masoud.kr@gmail.com; Fax: +61-98508313

^bHarvard-MIT Division of Health Sciences and Technology, Massachusetts Institute of Technology, Cambridge 02139, MA, USA

^cMining and Metallurgical Engineering Department, Amirkabir University of Technology, 424 Hafez Ave., Tehran 15875-4413, Iran

^dBiomaterials Innovation Research Center, Division of Biomedical Engineering, Department of Medicine, Brigham and Women's Hospital, Harvard Medical School, Boston 02139, MA, USA

† Electronic supplementary information (ESI) available: 1 and 2D NMR, IR, MS, and UV-Vis spectra and the synthesis procedures. See DOI: 10.1039/c6qo00653a

which successfully accomplishes the trögeration reaction. Afterwards, the nitro or halogen groups of these precursors become respectively reduced to or replaced by amino groups to generate the desired TB di-amino analogues listed in Table 1.

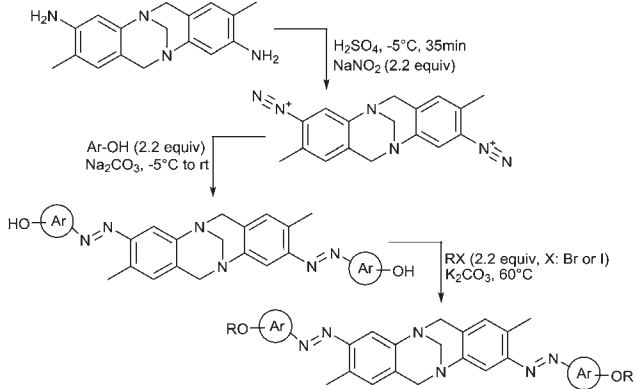
Converting a diamino compound to its azo derivatives results in having two photo-switchable units on the final products. These photoswitches change the shape of the molecule significantly upon receiving an external stimulant. This intense response is advantageous, *e.g.* in the case of applying such a material as a liquid crystal (LC) dopant, a lower concentration of it would be required to phototune the host LC. This helps to maintain physical properties of the host LC to be as desirable as expected. In addition, such symmetrical bisazo-compounds would be more useful for molecular recognition purposes or light-driven machine design. Having two photoswitchable moieties on HB's Λ -shaped scaffold means that the main structure resembles a pincer, made at the molecular scale. The claws of the pincer, which are the azo groups, start working upon receiving a certain wavelength of light. The claws' movement can be controlled by photo-isomerizing the azo groups. Photo-isomerization of the azo groups converts the thermally-stable photoisomer from *trans* to *cis* when the compound is illuminated by UV-light (~ 350 nm). Then, back-isomerization converts the *cis* to the *trans* gradually by undertaking thermal relaxation or more quickly when exposing the sample to a longer wavelength of light (within the visible range).

The addition of photo-responsive chiral materials to a liquid-crystalline host results in the enhancement of LCs' helical twisting power and the emergence of photo-tunable properties.²¹ The products presented in this work each have two photo-responsive groups and a resolvable TB core, as well as two modifiable phenolic extremities, which all sound promising for acting as LC dopants. These phenol groups confer the capability of hydrogen-bond interaction which would result in a wide-range tuning property.²² Furthermore, these phenol groups can also be alkylated to adjust the melting point, miscibility,²³ and dispersion of these molecules in a LC host, similar to those azo derivatives of spiroes,^{24–29} biphenyls^{26,28,29} or binaphthyls^{22,23,30,31} that have been already employed for such applications. To match up the solubility of these materials with their host LC, various alkyl chains are usually added to their structures. Considering that the alkylation of phenolic extremities may also lead to unwanted alkylation of the nitrogen atoms located on the diazocine bridge, this controversy was put to the test. To help alkylation of the phenol groups, this step was performed in the presence of a mineral base to turn them into phenoxy groups, which are more reactive than the bridges' tertiary hindered amine groups. To our delight, the alkylated derivatives of these materials were obtained in good yields (Table 2).

Results and discussion

In this study the starting material, freshly produced HB, was diazotized and coupled with a variety of phenols to afford the azo products listed in Table 2.

Table 2 The products' preparation



Compound	R	Ar ^a	Time (h)	Yield %	λ_{\max}
1	H		24	50	353
1a	Butyl		6	77	347
1b	Hexyl		12	72	346
1c	Octyl		12	75	346
2	H		15	90	361
3	H		15	~2	361
4	H		5	81	365
4a	Hexyl		12	88	349
5	H		4	60 ^b	384
5a	Hexyl		18	76	368
6	H		3	80	396
6a	Hexyl		48	58	370
7	H		5	70 ^b	NA ^b
8	H		5	70	408
8a	Hexyl		24	45	407
9	H		5	75	493
9a	Hexyl		24	52	393

^a The dots indicate where the azo group attaches. ^b Please check the ESI.

To improve the yield of the diazotization reaction and minimize decomposition of the produced bis-diazonium sulfate, this step was performed at a slightly lower temperature (-5 °C) than usual (0 °C) and with a higher concentration of sulfuric acid to lower the freezing point of the reaction mixture.³² In addition, sodium carbonate was used (instead of NaOH) in the coupling reaction to prevent an uncontrolled rise of temperature when merging the two acidic and alkaline solutions.

As expected, the produced bis-diazonium cation, as an electrophile, attacked the most electron-rich positions, which are *para/ortho* to the phenoxy groups, and the less hindered ones preferably, to generate these new products (Table 2).

The corresponding phenols in the preparation of **1** and **4–6** provide only one site for hosting the electrophiles; hence, these reactions resulted in a single product. Nonetheless, attempts at the synthesis of the 2nd compound led to cogeneration of the 3rd as a side-product (almost 2%). The negligible ratio of produced compound **3** compared to **2** may prove how effectively the phenoxy group enriches the electron density of the *para* rather than the two available *ortho* positions. Fortunately, the small differences between the **2**, **3** and **4** structural isomers vary their retardation factors enough to successfully separate them *via* chromatography.

In the case of the 7th entry, although the crude product signified the formation of a considerable amount of the expected compound, it was not retrieved from the chromatography columns and hence purification failed. It is postulated that the six phenol groups bind the product to the applied stationary phases. Similarly, the binding or degradation of **5** during column chromatography was considerable. Despite many attempts to find alternative ways to purify these two products and skip liquid chromatography, a shortcut was only found to purify **1**. Interestingly, purification of **1** through liquid-liquid extraction was achieved due to the fact that the most common impurity of the azo-coupling reaction is plausibly decomposed diazonium, which forms self-coupled molecules that hence leave some of the phenols unreacted. On one hand, the self-coupled molecules, which are rationally massive, are less likely to dissolve in a moistened organic solvent like 2-butanone. On the other hand, the chloro groups enhance the acidity of phenols, which facilitates the transfer of the unreacted 2,6-dichlorophenol to a basic-aqueous phase; meanwhile **1** remains in the organic layer due to its large hydrophobic structure and can be isolated as a pure compound.

Methylene groups of the diazocine ring prevent the resonance of TB aromatic moieties by bending the main scaffold around 90 degrees. This further explains why spectral properties of the chromophores appear almost identical³³ before and after being attached to a TB scaffold. As described, compounds **1–9** revealed a wavelength of maximum absorption almost identical to single chromophores (Fig. 1). Different phenols were employed in the design of **1–9** to vary their maximum wavelength of absorption and cover a broad range of the UV-Vis spectra. These products are expected to provide a handy tool-kit including a set of photoswitches with a specific response to external stimuli and various photo-isomerization rates (Fig. 2 and 3), molecular geometries and capacities of the voids (Table 2).

TB and its analogues have been resolved through the precipitation of diastereomeric salts,² the formation of diastereomers,¹⁴ high performance liquid chromatography (HPLC)³⁴ and stereo-selective crystallization with or without³⁵ the employment of chiral discriminators.³⁶ The chiral resolution of HB has also been achieved through the preparation of its

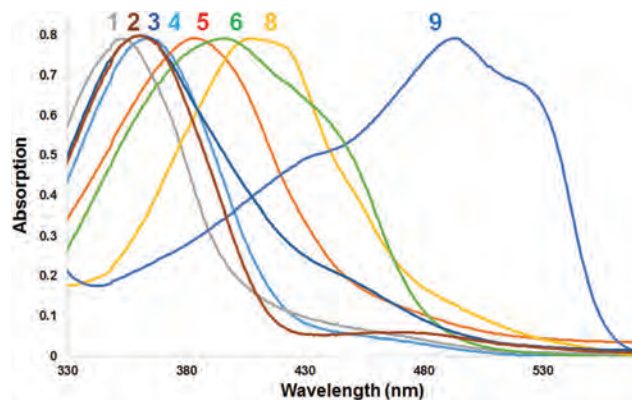


Fig. 1 UV/Vis absorption spectra of **1–6**, **8** and **9** in EtOAc.

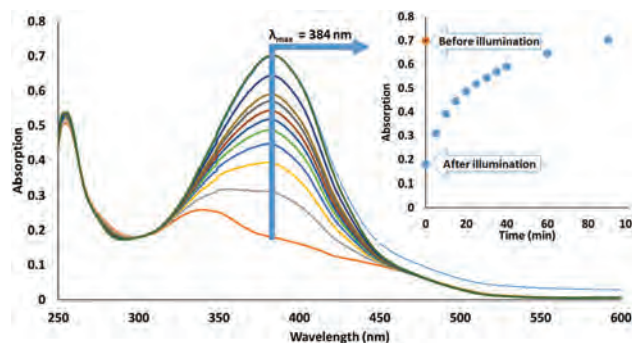


Fig. 2 Monitoring the photo-isomerization of **5** using UV/Vis.

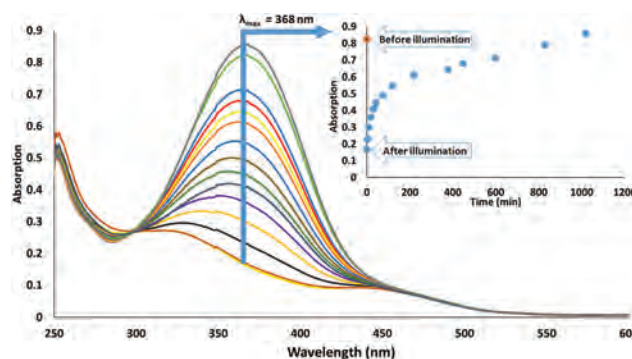
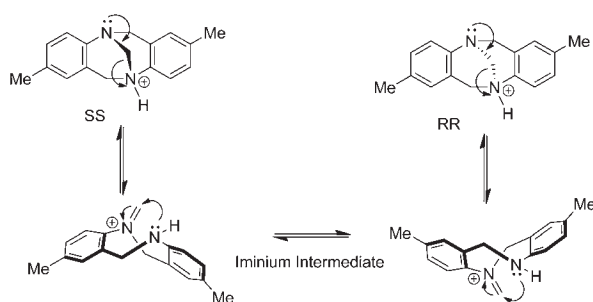


Fig. 3 Monitoring the photo-isomerization of **5A** using UV/Vis.

phenylalanine derivatives, separation of the obtained diastereomers using HPLC and then the basic hydrolysis of each one separately to obtain a single enantiomer.¹⁴ Unfortunately, such enantiomers in an acidic environment undergo racemization through the formation of an iminium intermediate (Scheme 1). Therefore, using one enantiomer as the starting material for producing its azo derivatives results in a racemate due to the acidic conditions of the diazotization reaction. On one hand, this racemization can be disadvantageous, as described; however, on the other hand, it can be taken as an advantage in order to prepare single enantiomers of TB



Scheme 1 Brønsted acids racemize Tröger's base.^{14,36}

analogues from racemates through crystallization-induced asymmetric enantiomer transformation in the presence of a chiral acid. A simple test was conducted to assess the chiral resolution of the products through the formation of an iminium intermediate, as described by Jameson *et al.*;³⁶ however, the focus of this work still remains on the synthesis and characterization. To put this to the test, initially **4** was alkylated to prevent the phenol groups interrupting the resolution process. Afterwards, the alkylated compound **4A** was refluxed in a solution of a single enantiomer of *O,O'*-dibenzoyl-tartaric acid in 1,2-dichloroethane and gradually cooled down. After rigorous work up using NaOH (aq) and ensuring total hydrolysis and elimination of the tartaric acid residues, the obtained partially-resolved product showed optical rotation. Although none of the crystallization conditions were optimized, achieving this partial resolution can be taken as proof of the concept.

Experimental

All the detailed preparation, synthesis and purification procedures are available in the ESI.†

Conclusions

In conclusion, the preparation of diamino analogues of Tröger's base is briefly reviewed, as well as the conversion of the Hünlich base to its bis-azo derivatives. We also highlighted that depending on which of these diamino precursors is chosen, the photoswitchable groups can be differently positioned on the TB scaffold. To simplify the production of the azo-derivatives, the Hünlich base was chosen as a building block, diazotized and coupled with several substituted phenols. The diverse design of these products resulted in the obtaining of various properties such as a different maximum wavelength of absorption, photo-isomerization rate, and capacity of the void. Tracking the photo-isomerisation of the selected products proved a totally repeatable and reversible process, in agreement with the NMR results, showing no signs of photo-degradation. Therefore, these new products can be considered as a handy tool-kit of Λ -shaped nanosize photo-

switches. Furthermore, these products have phenolic extremities that can be altered to form other functional groups and contribute to the preparation of photo-responsive copolymers or liquid crystal elastomers. These phenolic extremities can also be considered as interactive sites in molecular recognition studies, or attachment sites in molecular assembly. In addition, modification of the TB strap³⁷ may provide further attachment sites. Hence, these can be readily attached to porphyrins, peptides, DNAs, nanotubes, fullerenes, or even polymers to contribute to the design of novel light-driven molecular machines, photo-alignment films, smart drug-delivery systems and even liquid crystal displays.

Acknowledgements

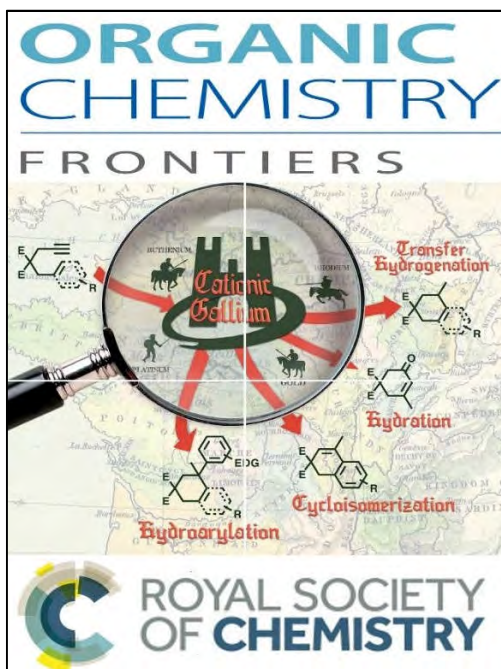
To pay tribute to our great teachers, this paper is dedicated to doctor Jennifer Rowland (Dean-HDR office, Macquarie University, Australia) and professor Ardeshtir Khazaei (Department of Chemistry, Bu-Ali Sina University, Iran). The corresponding author appreciates the Australian Government for awarding him with IPRS-2014004, Macquarie University for APA/HDR43010477 and PGRF2016R2-1672525 funds, and Mrs S. Kazem-Rostami for the graphics design.

Notes and references

- 1 J. Tröger, *J. Prakt. Chem.*, 1887, **36**, 225–245.
- 2 S. Sergeyev, *Helv. Chim. Acta*, 2009, **92**, 415–444.
- 3 Z. Wang, D. Wang, F. Zhang and J. Jin, *ACS Macro Lett.*, 2014, **3**, 597–601.
- 4 S. Satishkumar and M. Periasamy, *Tetrahedron: Asymmetry*, 2009, **20**, 2257–2262.
- 5 S. Goswami, K. Ghosh and S. Dasgupta, *J. Org. Chem.*, 2000, **65**, 1907–1914.
- 6 J. Adrian and C. Wilcox, *J. Am. Chem. Soc.*, 1989, **111**, 8055–8057.
- 7 J. Adrian and C. Wilcox, *J. Am. Chem. Soc.*, 1992, **114**, 1398–1403.
- 8 E. M. Boyle, S. Comby, J. K. Molloy and T. Gunnlaugsson, *J. Org. Chem.*, 2013, **78**, 8312–8319.
- 9 M. Valík, R. M. Strongin and V. Král, *Supramol. Chem.*, 2005, **17**, 347–367.
- 10 U. Kiehne, T. Weilandt and A. Lützen, *Org. Lett.*, 2007, **9**, 1283–1286.
- 11 A. Tatar, J. Cejka, V. Kral and B. Dolensky, *Org. Lett.*, 2010, **12**, 1872–1875.
- 12 S. Sergeyev and F. Diederich, *Angew. Chem., Int. Ed.*, 2004, **43**, 1738–1740.
- 13 M. Havlik, V. Kral, R. Kaplanek and B. Dolensky, *Org. Lett.*, 2008, **10**, 4767–4769.
- 14 S. Rigol, L. Beyer, L. Hennig, J. Sieler and A. Giannis, *Org. Lett.*, 2013, **15**, 1418–1420.
- 15 M. Havlík, V. Král and B. Dolenský, *Org. Lett.*, 2006, **8**, 4867–4870.

- 16 M. D. H. Bhuiyan, A. B. Mahon, P. Jensen, J. K. Clegg and A. C. Try, *Eur. J. Org. Chem.*, 2009, 687–698.
- 17 D. Didier and S. Sergeyev, *Tetrahedron*, 2007, **63**, 3864–3869.
- 18 J. Sturala and R. Cibulka, *Eur. J. Org. Chem.*, 2012, 7066–7074.
- 19 T. Weilandt, U. Kiehne, J. Bunzen, G. Schnakenburg and A. Lützen, *Chem. – Eur. J.*, 2010, **16**, 2418–2426.
- 20 A. Jarzebski, C. Bannwarth, C. Tenten, C. Benkhaeuser, G. Schnakenburg, S. Grimme and A. Lützen, *Synthesis*, 2015, 3118–3132.
- 21 T. J. White, M. E. McConney and T. J. Bunning, *J. Mater. Chem.*, 2010, **20**, 9832–9847.
- 22 O. Jin, D. Fu, Y. Ge, J. Wei and J. Guo, *New J. Chem.*, 2015, **39**, 254–261.
- 23 Q. Li, L. Green, N. Venkataraman, I. Shivanovskaya, A. Khan, A. Urbas and J. W. Doane, *J. Am. Chem. Soc.*, 2007, **129**, 12908–12909.
- 24 M. Zahangir Alam, T. Yoshioka, T. Ogata, T. Nonaka and S. Kurihara, *Liq. Cryst.*, 2007, **34**, 1215–1219.
- 25 J. G. Finden, E. Yuh, C. Huntley and R. P. Lemieux, *Liq. Cryst.*, 2007, **34**, 1095–1106.
- 26 Q. Cui and R. P. Lemieux, *J. Mater. Chem. C*, 2013, **1**, 1011–1017.
- 27 Q. Cui, C. M. Huntley and R. P. Lemieux, *J. Mater. Chem.*, 2009, **19**, 5188–5192.
- 28 C. J. Boulton, J. J. Sutherland and R. P. Lemieux, *J. Mater. Chem.*, 2003, **13**, 644–646.
- 29 C. J. Boulton, J. G. Finden, E. Yuh, J. J. Sutherland, M. D. Wand, G. Wu and R. P. Lemieux, *J. Am. Chem. Soc.*, 2005, **127**, 13656–13665.
- 30 S. M. Morris, M. M. Qasim, K. T. Cheng, F. Castles, D. H. Ko, D. J. Gardiner, S. Nosheen, T. D. Wilkinson, H. J. Coles, C. Burgess and L. Hill, *Appl. Phys. Lett.*, 2013, **103**, 101105.
- 31 H.-K. Kwon, K.-T. Lee, K. Hur, S. H. Moon, M. M. Quasim, T. D. Wilkinson, J.-Y. Han, H. Ko, I.-K. Han, B. Park, B. K. Min, B.-K. Ju, S. M. Morris, R. H. Friend and D.-H. Ko, *Adv. Energy Mater.*, 2015, **5**, 1–6.
- 32 T. Ohtake, *Tellus, Ser. B*, 1993, **45**, 138–144.
- 33 S. Sergeyev, D. Didier, V. Boitsov, A. Teshome, I. Asselberghs, K. Clays, C. M. L. Vande Velde, A. Plaquet and B. Champagne, *Chem. – Eur. J.*, 2010, **16**, 8181–8190.
- 34 S. Sergeyev and F. Diederich, *Chirality*, 2006, **18**, 707–712.
- 35 M. Valík, B. Dolenský, E. Herdtweck and V. Král, *Tetrahedron: Asymmetry*, 2005, **16**, 1969–1974.
- 36 D. L. Jameson, T. Field, M. R. Schmidt, A. K. DeStefano, C. J. Stiteler, V. J. Venditto, B. Krovic, C. M. Hoffman, M. T. Ondisco and M. E. Belowich, *J. Org. Chem.*, 2013, **78**, 11590–11596.
- 37 T. Kamiyama, L. Sigrist and J. Cvengroš, *Synthesis*, 2016, 3957–3964.

Paper II (Supporting Information)



Journal Impact Factor: 4.955

Notification

The following materials are *open access* and are available online free of charges *via* the Internet at: <https://doi.org/10.1039/c6qo00653a>. Every use of the following material has to be referred to the corresponding publication: *Org Chem Front* **2017**, *4*, 224–228.

Hünlich Base Derivatives as Photo-Responsive Λ -Shaped Hinges

Masoud Kazem-Rostami^{*a} and Amirhossein Moghanian^b

^a Department of Chemistry and Biomolecular Sciences, Macquarie University, North Ryde, NSW 2109, Australia.

^b Harvard-MIT Division of Health Sciences, Massachusetts Institute of Technology, Cambridge 02139, MA, USA; Mining and Metallurgical Engineering Department, Amirkabir University of Technology, 424 Hafez Ave., Tehran 15875-4413, Iran; Biomaterials Innovation Research Center, Division of Biomedical Engineering, Department of Medicine, Brigham and Women's Hospital, Harvard Medical School, Boston 02139, MA, USA.

* Emails: masoud.kazem-rostami@hdr.mq.edu.au, masoud.kr@gmail.com; Fax: 0061-9850 8313

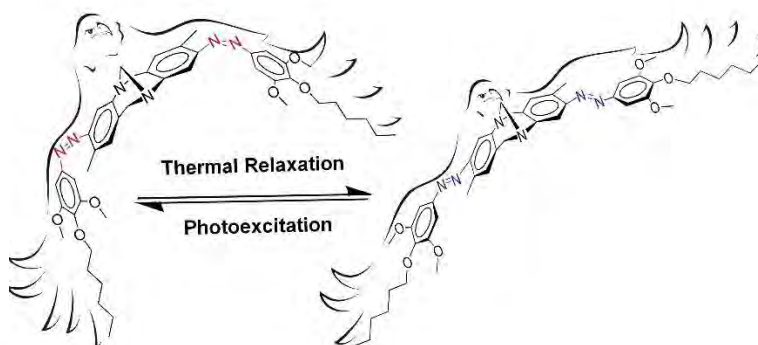


TABLE OF CONTENTS

General Remarks	107
Materials	107
Instrumentation	107
Synthesis and Characterization	108
1. Synthesis and Characterization of (\pm)-1	108
2. Synthesis and Characterization of (\pm)-2	110
3. Synthesis and Characterization of (\pm)-3	113
4. Synthesis and Characterization of (\pm)-4	116
5. Synthesis and Characterization of (\pm)-5	119
6. Synthesis and Characterization of (\pm)-6	122
7. Synthesis and Characterization of (\pm)-7	125
8. Synthesis and Characterization of (\pm)-8	127
9. Synthesis and Characterization of (\pm)-9	130
10. Synthesis and Characterization of (\pm)-1A	133
11. Synthesis and Characterization of (\pm)-1B	135
12. Synthesis and Characterization of (\pm)-1C	137
12. Synthesis and Characterization of (\pm)-4A	139
13. Synthesis and Characterization of (\pm)-5A	140
14. Synthesis and Characterization of (\pm)-6A	142
15. Synthesis and Characterization of (\pm)-8A	144
16. Synthesis and Characterization of (\pm)-9A	148
17. Preparation of the building block (Hünlich's base)	150
17. Partial resolution of 4A	152
Photo-excitation and thermal relaxation	152
1. Photo-isomerisation studies of (\pm)-6	153
2. Photo-isomerisation studies of (\pm)-6A	153
References	153

GENERAL REMARKS

Materials:

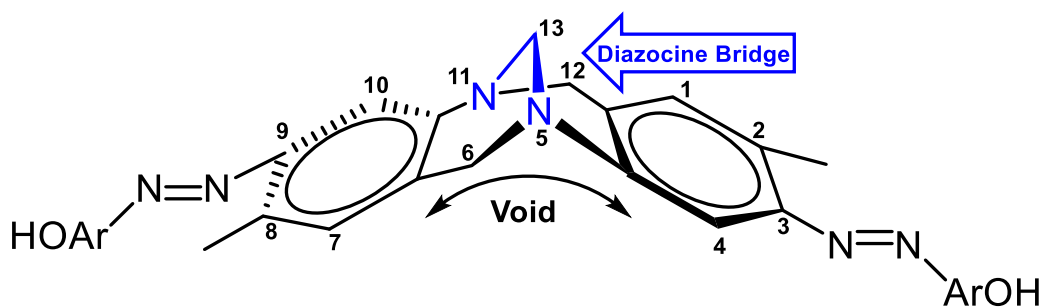
Pursuant to a procedure¹ adopted with minor modifications, described in section 17, pure Hünlich's base was prepared. The rest of the starting materials and solvents were purchased from Merck, Fluka and Sigma-Aldrich commercial suppliers and used without any further purification, except chloroform and acetone which were re-spectively deacidified and dried over anhydrous K₂CO₃ prior using.

Instrumentation:

The mass spectra were obtained by direct injections to Shimadzo-2010EV-LCMS or Agilent-6130-LCMS, set on Electro-Spray-Ionization (ESI) and using the described mobile phase for each compound. The UV-Vis and IR spectra were recorded by serving Varian-Cary-1 or Eppendorf-BioSpektrometer-kinetic and Thermo-Scientific-Nicolet-iS5/ATR10 spectrophotometers respectively. The reactions profile were monitored by Thin Layer Chromatography (TLC) on silica gel plates and colourless spots were visualized under 254 and 365nm UV lamps. The column chromatography was performed using 40-63 micron silica gel as the stationary phase and the applied mobile phases are described by a retention factor (*R_f*) for each compound. The organic elemental analysis was performed by using Vario-EL-Elementar or PerkinElmer-2400-series-II CHSNO elemental analysers. The NMR spectra acquisition were performed by running Topspin-3.2 on a Bruker-AVANCE-DRX400 NMR spectrometer for these nucleons and fields: ¹H: 400.0 MHz, ¹³C: 100.6 MHz. The chemical shifts were calibrated relative to the peaks of the applied deuterated solvents as shown below:

Deuterated Solvent	¹ H-NMR	¹³ C-NMR
CDCl ₃	7.26 ppm	77.16 ppm
DMSO- <i>d</i> ₆	2.50 ppm	39.52 ppm

The integrals are calibrated to the expected value for the most recognizable peak. The splitting patterns are abbreviated as **s** that stands for *singlet*, **d** for *doublet*, **t** for *triplet*, **q** for *quartet*; **b** for *broad*, **m** for *multiplet*. The coupling constants, rounded into one decimal, are indicated by *J* in Hertz. The NMR tests were all conducted at 298.15 K unless otherwise mentioned.

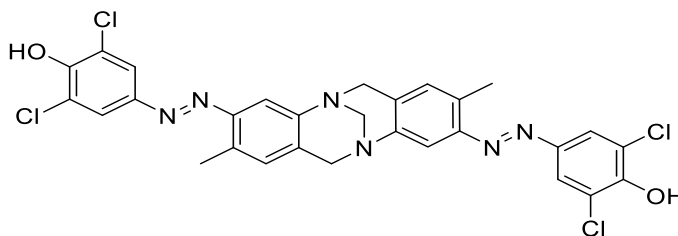


The numbering system used in the NMR interpretation

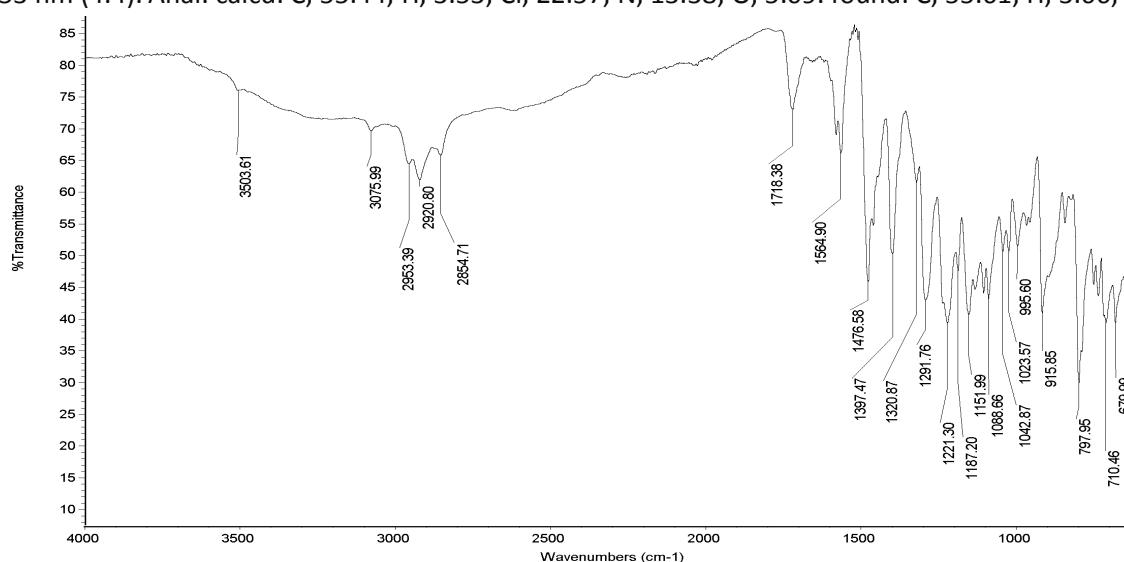
SYNTHESIS AND CHARACTERIZATION

1. Synthesis and Characterization of (\pm)-1

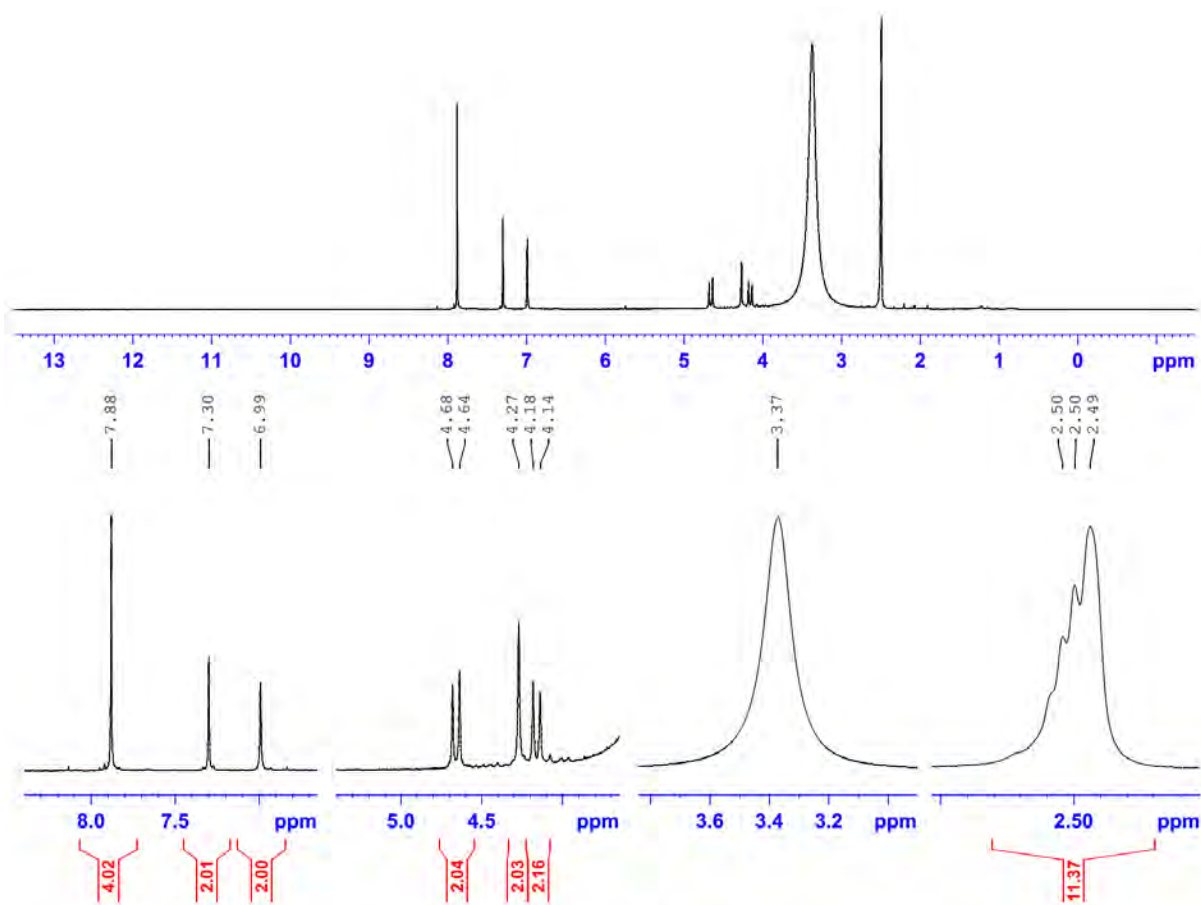
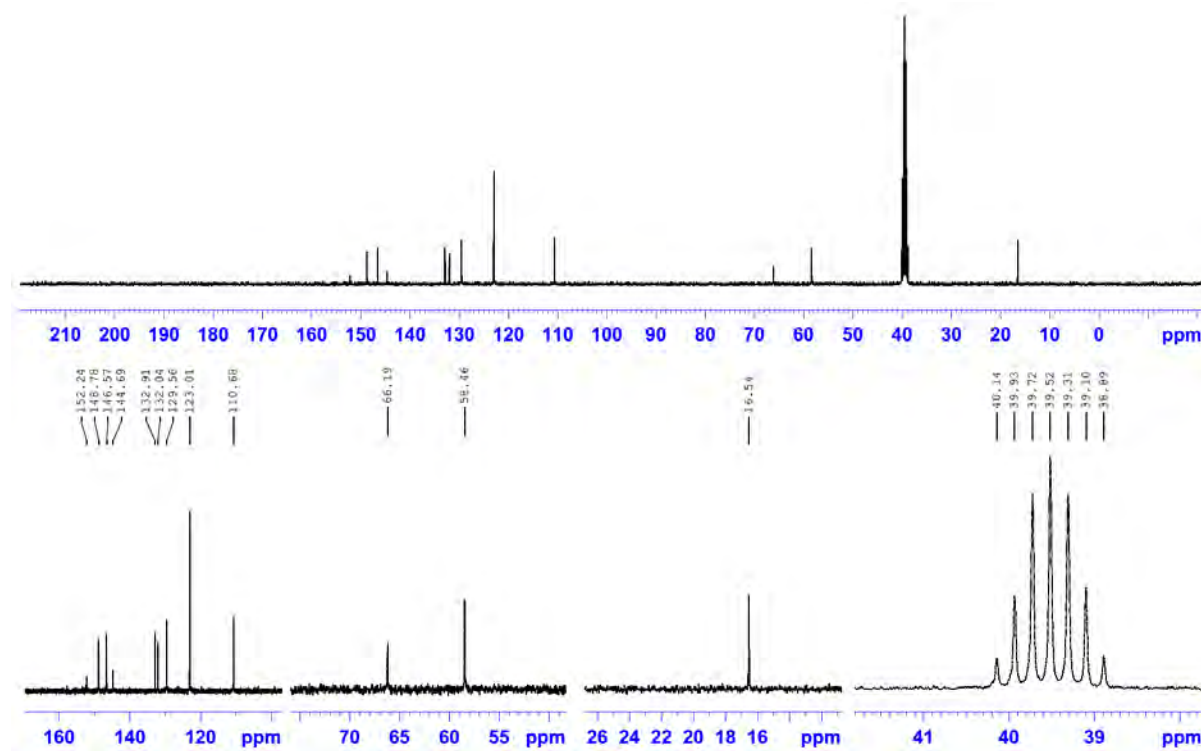
4,4'-((1E,1'E)-(2,8-dimethyl-6H,12H-5,11-methanodibenzo[b,f][1,5]diazocine-3,9-diyl)bis(diazene-2,1-diyl))bis(2,6-dichlorophenol)

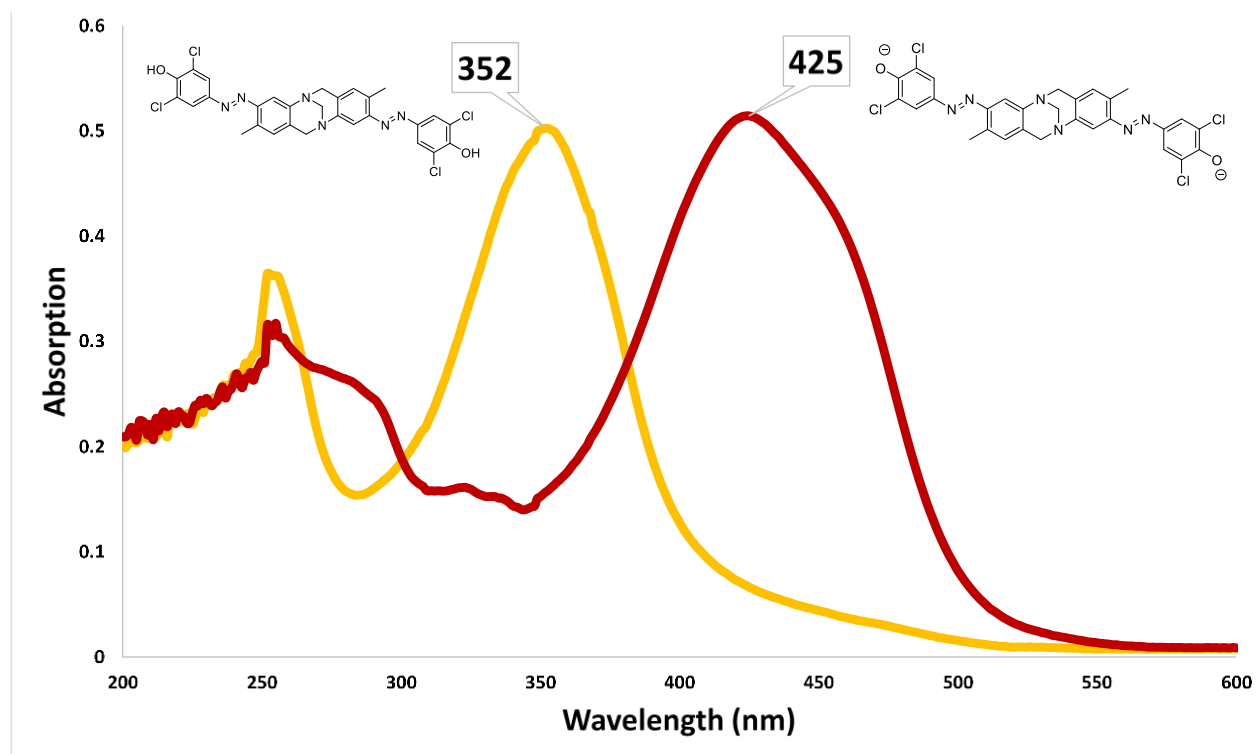


Hünlich's base (0.56 g, 2.0 mmol, 1.0 eq.) was dissolved in H_2SO_4 (6.5% v/v, 30 mL, aq.) at room temperature, then the reaction container was put in an ice/acetone bath to cool it down to -5°C . An aqueous solution of sodium nitrite (0.30 g, 4.4 mmol, 2.2 eq., 5 mL, 0°C) was dropped into the reaction mixture by 10 minutes and the stirring continued for 20 more minutes. The resulting yellowish solution was poured into a freshly prepared solution of 2,6-dichloro phenol (0.72 g, 4.4 mmol, 2.2 eq.) and Na_2CO_3 (2.0 g) in 100 mL of ice-cold water. Afterwards, two more grams of Na_2CO_3 gradually added to the mixture and stirred at 0°C for 23 hours. The final pH level of the reaction mixture was about 7 and a dark orange precipitate was filtered from it. The collected precipitate was properly washed with water and desiccated to obtain the crude. The crude was dissolved in 50 mL of 2-butanone, filtered and then shook with brine and NaOH solutions (3N, 100 mL x 5). Afterwards, this organic layer was separated, dried up over MgSO_4 and filtered. The purified compound **1** (0.63 g, 1.0 mmol, 50%) was obtained by addition of n-hexane to the 2-butanone solution, filtration and vacuum desiccation respectively. Chemical Formula: $\text{C}_{29}\text{H}_{22}\text{Cl}_4\text{N}_6\text{O}_2$, Molecular Weight: 628.34, R_f : 0.32 (DCM/ MeOH = 2% v/v) silica gel. $^1\text{H-NMR}$: (400 MHz, $\text{DMSO}-d_6$) δ [ppm] 2.49 (s, 6H, $2 \times -\text{CH}_3$), 4.16 (d, $J = 17.4$ Hz, 2H, H-6a, H-12a), 4.27 (s, 2H, $-\text{N}-\text{CH}_2-\text{N}-$), 4.66 (d, $J = 17.3$ Hz, 2H, H-6b, H-12b), 6.99 (s, 2H, H-1, H-7), 7.30 (s, 2H, H-4, H-10), 7.88 (s, 4H, $4 \times \text{CH}$). $^{13}\text{C-NMR}$: (100 MHz, $\text{DMSO}-d_6$) δ [ppm] 16.53, 58.46, 66.19, 110.68, 123.01, 129.56, 132.04, 132.91, 144.69, 146.57, 148.78, 152.24. IR: (Neat) ν_{max} (cm^{-1}) = 3503, 3076, 2953, 2920, 1718, 1565, 1476, 1397, 1291, 1221, 1151, 915, 797. MS (Acetonitrile 90%, EtOAc 5%, H_2O 5%): (ESI negative) calc. for $[\text{C}_{29}\text{H}_{21}\text{Cl}_4\text{N}_6\text{O}_2]^-$: $[\text{M}-\text{H}]^-$ 625.0, found: 625.2 and 627.3. UV (EtOAc): λ (lg ϵ) = 353 nm (4.4). Anal. calcd: C, 55.44; H, 3.53; Cl, 22.57; N, 13.38; O, 5.09. found: C, 55.61; H, 3.66; N, 13.14.



Compound 1, IR transmittance spectra (neat)

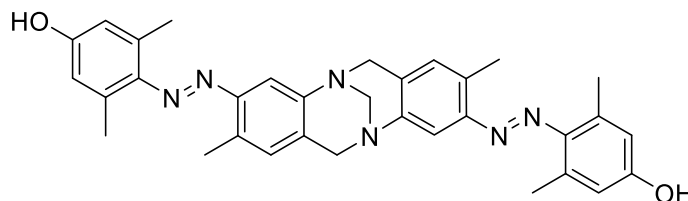
Compound 1, ¹H-NMR (400 MHz, DMSO-*d*₆)Compound 1, ¹³C-NMR (100 MHz, DMSO-*d*₆)



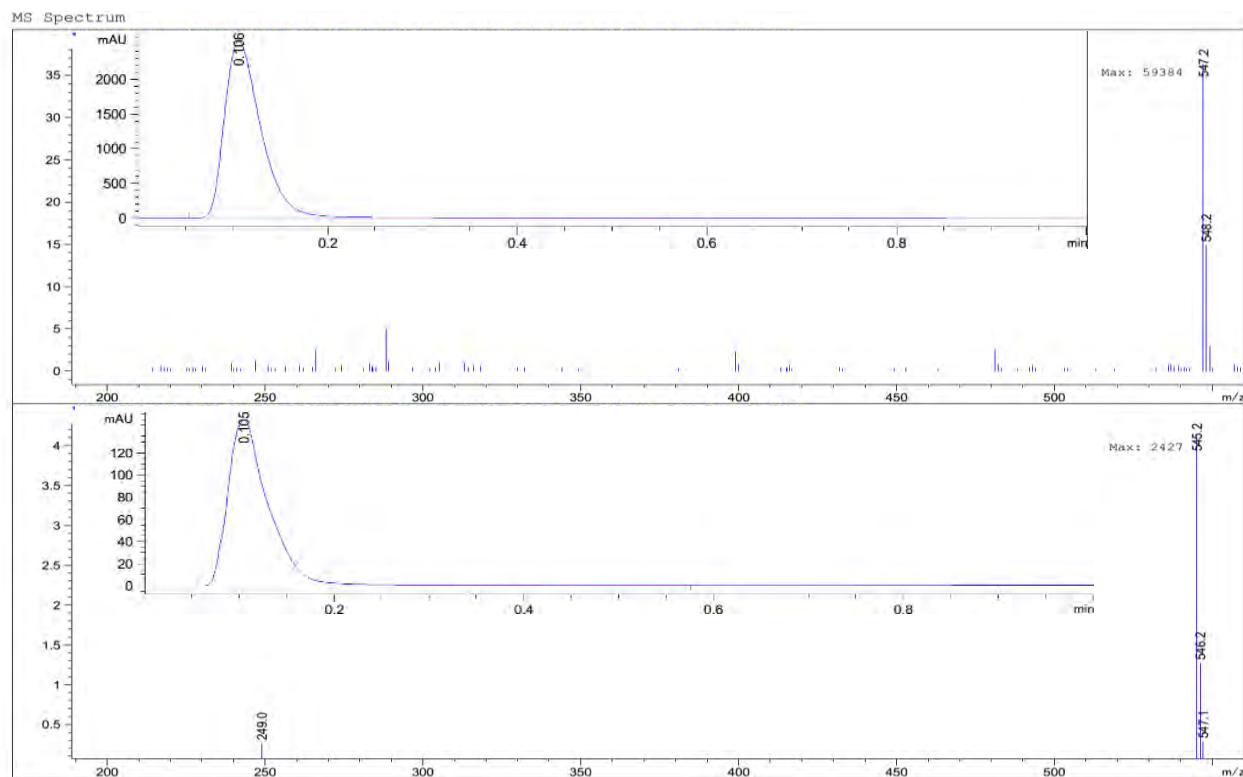
Compound 1 (rt, EtOAc), UV-Vis spectra in the absence (orange) and presence (red) of Et₃N

2. Synthesis and Characterization of (±)-2

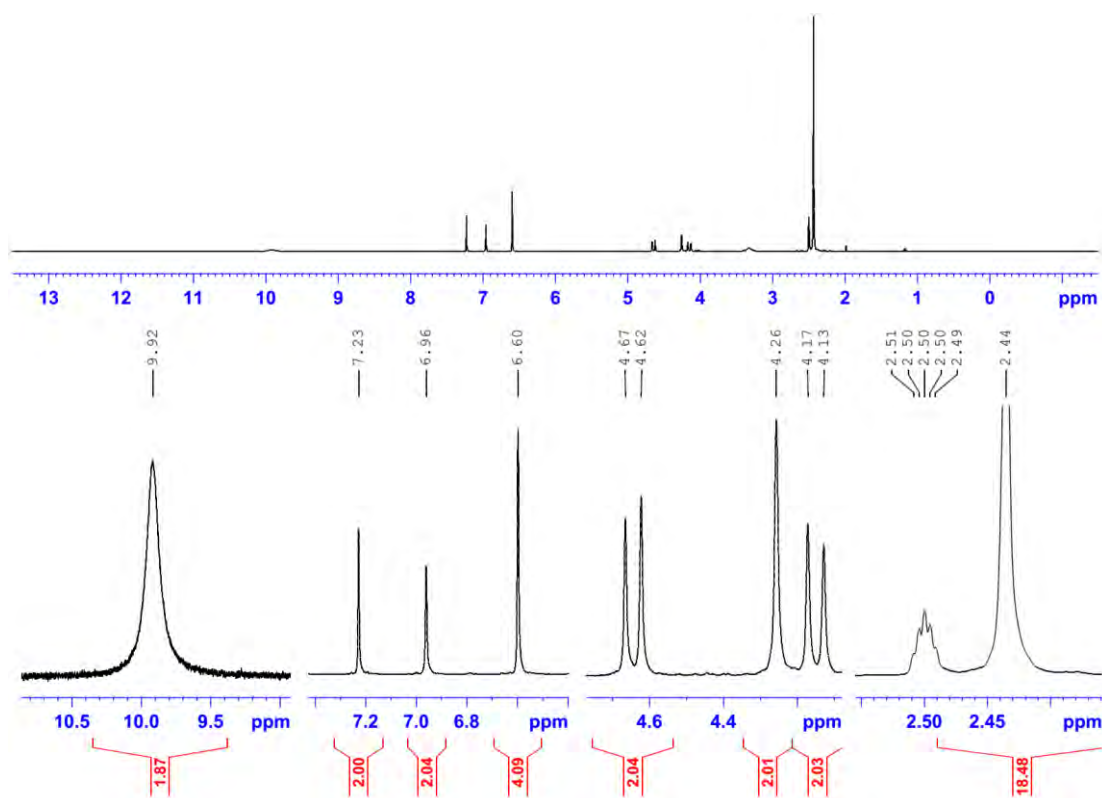
4,4'-((1E,1'E)-(2,8-dimethyl-6H,12H-5,11-methanodibenzo[b,f][1,5]diazocine-3,9-diyl)bis(diazene-2,1-diyl))bis(3,5-dimethylphenol)



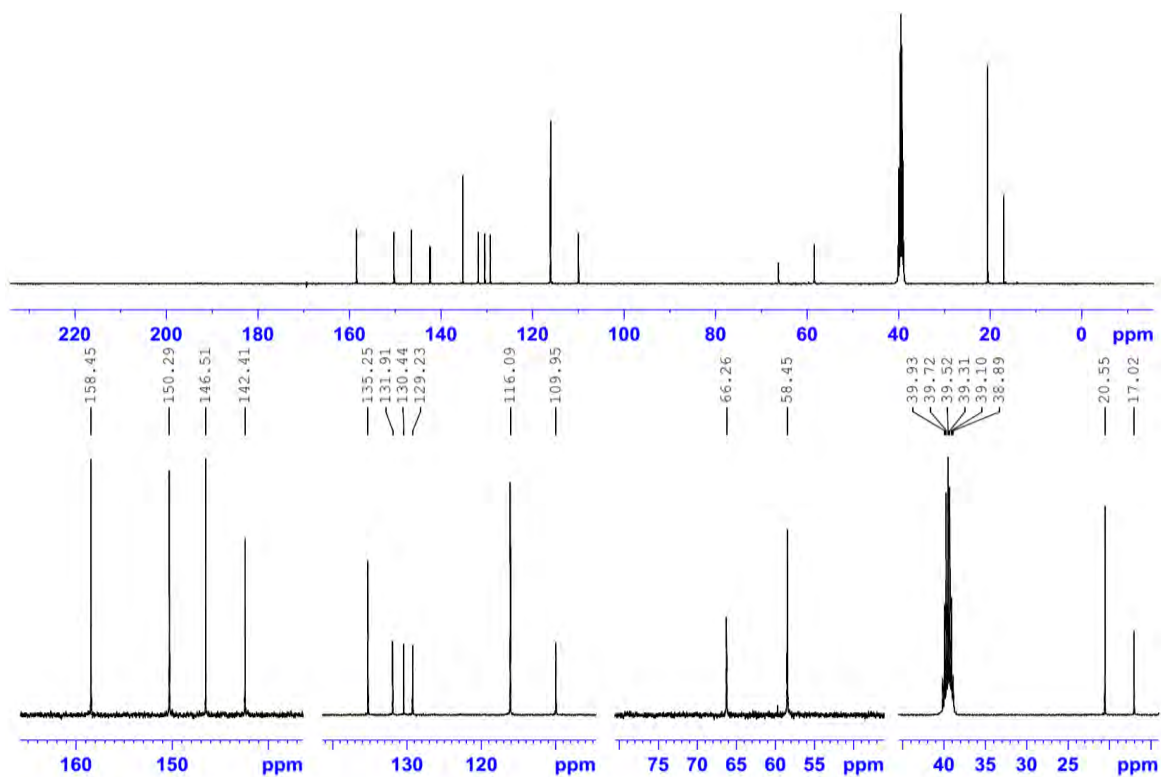
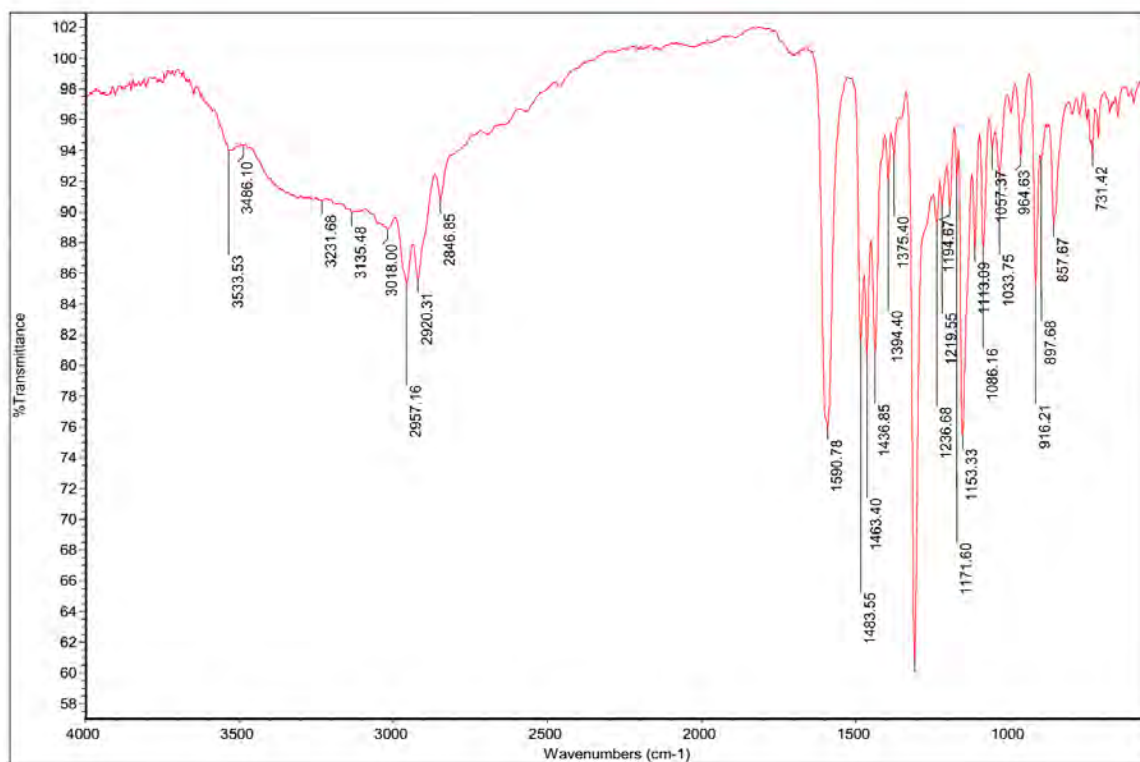
Hünlich's base (0.56 g, 2.0 mmol, 1.0 eq.) was dissolved in H₂SO₄ (6.5%, 30 mL, aq.) at room temperature, then cooled down to -5°C by placing the reaction container in ice/acetone bath. A sodium nitrite solution (0.3 g, 4.4 mmol, 2.2 eq.) in cold water (5 mL) was dropped into the reaction flask over 10 minutes. After continuing the stir for 25 more minutes, the resulting yellowish solution was poured into a prepared solution of 3,5-dimethylphenol (0.51 g, 4.2 mmol, 2.1 eq.) and Na₂CO₃ (2 g) in 100 mL of ice-cold water. The stirring continued for 2 h meanwhile two more grams of Na₂CO₃ was gradually added. After 12 more hours of stirring, an orange precipitate was filtered off from the aqueous mixture (pH=7), washed thoroughly with Milli-Q water and desiccated to obtain the product **2** (0.98 g, 1.8 mmol, 90%). Chemical Formula: C₃₃H₃₄N₆O₂, Molecular Weight: 546.68, *R*_f: 0.25 (EtOAc/ DCM = 5% v/v) silica gel. ¹H-NMR (400 MHz, DMSO-*d*₆) δ [ppm]: 2.44 (s, 18H, 6 × -CH₃), 4.15 (d, *J* = 17.3 Hz, 2H, H-6a, H-12a), 4.26 (s, 2H, -N-CH₂-N-), 4.65 (d, *J* = 17.2 Hz, 2H, H-6b, H-12b), 6.60 (s, 4H, 4 × CH), 6.96 (s, 2H, H-1, H-7), 7.23 (s, 2H, H-4, H-10), 9.92 (br, 2H, OH). ¹³C-NMR (100 MHz, DMSO-*d*₆) δ [ppm]: 17.02, 20.55, 58.45, 66.26, 109.95, 116.09, 129.23, 130.44, 131.91, 135.25, 142.41, 146.51, 150.29, 158.45. IR: (Neat) ν_{max} [cm⁻¹] = 3533, 3231, 3018, 2957, 2920, 1590, 1483, 1463, 1311, 1153 and 916. MS (EtOH 95%, EtOAc 5%): (ESI positive) calc. for [C₃₃H₃₅N₆O₂]⁺: [M+H]⁺ 547.27, found 547.2. (ESI negative) calc. for [C₃₃H₃₃N₆O₂]⁻: [M-H]⁻ 545.27, found 545.2. UV-Vis: (EtOAc) λ (lgε) = 361nm (4.5). Anal. calcd: C, 72.50; H, 6.27; N, 15.37; O, 5.85. found: C, 72.21; H, 6.45; N, 15.29.



Compound 2, LCMS results ESI+ (top) and ESI- (bottom)



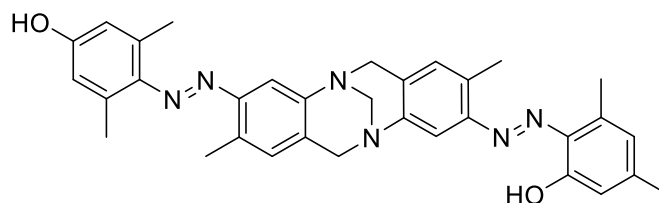
Compound 2, ¹H-NMR (400 MHz, DMSO-*d*₆)

Compound 2, ^{13}C -NMR (100 MHz, $\text{DMSO}-d_6$)

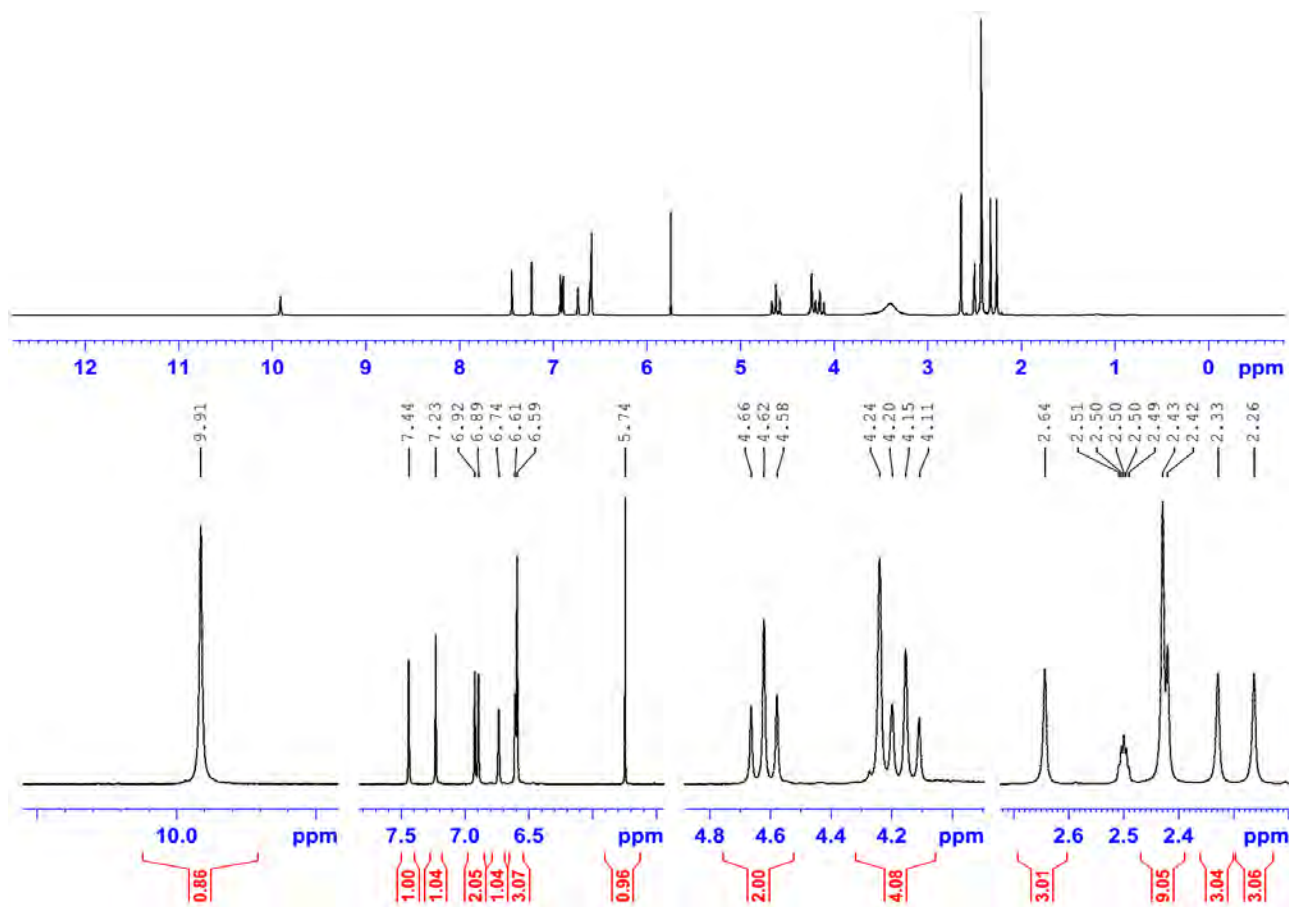
Compound 2, IR transmittance spectra (neat)

3. Synthesis and Characterization of (±)-3

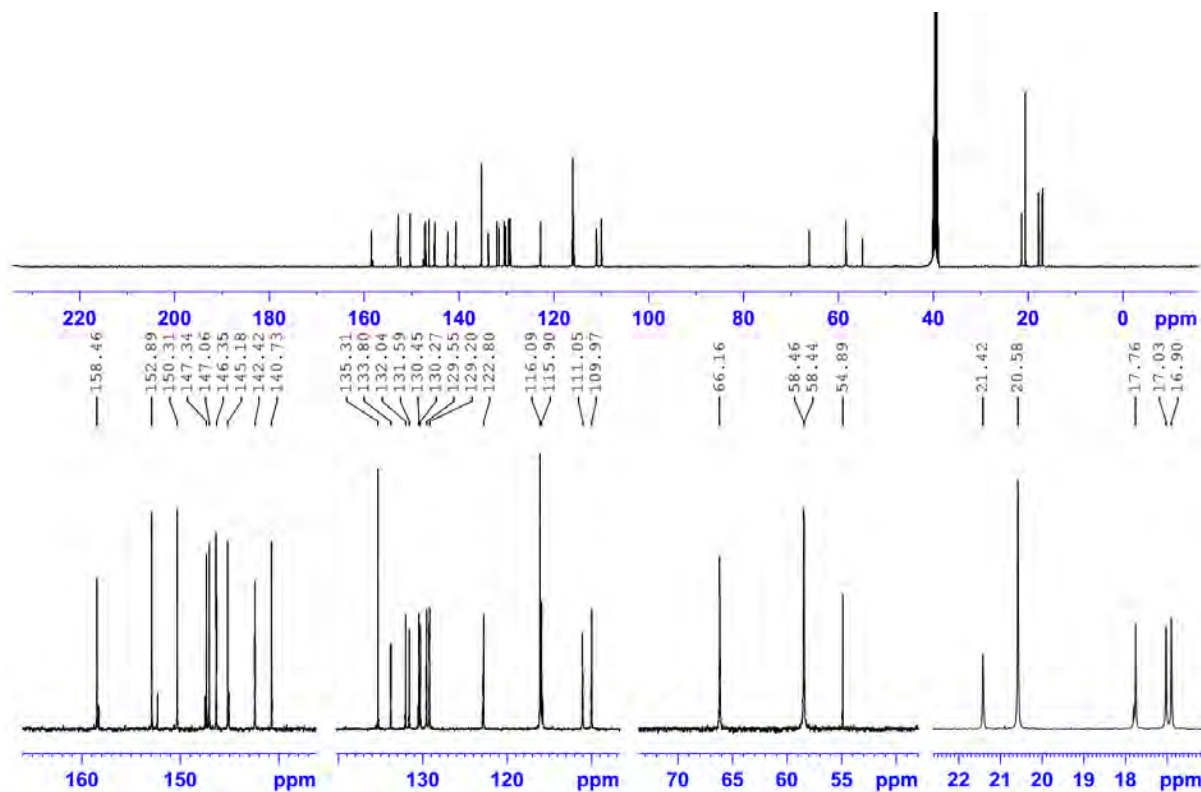
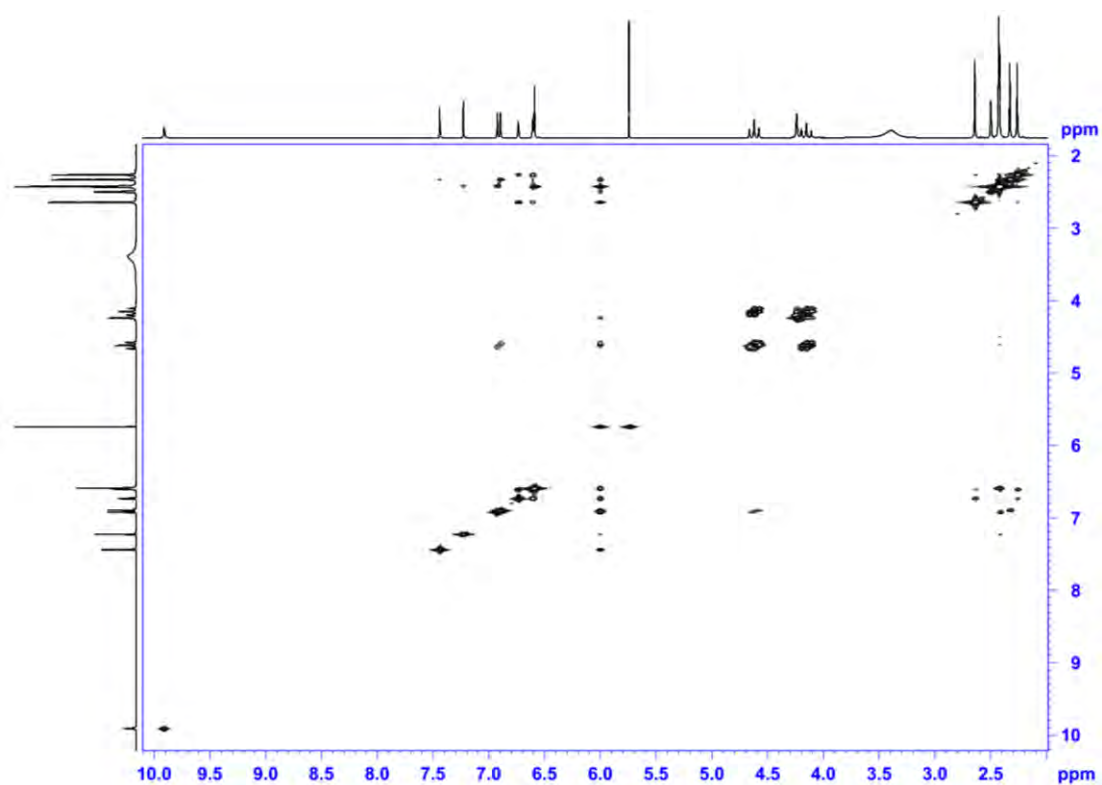
2-((E)-(9-((E)-(4-hydroxy-2,6-dimethylphenyl)diazenyl)-2,8-dimethyl-6H,12H-5,11-methanodibenzo[b,f][1,5]diazocin-3-yl)diazenyl)-3,5-dimethylphenol

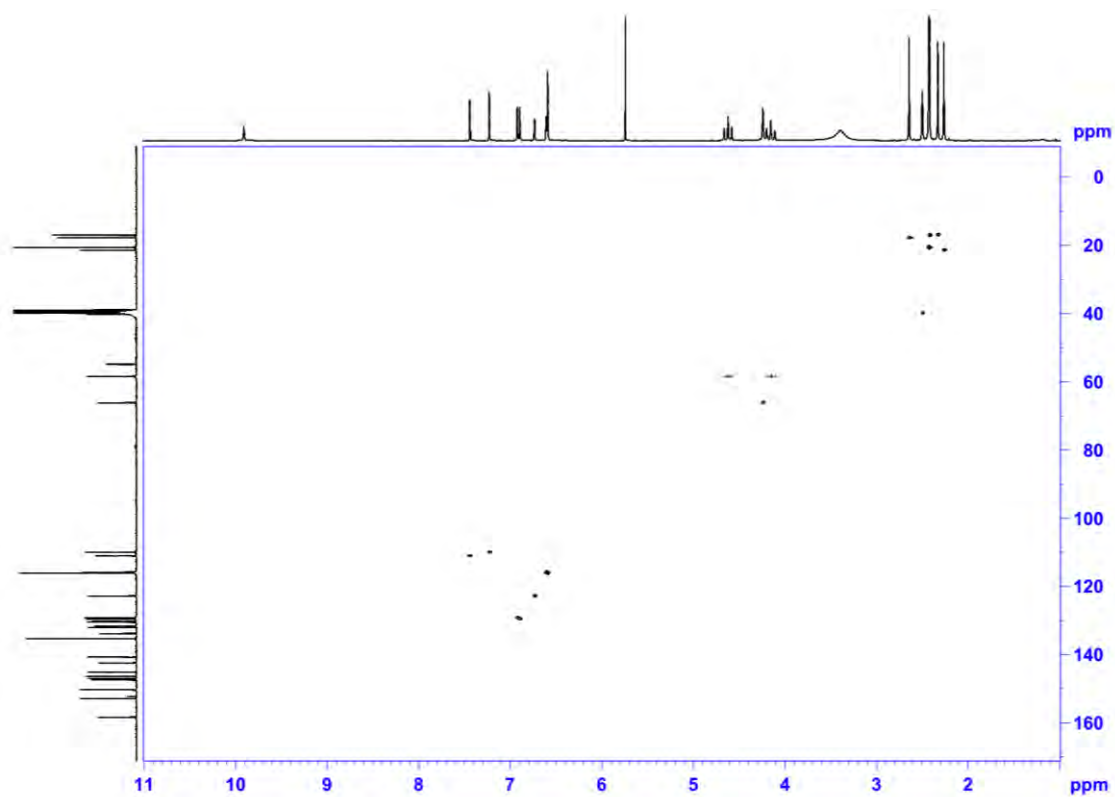


The side-product of the 2nd reaction, obtained during the column chromatography as a light orange solid (0.02 g, 0.03 mmol, 1.8%). Chemical Formula: $C_{33}H_{34}N_6O_2$, Molecular Weight: 546.68, R_f : 0.22 (MeOH/ DCM = 4% v/v) silica gel. **¹H-NMR** (400 MHz, DMSO- d_6) δ [ppm]: 2.26 (s, 3H, CH₃), 2.33 (s, 3H, CH₃), 2.42 (s, 3H, CH₃), 2.43 (s, 6H, 2 × -CH₃), 2.64 (s, 3H, CH₃), 4.11-4.24 (m, 2H), 4.24 (s, 2H, -N-CH₂-N-), 4.58-4.66 (m, 2H), 5.74 (s, 1H, OH), 6.59 (s, 2H, 2 × CH), 6.61 (s, 1H, CH), 6.74 (s, 1H, CH), 6.89 (s, 1H, CH), 6.92 (s, 1H, CH), 7.23 (s, 1H, CH), 7.44 (s, 1H, CH), 9.91 (s, 1H, OH). **¹³C-NMR** (100 MHz, DMSO- d_6) δ [ppm]: 16.90, 17.03, 17.76, 20.58, 21.42, 54.89, 58.44, 58.46, 66.16, 109.97, 111.05, 115.90, 116.09, 122.80, 129.20, 129.55, 130.27, 130.45, 131.59, 132.04, 133.80, 135.31, 140.73, 142.42, 145.18, 146.35, 147.06, 147.34, 150.31, 152.89, 158.46. **IR**: (Neat) ν_{max} [cm⁻¹] = 3521, 3236, 3022, 2949, 2932, 1585, 1479, 1458, 1316, 1144 and 928. **MS** (EtOH 95%, EtOAc 5%): (ESI positive) calc. for $[C_{33}H_{35}N_6O_2]^+$: $[M+H]^+$ 547.27, found 547.3. (ESI negative) calc. for $[C_{33}H_{33}N_6O_2]^-$: $[M-H]^-$ 545.27, found 545.2. **UV-Vis**: (EtOAc) λ (lge) = 361nm (4.5). Anal. calcd: C, 72.50; H, 6.27; N, 15.37; O, 5.85. found: C, 72.81; H, 6.46; N, 15.51.

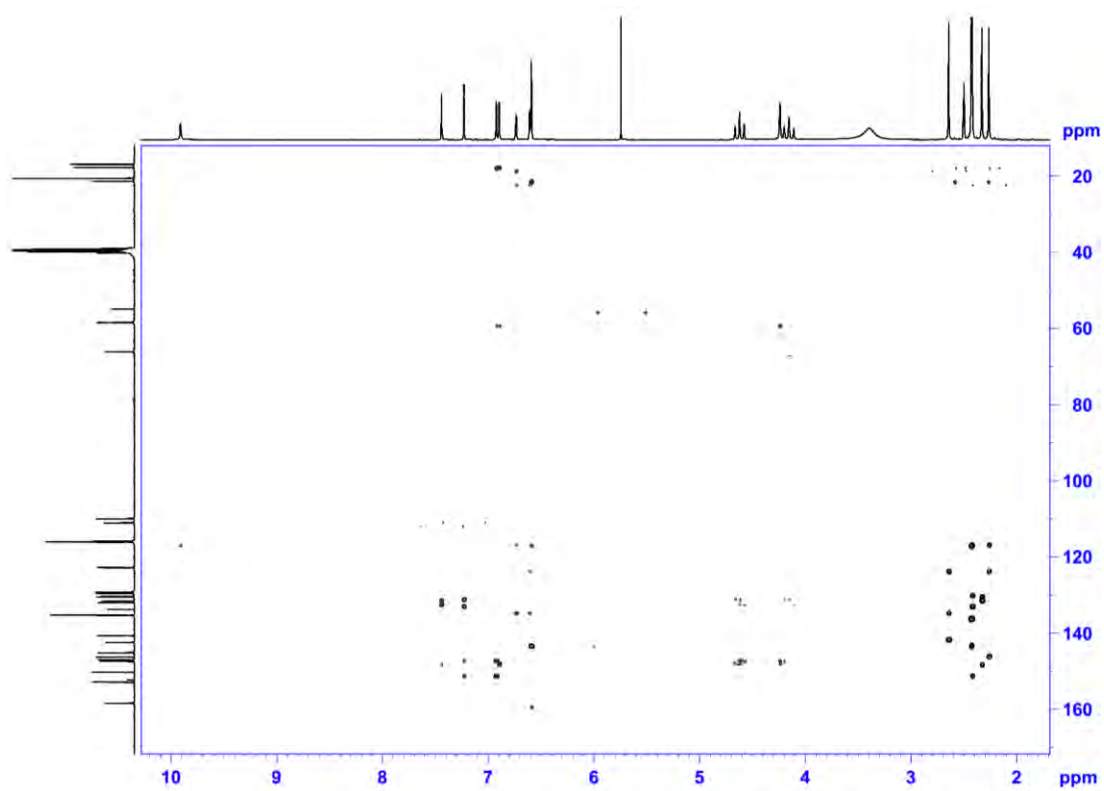


Compound 3, ¹H-NMR (400 MHz, DMSO- d_6)

Compound 3, ^{13}C -NMR (100 MHz, $\text{DMSO}-d_6$)Compound 3, COSY ($\text{DMSO}-d_6$)



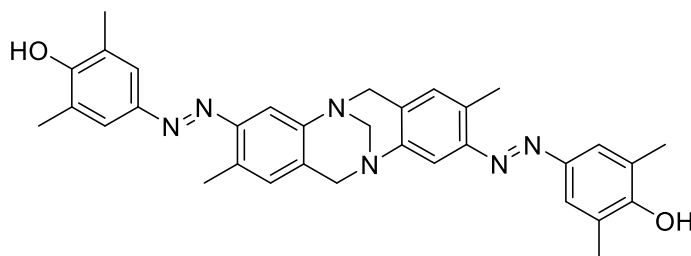
Compound 3, HSQC (DMSO- d_6)



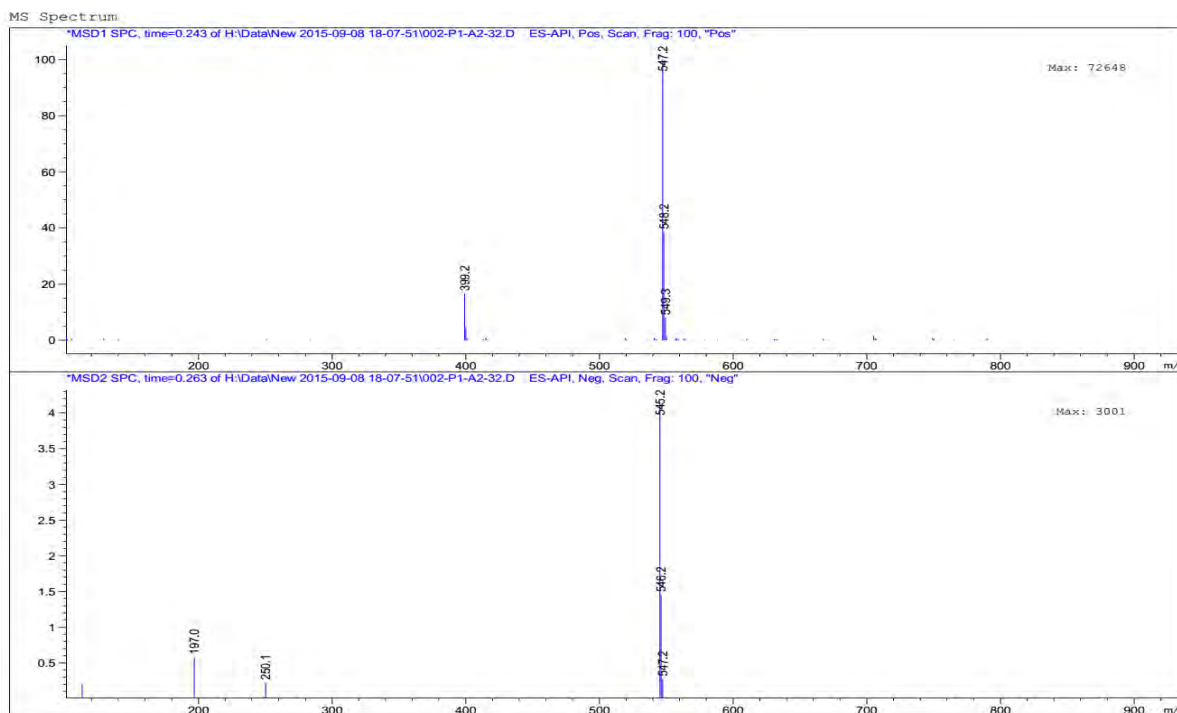
Compound 3, HMBC (DMSO- d_6)

4. Synthesis and Characterization of (±)-4

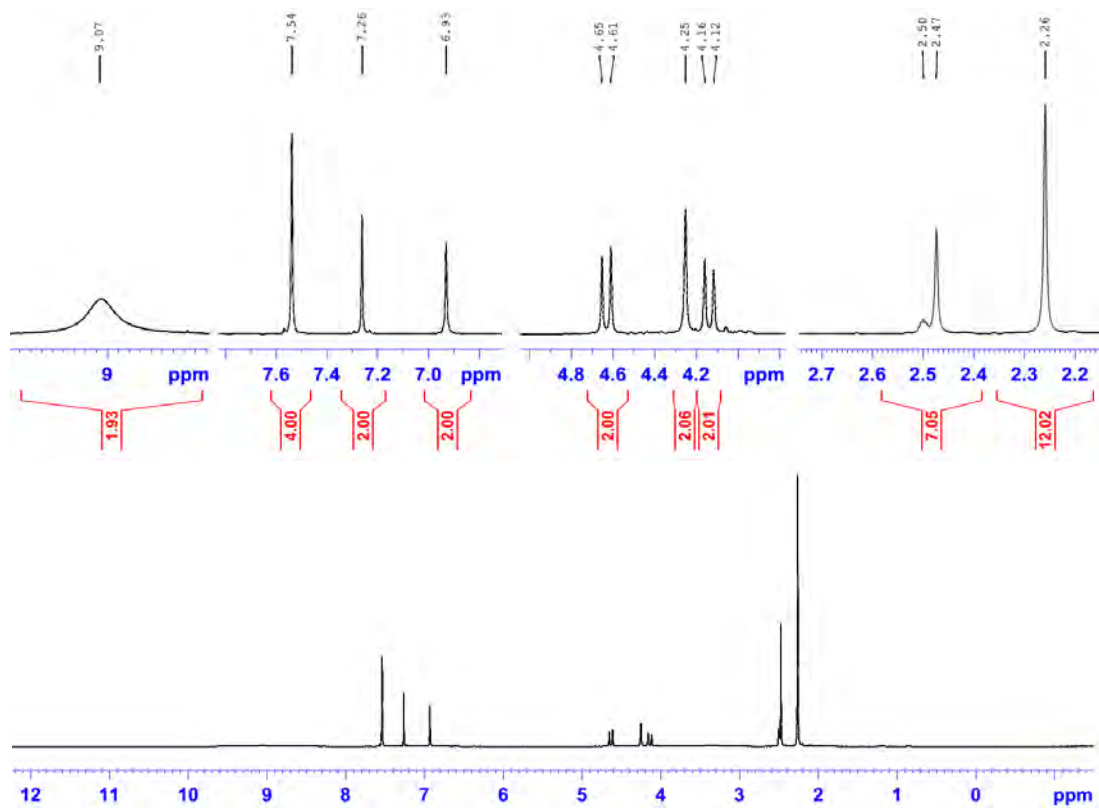
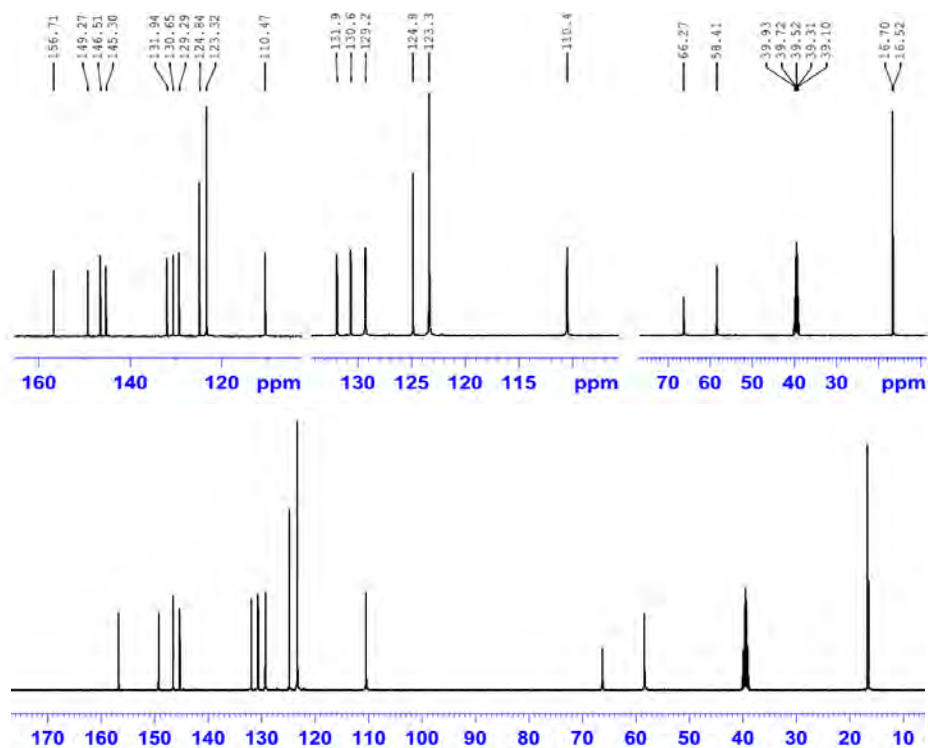
4,4'-((2,8-dimethyl-6H,12H-5,11-methanodibenzo[b,f][1,5]diazocine-3,9-diyl)bis(diazene-2,1-diyl))bis(2,6-dimethylphenol)

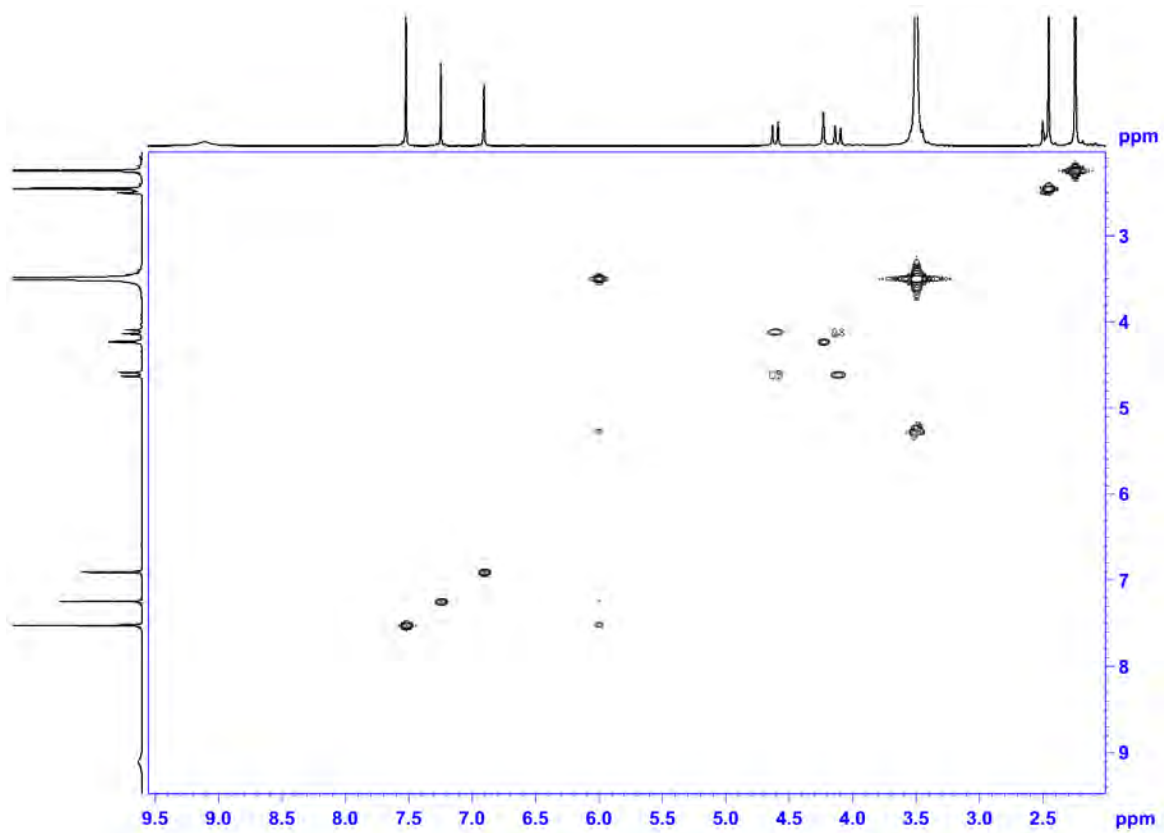


Hünlich's base (0.56 g, 2.0 mmol, 1.0 eq.) was dissolved in H_2SO_4 (6.5%, 30 mL) at room temperature, then cooled down to -5°C by placing the reaction container in ice/acetone bath. A sodium nitrite solution (0.30 g, 4.4 mmol, 2.2 eq.) in cold water (5 mL) was dropped into the reaction flask over 10 minutes. After continuing the stirring for another 25 minutes the resulting yellowish solution was poured into a prepared solution of 2,6-dimethylphenol (0.51 g, 4.2 mmol, 2.1 eq.) and Na_2CO_3 (2.0 g) in 100 mL of ice-cold water. The stirring was continued for 4 h meanwhile two more grams of Na_2CO_3 was gradually added. Afterwards, an orange precipitate was filtered off from the aqueous mixture (pH=7), washed thoroughly with Milli-Q water and desiccated to obtain the product **4** (0.88 g, 1.6 mmol, 81%). Chemical Formula: $\text{C}_{33}\text{H}_{34}\text{N}_6\text{O}_2$, Molecular Weight: 546.68, R_f : 0.33 (EtOAc/ n-hexane = 40% v/v) silica gel. $^1\text{H-NMR}$ (400 MHz, $\text{DMSO}-d_6$) δ [ppm]: 2.26 (s, 12H, 4 \times $-\text{CH}_3$), 2.47 (s, 6H, 2 \times $-\text{CH}_3$), 4.13 (d, J = 17.3 Hz, 2H, H-6a, H-12a), 4.25 (s, 2H, $-\text{N}-\text{CH}_2-\text{N}-$), 4.63 (d, J = 17.2 Hz, 2H, H-6b, H-12b), 6.92 (s, 2H, H-1, H-7), 7.26 (s, 2H, H-4, H-10), 7.53 (s, 4H, 4 \times CH), 9.07 (br, 2H, OH). $^{13}\text{C-NMR}$ (100 MHz, $\text{DMSO}-d_6$) δ [ppm]: 16.51, 16.70, 58.41, 66.27, 110.47, 123.32, 124.84, 129.29, 130.65, 131.94, 145.30, 146.51, 149.27, 156.71. IR: (Neat) ν_{max} [cm^{-1}] = 3563, 2946, 2914, 2843, 1592, 1480, 1417, 1298, 1182, 1111, 913, 728. MS (Acetonitrile 90%, EtOAc 5%, H_2O 5%): (ESI positive) calc. for $[\text{C}_{33}\text{H}_{35}\text{N}_6\text{O}_2]^+$: $[\text{M}+\text{H}]^+$ 547.2, found 547.2. (ESI negative) calc. for $[\text{C}_{33}\text{H}_{33}\text{N}_6\text{O}_2]^-$: $[\text{M}-\text{H}]^-$ 545.2, found 545.2. UV-Vis: (EtOAc) λ ($\text{lg}\epsilon$) = 365nm (4.5). Anal. calcd: C, 72.50; H, 6.27; N, 15.37. found: C, 72.63; H, 6.08; N, 14.98.

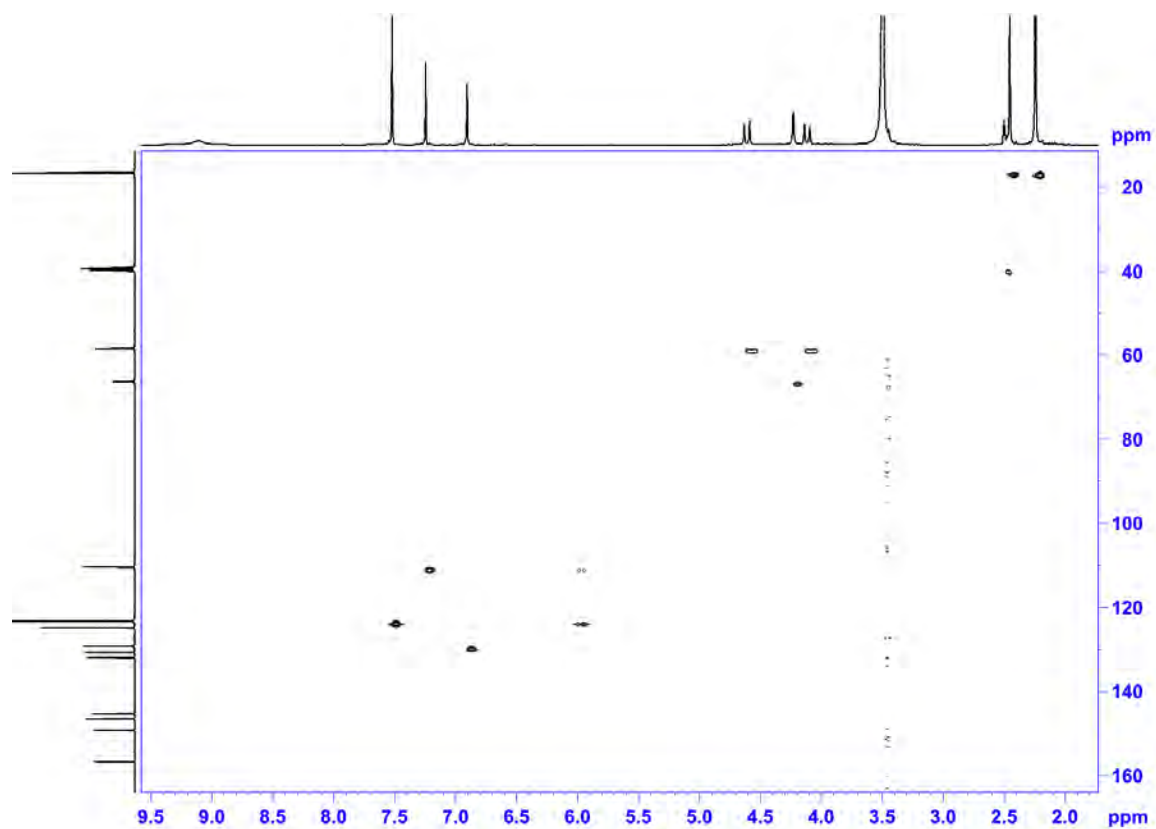


Compound 4, Mass Spectra ESI+ (top) and ESI- (bottom)

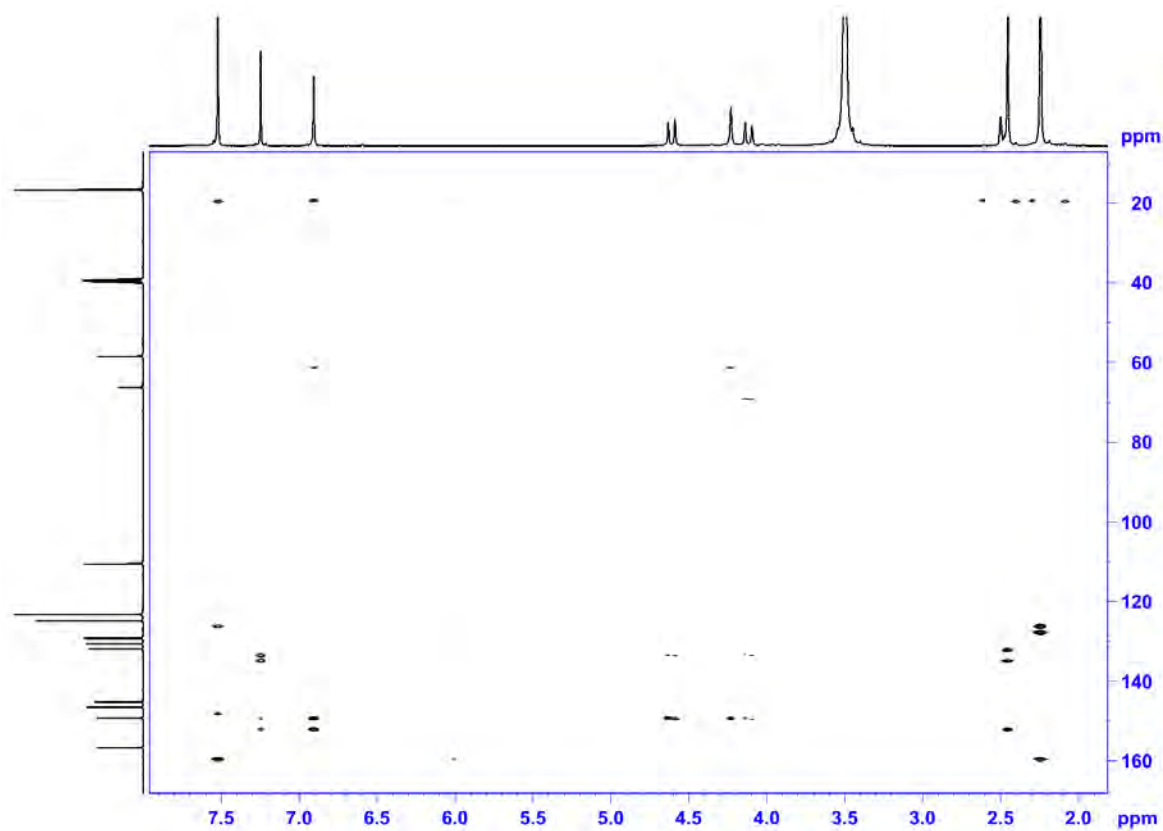
Compound 4, ¹H-NMR (400 MHz, DMSO-*d*₆)Compound 4, ¹³C-NMR (100 MHz, DMSO-*d*₆)



Compound 4, COSY (DMSO- d_6)

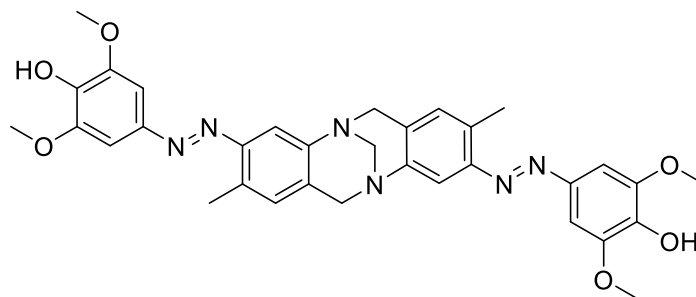


Compound 4, HSQC (DMSO- d_6)

Compound 4, HMBC (DMSO- d_6)

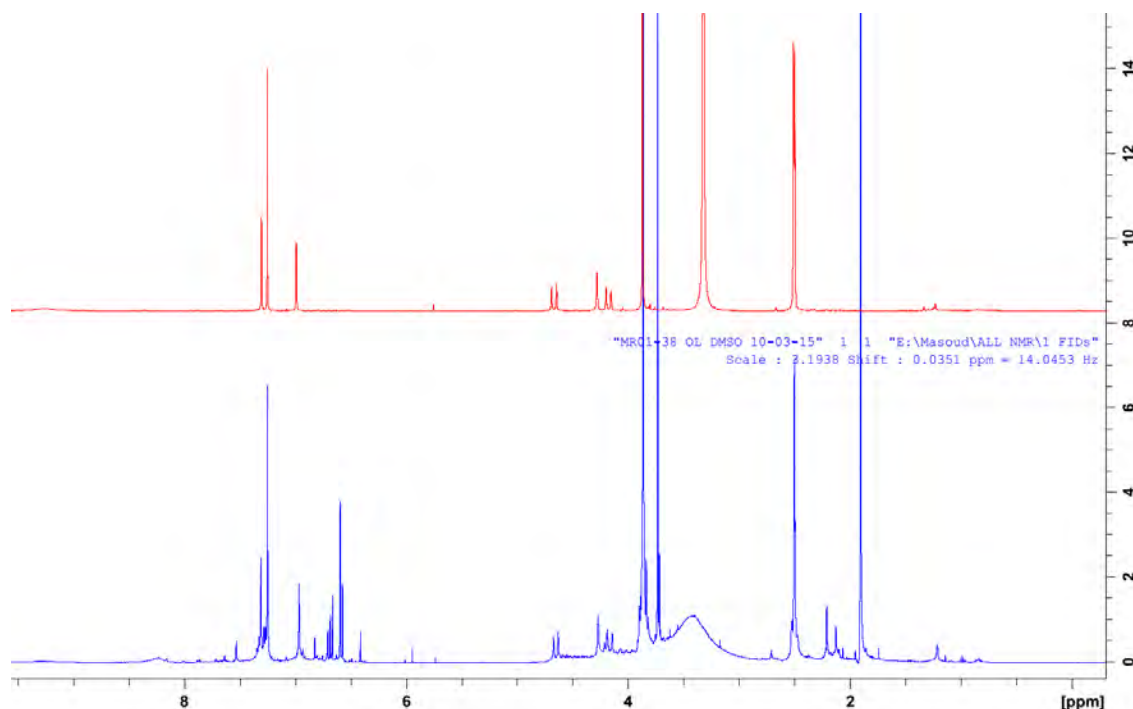
5. Synthesis and Characterization of (\pm)-5

4,4'-((2,8-dimethyl-6H,12H-5,11-methanodibenzo[b,f][1,5]diazocine-3,9-diyl)bis(diazene-2,1-diyl))bis(2,6-dimethoxyphenol)

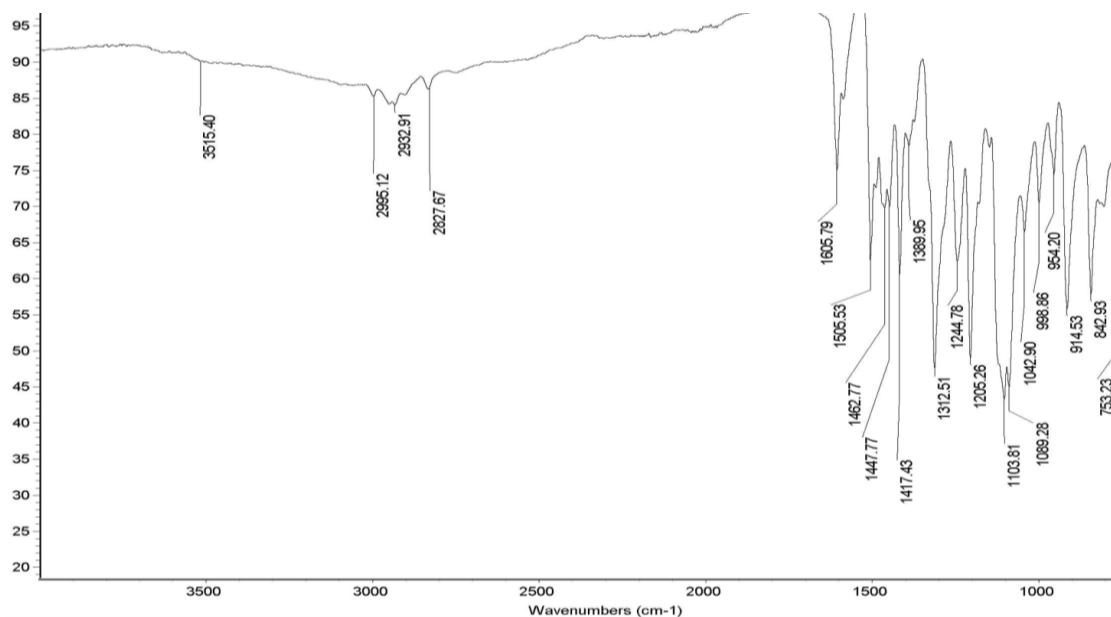


Hünlich's base (0.56 g, 2.0 mmol, 1.0 eq.) was dissolved in H_2SO_4 (6.5%, 30 mL, aq.) at room temperature, then cooled down to -5°C by putting the reaction container in an ice/acetone bath. A solution of sodium nitrite (0.30 g, 4.4 mmol, 2.2 eq.) in cold water (5 mL) was dropped into the reaction flask with continues stirring for 30 minutes. The resulting yellowish solution was poured into a freshly prepared solution of 2,6-dimethoxy phenol (1.0 g, 6.5 mmol, 3.3 eq.) and Na_2CO_3 (2.0 g) in 50 mL of acetonitrile/water 3:7 solution and stirred for 1 hour at -5°C . Two more grams of Na_2CO_3 was gradually added to neutralize the mixture and mixed two more hours until reached to the room temperature. After acidifying the reaction mixture (acetic acid, pH=5), an orange organic layer was extracted by ethyl acetate, washed with brine properly and evaporated to obtain the crude (0.93 g, contained almost 60% of the expected product based on the crude's NMR). Further purification was done by column chromatography to obtain a highly pure yellow solid however a significant portion of the product stuck

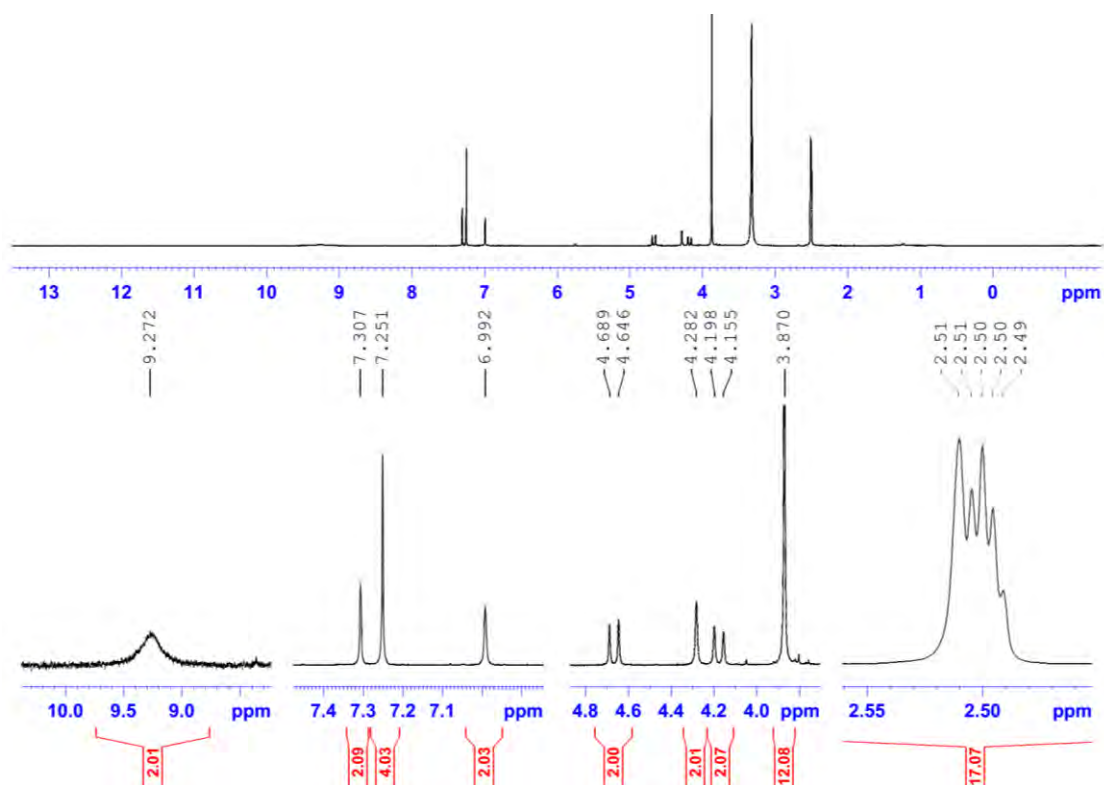
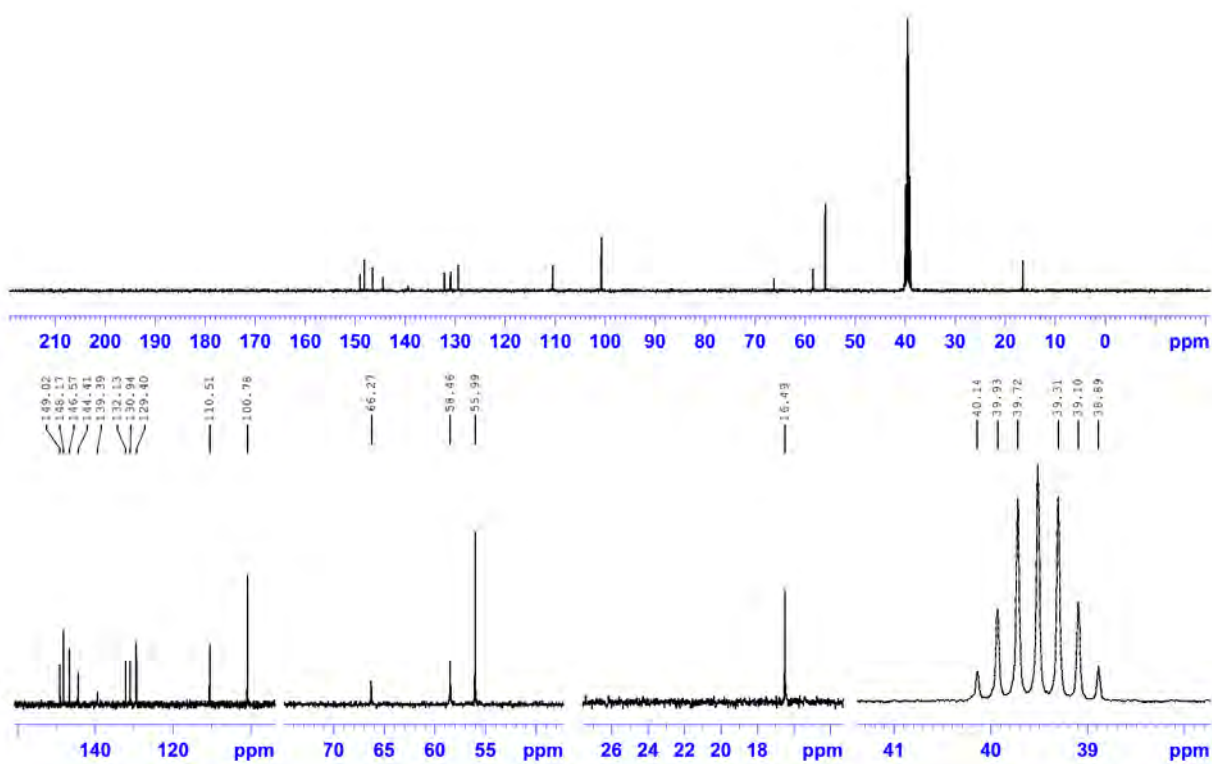
to the silica and the retrieved amount was (0.06 g, 0.1 mmol, 5%). Chemical Formula: $C_{33}H_{34}N_6O_6$, Molecular Weight: 610.67, R_f : 0.38 (MeOH/ DCM = 4% v/v) silica gel. **1H -NMR:** (400 MHz, DMSO- d_6) δ [ppm] 2.51 (s, 6H, 2 \times -CH₃), 3.87 (s, 12H, 4 \times -OCH₃), 4.17 (d, J = 17.30 Hz, 2H, H-6a, H-12a), 4.28 (s, 2H, -N-CH₂-N-), 4.66 (d, J = 17.22 Hz, 2H, H-6b, H-12b), 6.99 (s, 2H, H-1, H-7), 7.25 (s, 4H, 4 \times CH), 7.30 (s, 2H, H-4, H-10), 9.27 (br, 2H, OH). **^{13}C -NMR:** (100 MHz, DMSO- d_6) δ [ppm] 16.48, 55.99, 58.46, 66.27, 100.78, 110.5, 129.39, 130.94, 132.13, 139.39, 144.41, 146.57, 148.17, 149.01. **IR:** (Neat) ν_{max} (cm⁻¹) = 3515, 2995, 2827, 1605, 1505, 1417, 1312, 1205, 1103, 914, 842, 619. **MS:** (Acetonitrile 90%, EtOAc 5%, H₂O 5%): (ESI positive) calc., for $[C_{33}H_{35}N_6O_6]^+$: $[M+H]^+$ 611.25, found 611.5 (ESI negative) calc. for $[C_{33}H_{33}N_6O_6]^-$: $[M-H]^-$ 609.25, found 609.0. **UV:** (EtOAc) λ (lge) = 384 nm(4.5). Anal. calcd: C, 64.91; H, 5.61; N, 13.76; O, 15.72. found: C, 64.78; H, 5.97; N, 13.99.

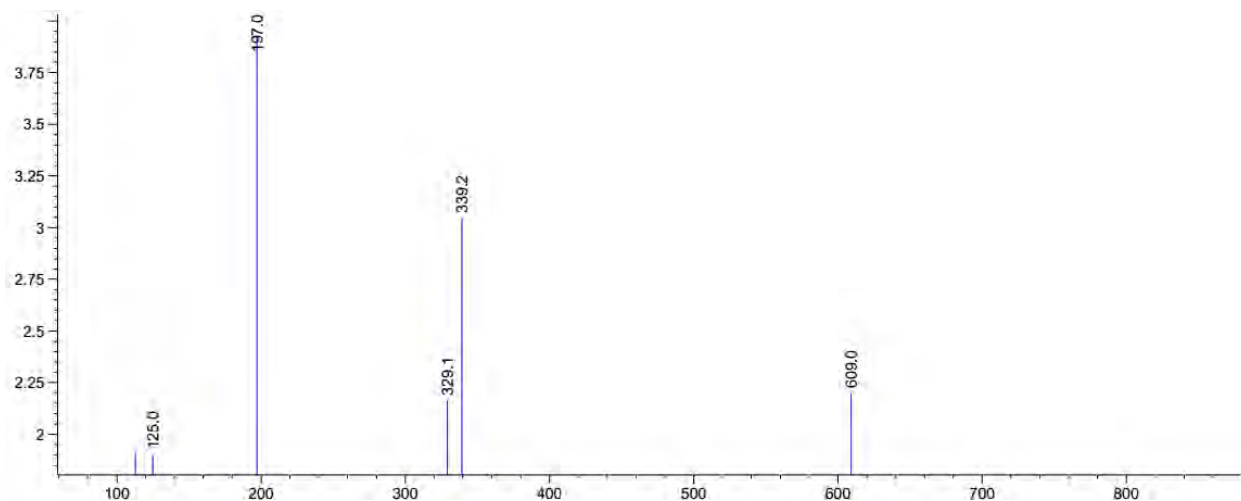


Compound 5 (top) and the Crude (bottom), 1H -NMR (400 MHz, DMSO- d_6)



Compound 5, IR transmittance spectra (neat)

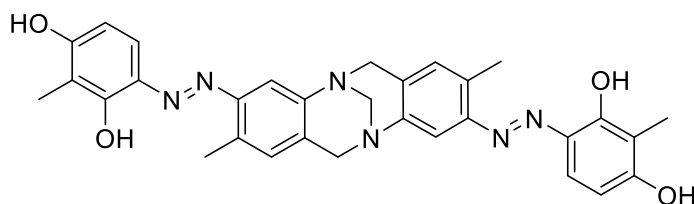
Compound 5, ¹H-NMR (400 MHz, DMSO-*d*₆)Compound 5, ¹³C-NMR (100 MHz, DMSO-*d*₆)



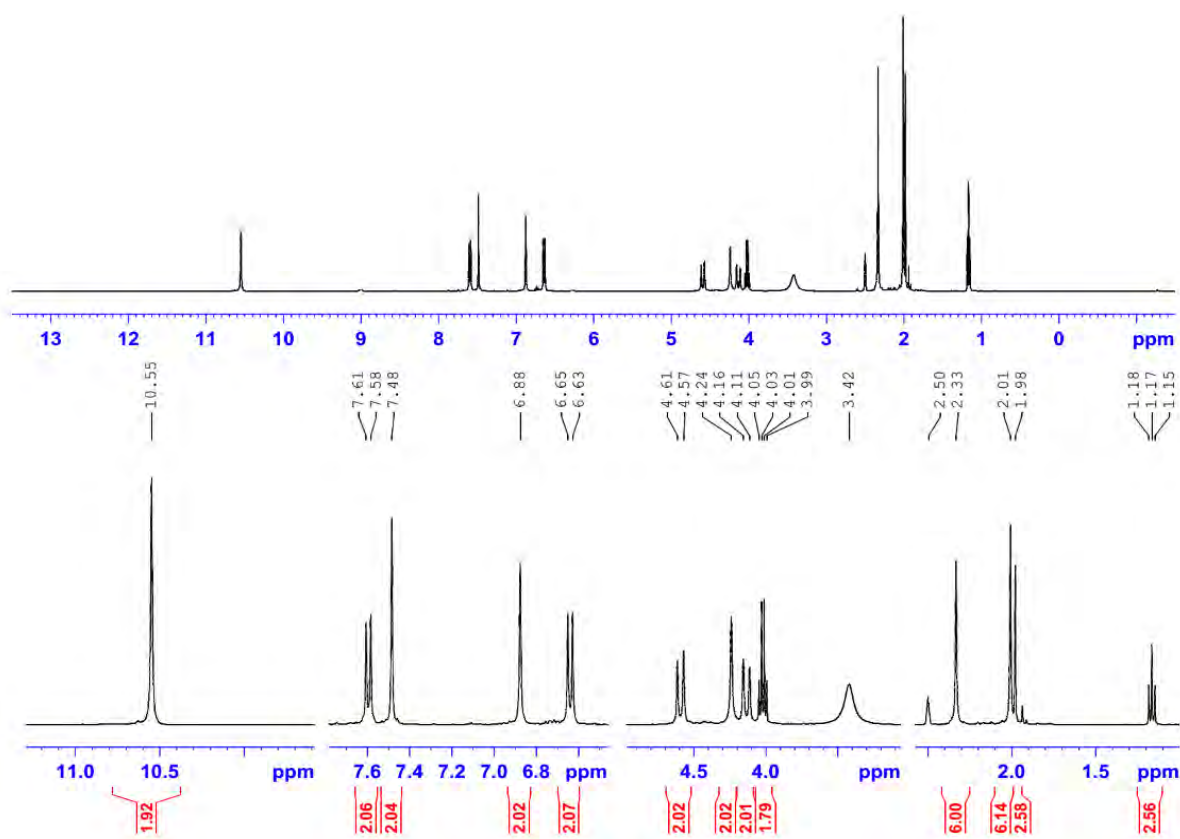
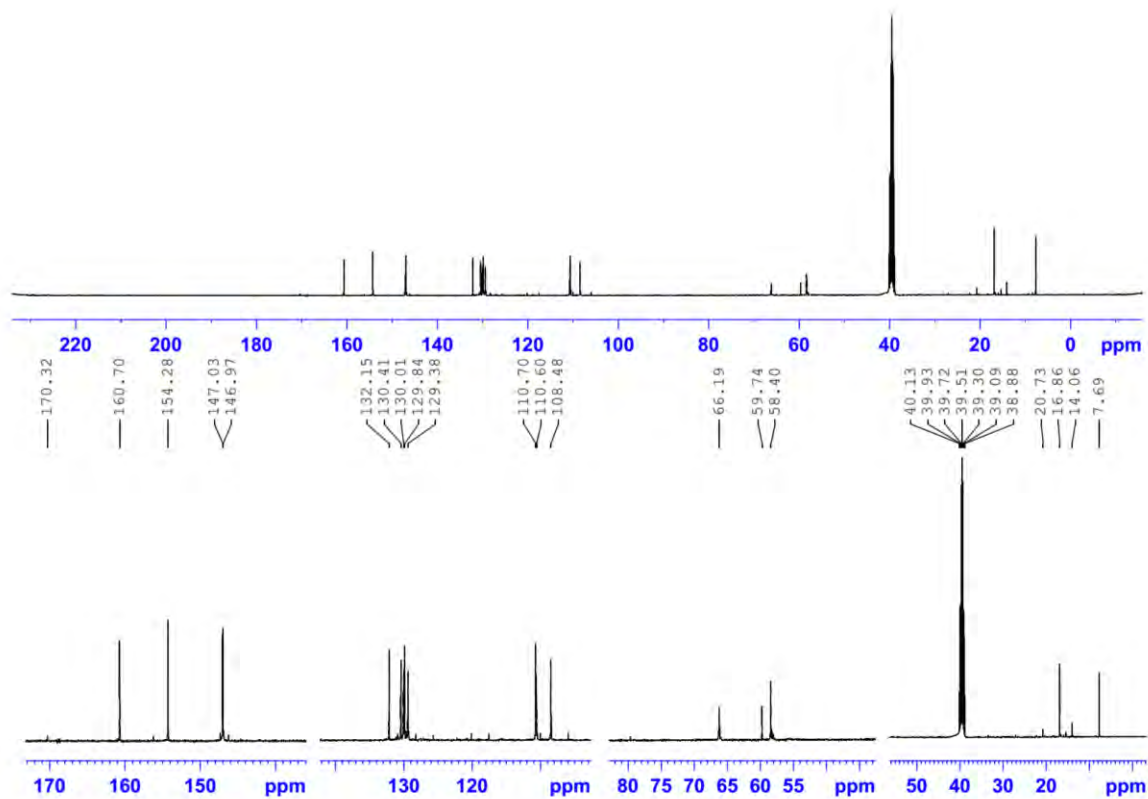
Compound 5, Mass spectra m/z (ESI negative)

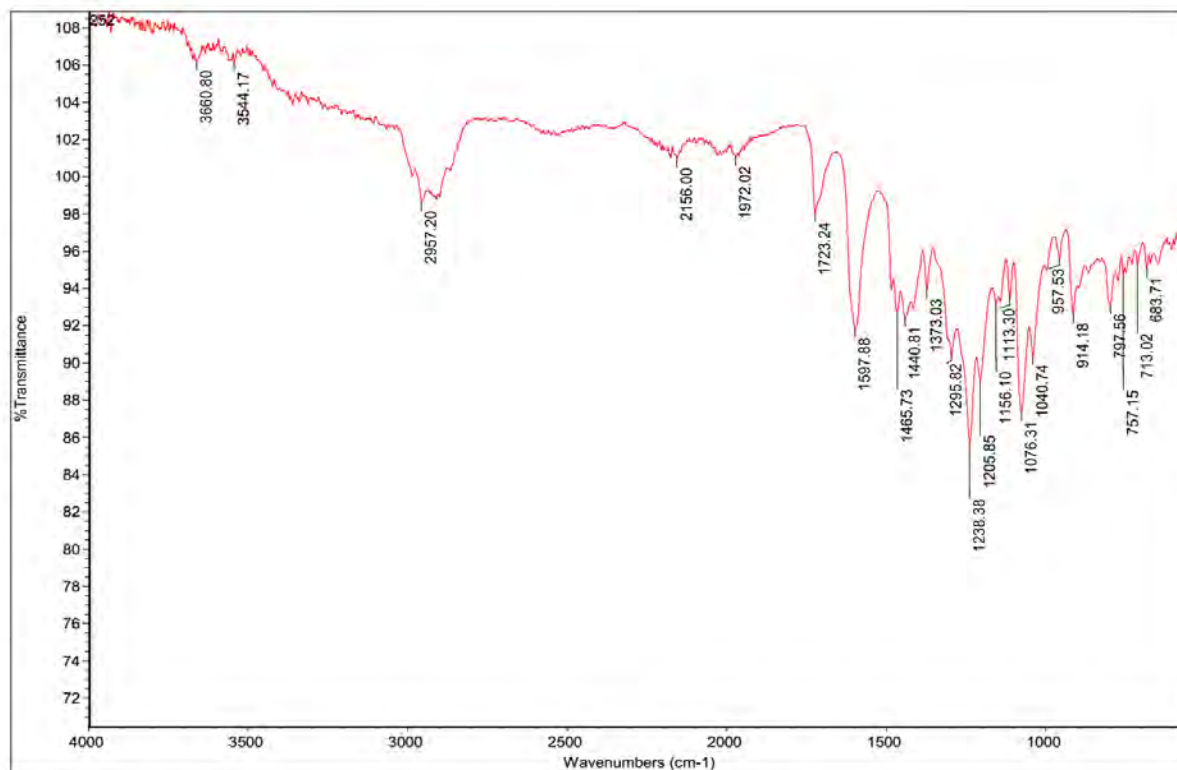
6. Synthesis and Characterization of (±)-6

4,4'-((1E,1'E)-(2,8-dimethyl-6H,12H-5,11-methanodibenzo[b,f][1,5]diazocine-3,9-diyl)bis(diazene-2,1-diyl))bis(2-methylbenzene-1,3-diol)

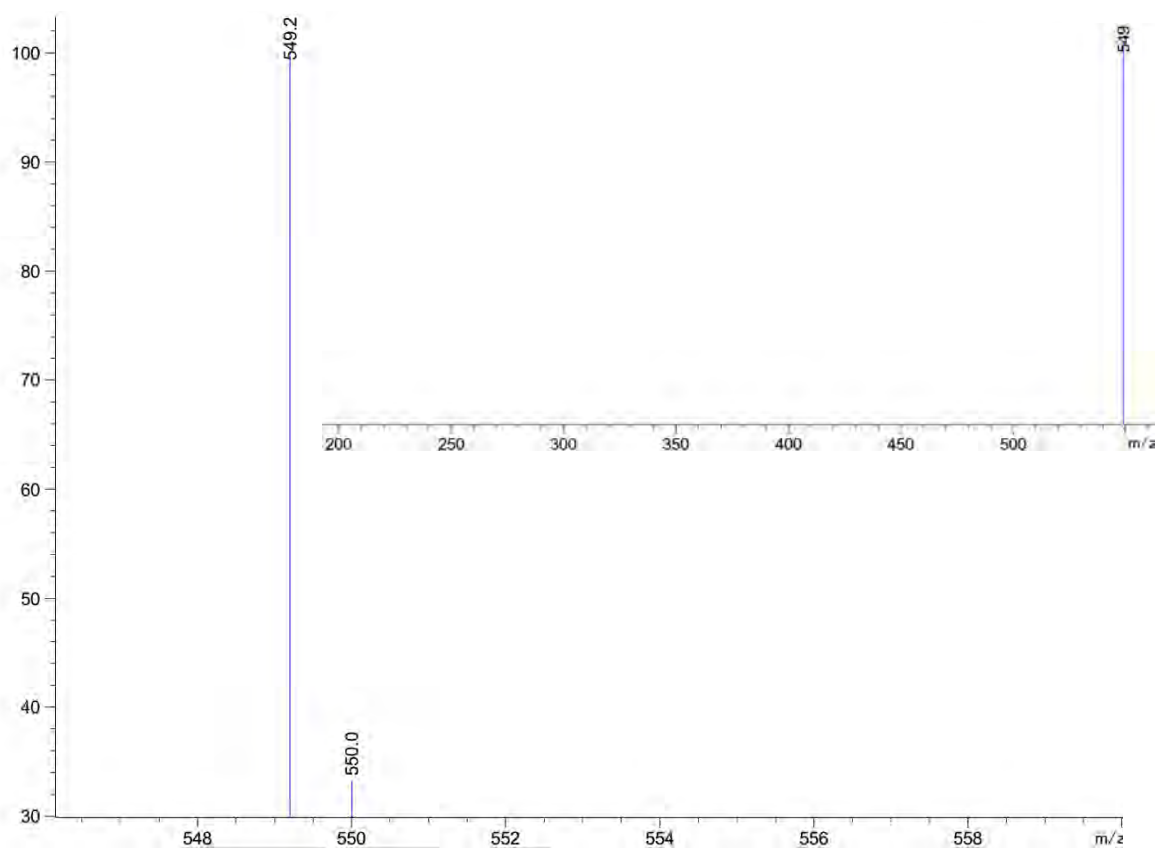


Hünlich's base (0.56 g, 2.0 mmol, 1.0 eq.) was dissolved in H₂SO₄ (6.5%, 30 mL, aq.) at room temperature, then cooled down to -5°C by placing the reaction container in an ice/acetone bath. A sodium nitrite solution (0.30 g, 4.4 mmol, 2.2 eq.) in cold water (5 mL) was dropped into the reaction flask and stirred for 30 minutes. The resulting yellowish solution was poured into a prepared solution of 2-methyl resorcinol (0.52 g, 4.2 mmol, 2.1 eq.) and Na₂CO₃ (2.0 g) in 100 mL of ice-cold water. Stirring was continued for 2 h at 0°C meanwhile two more grams of Na₂CO₃ was gradually added. Afterwards, a dark orange precipitate was extracted from the aqueous mixture (pH=7) by EtOAc (3 x 50 mL). The organic layers were combined, dried over MgSO₄ and evaporated to dryness (0.89 g, 1.62 mmol, 80%). Chemical Formula: C₃₁H₃₀N₆O₄, Molecular Weight: 550.62, **R_f**: 0.5 (EtOAc/ DCM = 50% v/v) silica gel. **¹H-NMR** (400 MHz, DMSO-*d*₆) δ [ppm]: 2.01 (s, 6H, 2 × -CH₃), 2.33 (s, 6H, 2 × -CH₃), 4.13 (d, *J* = 17.3 Hz, 2H, H-6a, H-12a), 4.24 (s, 2H, -N-CH₂-N-), 4.59 (d, *J* = 17.3 Hz, 2H, H-6b, H-12b), 6.64 (d, *J* = 8.85 Hz, 2H, CH), 6.88 (s, 2H, H-1, H-7), 7.48 (s, 2H, H-4, H-10), 7.59 (d, 2H, *J* = 8.80 Hz, CH), 10.55 (s, 2H, OH). **¹³C-NMR** (100 MHz, DMSO-*d*₆) δ [ppm]: 7.69, 16.86, 58.40, 66.19, 108.48, 110.60, 110.70, 129.38, 129.84, 130.01, 130.41, 132.15, 146.97, 147.03, 154.28 and 160.70. **IR**: (Neat) ν_{max} [cm⁻¹] = 3365, 3544, 2981, 1723, 1595, 1484, 1238, 1076 and 914. **MS** (Acetonitrile 48%, isopropyl alcohol 48%, MeOH 4%): (ESI positive) calc. for [C₃₁H₃₁N₆O₄]⁺: [M+H]⁺ 551.23, found 551.2. (ESI negative) calc. for [C₃₁H₂₉N₆O₄]⁻: [M-H]⁻ 549.23, found 549.2. **UV-Vis**: (EtOAc) λ (lgε) = 396nm (4.6). Anal. calcd: C, 67.62; H, 5.49; N, 15.26; O, 11.62. found: C, 68.01; H, 5.81; N, 14.98.

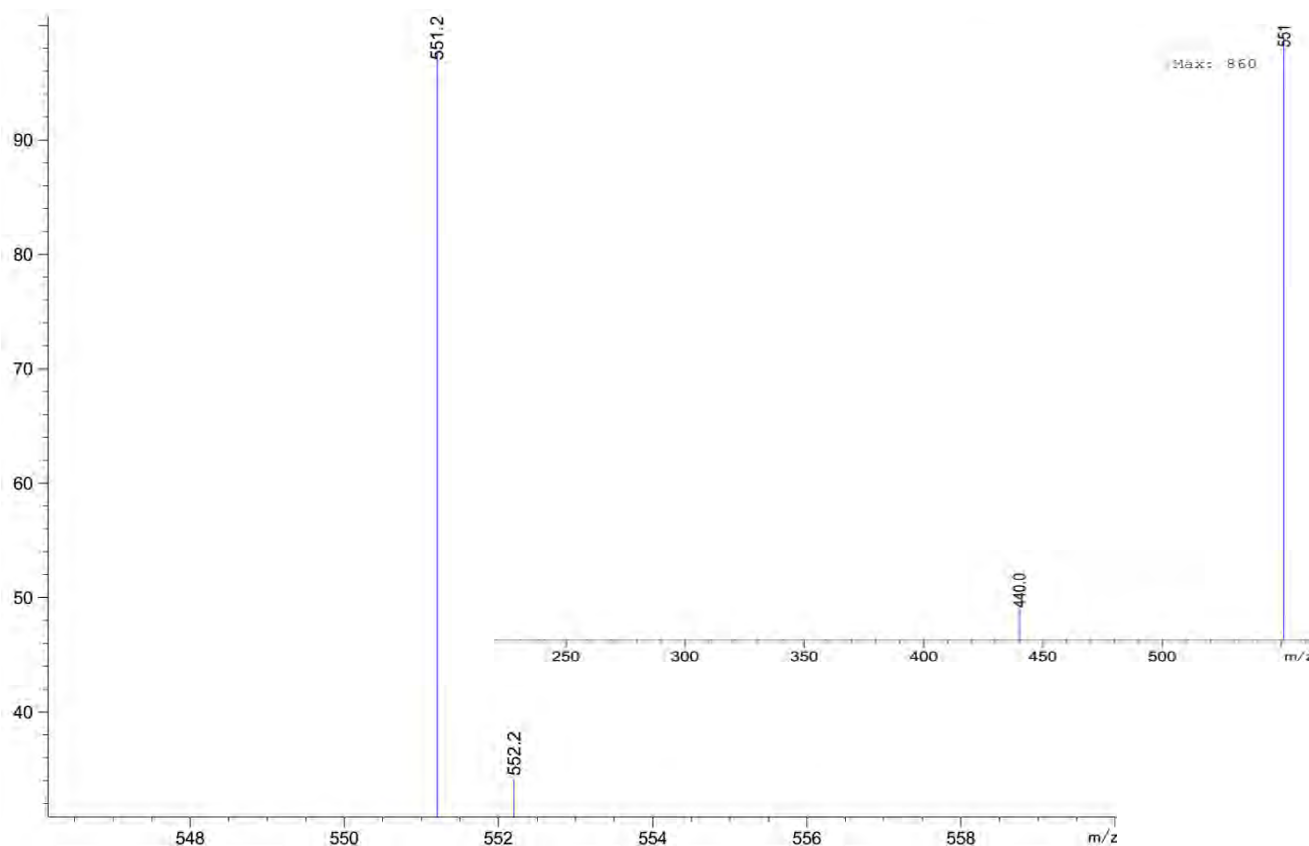
Compound 6, ¹H-NMR (400 MHz, DMSO-*d*₆)Compound 6, ¹³C-NMR (100 MHz, DMSO-*d*₆)



Compound 6, IR transmittance spectra (neat)



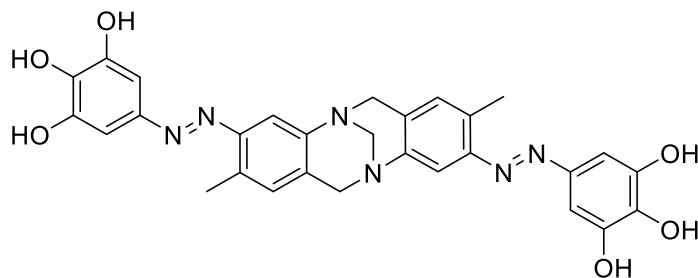
Compound 6, Mass spectra ESI (negative)



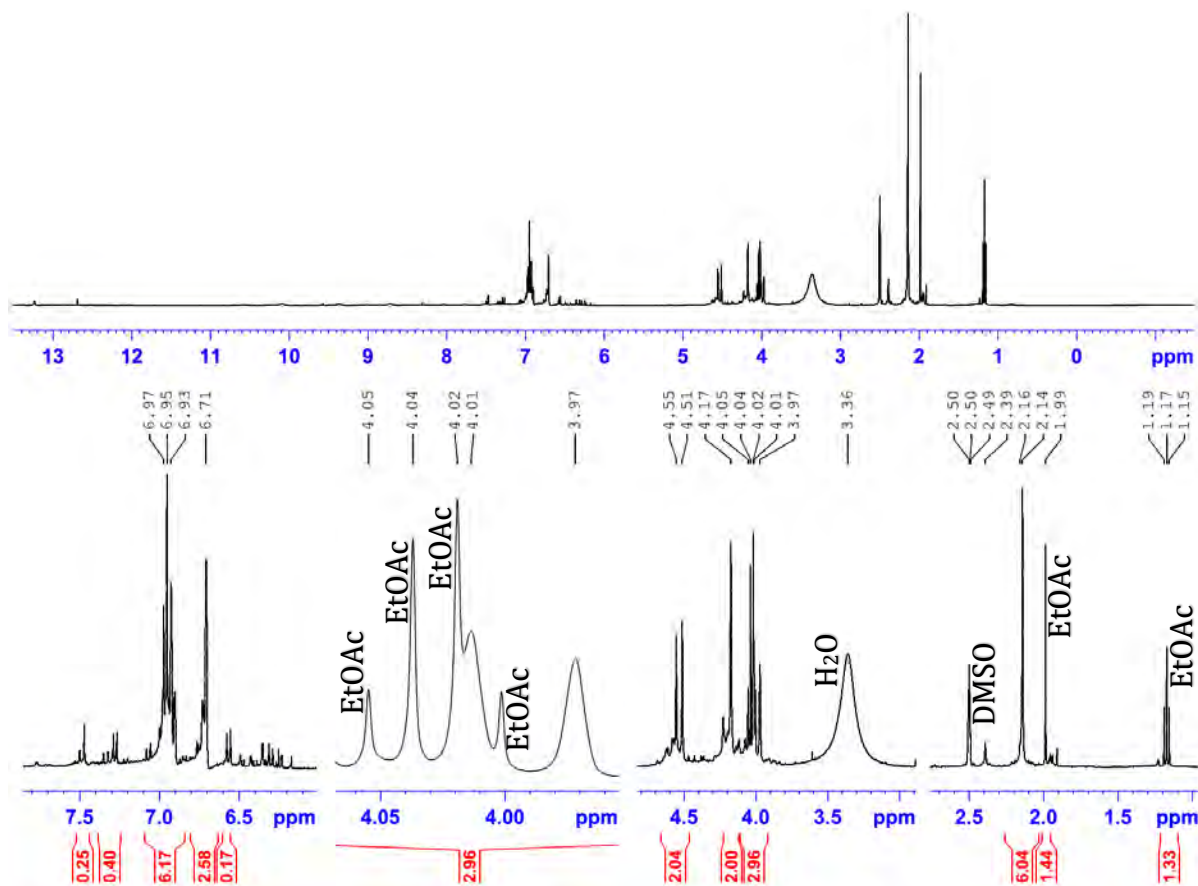
Compound 6, Mass spectra ESI (positive)

7. Synthesis and Characterization of (±)-7

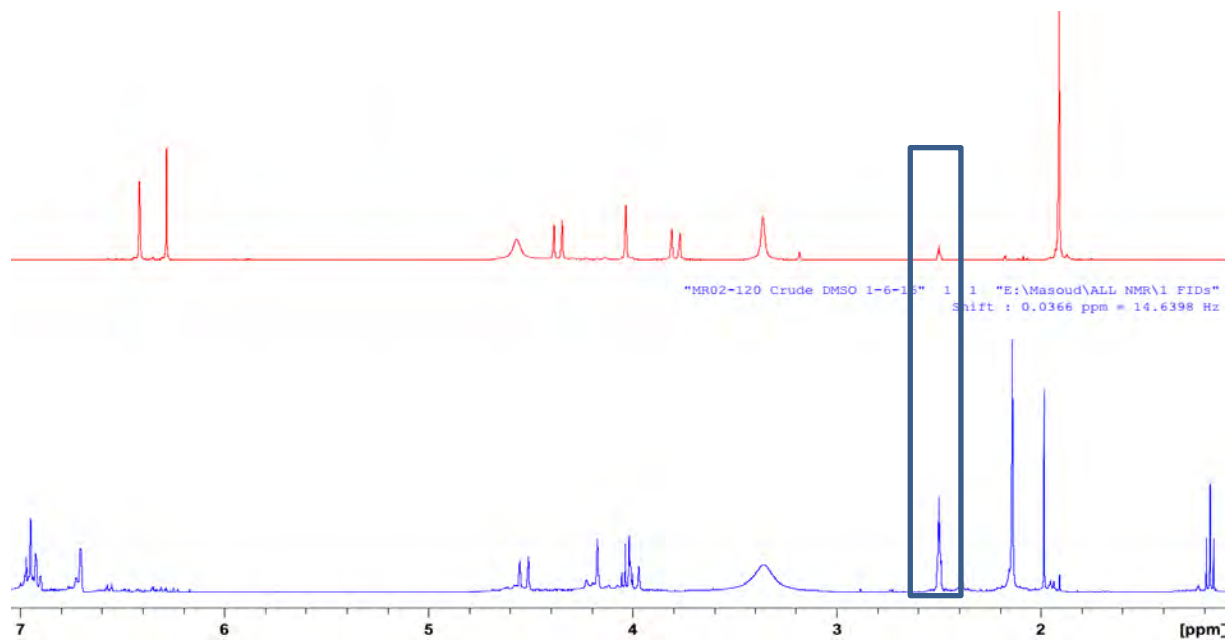
5,5'-((1E,1'E)-(2,8-dimethyl-6H,12H-5,11-methanodibenzo[b,f][1,5]diazocine-3,9-diyl))bis(diazene-2,1-diyl))bis(benzene-1,2,3-triol)



Hünlich's base (0.56 g, 2.0 mmol, 1.0 eq.) was dissolved in H₂SO₄ (6.5%, 30 mL) at room temperature, then cooled down to -5°C by placing the reaction container in ice/acetone bath. A sodium nitrite solution (0.30 g, 4.4 mmol, 2.2 eq.) in cold water (5 mL) was dropped into the reaction flask and stirred for 30 minutes. The resulting yellowish solution was poured into a freshly prepared solution of pyrogallol (1.0 g, excess) and Na₂CO₃ (2.0 g) in 100 mL of ice-cold water. The stirring continued for 4 h at 0°C meanwhile two more grams of Na₂CO₃ was gradually added. Afterwards, the reaction mixture pH was set between 4-5 by adding HCl. Then 3 grams of NaCl were added, and the crude was extracted by EtOAc (5x30 mL). The organic layers were combined, dried over MgSO₄ and evaporated under vacuum to obtain a brown solid (1.1 g). Chemical Formula: C₂₉H₂₆N₆O₆, Molecular Weight: 554.56, R_f: N/A. ¹H-NMR (400 MHz, CDCl₃) δ [ppm] : 2.14 (s, 6H, 2 × -CH₃), 4.00 (d, J = 16.8 Hz, 2H, H-6a, H-12a), 4.17 (s, 2H, -N-CH₂-N-), 4.53 (d, J = 16.6 Hz, 2H, H-6b, H-12b), 6.7 (s, 2H, CH), 6.90-7.00 (m, 6H, CH). Anal. calcd: C, 62.81; H, 4.73; N, 15.15; O, 17.31. found: C, 69.60; H, 6.53; N, 7.98.



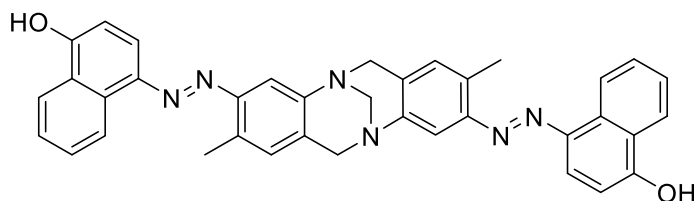
7th Reaction's Crude, ¹H-NMR (400 MHz, DMSO-*d*₆)



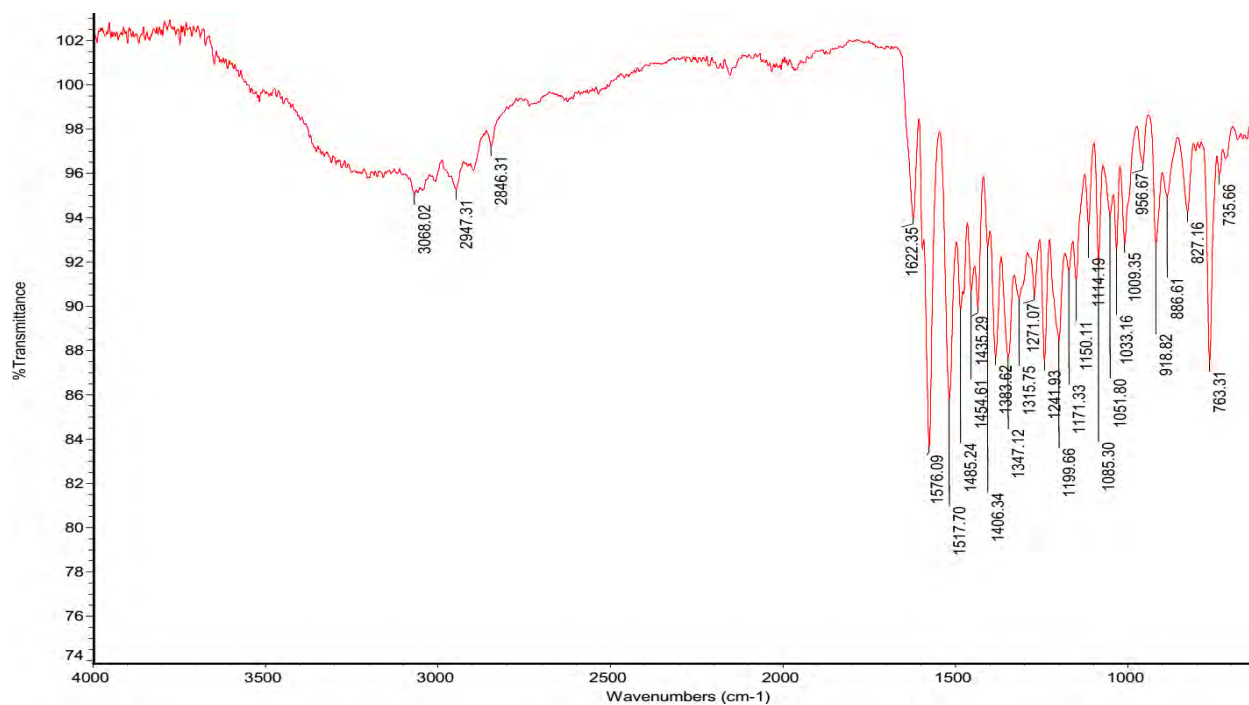
Comparative ¹H-NMR (400 MHz, DMSO-*d*₆, matched at the DMSO peak)
Starting material (top) and the 7th's crude (bottom)

8. Synthesis and Characterization of (±)-8

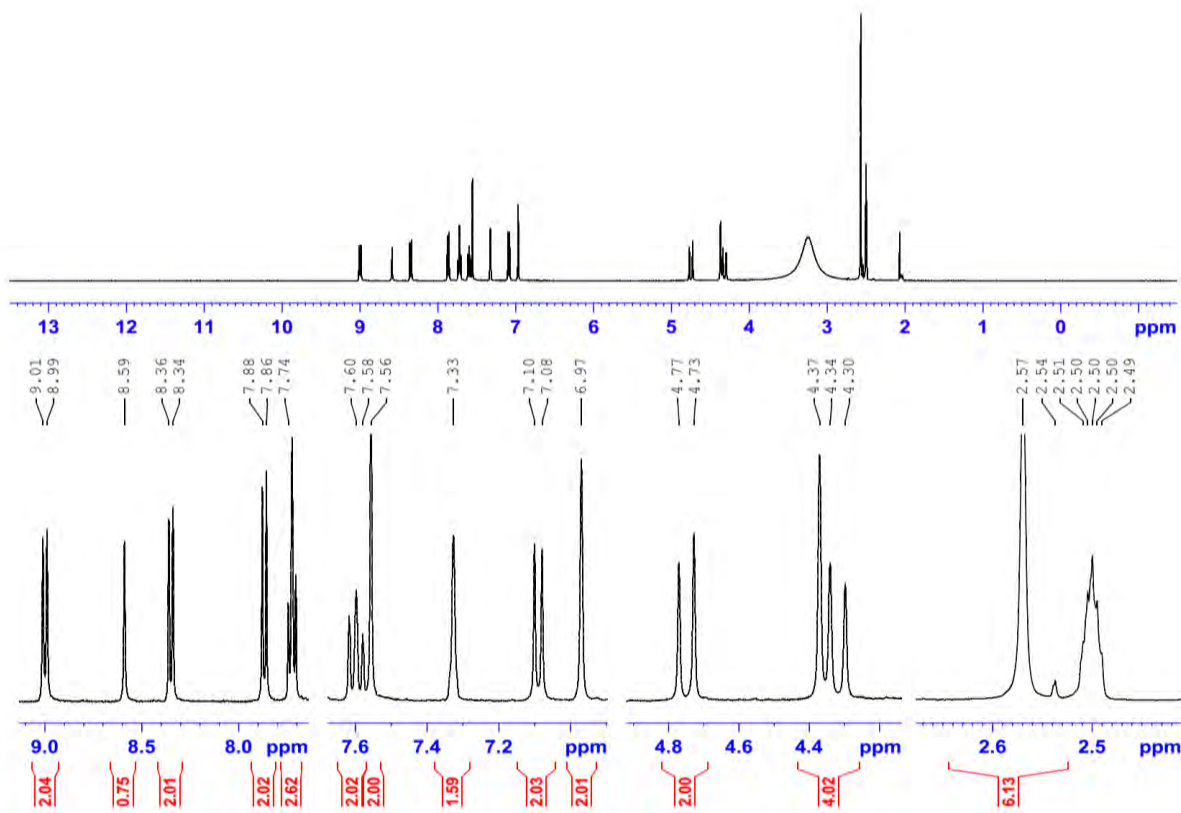
4,4'-((1E,1'E)-(2,8-dimethyl-6H,12H-5,11-methanodibenzo[b,f][1,5]diazocine-3,9-diyl))bis(diazene-2,1-diyl))bis(naphthalen-1-ol)



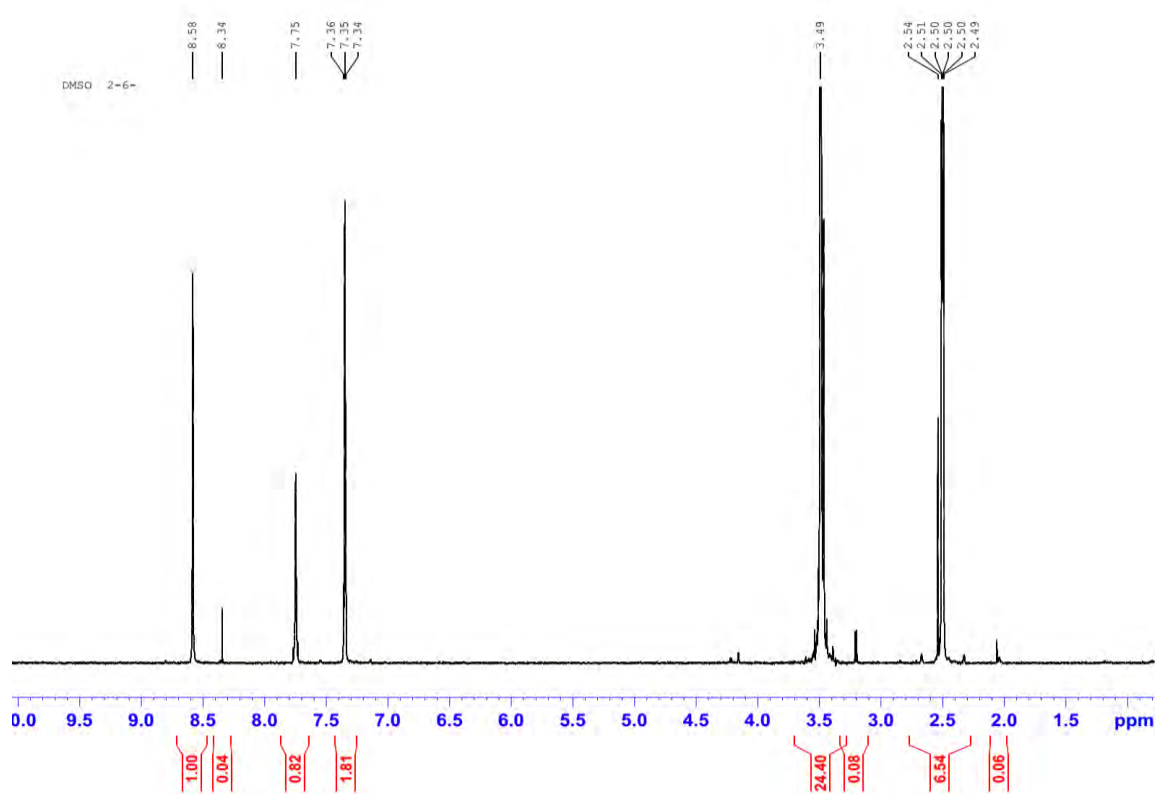
Hünlich's base (0.56 g, 2.0 mmol, 1.0 eq.) was dissolved in H₂SO₄ (6.5%, 30 mL, aq.) at room temperature, then cooled down to -5°C by placing the reaction container in an ice/acetone bath. A sodium nitrite solution (0.30 g, 4.4 mmol, 2.2 eq., in 5 mL of cold water) was dropped into the reaction flask over 10 minutes. After continuing the stirring for 25 more minutes the resulting yellowish solution was poured into a freshly prepared solution of 1-naphthol (0.61 g, 4.2 mmol, 2.1 eq.) and Na₂CO₃ (2.0 g) in 100 mL of ice-cold water. The reaction mixture was stirred for 4 h at 0°C and two more grams of Na₂CO₃ was gradually added into it. Afterwards, NaCl (3.0 g) was added and a brown precipitate was extracted by EtOAc (3 x 80 mL) from the aqueous mixture. The organic layers were combined, dried over MgSO₄ and evaporated to the dryness to obtain **8** (0.82 g, 1.4 mmol, 70%). Chemical Formula: C₃₇H₃₀N₆O₂, Molecular Weight: 590.69, *R_f*: 0.30 (EtOAc/ n-hexane = 40% v/v) silica gel. **¹H-NMR** (80 °C, 400 MHz, DMSO-*d*₆) δ [ppm]: 2.57 (s, 6H, 2 x -CH₃), 4.32 (d, *J* = 17.5 Hz, 2H, H-6a, H-12a), 4.37 (s, 2H, -N-CH₂-N-), 4.75 (d, *J* = 17.4 Hz, 2H, H-6b, H-12b), 6.97 (s, 2H, CH), 7.08 (d, *J* = 8.5 Hz, 2H, CH), 7.56 (s, 2H, CH), 7.60 (t, *J* = 7.8 Hz, 2H, CH), 7.72 (t, *J* = 7.9 Hz, 2H, CH), 7.86 (d, *J* = 8.4 Hz, 2H, CH), 8.35 (d, 2H, *J* = 8.5 Hz, CH), 8.99 (d, 2H, *J* = 8.5 Hz, CH). **¹³C-NMR** (80 °C, 100 MHz, DMSO-*d*₆) δ [ppm]: 16.09, 58.27, 66.27, 108.29, 110.99, 114.29, 122.04, 122.37, 124.40, 124.81, 127.16, 128.88, 130.19, 132.10, 146.47, 149.87 and 205.43. **IR**: (Neat) *v*_{max} [cm⁻¹] = 3412, 3068, 2947, 2846, 1622, 1576, 1485, 1406, 1347, 1315, 1271, 1241, 1199, 1171, 1150, 1085, 1051, 1033, 1009, 956, 918, 886, 827, 763, 735. **MS** (EtOH 60%, EtOAc 40%): (ESI positive) calc. for [C₃₇H₃₁N₆O₂]⁺: [M+H]⁺ 591.24, found 591.2. (ESI negative) calc. for [C₃₇H₂₉N₆O₂]⁻: [M-H]⁻ 589.24, found 589.2. **UV-Vis**: (EtOAc) λ (lge) = 408nm (4.6). **Anal.**: calc. C, 75.24; H, 5.12; N, 14.23; found: C, 75.39; H, 5.23; N, 14.49.



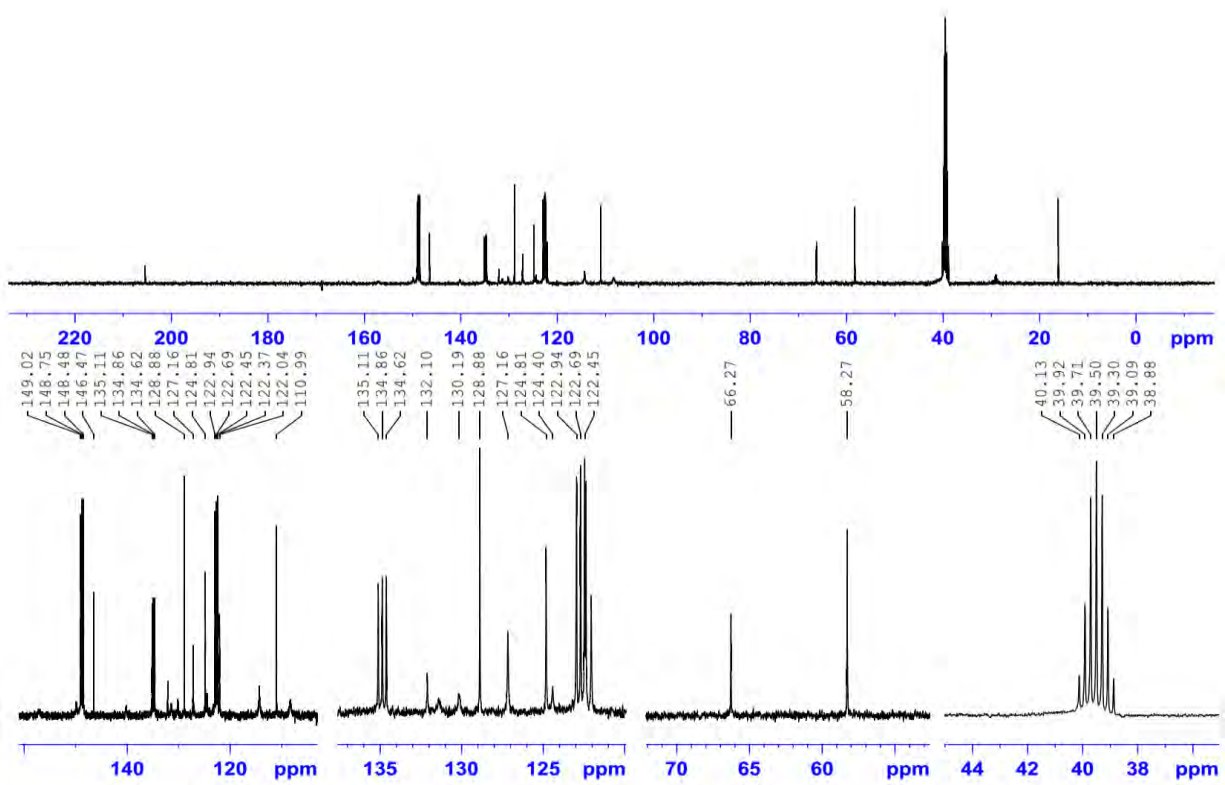
Compound 8, IR transmittance spectra (neat)



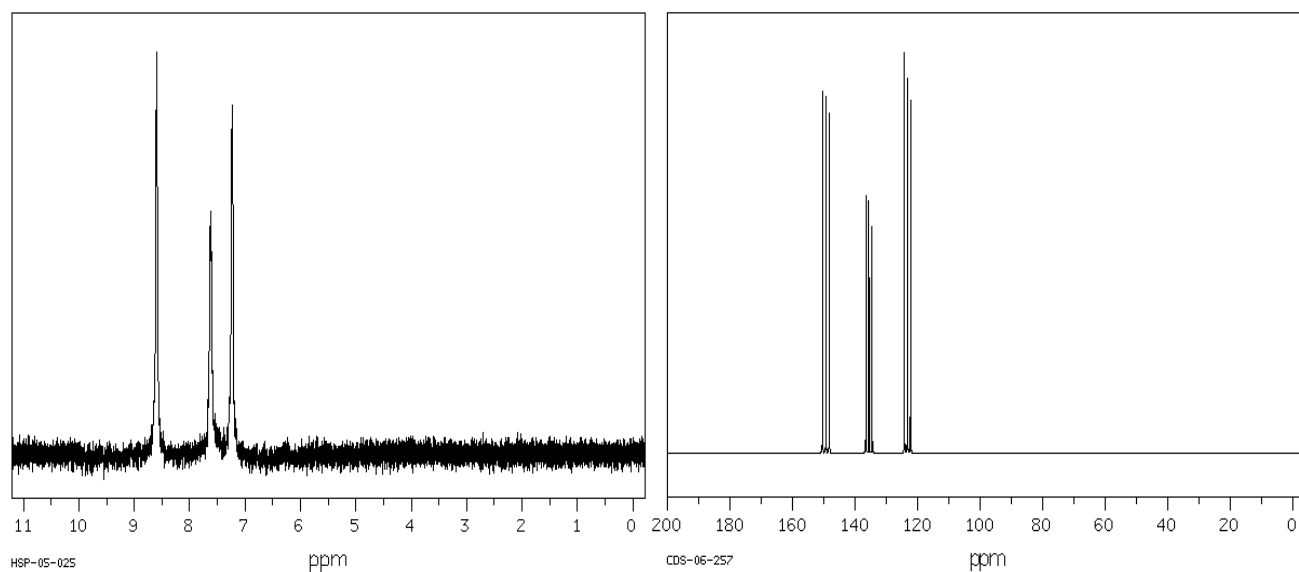
Compound 8, ^1H -NMR (353°K, 400 MHz, $\text{DMSO}-d_6$ and $\text{Pyridine}-d_5$)



^1H NMR 400MHz, $\text{Pyridine}-d_5$ in $\text{DMSO}-d_6$

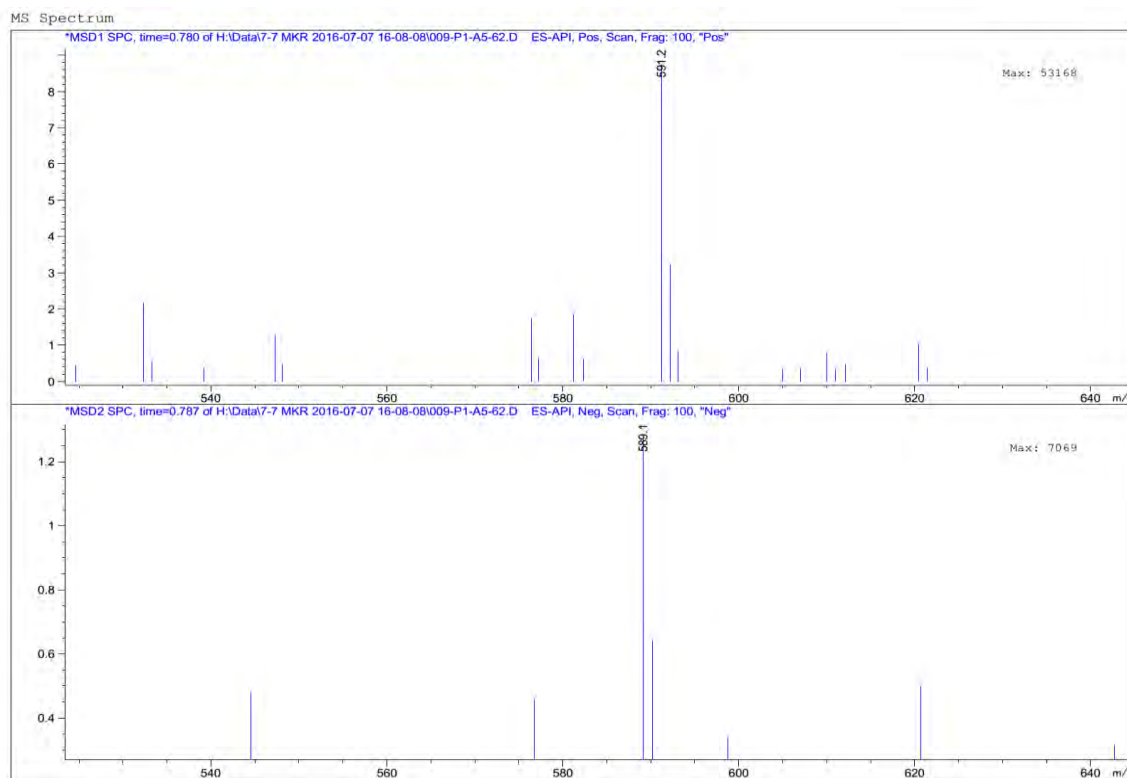


Compound 8, ^{13}C -NMR (353°K, 100 MHz, $\text{DMSO}-d_6$ and $\text{Pyridine}-d_5$)



^1H - (Left, 89.56 MHz) and ^{13}C -NMR (Right, 25.16 MHz) spectra*, Neat $\text{pyridine}-d_5$

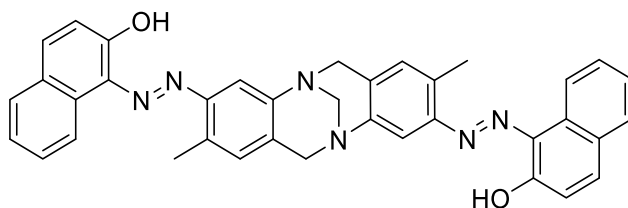
*The spectral data adopted from: <http://sdb.sdb.aist.go.jp> (National Institute of Advanced Industrial Science and Technology, 10/23/2016)



Compound 8, Mass Spectra ESI+ (top) and ESI- (bottom)

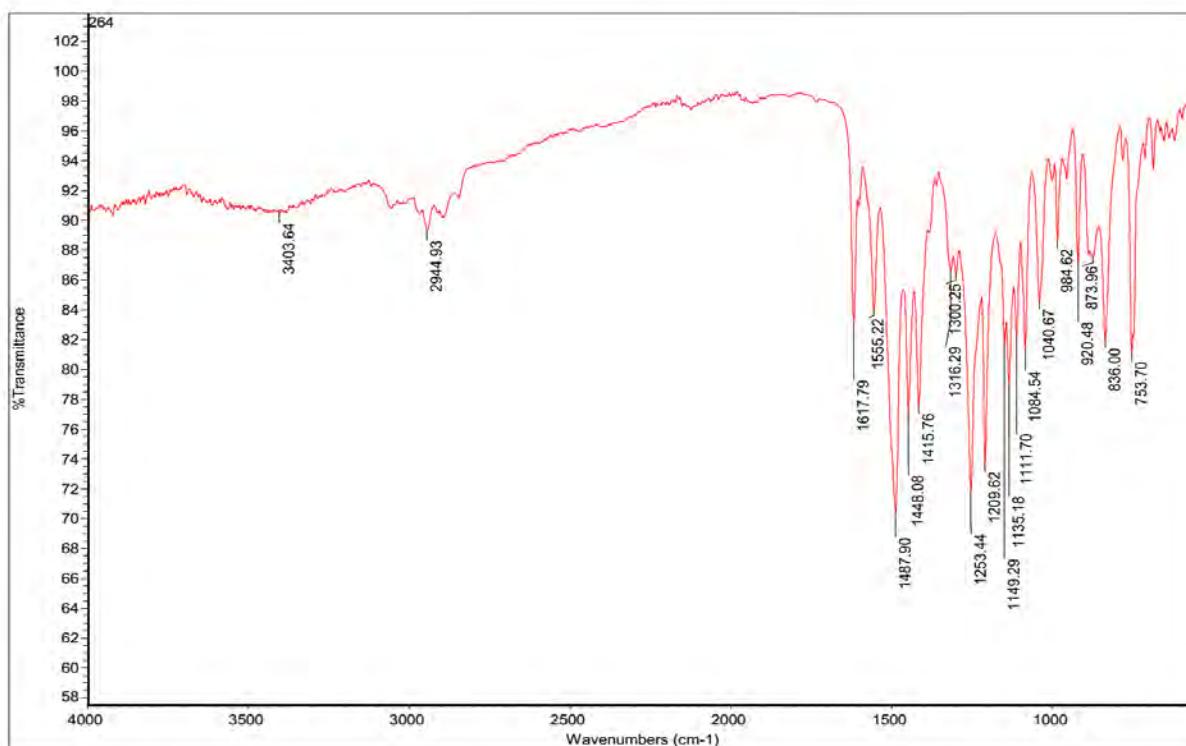
9. Synthesis and Characterization of (±)-9

1,1'-((1E,1'E)-(2,8-dimethyl-6H,12H-5,11-methanodibenzo[b,f][1,5]diazocine-3,9-diyl)bis(diazene-2,1-diyl))bis(naphthalen-2-ol)

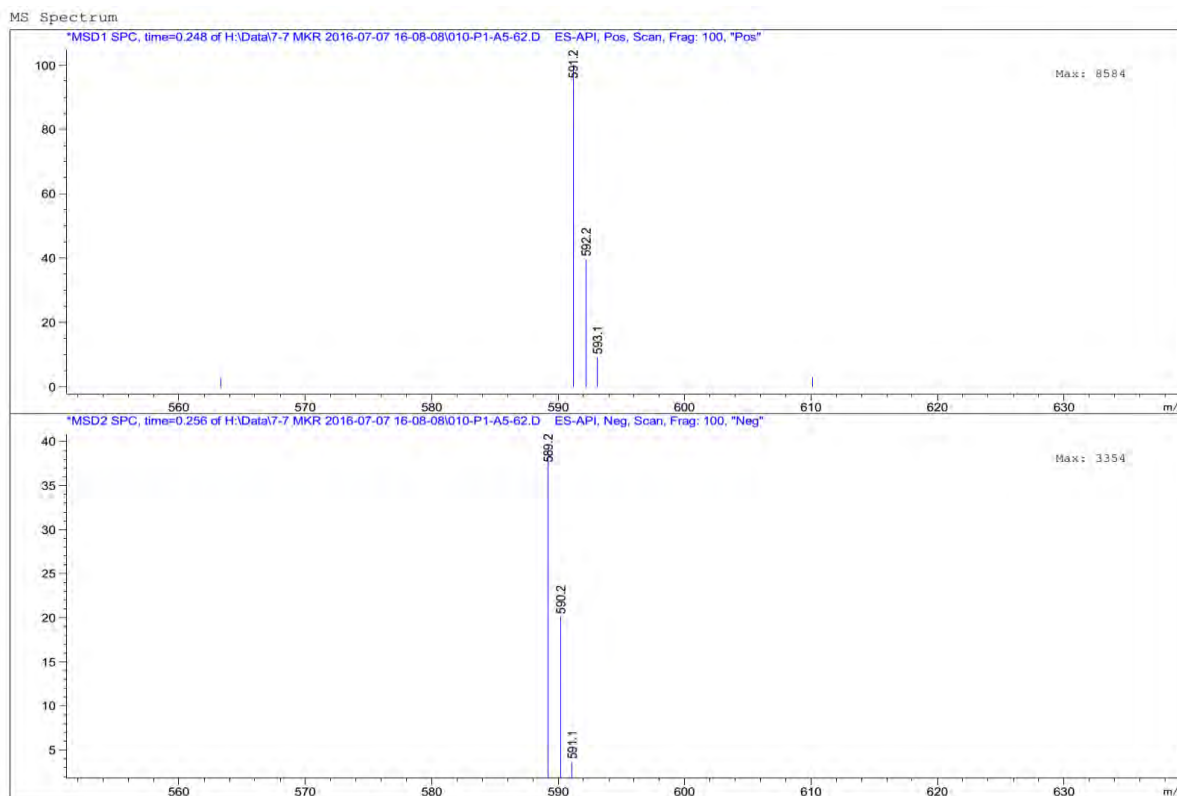


Hünlich's base (0.56 g, 2.0 mmol, 1.0 eq.) was dissolved in H₂SO₄ (6.5%, 30 mL, aq.) at room temperature, then cooled down to -5°C by placing the reaction container in an ice/acetone bath. A sodium nitrite solution (0.30 g, 4.4 mmol, 2.2 eq., in cold water 5 mL) was dropped into the reaction flask over 10 minutes. The stirring continued for 25 more minutes and then the resulting yellowish solution was poured into a fresh solution of 2-naphthol (0.61 g, 4.2 mmol, 2.1 eq.) and Na₂CO₃ (2.0 g) in 100 mL of ice-cold water. The stirring continued for 4 h at 0°C meanwhile two more grams of Na₂CO₃ were gradually added. Afterwards, NaCl (3.0 g) was added and the aqueous mixture was acidified by addition of 5% H₂SO₄ (pH=3) to form a hot-pink precipitate which finally was collected by vacuum filtration. The precipitate was rinsed with distilled water and then desiccated under high-vacuum to obtain **9** (0.88 g, 1.49 mmol, 75%). Chemical Formula: C₃₇H₃₀N₆O₂, Molecular Weight: 590.69, **R_f**: 0.50 (EtOAc/ n-hexane = 40% v/v) silica gel. **¹H-NMR** (400 MHz, CDCl₃) δ [ppm]: 2.41 (s, 6H, 2 × -CH₃), 4.35 (d, *J* = 17.0 Hz, 2H, H-6a, H-12a), 4.42 (s, 2H, -N-CH₂-N-), 4.79 (d, *J* = 17.3 Hz, 2H, H-6b, H-12b), 6.85-6.88 (m, 4H, CH), 7.40-7.44 (m, 2H, CH), 7.57-7.62 (m, 4H, CH), 7.72 (d, 2H, *J* = 9.5 Hz, CH), 7.86 (s, 2H, CH), 8.63 (d, 2H, *J* = 8 Hz, CH). **¹³C-NMR** (100 MHz, CDCl₃) δ [ppm]: 17.18, 59.11, 67.18, 109.75, 111.87, 121.93, 125.14, 125.20, 125.99, 127.08, 128.18, 128.84, 129.07, 129.59, 130.87, 133.68, 140.42, 142.15, 147.55 and 173.14. **IR**: (Neat) ν_{max} [cm⁻¹] = 3403, 2944, 2925, 1617, 1555, 1487, 1448, 1415, 1253, 1209, 1135, 1084, 836 and 753. **MS** (EtOH 80%, EtOAc 20%): (ESI positive)

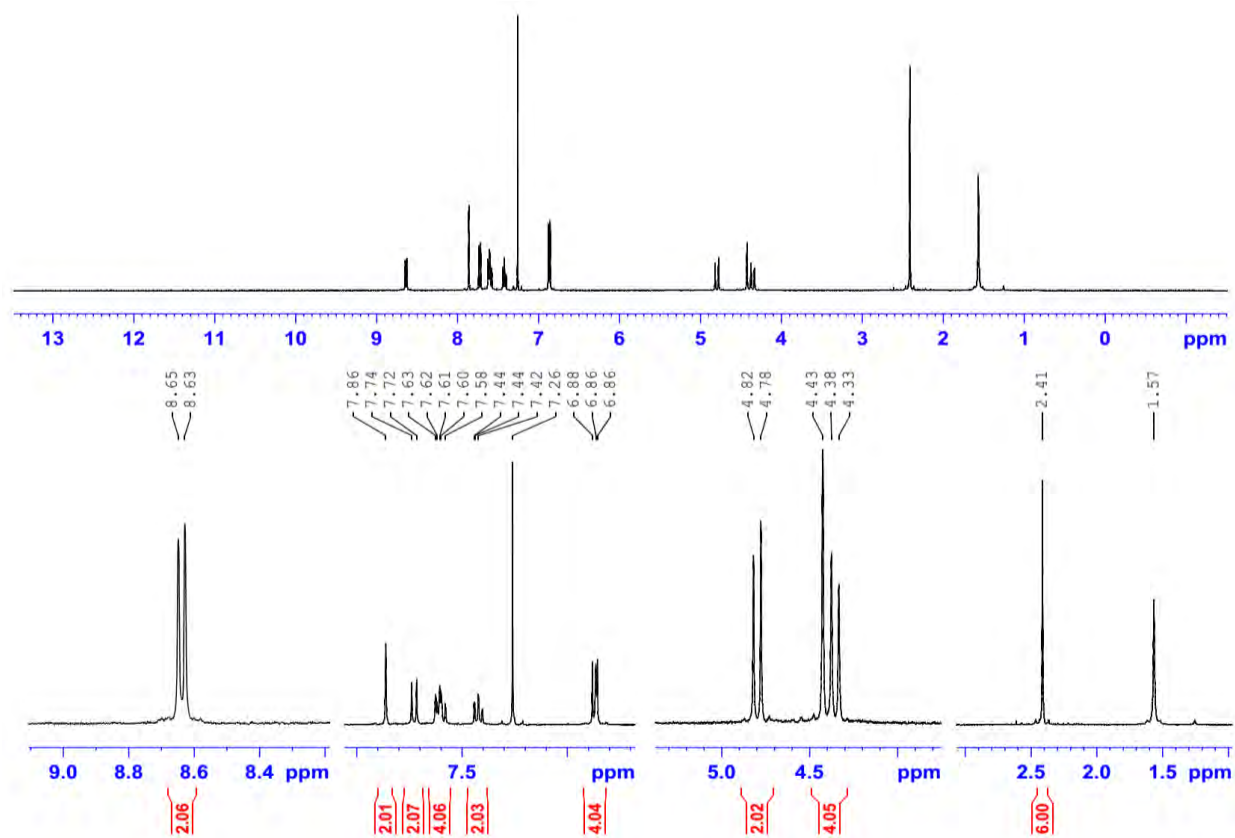
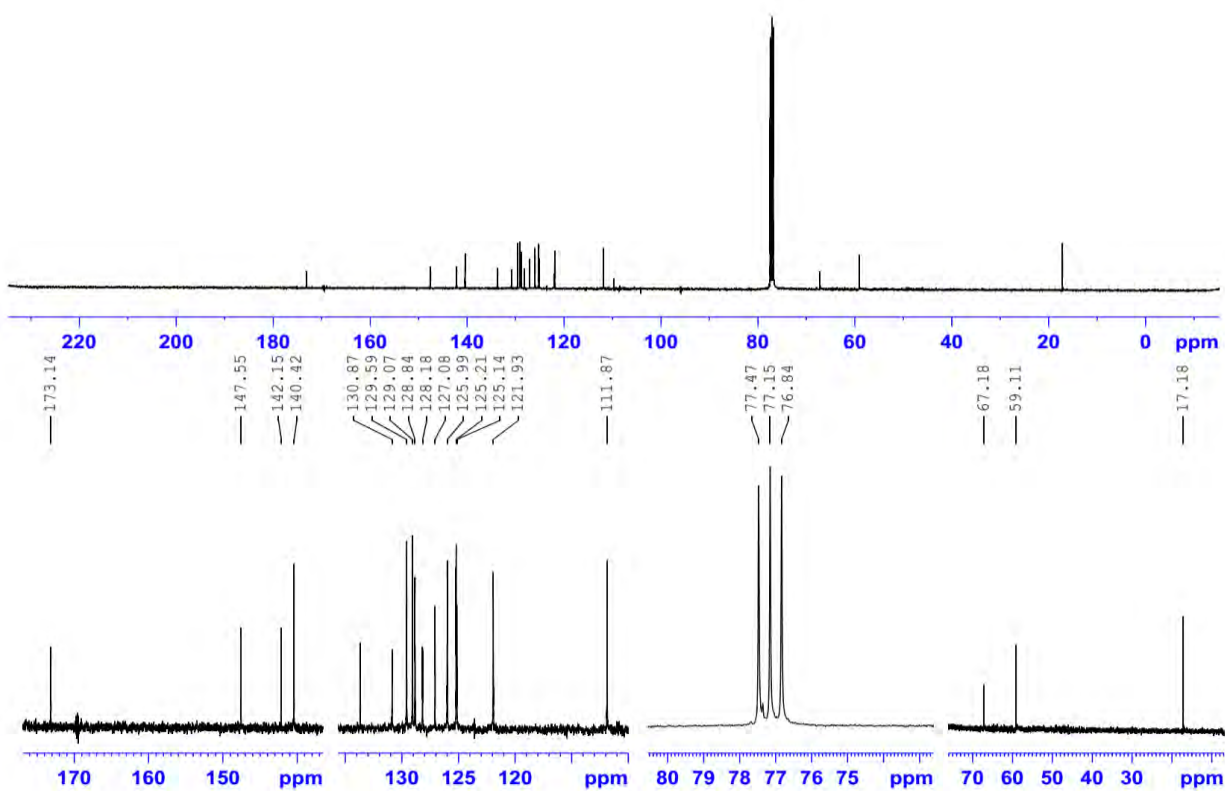
calc. for $[C_{37}H_{31}N_6O_2]^+$: $[M+H]^+$ 591.24, found 591.2. (ESI negative) calc. for $[C_{37}H_{29}N_6O_2]^-$: $[M-H]^-$ 589.24, found 589.2. **UV-Vis:** (EtOAc) λ (lg ϵ) = 493nm (4.4). Anal. calcd: C, 75.24; H, 5.12; N, 14.23; O, 5.42. found: C, 75.02; H, 5.03; N, 14.51.



Compound 9, IR transmittance spectra (neat)

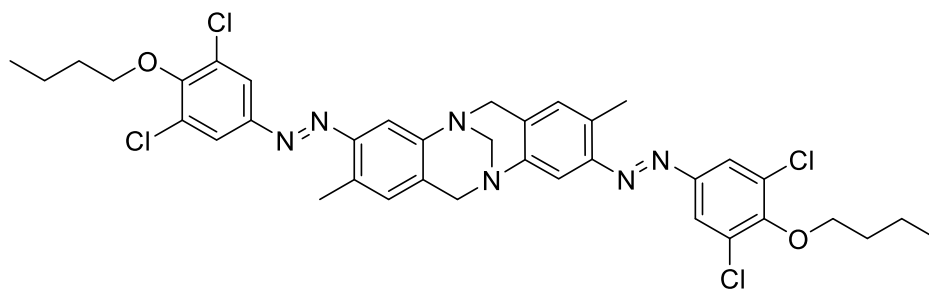


Compound 9, Mass Spectra ESI+ (top) and ESI- (bottom)

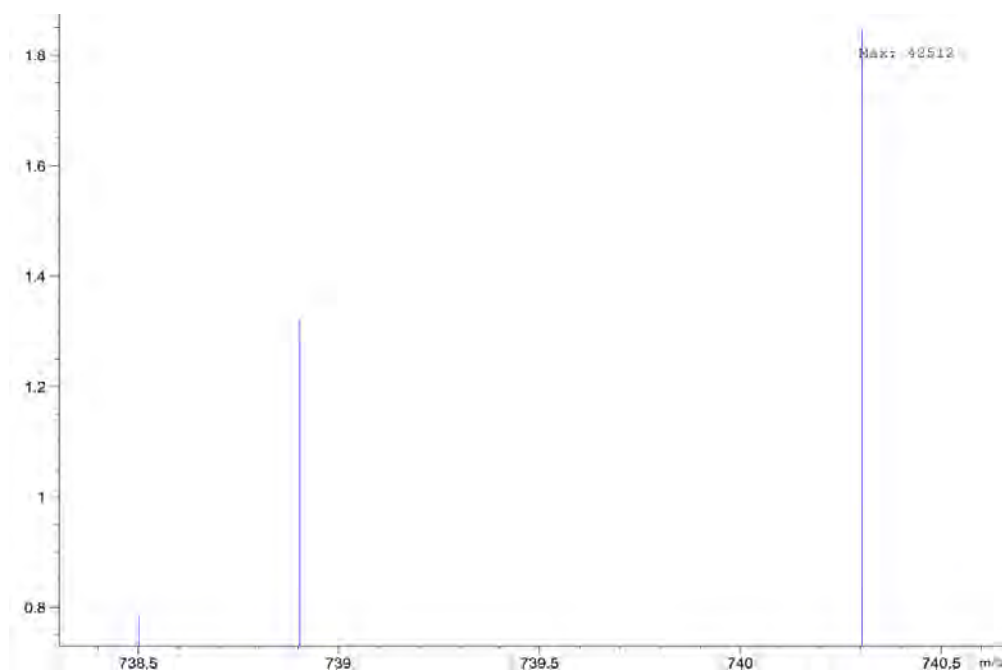
Compound 9, ¹H-NMR (400 MHz, CDCl₃)Compound 9, ¹³C-NMR (100 MHz, CDCl₃)

10. Synthesis and Characterization of (±)-1A

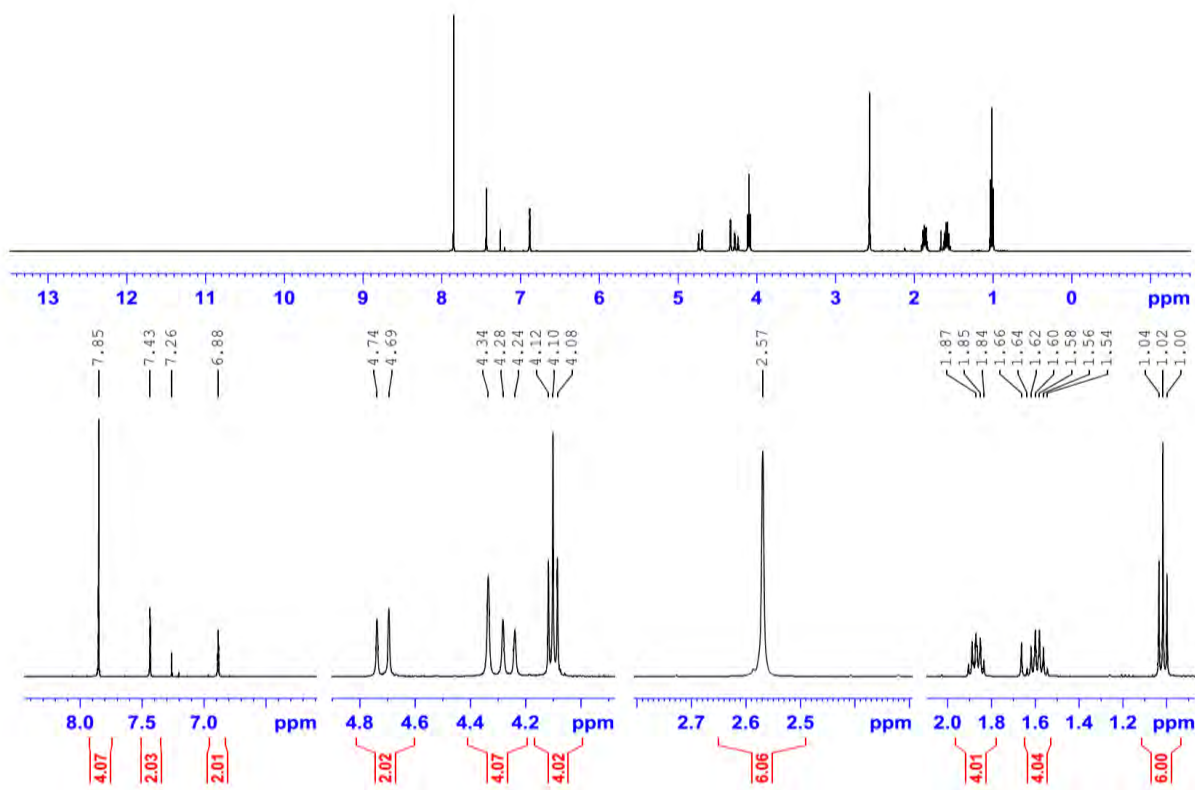
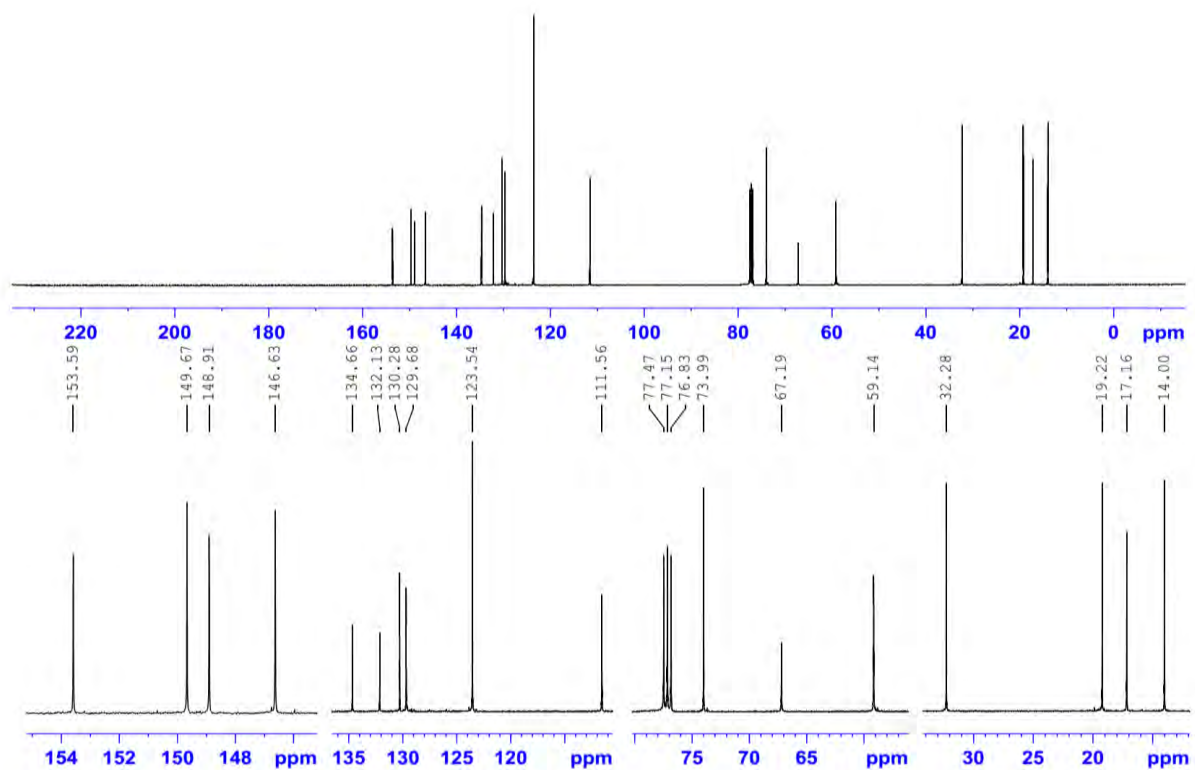
3,9-bis((E)-(4-butoxy-3,5-dichlorophenyl)diazenyl)-2,8-dimethyl-6H,12H-5,11-methanodibenzo[b,f][1,5]diazocine



Compound **1** (0.31 g, 0.50 mmol, 1.0 eq.) and K_2CO_3 (0.55 g, 4 mmol) were mixed in dried acetone (5 mL) at room temperature for 15 minutes in a sealed round-bottom flask. Then, 1-iodobutane (0.24 g, 1.2 mmol, 2.4 eq.) was injected into the mixture and refluxed for 6 hours at 55°C in darkness. The reaction profile was monitored by TLC, which showed a single spot at the conclusion of the reaction. Then the resulting mixture was added to 50 ml of distilled water and the crude was extracted by EtOAc (3 x 30 ml). The organic layers were combined, dried over $MgSO_4$ and filtered. After solvent removal under reduced pressure, the solid residue was chromatographed to obtain a shiny orange solid **1A** (0.29 g, 0.39 mmol, 77%). Chemical Formula: $C_{37}H_{38}Cl_4N_6O_2$, Molecular Weight: 740.55, R_f : 0.5 (EtOAc/ n-hexane = 20% v/v) silica gel. 1H -NMR (400 MHz, $CDCl_3$) δ [ppm]: 1.02 (t, J = 7.6 Hz, 6H, CH_3), 1.59 (m, 4H, CH_2), 1.85 (m, 4H, CH_2), 2.57 (s, 6H, CH_3), 4.10 (t, J = 7.9 Hz, 4H, CH_2), 4.26 (d, J = 17.1 Hz, 2H, H-6a, H-12a), 4.34 (s, 2H, -N- CH_2 -N-), 4.72 (d, J = 17.1 Hz, 2H, H-6b, H-12b), 6.88 (s, 2H, H-1, H-7), 7.43 (s, 2H, H-4, H-10), 7.85 (s, 4H, CH). ^{13}C -NMR (100 MHz, $CDCl_3$) δ [ppm]: 14.00, 17.16, 19.22, 32.28, 59.14, 67.19, 73.99, 111.56, 123.54, 129.68, 130.28, 132.13, 134.66, 146.63, 148.91, 149.67 and 153.59. IR: (Neat) ν_{max} [cm^{-1}] = 2929, 2858, 1561, 1482, 1447, 1381, 1254, 1233, 1081, 984, 930, 899, 802, 729. MS (Acetonitrile 45%, isopropyl alcohol 45%, EtOAc 5%, MeOH 5%): (ESI positive) calc. for $[C_{37}H_{39}Cl_4N_6O_2]^+$: $[M+H]^+$ 739.18, found 738.9 and 740.3. UV-Vis: (EtOAc) λ (lg ϵ) = 347 nm (4.5). Anal. calcd: C, 60.01; H, 5.17; Cl, 19.15; N, 11.35; O, 4.32. found: C, 59.71; H, 5.36; N, 11.51.

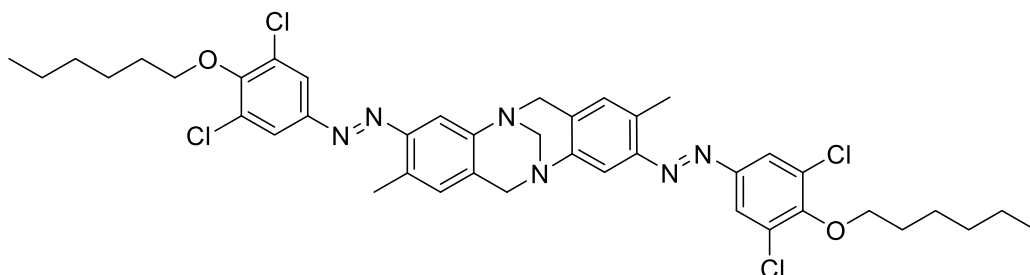


Compound 1A, Mass spectra (ESI positive)

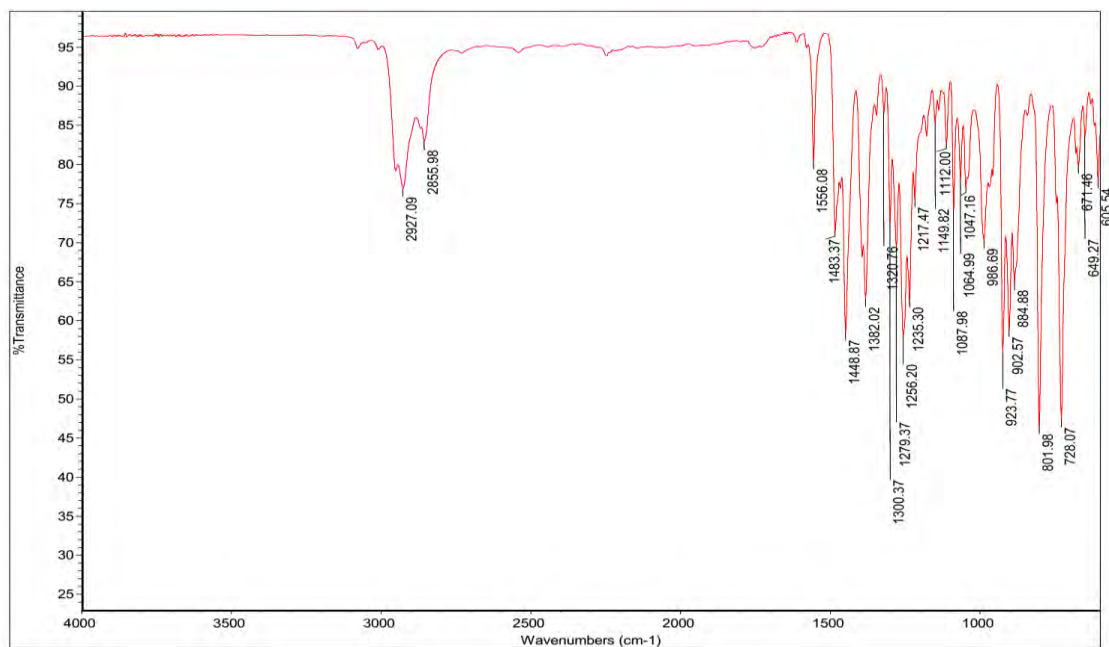
Compound 1A, ¹H-NMR (400 MHz, CDCl₃)Compound 1A, ¹³C-NMR (100 MHz, CDCl₃)

11. Synthesis and Characterization of (±)-1B

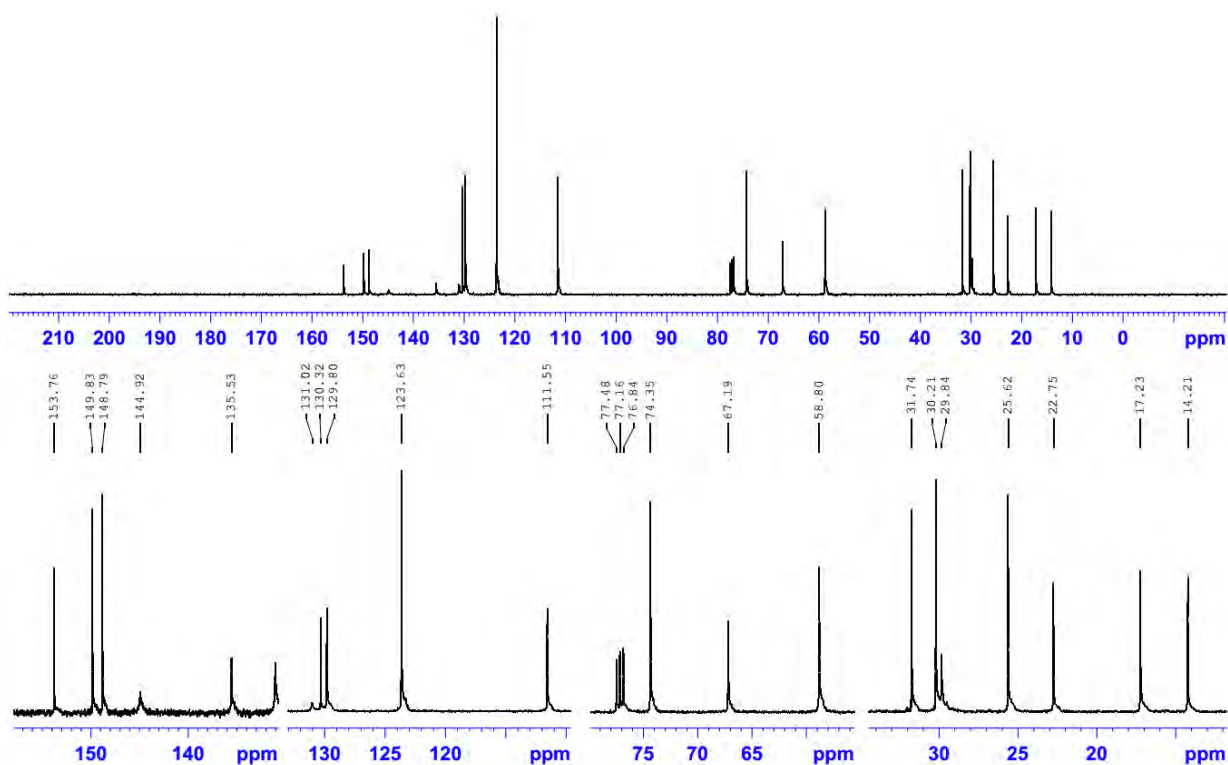
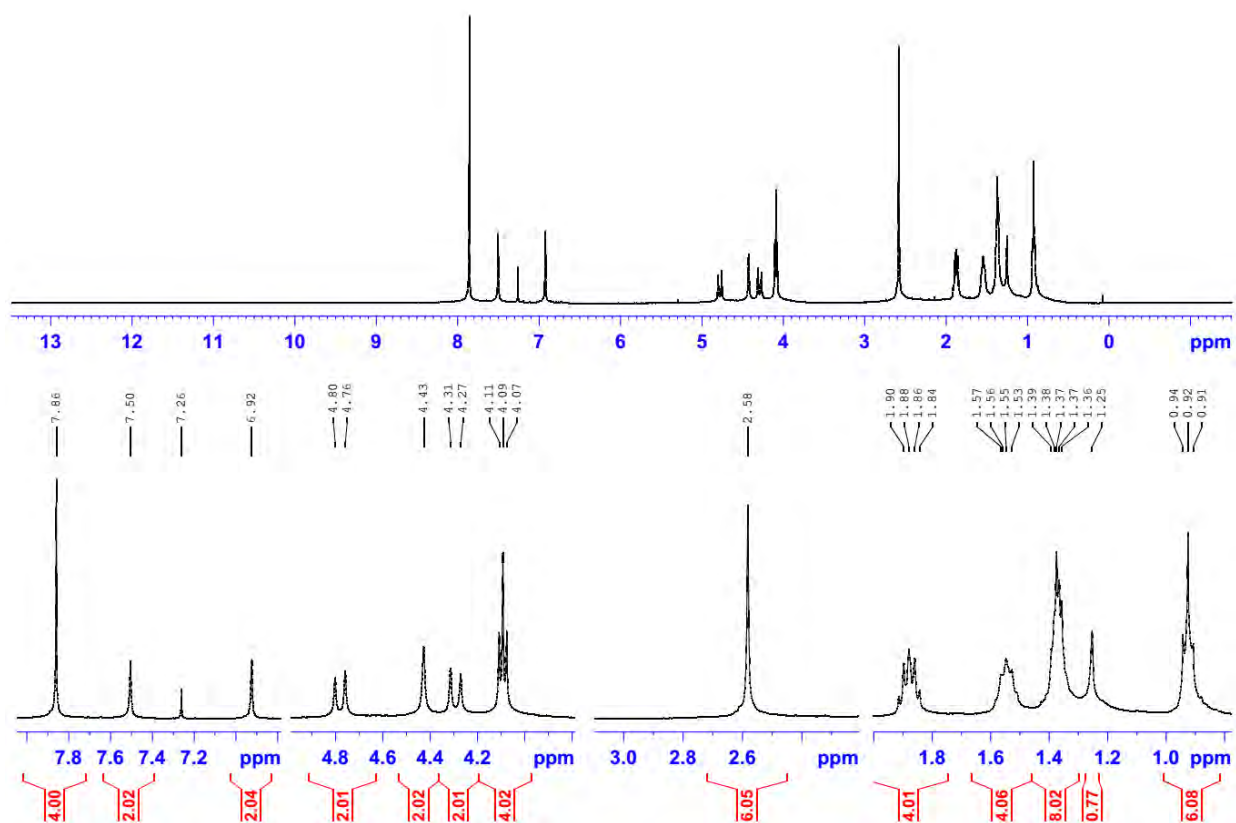
3,9-bis((E)-(3,5-dichloro-4-(hexyloxy)phenyl)diazenyl)-2,8-dimethyl-6H,12H-5,11-methanodibenzo[b,f][1,5]diazocine



1 (0.31 g, 0.5 mmol, 1eq.), K_2CO_3 (0.55 g, 4 mmol) and a catalytic amount of KI (~0.01 g) were mixed in dried acetone (10 mL) at room temperature for 15 minutes in a sealed round bottom flask, then 1-bromohexane (0.22 g, 1.3 mmol, 2.6 eq.) was injected into the mixture and refluxed for 12 hours at 55°C in darkness. After monitoring the TLC profile which showed a single spot, the resulting orange mixture was poured into 50 ml of cold water, and extracted by ethyl acetate (3 x 30 ml). The organic layers were combined, dried up over $MgSO_4$ and kept under the reduced pressure to the dryness. Afterwards, the purification was done by column chromatography on silica gel in dark to obtain a shiny orange solid **1B** (0.29 g, 0.36 mmol, 72%). Chemical Formula: $C_{41}H_{46}Cl_4N_6O_2$, Molecular Weight: 796.66, R_f : 0.62 (MeOH/ DCM = 4% v/v) silica gel. 1H -NMR (400 MHz, $CDCl_3$) δ [ppm]: 0.92 (t, J = 7.8 Hz, 6H, CH_3), 1.37 (m, 8H, CH_2), 1.55 (m, 4H, CH_2), 1.88 (m, 4H, CH_2), 2.58 (s, 6H, CH_3), 4.10 (t, J = 8.1 Hz, 4H, CH_2), 4.29 (d, J = 17.2 Hz, 2H, H-6a, H-12a), 4.42 (s, 2H, -N- CH_2 -N-), 4.77 (d, J = 17.2 Hz, 2H, H-6b, H-12b), 6.92 (s, 2H, H-1, H-7), 7.50 (s, 2H, CH), 7.85 (s, 4H, H-4, H-10). ^{13}C -NMR (100 MHz, $CDCl_3$) δ [ppm]: 14.21, 17.23, 22.75, 25.62, 29.83, 30.20, 31.74, 58.80, 67.18, 74.34, 111.54, 123.62, 129.79, 130.32, 131.02, 135.52, 144.91, 148.79, 149.83, 153.75. IR: (Neat) ν_{max} (cm^{-1}) = 2927, 2855, 1556, 1483, 1448, 1382, 1256, 1235, 1087, 986, 923, 902, 801, 728. MS (Acetonitrile 90%, EtOAc 10%): (ESI positive) calc. for $[C_{41}H_{47}Cl_4N_6O_2]^+$: $[M+H]^+$ 795.24, found 795.6. UV: (ethyl acetate) λ (lg ϵ) = 346 nm. Anal. calcd: C, 61.81; H, 5.82; Cl, 17.80; N, 10.55; O, 4.02. found: C, 61.93; H, 5.51; N, 10.33.

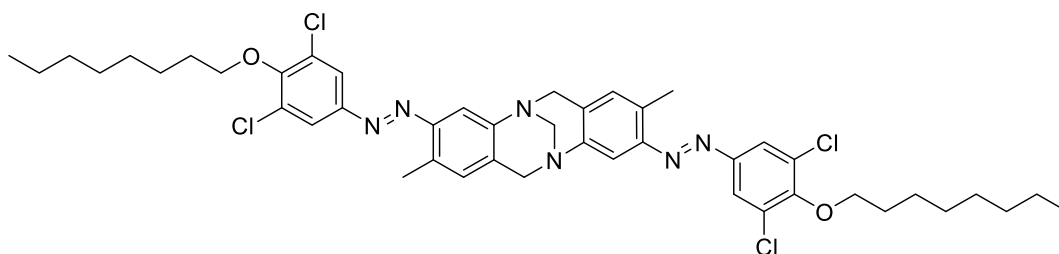


Compound 1B, IR transmittance spectra (neat)

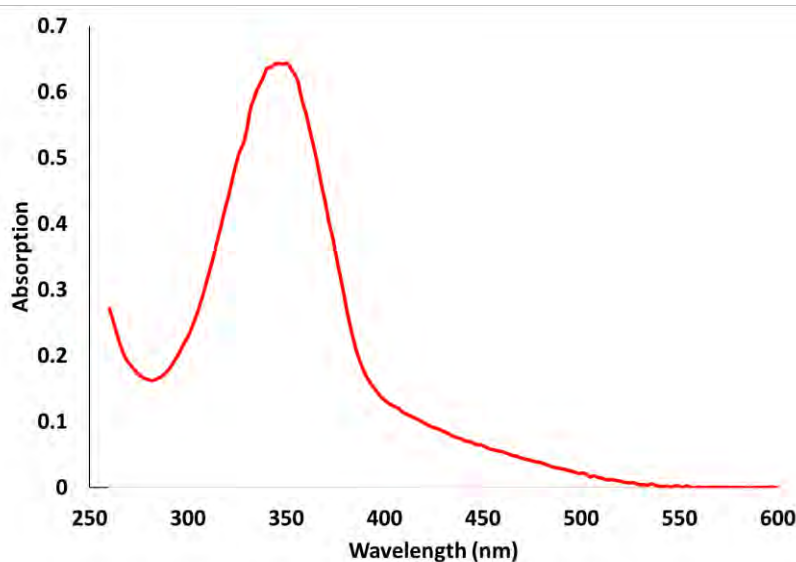


12. Synthesis and Characterization of (±)-1C

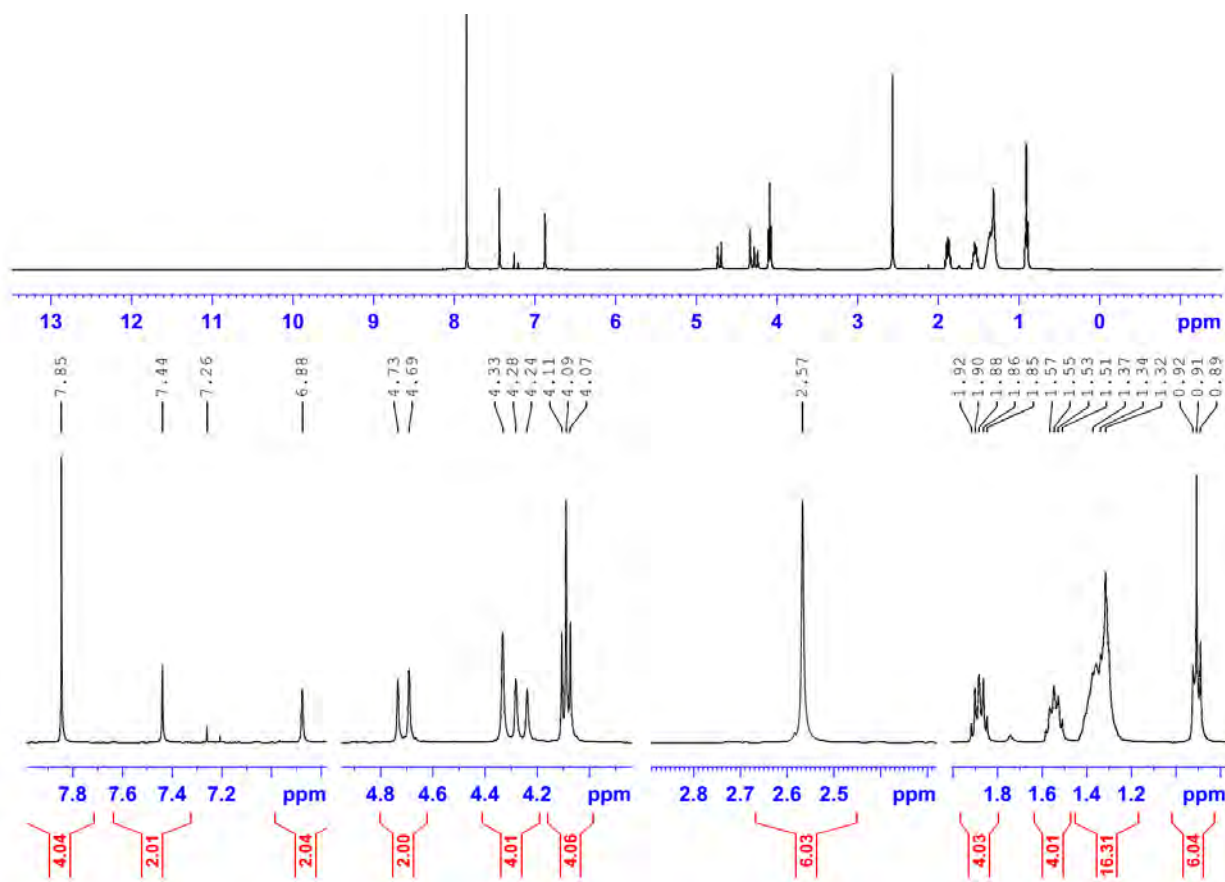
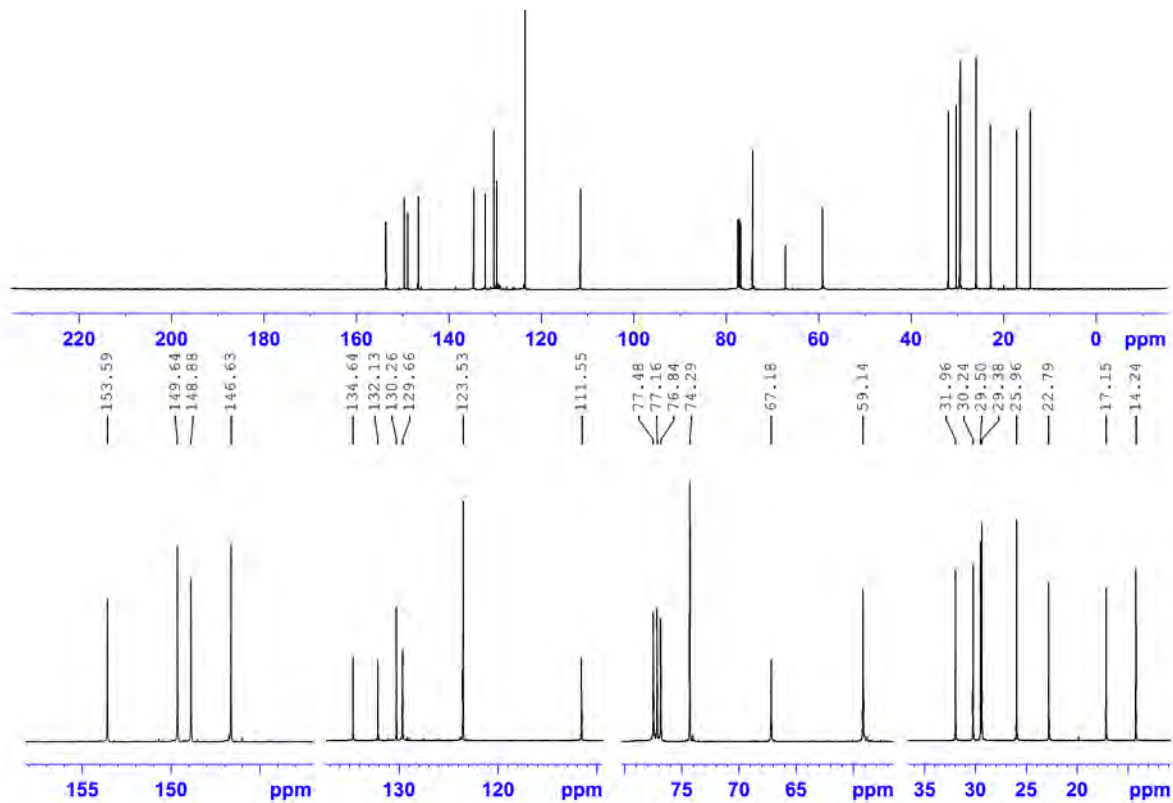
3,9-bis((E)-(3,5-dichloro-4-(octyloxy)phenyl)diazenyl)-2,8-dimethyl-6H,12H-5,11-methanodibenzo[b,f][1,5]diazocine



Compound **1** (0.31 g, 0.50 mmol, 1.0 eq.) and K_2CO_3 (0.55 g, 4.0 mmol) were mixed in dried acetone (10 mL) at room temperature for 15 minutes in a sealed round-bottom flask. Then, 1-bromo octane (0.23 g, 1.2 mmol, 2.4 eq.) was injected into the mixture and refluxed for 12 hours at 55°C in darkness. The reaction profile was monitored by TLC which showed a single spot at the conclusion. Afterwards, the reaction mixture was added to 50 ml of distilled water and the crude was extracted by DCM (3 x 50 ml). The organic layers were combined, dried over $MgSO_4$ and filtered. After solvent removal under reduced pressure, the solid residue was chromatographed to obtain a shiny orange solid **1C** (0.32 g, 0.38 mmol, 75%). Chemical Formula: $C_{45}H_{54}Cl_4N_6O_2$, Molecular Weight: 852.77, **R_f**: 0.50 (EtOAc/ n-Hex = 20% v/v) silica gel. **¹H-NMR** (400 MHz, $CDCl_3$) δ [ppm] : 0.91 (t, J = 7.8 Hz, 6H, CH_3), 1.34 (m, 16H, CH_2), 1.54 (m, 4H, CH_2), 1.88 (m, 4H, CH_2), 2.57 (s, 6H, CH_3), 4.09 (t, J = 8.1 Hz, 4H, CH_2), 4.26 (d, J = 17.2 Hz, 2H, H-6a, H-12a), 4.33 (s, 2H, -N- CH_2 -N-), 4.71 (d, J = 17.1 Hz, 2H, H-6b, H-12b), 6.88 (s, 2H, H-1, H-7), 7.44 (s, 2H, H-4, H-10), 7.85 (s, 4H, CH). **¹³C-NMR** (100 MHz, $CDCl_3$) δ [ppm]: 14.24, 17.15, 22.79, 25.96, 29.38, 29.50, 30.24, 31.96, 59.14, 67.18, 74.29, 111.55, 123.53, 129.66, 130.26, 132.13, 134.64, 146.63, 148.88, 149.64 and 153.59. **IR**: (Neat) ν_{max} [cm^{-1}] = 2926, 2856, 1555, 1481, 1452, 1379, 1253, 1229, 1088, 989, 921, 801, 725. **MS** (Acetonitrile 45%, isopropyl alcohol 45%, EtOAc 5%, MeOH 5%): (ESI positive) calc. for $[C_{45}H_{55}Cl_4N_6O_2]^+$: $[M+H]^+$ 851.31, found 851.2, 851.9 and 853.0. **UV-Vis**: (EtOAc) λ ($\lg\epsilon$) = 346 nm (4.5). Anal. calcd: C, 63.38; H, 6.38; Cl, 16.63; N, 9.86; O, 3.75. found: C, 63.57; H, 6.54; N, 9.62.

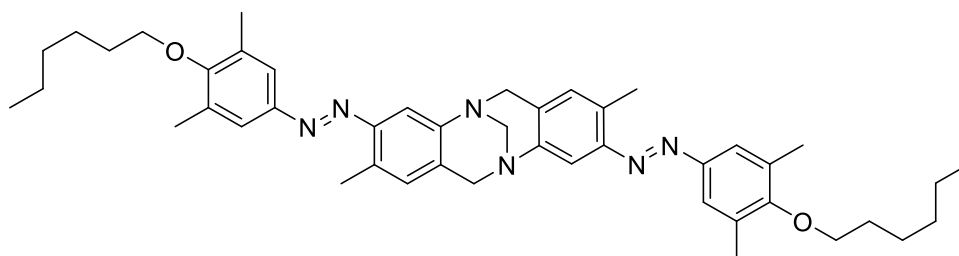


Compound **1C**, UV-Vis spectra (EtOAc, r.t.)

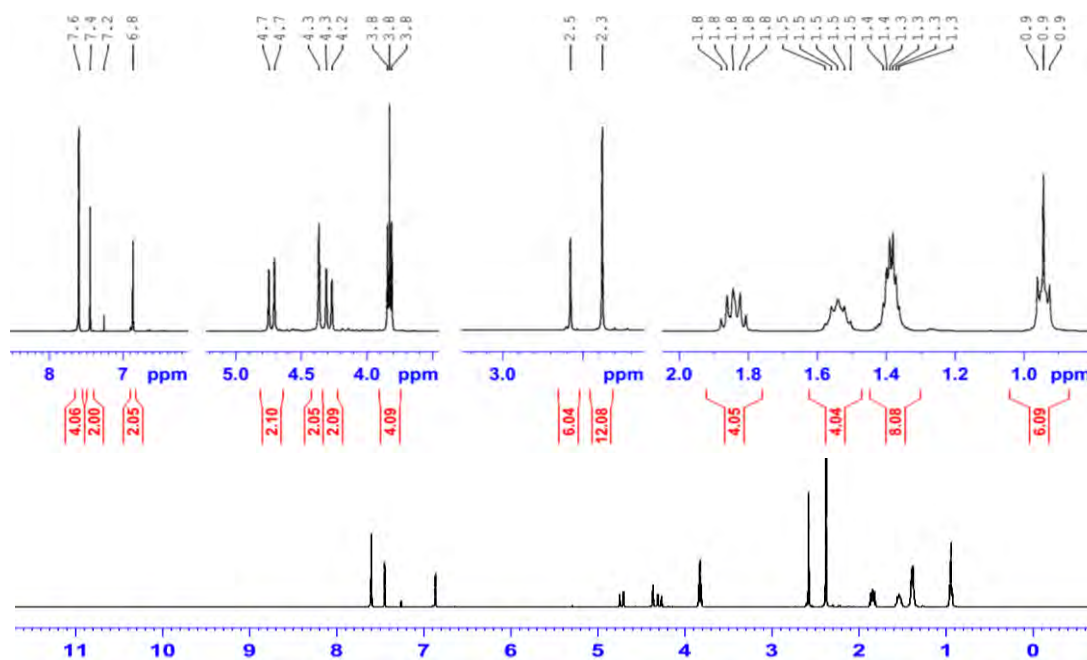
Compound 1C, ¹H-NMR (400 MHz, CDCl₃)Compound 1C, ¹³C-NMR (100 MHz, CDCl₃)

12. Synthesis and Characterization of (\pm)-4A

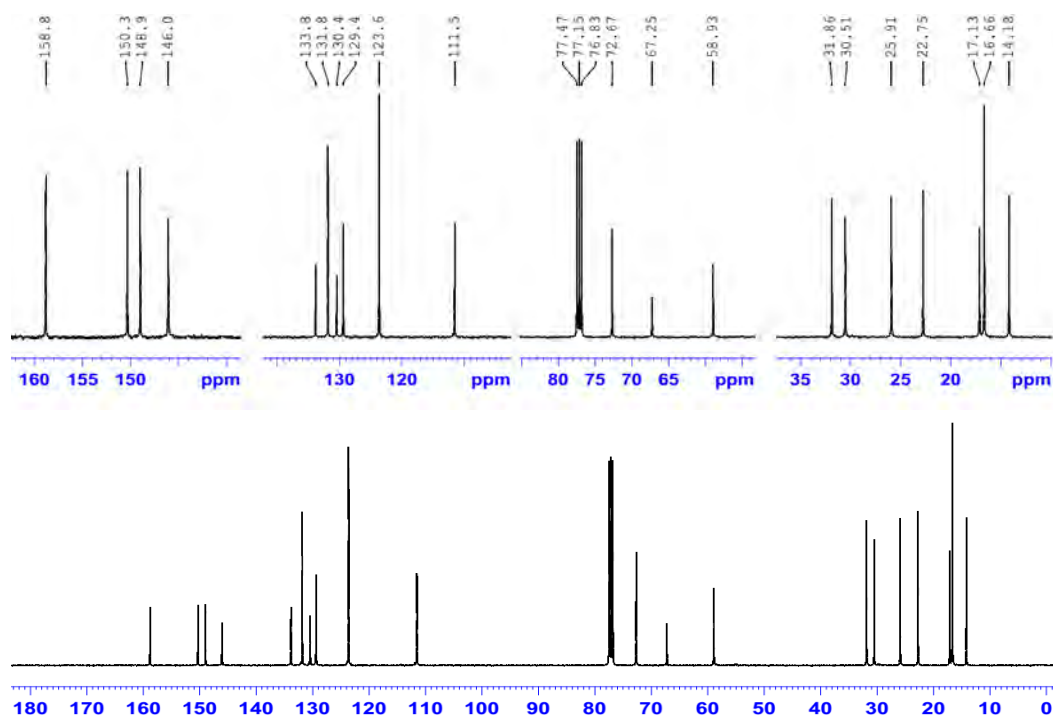
3,9-bis((E)-4-(hexyloxy)-3,5-dimethylphenyl)diazenyl)-2,8-dimethyl-6H,12H-5,11-methanodibenzo[b,f][1,5]diazocine



Compound **4** (0.55 g, 1.0 mmol, 1.0 eq.), a catalytic amount of KI (0.01 g, 0.06 mmol) and K_2CO_3 (0.69 g, 5.0 mmol) were mixed in dried acetone (10 mL) at room temperature for 15 minutes in a sealed round-bottom flask. Then, 1-bromohexane (0.50 g, 3.0 mmol, 1.5 eq.) was injected into the mixture and refluxed for 12 hours at 60°C in darkness. The reaction profile was monitored by TLC which showed a single spot at the conclusion. Afterwards, the reaction mixture was added to 50 ml of distilled water and the crude was extracted by DCM (3 x 50 ml). The organic layers were combined, dried over $MgSO_4$ and filtered. After solvent removal under reduced pressure, the solid residue was chromatographed to obtain a shiny orange solid **4A** (0.63 g, 0.88 mmol, 88%). Chemical Formula: $C_{45}H_{58}N_6O_2$, Molecular Weight: 715.00, R_f : 0.63 (EtOAc/ n-hexane = 30% v/v) silica gel. 1H -NMR (400 MHz, $CDCl_3$) δ [ppm]: 0.93-0.96 (t, J = 7.1 Hz, 6H, CH_3), 1.36-1.41 (m, 8H, CH_2), 1.50-1.58 (m, 4H, CH_2), 1.81-1.88 (m, 4H, CH_2), 2.38 (s, 12H, CH_3), 2.58 (s, 6H, CH_3), 3.81-3.84 (t, J = 6.6 Hz, 4H, CH_2), 4.27-4.31 (d, J = 16.7 Hz, 2H, H-6a, H-12a), 4.37 (s, 2H, -N- CH_2 -N-), 4.71-4.75 (d, J = 16.8 Hz, 2H, H-6b, H-12b), 6.82 (s, 2H, H-1, H-7), 7.45 (s, 2H, H-4, H-10), 7.60 (s, 4H, CH). ^{13}C -NMR (100 MHz, $CDCl_3$) δ [ppm]: 158.8, 150.3, 148.9, 146.0, 133.8, 131.8, 130.4, 129.4, 123.6, 111.5, 72.6, 67.2, 58.9, 31.8, 30.5, 25.9, 22.7, 17.1, 16.6, 14.1. IR: (Neat) ν_{max} [cm^{-1}] = 2926, 2858, 1586, 1474, 1375, 1302, 1208, 1111, 1086, 999, 920, 898, 748, 609. MS (ACN 90%, EtOAc 5%, H_2O 5%): (ESI positive) calc. for $[C_{45}H_{59}N_6O_2]^+$: $[M+H]^+$ 715.4, found 715.7. UV-Vis: (EtOAc) λ (lg ϵ) = 349 nm (4.572). Anal. calcd: C, 75.59; H, 8.18; N, 11.75. found: C, 75.83; H, 7.94; N, 11.60.

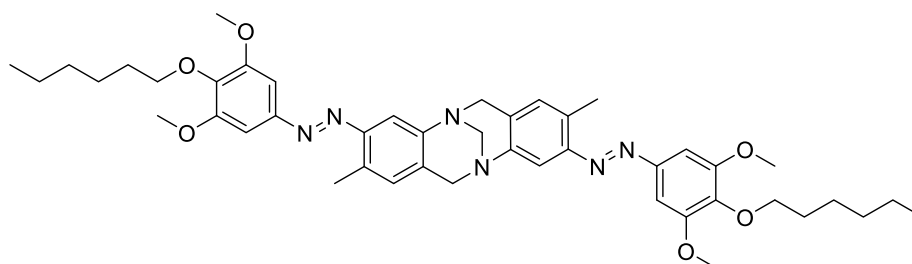


Compound **4A**, 1H -NMR (400 MHz, $CDCl_3$)

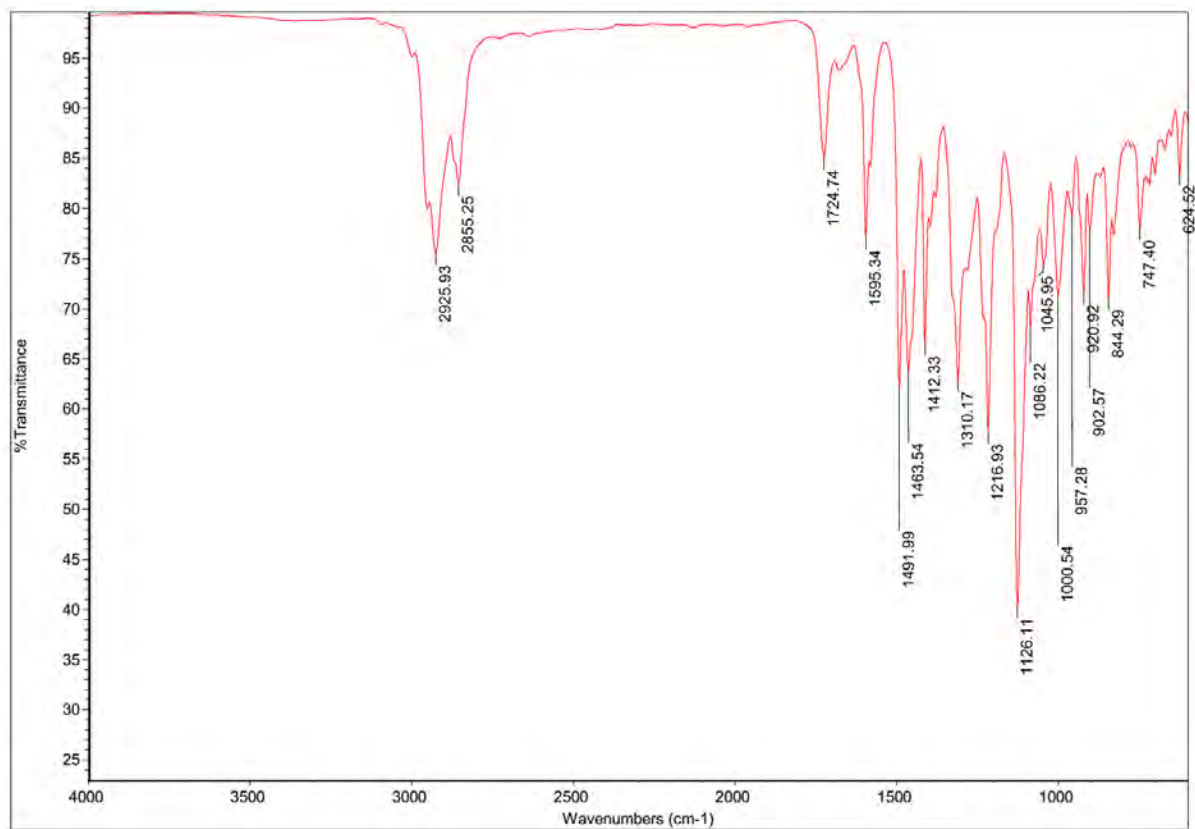
Compound 4A, ^{13}C -NMR (100 MHz, CDCl_3)

13. Synthesis and Characterization of (\pm)-5A

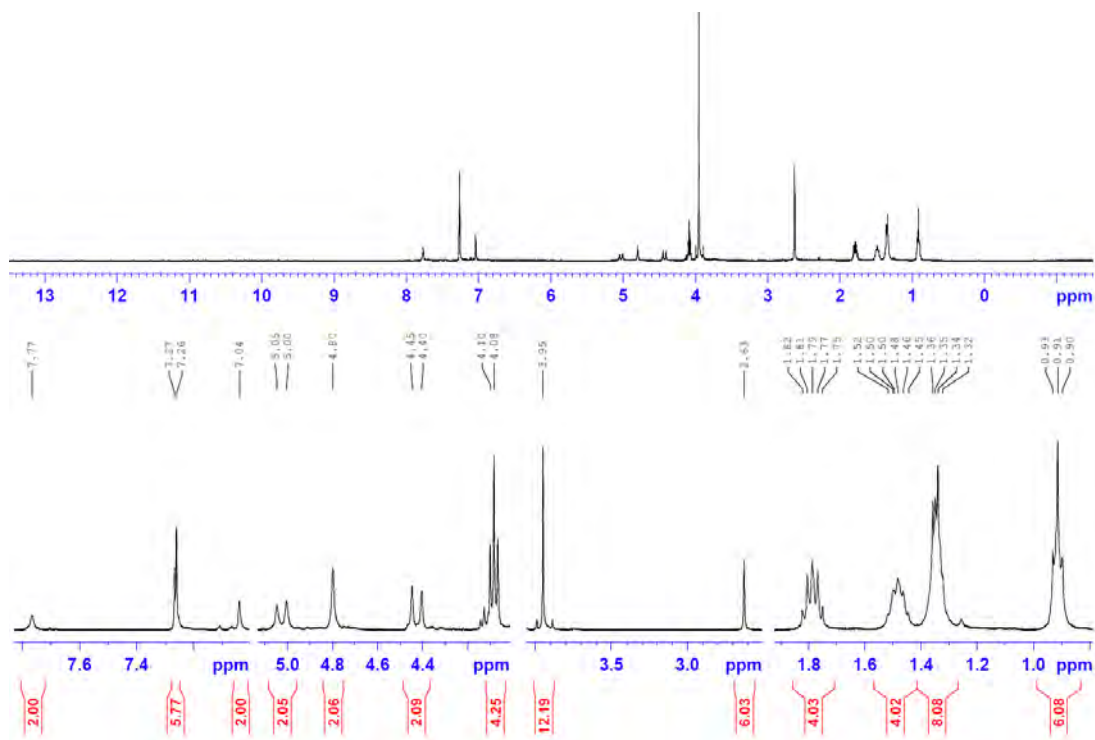
3,9-bis((E)-(4-(hexyloxy)-3,5-dimethoxyphenyl)diazenyl)-2,8-dimethyl-6H,12H-5,11-methanodibenzo[b,f][1,5]diazocine

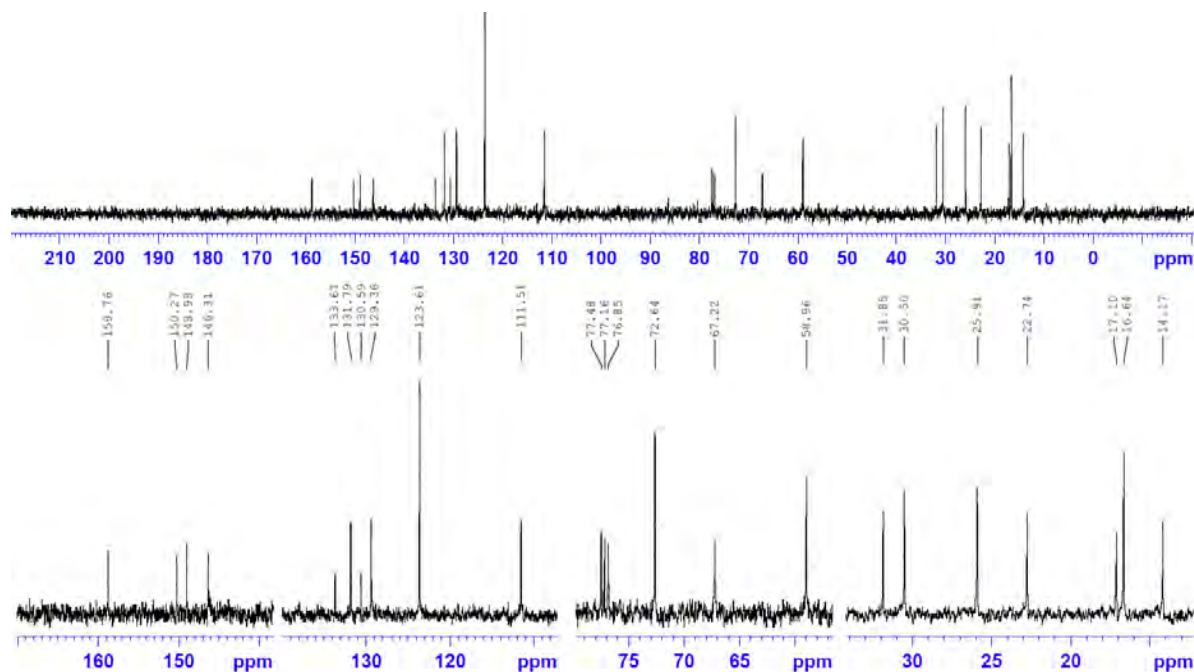


5 (0.31 g, 0.50 mmol, 1.0 eq.), K_2CO_3 (0.55 g, 4.0 mmol) and a catalytic amount of KI (~0.01 g) were mixed in dried acetone (10 mL) at room temperature for 15 minutes in a sealed round bottom flask. Then, 1-bromohexane (0.22 g, 1.3 mmol, 2.6 eq.) was injected into the mixture and refluxed for 18 hours at 58°C in darkness. After monitoring the TLC profile which showed a single spot, the resulting orange mixture was poured into cold water. The crude was extracted by ethyl acetate (3 x 30 mL). The organic layers were combined and dried over MgSO_4 and the solvent was removed under reduced pressure. Afterwards, the purification was done by column chromatography in dark to obtain a sticky orange substance **5A** (0.30 g, 0.39 mmol, 76%). Chemical Formula: $\text{C}_{45}\text{H}_{58}\text{N}_6\text{O}_6$, Molecular Weight: 779.00, R_f : 0.73 (MeOH/ DCM = 4% v/v) silica gel. ^1H -NMR (400 MHz, CDCl_3) δ [ppm] : 0.91 (t, 6H, CH_3), 1.34 (m, 8H, CH_2), 1.48 (m, 4H, CH_2), 1.78 (m, 4H, CH_2), 2.62 (s, 6H, CH_3), 3.95 (s, 12H, OCH_3), 4.08 (t, 4H, CH_2), 4.42 (d, $^2J_{\text{H,H}} = 17.0$ Hz, 2H, H-6a, H-12a), 4.79 (s, 2H, -N- CH_2 -N-), 5.02 (d, $^2J_{\text{H,H}} = 17.0$ Hz, 2H, H-6b, H-12b), 7.04 (s, 2H, H-1, H-7), 7.25 (s, 4H, CH), 7.76 (s, 2H, H-4, H-10). ^{13}C -NMR (100 MHz, CDCl_3) δ [ppm] : 14.23, 17.30, 22.80, 25.65, 30.24, 31.78, 56.31, 58.06, 67.31, 73.94, 100.92, 111.60, 129.79, 140.63, 148.56, 150.70, 153.92. IR: (Neat) ν_{max} (cm^{-1}) = 2925, 2855, 1724, 1595, 1491, 1463, 1412, 1310, 1216, 1126, 1000, 920, 844, 747. MS (Acetonitrile 90%, EtOAc 5% (ESI positive) calc. for $[\text{C}_{45}\text{H}_{59}\text{N}_6\text{O}_6]^+$: $[\text{M}+\text{H}]^+$ 779.44, found 779.1. UV: (DCM) λ (lge) = 368 nm. Anal. calcd: C, 69.38; H, 7.51; N, 10.79; O, 12.32. found: C, 69.57; H, 7.70; N, 10.98.



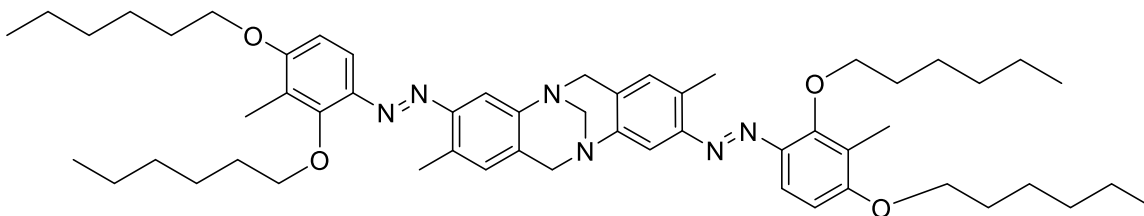
Compound 5A, IR transmittance spectra (neat)

Compound 5A, ¹H-NMR (400 MHz, CDCl₃)

Compound 5A, ^{13}C -NMR (100 MHz, CDCl_3)

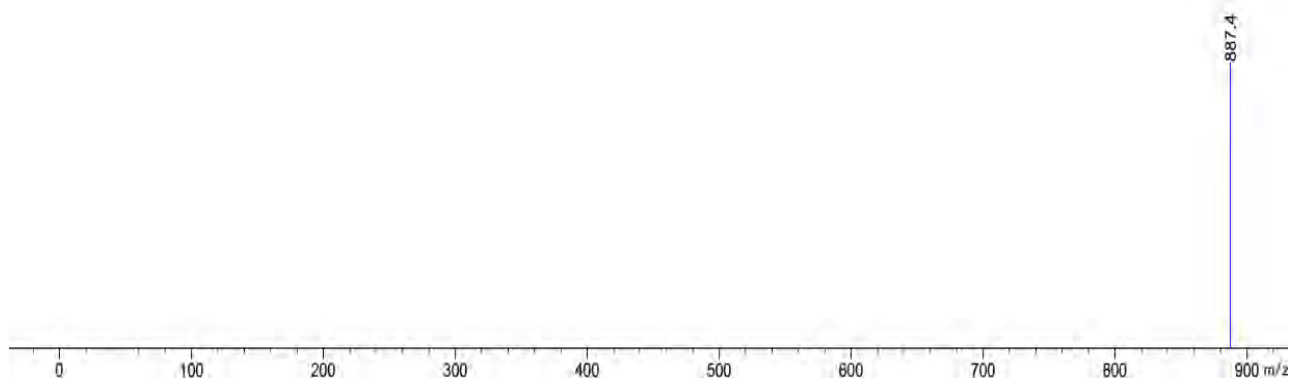
14. Synthesis and Characterization of (\pm)-6A

3,9-bis((E)-(2,4-bis(hexyloxy)-3-methylphenyl)diazenyl) -2,8-dimethyl-6H,12H-5,11-methano dibenzo [b,f][1,5] diazocine

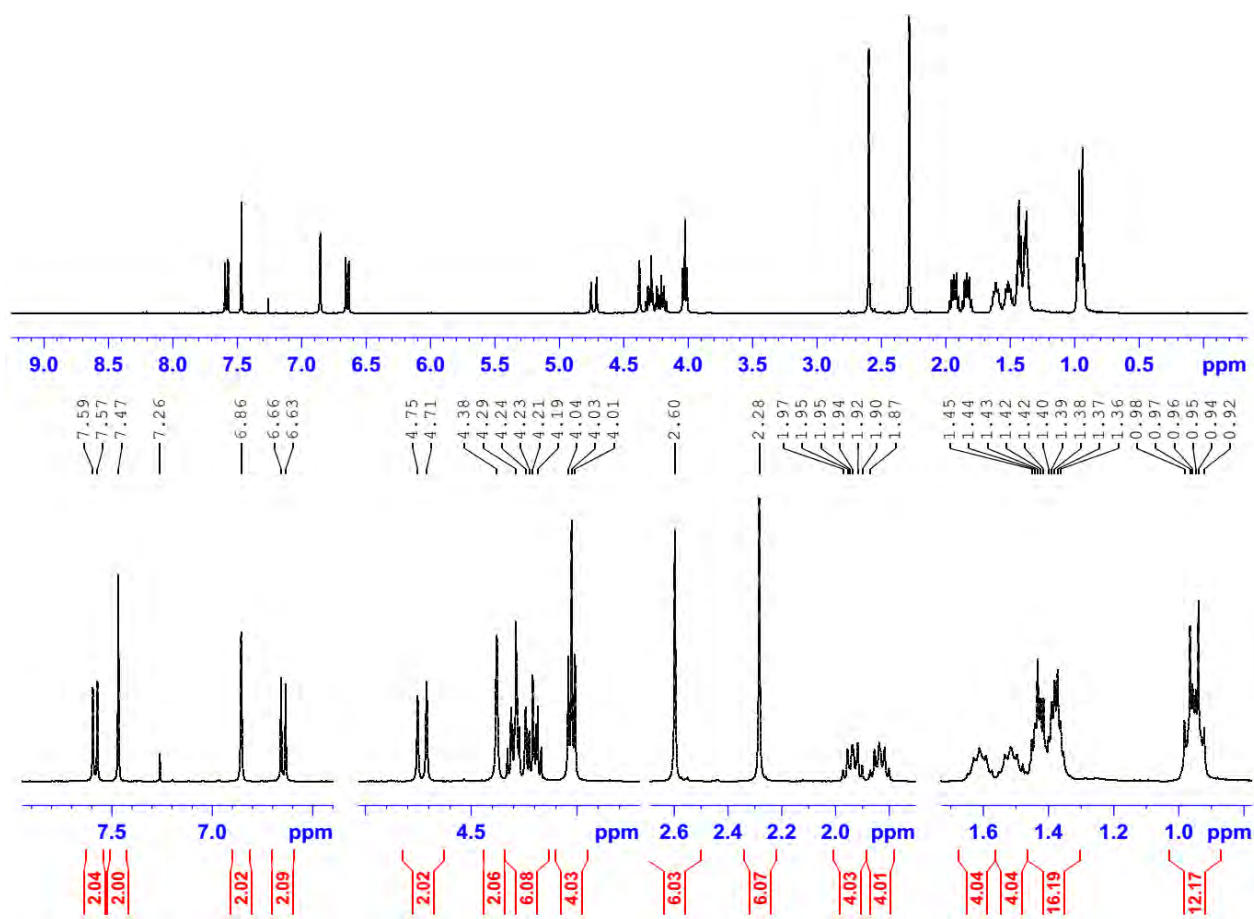


6 (0.28 g, 0.5 mmol, 1.0 eq.), K_2CO_3 (0.55 g, 4.0 mmol, excess) and a catalytic amount of KI (~ 0.02 g) were mixed in dried acetone (6 mL) at room temperature for 15 minutes in a sealed round bottom flask. Then, 1-bromohexane (0.36 g, 2.2 mmol, 4.4 eq.) was injected into the mixture and refluxed for 48 hours at 60°C in darkness. After monitoring the TLC profile, the final red mixture was poured into 50 ml of cold water. The crude was extracted by DCM (2 x 50ml) and the DCM layers were combined, dried over MgSO_4 and filtered. Afterwards, the volatiles were removed under reduced pressure to obtain a red residue which then purified by column chromatography to obtain a red-orange semisolid substance **6B** (0.26 g, 0.29 mmol, 58%). Chemical Formula: $\text{C}_{55}\text{H}_{78}\text{N}_6\text{O}_4$, Molecular Weight: 887.27, R_f : 0.75 (EtOAc/ n-Hex = 5% v/v) silica gel. ^1H -NMR (400 MHz, CDCl_3) δ [ppm]: 0.92-0.98 (m, 12H, CH_3), 1.36-1.45 (m, 16H, CH_2), 1.47-1.58 (m, 4H, CH_2), 1.57-1.65 (m, 4H, CH_2), 1.87-1.94 (m, 4H, CH_2), 1.96-1.98 (m, 4H, CH_2), 2.28 (s, 6H, CH_3), 2.60 (s, 6H, CH_3), 4.01-4.04 (t, $J = 7.8$ Hz, 4H, CH_2), 4.19-4.29 (m, 6H), 4.38 (s, 2H, -N- CH_2 -N-), 4.71-4.75 (d, $J = 17.2$ Hz, 2H, H-6b, H-12b), 6.63-6.66 (d, $J = 8.9$ Hz, 2H), 6.86 (s, 2H, CH), 7.47 (s, 2H, CH), 7.57-7.59 (d, $J = 8.7$ Hz, 2H). ^{13}C -NMR (100 MHz, CDCl_3) δ [ppm]: 9.15, 14.12, 14.24, 17.17, 22.71, 22.82, 25.88, 26.08, 29.36, 30.69, 31.66, 31.98, 59.05, 67.29, 68.56, 76.67, 106.62, 111.61, 114.68, 120.45, 129.30, 130.16, 133.66, 140.51, 146.30, 150.60, 157.50, 160.66.

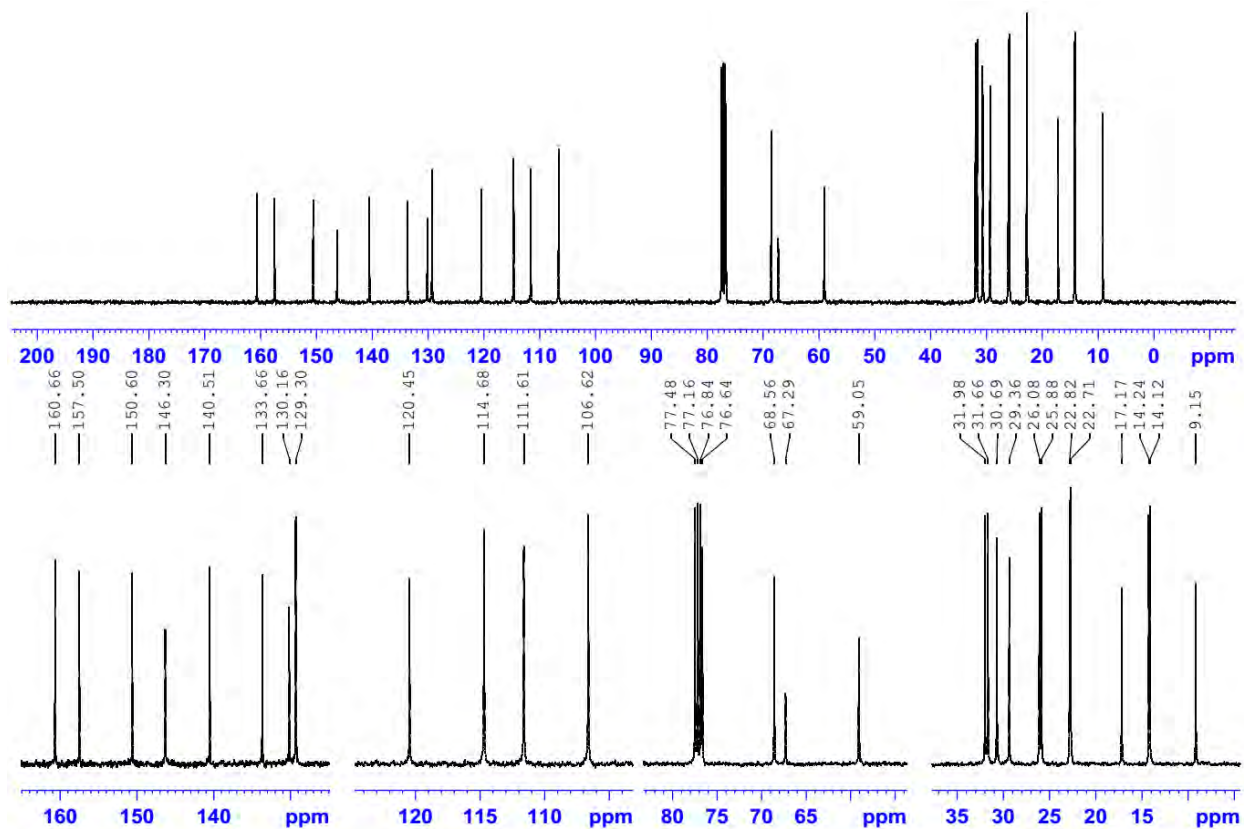
IR: (Neat) ν_{\max} (cm^{-1}) = 2929, 2853, 1550, 1479, 1452, 1379, 1254, 1077, 976, 943, 907, 851. **MS** (Isopropyl alcohol, formic acid 0.05 %): (ESI positive) calc. for $[\text{C}_{55}\text{H}_{79}\text{N}_6\text{O}_4]^+$: $[\text{M}+\text{H}]^+$ 887.61, found 887.4. UV: (ethyl acetate) λ ($\text{lg}\epsilon$) = 370 nm (4.6).



Compound 6A, Mass spectra ESI (positive)

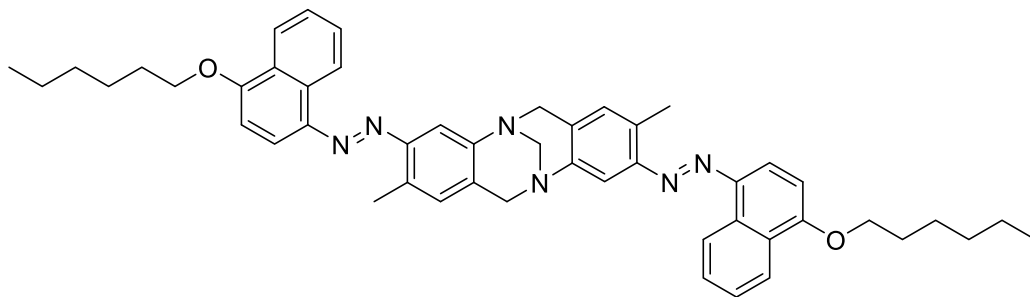


Compound 6A, ^1H -NMR (400 MHz, CDCl_3)

Compound 6A, ^{13}C -NMR (100 MHz, CDCl_3)

15. Synthesis and Characterization of (\pm)-8A

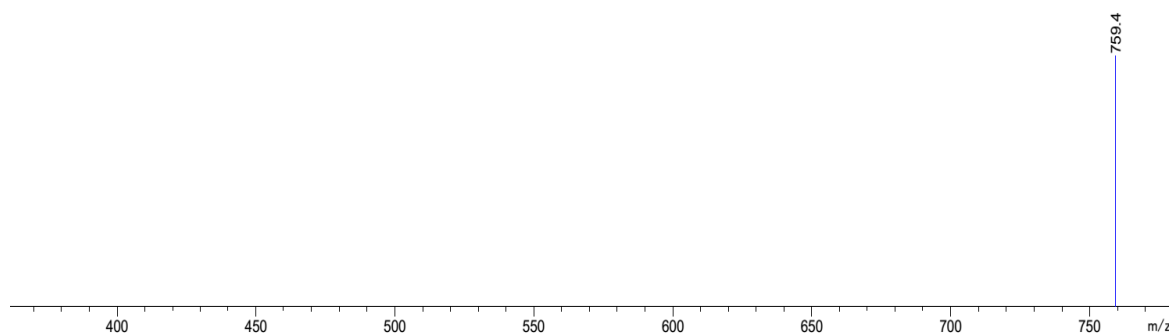
3,9-bis((E)-(4-(hexyloxy)naphthalen-1-yl)diazenyl)-2,8-dimethyl-6H,12H-5,11-methanodibenzo[b,f][1,5]diazocine



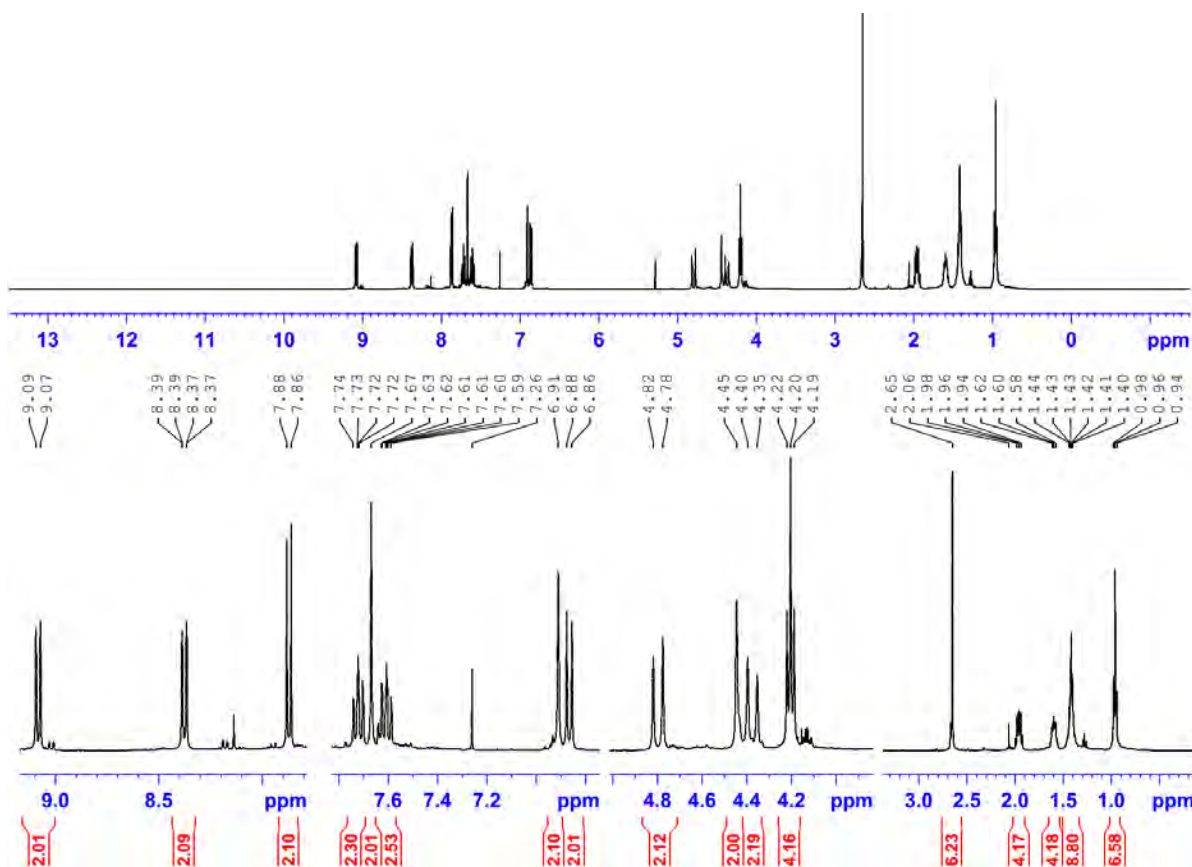
8 (0.59 g, 1.0 mmol, 1.0 eq.), K_2CO_3 (0.55 g, 4.0 mmol) and a catalytic amount of KI (~0.01 g) were sonicated in dried DMF (8 mL) at 40°C for 15 minutes in a sealed round bottom flask; then, 1-bromohexane (0.36 g, 2.2 mmol, 1.1 eq.) was injected into the mixture and stirred for 24 hours at 110°C in darkness. Then, the resulting solution was poured into cold water, and the crude was extracted by DCM (3 x 50 ml). The DCM layers were combined, washed with brine, dried over MgSO_4 , filtered and then evaporated under reduced pressure. Afterwards, further purification was done by column chromatography on silica gel in dark to obtain a sticky maroon substance **8A** (0.34 g, 0.45 mmol, 45%). Chemical Formula: $\text{C}_{49}\text{H}_{54}\text{N}_6\text{O}_2$, Molecular Weight: 759.01, R_f : 0.8 (EtOAc/n-Hex = 40% v/v) silica gel. ^1H -NMR (400 MHz, CDCl_3) δ [ppm]: 0.96 (t, J = 7.8 Hz, 6H, CH_3), 1.41 (m, 8H, CH_2), 1.59 (m, 4H, CH_2), 1.96 (m, 4H, CH_2), 2.65 (s, 6H, CH_3), 4.20 (t, J = 7.6 Hz, 4H, CH_2), 4.37 (d, J = 17.2 Hz, 2H, H-6a, H-12a), 4.44 (s, 2H, -N- CH_2 -N-), 4.79 (d, J = 17.1 Hz, 2H, H-6b, H-12b), 6.86 (d, J = 8.6 Hz, 2H, CH), 6.91 (s, 2H, CH), 7.60 (t, J = 7.6 Hz, 2H, CH), 7.66 (s, 2H, CH), 7.72 (t, J = 7.6 Hz, 2H, CH), 7.87 (d, J = 8.5 Hz, 2H, CH), 8.37 (d, J = 8.5 Hz, 4H, CH), 9.08 (d, J = 8.5 Hz, 4H, CH). ^{13}C -NMR (100 MHz, CDCl_3) δ [ppm]: 14.16, 17.28, 22.77, 26.02, 29.29, 31.72, 59.13, 67.28,

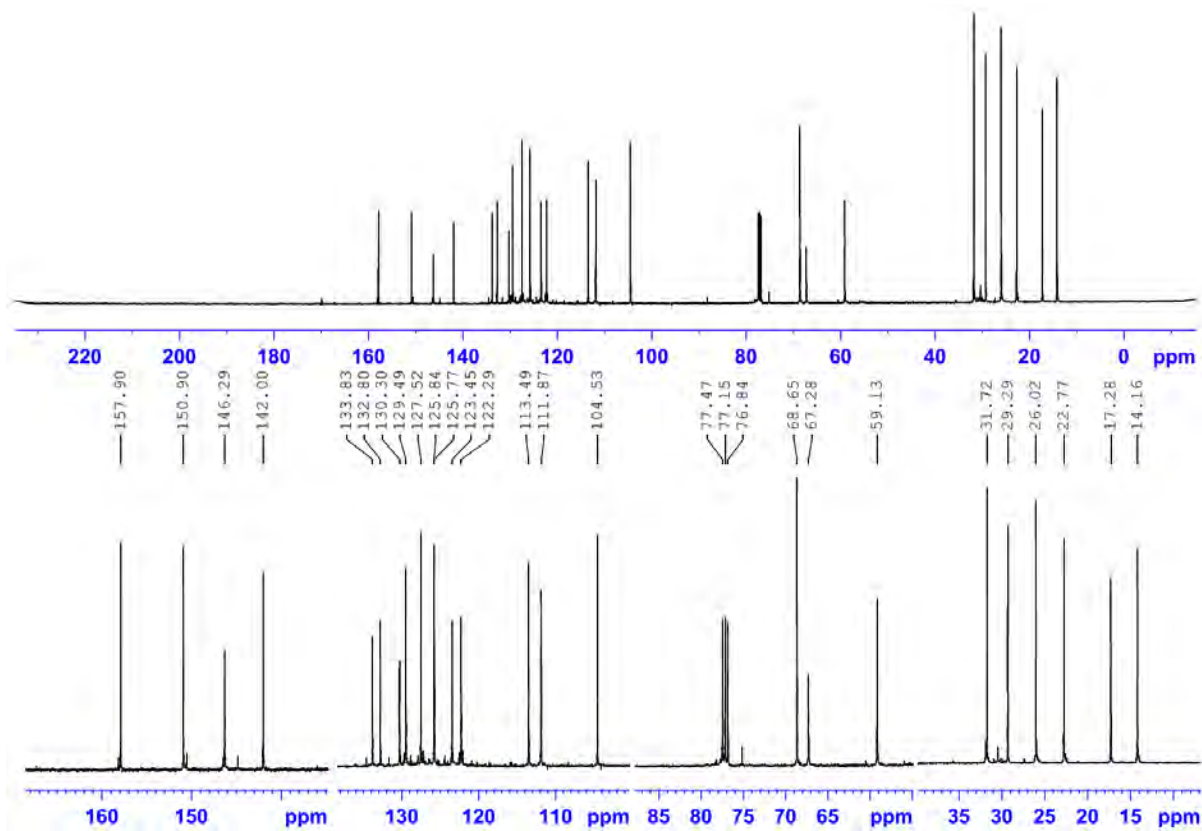
68.64, 104.53, 111.87, 113.49, 122.29, 123.45, 125.77, 125.84, 127.52, 129.49, 130.30, 132.80, 133.83, 142.00, 146.29, 150.90, 157.90. **IR:** (Neat) ν_{max} (cm^{-1}) = 2927, 2856, 1576, 1507, 1459, 1385, 1319, 1237, 1087, 920, 764, 728. **MS** (Acetonitrile 20%, EtOAc 80%) (ESI positive) calc. for $[\text{C}_{49}\text{H}_{55}\text{N}_6\text{O}_2]^+$: $[\text{M}+\text{H}]^+$ 759.43, found 759.4. **UV:** (DCM) λ (lg ϵ) = 407(4.6) nm. Anal. calcd: C, 77.54; H, 7.17; N, 11.07; O, 4.22. found: C, 77.46; H, 7.47; N, 11.35.

Max: 2335

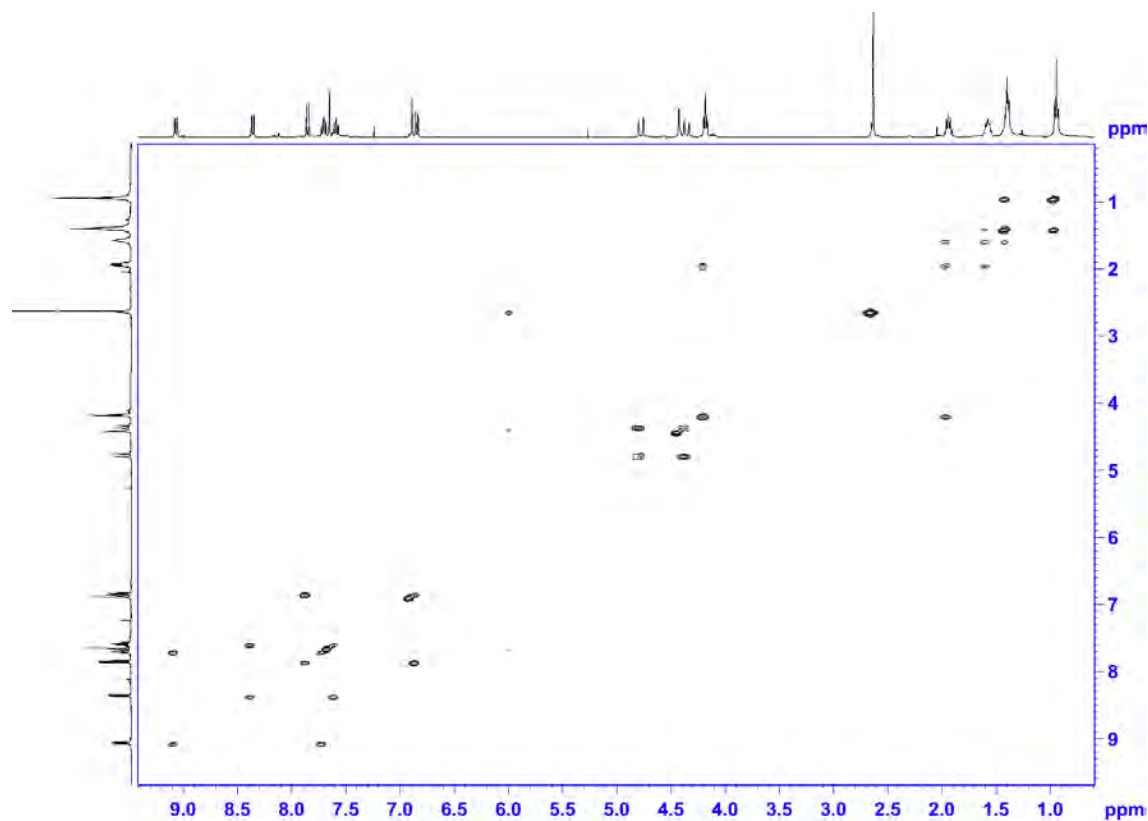


Compound 8A, Mass Spectra ESI +

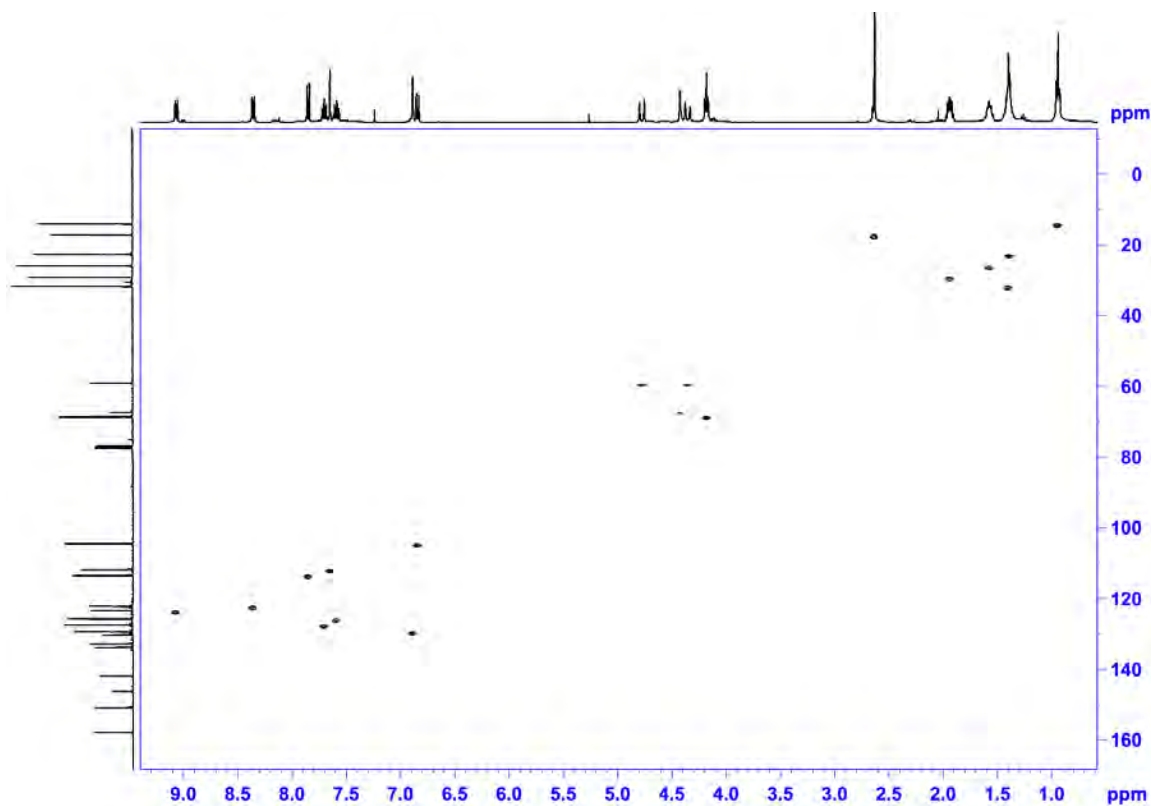
Compound 8A, ^1H -NMR (400 MHz, CDCl_3)



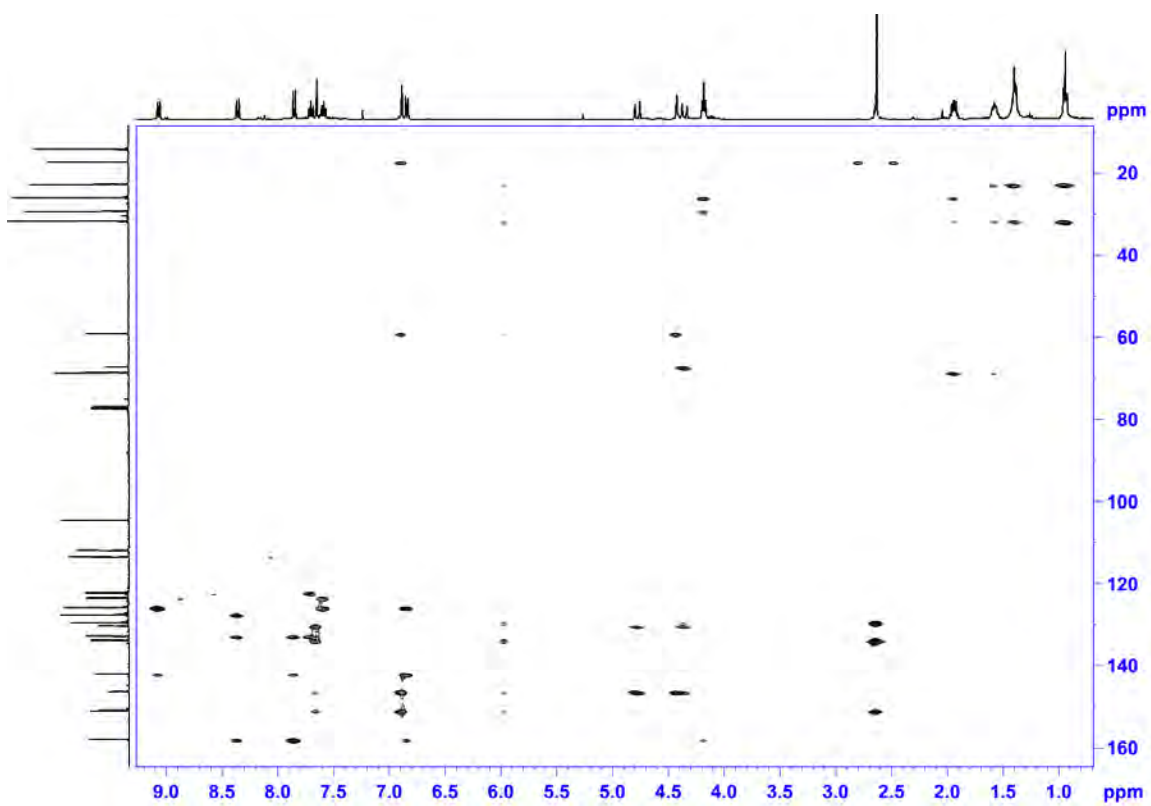
Compound 8A, ^{13}C -NMR (100 MHz, CDCl_3)



Compound 8A, COSY



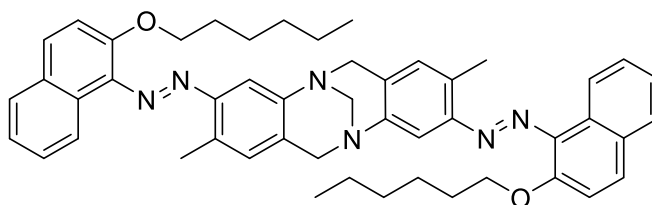
Compound 8A, HSQC



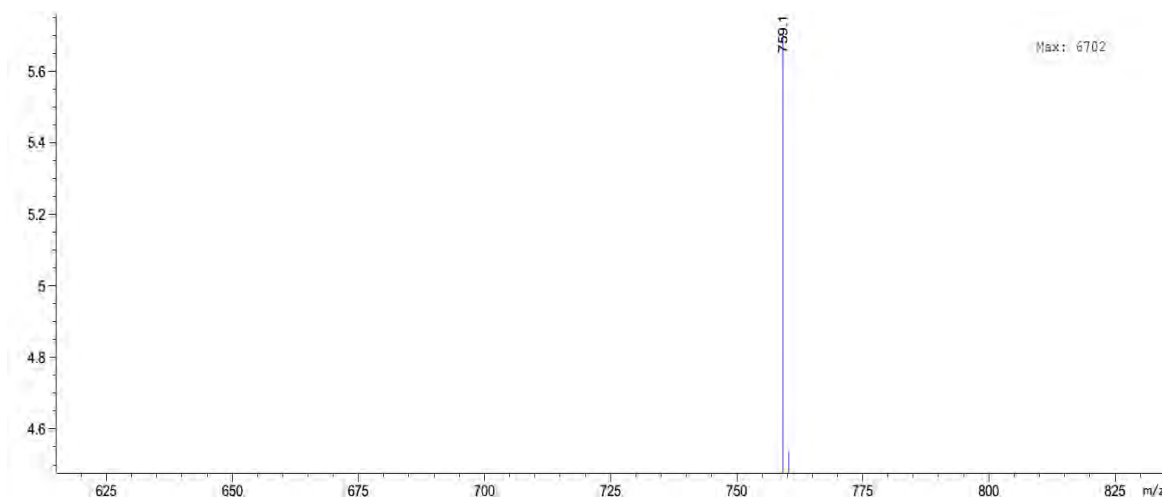
Compound 8A, HMBC

16. Synthesis and Characterization of (±)-9A

3,9-bis((E)-(2-(hexyloxy)naphthalen-1-yl)diazenyl)-2,8-dimethyl-6H,12H-5,11-methanodibenzo[b,f][1,5]diazocine



9 (0.59 g, 1.0 mmol, 1.0 eq.), K_2CO_3 (0.55 g, 4.0 mmol) and a catalytic amount of KI (~0.01 g) were sonicated in dried DMF (8 mL) at 40°C for 15 minutes in a sealed round bottom flask, then 1-bromohexane (0.36 g, 2.2 mmol, 1.1 eq.) was injected into the mixture and stirred for 24 hours at 110°C in darkness. Then, the resulting mixture was poured into 100 ml of cold water and the crude was extracted by DCM (3 x 20 ml). The DCM layers were combined, dried over $MgSO_4$, filtered and evaporated under reduced pressure respectively. Afterwards, the purification was done by column chromatography to obtain a sticky dark red substance **9A** (0.39 g, 0.52 mmol, 52%). Chemical Formula: $C_{49}H_{54}N_6O_2$, Molecular Weight: 759.01, R_f : 0.6 (EtOAc/n-Hex = 40% v/v) silica gel. **1H -NMR** (400 MHz, $CDCl_3$) δ [ppm] : 0.86 (t, J = 7.8 Hz, 6H, CH_3), 1.30 (m, 8H, CH_2), 1.46 (m, 4H, CH_2), 1.81 (m, 4H, CH_2), 2.64 (s, 6H, CH_3), 4.17 (m, 4H, CH_2), 4.38 (d, J = 17.0 Hz, 2H, H-6a, H-12a), 4.44 (s, 2H, -N- CH_2 -N-), 4.79 (d, J = 17.1 Hz, 2H, H-6b, H-12b), 6.95 (s, 2H), 7.39 (d, 2H, CH), 7.43 (t, 2H), 7.54 (t, 2H), 7.62 (s, 2H), 7.83 (t, 4H), 8.47 (d, 2H). **^{13}C -NMR** (100 MHz, $CDCl_3$) δ [ppm] : 14.00, 17.23, 22.56, 25.71, 29.56, 31.57, 59.00, 67.15, 70.69, 111.24, 116.31, 123.39, 124.34, 127.43, 127.81, 128.98, 129.17, 129.35, 130.71, 130.87, 133.67, 136.85, 146.51, 147.99, 151.41. **IR**: (Neat) ν_{max} (cm^{-1}) = 2924, 2854, 1591, 1463, 1271, 1241, 1086, 1016, 919, 805, 746. **MS** (Acetonitrile 20%, EtOAc 80%) (ESI positive) calc. for $[C_{49}H_{54}N_6O_2]^+$: $[M+H]^+$ 759.43, found 759.1. **UV**: (DCM) λ (lg ϵ) = 393(4.7) nm. Anal. calcd: C, 77.54; H, 7.17; N, 11.07; O, 4.22. found: C, 77.63; H, 7.33; N, 10.89.



Compound 9A, Mass Spectra ESI +

Four stacked ^{13}C NMR spectra of compound **1** are shown. The top spectrum is the full range from 0 to 220 ppm. The three spectra below are zoomed-in regions of the full spectrum.

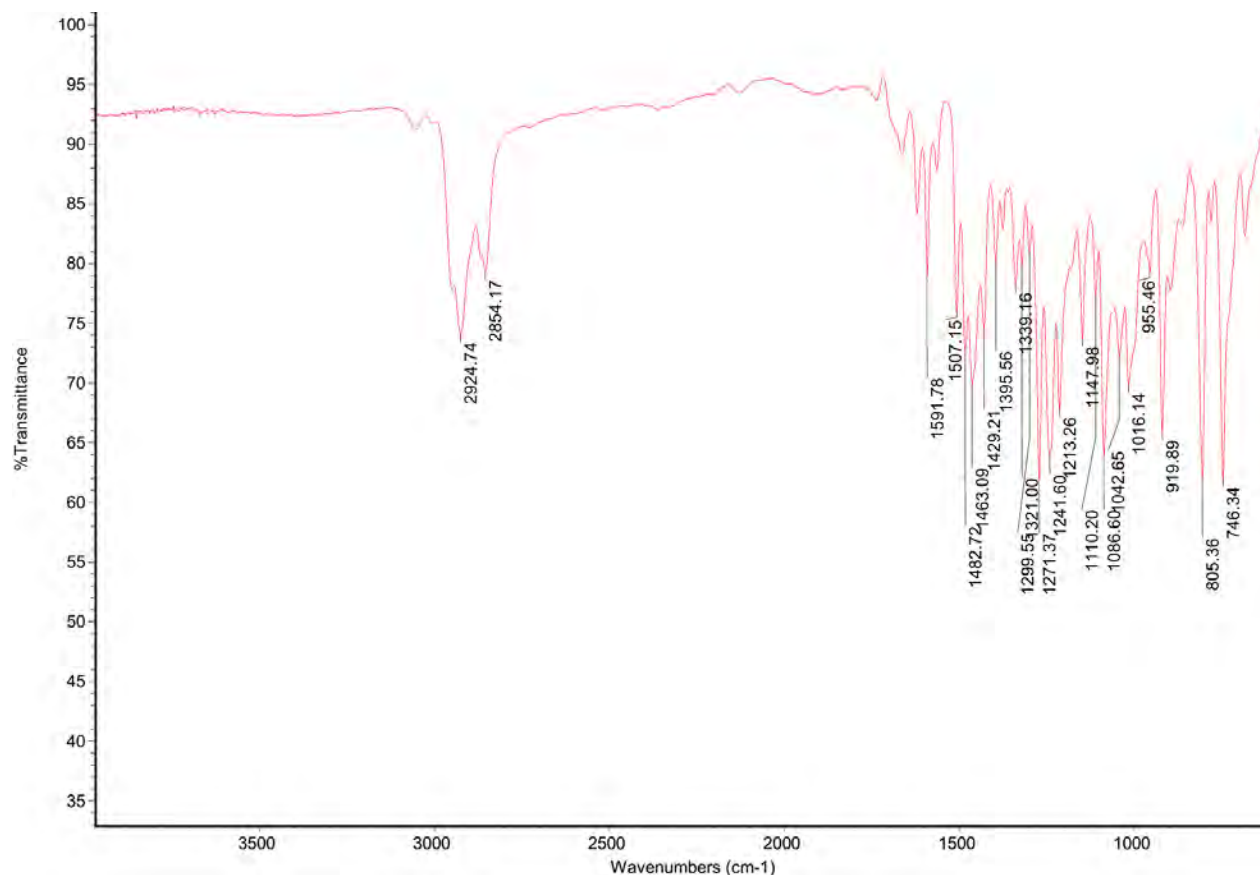
Full Spectrum (0-220 ppm):

- 151.41
- 147.99
- 146.51
- 133.67
- 130.87
- 130.71
- 129.35
- 129.17
- 128.98
- 127.81
- 127.43
- 124.34
- 123.39
- 116.31
- 111.24
- 77.48
- 77.16
- 76.84
- 70.69
- 67.15
- 59.00
- 31.57
- 29.56
- 25.71
- 22.56
- 17.23
- 14.00

Zoomed-in Regions:

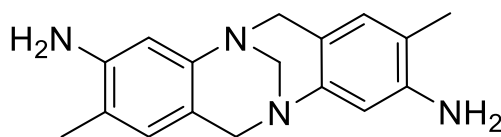
- 155-145 ppm:** 151.41, 147.99, 146.51
- 135-115 ppm:** 133.67, 130.87, 130.71, 129.35, 129.17, 128.98, 127.81, 127.43, 124.34, 123.39, 116.31, 111.24
- 80-55 ppm:** 77.48, 77.16, 76.84, 70.69, 67.15, 59.00
- 35-15 ppm:** 31.57, 29.56, 25.71, 22.56, 17.23, 14.00

149

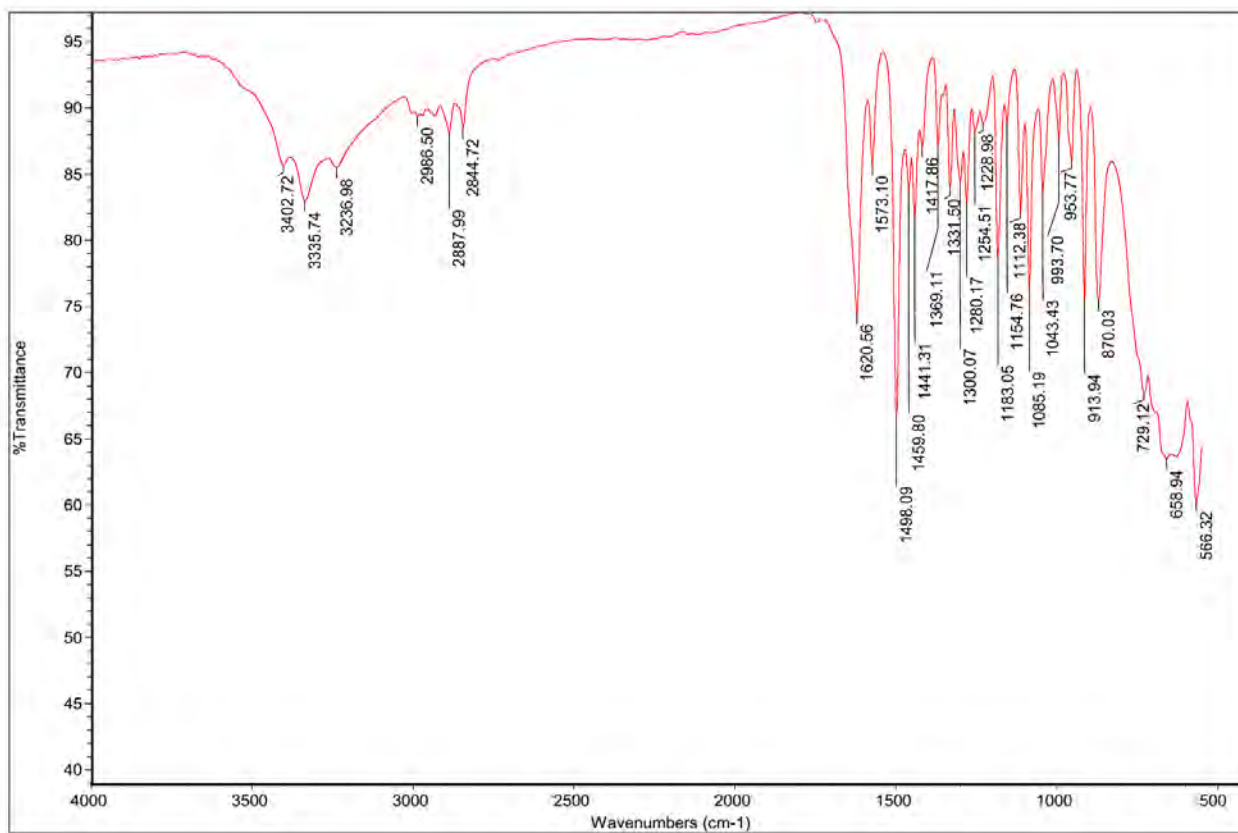


Compound 9A, Infrared Transmittance Spectra (neat)

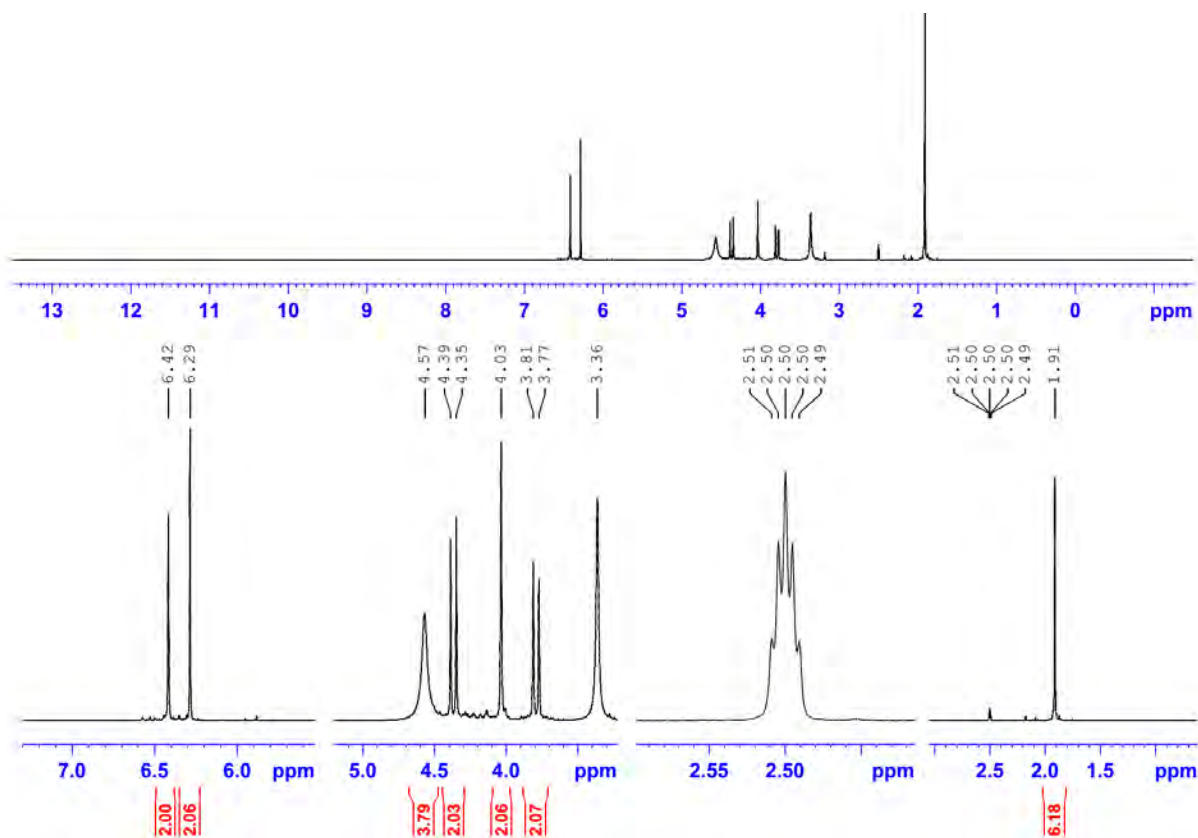
17. Preparation of the building block (*Hünlich's base*)



2,4-diaminotoluene (36.6 g, 300 mmol, 2.05 eq.) was dissolved in an aqueous solution of sulfuric acid (5 %, 1000 ml). Then, formaldehyde (37 % in H₂O, 10.9 ml, 11.9 g, 146 mmol, 1.00 eq.) was slowly added to the solution and stirred for 48 hours at room temperature in a sealed container kept away from light. After checking the completion of the reaction by TLC, ice (300 g) and ammonia (25 %, 300 ml) were added and the precipitated crude product was filtrated. The crude was dissolved in boiling methanol (200 ml) and gradually cooled down to -20°C. Filtration yielded Hünlich's base (14.2 g, 50.8 mmol, 34.7 %) as an off-white solid. Chemical Formula: C₁₇H₂₀N₄, Molecular Weight: 280.38, R_f: 0.5 (MeOH/ DCM = 10% v/v) silica gel. ¹H-NMR (400 MHz, DMSO-*d*₆) δ [ppm] : 6.24 (s, 2H, CH), 6.29 (s, 2H, CH), 4.57 (b, 4H, NH), 4.35-4.39 (d, *J* = 16.2 Hz, 2H, H-6b, H-12b), 4.03 (s, 2H, -N-CH₂-N-), 3.77-3.81 (d, *J* = 16.3 Hz, 2H, H-6a, H-12a), 1.91 (s, 6H, 2 × -CH₃). IR: (Neat) ν_{max} [cm⁻¹] = 3402, 3335, 3236, 2986, 2887, 2844, 1620, 1573, 1498, 1441, 1183, 1085, 913, 870. MS (EtOH): (ESI positive) calc. for [C₁₇H₂₁N₄]⁺: [M+H]⁺ 281.17, found 281.2.



Hünlich's base, IR spectra (neat)

Hünlich's base, ¹H-NMR (400 MHz, DMSO-*d*₆)

17. Partial resolution of 4A

(-)-O,O'-dibenzoyl-L-tartaric acid (0.36 g, 1.0 mmol, 1.0 eq.) was carefully boiled in 1,2-dichloroethane (6 ml) under a flow of nitrogen gas (to reduce the solution volume up to 4ml) for making sure that the solution is moisture free.² Then, compound **4A** (0.72 g, 1.0 mmol, 1.0 eq.) was added to the solution and refluxed for 2h at 85°C. Afterwards, the container was sealed, kept at 55°C for three days and then gradually cooled down to the rt in darkness over three more days. Then, the reaction flask was put in a heat-insulator container and slowly refrigerated and kept at -20°C for two days. Afterwards, the remaining 1,2-dichloroethane was removed by vacuum, the solid residue was sonicated with NaOH (aq, 6N, 10ml) and then DCM (10 ml) was added. The DCM layer quickly turned orange and was separated and was rigorously worked up with NaOH (aq, 1N, 30ml X 5) for ensuring a total hydrolysis and elimination of the tartaric acid residues. The organic layer was finally separated, dried over Na₂SO₄ and filtered. The solvent was removed under reduced pressure to obtain a partially-resolved product (0.68 g, 0.95 mmol, 0.95 eq., [α]_D^{15.5}=-43 in DCM).

Similarly, this test was performed with (+)-O,O'-dibenzoyl-R-tartaric acid which gave another partially-resolved product (0.66 g, 0.93 mmol, 0.93 eq. [α]_D^{16.2}=+39 in DCM).

To the DCM solutions of these products were added an excess amount of trichloroacetic acid (2.0 mmol, 0.33 g) and stirred at rt for 48 hours. Afterwards, the mixture was neutralized and worked up by NaOH (aq, 1N, 30ml X 3) and the optical rotation was finally recalculated which was almost zero.

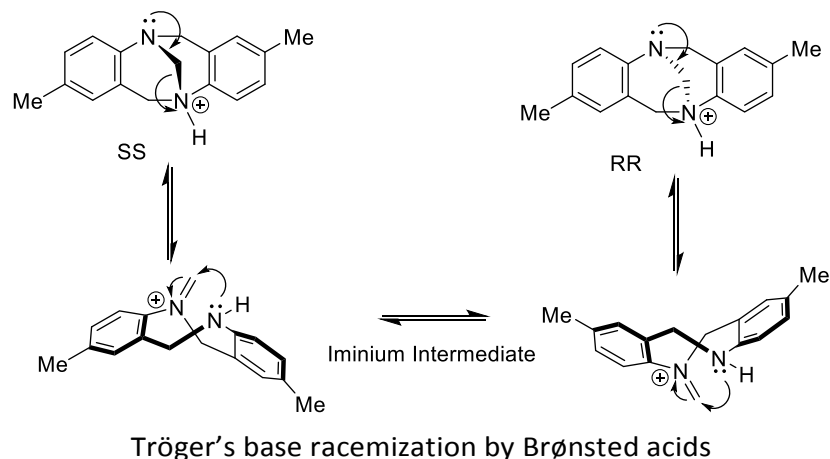
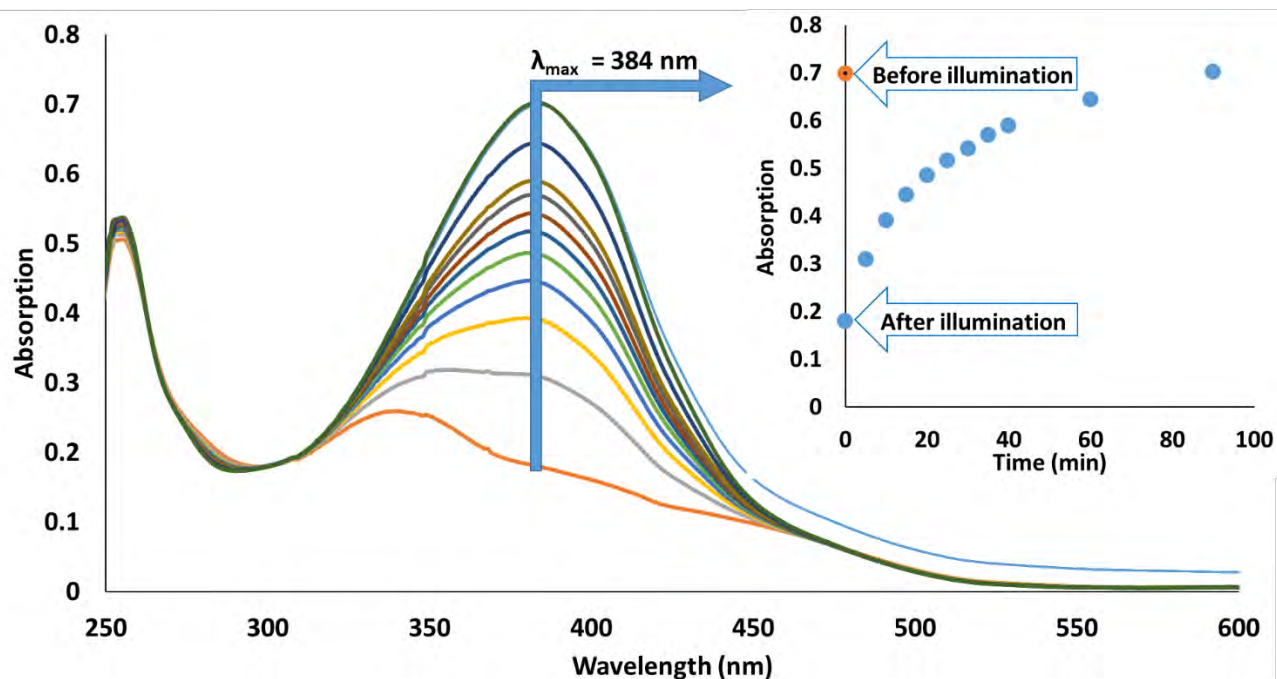
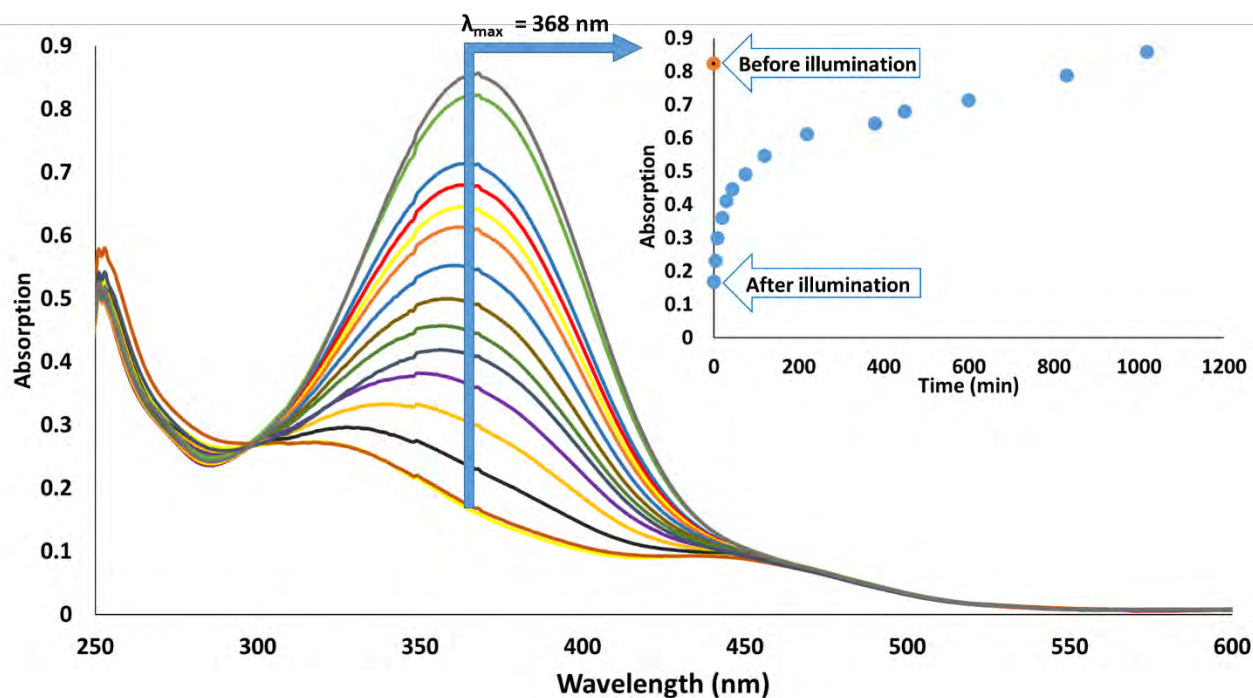


PHOTO-EXCITATION AND THERMAL RELAXATION

A solution of the selected compound in EtOAc at r.t. (2×10^{-5} mol.L⁻¹) was prepared in darkness and loaded into a tightly sealed quartz cuvette. The UV-Vis absorption spectra of this solution was obtained indicating a dominant population of the *trans* isomer. Afterwards, the cuvette was illuminated by a 365 nm UV light-source (Spectroline® ENF-260C/FE [230V, 50Hz, 0.17A], Spectronics Corporation, Westbury, New York, USA) installed on a standard fluorescence cabinet (Spectroline® CM10) for 5 minutes and instantly rescanned to obtain the UV-Vis spectra when the *cis* isomer reaches to its maximum possible population. Then, rescanning process of the sample, (incubated in darkness at the room temperature), continued to track its thermal back-isomerization until when the spectra reached to its initial shape. Tracking the photo-isomerisation proved a totally repeatable and reversible process in agreement with the NMR results showing no sign of photo-degradation. To simplify the photo-isomerisation results, only one cycle of photo-excitation /thermal relaxation is shown.

1. Photo-isomerisation studies of (\pm)-6

Monitoring the changes in UV-vis spectra of 6 in EtOAc at r.t.

2. Photo-isomerisation studies of (\pm)-6A

Monitoring the changes in UV-vis spectra of 6A in EtOAc at r.t.

REFERENCES:

1. S. Rigol, L. Beyer, L. Hennig, J. Sieler and A. Giannis, *Org. Lett.*, 2013, **15**, 1418-1420.
2. D. L. Jameson, T. Field, M. R. Schmidt, A. K. DeStefano, C. J. Stiteler, V. J. Venditto, B. Krovic, C. M. Hoffman, M. T. Ondisco and M. E. Belowich, *J. Org. Chem.*, 2013, **78**, 11590-11596.

RESEARCH CHAPTER THREE

Paper III (Main Article)



Journal Impact Factor: 2.419

Disclaimer Notification

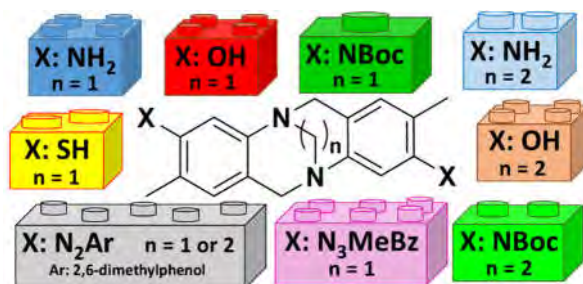
The following copyrighted materials are reproduced with a license, numbered 4119030834308, obtained from *Thieme publisher* on May 30, 2017. In accordance with an agreement between the author and the publisher, the accepted version of the publication is restrictedly allowed to be presented in this copy of the thesis only. Any other use of the following material has to be authorised by the copyright holder of *Synlett*© 2017 Georg Thieme Verlag KG.

M. Kazem-Rostami, *Synlett* 2017, 28, 1641–1645. (accepted version before publication)
Facile preparation of Λ -shaped building blocks: Hünlich's base derivatization

Masoud Kazem-Rostami *

*Department of Chemistry and Biomolecular Sciences,
 Macquarie University, North Ryde, NSW 2109, Australia.

masoud.kazem-rostami@hdr.mq.edu.au,
masoud.kr@gmail.com



Received:
 Accepted:
 Published online:
 DOI:

Abstract Hünlich's base modification has resulted in introducing a series of versatile Λ -shaped building blocks presented in this work. The methods are optimized to provide convenient approaches in the quicker production of these new building blocks in low-cost and low-risk.

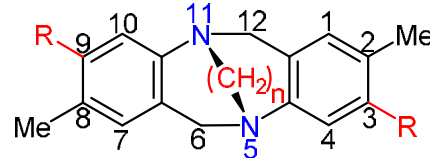
Key words: amines, bicyclic compounds, azo compounds, diazo compounds, nucleophilic aromatic substitution, phenols, protecting groups, thiols.

Tröger's Base Analogues (TBAs) are tetracyclic boomerang-shaped molecules whose aromatic moieties nearly stand in a perpendicular dihedral angle to one another. The bent shaped chiral core of TBAs is generated by two tertiary amine groups which flank a diazocine strap. Depending on which side of the molecule the strap is located, the handedness of TBAs is determined as an *SS* or *RR* enantiomer. Various TBAs structures have been elucidated by single-crystal X-ray crystallography.^{1,2}

TBAs have played a substantial role as versatile building blocks employed in the design of Λ -shaped photo-switchable molecular hinges,^{3, 4} chiral ligands,⁵ catalysts,⁶ receptors,^{7, 8, 9} supermolecules,¹⁰ sensors,^{7, 11} polymers,¹² molecular tweezers, and leashes.¹³ Although numerous methods have reported the production of TBAs including azide or triazole carrying ones;^{2, 14} up to the date, no TBA has been produced carrying triazene or sulfhydryl functional groups which would be useful in coordination,¹⁵ polymer,^{16, 17} surface,¹⁸ and organometallic/heterocyclic¹⁹ chemistries. Triazene group can be converted to functionalized lactams,²⁰ triazoles,²¹ dibenzopyranones and coumarins,²² or be utilized as a substrate for perfluoroalkylation reactions.²³ Furthermore, the triazene group can be replaced with many other functional groups^{24, 25} by being consumed as a diazonium source in organic solutions²⁵ or ionic liquids.²⁶ For instance; herein, a bis-triazene TBA **1** (Table 1) is produced and converted to its corresponding bis-thiophenol

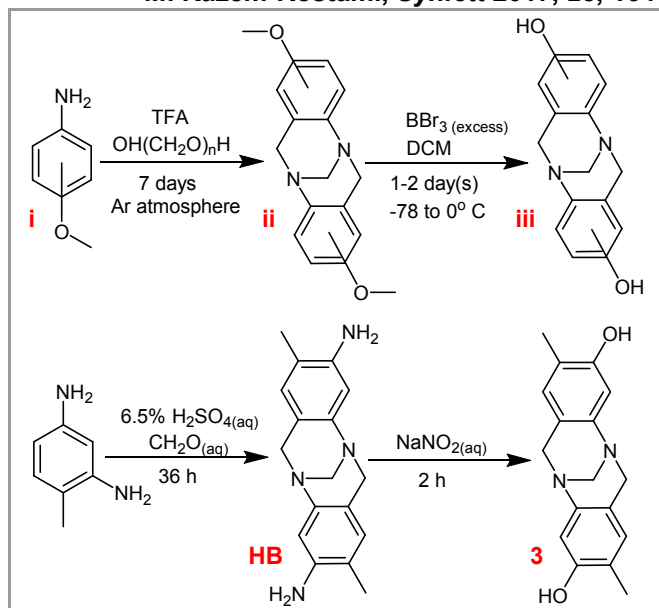
derivative **2** to introduce the first TBA possessing sulfhydryl groups. This conversion achieved under a method reported in 2012.²⁵ This work not only introduces the first sulfhydryl and triazene carrying TBAs but also elaborates a quicker and much safer method of the preparation of bis-hydroxyl and ethano-strapped TBAs using inexpensive materials.

Table 1 The synthesis of the building blocks

				
Entry	Cpd ^a	Time (h)	R Substituents ^b ; [n] ^{Notes}	Yield%
1	1	3.5	3-benzyl-3-methyl-1-triazene; [1] ³⁵	60
2	2	2.5	SH; [1] ³⁶	19
3	3	2.5	OH; [1] ³⁷	96
4	4	6	tert-butyl carbamate; [1]	92
5	5	12	tert-butyl carbamate; [2]	77
6	6	9	4-hydroxy-3,5-dimethylphenyl diazene; [1]	83
7	7	12	4-butoxy-3,5-dimethylphenyl diazene; [1]	71
8	8	8	4-hydroxy-3,5-dimethylphenyl diazene; [2]	78
9	9	24	4-butoxy-3,5-dimethylphenyl diazene; [2]	22
10	10	1	NH ₂ ; [2]	96
11	11	2.5	OH; [2]	91
12	12	18	OH; [0]	trace
13	13	2.5	H; [1]; 1,7: OH; and 4,10: CH ₃	92

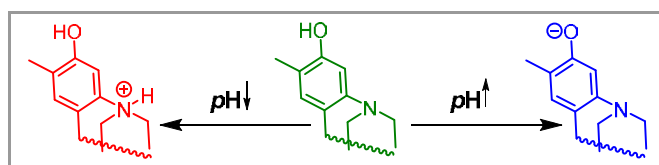
^a Compound (racemate). ^b R is symmetrically positioned on 3 and 9 positions.

The preparation of dihydroxy-TBAs (Scheme 1, **iii**) has been performed by using the excess amounts of extremely hazardous and expensive reagents such as boron tribromide and trifluoroacetic acid (TFA).^{9, 27}

M. Kazem-Rostami, *Synlett* 2017, 28, 1641–1645. (accepted version before publication)

Scheme 1 The previously reported method on the preparation of di-hydroxyl TBAs (top) and the inexpensive shortcut introduced in this work (bottom).

The production of **iii** is time-consuming and requires several days to complete the trogeration (Scheme 1, the conversion of **i** to **ii**) and the demethylation steps (the conversion of **ii** to **iii**).²⁷ Furthermore, due to the low solubility of the produced bis-hydroxyl TBA **iii** in organic solvents, the separation of the product is problematic. In fact, every slight increase or decrease of pH value can easily transform the product into phenoxy form or quaternary amine salt, respectively (Scheme 2); which both tend to remain in the aqueous layer and hence the extraction becomes troublesome.²⁷ To display the pH sensitive features of such molecules, the UV-Vis spectra of **3** was obtained in the presence of strong protonating and deprotonating reagents (Page 46, Supp. Info.). Compound **3** experienced a tremendous bathochromic shift upon deprotonation and turned red in color; however, the protonation led to a normal hypsochromic shift.



Scheme 2 The pH sensitive nature of typical dihydroxy-TBAs, e.g. **3**

The attempts on demethylation of **ii** in harsh and acidic conditions, HCl–AcOH (1:1, 110°C, 48 h) instead of using BBr₃, only gave a mixture of **iii** and its asymmetrically methylated derivative which carries a hydroxyl group as well as an intact methoxy.⁹

The literature also introduces the preparation of dihydroxyl TBAs by the reduction of benzyl ether carrying analogues in the presence of hydrogen gas, and Pd/C catalyst.²⁷ This method is as costly as the previous ones, in addition, requires the stream of an explosive gas or specialized hydrogenation reactor(s) which are only applicable in small batches. Although BBr₃ has apparently^{9, 27, 28} covered the tedious production of hydroxyl-carrying TBAs, the involved risks and costs cannot be ignored and yet an

alternative method is needed to be found. Therefore, an easier method (Scheme 1, bottom) on the production of dihydroxy-TBAs (Table 1, compounds **3**, **11**, and **13**) is described in this work. Hünlich's base (Scheme 1, HB) is an affordable diamino-TBA that facilitates the synthesis in the big scale in much lower costs. Furthermore, additionally-introduced methyl groups significantly increase the hydrophobicity of **3**, **11**, and **13** products which helps their extraction during the work up.

The applied method in the production of **3**, **11**, and **13**, is known as the decomposition of diazonium salts in aqueous media¹⁶ which is optimized here to result in the facile production of the dihydroxy TBAs. This method¹⁶ uses a diluted aqueous solution of sulfuric acid (H₂SO₄:H₂O, v/v 6.5%) instead of an expensive and fuming acid (neat TFA), and a harmless sodium nitrite solution (NaNO₂ in H₂O, w/v 3%) instead of boron tribromide which is violently corrosive, expensive, problematic to store and handle. Delightfully, the production of **3**, **11**, and **13** included none of the aforementioned drawbacks and resulted in the excellent amount of yields (91–96%).

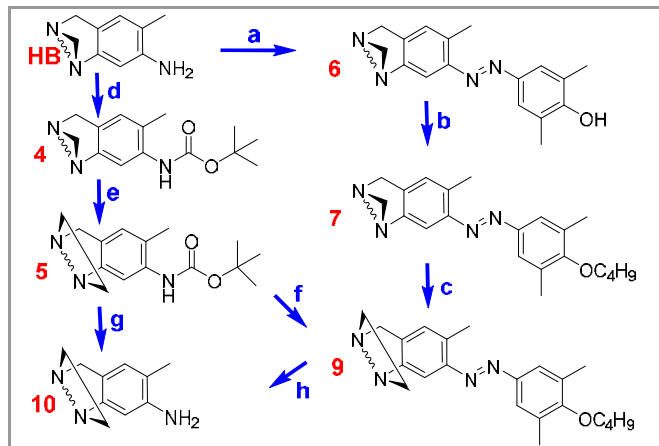
TBAs structure has been modified by replacing the diazocine strap as well as changing the substituents.^{29, 30} Such structural modifications result in the emergence of enhanced properties. For instance, replacing the methylene group of the diazocine bridge by an ethylene group simply prevents the racemisation⁴ of TBAs in acidic media. Furthermore, such a modification gives new features to these valuable building blocks such as changing the size of their Δ -shape void and the dihedral angle (ca. up to 20°) of the scaffold.^{29, 31}

Compounds **6** and **7** are previously introduced as molecular photo-switches with the potential of being utilised for various purposes.³ The strap modification can make the chirality of such compounds resistant to acids and tightens their scaffold which may be beneficial in molecule recognition studies. Therefore, the change of strap was herein performed on compound **7** to obtain its ethano-strapped derivative **9**. The strap-change operation (Scheme 3, step c) usually ends up with a mixture of both methano- and ethano-strapped TBAs, especially when TBAs carry electron-withdrawing groups. Despite many attempts, in optimising the conversion of **7** to **9**, neither the higher ratio of alkyl halide–TBA nor elongated reaction time did improve the conversion yield beyond 30%. Also, the separation of these two is challenging because the butyl groups make the retardation factors of **7** and **9** very close to one another. Hence, the separation of product **9** from the starting material **7** was a challenge for common liquid chromatography. Also, modifying a compound like **7** only gives a specialised product with specific properties which cannot be considered as a versatile building block. Therefore, as the ultimate goal of this project, a versatile and affordable building block had to be found e.g. a modified diamino TBA.

Although **8**'s or **9**'s reduction gives the desired ethano-strapped diamino building block **10** (Scheme 2, step h), such conversion is not convenient due to multiple steps and instability of **10**. A modified building block needs to be easily produced, stored and be readily available for straightforward applications.

M. Kazem-Rostami, *Synlett* 2017, 28, 1641–1645. (accepted version before publication)

Having all these in mind, the preparation of **5** as an ethano-strapped versatile building block is reported in satisfactory yield without any of the aforementioned issues. In fact, the *N*-Boc protected groups moderately activate the substrate compound **4** during the strap-change operation and also prevent the unwanted *N*-alkylation reactions.



Scheme 3 Due to the symmetry of the products, they are presented as half. **a:** i) $\text{H}_2\text{SO}_4/\text{NaNO}_2$, ii) 2, 6-dimethylphenol/ Na_2CO_3 ; **b:** $\text{C}_4\text{H}_9\text{Br}/\text{K}_2\text{CO}_3$; **c:** $\text{C}_2\text{H}_4\text{Br}_2/\text{Li}_2\text{CO}_3$; **d:** $\text{Boc}(\text{anhyd})/\text{I}_2$; **e:** $\text{C}_2\text{H}_4\text{Br}_2/\text{Li}_2\text{CO}_3$; **f:** i) $\text{H}_2\text{SO}_4/\text{NaNO}_2$, ii) 2, 6-dimethylphenol/ Na_2CO_3 , iii) $\text{C}_4\text{H}_9\text{Br}/\text{K}_2\text{CO}_3$; **g:** H_2SO_4 ; **h:** $\text{Na}_2\text{S}_2\text{O}_6$.

Therefore, **4**'s strap-change operation accomplished in good yields (up to 96% converted based on the crude's NMR, 77% isolated by chromatography). The obtained ethano-strapped TBA **5** can be readily unprotected and be converted to other functional groups as earlier performed on the methano-strapped analogues.

Exposure of diamino-TBAs, e.g. **10** (Table 1) and HB (Scheme 1), to air and light quickly decomposes them. This can be detected by the fast change of colour from white to brown. To prevent the decomposition, Boc-protection of the amine groups was performed which significantly elongated the shelf life of these sensitive materials. The unprotection of **4** and **5** is fast and easy³² and releases the corresponding diamino-TBAs which can be easily converted to the other desired compounds as described.

The generality of the applied methodologies are well documented in the literature, and rescaling the reactions up to tenfold showed not a considerable change of the yields percentage.

To conclude, a group of novel TBAs is safely prepared out of inexpensive materials. The illustrated structural modifications in this work can be considered as the reincarnation of this hundred-year-old compound. These novel products can be utilised as Λ -shape building blocks in the design of photonic crystals,³³ chiral ligands, receptors, catalysts, molecular machines, porous and conductive^{16, 34} polymers.

Acknowledgment

The author wholeheartedly appreciates the Australian Government for providing him with a Research Training Program Scholarship (IPRS-2014004) and Macquarie University for the provided facilities, HDR43010477 grant and PGRF2016R2-1672525 fund. Dr Andrew Piggott and respected Jamie family are thanked for the provided lab space, and partial access to the departmental facilities.

Supporting Information

Detailed procedures and the NMR, MS, IR, and UV/Vis spectra are available *via* the Internet at (links)

References and Notes

- (1) Solano, C.; Svensson, D.; Olomi, Z.; Jensen, J.; Wendt, O. F.; Wärnmark, K. *Eur. J. Org. Chem.* **2005**, 2005, 3510.
- (2) Bosmani, A.; Pujari, S.; Guenee, L.; Besnard, C.; Poblador Bahamonde, A. I.; Lacour, J. *Chem. Eur. J.* **2017**, In press: 10.1002/chem.201700845.
- (3) Kazem-Rostami, M. *Synthesis* **2017**, 49, 1214.
- (4) Kazem-Rostami, M.; Moghanian, A. *Org Chem Front* **2017**, 4, 224.
- (5) Harmata, M.; Kahraman, M. *Tetrahedron Asymmetry* **2000**, 11, 2875.
- (6) Goldberg, Y.; Alper, H. *Tetrahedron Lett.* **1995**, 36, 369.
- (7) Boyle, E. M.; Comby, S.; Molloy, J. K.; Gunnlaugsson, T. *J. Org. Chem.* **2013**, 78, 8312.
- (8) Webb, T. H.; Suh, H.; Wilcox, C. S. *J. Am. Chem. Soc.* **1991**, 113, 8554; Bhaskar Reddy, M.; Shailaja, M.; Manjula, A.; Premkumar, J. R.; Sastry, G. N.; Sirisha, K.; Sarma, A. V. S. *Org. Biomol. Chem.* **2015**, 13, 1141; Wilcox, C. S.; Cowart, M. D. *Tetrahedron Lett.* **1986**, 27, 5563; Kejřk, Z.; Břřza, T.; Havřík, M.; Dolenský, B.; Kapláneř, R.; Králová, J.; Mikula, I.; Martásek, P.; Král, V. *Dyes Pigm* **2016**, 134, 212.
- (9) Tatar, A.; Valřk, M.; Novotná, J.; Havřík, M.; Dolenský, B.; Král, V.; Urbanová, M. *Chirality* **2014**, 26, 361.
- (10) Kiehne, U.; Weilandt, T.; Lützen, A. *Org. Lett.* **2007**, 9, 1283; Banerjee, S.; Bright, S. A.; Smith, J. A.; Burgeat, J.; Martinez-Calvo, M.; Williams, D. C.; Kelly, J. M.; Gunnlaugsson, T. *J. Org. Chem.* **2014**, 79, 9272.
- (11) Satishkumar, S.; Periasamy, M. *Tetrahedron Asymmetry* **2009**, 20, 2257; Goswami, S.; Ghosh, K.; Dasgupta, S. *J. Org. Chem.* **2000**, 65, 1907; Adrian, J.; Wilcox, C. J. *Am. Chem. Soc.* **1989**, 111, 8055; Adrian, J.; Wilcox, C. J. *Am. Chem. Soc.* **1992**, 114, 1398; Valřk, M.; Strongin, R. M.; Král, V. *Supramol. Chem.* **2005**, 17, 347; Adrian Jr, J. C.; Wilcox, C. S. *J. Am. Chem. Soc.* **1989**, 111, 8055; Cowart, M. D.; Sucholeiki, I.; Bukownik, R. R.; Wilcox, C. S. *J. Am. Chem. Soc.* **1988**, 110, 6204.
- (12) Abdolmaleki, A.; Heshmat-Azad, S.; Kheradmand-fard, M. *J. Appl. Polym. Sci.* **2011**, 122, 282; Shishkanova, T. V.; Havřík, M.; Král, V.; Kopecký, D.; Matěřka, P.; Dendisová, M.; Mirsky, V. M. *Electrochim. Acta* **2017**, 224, 439.
- (13) Tatar, A.; Cejka, J.; Král, V.; Dolenský, B. *Org. Lett.* **2010**, 12, 1872; Sergeyev, S.; Diederich, F. *Angew. Chem. Int. Ed.* **2004**, 43, 1738; Havřík, M.; Král, V.; Kaplanek, R.; Dolenský, B. *Org. Lett.* **2008**, 10, 4767.
- (14) Rigol, S.; Beyer, L.; Hennig, L.; Sieler, J.; Giannis, A. *Org. Lett.* **2013**, 15, 1418.
- (15) Vajs, J.; Steiner, I.; Brozovic, A.; Pevec, A.; Ambriović-Ristov, A.; Matković, M.; Piantanida, I.; Urankar, D.; Osmak, M.; Kořmrlj, J. *J. Inorg. Biochem.* **2015**, 153, 42; Rofouei, M. K.; Soleymani, R.; Aghaei, A.; Mirzaei, M. *J. Mol. Struct.* **2016**, 1125, 247; Blower, P. J.; Dilworth, J. R. *Coord. Chem. Rev.* **1987**, 76, 121; Gholivand, M. B.; Mohammadi, M.; Rofouei, M. K. *Mater Sci Eng C Mater Biol Appl* **2010**, 30, 847.
- (16) Khazaei, A.; Kazem-Rostami, M.; Zare, A.; Moosavi-Zare, A. R.; Sadehpour, M.; Afkhami, A. *J. Appl. Polym. Sci.* **2013**, 129, 3439.

M. Kazem-Rostami, *Synlett* 2017, 28, 1641–1645. (accepted version before publication)

- (17) Schneider, P. Masticating synthetic rubber, U.S. Patents 2,784,167. 1957.
- (18) Gholivand, M. B.; Mohammadi, M.; Khodadadian, M.; Rofouei, M. K. *Talanta* **2009**, 78, 922; Chen, B.; Flatt, A. K.; Jian, H.; Hudson, J. L.; Tour, J. M. *Chem. Mater.* **2005**, 17, 4832; Lu, M.; He, T.; Tour, J. M. *Chem. Mater.* **2008**, 20, 7352; Riskin, M.; Tel-Vered, R.; Willner, I. *Adv. Mater.* **2010**, 22, 1387.
- (19) Takacs, J. M.; Vayalakkada, S.; Jiang, X., *Organometallics. In Science of Synthesis: Houben-Weyl methods of molecular transformations*, 1 ed.; Lautens, M., Ed. Georg Thieme Verlag: Stuttgart and Thieme Publishing Group: New York, 2001; Vol. 1, pp 304-313.
- (20) Petrovic, M.; Scarpi, D.; Nieger, M.; Jung, N.; Occhiato, E. G.; Brase, S. *RSC Adv.* **2017**, 7, 9461.
- (21) Takagi, K.; Al-Amin, M.; Hoshiya, N.; Wouters, J.; Sugimoto, H.; Shiro, Y.; Fukuda, H.; Shuto, S.; Arisawa, M. *J. Org. Chem.* **2014**, 79, 6366.
- (22) Shang, X.; Xu, L.; Yang, W.; Zhou, J.; Miao, M.; Ren, H. *Eur. J. Org. Chem.* **2013**, 2013, 5475.
- (23) Hafner, A.; Hussal, C.; Bräse, S. *Synthesis* **2014**, 46, 1448.
- (24) Sun, H.; Huang, Y. *Synlett* **2015**, 26, 2751; Zhang, Y.; Cao, D.; Liu, W.; Hu, H.; Zhang, X.; Liu, C. *Curr. Org. Chem.* **2015**, 19, 151.
- (25) Khazaei, A.; Kazem-Rostami, M.; Moosavi-Zare, A. R.; Bayat, M.; Saednia, S. *Synlett* **2012**, 23, 1893.
- (26) Cao, D.; Zhang, Y.; Liu, C.; Wang, B.; Sun, Y.; Abdukadera, A.; Hu, H.; Liu, Q. *Org. Lett.* **2016**, 18, 2000; Zhang, Y.; Hu, H.; Liu, C.-J.; Cao, D.; Wang, B.; Sun, Y.; Abdukader, A. *Asian J. Org. Chem.* **2016**, 6, 102.
- (27) Malik, Q. M.; Ijaz, S.; Craig, D. C.; Try, A. C. *Tetrahedron* **2011**, 67, 5798.
- (28) Kiehne, U.; Lützen, A. *Synthesis* **2004**, 2004, 1687.
- (29) Faroughi, M.; Try, A. C.; Klepetko, J.; Turner, P. *Tetrahedron Lett.* **2007**, 48, 6548.
- (30) Kamiyama, T.; Sigrist, L.; Cvengroš, J. *Synthesis* **2016**, 48, 3957; Michon, C.; Sharma, A.; Bernardinelli, G.; Francotte, E.; Lacour, J. *Chem. Commun.* **2010**, 46, 2206; Hamada, Y.; Mukai, S. *Tetrahedron Asymmetry* **1996**, 7, 2671.
- (31) Sergeev, S. *Helv. Chim. Acta* **2009**, 92, 415.
- (32) Zinelaabidine, C.; Souad, O.; Zoubir, J.; Malika, B.; Nour-Eddine, A. *Int. J. Chem.* **2012**, 4, 73.
- (33) Hu, Y.; Miles, B. T.; Ho, Y.-L. D.; Taverne, M. P. C.; Chen, L.; Gersen, H.; Rarity, J. G.; Faul, C. F. J. *Adv. Opt. Mater.* **2017**, 5, 1600458.
- (34) Liao, Y.; Weber, J.; Mills, B. M.; Ren, Z.; Faul, C. F. J. *Macromolecules* **2016**, 49, 6322.

(35) Synthesis and Characterisation of Compound 1

Hünlich's base (0.56 g, 2.0 mmol, 1.0 eq.) solution in H₂SO₄ (6.5%, 30 mL) was cooled down to -5°C. A sodium nitrite solution (0.30 g, 4.4 mmol, 2.2 eq. in 5 mL cold water) was dropped into the reaction flask and stirred for 30 min. The resulting yellowish solution was poured into a solution consisting *N*-benzylmethylamine (3 mL, excess), Na₂CO₃ (4.5 g), 60 mL of water, and 30 mL of ACN chilled at -10°C. The stirring was continued for 3 h meanwhile the temperature was gradually raised to r.t.; afterward, a beige precipitate was extracted from the aqueous mixture by DCM (3x50 mL). The DCM layers were combined, dried over Na₂SO₄ and filtered. The evaporation of the DCM gave the crude product which was then purified by

chromatography to furnish the purified bis-triazene compound **1** as a light-yellow solid. Yield: 0.65 g (1.2 mmol, 60%); *R*_f: 0.3 (silica gel; MeOH–DCM, 2% v/v). IR (neat): 3027, 2941, 2893, 2844, 1610, 1486, 1441, 1341, 1173, 1047, 921 and 697 cm⁻¹. ¹H NMR (400 MHz, CDCl₃): δ = 7.28–7.38 (m, 12H, CH), 6.74 (s, 2H, CH), 4.91–5.02 (q, *J* = 16.1 Hz, 4H, NCH₂), 4.66–4.70 (d, *J* = 16.6 Hz, 2H, CH₂), 4.36 (s, 2H, NCH₂N), 4.22–4.26 (d, *J* = 16.8 Hz, 2H, CH₂), 3.15 (b, 6H, NCH₃), 2.30 (s, 6H, CH₃). ¹³C NMR (100 MHz, CDCl₃): δ = 147.9, 146.3, 137.1, 129.0, 128.7, 128.6, 128.0, 127.7, 125.1, 112.7, 67.3, 58.8, 34.4, 17.2. MS (ESI +; *i*-PrOH): *m/z* [M + H]⁺ calcd for [C₃₃H₃₇N₈]⁺: 545.31; found 545.2. UV/Vis: (EtOAc): λ (lg ε) = 297 (4.465) nm. Anal. Calcd for C₃₃H₃₆N₈: C, 72.77; H, 6.66; N, 20.57. Found: C, 72.56; H, 6.85; N, 20.18.

(36) Synthesis and Characterisation of Compound 2

The bis-triazene compound **1** (0.54 g, 1.0 mmol, 1.0 eq.) was poured into a 50 mL round-bottom flask containing DCM (20 mL). A solution of trichloroacetic acid (5.0 g, 30 mmol, excess, in DCM 20 mL) was added and stirred for 2 min. Afterward, Na₂S (0.70 g, 9 mmol, excess) was slowly added to the reaction flask, as shown in the following figure, and remained sealed when stirred for 2 hours at rt. The volume of the resulting yellowish suspension was then reduced to half by nitrogen gas flow and then refluxed for 30 min. The reaction mixture cooled down to rt and diluted with DCM (100 mL), and filtered. The DCM layer was rinsed with cold water (5 X 100 mL), dried over Mg₂SO₄ and filtered. The DCM was removed and the residue was purified by column chromatography to obtain a pale-lemon substance with a mild rotten-egg odour which was then stored under argon in darkness. Yield: 0.06 g (0.19 mmol, 19 %); *R*_f: 0.2 (silica gel; MeOH–DCM, 4% v/v). IR (neat): 2896, 2847, 2560, 1608, 1492, 1474, 1205, 1091, 1010, 811 cm⁻¹. ¹H NMR (400 MHz, CDCl₃): δ = 7.62 (br, 2 H, SH), 6.65 (s, 2 H, CH), 6.17 (s, 2 H, CH), 4.56–4.60 (d, *J* = 16.7 Hz, 2 H), 4.28 (s, 2 H, NCH₂N), 4.17–4.13 (d, *J* = 16.8 Hz, 2 H), 2.10 (s, 6 H, 2CH₃). ¹³C NMR (100 MHz, CDCl₃): δ = 143.8, 134.5, 128.6, 127.4, 126.8, 124.7, 67.1, 58.4, 20.9. MS (ESI +; *i*-PrOH–EtOAc–H₂O/0.5% HCO₂Na, 90:5:5): *m/z* [M + Na]⁺ calcd for [C₁₇H₁₈N₂S₂Na]⁺: 337.08; found: 337.0. MS (ESI –): *m/z* [M – H][–] calcd for [C₁₇H₁₇N₂S₂][–]: 313.09; found: 313.1. MS (ESI +; ACN/Δ): *m/z* [M + 2ACN + H]⁺ calcd for [C₂₁H₂₅N₄S₂]⁺: 397.14; found: 397.1. UV/Vis: (EtOAc): λ (lg ε) = 277 (3.583) nm. Anal. Calcd for C₁₇H₁₈N₂S₂: C, 64.93; H, 5.77; N, 8.91; S, 20.39. Found: C, 65.08; H, 5.83; N, 9.22.

(37) Synthesis and Characterisation of Compound 3

Hünlich's base (0.56 g, 2.0 mmol, 1.0 eq.) was dissolved in H₂SO₄ (6.5%, 90 mL), then cooled down to -5°C. A sodium nitrite solution (0.30 g, 4.4 mmol, 2.2 eq.) in cold water (10 mL) was dropped into the reaction flask and stirred for 30 min. Afterward, the solution's temperature was gradually raised to boil, over two hours (Attention: this step releases nitrogen gas; hence, rapid heating and sealing the container may lead to explosion). The reaction mixture was cooled down to r.t., its pH was adjusted to 5 (by adding Na₂CO₃ saturated solution) and extracted with EtOAc (30 mL x 5), the organic layers were combined, dried over Na₂SO₄ and evaporated to dryness to obtain the product as a light-grey powder. Yield: 0.54 g (1.9 mmol, 96%). *R*_f: 0.3 (silica gel; MeOH–DCM, 8% v/v). IR (neat): 3649, 3549, 3012, 2948, 2904, 2857, 1620, 1508, 1368, 1081 and 910 cm⁻¹. ¹H

M. Kazem-Rostami, *Synlett* 2017, 28, 1641–1645. (accepted version before publication)

NMR (400 MHz, DMSO- d_6): δ = 9.06 (s, 2H, OH), 6.56 (s, 2H, CH), 6.45 (s, 2H, CH), 4.39–4.43 (d, J = 16.4 Hz, 2H, CH₂), 4.07 (s, 2H, NCH₂N), 3.81–3.85 (d, J = 16.4 Hz, 2H, CH₂), 1.97 (s, 6H, CH₃). ¹³C-NMR (100 MHz, DMSO- d_6): δ = 154.1, 146.5, 128.2, 119.9, 117.9, 110.0, 66.5, 57.8, 15.5. MS (ESI +; EtOH–EtOAc–H₂O, 90:5:5): m/z [M + H]⁺ calcd for [C₁₇H₁₉N₂O₂]⁺: 283.14; found 283.1. MS (ESI –): m/z [M – H][–] calcd for [C₁₇H₁₇N₂O₂][–]: 281.14; found 281.1. UV/Vis: (EtOAc): λ (lg ϵ) = 292 (3.643) nm. Anal. calcd for C₁₇H₁₈N₂O₂: C, 72.32; H, 6.43; N, 9.92; O, 11.33. Found: C, 72.21; H, 6.61; N, 9.74.

Paper III (Supporting Information)



Journal Impact Factor: 2.419

Notification

The following materials are *open access* and are available online free of charges *via* the Internet at: <https://doi.org/10.1055/s-0036-1588180>. Any other use of the following material has to be referred to the corresponding publication: *Synlett*, **2017**, 28, 1641–1645.

Supporting Information
for DOI: 10.1055/s-0036-**1588180**
© Georg Thieme Verlag KG Stuttgart · New York 2017

Supporting Information

Facile preparation of Λ -shaped building blocks: Hünlich-base derivatization

Masoud Kazem-Rostami^{*a}

^a Department of Chemistry and Biomolecular Sciences, Macquarie University, North Ryde, NSW 2109, Australia.

* Emails: masoud.kazem-rostami@hdr.mq.edu.au, masoud.kr@gmail.com; Fax: 0061-9850 8313

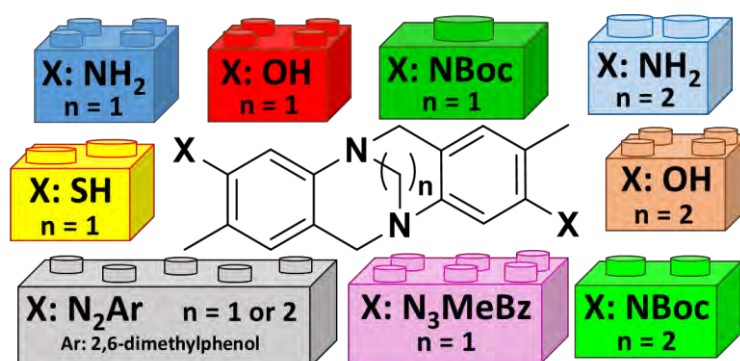
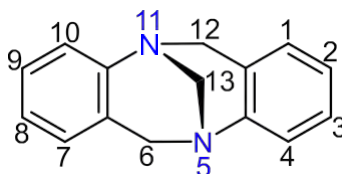


Table of Contents

Materials and Methods	2
1. Preparation and Purification of Compound (1)	2
2. Preparation and Purification of Compound (2)	5
3. Preparation and Purification of Compound (3)	9
4. Preparation and Purification of Compound (4)	13
5. Preparation and Purification of Compound (5)	16
6. Preparation and Purification of Compound (6)	19
7. Preparation and Purification of Compound (7)	21
8. Preparation and Purification of Compound (8)	22
9. Preparation and Purification of Compound (9)	26
10. Preparation and Purification of Compound (10)	29
11. Preparation and Purification of Compound (11)	34
12. Preparation and Purification of Compound (12)	39
13. Preparation and Purification of Compound (13)	40
14. UV/Vis Studies of Compound (3)	46
Relevant Mechanisms	47
Starting Materials	48
15. Hünlich's base preparation	48
16. 1,2-dibromoethane	49
References	51

Materials and Methods:

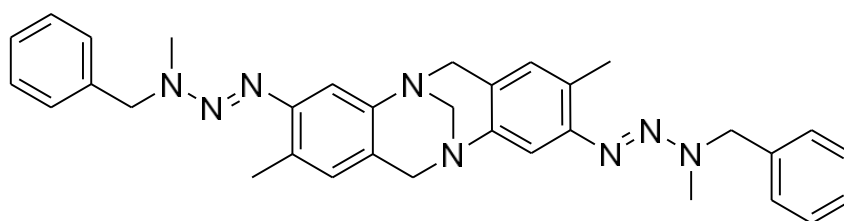
Except for Hünlich's base and 1,2-dibromoethane, all other chemicals were supplied by Sigma-Aldrich, Merck, BOC and Fluka companies. Agilent-6130 or Shimadzo-2010EV mass spectrometers, Varian-Cary-1 and Eppendorf-BioSpektrometer-kinetic spectrophotometers and Thermo-Scientific-Nicolet-iS5/ATR10 spectrophotometer recorded the MS, UV/Vis, and IR spectra. The reaction completion was checked by Thin Layer Chromatography (TLC) on UV-activate silica gel plates of 256nm. Chromatography columns were filled with silica gel (40–63 μm) and mobile phases are displayed by a retardation factor (R_f) for each product. Elemental analysers Vario-EL-Elementar and PerkinElmer-2400-series-II performed the micro-elemental analysis. Bruker-AVANCE-DRX NMR spectrometer and Topspin[®] software were used to obtain NMR spectra calibrated depending on the applied solvent and the chosen nucleon as follow: ^1H (400.0 MHz): 7.26 and 2.50 ppm, and ^{13}C (100.6 MHz): 77.16 and 39.52 ppm for CDCl_3 and $\text{DMSO}-d_6$, respectively. The NMR splitting, integrals, and coupling constants, are displayed by the common standards.



Numbering the atoms on Hünlich-base scaffold

1. Preparation and Purification of Compound (1)

3,9-bis((E)-3-benzyl-3-methyltriaz-1-en-1-yl)-2,8-dimethyl-6H,12H-5,11-methanodibenzo[b,f][1,5] diazocine



Hünlich's base (0.56 g, 2.0 mmol, 1.0 eq.) solution in H_2SO_4 (6.5%, 30 mL) was cooled down to -5°C . A sodium nitrite solution (0.30 g, 4.4 mmol, 2.2 eq. in 5 mL cold water) was dropped into the reaction flask and stirred for 30 min. The resulting yellowish solution was poured into a solution consisting *N*-benzylmethylamine (3 mL, excess), Na_2CO_3 (4.5 g), 60 mL of water, and 30 mL of ACN chilled at -10°C . The stirring was continued for 3 h meanwhile the temperature was gradually raised to r.t.; afterward, a beige precipitate was extracted from the aqueous mixture by DCM (3x50 mL). The DCM layers were combined, dried over Na_2SO_4 and filtered. The evaporation of the DCM gave the crude product which was then purified by chromatography to furnish the purified bis-triazene compound **1** as a light-yellow solid.

Yield: 0.65 g (1.2 mmol, 60%); R_f : 0.3 (silica gel; MeOH–DCM, 2% v/v).

IR (neat): 3027, 2941, 2893, 2844, 1610, 1486, 1441, 1341, 1173, 1047, 921 and 697 cm^{-1} .

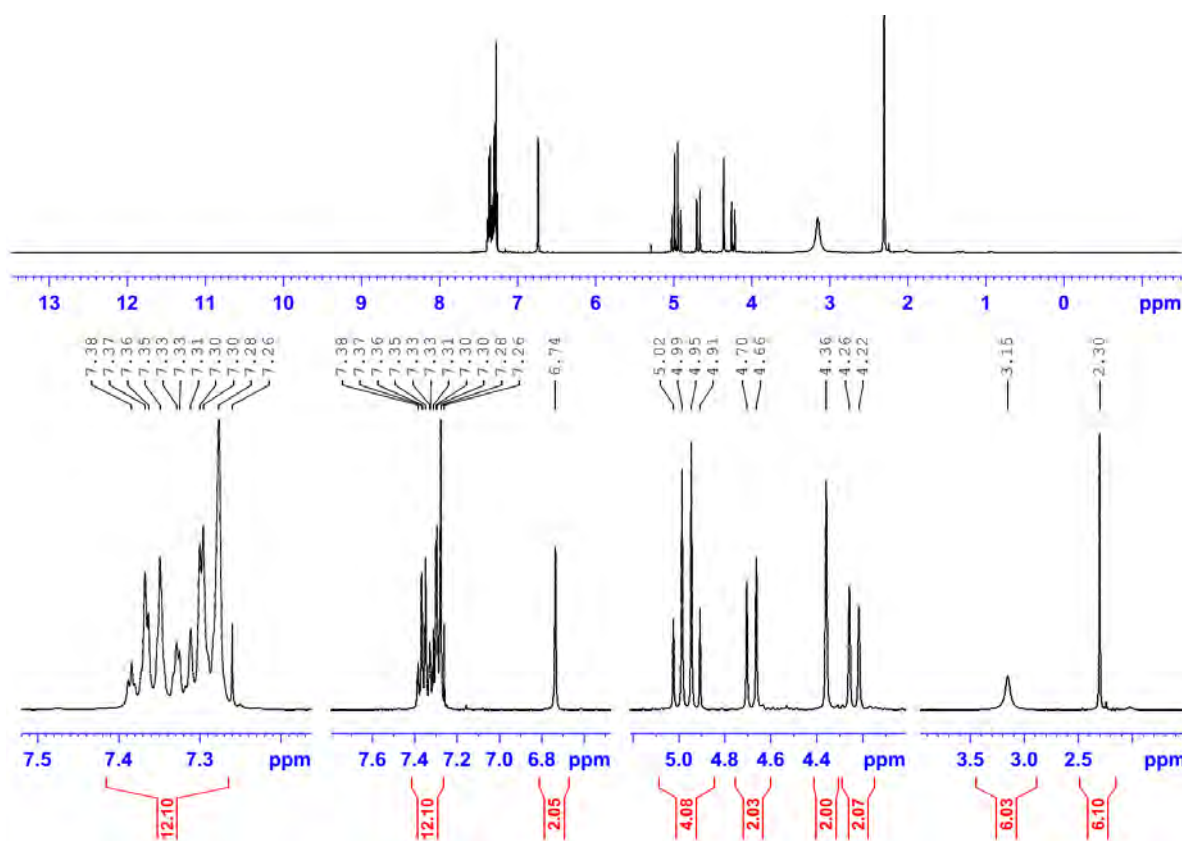
^1H NMR (400 MHz, CDCl_3): δ = 7.28–7.38 (m, 12H, CH), 6.74 (s, 2H, CH), 4.91–5.02 (q, J = 16.1 Hz, 4H, NCH_2), 4.66–4.70 (d, J = 16.6 Hz, 2H, CH_2), 4.36 (s, 2H, NCH_2N), 4.22–4.26 (d, J = 16.8 Hz, 2H, CH_2), 3.15 (b, 6H, NCH_3), 2.30 (s, 6H, CH_3).

^{13}C NMR (100 MHz, CDCl_3): δ = 147.9, 146.3, 137.1, 129.0, 128.7, 128.6, 128.0, 127.7, 125.1, 112.7, 67.3, 58.8, 34.4, 17.2.

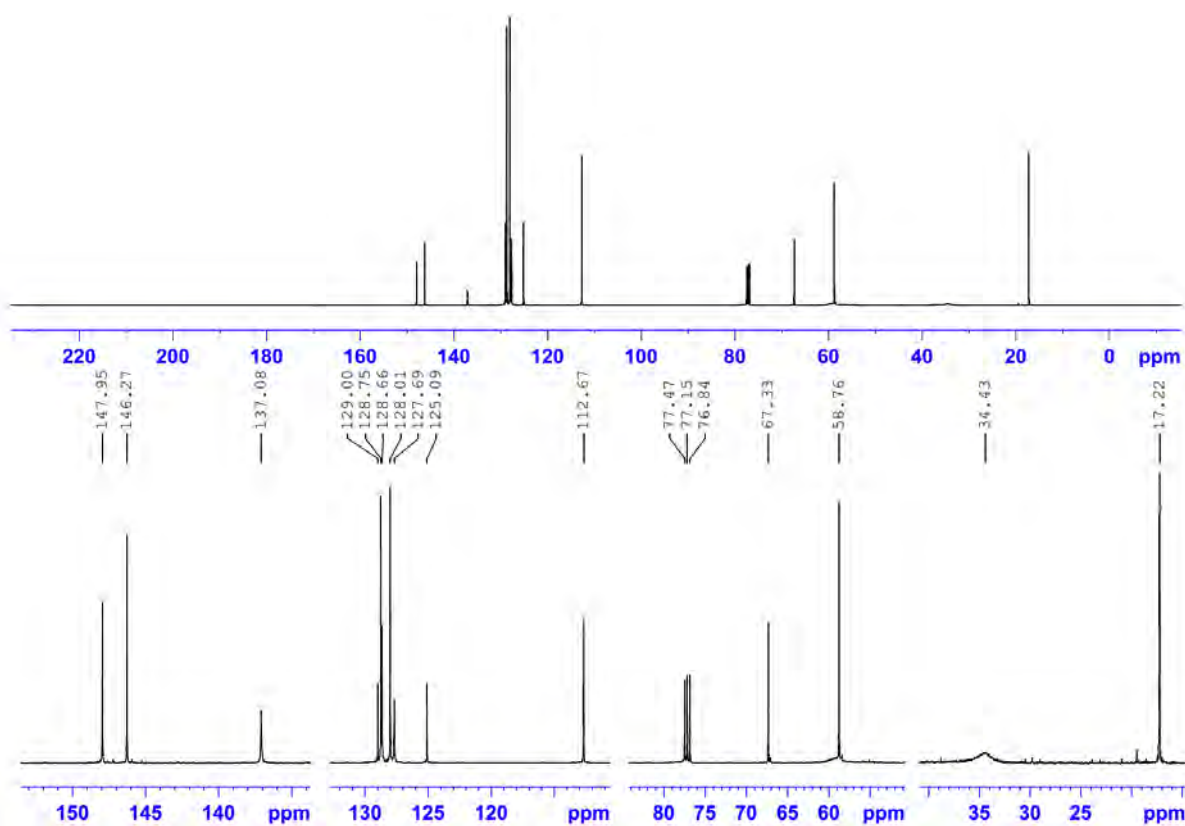
MS (ESI +; i -PrOH): m/z $[\text{M} + \text{H}]^+$ calcd for $[\text{C}_{33}\text{H}_{37}\text{N}_8]^+$: 545.31; found 545.2.

UV/Vis: (EtOAc): λ (lg ϵ) = 297 (4.465) nm.

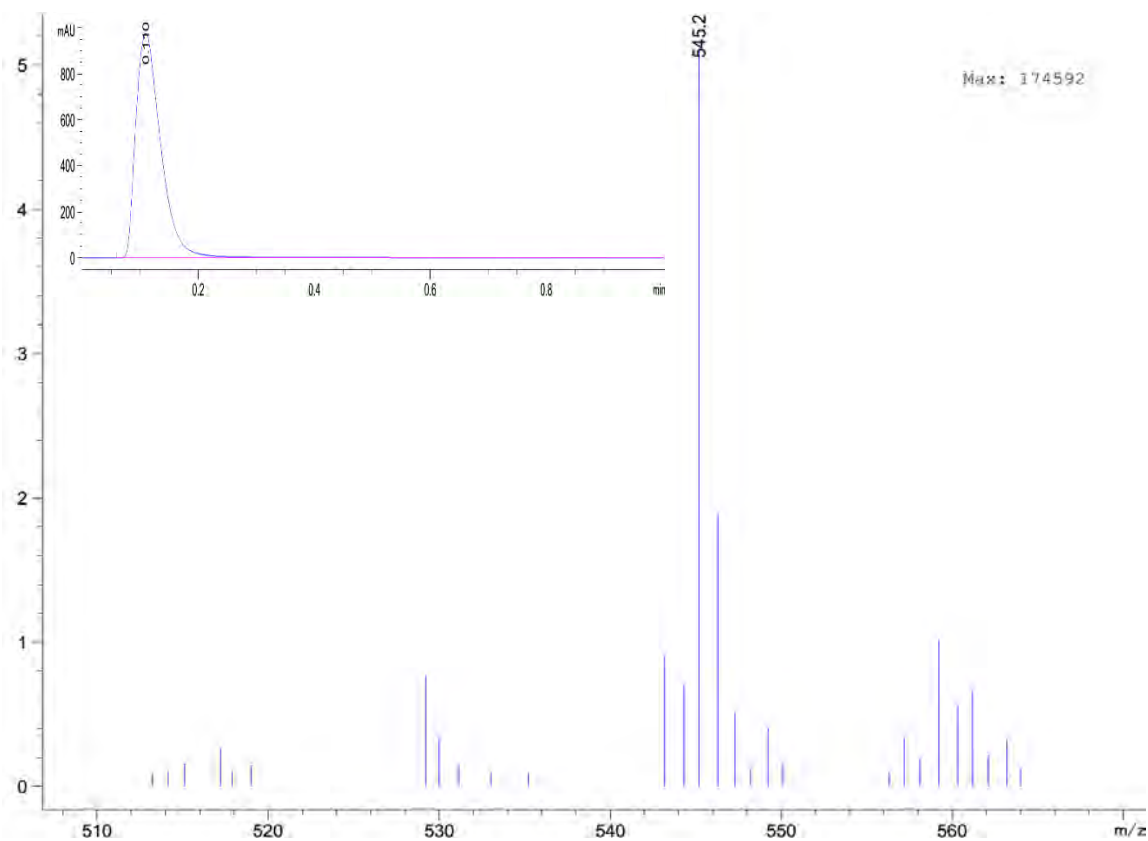
Anal. Calcd for $\text{C}_{33}\text{H}_{36}\text{N}_8$: C, 72.77; H, 6.66; N, 20.57. Found: C, 72.56; H, 6.85; N, 20.18.



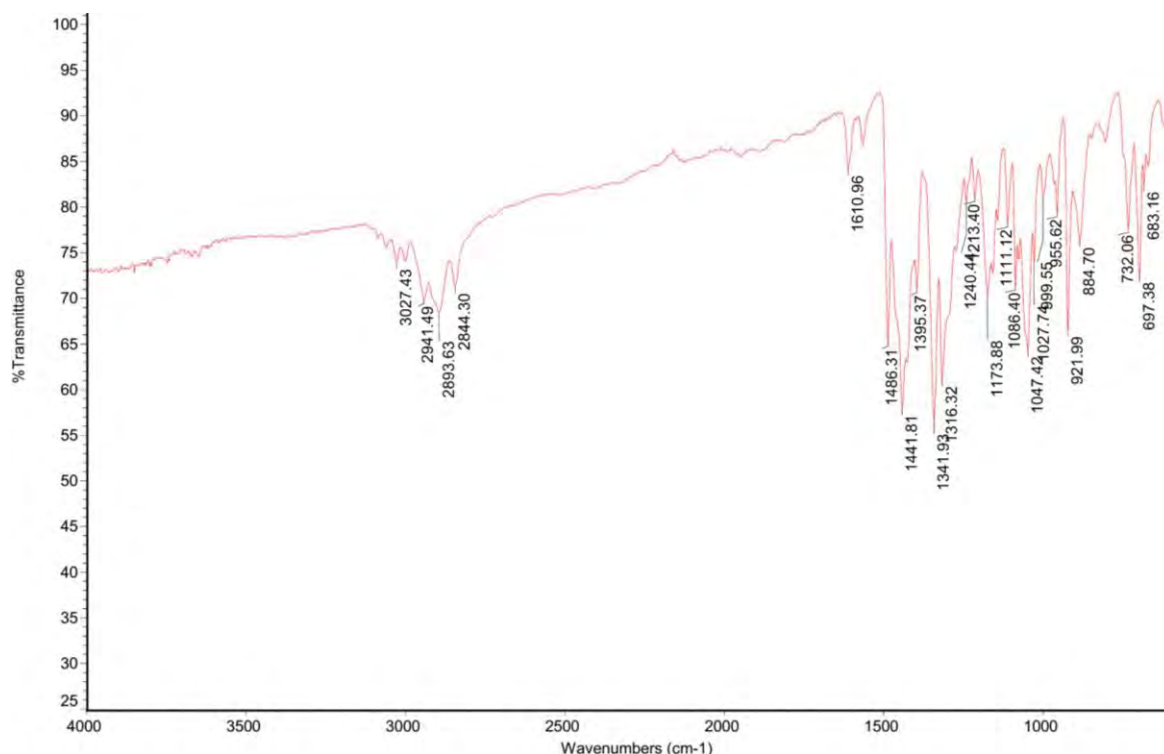
Compound 1, ^1H NMR (400 MHz, CDCl_3)



Compound 1, ^{13}C NMR (100 MHz, CDCl_3)



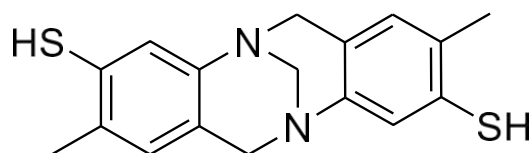
Compound 1, MS (ESI+)



Compound 1, IR transmittance (neat)

2. Preparation and Purification of Compound (2)

2,8-dimethyl-6H,12H-5,11-methanodibenzo[b,f][1,5]diazocine-3,9-dithiol



The bis-triazene compound **1** (0.54 g, 1.0 mmol, 1.0 eq.) was poured into a 50ml round-bottom flask containing DCM (20 mL). A solution of trichloroacetic acid (5.0 g, 30 mmol, excess, in DCM 20 mL) was added and stirred for 2 min. Afterward, Na₂S (0.70 g, 9 mmol, excess) was slowly added to the reaction flask, as shown in the following figure, and remained sealed when stirred for 2 hours at rt. The volume of the resulting yellowish suspension was then reduced to half by nitrogen gas flow and then refluxed for 30 min. The reaction mixture cooled down to rt and diluted with DCM (100 mL), and filtered. The DCM layer was rinsed with cold water (5 X 100 mL), dried over Mg₂SO₄ and filtered. The DCM was removed and the residue was purified by column chromatography to obtain a pale-lemon substance with a mild rotten-egg odour which was then stored under argon in darkness.

Yield: 0.06 g (0.19 mmol, 19 %); R_f = 0.2 (silica gel; MeOH–DCM, 4% v/v).

IR (neat): 2896, 2847, 2560, 1608, 1492, 1474, 1205, 1091, 1010, 811 cm^{-1} .

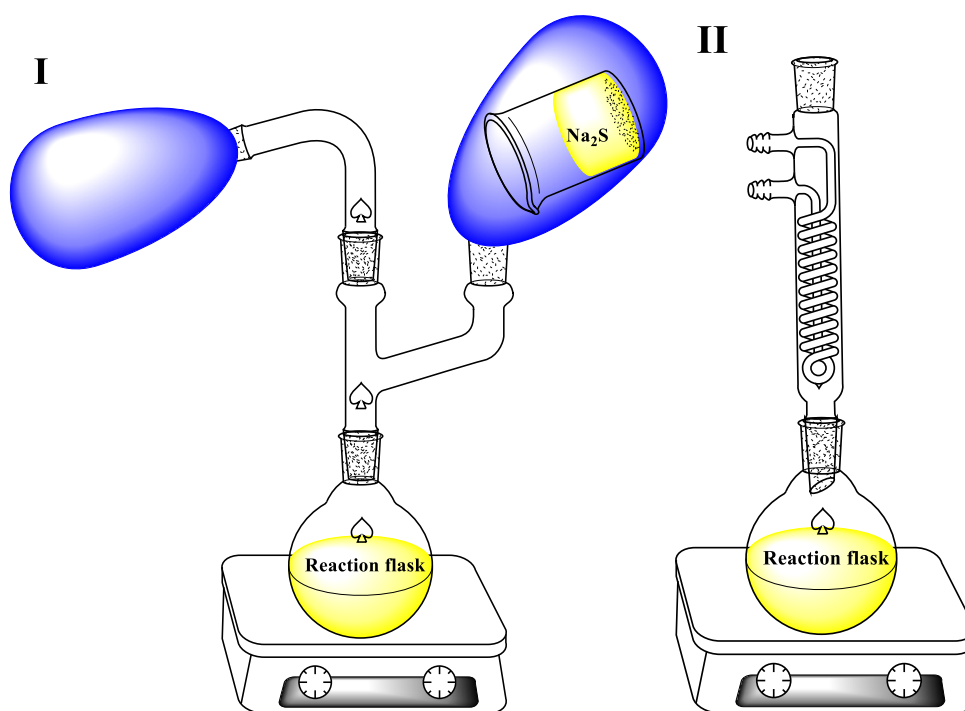
^1H NMR (400 MHz, CDCl_3): δ = 7.62 (br, 2 H, SH), 6.65 (s, 2 H, CH), 6.17 (s, 2 H, CH), 4.56–4.60 (d, J = 16.7 Hz, 2 H), 4.28 (s, 2 H, NCH_2N), 4.17–4.13 (d, J = 16.8 Hz, 2 H), 2.10 (s, 6 H, 2 CH_3).

^{13}C NMR (100 MHz, CDCl_3): δ = 143.8, 134.5, 128.6, 127.4, 126.8, 124.7, 67.1, 58.4, 20.9.

MS (ESI +; *i*-PrOH–EtOAc– H_2O /0.5% HCO_2Na , 90:5:5): m/z $[\text{M} + \text{Na}]^+$ calcd for $[\text{C}_{17}\text{H}_{18}\text{N}_2\text{S}_2\text{Na}]^+$: 337.08; found: 337.0. MS (ESI –): m/z $[\text{M} - \text{H}]^-$ calcd for $[\text{C}_{17}\text{H}_{17}\text{N}_2\text{S}_2]^-$: 313.09; found: 313.1. MS (ESI +; ACN/ Δ): m/z $[\text{M} + 2\text{ACN} + \text{H}]^+$ calcd for $[\text{C}_{21}\text{H}_{25}\text{N}_4\text{S}_2]^+$: 397.14; found: 397.1.

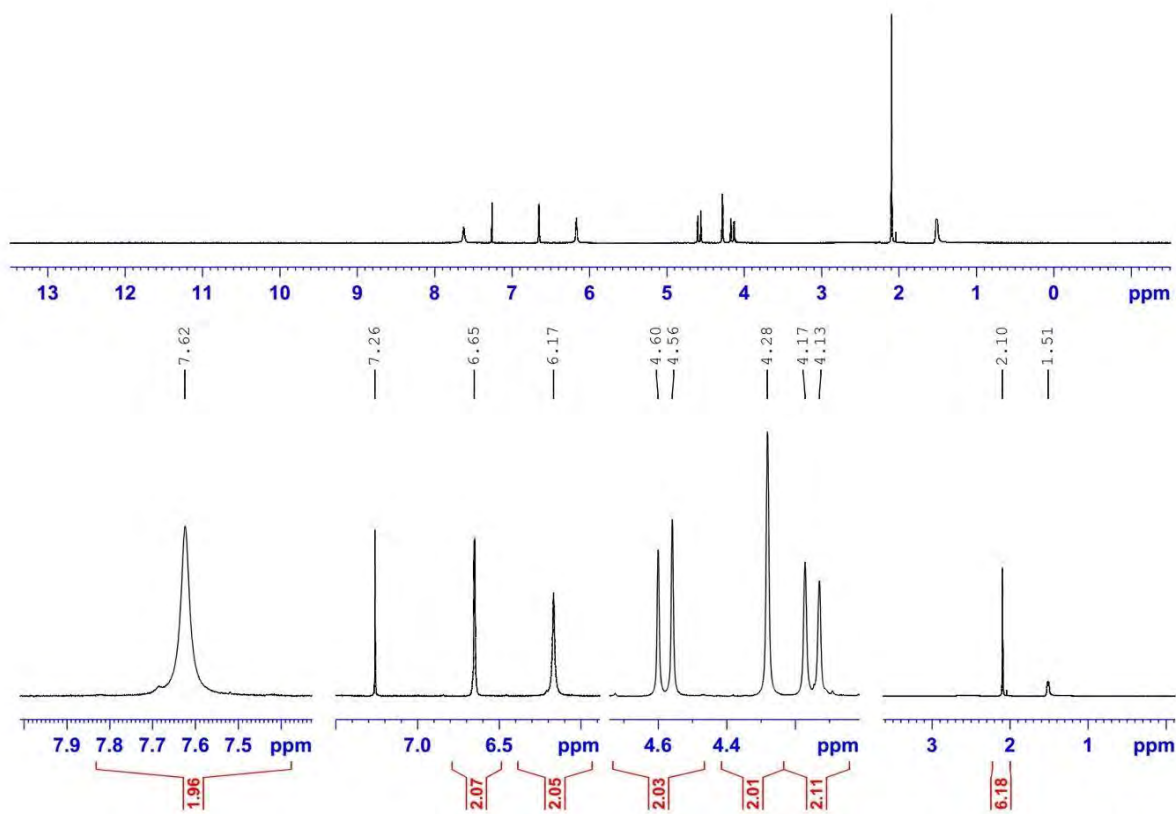
UV/Vis: (EtOAc): λ (lg ϵ) = 277 (3.583) nm.

Anal. Calcd for $\text{C}_{17}\text{H}_{18}\text{N}_2\text{S}_2$: C, 64.93; H, 5.77; N, 8.91; S, 20.39. Found: C, 65.08; H, 5.83; N, 9.22.

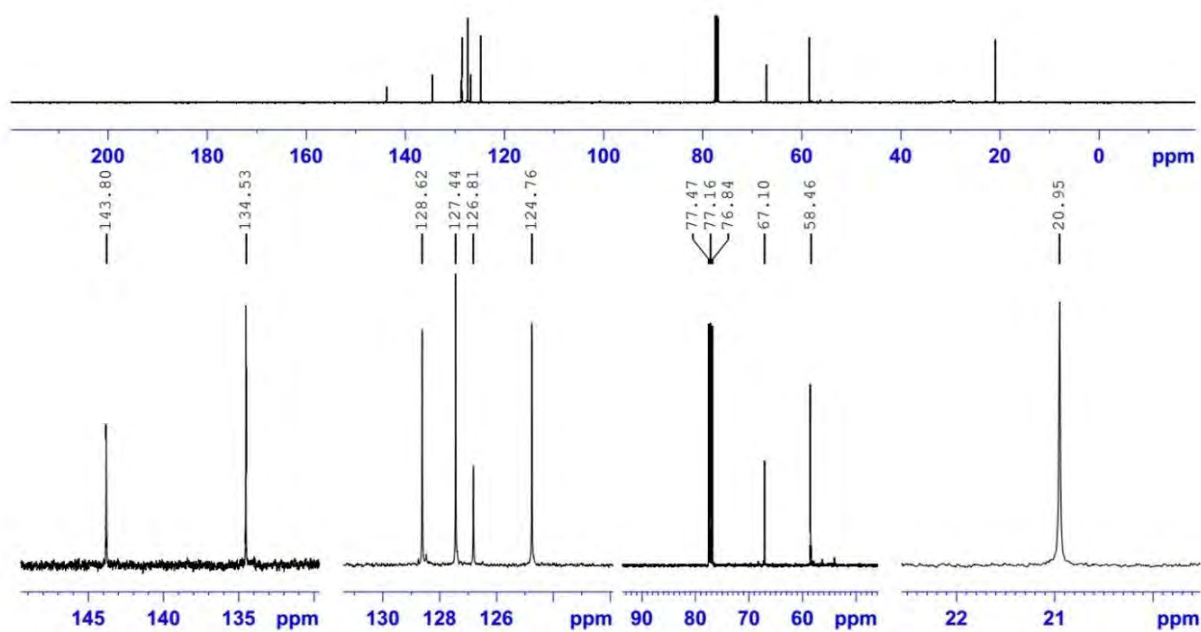


The apparatus used for compound 2 synthesis

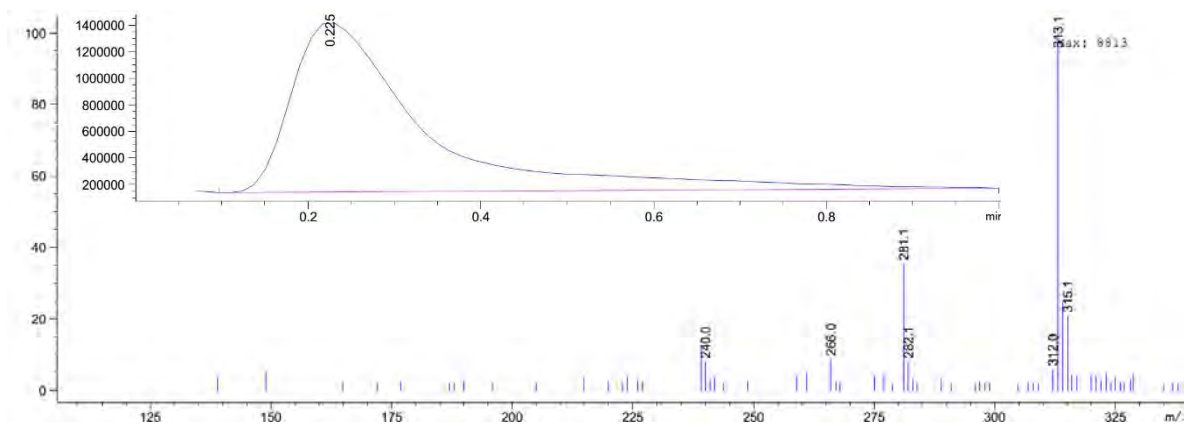
The balloons (shown in blue) prevent moisture/ Na_2S contact as well as O_2 /thiophenol contact, and stop H_2S escaping from the container and regulate $\text{H}_2\text{S}/\text{N}_2$ gases pressure



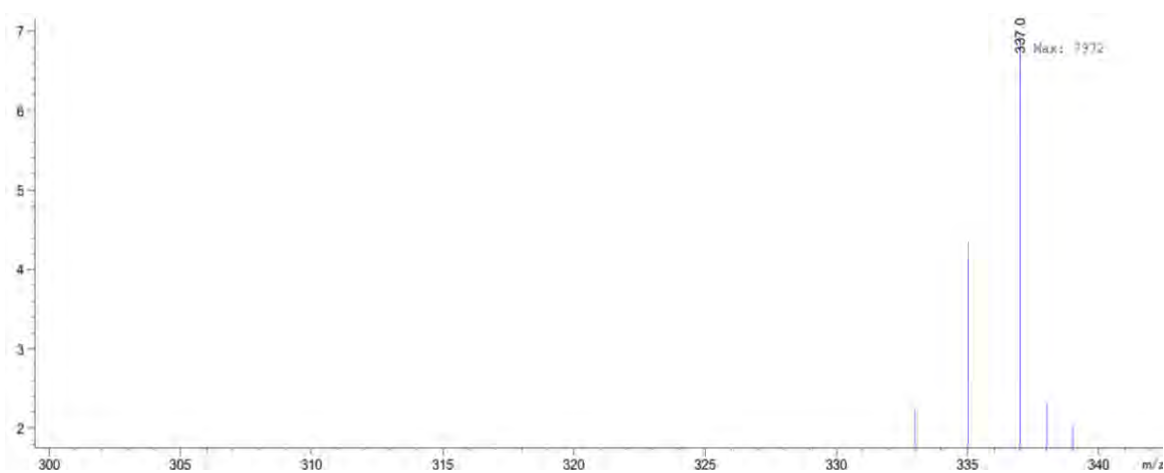
Compound 2, ¹H NMR (400 MHz, CDCl₃)



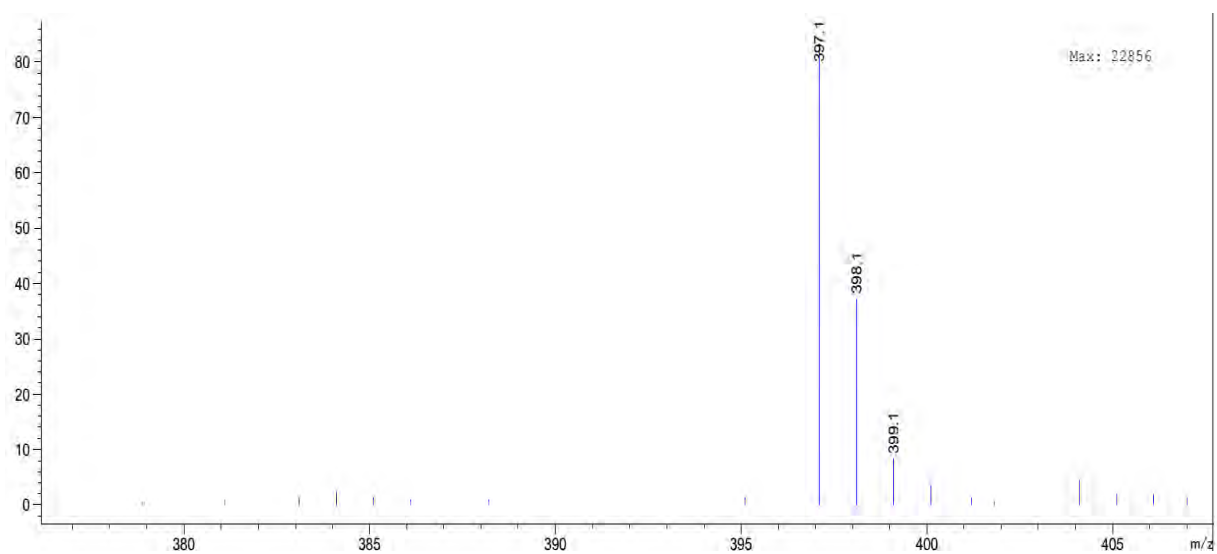
Compound 2, ¹³C NMR (100 MHz, CDCl₃)



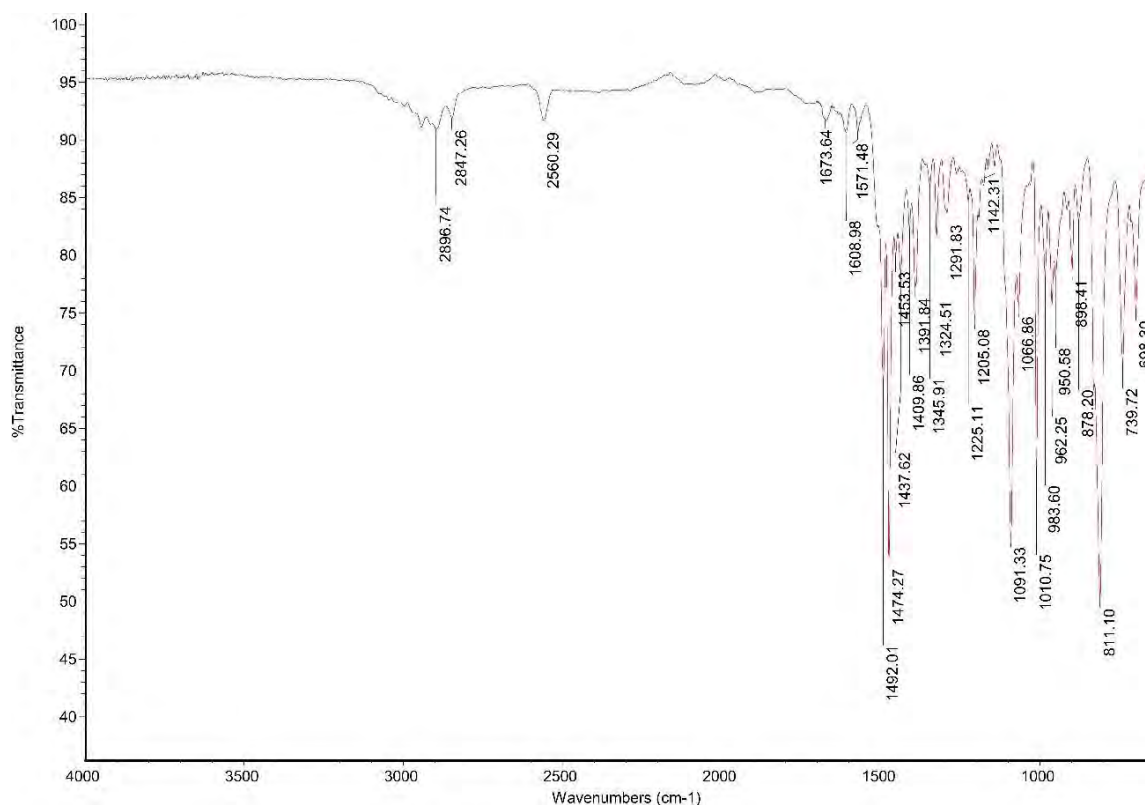
Compound 2, MS [M – H]



Compound 2, MS [M + Na]



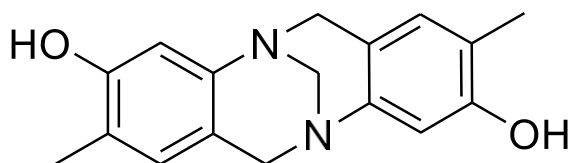
Compound 2, MS [M+ 2 ACN + H]



Compound 2, IR transmittance (neat)

3. Preparation and Purification of Compound (3)

2,8-dimethyl-6H,12H-5,11-methanodibenzo[b,f][1,5]diazocine-3,9-diol



Hünlich's base (0.56 g, 2.0 mmol, 1.0 eq.) was dissolved in H₂SO₄ (6.5%, 90 mL), then cooled down to -5°C . A sodium nitrite solution (0.30 g, 4.4 mmol, 2.2 eq.) in cold water (10 mL) was dropped into the reaction flask and stirred for 30 min. Afterward, the solution's temperature was gradually raised to boil, over two hours (Attention: this step releases nitrogen gas; hence, rapid heating and sealing the container may lead to explosion). The reaction mixture was cooled down to r.t., its pH was adjusted to 5 (by adding Na₂CO₃ saturated solution) and extracted with EtOAc (30 mL x 5), the organic layers were combined, dried over Na₂SO₄ and evaporated to dryness to obtain the product as a light-grey powder.

Yield: 0.54 g (1.9 mmol, 96%). R_f = 0.3 (silica gel; MeOH–DCM, 8% v/v).

IR (neat): 3649, 3549, 3012, 2948, 2904, 2857, 1620, 1508, 1368, 1081 and 910 cm^{-1} .

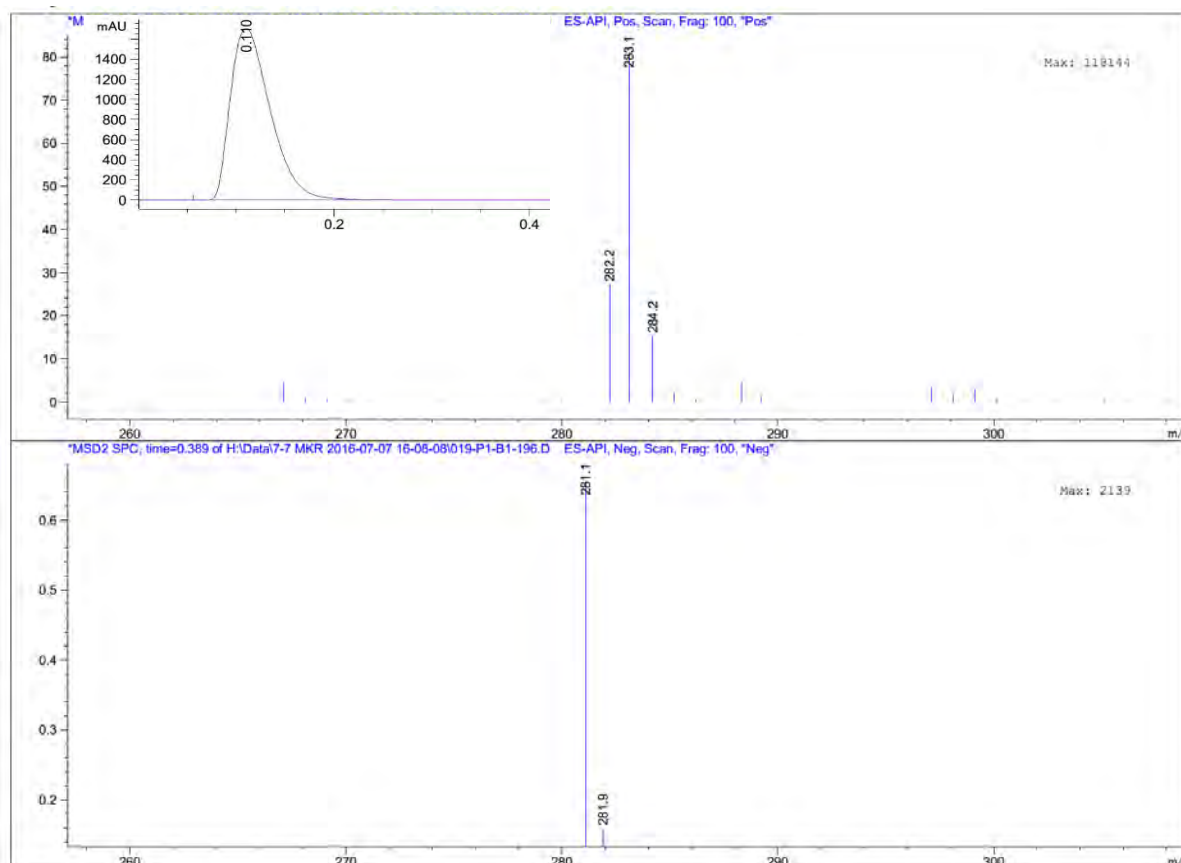
^1H NMR (400 MHz, DMSO- d_6): δ = 9.06 (s, 2H, OH), 6.56 (s, 2H, CH), 6.45 (s, 2H, CH), 4.39–4.43 (d, J = 16.4 Hz, 2H, CH_2), 4.07 (s, 2H, NCH_2N), 3.81–3.85 (d, J = 16.4 Hz, 2H, CH_2), 1.97 (s, 6H, CH_3).

^{13}C -NMR (100 MHz, DMSO- d_6): δ = 154.1, 146.5, 128.2, 119.9, 117.9, 110.0, 66.5, 57.8, 15.5.

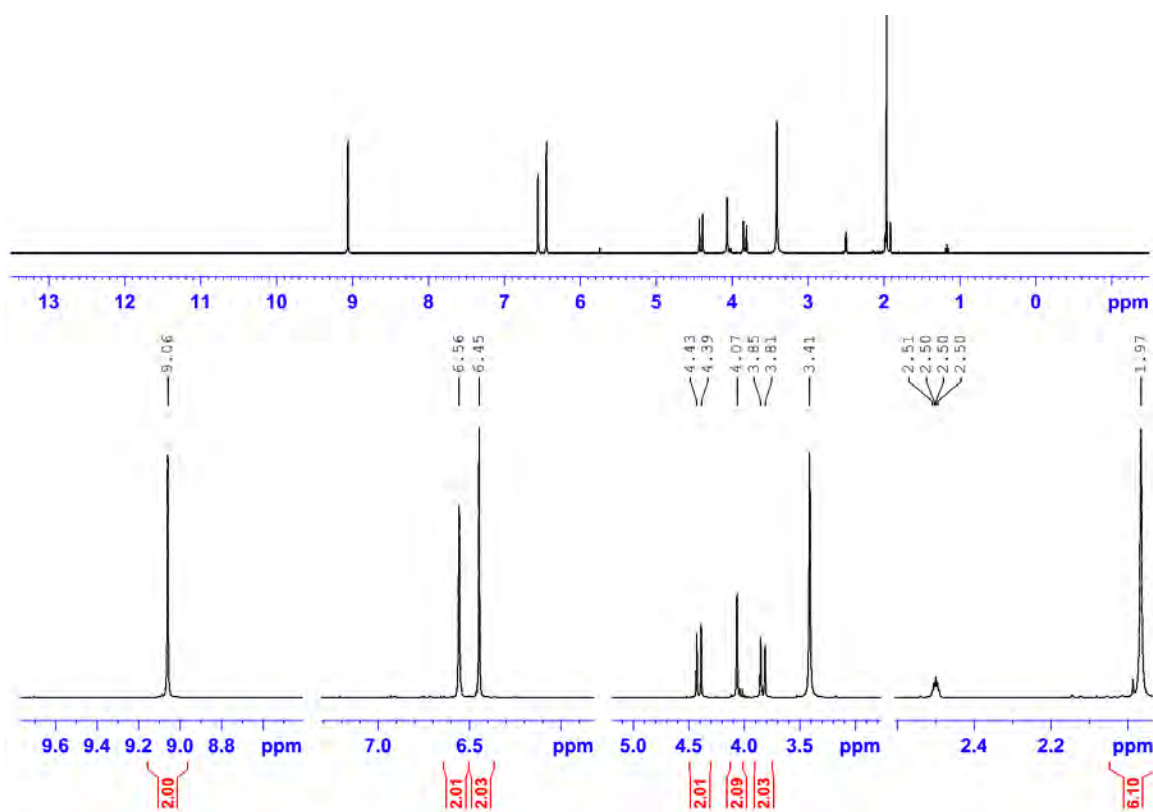
MS (ESI +; EtOH–EtOAc– H_2O , 90:5:5): m/z $[\text{M} + \text{H}]^+$ calcd for $[\text{C}_{17}\text{H}_{19}\text{N}_2\text{O}_2]^+$: 283.14; found 283.1. MS (ESI –): m/z $[\text{M} - \text{H}]^-$ calcd for $[\text{C}_{17}\text{H}_{17}\text{N}_2\text{O}_2]^-$: 281.14; found 281.1.

UV/Vis: (EtOAc): λ (lg ϵ) = 292 (3.643) nm.

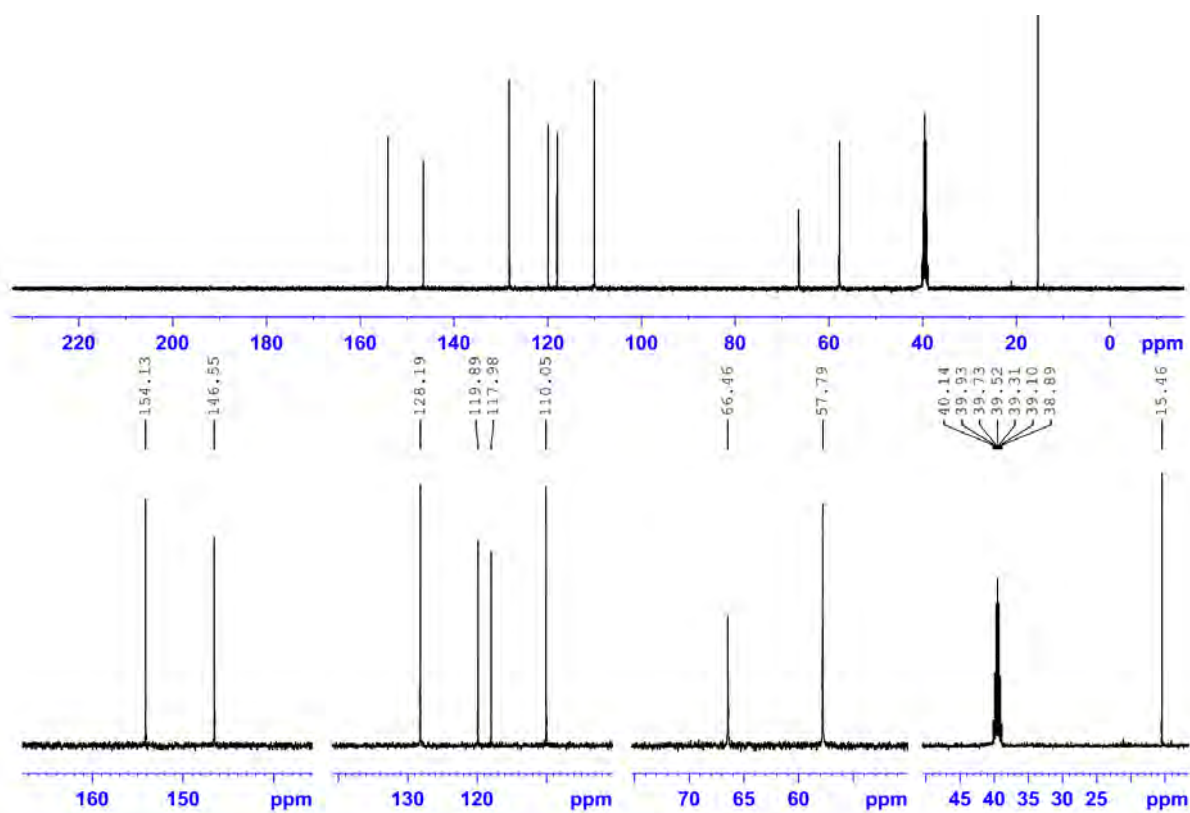
Anal. calcd for $\text{C}_{17}\text{H}_{18}\text{N}_2\text{O}_2$: C, 72.32; H, 6.43; N, 9.92; O, 11.33. Found: C, 72.21; H, 6.61; N, 9.74.



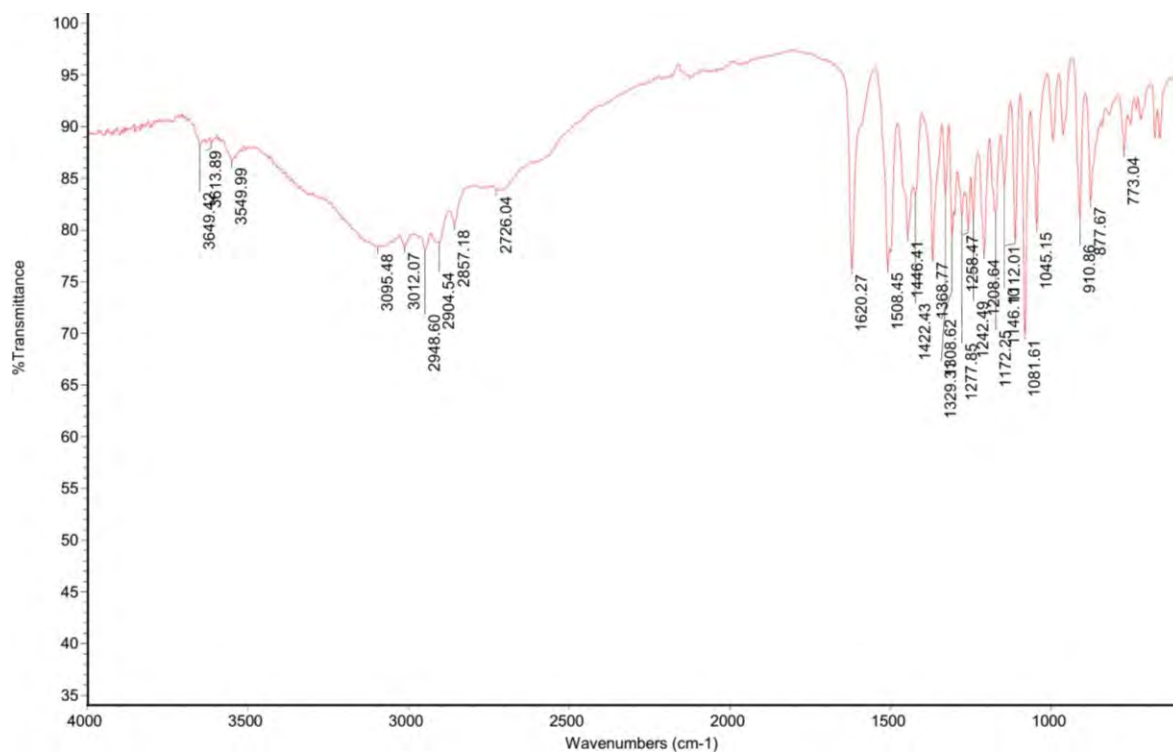
Compound 3, MS (ESI + and ESI –)



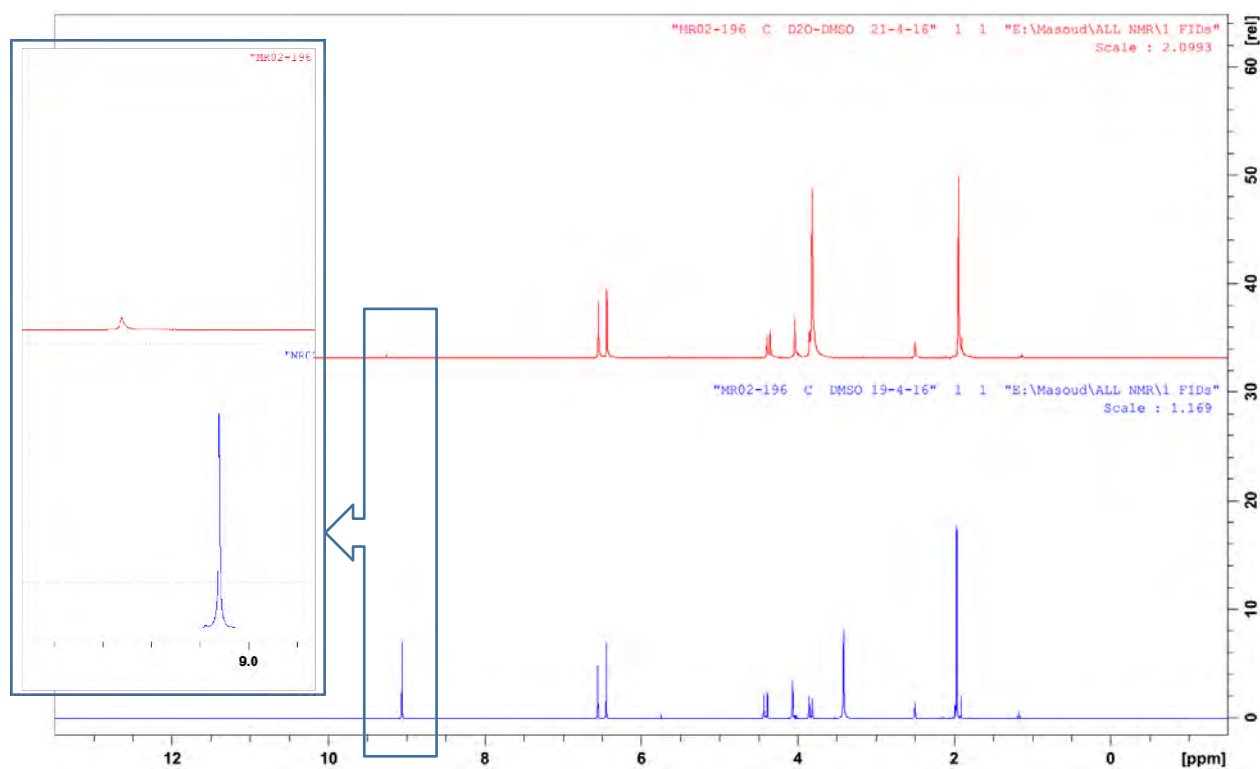
Compound 3, ^1H NMR (400 MHz, $\text{DMSO-}d_6$)



Compound 3, ^{13}C NMR (100 MHz, $\text{DMSO-}d_6$)



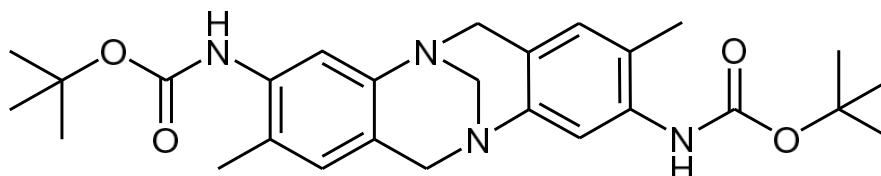
Compound 3, IR transmittance (neat)



Compound 3, ^1H NMR 400 MHz, $\text{DMSO}-d_6$ (in blue) and $\text{D}_2\text{O}/\text{DMSO}-d_6$ (in red)

4. Preparation and Purification of Compound (4)

di-tert-butyl (2,8-dimethyl-6H,12H-5,11-methanodibenzo[b,f][1,5]diazocine-3,9-diyl) dicarbamate



Hünlich's base (0.28 g, 1 mmol, 1eq.) and di-tert-butyl dicarbonate (0.458 g, 2.1 mmol, 1.05eq.) were dissolved in MeOH (7 mL) then a catalytic amount of iodine (0.025 g, 0.1 mmol, 0.1eq.) was added to the solution and stirred at room temperature in darkness for 6 hours (Attention: This step releases CO₂ gas and the container should not be tightly sealed). Finally, the suspension was filtered by paper and its filtrate was neutralized by sodium thiosulfate before discarding. The obtained white precipitate was washed with few drops of cold MeOH and then desiccated under high-vacuum to obtain neat **4**.

The catalytic role of iodine is proven within the literature.¹

Yield: 0.44 g (0.92 mmol, 92%); *R*_f: 0.5 (silica gel; EtOAc–DCM= 40% v/v).

IR: (neat): 3232, 2976, 1645, 1515, 1248, 1069 and 593 cm⁻¹.

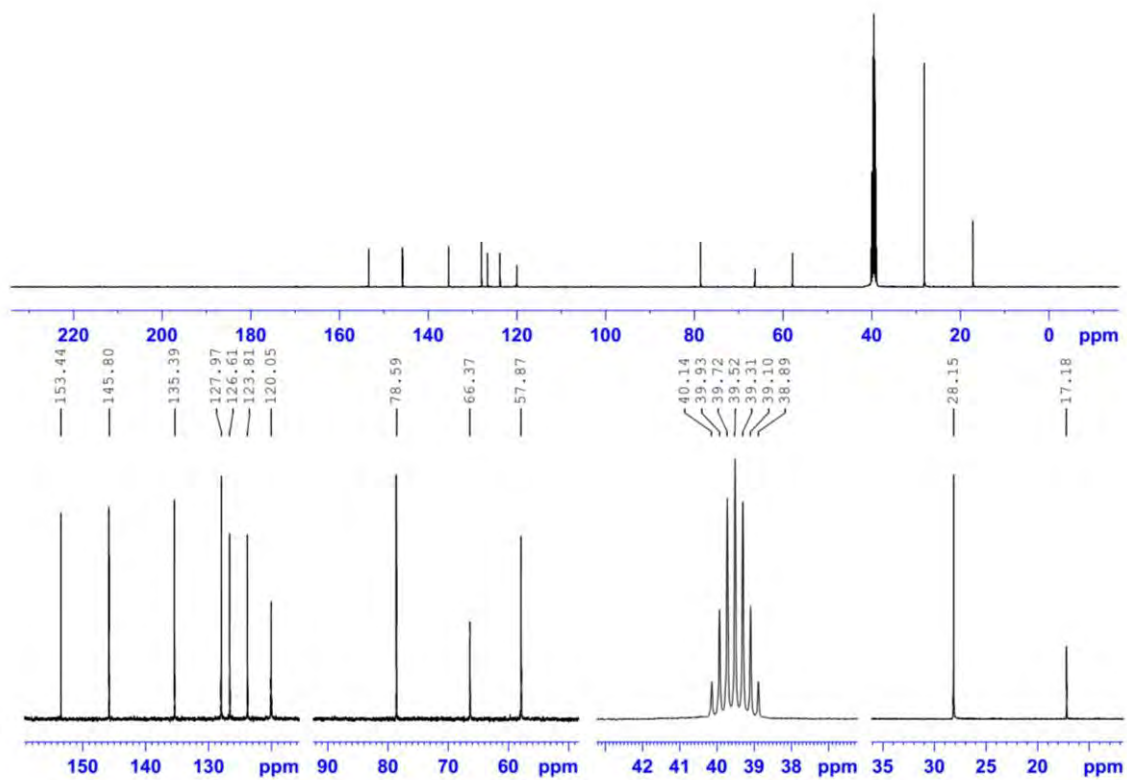
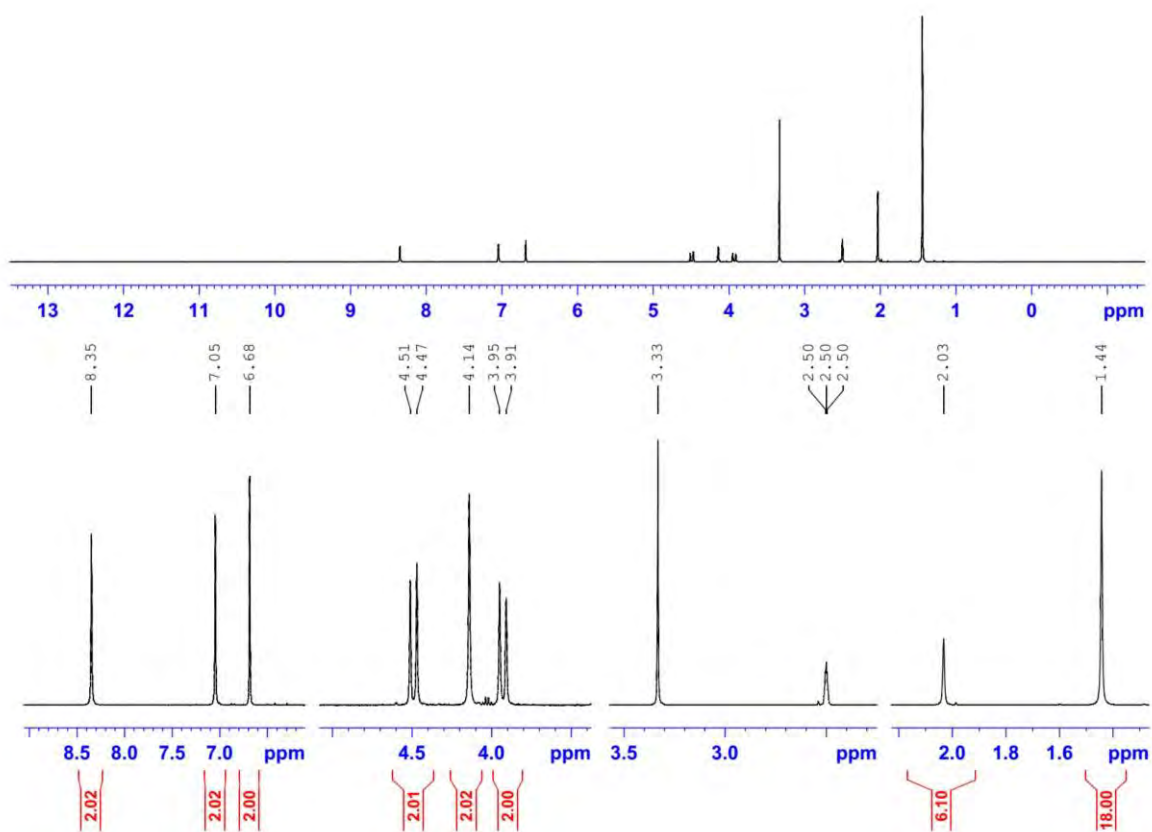
¹H NMR (400 MHz, DMSO-*d*₆): δ = 8.35 (s, 2H, NH), 7.05 (s, 2H, CH), 6.68 (s, 2H, CH), 4.47–4.51 (d, *J* = 16.6 Hz, 2H, CH₂), 4.14 (s, 2H, NCH₂N), 3.91–3.95 (d, *J* = 16.8 Hz, 2H, CH₂), 2.03 (s, 6H, CH₃), 1.44 (s, 18H, CH₃).

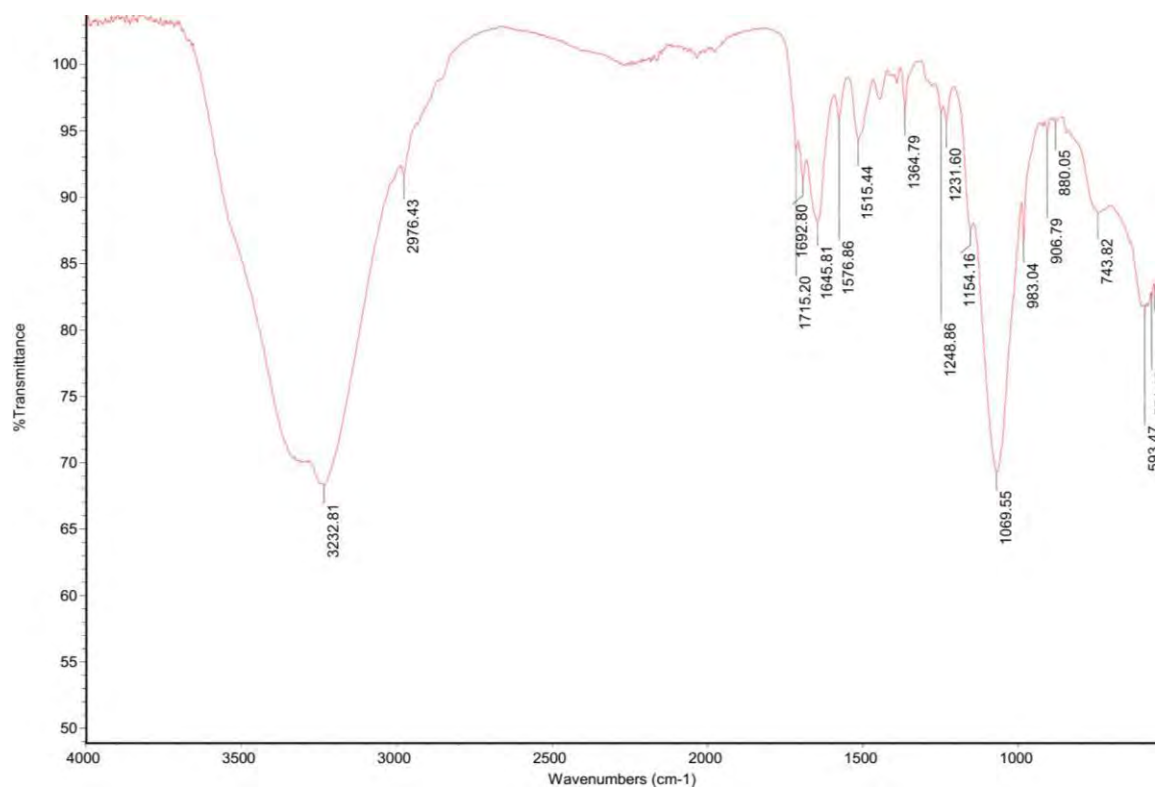
¹³C NMR (100 MHz, DMSO-*d*₆): δ = 153.4, 145.8, 135.4, 127.9, 126.6, 123.8, 120.0, 78.6, 66.4, 57.9, 28.1, 17.2.

MS (ESI +; EtOH): *m/z* [M + H]⁺ calcd for [C₂₇H₃₇N₄O₄]⁺: 481.27; found 481.3.

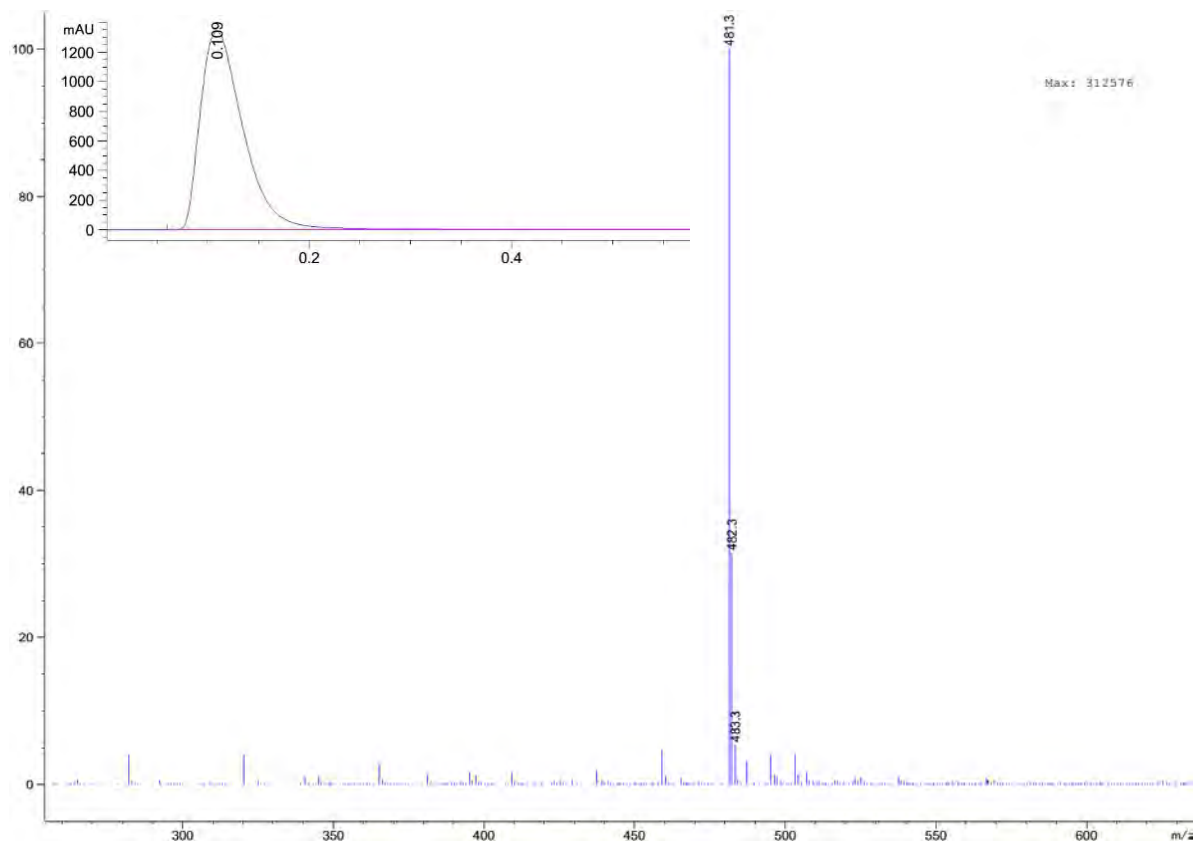
UV/Vis: (EtOAc): λ (lg ε) = 296 (3.647) nm.

Anal. calcd for C₂₇H₃₆N₄O₄: C, 67.48; H, 7.55; N, 11.66; O, 13.32. Found: C, 67.57; H, 7.60; N, 11.84.





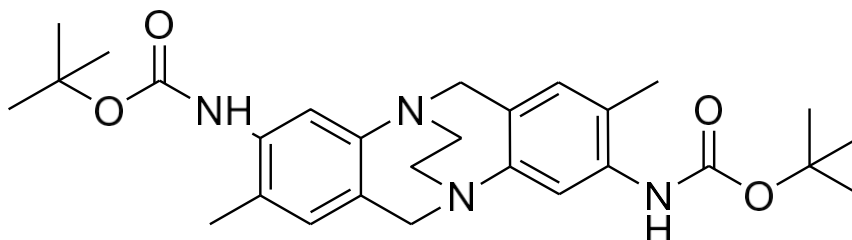
Compound 4, IR transmittance (neat)



Compound 4, MS (ESI +)

5. Preparation and Purification of Compound (5)

di-tert-butyl (2,8-dimethyl-6H,12H-5,11-ethanodibenzo[b,f][1,5]diazocine-3,9-diyl)dicarbamate



Compound **4** (0.24 g, 0.5 mmol, 1.0 eq.), 1,2-dibromoethane (0.47 g, 2.5 mmol, excess) and Li_2CO_3 (0.37 g, 5.0 mmol, excess) were mixed in DMF (1.5 mL) and heated at 105°C for 12 hours under argon atmosphere in darkness. Afterwards, the reaction mixture was added to 100ml of cold water containing 8 g of NaCl; then the obtained suspension was filtered by sintered funnel and vacuum pump. The collected light-brown precipitate was rinsed with few more drops of cold water and purified by column chromatography to obtain an extra-pure white product. (The reaction rescaled tenfold, gave 80% yield)

Yield: 0.19 g (0.39 mmol, 77%); R_f : 0.3 (silica gel; EtOAc–DCM= 30% v/v).

IR (neat): 3242, 2976, 1692, 1648, 1515, 1364, 1232, 1154, 1069 and 601 cm^{-1} .

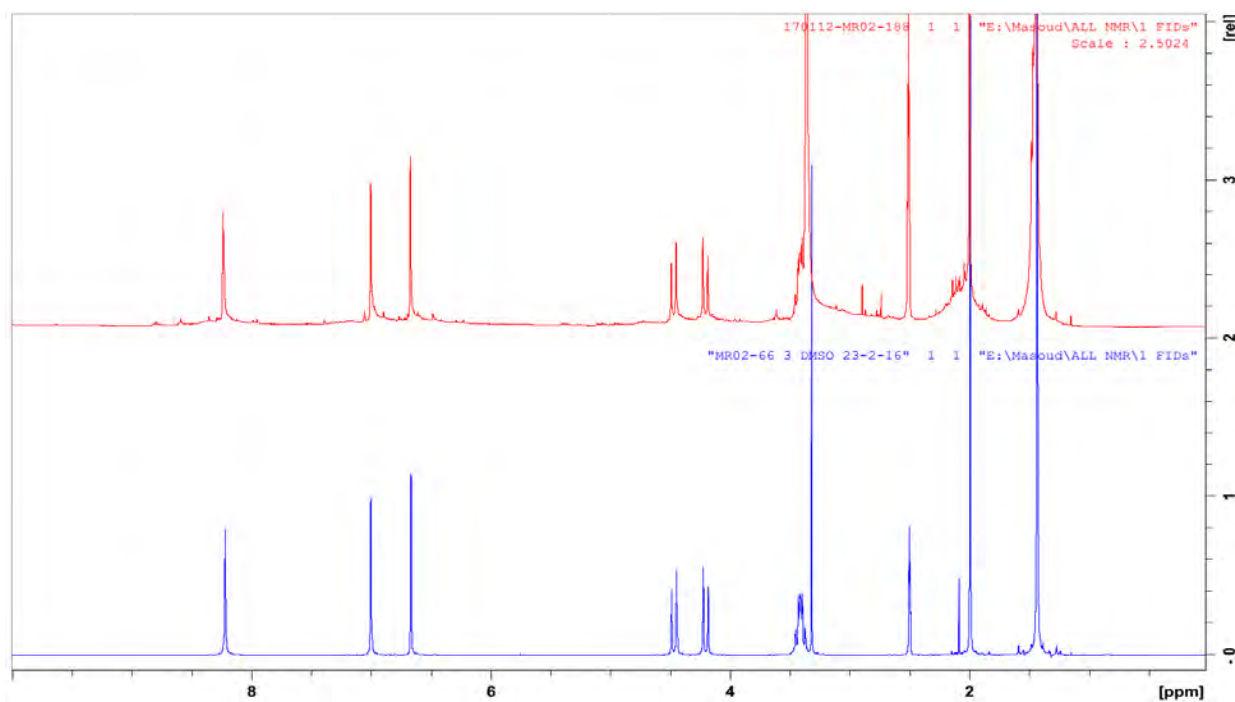
^1H NMR (400 MHz, $\text{DMSO}-d_6$): δ = 8.22 (s, 2H, NH), 7.00 (s, 2H, CH), 6.67 (s, 2H, CH), 4.45–4.49 (d, J = 17.2 Hz, CH_2), 4.18–4.22 (d, J = 17.2 Hz, CH_2), 3.36–3.47 (m, 4H, CH_2), 1.99 (s, 6H, CH_3), 1.43 (s, 18H, CH_3).

^{13}C NMR (100 MHz, $\text{DMSO}-d_6$): δ = 153.4, 148.2, 135.0, 132.9, 129.8, 127.2, 123.3, 78.5, 57.9, 54.3, 28.1, 17.1.

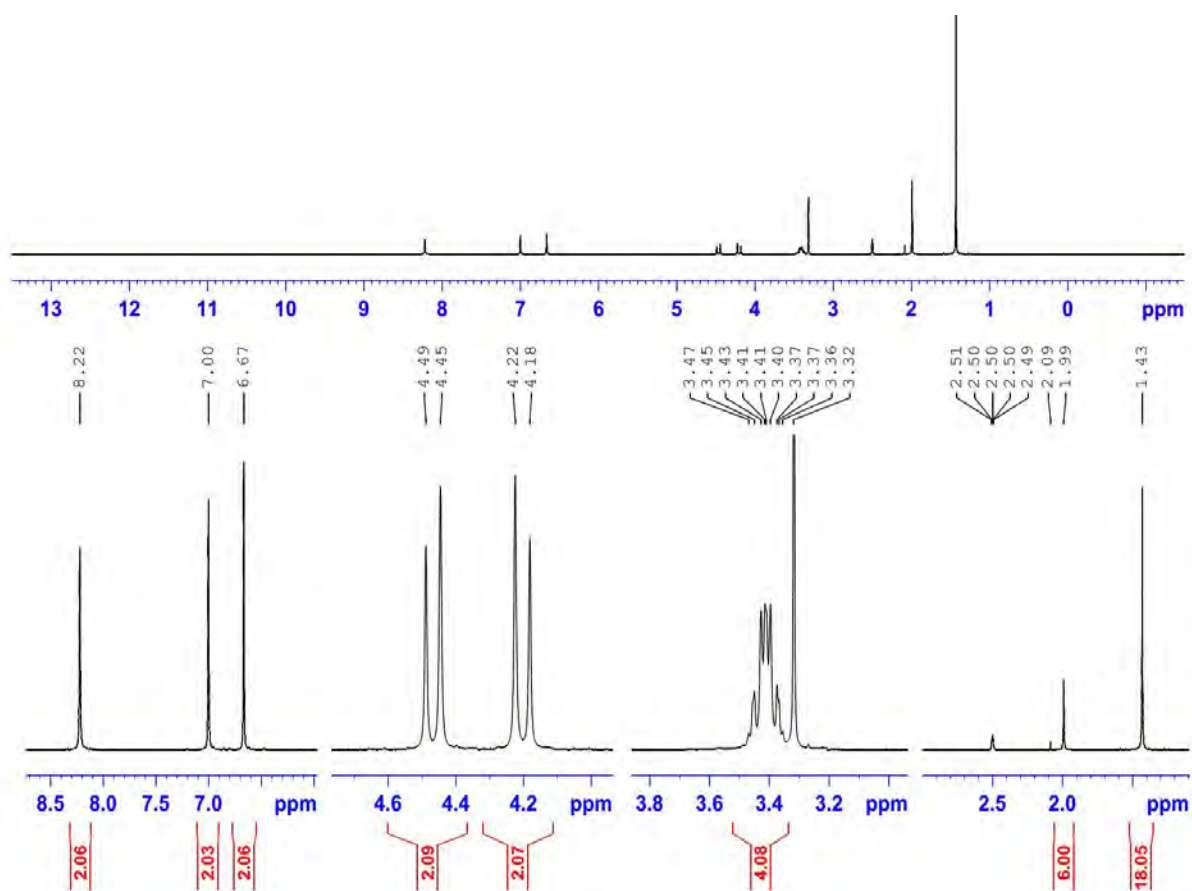
MS (ESI +; EtOH): m/z $[\text{M} + \text{H}]^+$ calcd for $[\text{C}_{28}\text{H}_{39}\text{N}_4\text{O}_4]^+$: 495.29; found 495.3.

UV/Vis: (EtOAc): λ (lg ϵ) = 295 (3.597) nm.

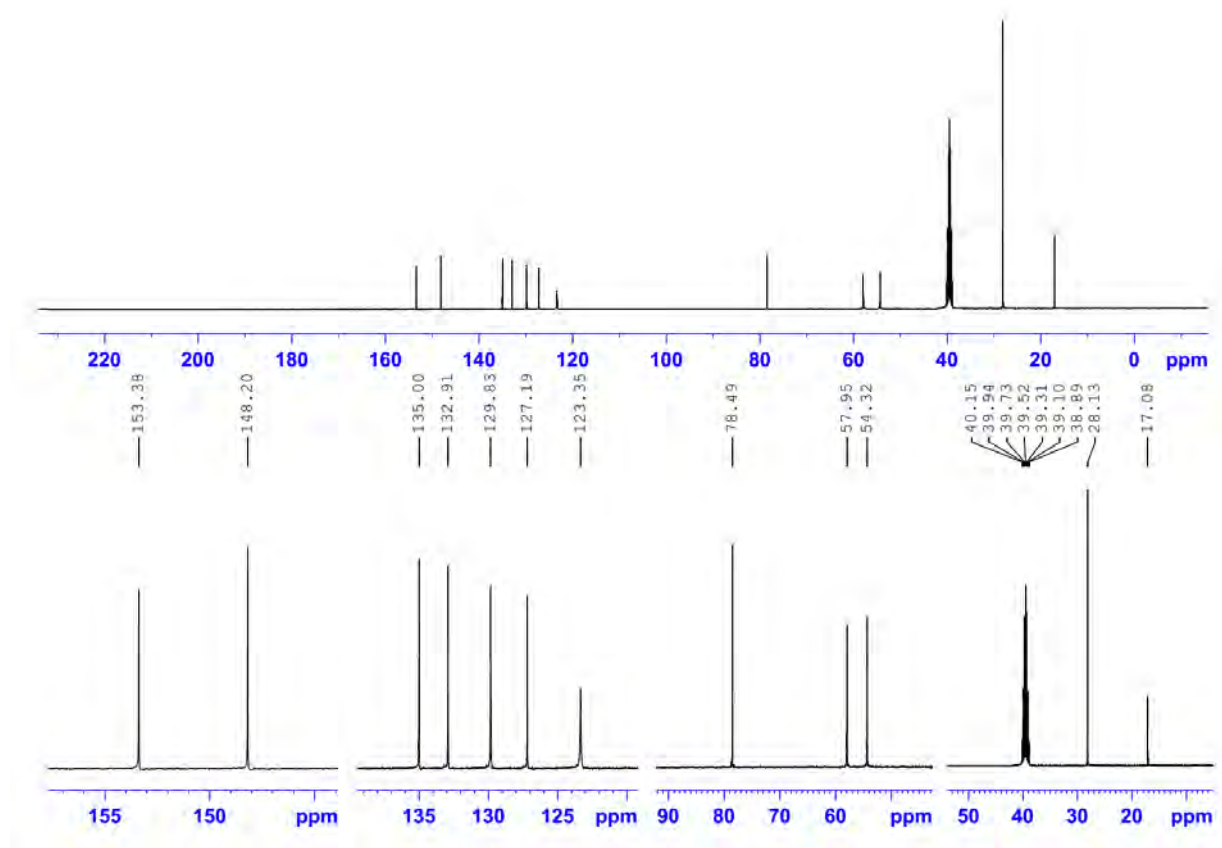
Anal. Calcd for $\text{C}_{28}\text{H}_{38}\text{N}_4\text{O}_4$: C, 67.99; H, 7.74; N, 11.33; O, 12.94. Found: C, 67.86; H, 7.53; N, 11.21.



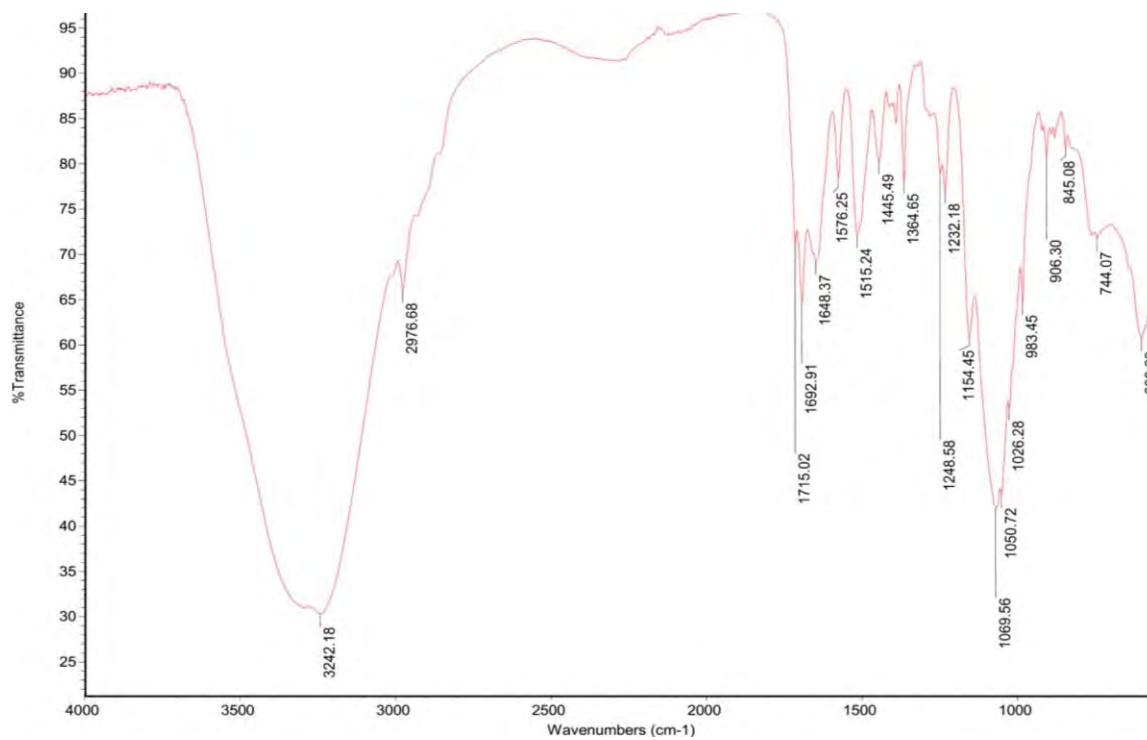
Compound 5 crude (top) and pure (bottom), ¹H NMR (400 MHz, DMSO-*d*₆)



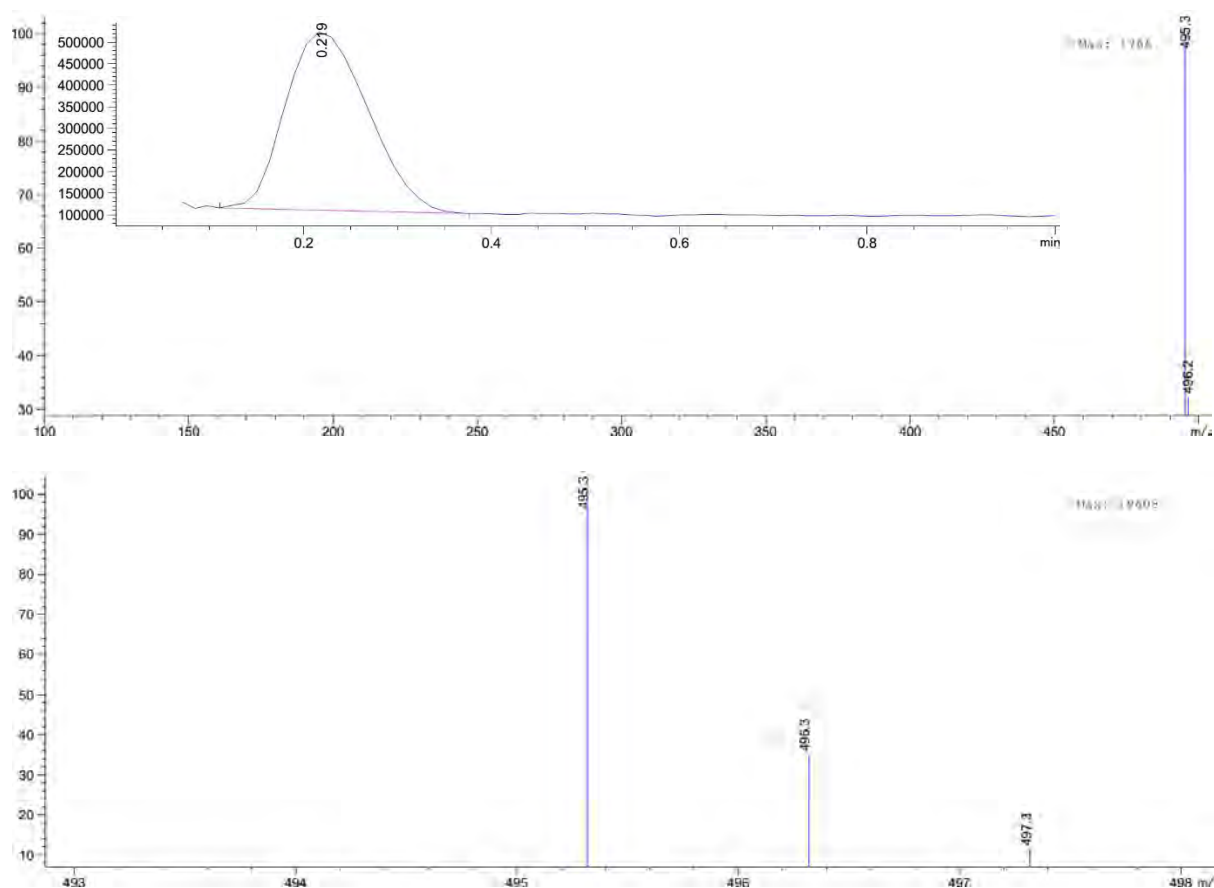
Compound 5, ¹H NMR (400 MHz, DMSO-*d*₆)



Compound 5, ¹³C NMR (100 MHz, DMSO-*d*₆)



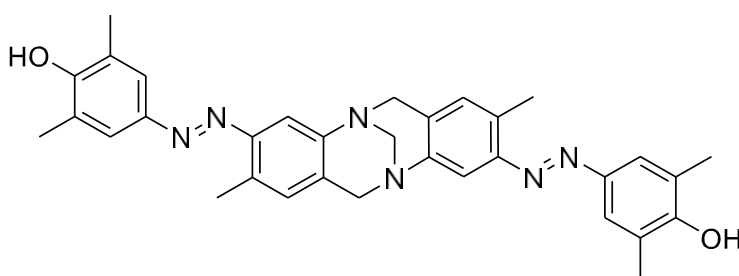
Compound 5, IR (neat)



Compound 5, MS (ESI +)

6. Preparation and Purification of Compound (6)

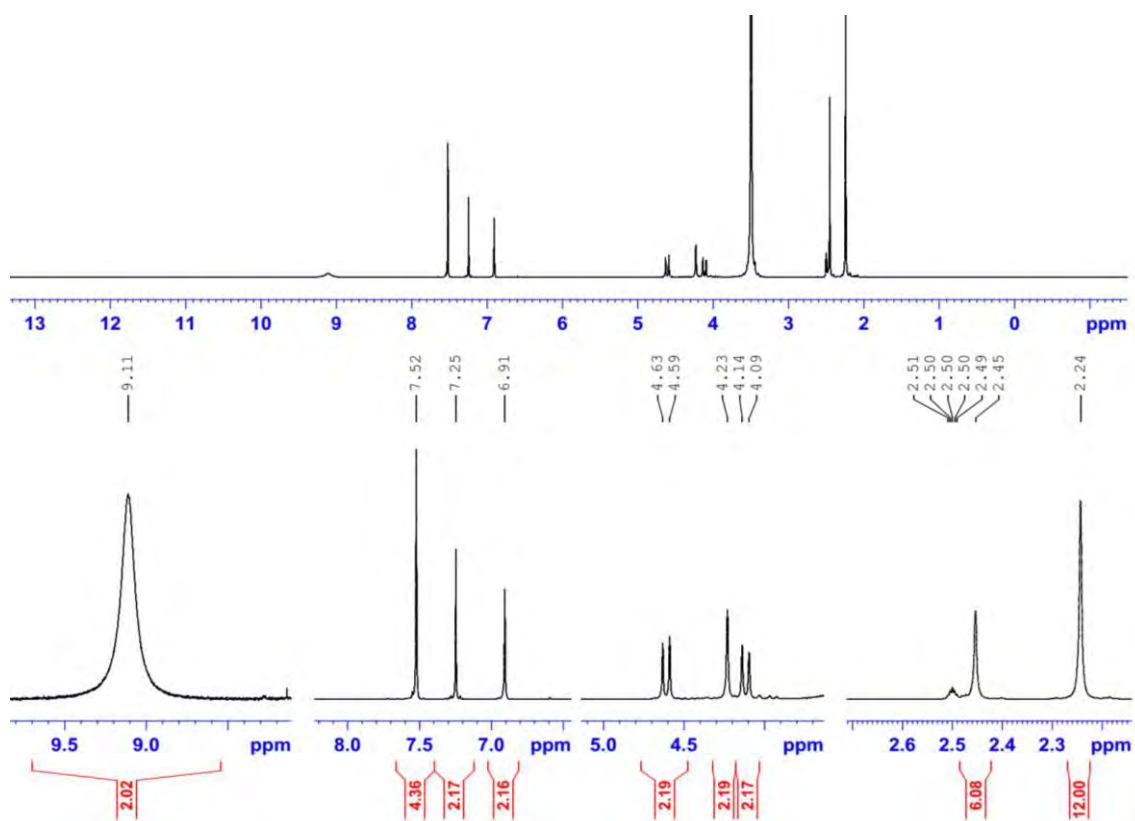
4,4'-((1E,1'E)-(2,8-dimethyl-6H,12H-5,11-methanodibenzo[b,f][1,5]diazocine-3,9-diyl) bis (diazene-2,1-diyl)) bis (2,6-dimethylphenol)



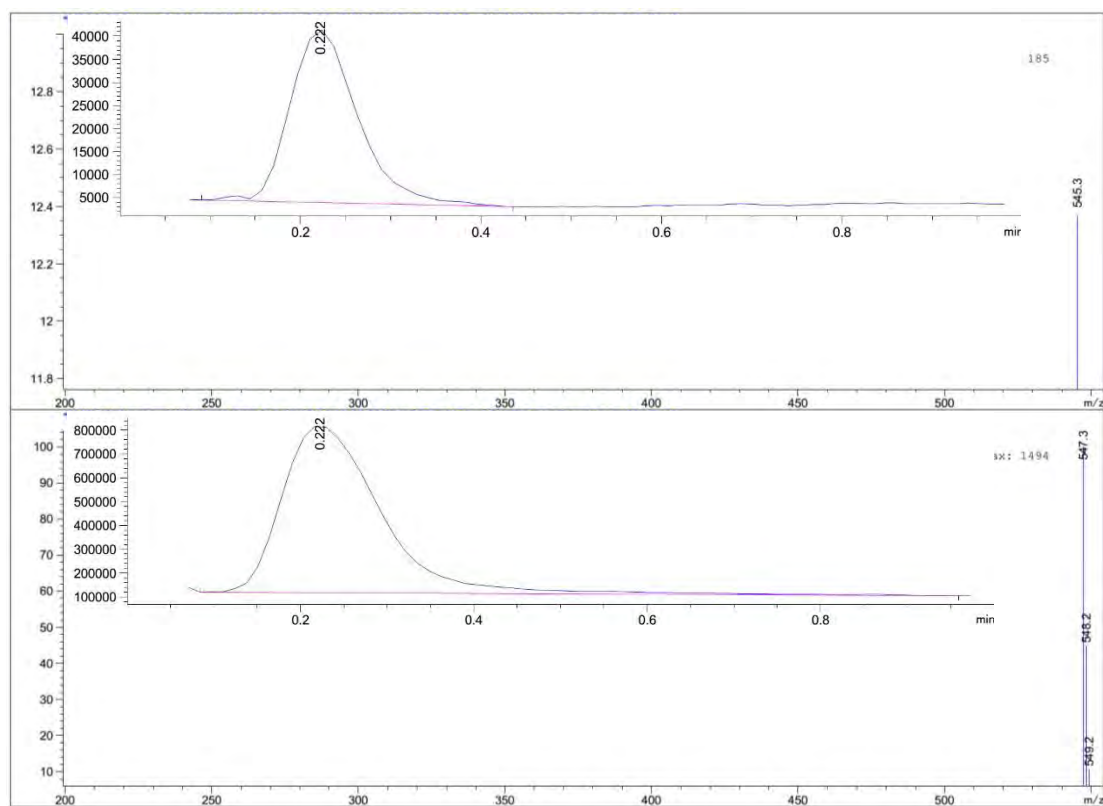
Prepared according to the literature.²

¹H-NMR (400 MHz, DMSO-*d*₆) δ [ppm]: 9.11 (br, 2H, OH) , 7.52 (s, 4H, CH), 7.25 (s, 2H, CH), 6.91 (s, 2H, CH), 4.59–4.63 (d, *J* = 17.2 Hz, 2H, CH₂), 4.23 (s, 2H, NCH₂N), 4.09–4.14 (d, *J* = 17.3 Hz, 2H, CH₂) , 2.45 (s, 6H, CH₃), 2.24 (s, 12H, CH₃).

MS (ESI +; EtOAc): *m/z* [M+H]⁺ calcd for [C₃₃H₃₅N₆O₂]⁺: 547.27; found: 547.3. MS (ESI –): *m/z* [M – H][–]calcd for [C₃₃H₃₃N₆O₂][–]: 545.27; found: 545.3.



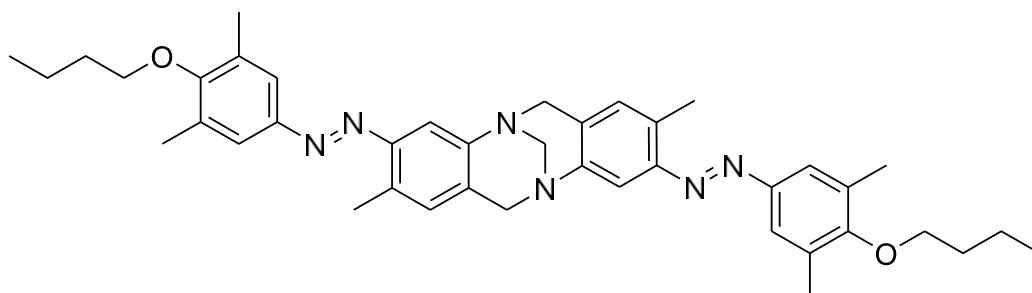
Compound 6, ¹H NMR (400 MHz, DMSO-*d*₆)



Compound 6, MS (ESI + and ESI -)

7. Preparation and Purification of Compound (7)

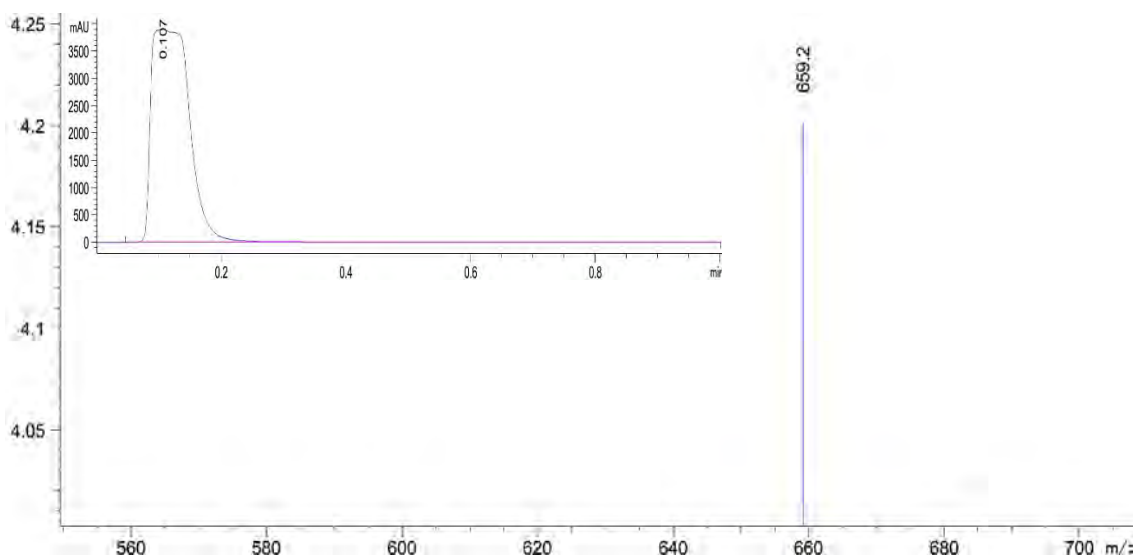
3,9-bis((E)-(4-butoxy-3,5-dimethylphenyl)diazenyl)-2,8-dimethyl-6H,12H-5,11-methanodibenzo [b,f][1,5]diazocine



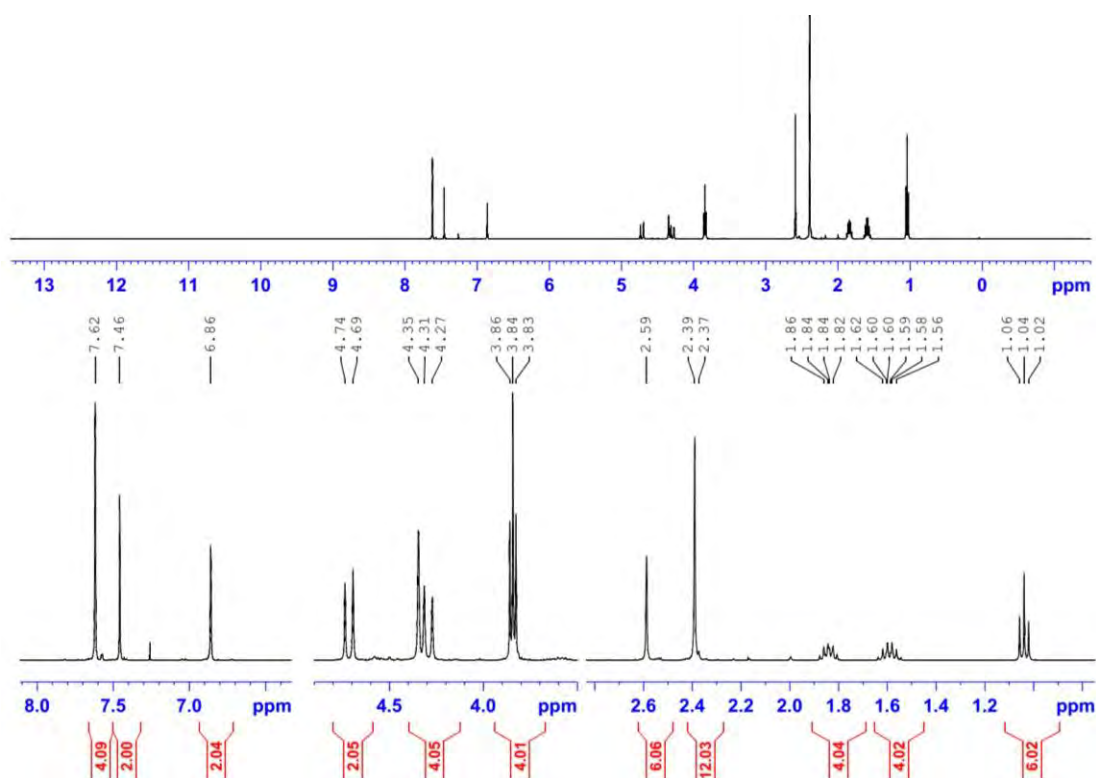
Prepared according to the literature. ²

¹H NMR (400 MHz, CDCl₃): δ = 7.62 (s, 4 H, CH), 7.46 (s, 2 H, CH), 6.86 (s, 2 H, CH), 4.69–4.74 (d, J = 17.1 Hz, 2 H, CH₂), 4.35 (s, 2 H, NCH₂N), 4.27–4.31 (d, J = 17.2 Hz, 2 H, CH₂), 3.83–3.86 (t, J = 8.1 Hz, 4 H, CH₂), 2.59 (s, 6 H, CH₃), 2.39 (s, 12 H, CH₃), 1.81–1.86 (m, 4 H, CH₂), 1.54–1.62 (m, 4 H, CH₂), 1.02–1.06 (t, J = 8.1 Hz, 6 H, CH₃).

MS (ESI +; MeCN–EtOAc–H₂O, 90:5:5): m/z [M + H]⁺ calcd for [C₄₁H₅₁N₆O₂]⁺: 659.40; found: 659.2.



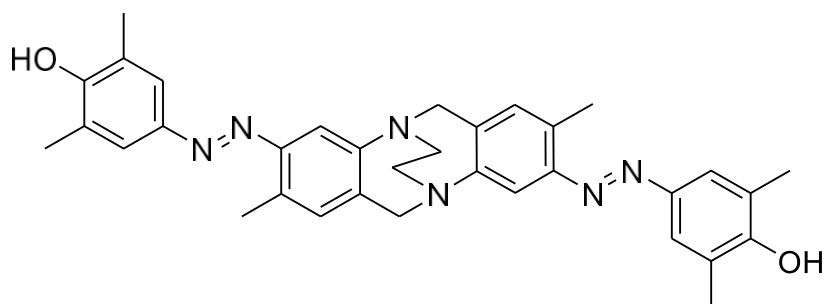
Compound 7, MS (ESI +)



Compound 7, ^1H NMR (400 MHz, CDCl_3)

8. Preparation and Purification of Compound (8)

4,4'-((1E,1'E)-(2,8-dimethyl-6H,12H-5,11-ethanodibenzo[b,f][1,5]diazocine-3,9-diyl)bis(diazene-2,1-diyl))bis(2,6-dimethylphenol)



Compound **5** (0.49 g, 1.0 mmol, 1.0 eq.) was sonicated and dissolved in H_2SO_4 (6.5%, 30 mL) at 95°C , then cooled down to -5°C by placing the reaction container in ice/acetone bath. A sodium nitrite solution (0.30 g, 4.4 mmol, excess, in 5 mL of cold water) was dropped into the reaction flask and stirred for 15 minutes. The resulting solution was poured into a solution consisting 2,6-dimethylphenol (0.25 g, 2.1 mmol, 1.0 eq), Na_2CO_3 (4.0 g, 38 mmol) and 50 mL of ice-cold water and stirred for 8 h. The crude was extracted by EtOAc (30 mL x 3), the organic layers were combined, dried over MgSO_4 and filtered. After solvent removal under reduced pressure, the solid residue was chromatographed (silica gel in dark) to obtain a shiny orange solid.

Yield: 0.44 g (0.78 mmol, 78%); R_f : 0.4 (silica gel; EtOAc–*n*-hexane, 40% v/v). IR (neat): 3331, 2917, 2849, 1719, 1674, 1595, 1490, 1287, 1183, 1113, 1017, 825 cm^{-1} .

^1H NMR (400 MHz, $\text{DMSO-}d_6$): δ = 9.16 (s, 2H, OH), 7.55 (s, 4H, CH), 7.42 (s, 2H, CH), 7.05 (s, 2H, CH),

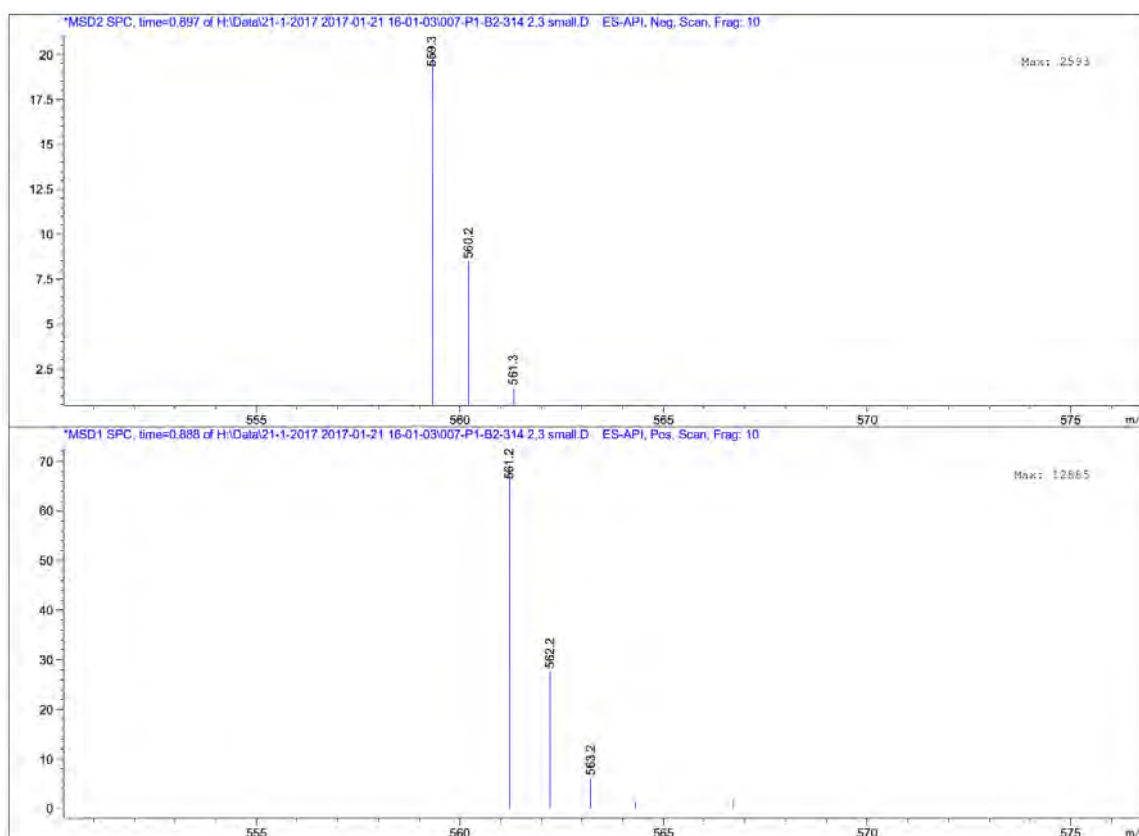
4.50–4.55 (d, J = 17.2, 2H, CH_2), 4.75–4.79 (d, J = 17.3, 2H, CH_2), 3.59–3.71 (br, 4H, $\text{NCH}_2\text{CH}_2\text{N}$), 2.47 (s, 6H, CH_3), 2.30 (s, 12H, CH_3).

^{13}C NMR (100 MHz, CDCl_3) δ [ppm]: 156.6, 149.2, 146.4, 142.1, 131.9, 129.2, 126.7, 124.8, 123.3, 110.4, 58.4, 53.9, 16.6, 16.4.

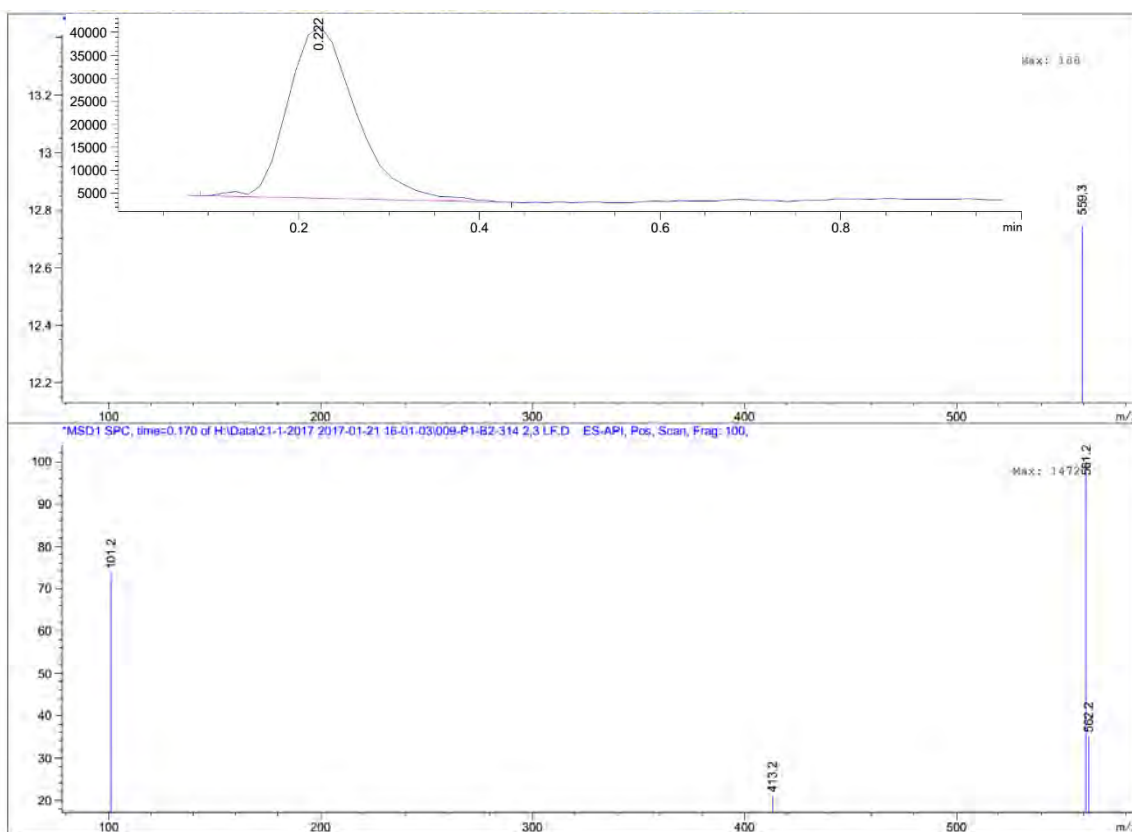
MS (ESI +; EtOAc): m/z $[\text{M} + \text{H}]^+$ calcd for $[\text{C}_{34}\text{H}_{37}\text{N}_6\text{O}_2]^+$: 561.29, found 561.2. (ESI –): m/z $[\text{M} - \text{H}]^-$ calcd for $[\text{C}_{34}\text{H}_{35}\text{N}_6\text{O}_2]^+$: 559.29, found 559.3.

UV/Vis: (EtOAc): λ (lg ϵ) = 349 (4.619) nm.

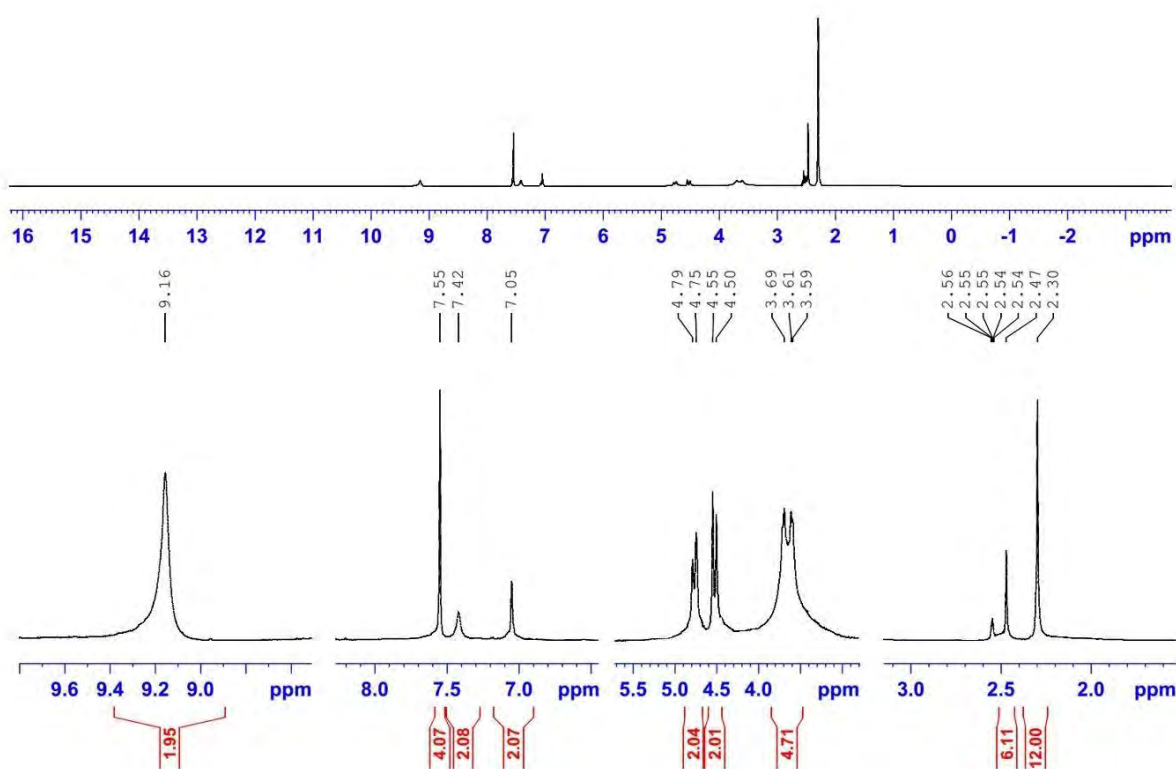
Anal. Calcd for $\text{C}_{34}\text{H}_{36}\text{N}_6\text{O}_2$: C, 72.83; H, 6.47; N, 14.99; O, 5.71. Found: C, 72.69; H, 6.81; N, 15.13.



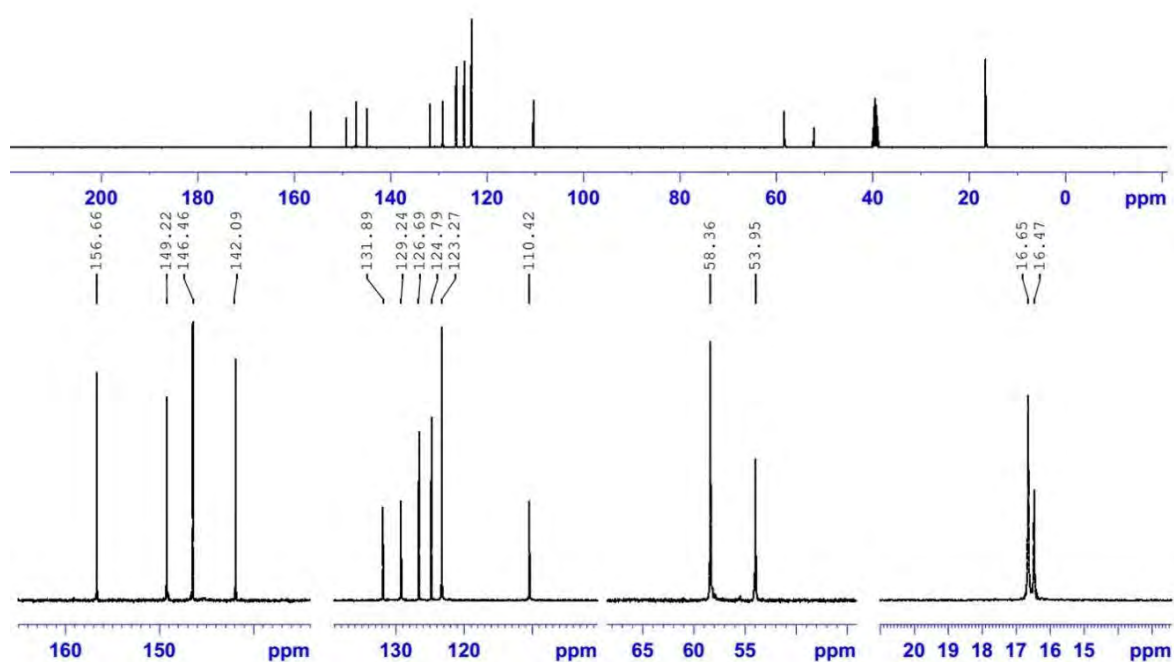
Compound 8, MS ESI + (bottom) and ESI – (top)



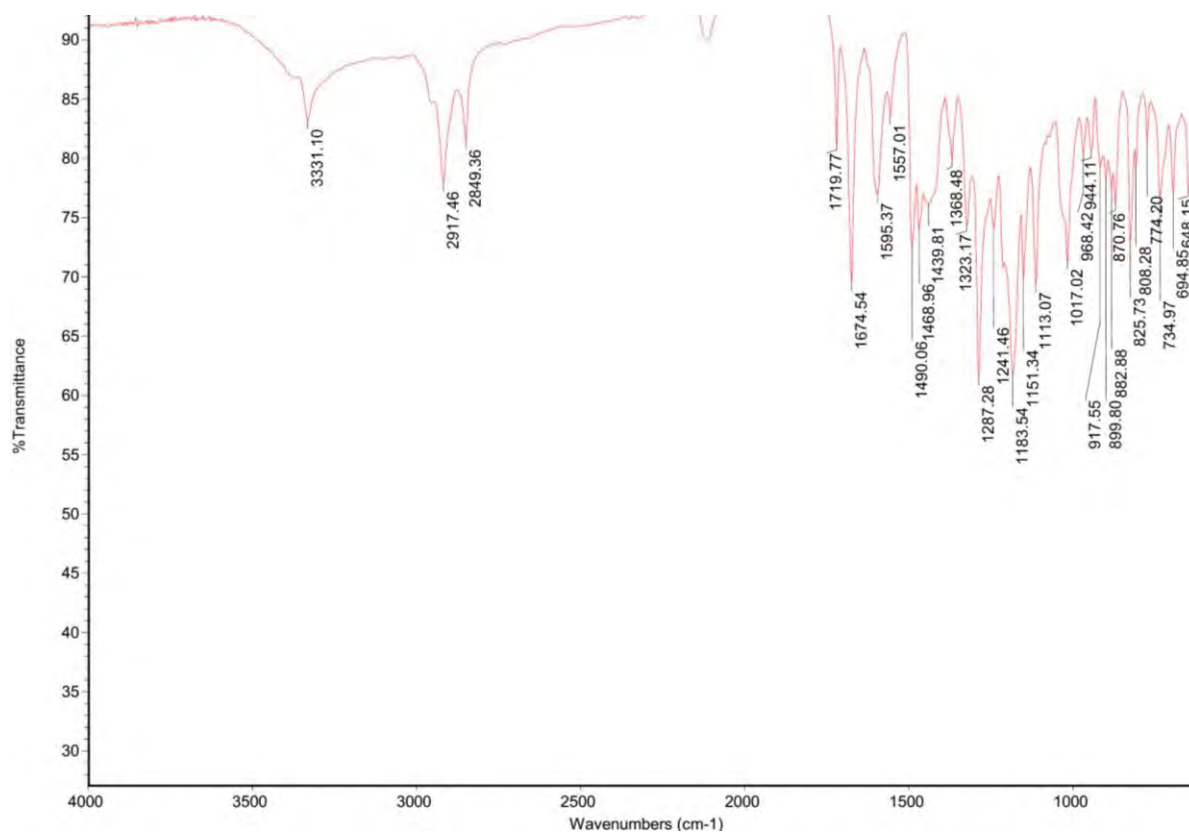
Compound 8, MS ESI + (bottom) and ESI – (top)



Compound 8, ¹H NMR (400 MHz, DMSO-d₆)



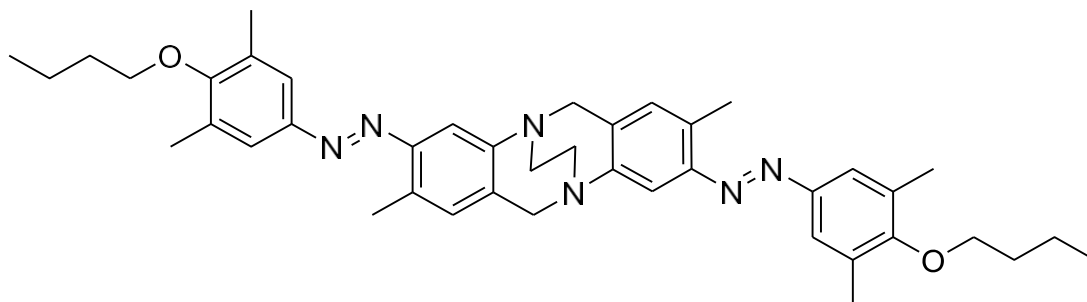
Compound 8, ¹³C NMR (100 MHz, DMSO-*d*₆)



Compound 8, IR transmittance (neat)

9. Preparation and Purification of Compound (9)

3,9-bis((E)-(4-butoxy-3,5-dimethylphenyl)diazenyl)-2,8-dimethyl-6H,12H-5,11-ethanodibenzo [b,f][1,5]diazocine



Compound **7** (1.31 g, 2.0 mmol, 1.0 eq.), 1,2-dibromoethane (0.75 g, 4.0 mmol, 2.0 eq.) and Li_2CO_3 (0.59 g, 8.0 mmol) were mixed in dried DMF (10 mL) and refluxed for 24 hours at 110°C under nitrogen atmosphere in darkness and then the reaction mixture was poured into cold water and the crude was extracted by EtOAc (50 mL x 3). The organic layer was collected, dried over MgSO_4 and filtered. After solvent removal under reduced pressure, the solid residue was chromatographed (silica gel in dark) to obtain a shiny orange solid.

Yield: 0.29 g (0.44 mmol, 22%); R_f : 0.45 (silica gel; MeOH–DCM = 2% v/v).

IR (neat): 2956, 2927, 2868, 1589, 1480, 1208, 1115, 956 and 890 cm^{-1} .

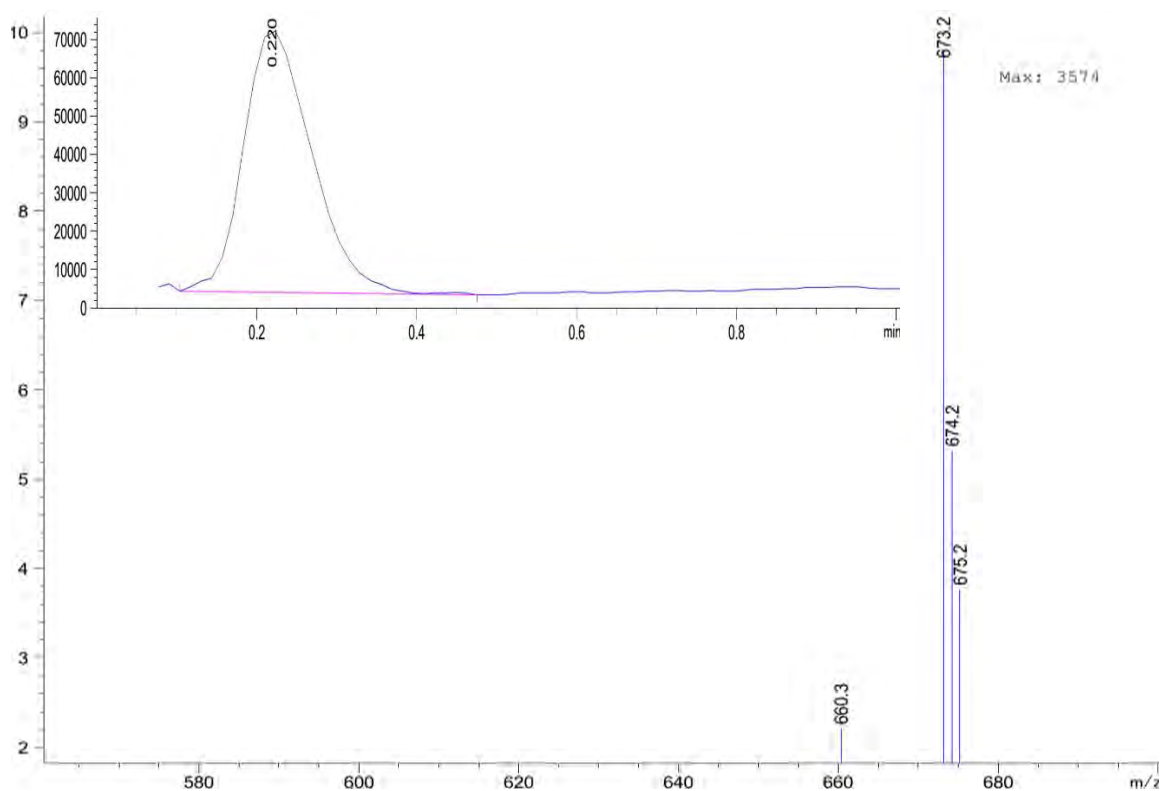
^1H NMR (400 MHz, CDCl_3): δ = 7.57 (s, 4H, CH), 7.43 (s, 2H, CH), 6.86 (s, 2H, CH), 4.51–4.65 (m, 4H, CH_2), 3.81–3.84 (t, 4H, CH_2), 3.55–3.65 (m, 4H, CH_2), 2.52 (s, 6H, CH_3), 2.37 (s, 12H, CH_3), 1.79–1.83 (m, 4H, CH_2), 1.53–1.62 (m, 4H, CH_2), 1.01–1.04 (t, J = 8.2, 6H, CH_3).

^{13}C NMR (100 MHz, CDCl_3) δ [ppm]: 158.6, 150.0, 149.0, 148.7, 139.7, 134.3, 131.7, 131.4, 123.5, 114.6, 72.3, 59.0, 54.8, 32.6, 19.5, 17.0, 16.6, 14.1.

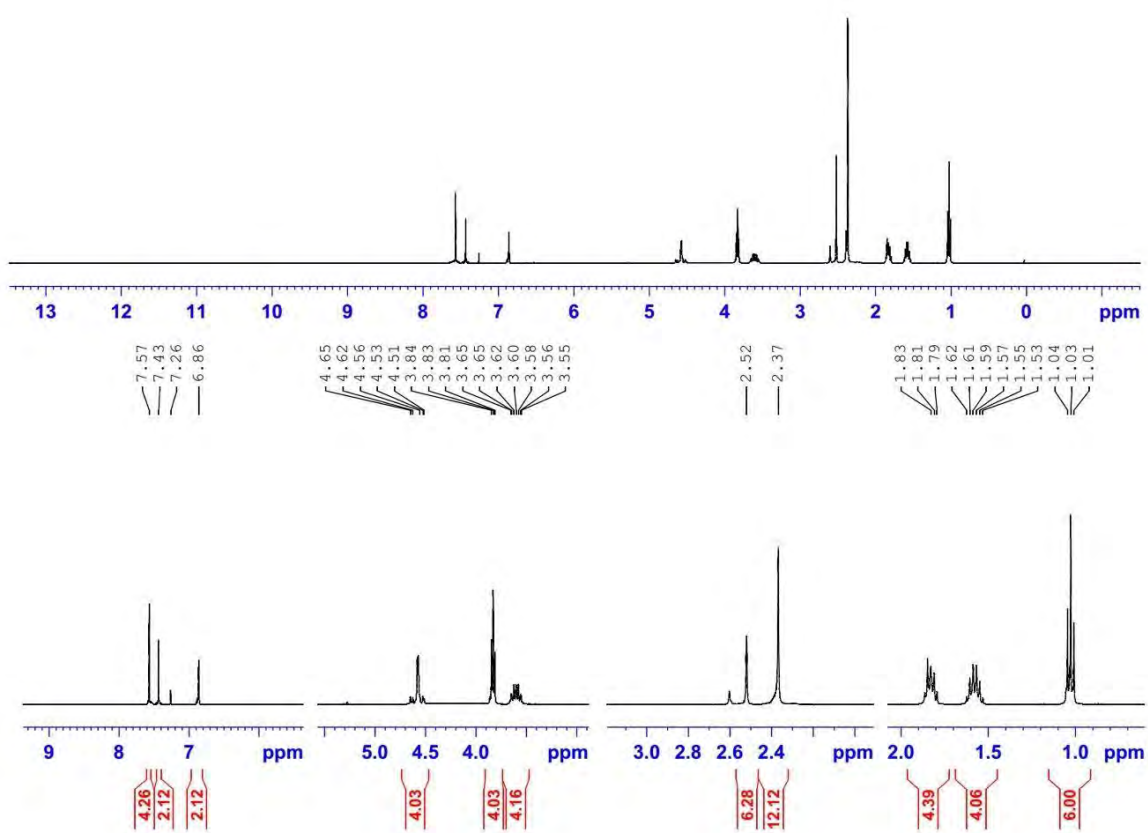
MS (ESI +; ACN–EtOAc– H_2O /HCO $_2\text{H}$, 90:5:5): m/z $[\text{M} + \text{H}]^+$ calcd for $[\text{C}_{42}\text{H}_{53}\text{N}_6\text{O}_2]^+$: 673.42, found 673.2.

UV/Vis: (EtOAc): λ (lg ϵ) = 349 (4.569) nm.

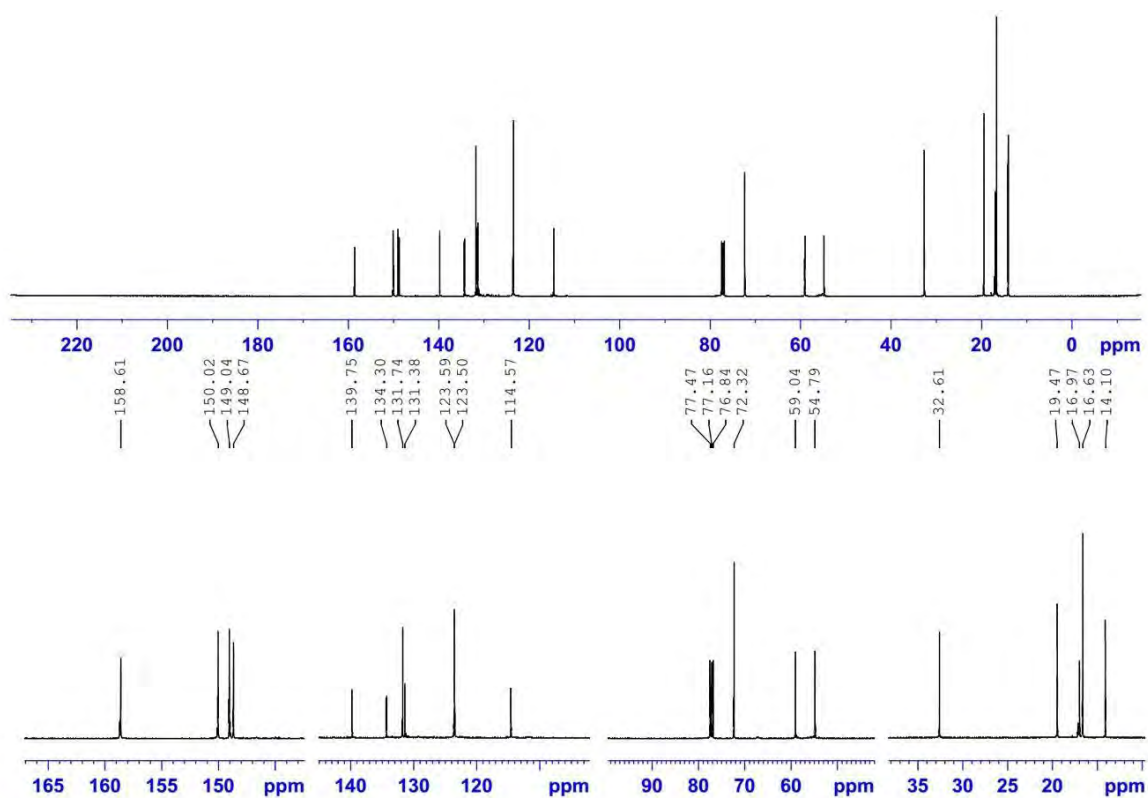
Anal. Calcd for $\text{C}_{42}\text{H}_{52}\text{N}_6\text{O}_2$: C, 74.97; H, 7.79; N, 12.49; O, 4.76. Found: C, 74.75; H, 7.91; N, 12.68.



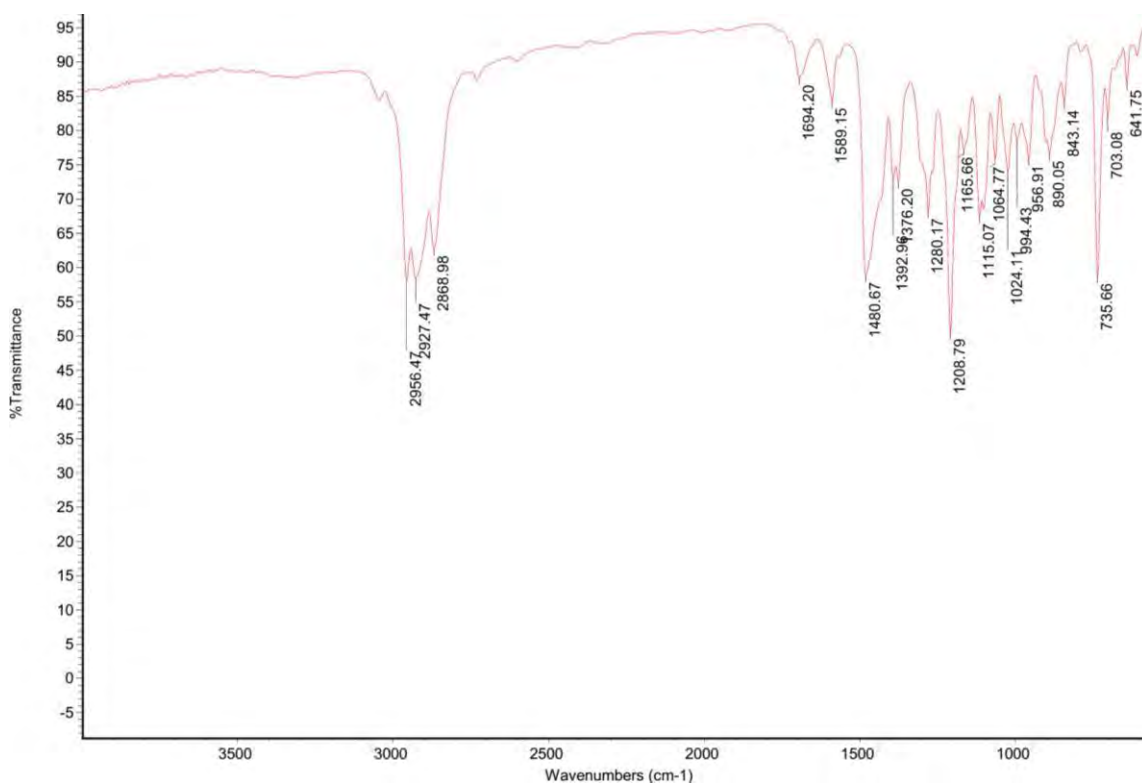
Compound 9, MS (ESI +)



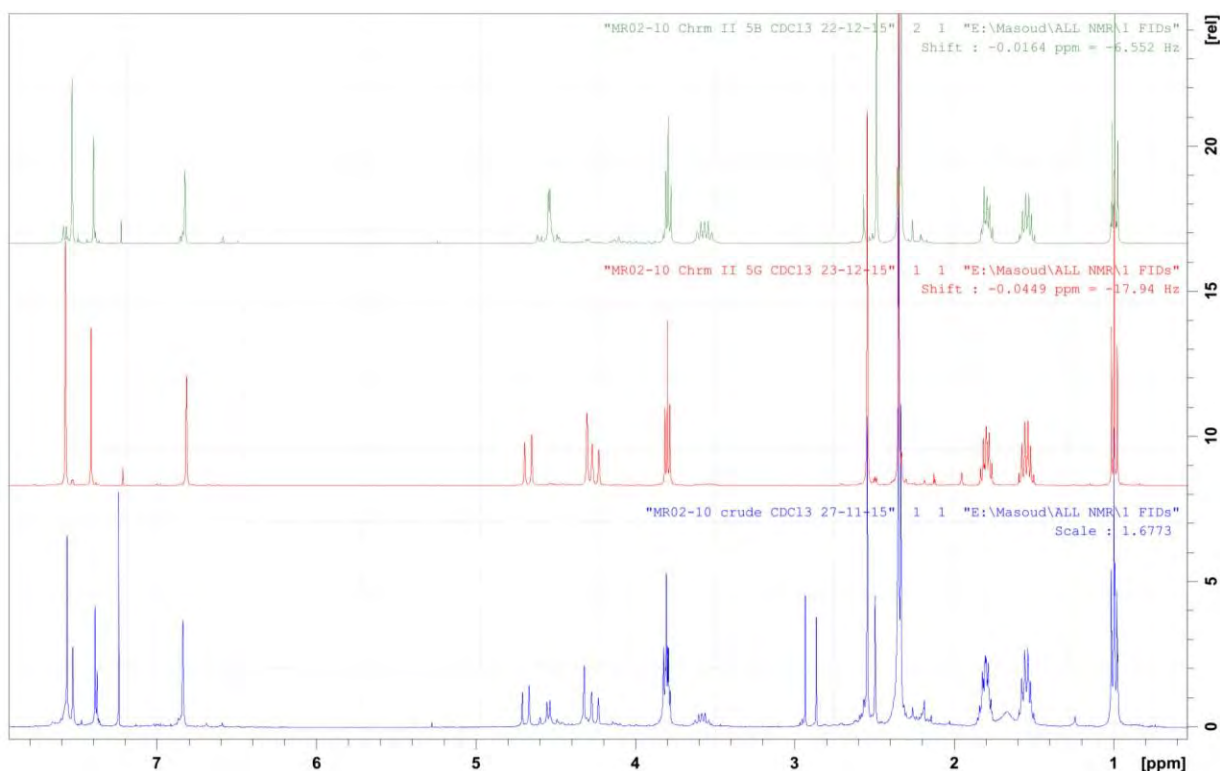
Compound 9, ¹H NMR (400 MHz, CDCl₃)



Compound 9, ¹³C NMR (100 MHz, CDCl₃)



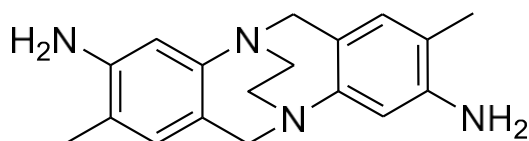
Compound 9, IR transmittance (neat)



¹H NMR (400 MHz, CDCl₃), 9 (ethano-strap, in green), 7 (methano strap, in red), reaction mixture containing 7 and 9 (in blue)

10. Preparation and Purification of Compound (10)

2,8-dimethyl-6H,12H-5,11-ethanodibenzo[b,f][1,5]diazocine-3,9-diamine



Method G: Sonicating compound **5** (0.49 g, 1.0 mmol in H₂SO₄ 12%, 15 mL) gave a milky suspension; which was then heated (80°C, 15-20 min) under argon atmosphere until turned to a clear colourless solution. Afterwards, the solution was neutralized by Na₂CO₃ (3.5 g) and basified by adding ammonium solution (28%, 5 mL) and was then extracted by DCM (30 mL x 5). DCM layers were combined and washed with brine, dried over Na₂SO₄ and filtered. DCM was removed under reduced pressure at 15°C in darkness to obtain pure **10** as a cream-coloured solid. Yield: 0.28 g (0.96 mmol, 96%).

Method H: Compound **9** (0.67 g, 1 mmol, 1eq.), was dissolved in boiling MeOH (30 mL). Then, sodium dithionite ($\text{Na}_2\text{S}_2\text{O}_4$, 4 g, excess) was gradually added. The suspension was refluxed until obtaining a total discoloration from orange to milky white (3-4 h). The suspension was cooled down to r.t., DCM (120 mL) was added and the suspension was filtered off. The solvents were removed under reduced pressure and the remaining residue was chromatographed to obtain purified **10**. (This product has to be stored under inert atmosphere in dark and cold otherwise darkens fast). Yield: 0.18 g (0.62 mmol, 62%); R_f : 0.6 (silica gel; MeOH–DCM = 10% v/v).

IR (neat): 3338, 3227, 2894, 2855, 1619, 1501, 1440, 1287, 1117, 876 cm^{-1} .

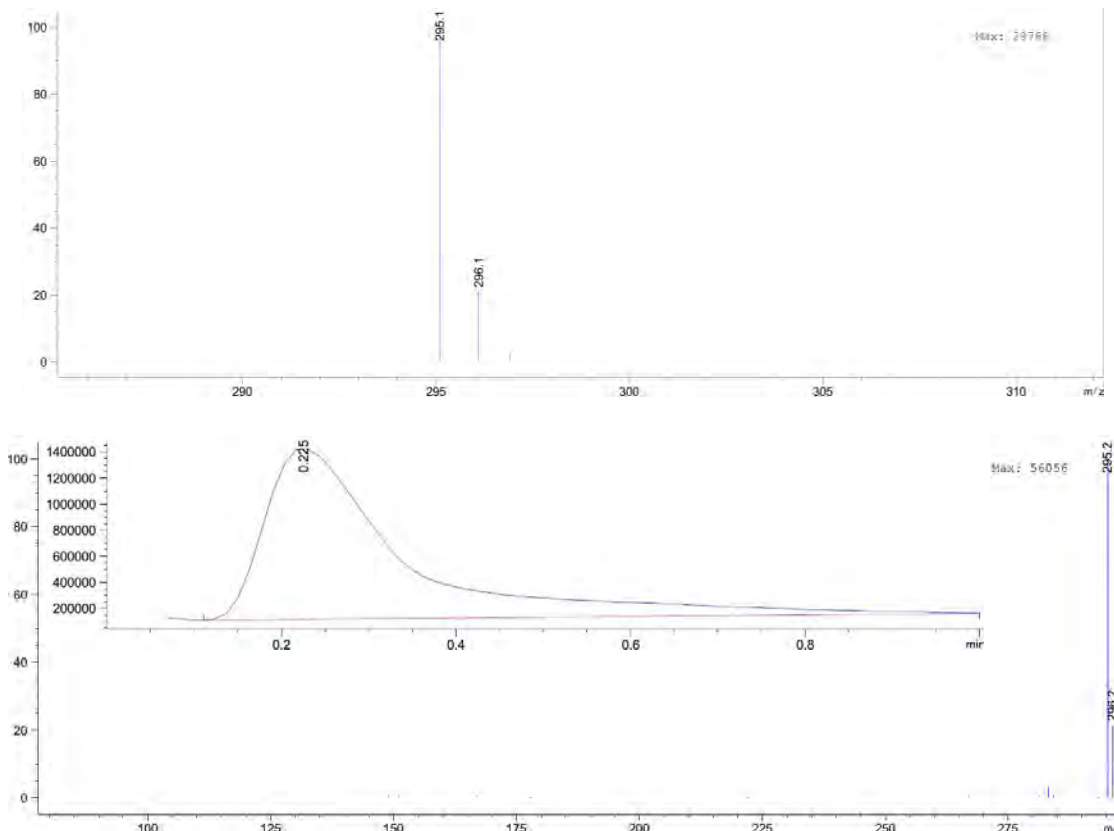
^1H NMR (400 MHz, $\text{DMSO}-d_6$): δ = 6.40 (s, 2H, CH), 6.27 (s, 2H, CH), 4.47 (br, 4H, NH), 4.30–4.34 (d, J = 16.6 Hz, 2H, CH_2), 4.01–4.05 (d, J = 16.7 Hz, 2H, CH_2), 3.34 (br, 4H, $\text{N}(\text{CH}_2)_2\text{N}$), 1.86 (s, 6H, CH_3).

^{13}C NMR (100 MHz, $\text{DMSO}-d_6$): δ = 149.0, 144.8, 129.6, 124.3, 117.4, 112.8, 58.2, 54.44, 16.7.

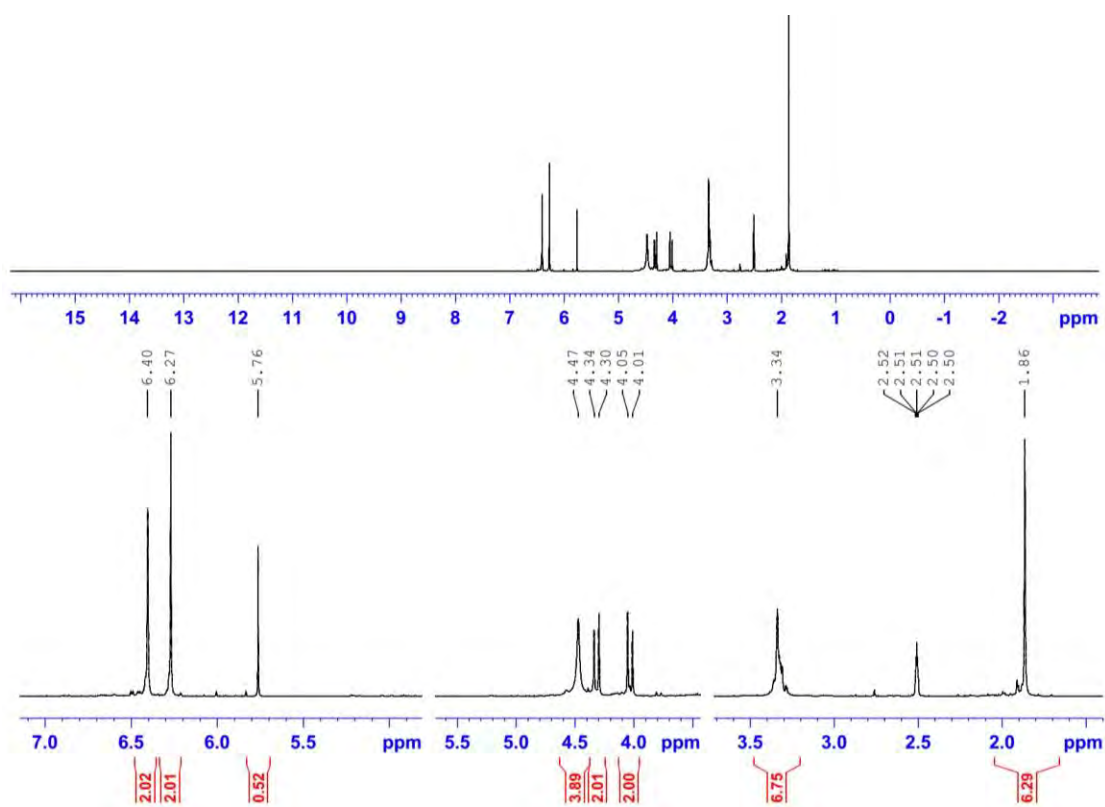
MS (ESI +; MeOH): m/z $[\text{M} + \text{H}]^+$ calcd for $[\text{C}_{18}\text{H}_{23}\text{N}_4]^+$: 295.18, found 295.1.

UV/Vis: (ACN): λ (lg ϵ) = 225 (4.569), 304 (4.009) nm.

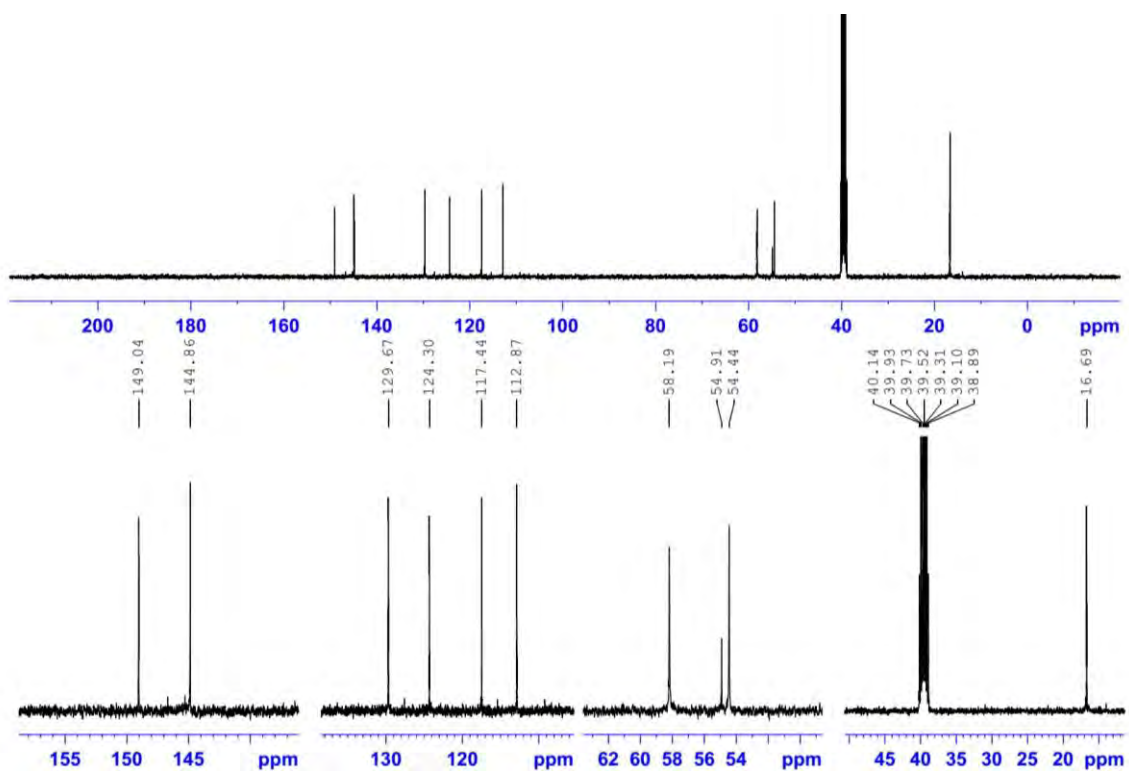
Anal. Calcd for $\text{C}_{18}\text{H}_{22}\text{N}_4$: C, 73.44; H, 7.53; N, 19.03. Found: C, 73.23; H, 7.70; N, 19.14.



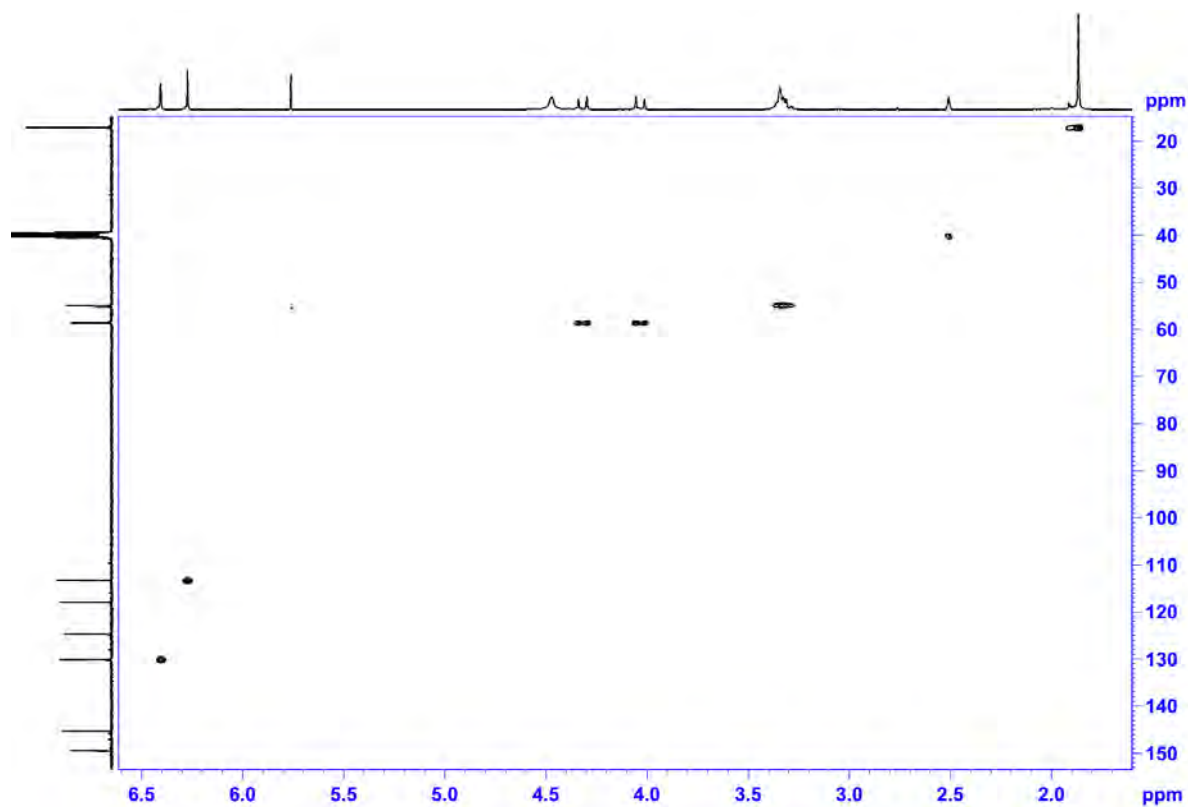
Compound 10, MS (ESI +)



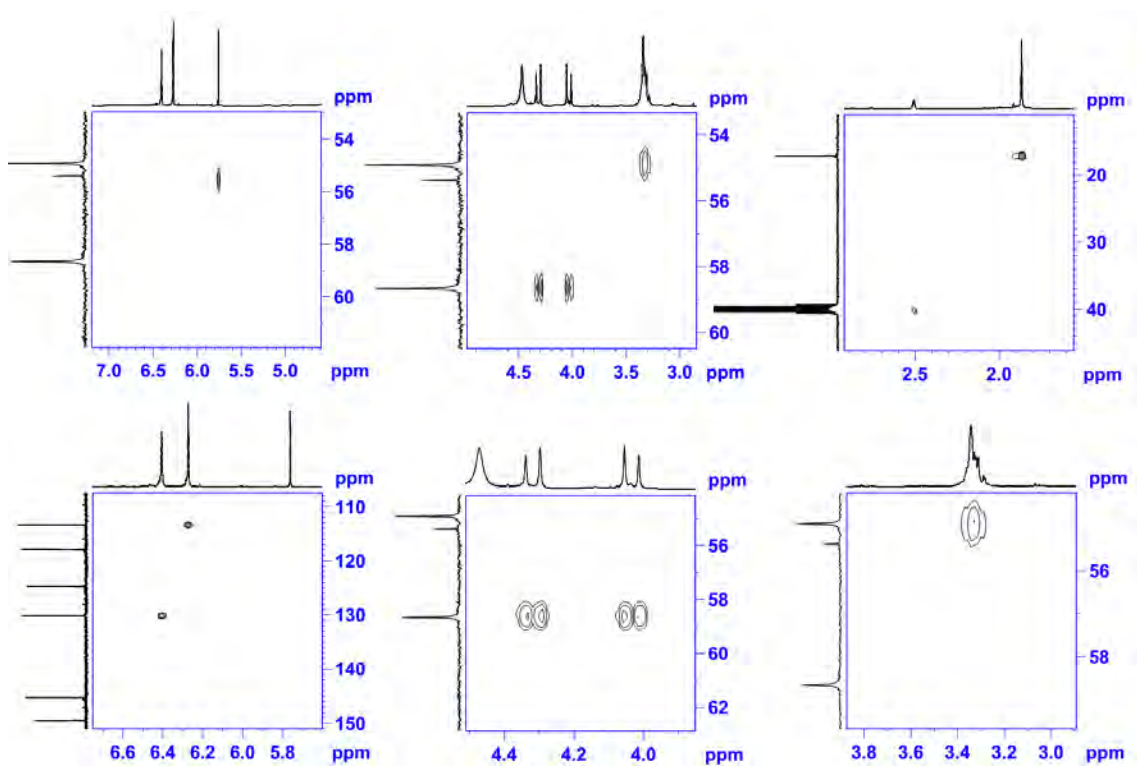
Compound 10, ¹H NMR (400 MHz, DMSO-*d*₆)



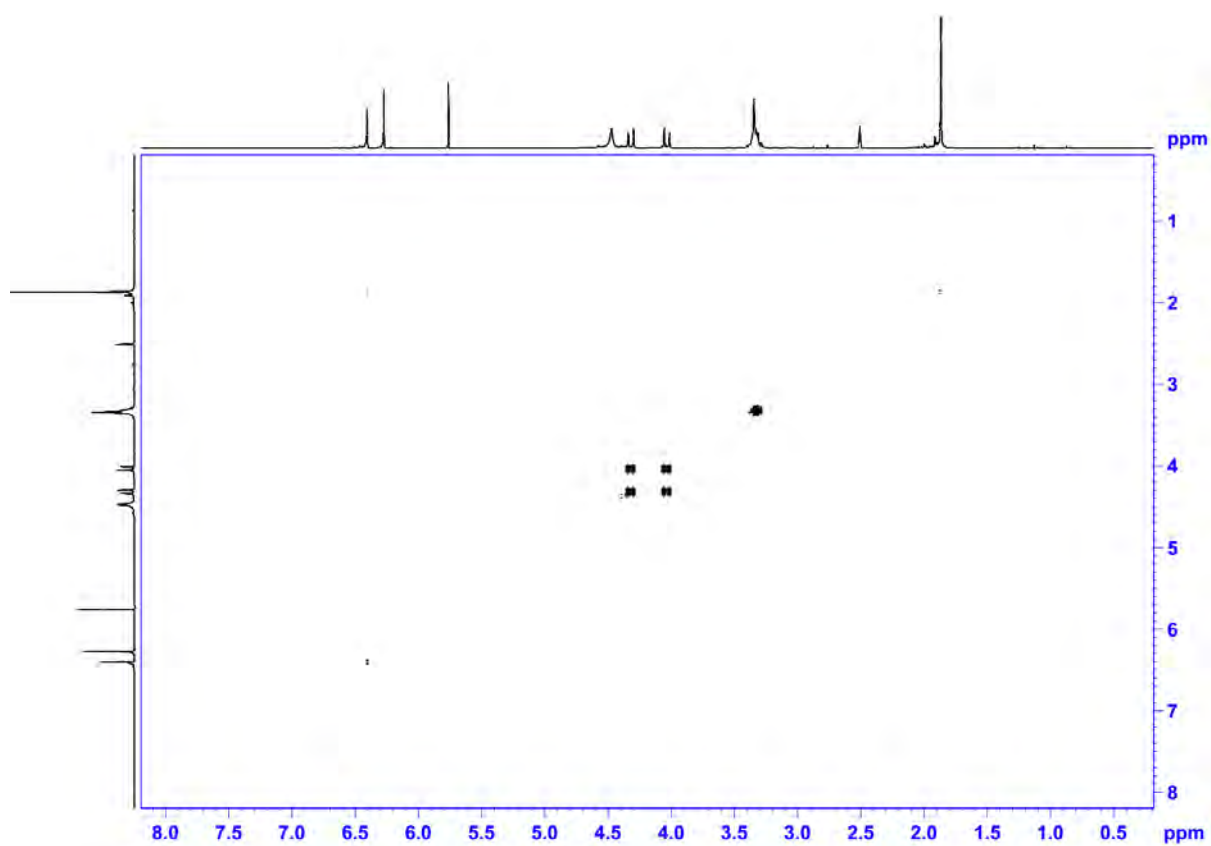
Compound 10, ¹³C NMR (100 MHz, DMSO-*d*₆)



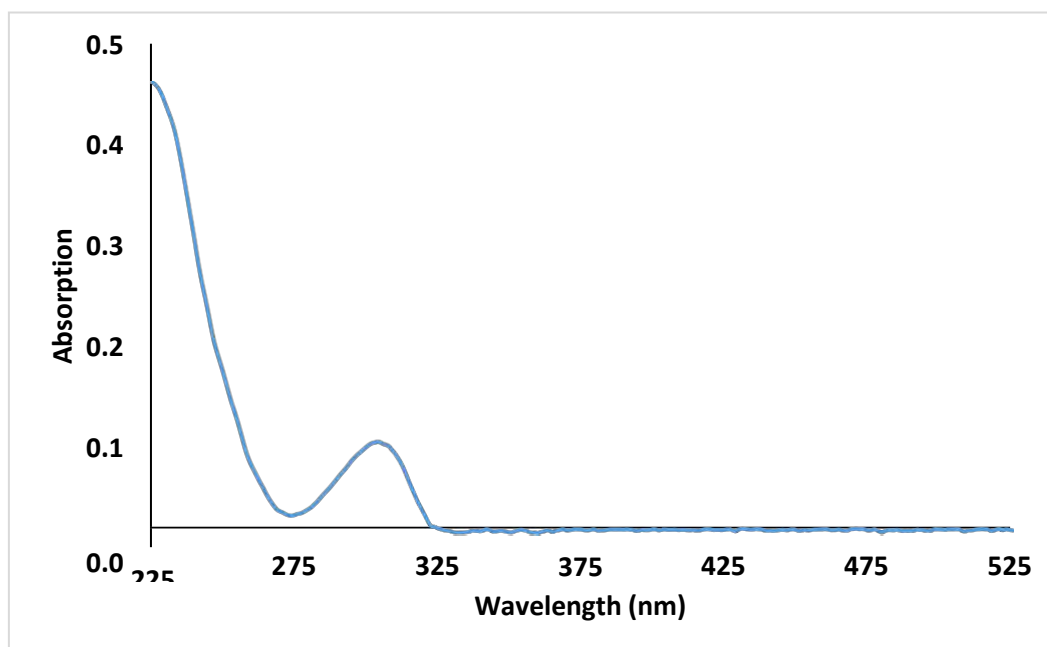
Compound 10, HSQC (DMSO- d_6)



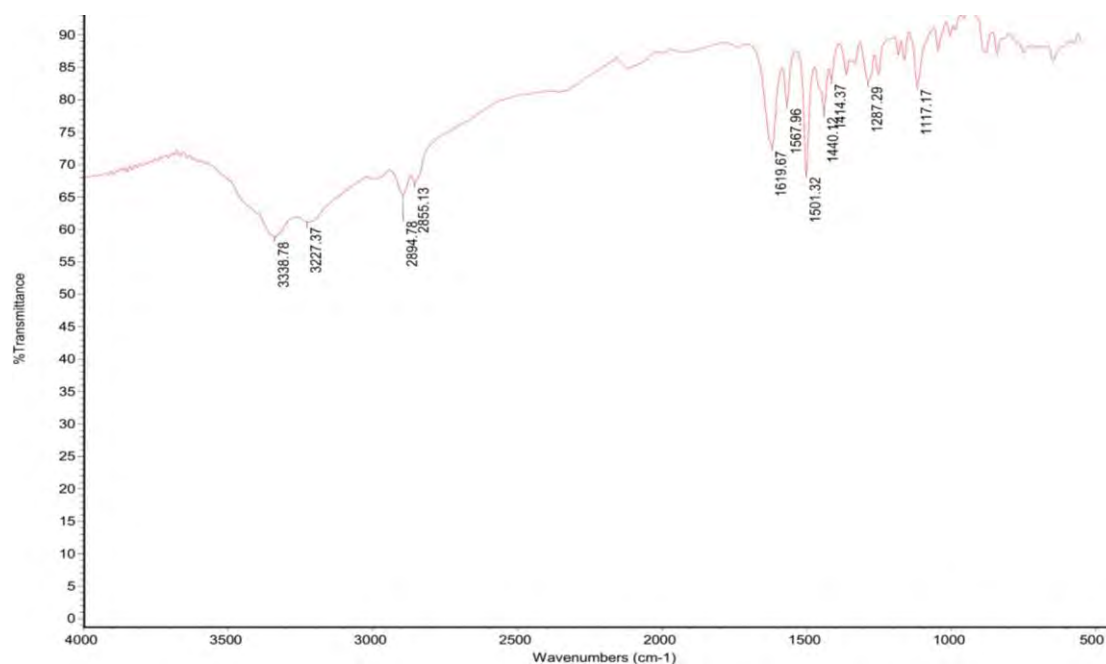
Compound 10, HSQC (DMSO- d_6)



Compound 10, COSY (DMSO- d_6)



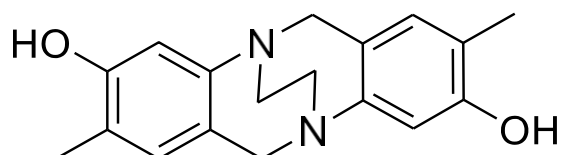
Compound 10, UV/Vis (ACN, r.t.)



Compound 10, IR transmittance (neat)

11. Preparation and Purification of Compound (11)

2,8-dimethyl-6H,12H-5,11-ethanodibenzo[b,f][1,5]diazocine-3,9-diol



Compound **5** (0.49 g, 1 mmol, 1eq.) was dispersed in H_2SO_4 (6.5%, 30 mL) by sonication for 5 min. Then, the obtained milky suspension was refluxed under nitrogen atmosphere in darkness until turned to a clear colourless solution. The solution was cooled down to -5°C and sodium nitrite solution (0.3 g, 4.4 mmol, 2.2 eq.) in cold water (10 mL) was added dropwise and stirring continued for 30 min at -5°C . Afterwards, the solution's temperature was gradually raised until boil over two hours (Attention: this step releases nitrogen gas; hence, rapid heating of a sealed container may lead to explosion). The reaction mixture was cooled down to r.t., its pH was adjusted to 5 (by adding Na_2CO_3 saturated solution) and extracted by EtOAc (30ml x 5), the organic layers were combined, dried over Na_2SO_4 and evaporated until dryness to obtain the pure product as an off-white powder.

Yield: 0.27 g (0.91 mmol, 91%). R_f = 0.4 (silica gel; MeOH–DCM, 8% v/v).

IR (neat): 3190, 2949, 2914, 1704, 1616, 1500, 1440, 1220, 1042, 879, 716 cm^{-1} .

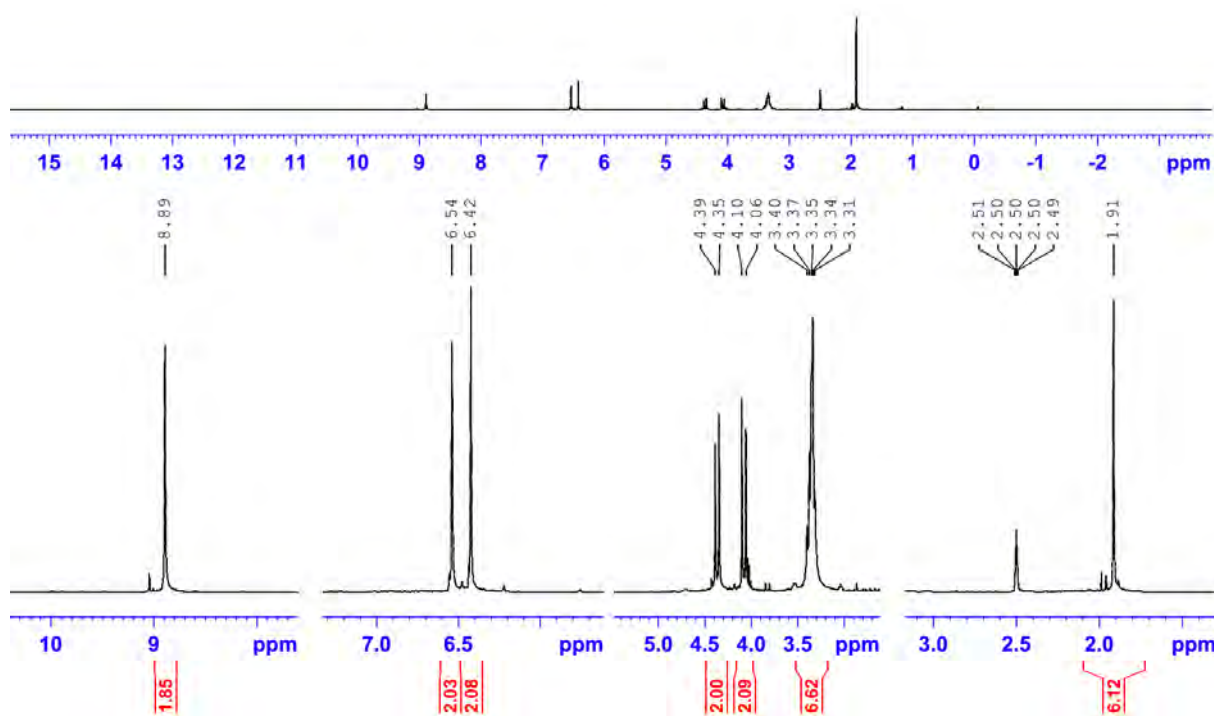
^1H NMR (400 MHz, $\text{DMSO}-d_6$): δ = 8.89 (s, 2H, OH), 6.54 (s, 2H, CH), 6.42 (s, 2H, CH), 4.34–4.38 (d, J = 16.7 Hz, 2H, CH_2), 4.05–4.10 (d, J = 16.8 Hz, 2H, CH_2), 3.29–3.39 (m, 4H, CH_2), 1.91 (s, 6H, CH_3).

^{13}C NMR (100 MHz, $\text{DMSO}-d_6$): δ = 153.7, 148.8, 130.1, 126.8, 119.8, 113.4, 58.0, 54.4, 15.3.

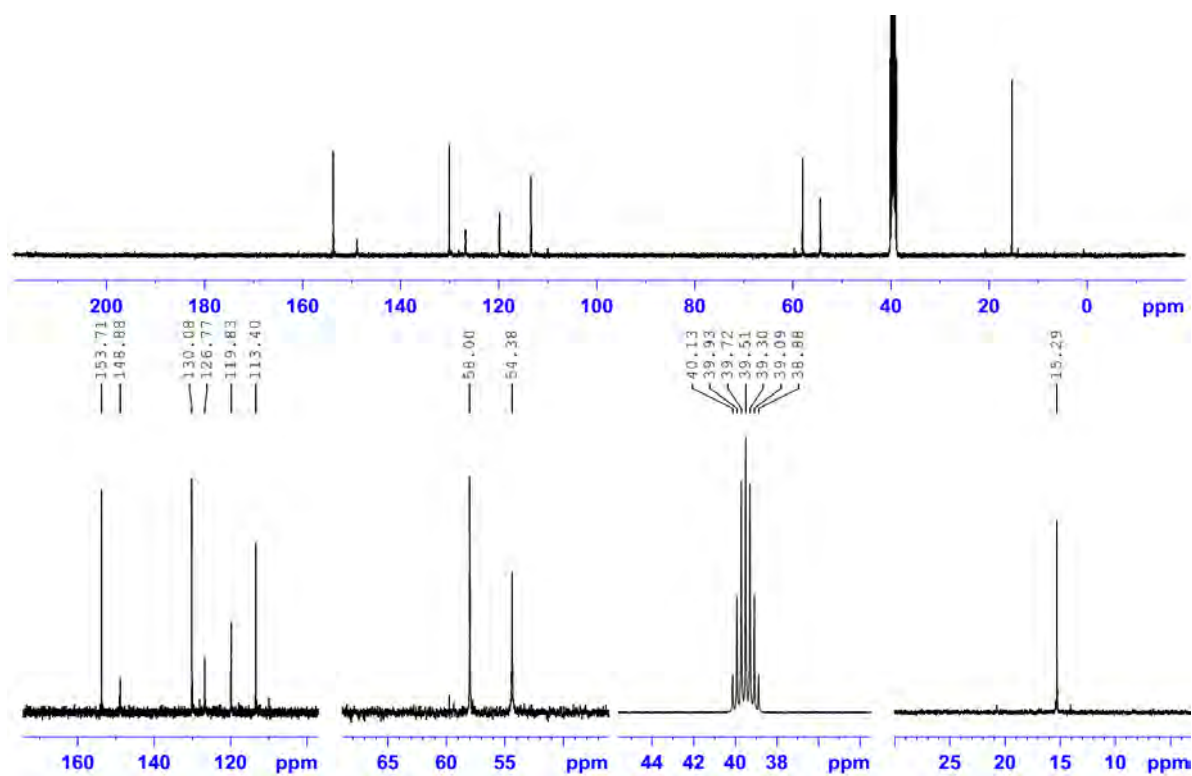
MS (ESI +; EtOH–EtOAc– H_2O , 90:5:5): m/z $[\text{M} + \text{H}]^+$ calcd for $[\text{C}_{18}\text{H}_{21}\text{N}_2\text{O}_2]^+$: 297.15; found 297.1. MS (ESI –): m/z $[\text{M} - \text{H}]^-$ calcd for $[\text{C}_{18}\text{H}_{19}\text{N}_2\text{O}_2]^-$: 295.15; found 295.1.

UV/Vis: (EtOAc): λ (lg ϵ) = 294 (3.655) nm.

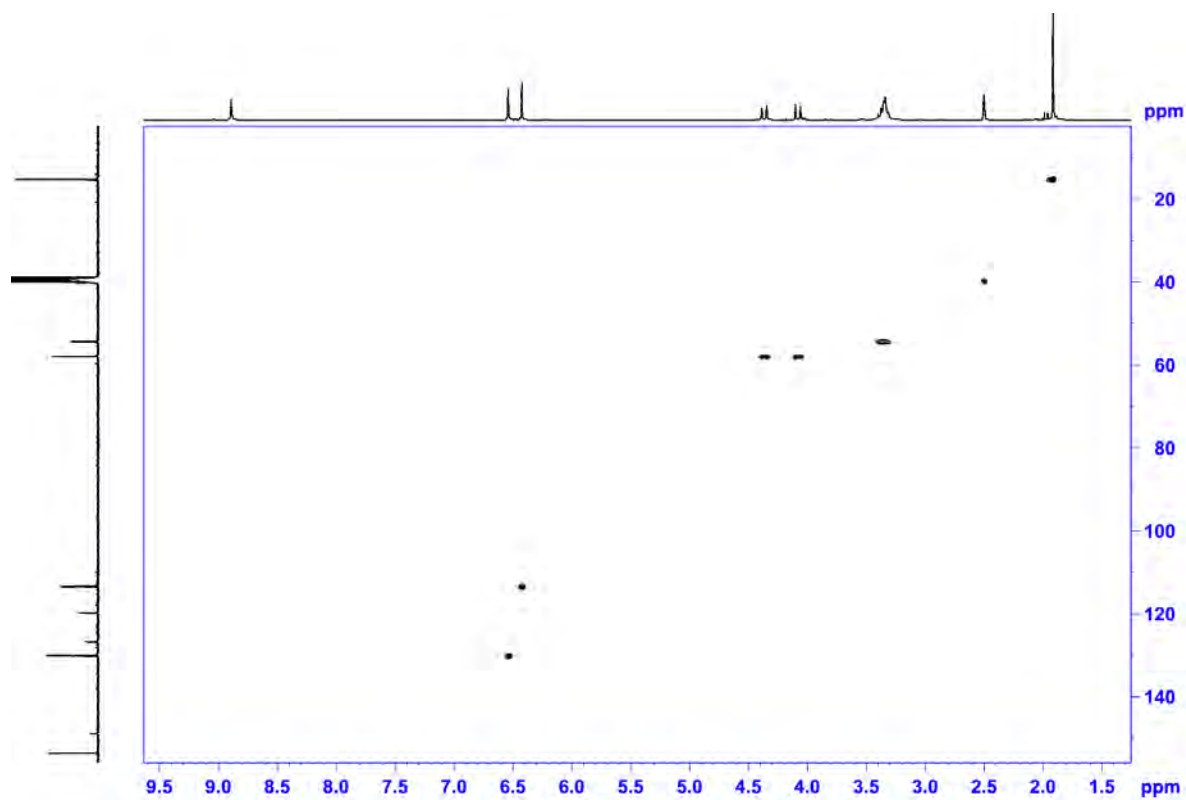
Anal. calcd for $\text{C}_{18}\text{H}_{20}\text{N}_2\text{O}_2$: C, 72.95; H, 6.80; N, 9.45; O, 10.80. Found: C, 72.67; H, 6.64; N, 9.83.



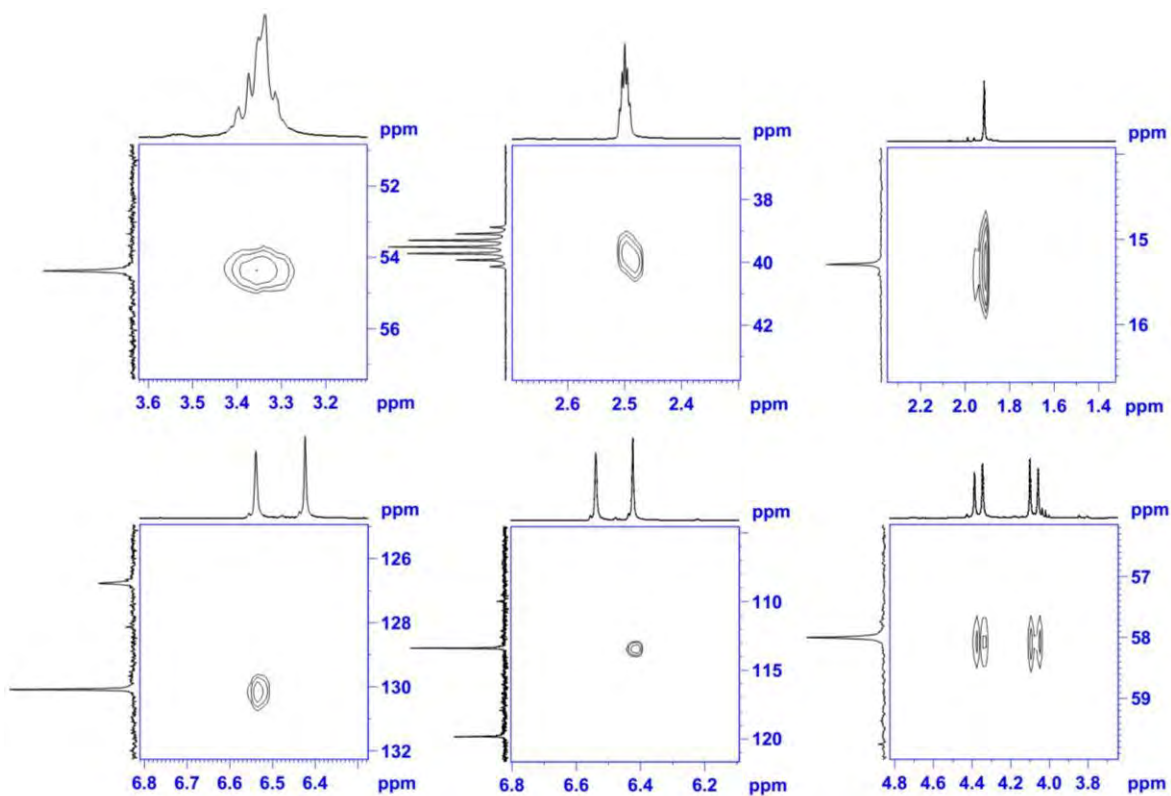
Compound 11, ^1H NMR (400 MHz, $\text{DMSO}-d_6$)



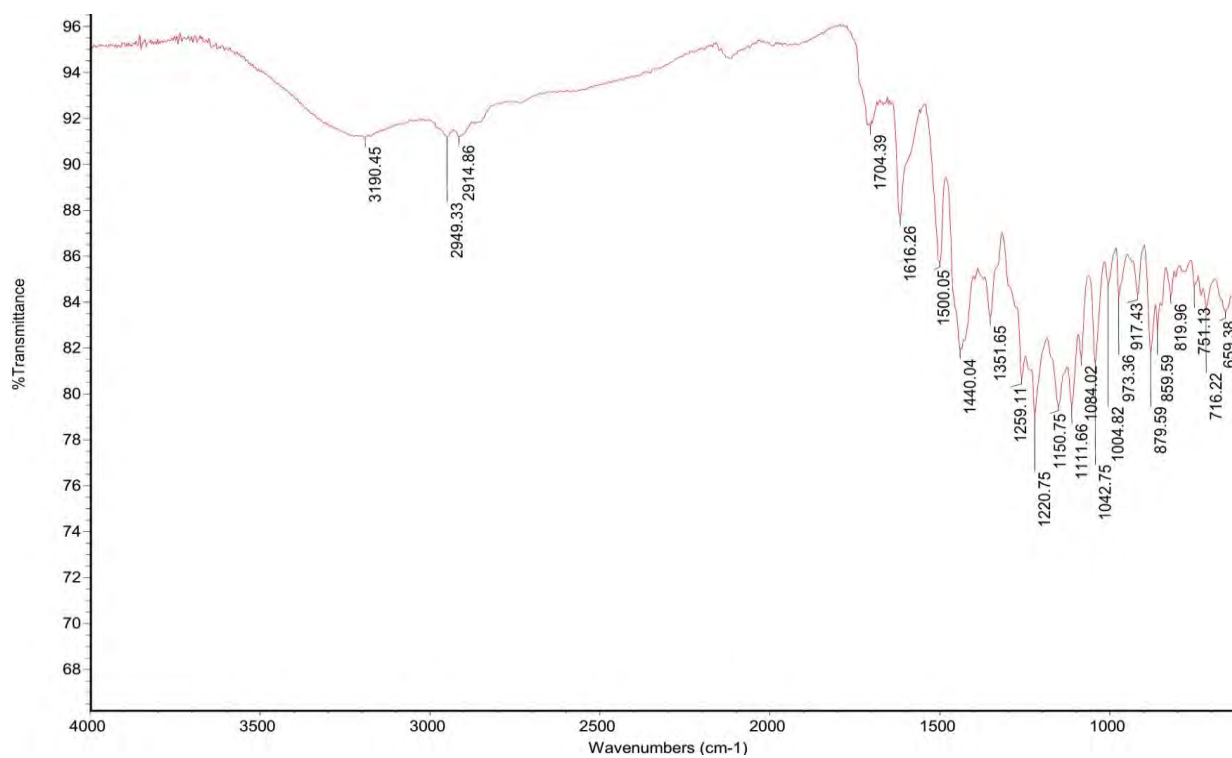
Compound 11, ¹³C NMR (100 MHz, DMSO-*d*₆)



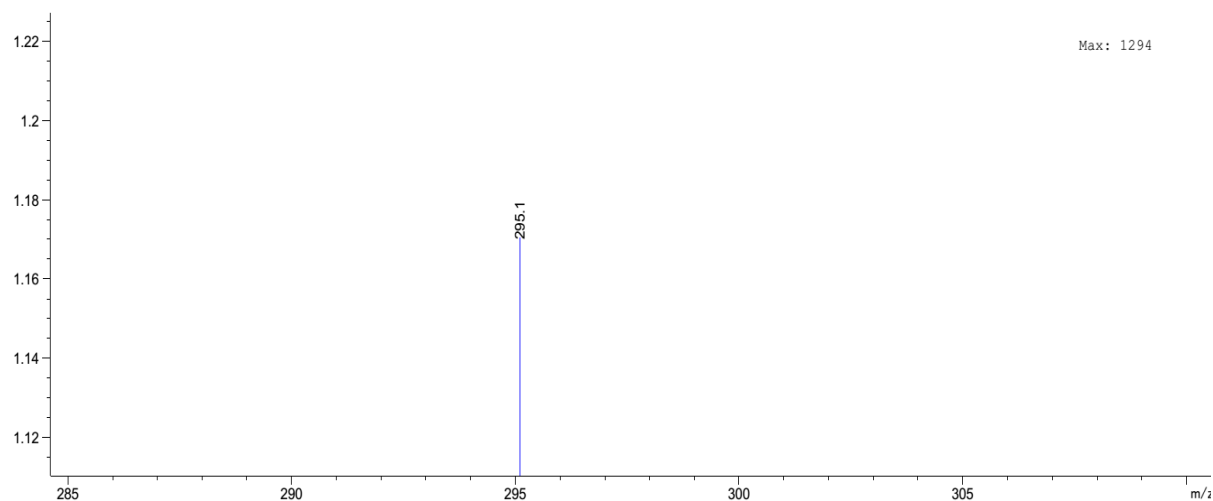
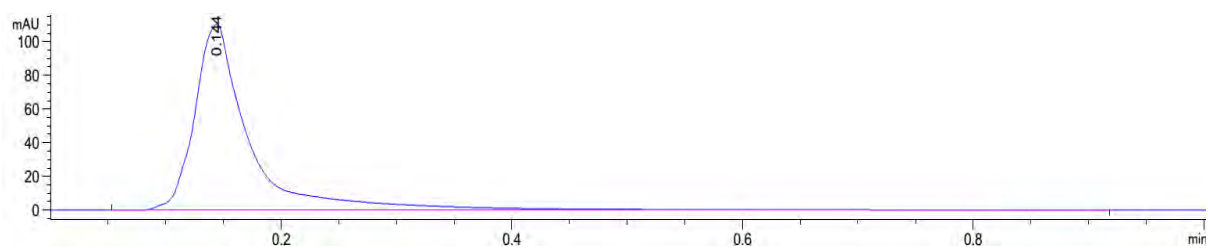
Compound 11 (HSQC, DMSO-*d*₆)



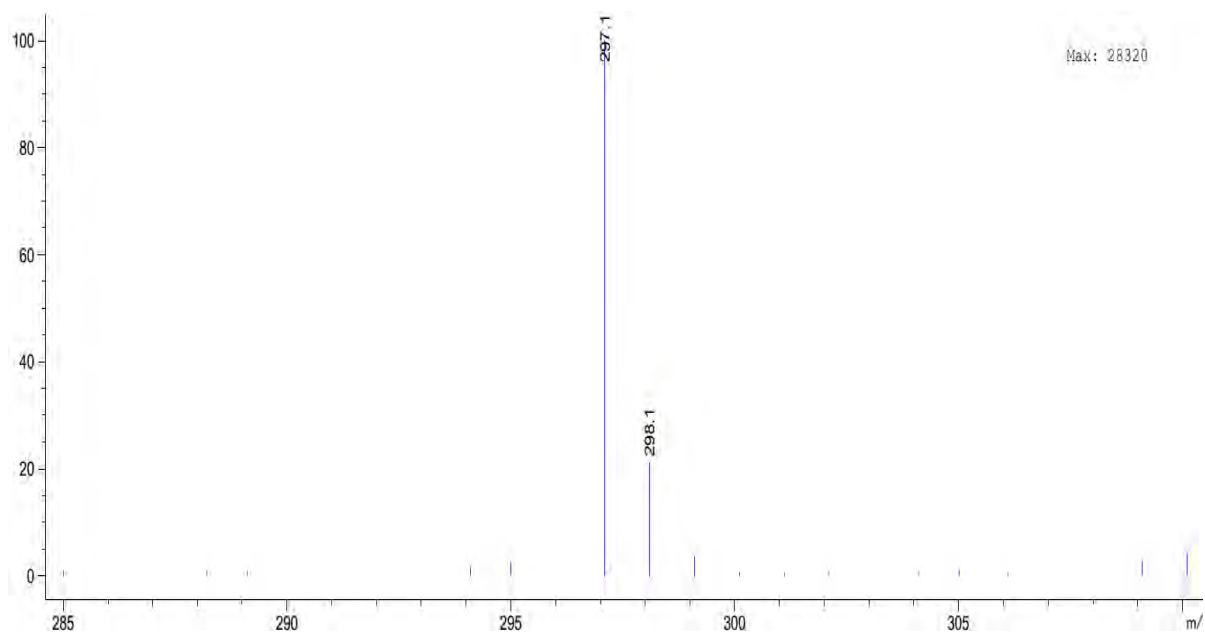
Compound 11 (HSQC, DMSO- d_6)



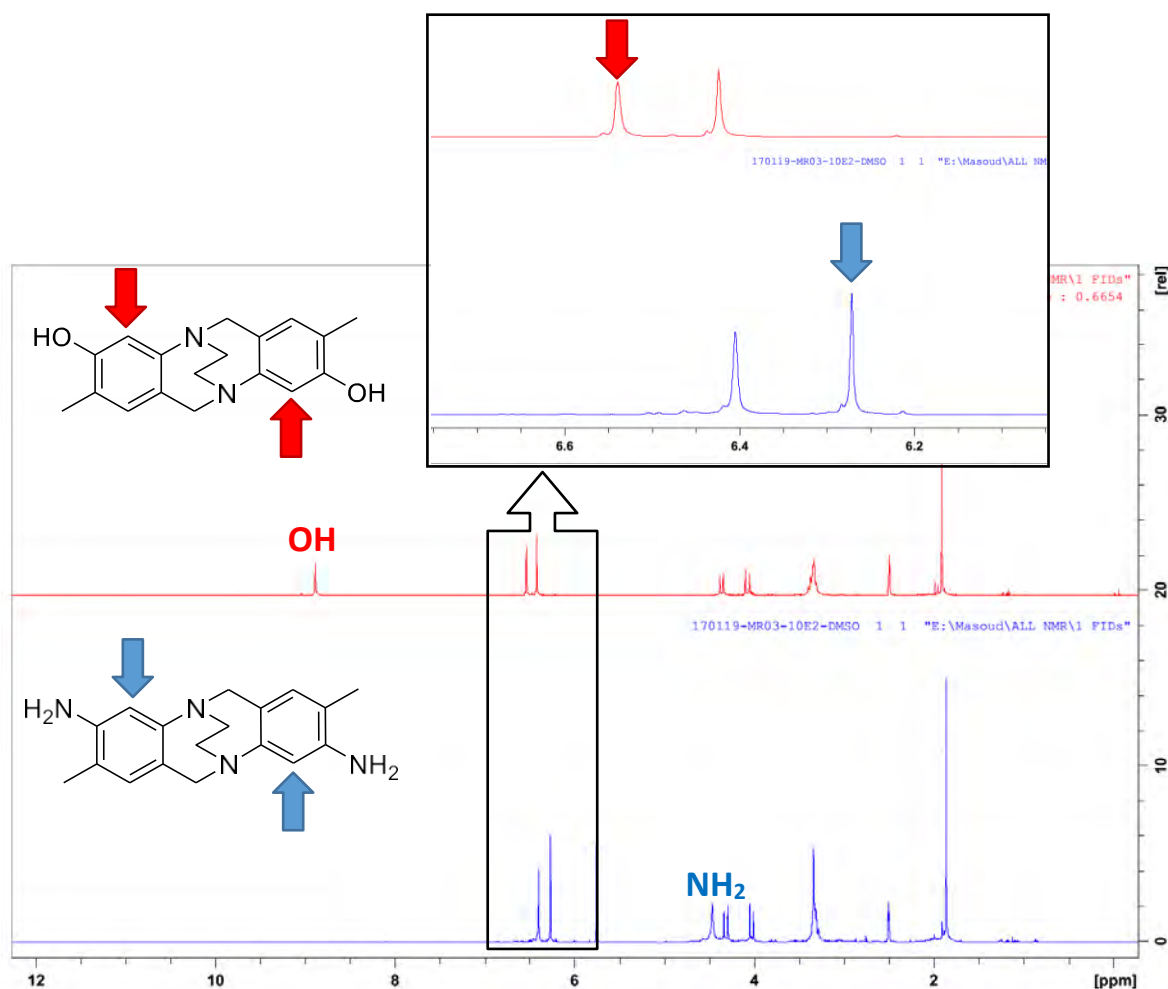
Compound 11, IR (neat)



Compound 11, MS (ESI -)



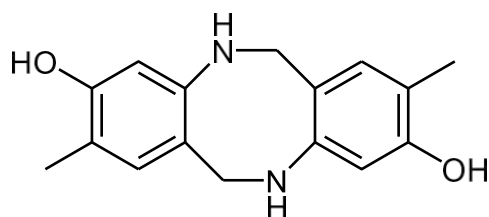
Compound 11, MS (ESI +)



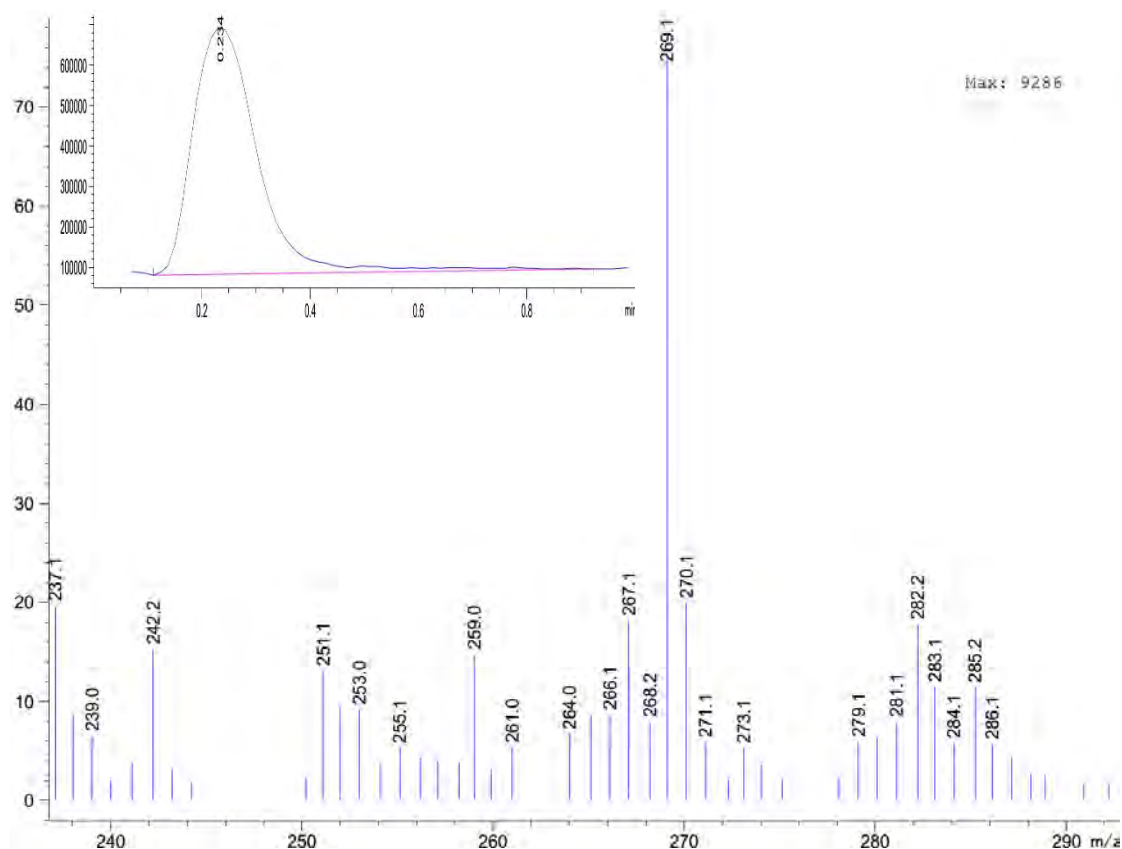
Comparative ^1H NMR spectra of 10 and 11, $\text{DMSO}-d_6$

12. Preparation and Purification of Compound (12)

2,8-dimethyl-5,6,11,12-tetrahydrodibenzo[b,f][1,5]diazocine-3,9-diol



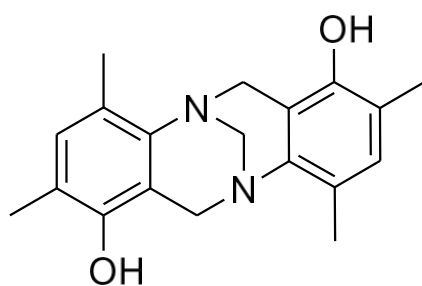
Hünlich's base was subjected to the method described in the literature.³ The amount of obtained product was not sufficient to be properly characterized, despite scaling up the reaction tenfold. Yield: trace. MS (ESI +; ACN–MeOH, 90:10): m/z $[\text{M} - \text{H}]^-$ calcd for $[\text{C}_{16}\text{H}_{17}\text{N}_2\text{O}_2]^-$: 269.14; Found: 269.1.



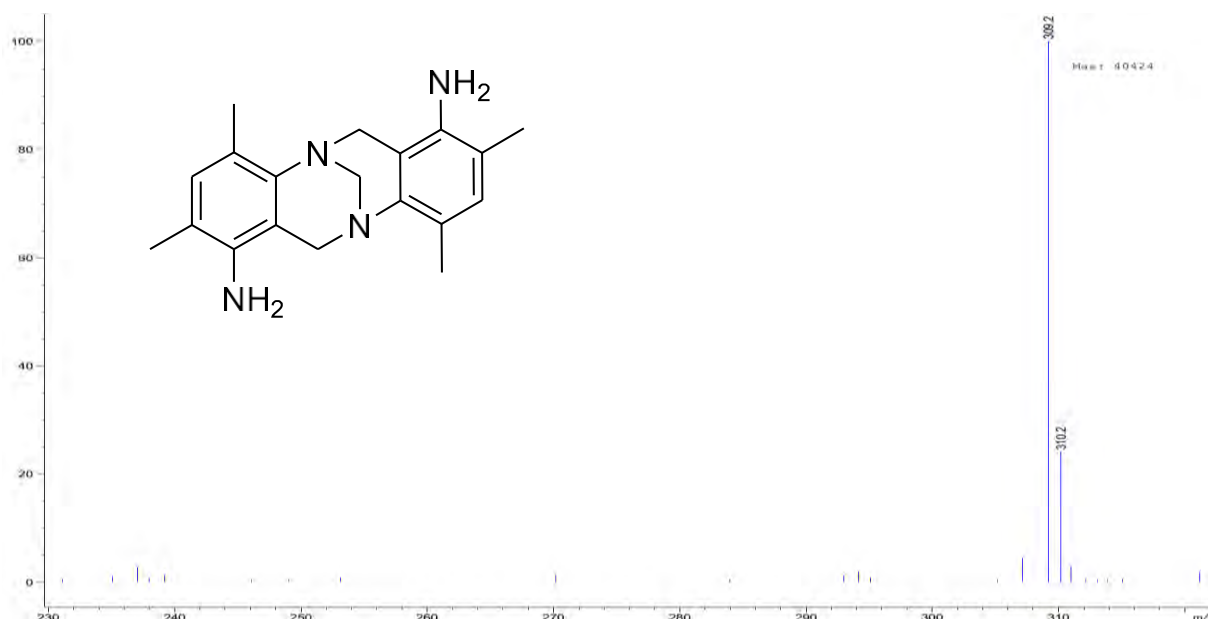
Compound 12, MS (ESI -)

13. Preparation and Purification of Compound (13)

2,4,8,10-tetramethyl-6H,12H-5,11-methanodibenzo[b,f][1,5]diazocine-1,7-diol



First, “2,4,8,10-tetramethyl-6H,12H-5,11-methanodibenzo[b,f][1,5]diazocine-1,7-diamine” was prepared according to the literature.⁴ MS (ESI +; EtOAc): m/z $[M + H]^+$ calcd for $[C_{19}H_{25}N_4]^+$: 309.20; found 309.2.



**2,4,8,10-tetramethyl-6H,12H-5,11-methanodibenzo[b,f][1,5]diazocine-1,7-diamine, MS
(ESI +)**

Afterwards, 2,4,8,10-tetramethyl-6H,12H-5,11-methanodibenzo [b,f][1,5] diazocine-1,7-diamine (0.60 g, 2.0 mmol, 1.0 eq.) was dissolved in H₂SO₄ (6.5%, 90 mL), and cooled down to -5°C. A sodium nitrite solution (0.30 g, 4.4 mmol, 2.2 eq.) in cold water (10 mL) was dropped into the reaction flask and stirred for 30 min at -5°C. Then, the solution's temperature was gradually raised until boil, by two hours (Attention: this step releases nitrogen gas; hence, rapid heating and sealing the container may lead to explosion). The reaction mixture was cooled down to r.t., its pH was adjusted to 5 (by adding 6–8 g of Na₂CO₃) and extracted with EtOAc (30ml x 5). The organic layers were combined, dried over MgSO₄ and evaporated until dryness to obtain the product as a white powder. Yield: 0.57 g (1.8 mmol, 92%). *R_f* = 0.5 (silica gel; MeOH–DCM, 8% v/v).

IR (neat): 3253, 2970, 1615, 1482, 1216, 1035, 870, 615 cm⁻¹.

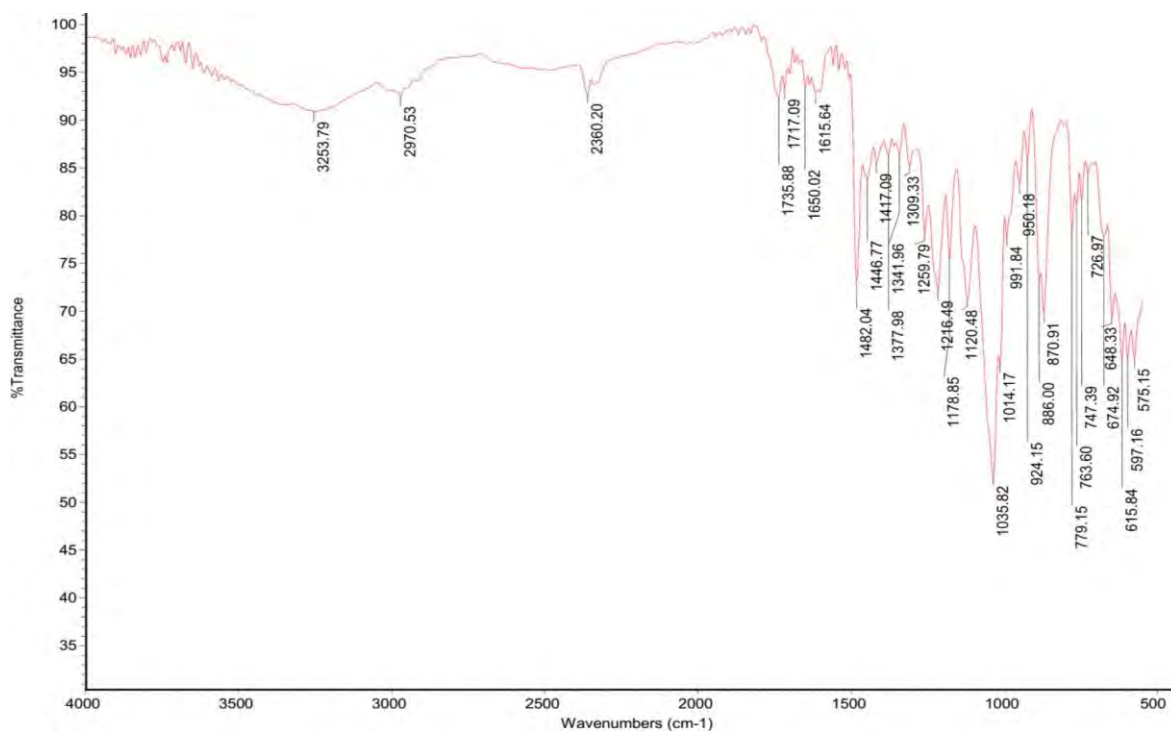
¹H NMR (400 MHz, DMSO-*d*₆): δ = 8.46 (s, 2H, OH), 6.89 (s, 2H, CH), 4.56 (s, 2H, NCH₂N), 4.44–4.48 (d, *J* = 17.0 Hz, 2H, CH₂), 4.08–4.04 (d, *J* = 17.2 Hz, 2H, CH₂), 2.29 (s, 6H, CH₃), 2.06 (s, 6H, CH₃).

¹³C NMR (100 MHz, DMSO-*d*₆): δ = 149.8, 146.7, 132.3, 131.3, 131.0, 122.1, 66.4, 51.2, 15.9, 15.9.

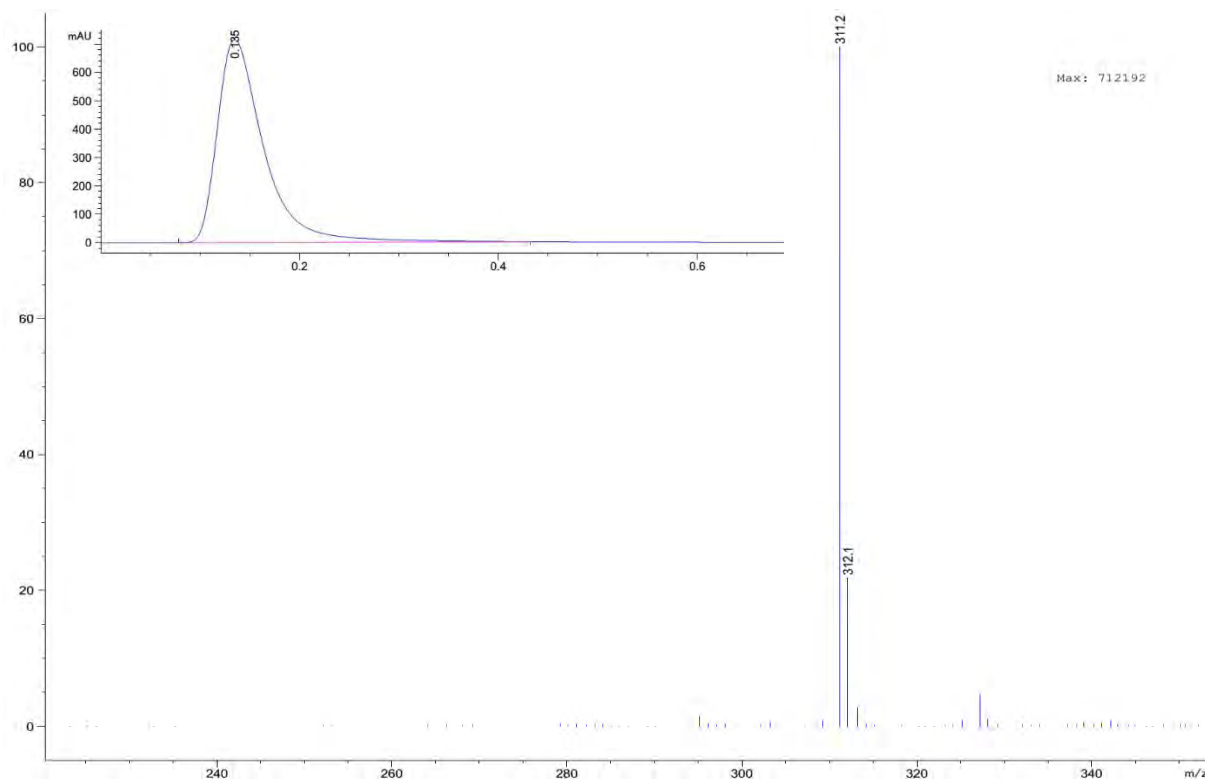
MS (ESI +; EtOAc): *m/z* [M + H]⁺ calcd for [C₁₉H₂₃N₂O₂]⁺: 311.17; found 311.2.

UV/Vis: (ACN): λ (lg ε) = 285 (3.563) nm.

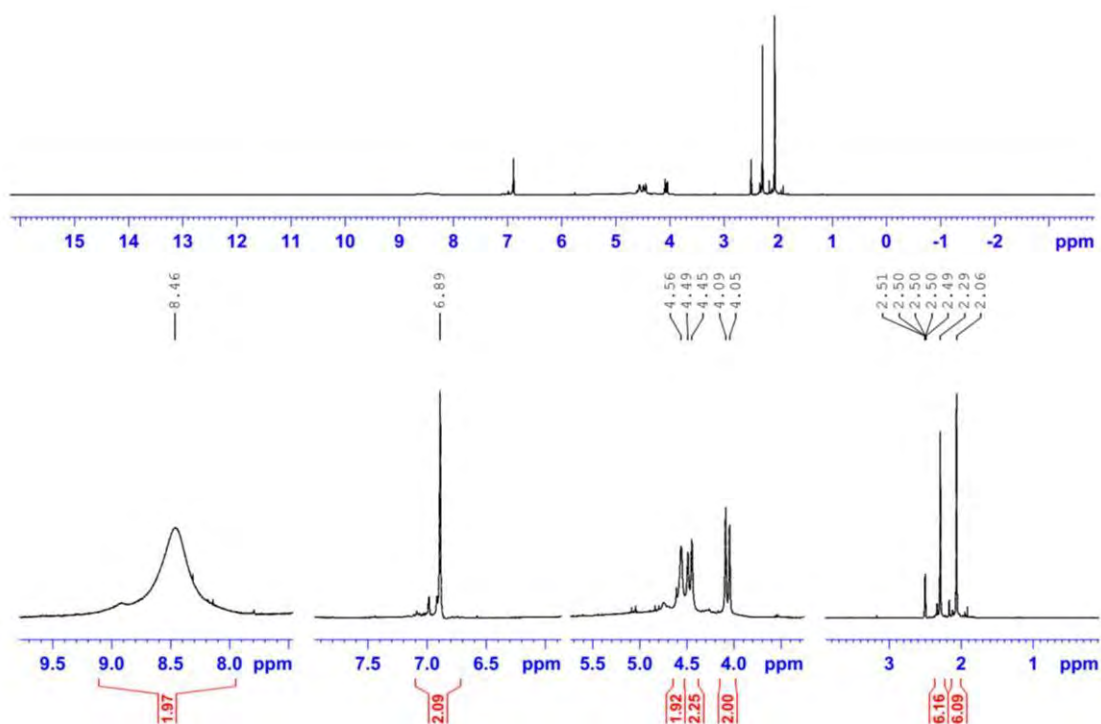
Anal. calcd for C₁₉H₂₂N₂O₂: C, 73.52; H, 7.14; N, 9.03. Found: C, 73.44; H, 6.96; N, 8.84.



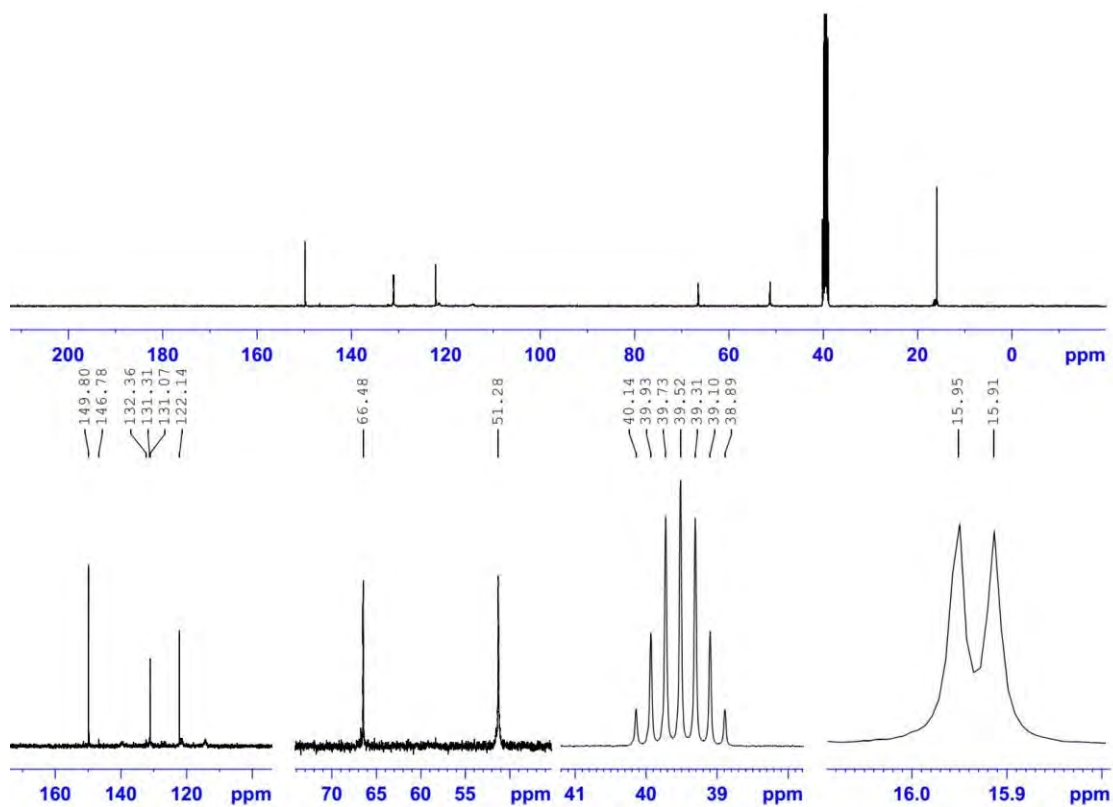
Compound 13, IR transmittance (neat)



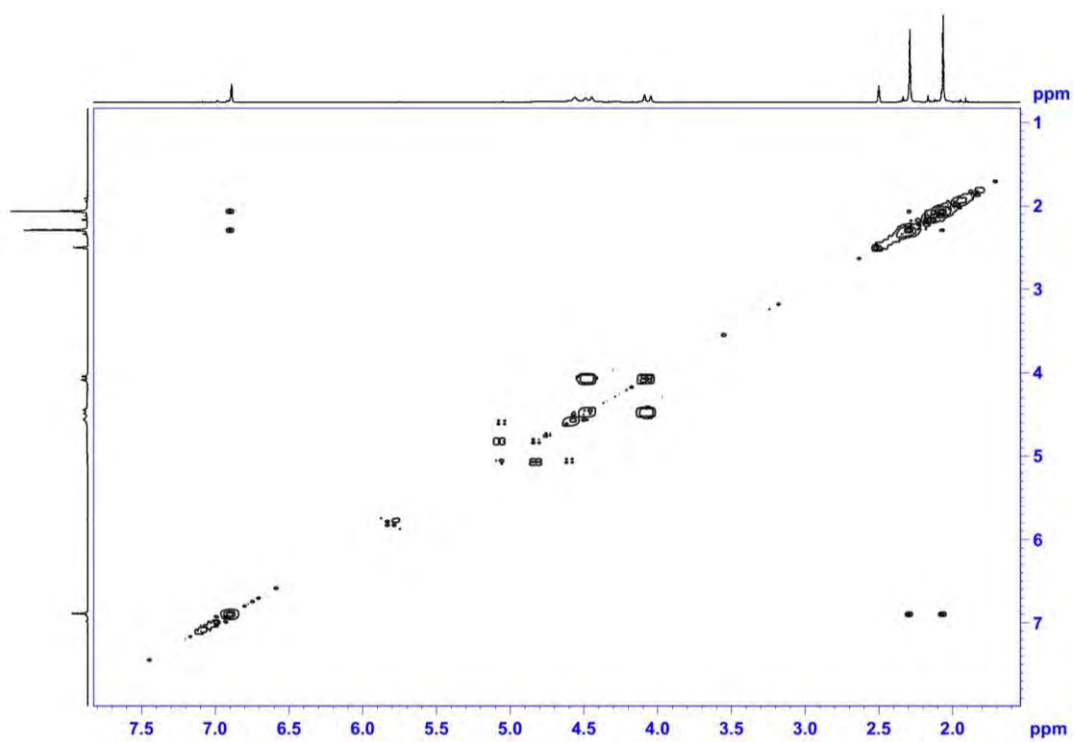
Compound 13, MS (ESI +)



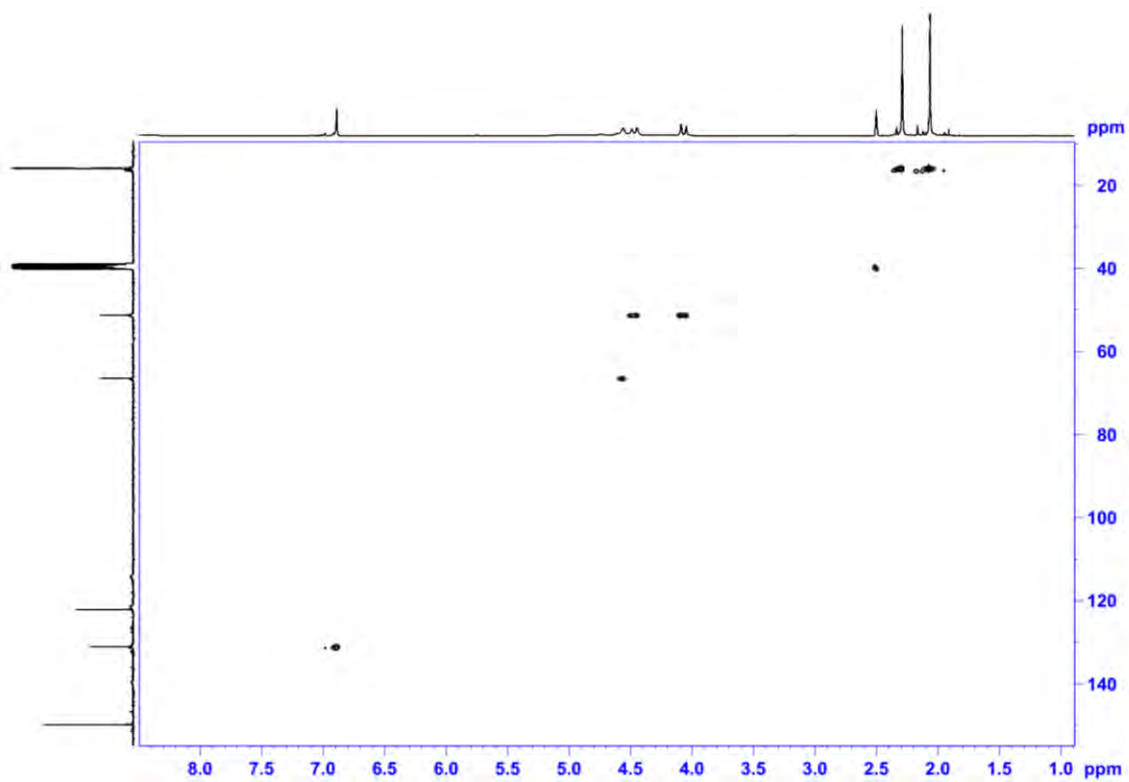
Compound 13, ¹H NMR (400 MHz, DMSO-*d*₆)



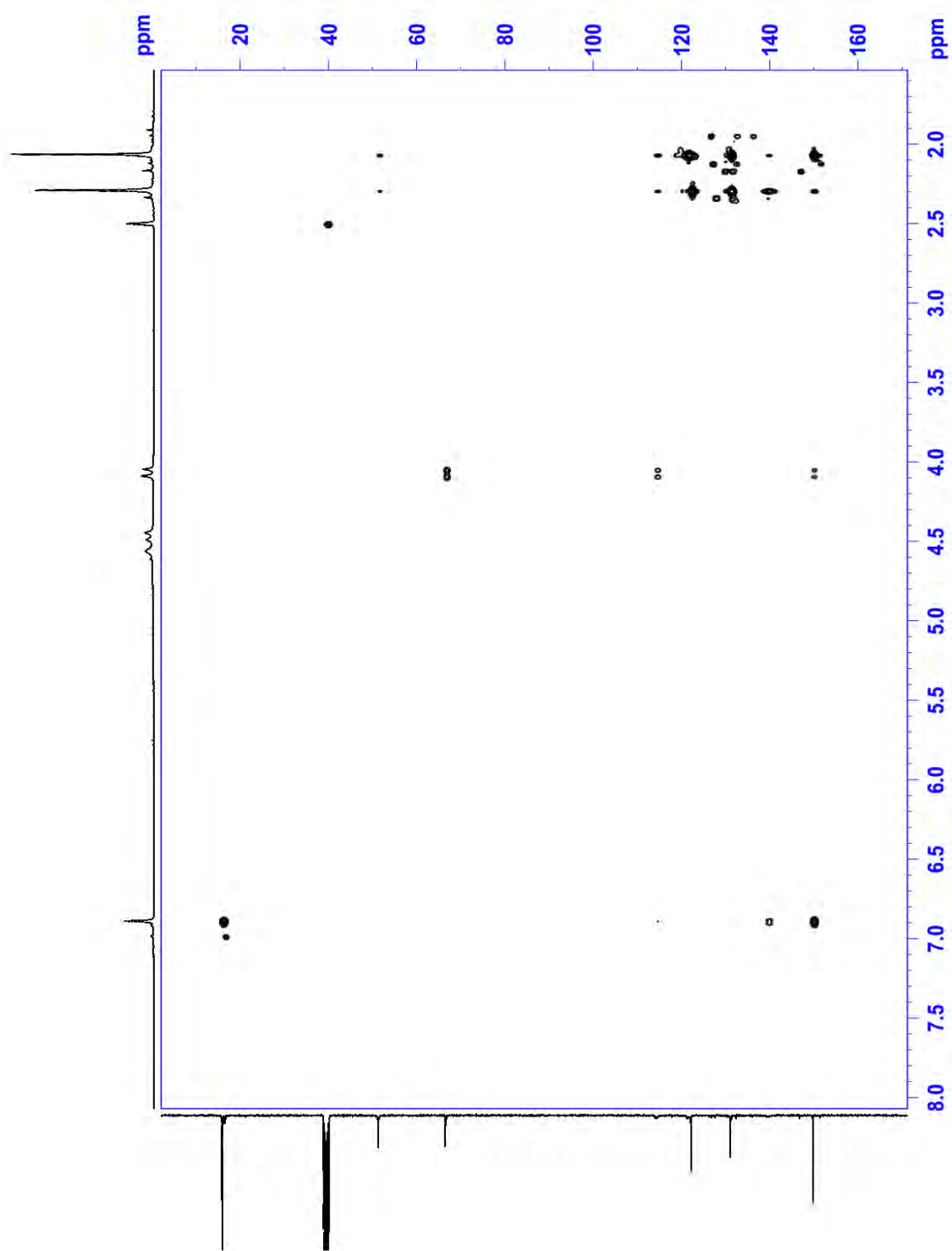
Compound 13, ¹³C NMR (100 MHz, DMSO-*d*₆)



Compound 13, COSY (DMSO- d_6)



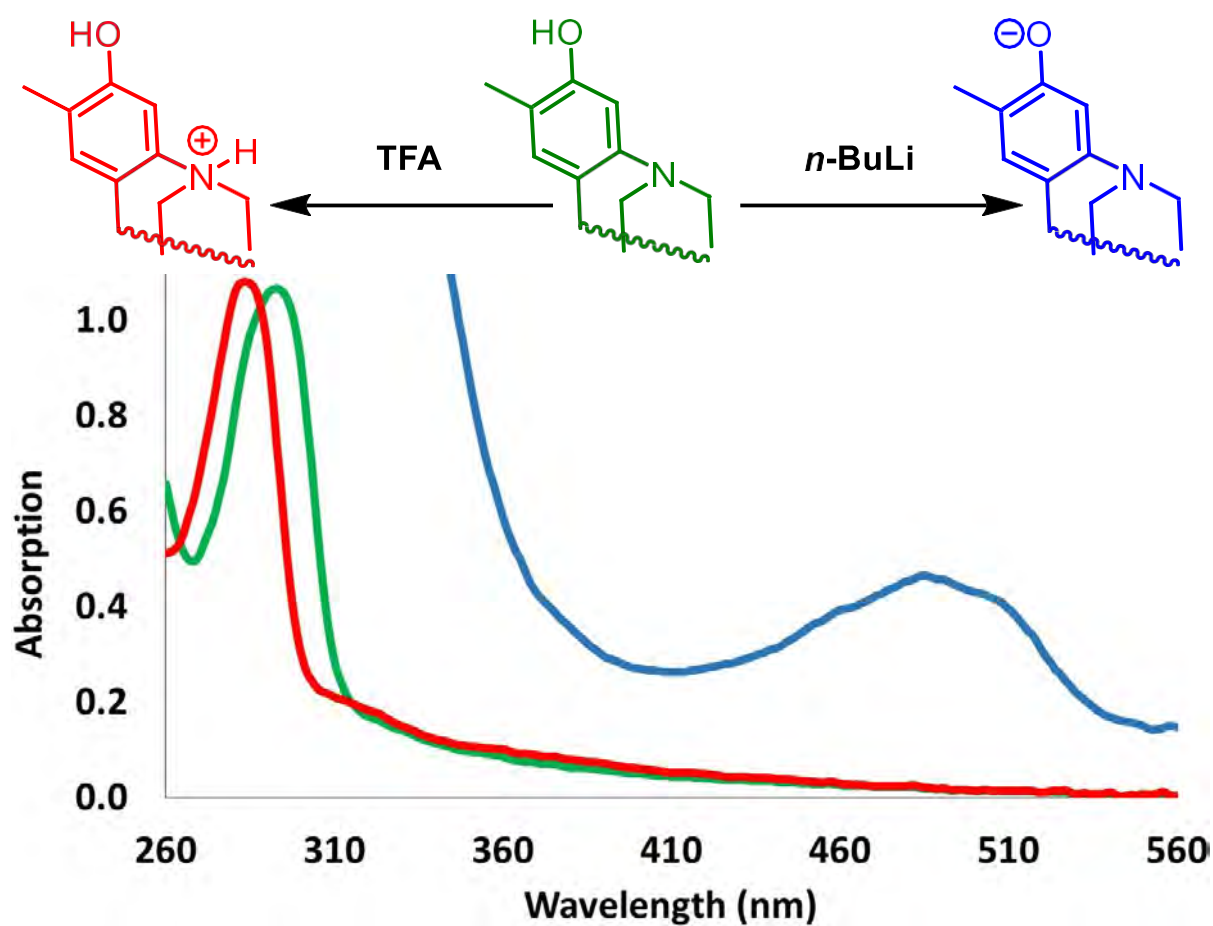
Compound 13, HSQC (DMSO- d_6)



Compound 13, HMBC(DMSO- d_6)

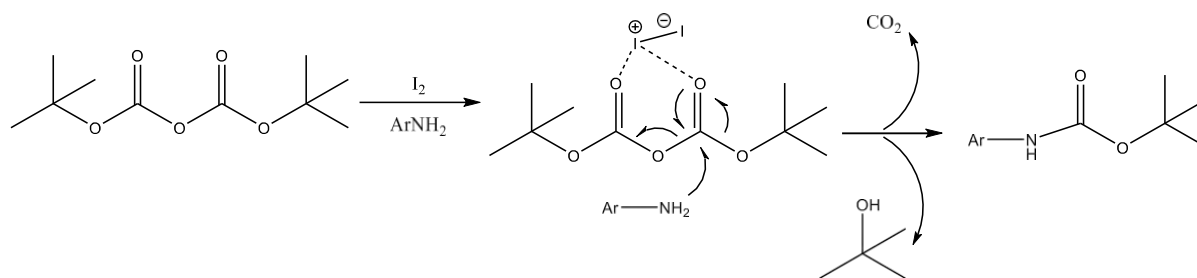
14. UV/Vis Studies of Compound (3)

2,8-dimethyl-6H,12H-5,11-methanodibenzo[b,f][1,5]diazocine-3,9-diol

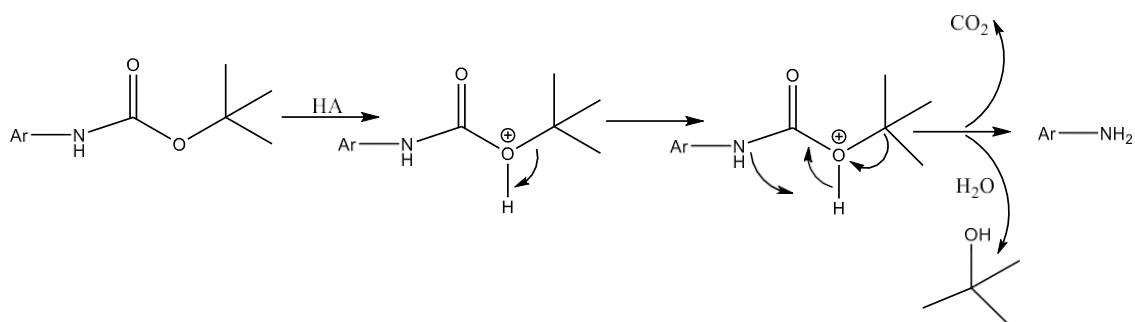


Compound 3, UV/Vis spectra in acetonitrile (in green), in the presence of TFA (in red), and in the presence of *n*-BuLi (in Blue).

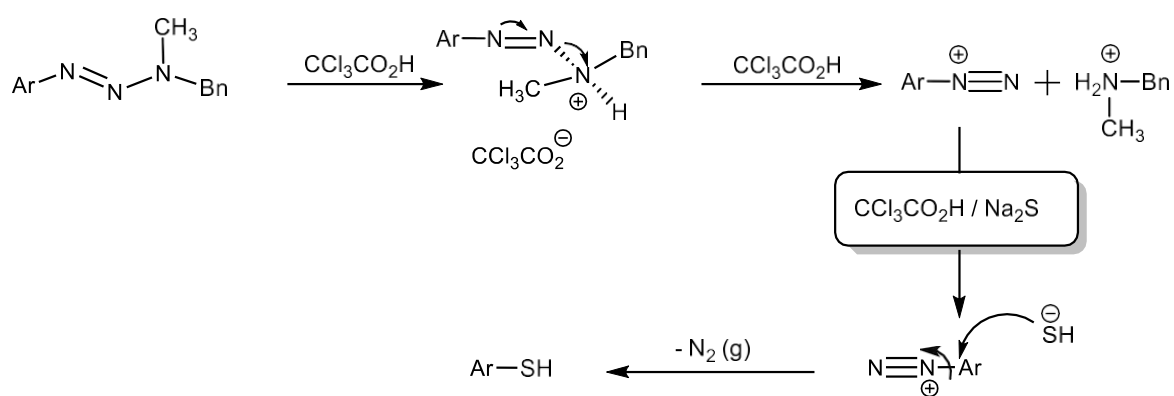
Relevant mechanisms



Iodine-catalyzed *N*-Boc protection ¹



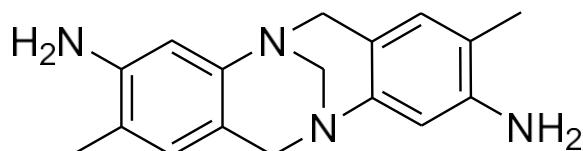
Acid-catalyzed *N*-Boc deprotection in aqueous solution ⁵



Acid-catalyzed cleavage of triazene and its transformation to thiophenol ⁶

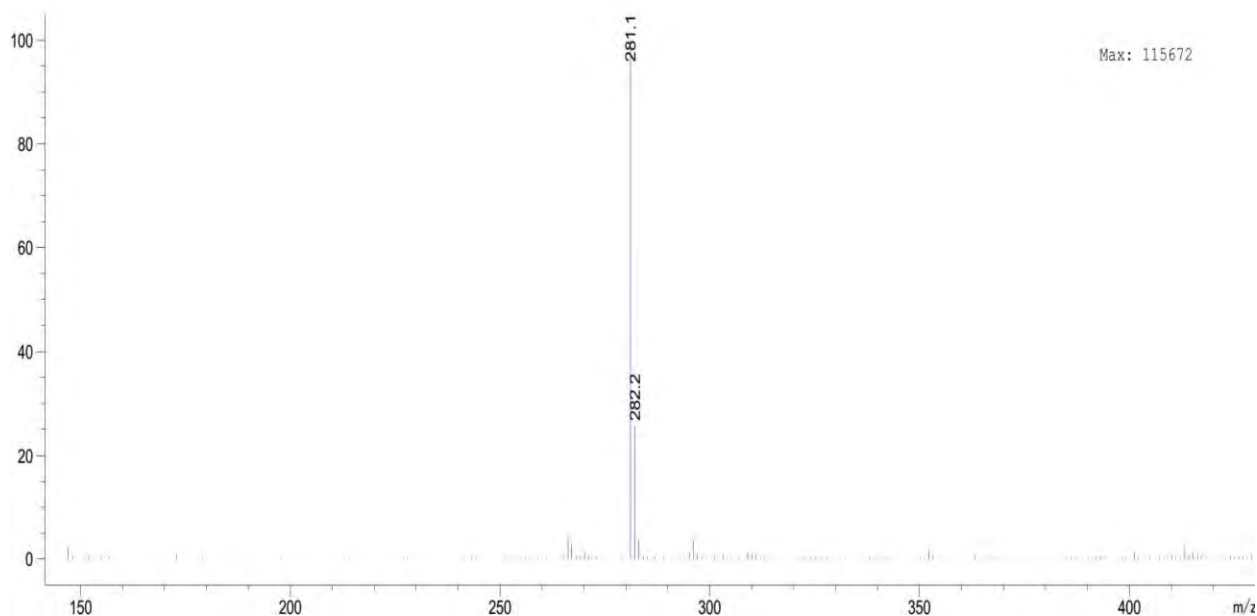
Starting materials

15. Hünlich's base preparation

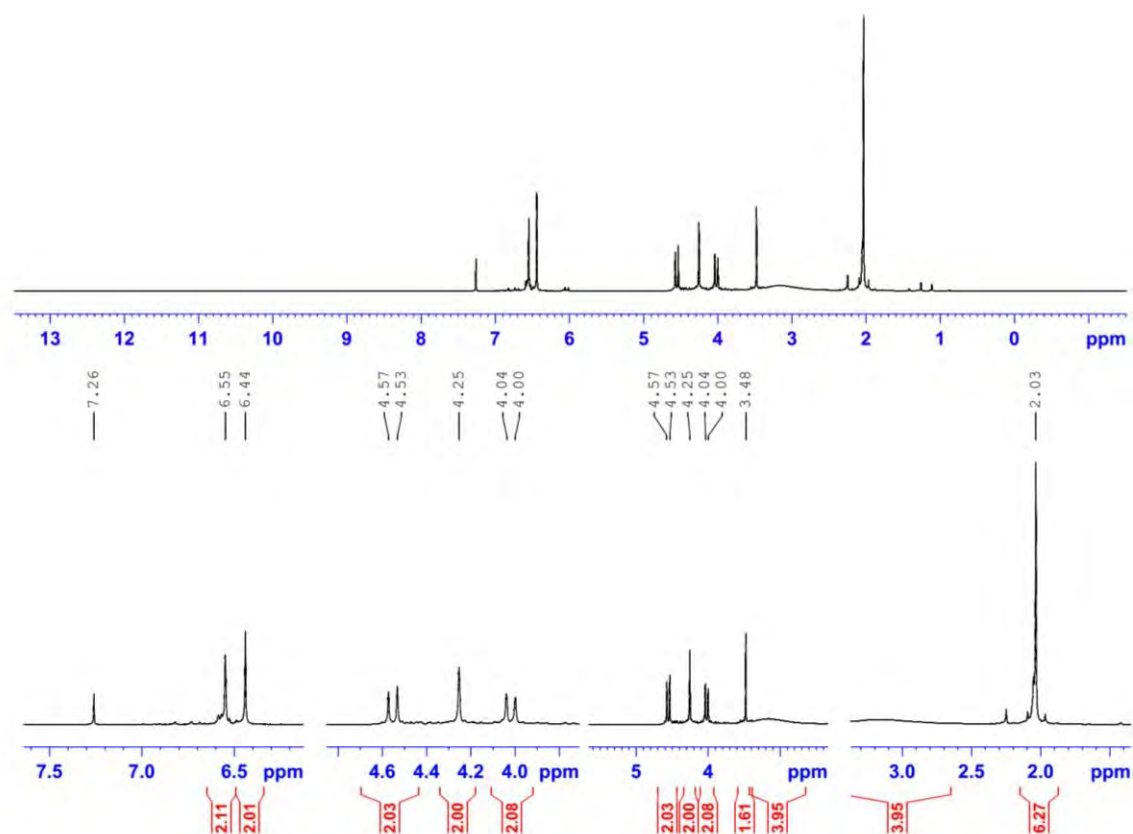


Hünlich's base was prepared according to a previous report.⁷

¹H NMR (400 MHz, CDCl₃ – CD₃OD, 2:1): δ = 6.55 (s, 2 H, CH), 6.44 (s, 2 H, CH), 4.53–4.57 (d, J = 16.2 Hz, 2 H, CH₂), 4.25 (s, 2 H, NCH₂N), 4.00–4.04 (d, J = 16.3 Hz, 2 H, CH₂), 2.35–3.45 (br, 4 H, NH₂), 2.03 (s, 6 H, CH₃). MS (ESI +; MeOH): m/z [M + H]⁺ calcd for [C₁₇H₂₁N₄]⁺: 281.17; found: 281.1 and 282.2.

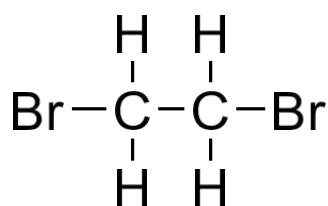


Hünlich's base, MS (ESI +)



Hünlich's base, ^1H NMR (400 MHz, $\text{CDCl}_3 - \text{CD}_3\text{OD}$, 2:1 v/v)

16. 1,2-dibromoethane



Bromine (200.0 g, 1.25 mol) was cooled down to -5°C into a reactor equipped with a stirring magnet bar, condenser, and thermometer. A constant stream of ethylene gas was gently injected, by immersing a gas distribution tube, into the bromine. This process continued for 40-60 min until achieving a total discolouration of the bromine and seeing the crude starts freezing. The obtained yellowish liquid was then rinsed by NaOH (1M, 100 ml X 3), saturated sodium thiosulfate solution (20 ml), and then dried over MgSO_4 and filtered. The obtained colourless liquid was then distilled twice and passed through a column filled with anhydrous NaHCO_3 before bottling it in an amber glass bottle and tightly sealing its cap.

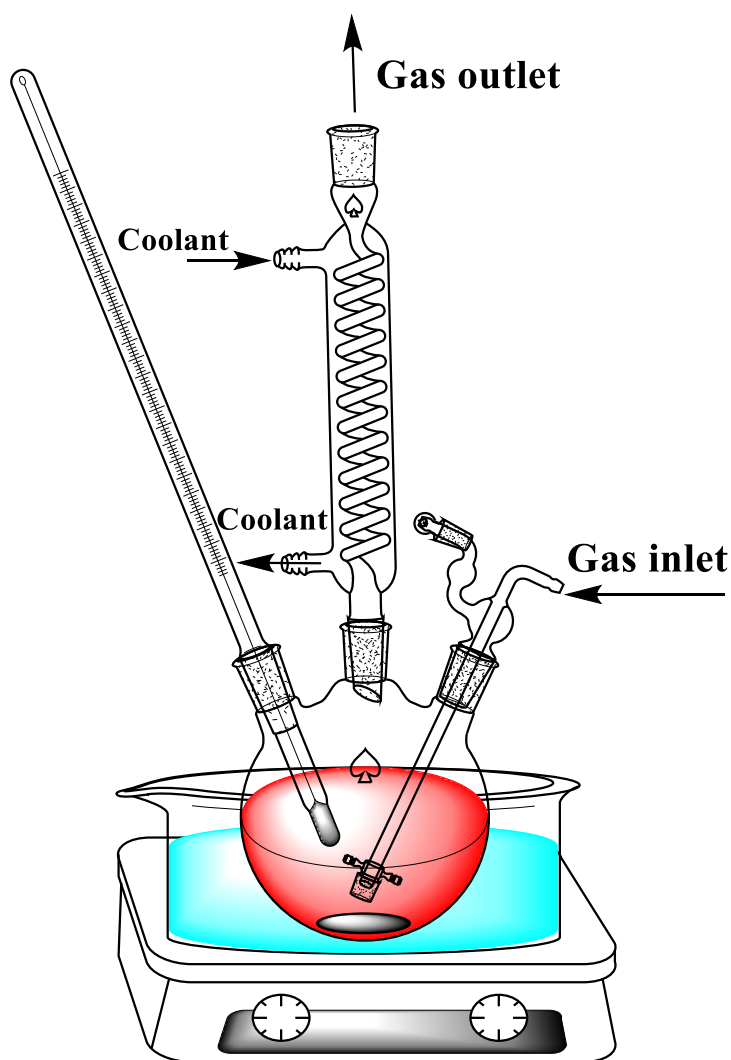
Notification: This reaction is extremely exothermic and the flow of the gas should be very slow to avoid bumping and boiling the bromine over. Using appropriate gas-mask and adequate ventilation are crucial.

Yield: 214.16 g (1.14 mol, 91%); R_f : N/A.

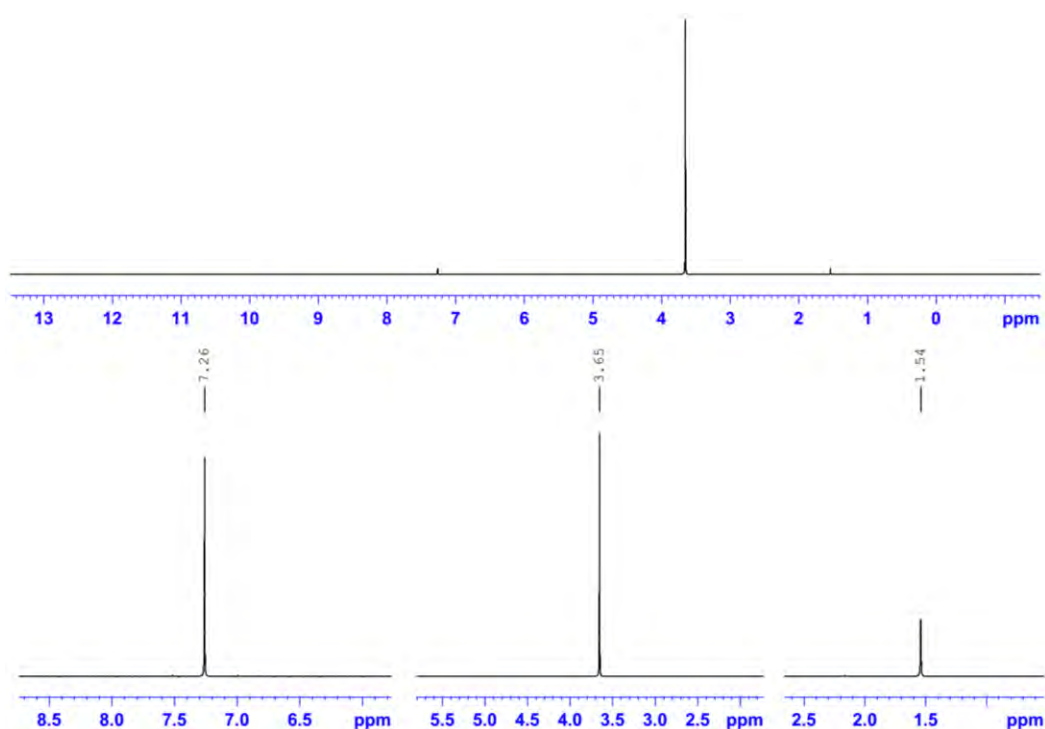
^1H NMR (400 MHz, CDCl_3): $\delta = 3.65$ (s, CH_2).

MS: m/z $[\text{M} - \text{Br}]^+$ calcd for $[\text{C}_2\text{H}_4\text{Br}]^+$: 106.96, found 106.95.

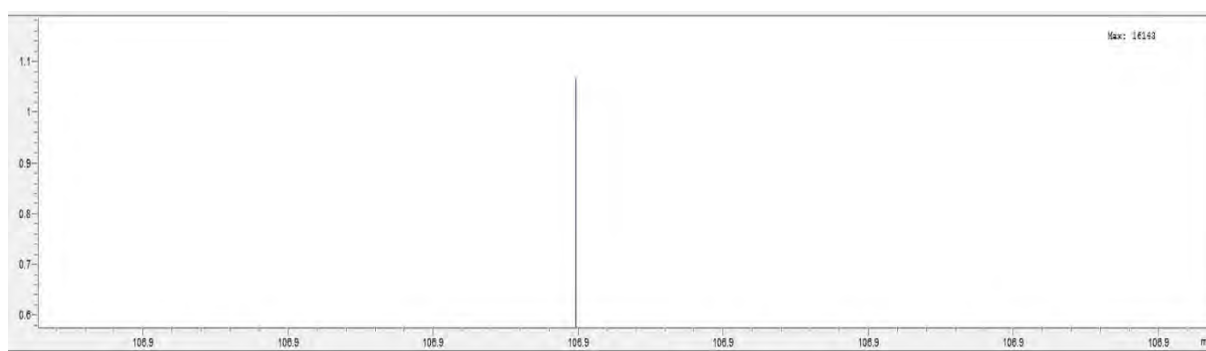
Boiling point: $131 \pm 1^\circ\text{C}$, Melting point: $9.5 \pm 0.2^\circ\text{C}$.



Bromination reactor



1, 2-Dibromoethane, ^1H NMR (400 MHz, CDCl_3)



1, 2-Dibromoethane, MS

References

- (1) Varala, R.; Nuvula, S.; Adapa, S. R. *J. Org. Chem.* **2006**, 71, 8283.
- (2) Kazem-Rostami, M. *Synthesis* **2017**, 49, 1214.
- (3) Mahon, A. B.; Craig, D. C.; Try, A. C. *Arkivoc* **2008**, 12, 148.
- (4) Bhuiyan, M. D. H.; Mahon, A. B.; Jensen, P.; Clegg, J. K.; Try, A. C. *Eur. J. Org. Chem.* **2009**, 2009, 687.
- (5) Zinelaabidine, C.; Souad, O.; Zoubir, J.; Malika, B.; Nour-Eddine, A. *Int. J. Chem.* **2012**, 4, 73.
- (6) Khazaei, A.; Kazem-Rostami, M.; Moosavi-Zare, A. R.; Bayat, M.; Saednia, S. *Synlett* **2012**, 23, 1893.
- (7) Rigol, S.; Beyer, L.; Hennig, L.; Sieler, J.; Giannis, A. *Org. Lett.* **2013**, 15, 1418.

Significance and future directions

This project describes the synthesis of a new family of azo-carrying TBAs that can act as molecular photo-switches. The unique Λ -shaped structure of the obtained products, which possess two abreast photo-isomerisable groups, gives them special features that could be of interest in the field of molecular recognition⁵⁻¹² studies, the design of light-driven molecular machines, chiral light-responsive LC dopants, and photo-alignment agents. Some features and possible applications of these novel materials are elaborated in the following subsections by the existing examples found in the chemical literature.

Photo-alignment agents

The synthesised azo-carrying TBAs have two azo groups that are in the plane with the aromatic moieties of the TB scaffold (Figure 34). This planar positioning is anticipated to elongate the Λ -shaped structure of the TB scaffold and facilitate the resonance between the aromatic rings of each side separately (Figure 34). According to the descriptions previously given in Section 2.1.4, and the bisazo examples (shown in Figure 12 and Figure 14), it was postulated that bisazo carrying TBAs as the main products of this thesis may exhibit interesting photo-alignment properties owing to the azo groups positioned perpendicularly to one another (Figure 35). This provides fewer degrees of freedom and hence may provide a better photo-alignment than planar and single chromophore carrying azo molecules.

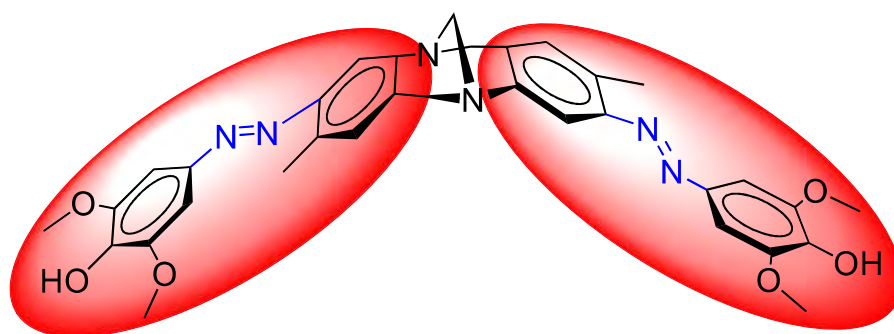


Figure 34 A typical example of the Λ -shaped products having two oscillators in a roughly perpendicular angle

These Λ -shaped products may form more limited intermolecular interactions and π -stacking, due to the bent shape of the molecule; hence, solidification within the LC phase is less probable. Furthermore, these products each carry two azo groups, which will likely confer a stronger response to the stimuli (Figure 35).

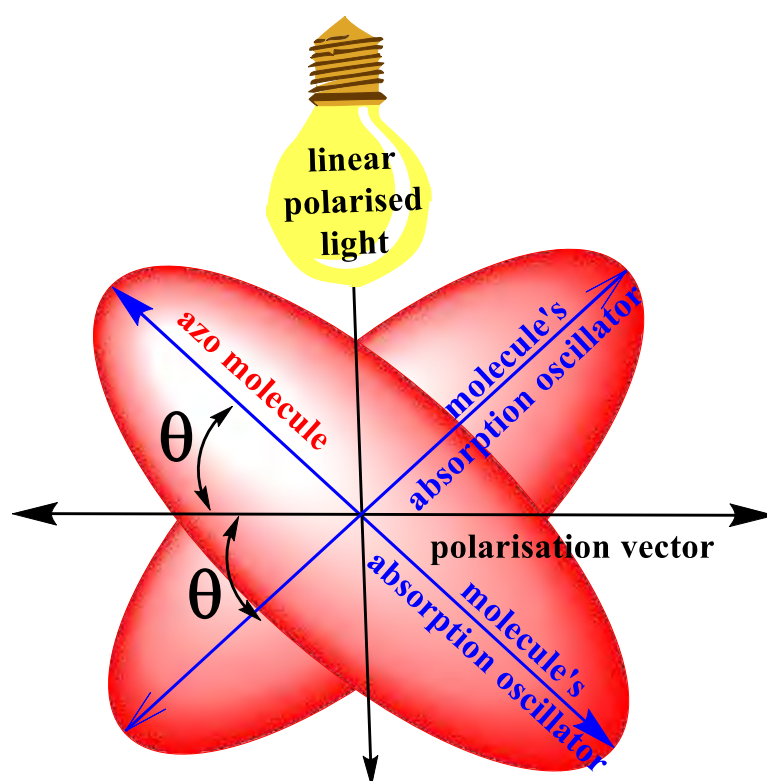


Figure 35 A schematic view of the crossed oscillators and the polarisation vector

The unique shape of azo-carrying TBAs (Figure 34) suggests a new possibility for azo materials application in LC photo-alignment. Additional details of this topic are beyond the scope of this thesis.

Photo-responsive elastomers

Photo-responsive¹⁷⁵ groups have been added in the structure of LC elastomers¹⁷⁶ to contribute to the design of light-driven artificial muscles.^{54-56, 176, 177} For example in Figure 36,¹⁷⁸ a thin polymeric film consisting of azo groups is illuminated by a linearly polarised light source whose polarisation direction is variable. This results in a selective photo-isomerisation of the azo groups in a specific domain and consequently a directed deformation of the film. In this example of light-driven deformation of the LC network (Figure 36),¹⁷⁸ azo molecules **1** and **2** are used in the preparation of the film as the LC monomer and a cross-linker, respectively. Changing the direction of the polarised light source, shown as the white arrows in Figure 36, results in differently bent forms of the film. To accelerate the back isomerisation, a longer wavelength of light (540 nm) is used in this example, which eventually flattens the film.

The following reactions shown in Figure 37 can simply provide the desired monomers for the design of new photo-responsive elastomers consisting TBAs. These materials may provide a more specific and intense response due to the existence of two switching units per molecule. The desired switchable monomers can be directly produced by reacting **1** and **13** (introduced in Paper I) with acryloyl chloride and a base, respectively (Figure 37).

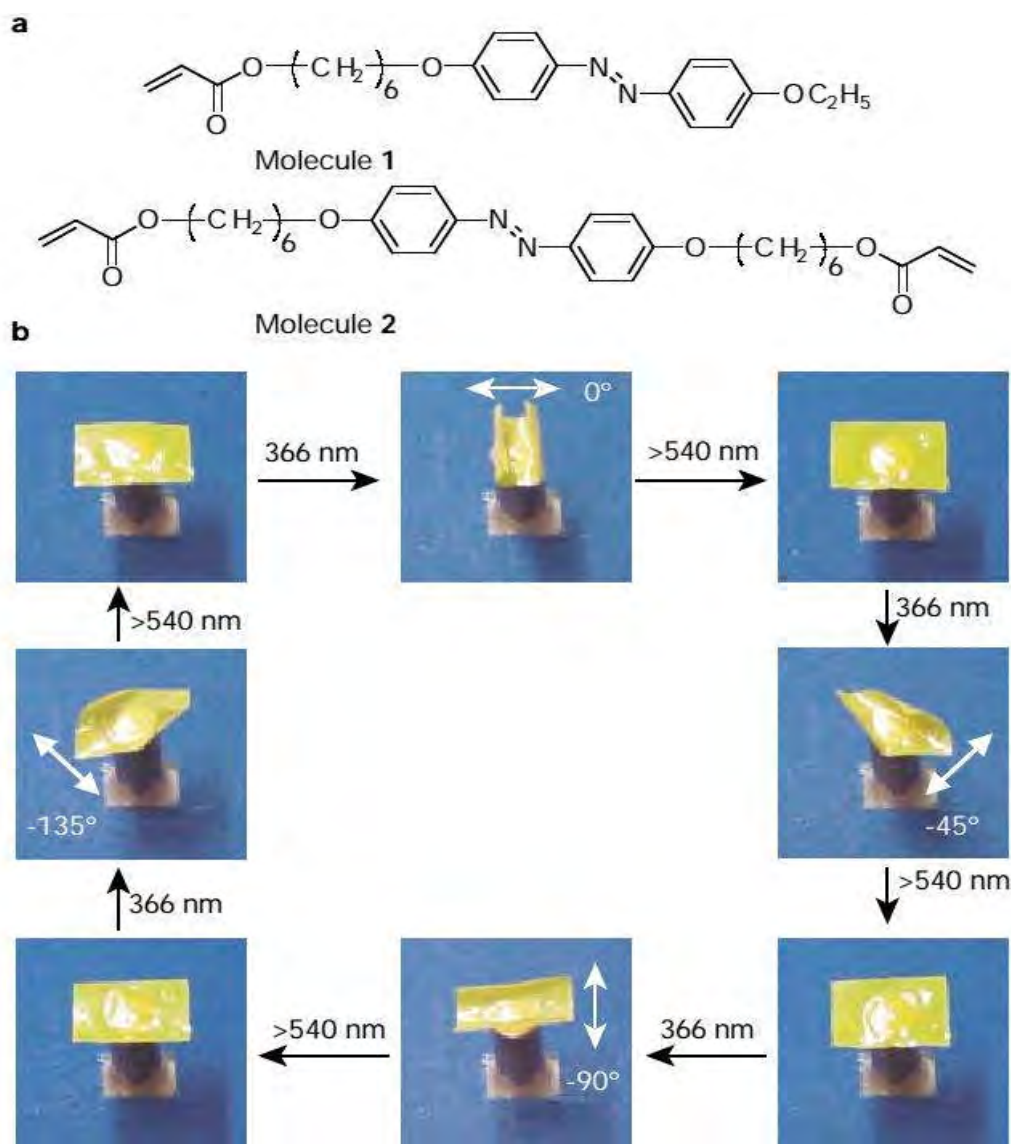


Figure 36 Light-driven deformation of a polymeric LC network¹⁷⁸

To modify the monomers' geometries and their response to the light, compounds **1–9** (Paper II) might be used instead of **1** (Paper I). In addition, compounds **8** and **9** (Paper III) and the other new ethano-strapped building blocks (introduced in Paper III) may change the porosity and the intermolecular interactions of the obtained elastomers owing to the tightened dihedral angle (Table 5) of the modified TB scaffold. Furthermore, using compounds **14** and **15** instead of **13** (Paper I) can provide more flexible elastomers. The building blocks introduced *via* this thesis provide a broad range of possibilities to design novel photo-responsive elastomers and multifunctional enes.^{179, 180}

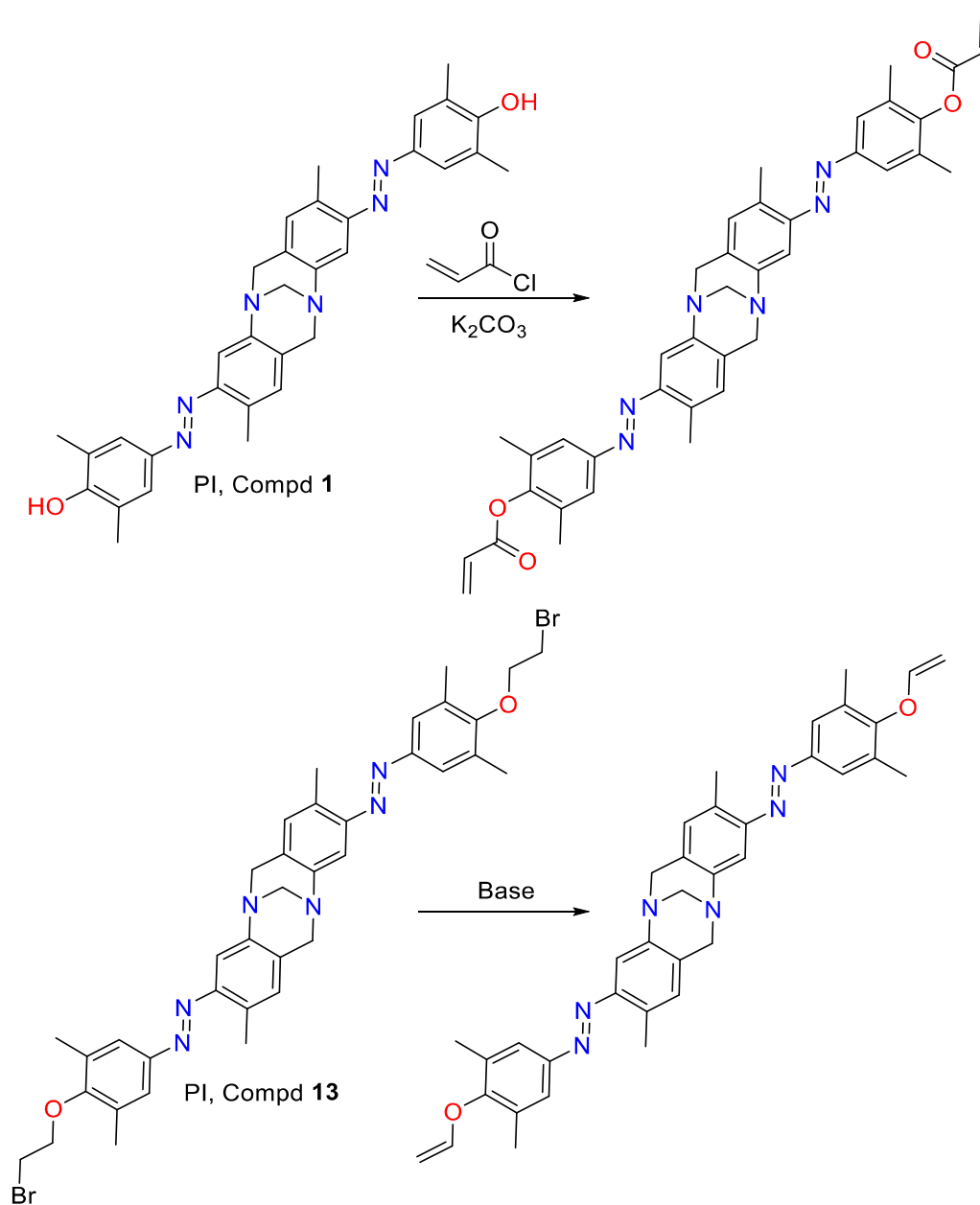


Figure 37 Suggested compounds for photo-driven elastomers design

Design of light-driven machines

Azo compounds, owing to their reversible and efficient photo-isomerisation, have been utilised in the design of photo-driven machines, namely photo-mobiles, and photo-responsive actuators.^{115, 177} Figure 38 displays an azo compound that is employed in the preparation of a polymeric film. This film is introduced as a light-driven poly belt (displayed

in Figure 38) by the corresponding references.^{181, 182} This belt deforms upon illumination by certain wavelengths of light and this results in a momentum that spins the pulleys (Figure 38).

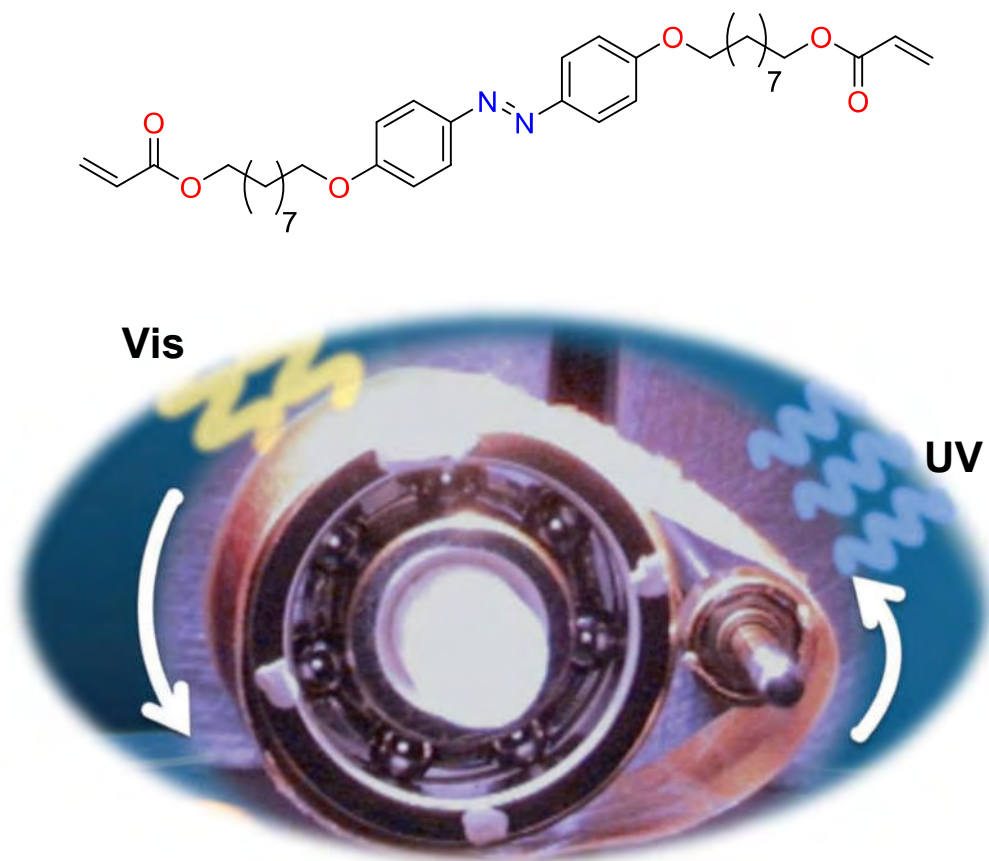


Figure 38 A light-driven liquid-crystalline elastomer namely, plastic photo-mobile^{181, 182}

Most of the new products introduced in this thesis, due to their unique molecular geometry and properties, can be used in the design of light-driven machines. For instance, products **13–15** in Paper I can be easily copolymerised with diols, diamines, dithiols, or even compounds **2**, **3**, **10**, **11**, and **13** introduced in Paper III, to form the corresponding photo-responsive copolymers.^{85, 183} Compounds **1** in Paper I, **1–9** in Paper II, and **6** and **8** in Paper III can be copolymerised with the mole-equivalent of alkyl-dibromides or alkyl-diiodides to form novel photo-responsive copolymers (Figure 39, bottom). These linear polymer chains can be used in the design of new photo-responsive elastomers.

In Paper I the ratio of the TBA **1** to the alkyl dibromides was almost 1:2 and as a result, compounds **13–15** were obtained as the main products in Paper I (Figure 39, top). A mole-equivalent of TBA to alkyl dibromides may guide the alkylation toward polymerisation as shown at the bottom of Figure 39.

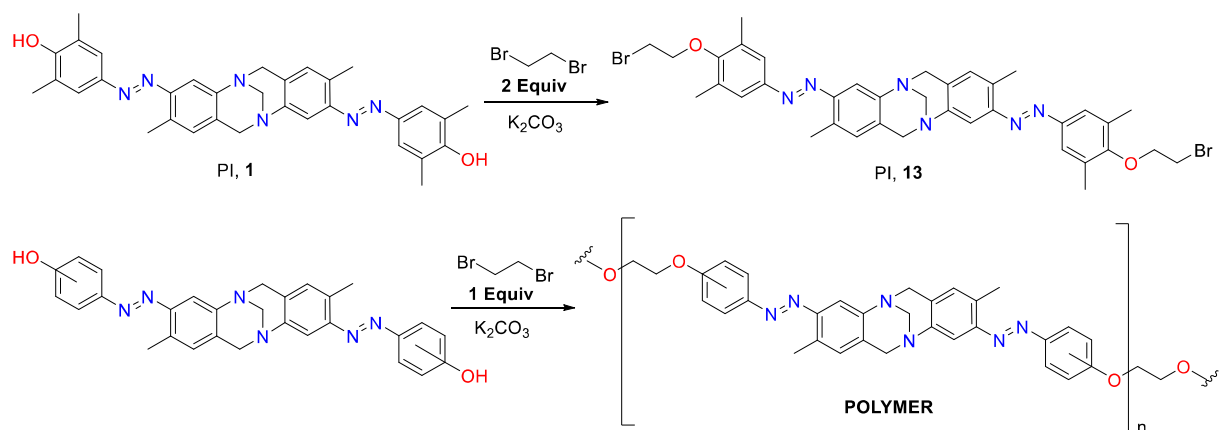


Figure 39 Copolymerisation of azo-carrying TBAs

Design of light-driven molecular machines

Azo compounds, owing to their efficient photo-isomerisation and the predictable molecular geometries of their photo-isomers, have been utilised in the design of molecule-sized hinges.¹⁸⁴ The photo-isomerisation of the azo group fulfils the opening or closing function of the hinge. The following example shown in Figure 40 depicts how a bis-azo compound can be utilised as a molecular photo-switchable hinge.

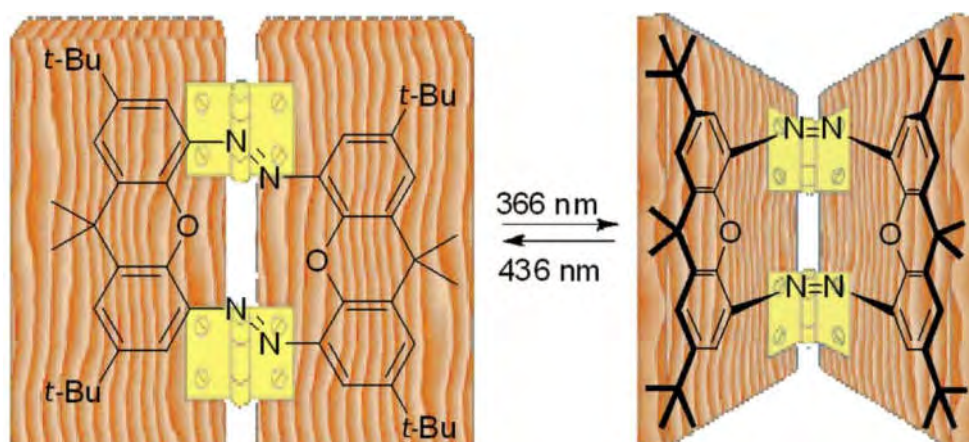


Figure 40 A typical bis-azo molecular hinge¹⁸⁴

The addition of photo-switchable groups to the TB scaffold resembles the main structure of a pincer made at the molecular scale. The claws of the pincer, which are the azo groups, start working upon receiving a certain wavelength of light. The movement of the claws can be controlled by photo-isomerising the azo groups (Figure 34). The photo-isomerisation of azo groups converts the thermally-stable photo-isomer the *trans* to the *cis* when the compound is illuminated by UV-light (Figure 18). Then, back-isomerisation gradually converts the *cis* isomer to the *trans* form by undertaking thermal relaxation or more quickly when exposing the sample to a longer wavelength of light (within the visible range). When a bis-azo TBA is attached to other molecules, e.g. peptides, the movement of the azo groups would resemble a Λ -shaped hinge (Figure 41). This phenomenon is elaborated within the following sections and Paper II.

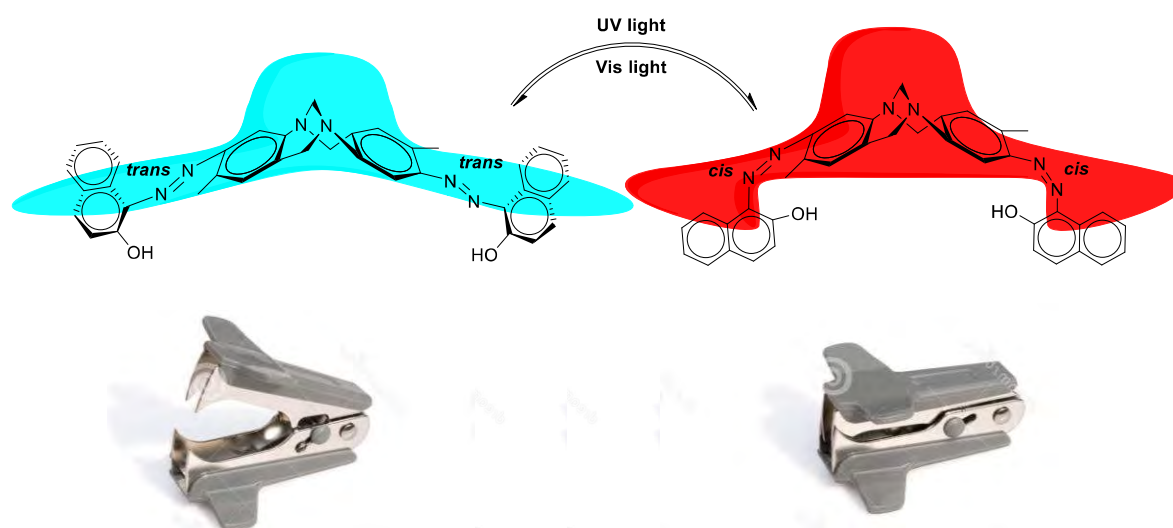


Figure 41 Hinge-like feature of azo-carrying TBAs

Smart drug delivery systems

Azo compounds have also been used in the design of smart molecular gates owing to their repeatable and reversible photo-isomerisation. These gates can control the release of drugs, antigens or even ions (Figure 42).^{185, 186}

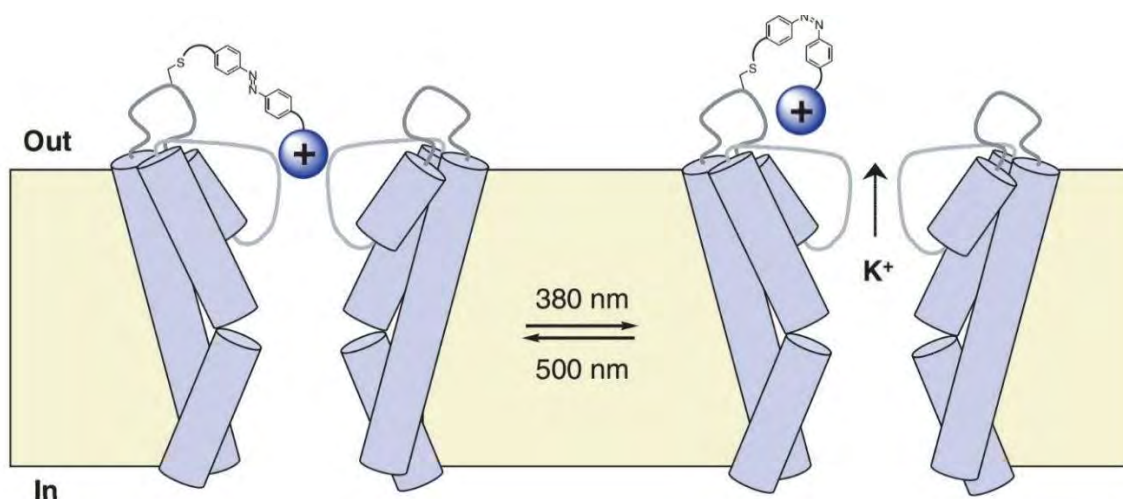


Figure 42 A photo-switchable ion-channel^{185, 186}

The azo products introduced in this project, owing to their unique molecular geometry and properties, are anticipated to be useful as photo-switchable gates.^{115, 185, 187} These should be easily attached to various surfaces/structures from their reactive and modifiable extremities (Figure 43).^{14, 122} These extremities should be easily modified to match the reactivity of TBAs for their convenient assembly on larger molecules or structures. These modifications are comprehensively explained within Research Chapters One and Three; for instance, thiophenol and bis-triazene-carrying TBAs can even be attached to various surfaces like gold,^{188, 189} graphene,¹⁹⁰ polymer,^{179, 191} silica/glass,¹⁹² and others.⁶⁸

In addition, the modification of the diazocine bridge (Table 5) may provide further attachment sites.^{2, 193-195} Hence, these molecules can be readily attached to porphyrins, peptides, DNA, nanotubes, fullerenes,¹⁵²⁻¹⁵⁸ or even polymers to contribute to the design of novel light-driven gates or smart drug-delivery systems.^{14, 122} For instance, the following example describes a potential use of such material, *e.g.* **13** introduced in Paper I (Figure 43 and Figure 44).

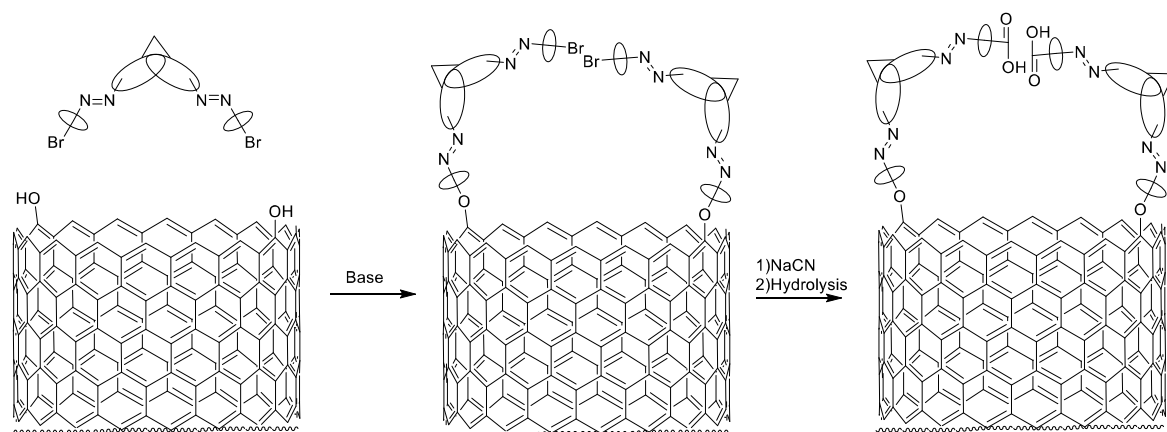


Figure 43 The assembly of light-triggered gates

Figure 43 displays how a bis-azo-carrying TBA (Paper I, **13**) could be attached to a functionalised carbon nanotube by a simple etherification reaction. Afterwards, the remaining alkyl halides could be replaced by cyano groups through a nucleophilic substitution reaction. The cyano group could be hydrolysed and converted to a carboxylic acid, which should be capable of forming hydrogen-bond interactions and holding the gate components paired (Figure 44, left). Therefore, the dark incubated azo groups should remain in the *trans* form, which elongates the V-shaped structure of the TB scaffold and hence keeps the gate closed (Figure 44, left). The illumination of the azo groups turns them from the *trans* to the *cis* form. This action should impair the gate components and open the gate by holding the aromatic moieties twisted (Figure 44, right).

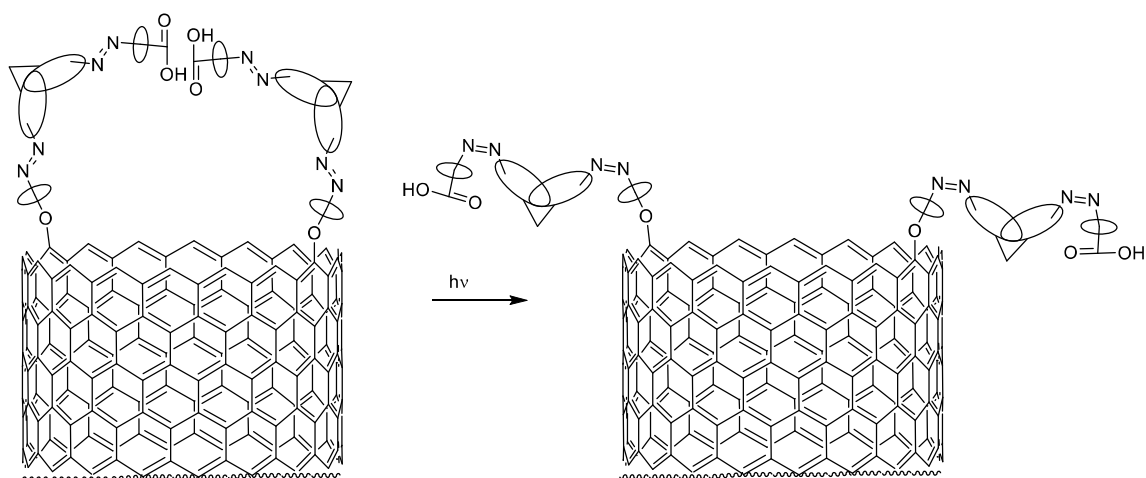


Figure 44 Light-triggered gates in action

Molecular recognition

In molecular recognition experiments, azo compounds are often used in their *cis* form to tighten their grip on the targeted molecules¹⁹⁶ and obviously the unstable *cis* form has to undergo back-isomerisation (Figure 45). This relaxation may cause complexity of the studies and less efficiency due to fact that the major population of the molecules are normally in the *trans* form.

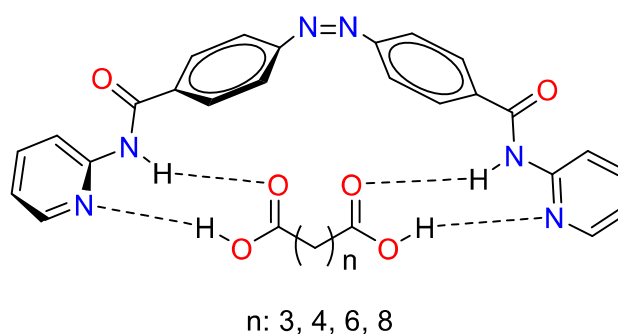


Figure 45 The *cis* photo-isomer provides a grip
Adapted from prof. S. Goswami's pioneering studies in 1999¹⁹⁶

The presented products in this work obviously provide a unique grip as the TB scaffold dictates their spatial Λ -shaped feature (Figure 24). Various products presented in this project have interactive/modifiable extremities. They are capable of forming intermolecular hydrogen-bond interactions and hosting other molecules in their Λ -shaped voids (Figure 24). This phenomenon was earlier elaborated on in the introduction section due to the fact that the Λ -shaped scaffold of TBAs possess a void that can host smaller molecules inside and hence has been used in molecular recognition studies.⁵⁻¹²

In Research Chapter Two, various substituted phenols were coupled with a bis-diazonium-carrying building block to obtain a set of molecular switches with different sizes of the void and differently positioned substituents in or around it. Therefore, these products may

selectively host and respond to different molecules. The second paper and Appendices 2 – 4 display the corresponding products in more detail. The host-guest chemistry of these products will be studied in the future.

Design of membranes and polymers

In addition to the TBA-carrying membranes^{159, 163, 164} listed in Section 3.2.2, triazenes are found in the chemical literature employed in the design of various membranes.^{24, 197-199} Triazene-carrying membranes can be used for the selective detection of cations, *e.g.* mercury (II) or platinum (II) ions (Figure 46).^{21, 24, 197}

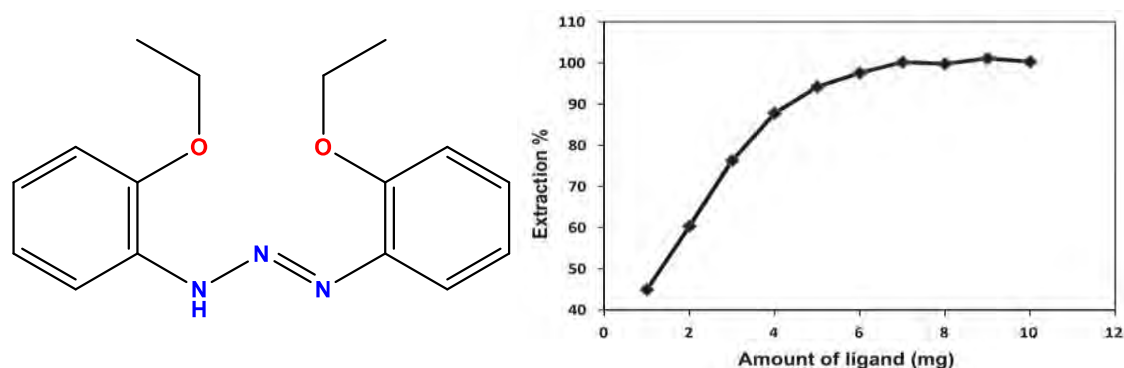


Figure 46 The chemical structure of a triazene-based ligand and its dosage effect on the performance of an ion-selective membrane¹⁹⁷

These two concepts encouraged the design of the very first triazene-carrying TBA (Figure 47, top) in this thesis reported as compound **1** in the third paper. Triazene-carrying TBAs may be able to coordinate large cationic molecules selectively by hosting them in the TB scaffold's void (Figure 47, shown in the 3D images).

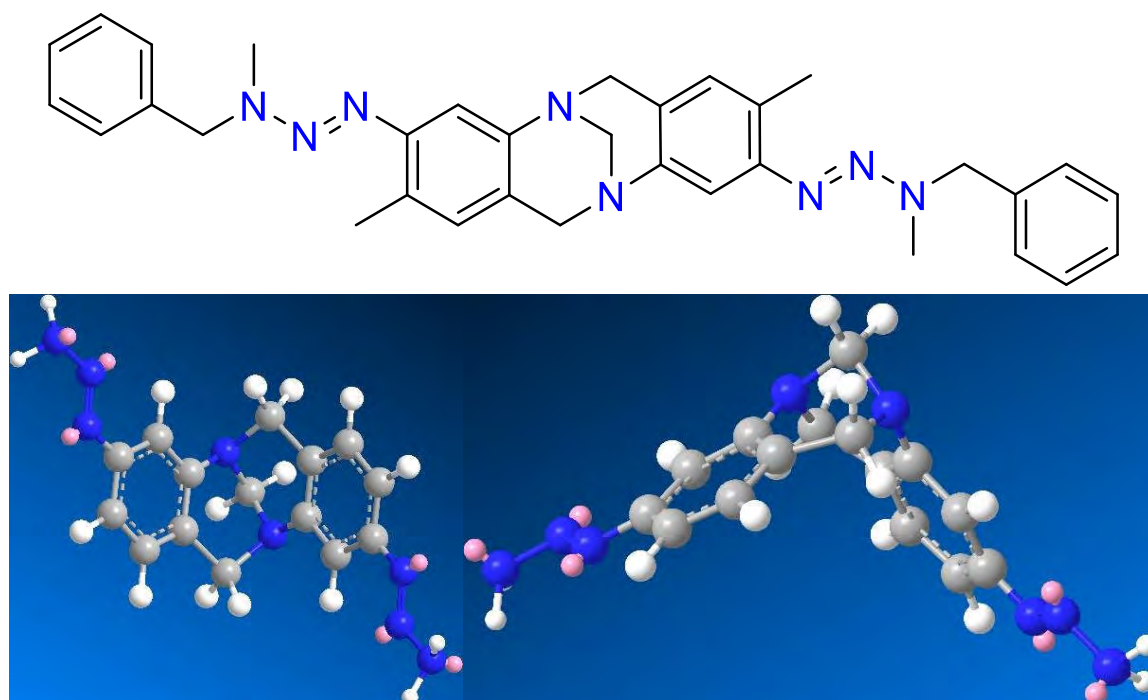


Figure 47 2D and simplified 3D presentation of a triazene-carrying-TBA¹⁵

Triazene-carrying polymers are able to absorb cationic molecules and they have been used as the cationic-dyes absorbent and cation-doped conductive polymers.^{22, 200} Figure 48 (top) displays a triazene-carrying polysulfone as an example of a cation absorbent, which is used in water treatment.²²

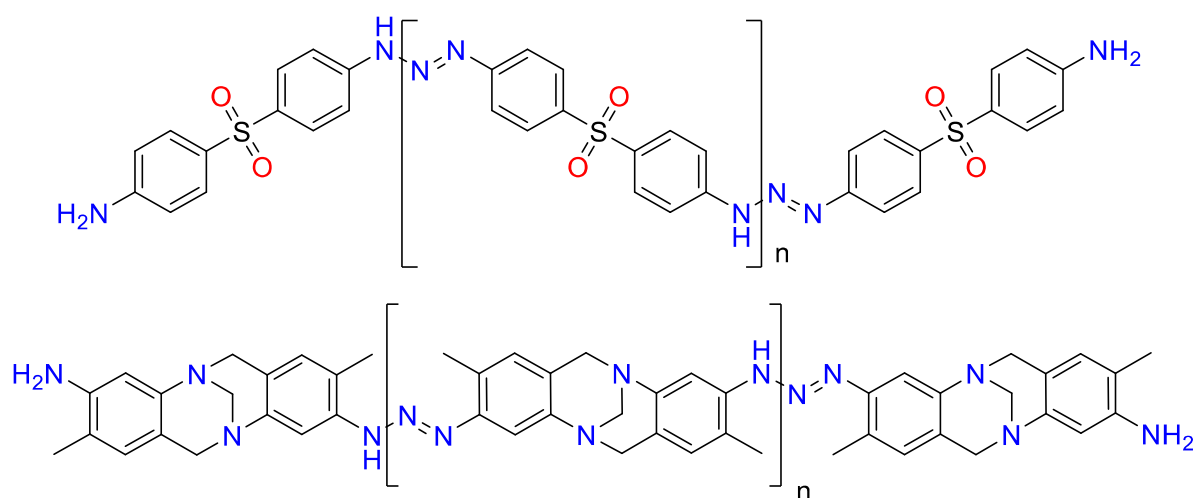


Figure 48 Triazene-based polymers

The polymerised triazene-carrying TBA shown in Figure 48 (bottom) was also prepared during this project; however, reporting further on its preparation and applications are beyond the scope of this thesis. The TBAs introduced throughout this project, especially those reported in Paper III, have a great potential of being utilised as Λ -shaped building blocks in the design of various novel materials *e.g.* photo-degradable polymers²⁰¹ or membranes.²⁰²

This thesis introduces a variety of photo-switchable and non-switchable TBA-possessing reactive extremities. For instance, compounds **13–15** in Paper I could be easily polymerised with diols, diamines, dithiols or even compounds **2**, **3**, **10**, **11**, and **13** in Paper III to form the corresponding photo-responsive copolymers (Figure 49). Compounds **1** in Paper I, **1–9** in Paper II, and **6** or **8** in Paper III should be readily copolymerised^{85, 183} with alkyl dibromides or iodides to form novel photo-responsive copolymers, as already displayed in Figure 39. TBA-carrying polymer applications were also briefly reviewed in Section 3.2.2.

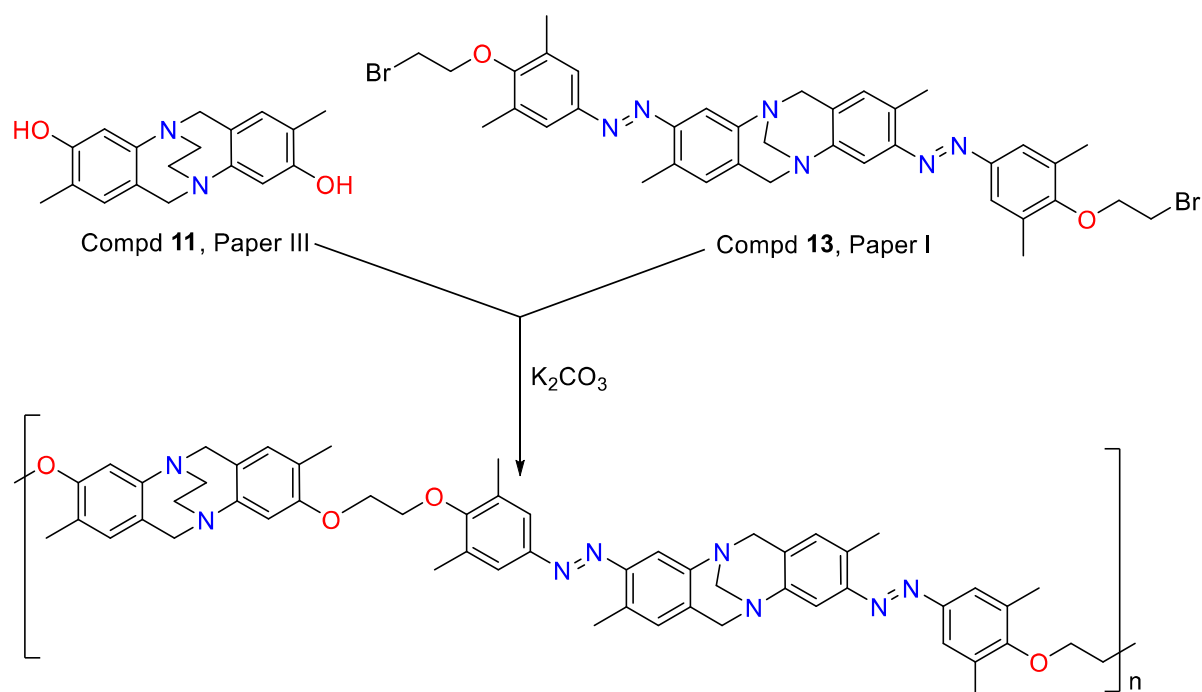


Figure 49 Proposed copolymerisation of TBAs

Fluorescent and pH sensing analogues

Photo-switchable, fluorescent²⁰³ and pH sensing⁴² azo materials can be used in live cell studies,²⁰⁴ and the production of chemosensors.^{205, 206} Various TBAs with such desirable properties were designed, and characterised (Figure 50 and Figure 51) during this project. For reasons of confidentiality, the structures of the represented examples are not provided in Figures 50 – 54. Determination of the quantum yields of photoisomerisation and fluorescence, wavelength-dependent plots, and establishing the photophysical behaviour of the materials presented in this thesis will remain as a part of the future explorations. Quantum yield of photoisomerisation would particularly determine the efficiency of *trans* – *cis* photoisomerisation in regard to the number of photons absorbed by the molecules. Photophysical studies and advanced NMR spectroscopy may also provide a better understanding of how bisazo TBAs can be employed as dual-switches in the design of molecular machines.

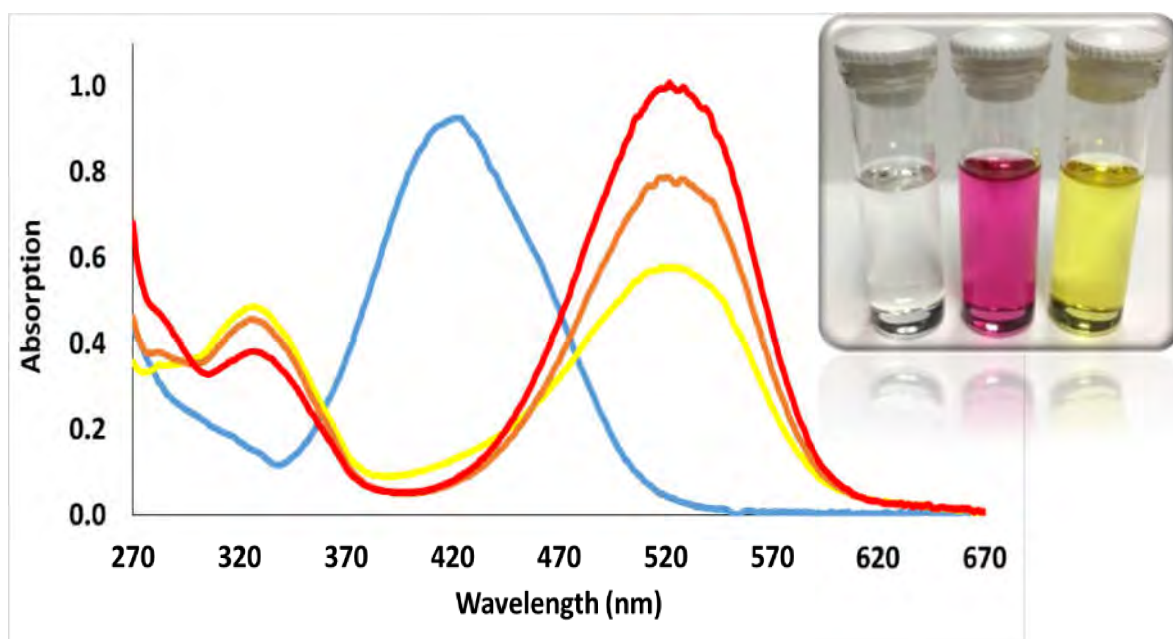


Figure 50 Absorption spectra and the appearance of a new TBA in different pH values

An example of a base-sensing TBA was introduced in Paper II (Compd 1). Figure 50 shows the UV-Vis spectra of an acid-sensing TBA following the addition of an organic acid.

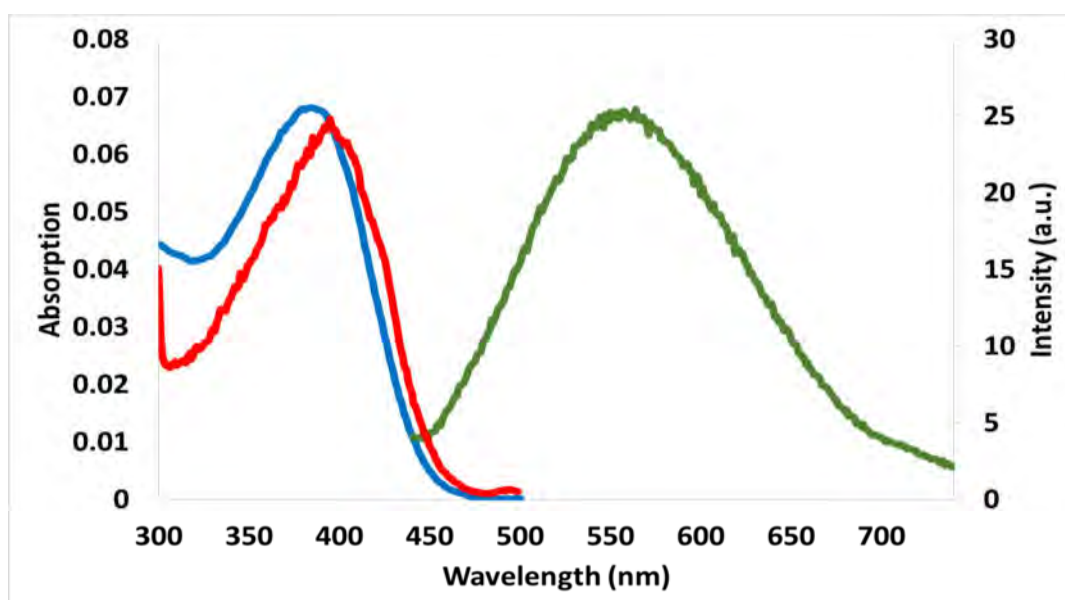
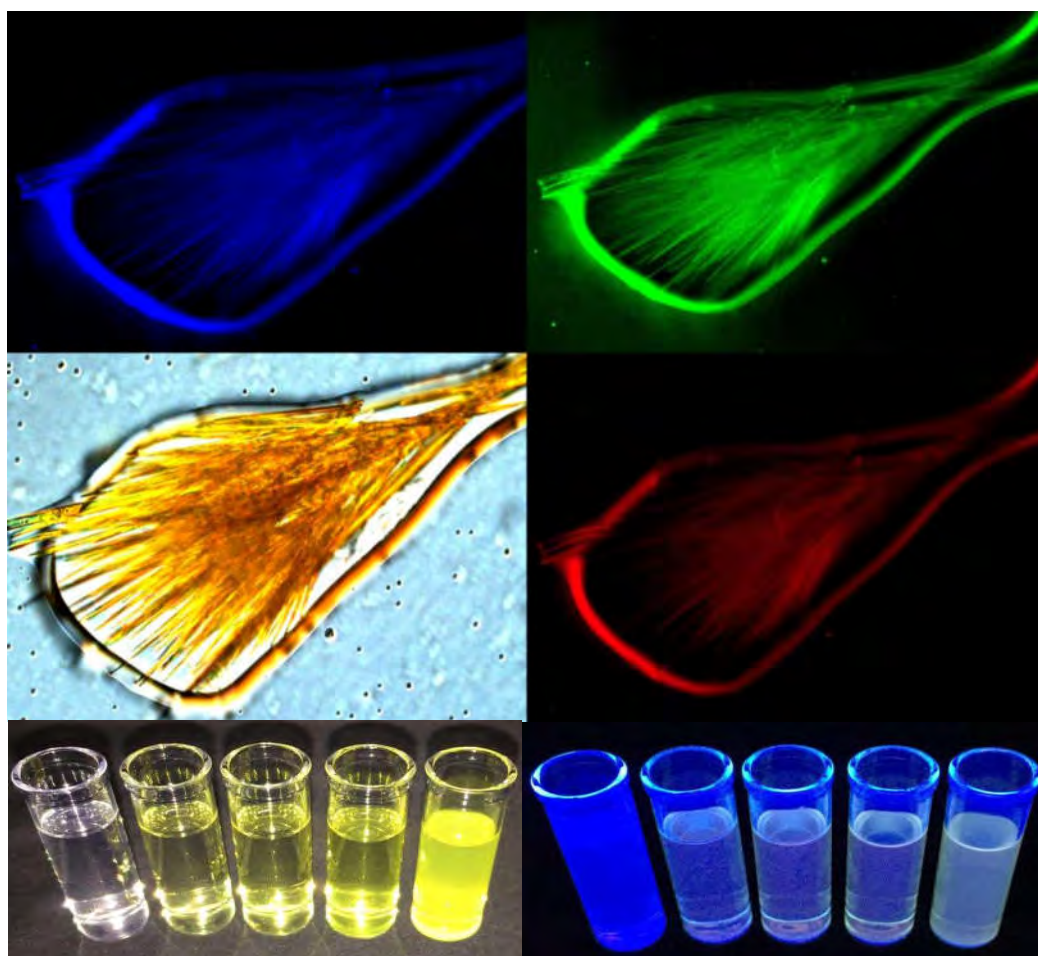


Figure 51 Absorption, emission and excitation spectra and the appearance of a fluorescent TBA under different wavelengths of light

Magnetic and photochromism studies

The building blocks introduced in this thesis can be symmetrically and asymmetrically modified. For instance, they can be turned into amine oxide, nitrosoamine²⁰⁷ or quaternary TB salts or be equipped with nitroxide radicals^{208, 209} or a spirooxazine.^{107, 210, 211} These enable spin-labelling,²¹² photo-magnetic activities,^{107, 210, 211} tunable photochromism,²¹³ phase transfer and green azo chemistry.⁴² Asymmetric positioning of different chromophores on the TB scaffold were also performed during this project. Further characterisation details of the products remain beyond the scope of this thesis.

Crystallography and aggregation studies

The products introduced in this thesis were prepared as crystals (Figure 52 and Figure 53) and spherical aggregates (Figure 54). The crystals will be investigated in the future to reveal their stacking pattern, fluorescence, and photochromism in the solid state. For reasons of confidentiality, the specific structures of these TBAs are not provided.

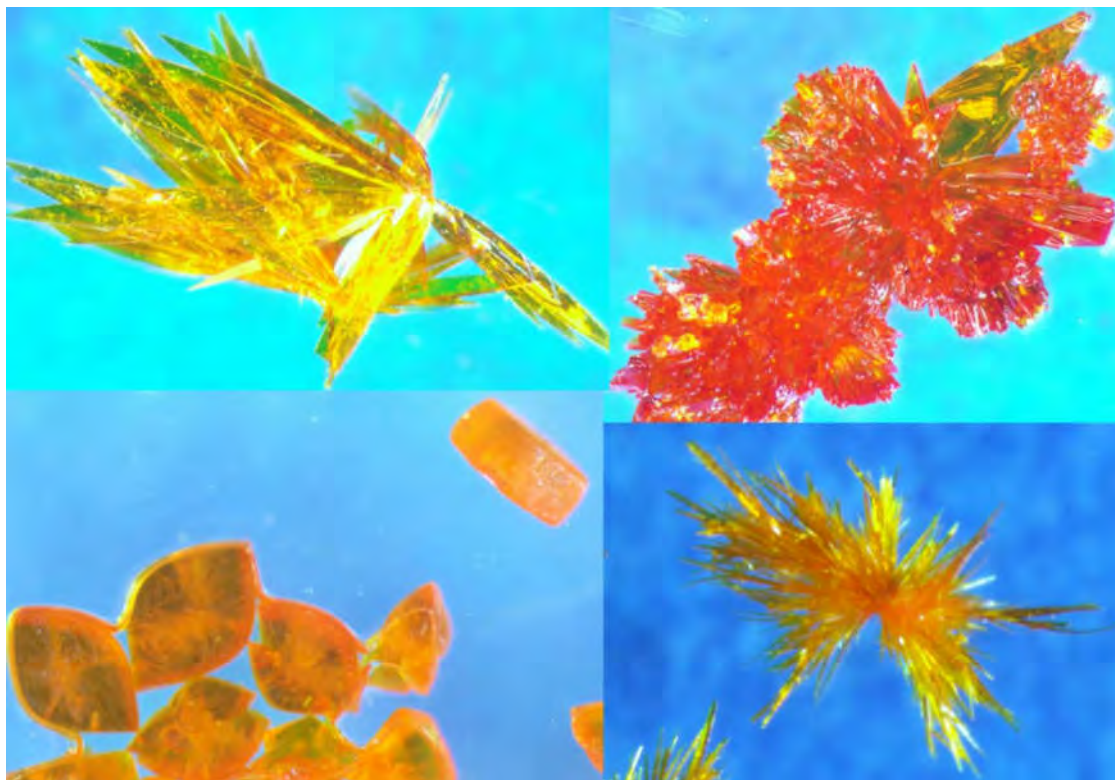


Figure 52 Images of the crystallised azo-carrying TBAs

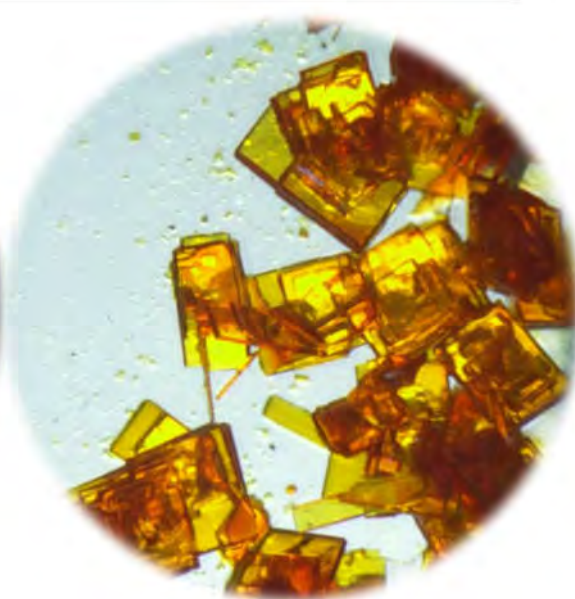
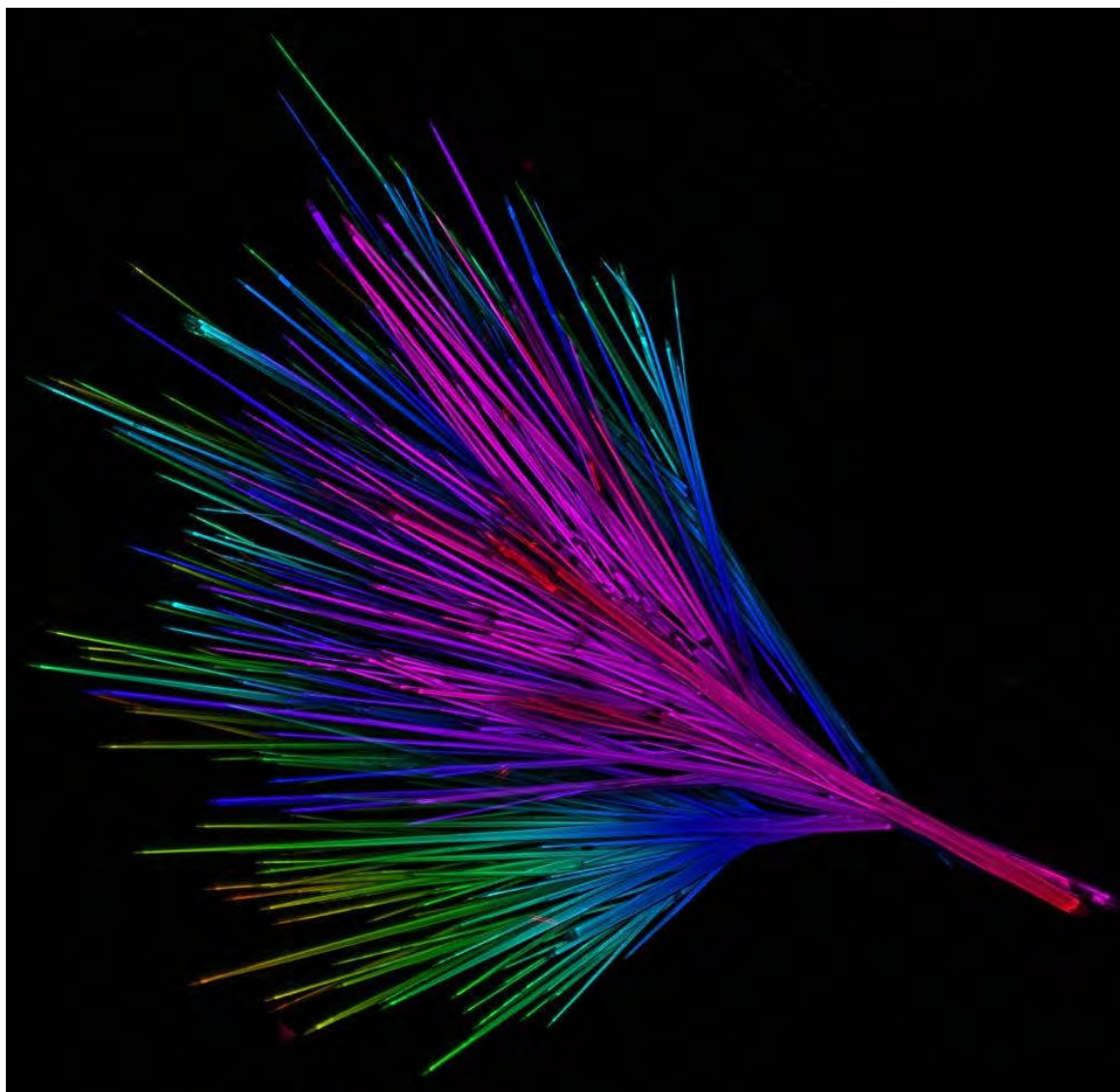


Figure 53 Images of the produced crystals of TBAs

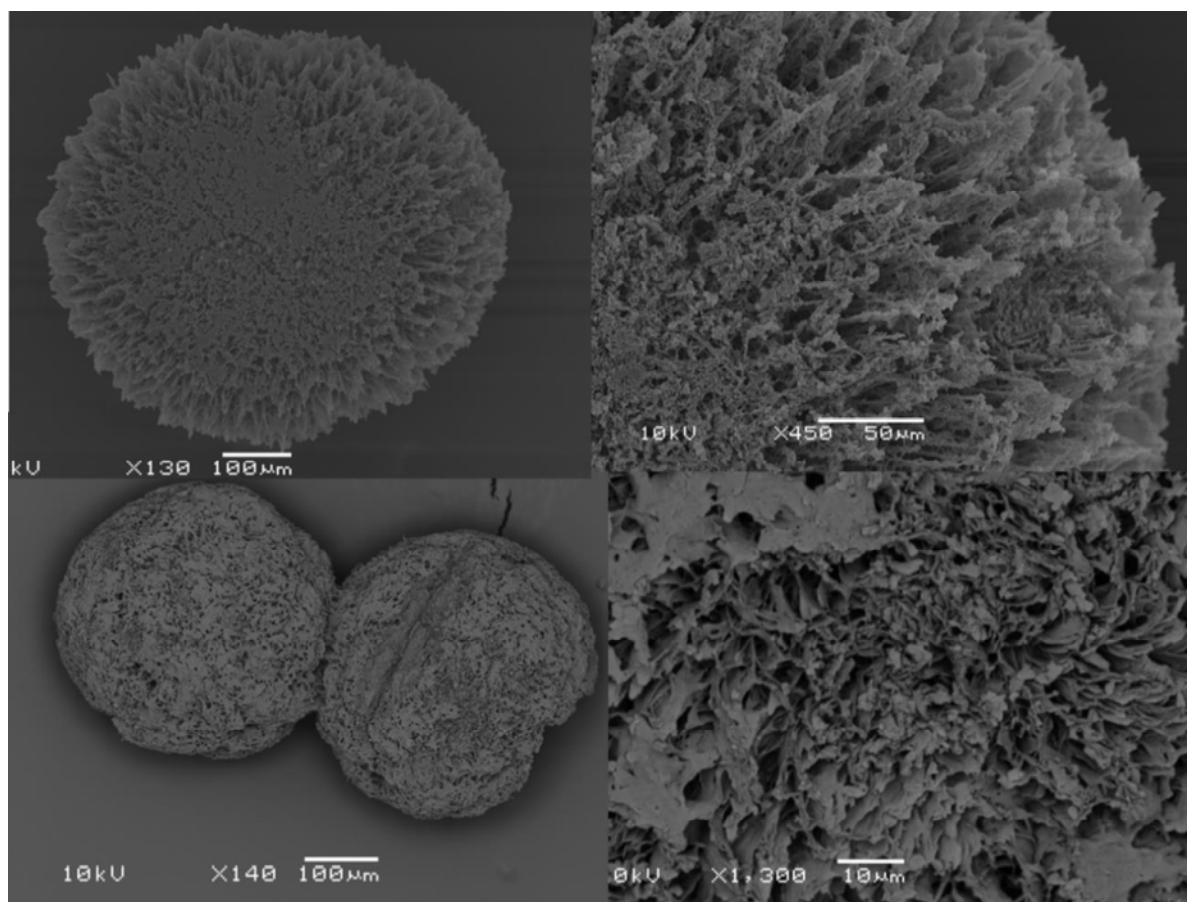


Figure 54 SEM images of the produced TBAs spherical aggregates

The SEM images (Figure 54) showed that the aggregates are porous and have high permeability. Further analysis of the aggregates properties and their applications will be explored in the future.

The design of sensing surfaces

The photo-switches introduced in this thesis can be mounted on glass,¹⁹² gold,^{188, 189} graphene or nanodiamonds,¹⁹⁰ polymer,^{179, 191} and other⁶⁸ surfaces to contribute to the modification of the surface and enable laser-induced lithography (Figure 55).¹⁹² These applications will be developed in the future.

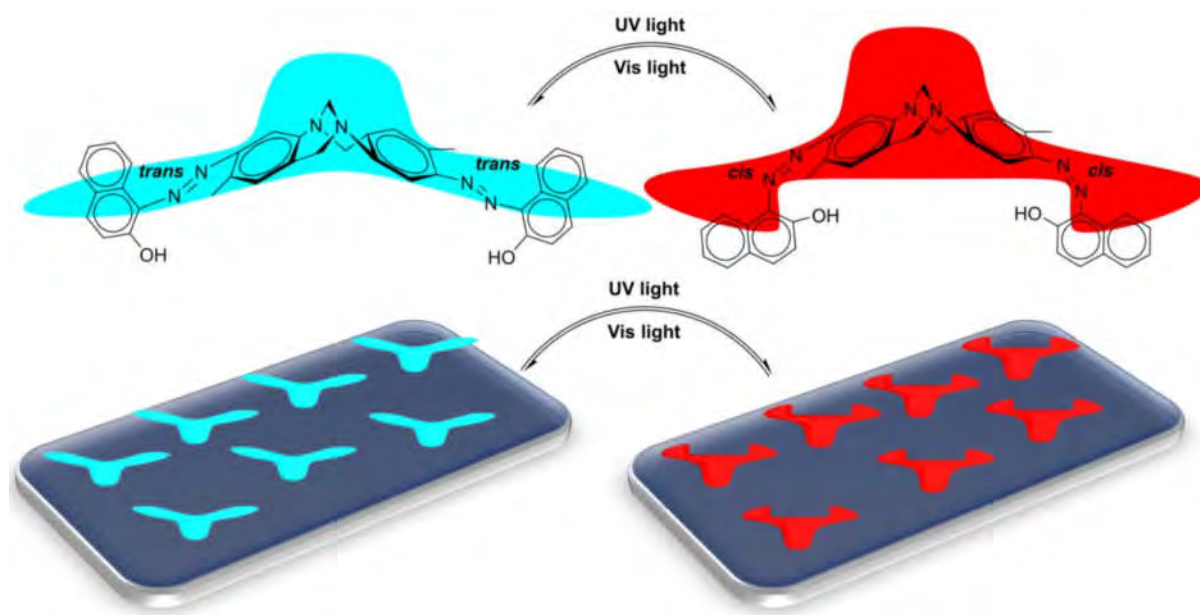


Figure 55 Proposed surface modification by TBAs

LC dopants: contribution in the design of smart LCDs

The idea of utilising azo materials in the design of flexible (Figure 10) and reflective (Figure 14) displays,⁶⁶ and enabling LCDs to work without a connection to electronics, encourages the application of the products of this project for such purposes (Figure 56).

To illustrate this application, a change of vision to molecular scale is required. For instance, Figure 56 (bottom) shows a sample²¹⁴ that displays an image in two colours. In fact, these orange and green areas on the screen are created by the different arrangement of molecules. To arrange these molecules in a specific way to produce the desired colours, photo-switchable materials are required. Due to the existing resemblance between the switches introduced by this thesis to flying birds, they are depicted as eagles with open or closed wings in Figure 56 (top).¹⁴ Opening and closing the wings can change the arrangement of neighbouring molecules and consequently results in the appearance of a different colour on the screen.

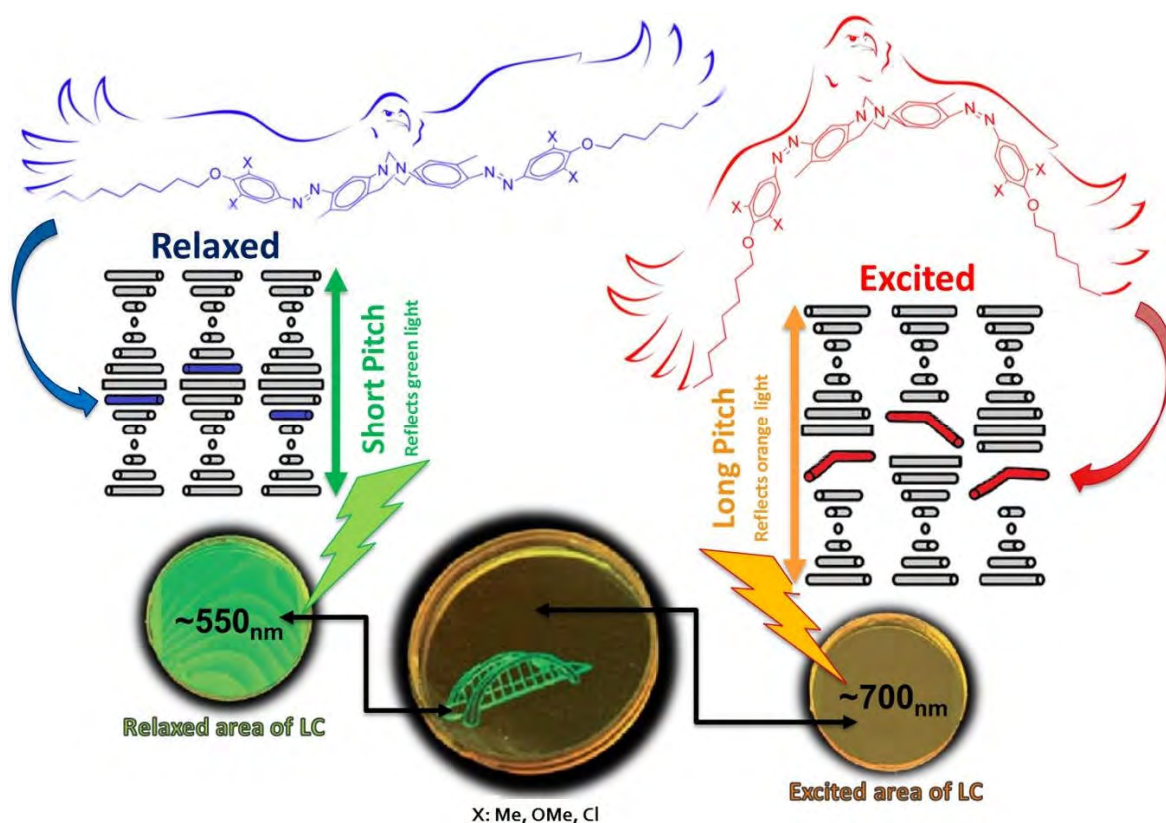


Figure 56 Visualisation of image on photo-tunable LC phase
This figure is partially adapted from references¹⁴ and 214

Furthermore, depending on the quantity of the applied switches, a wider range of colours can be obtained. For instance, the displayed RGB colours in Figure 57 show the concentration effect (left to right more dilute) produced following the addition of a chiral azo-carrying TBA to 7CB (Figure 7). This phenomenon is directly related to the pitch length changes (shown in Figure 2 and Table 3). In fact, the higher the concentration of dopant used, the stronger helical twisting power will be obtained. This shortens the pitch length, which results in the reflection of a shorter wavelength of light (Table 3). For example, in Figure 57 by an increase of the applied dopant, the reflected colour shifted from red to green, and later to blue (Table 3). For reasons of confidentiality, the specific structures of the chiral azo-carrying TBA is not provided.



Figure 57 RGB colour cells
obtained from an azo-carrying TBA in an achiral LC host (7CB)

The RGB primary colours (Figure 58) are sufficient for designing an LCD capable of displaying an unlimited number of vivid colours. In fact, every conventional LCD consists of only three colour filters, as displayed in Figure 1. Manipulating the amount of light passing through these colour filters creates a different combination of the wavelengths, which eventually results in the formation of new colours on the screen. Accordingly, a broad array of colours can be produced from the primary colours (Figure 58).

These three basic colours (Figure 58) used to be produced with plastic-made colour filters in conventional LCDs (Figure 1). These colour filters (Figure 1) are not needed in the design of smart LCDs owing to the fact that novel doped LCs (Figure 57) can create the desired colours within the LC layer (Table 3). This facilitates the design of ultra-thin LCDs.

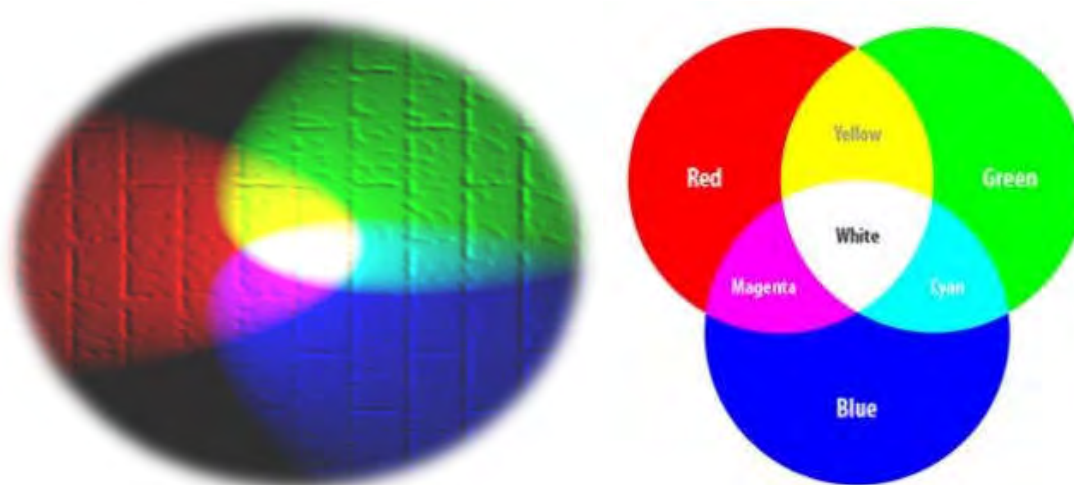


Figure 58 Colours created by manipulation of the RGB ratio
Images are adapted from Wikipedia

Conclusion

The first family of photo-switchable Tröger's base analogues (TBAs) was introduced in Paper I. The possibility of the synthesis was evaluated as well as optimising the reaction conditions. Afterward, various derivatives with modified extremities were reported along with their potential applications. The photo-isomerisation of these products was also studied and no sign of photo-degradation of the products was detected after their exposure to UV light.

The second generation of these products with modified molecular geometries as well as the capacity of their voids was introduced in Paper II. The various applied phenols resulted in obtaining a broad coverage of the UV-Vis spectrum and varying of the products response to the electromagnetic stimuli.

The third family of these products was produced with the priority of having an acid-resistant optical activity. This will facilitate the separation of the single enantiomers of the products. Changing the applied methodologies was inevitable due to the limited number of available building blocks. Therefore, novel TBAs carrying various functional groups were designed and reported in Paper III.

The complexity of producing such functional compounds was discussed in this thesis and the solutions were elaborated. The LCD application of these novel products were also elaborated in detail.

To sum up, this project has proved that the Tröger's base scaffold does not interfere with the photo-switching mechanism and can be employed in the design of novel chiral photo-responsive liquid crystal dopants. Therefore, this work can be considered as the beginning of a new chapter in TBAs applications, and LC dopants design.

References and Notes

- 1 A. B. Mahon, D. C. Craig and A. C. Try, *Arkivoc*, **2008**, 12, 148-163.
- 2 C. Michon, A. Sharma, G. Bernardinelli, E. Francotte and J. Lacour, *Chem. Commun.*, **2010**, 46, 2206-2208.
- 3 O. Trapp, G. Trapp, J. Kong, U. Hahn, F. Vögtle and V. Schurig, *Chem. Eur. J.*, **2002**, 8, 3629-3634.
- 4 D. R. Bond and J. L. Scott, *J. Chem. Soc., Perkin. Trans. 2*, **1991**, 2, 47-51.
- 5 T. H. Webb, H. Suh and C. S. Wilcox, *J. Am. Chem. Soc.*, **1991**, 113, 8554-8555.
- 6 S. Satishkumar and M. Periasamy, *Tetrahedron Asymmetry*, **2009**, 20, 2257-2262.
- 7 Z. Kejík, T. Bříza, M. Havlík, B. Dolenský, R. Kaplánek, J. Králová, I. Mikula, P. Martásek and V. Král, *Dyes Pigm.*, **2016**, 134, 212-218.
- 8 M. D. Cowart, I. Sucholeiki, R. R. Bukownik and C. S. Wilcox, *J. Am. Chem. Soc.*, **1988**, 110, 6204-6210.
- 9 S. Banerjee, S. A. Bright, J. A. Smith, J. Burgeat, M. Martinez-Calvo, D. C. Williams, J. M. Kelly and T. Gunnlaugsson, *J. Org. Chem.*, **2014**, 79, 9272-9283.
- 10 J. C. Adrian Jr and C. S. Wilcox, *J. Am. Chem. Soc.*, **1989**, 111, 8055-8057.
- 11 J. Adrian and C. Wilcox, *J. Am. Chem. Soc.*, **1992**, 114, 1398-1403.
- 12 J. Adrian and C. Wilcox, *J. Am. Chem. Soc.*, **1989**, 111, 8055-8057.
- 13 S. M. Morris, M. M. Qasim, K. T. Cheng, F. Castles, D. H. Ko, D. J. Gardiner, S. Nosheen, T. D. Wilkinson, H. J. Coles, C. Burgess and L. Hill, *Appl. Phys. Lett.*, **2013**, 103, 101105-101110.
- 14 M. Kazem-Rostami and A. Moghanian, *Org. Chem. Front.*, **2017**, 4, 224-228.
- 15 M. Kazem-Rostami, *Synlett*, **2017**, 28, 1641-1645.
- 16 A. Bosmani, S. Pujari, L. Guenee, C. Besnard, A. I. Poblador Bahamonde and J. Lacour, *Chem. Eur. J.*, **2017**, 23, 8678-8684.
- 17 S. Rigol, L. Beyer, L. Hennig, J. Sieler and A. Giannis, *Org. Lett.*, **2013**, 15, 1418-1420.
- 18 J. Vajs, I. Steiner, A. Brozovic, A. Pevec, A. Ambriović-Ristov, M. Matković, I. Piantanida, D. Urankar, M. Osmak and J. Košmrlj, *J. Inorg. Biochem.*, **2015**, 153, 42-48.
- 19 M. K. Rofouei, R. Soleymani, A. Aghaei and M. Mirzaei, *J. Mol. Struct.*, **2016**, 1125, 247-259.
- 20 P. J. Blower and J. R. Dilworth, *Coord. Chem. Rev.*, **1987**, 76, 121-185.
- 21 M. B. Gholivand, M. Mohammadi and M. K. Rofouei, *Mater Sci Eng C Mater Biol Appl*, **2010**, 30, 847-852.
- 22 A. Khazaei, M. Kazem-Rostami, A. Zare, A. R. Moosavi-Zare, M. Sadeghpour and A. Afkhami, *J. Appl. Polym. Sci.*, **2013**, 129, 3439-3446.
- 23 P. Schneider, **1957**, *Masticating synthetic rubber*, U.S. Patents 2,784,167, USA.
- 24 M. B. Gholivand, M. Mohammadi, M. Khodadadian and M. K. Rofouei, *Talanta*, **2009**, 78, 922-928.
- 25 B. Chen, A. K. Flatt, H. Jian, J. L. Hudson and J. M. Tour, *Chem. Mater.*, **2005**, 17, 4832-4836.
- 26 M. Lu, T. He and J. M. Tour, *Chem. Mater.*, **2008**, 20, 7352-7355.

- 27 M. Riskin, R. Tel-Vered and I. Willner, *Adv. Mater.*, **2010**, 22, 1387-1391.
- 28 J. M. Takacs, S. Vayalakkada and X. Jiang, in *Science of Synthesis: Houben-Weyl methods of molecular transformations*, ed. M. Lautens, Georg Thieme Verlag: Stuttgart and Thieme Publishing Group: New York, 1 edn., **2001**, vol. 1, pp. 304-313.
- 29 M. Petrovic, D. Scarpi, M. Nieger, N. Jung, E. G. Occhiato and S. Bräse, *RSC Adv.*, **2017**, 7, 9461-9464.
- 30 K. Takagi, M. Al-Amin, N. Hoshiya, J. Wouters, H. Sugimoto, Y. Shiro, H. Fukuda, S. Shuto and M. Arisawa, *J. Org. Chem.*, **2014**, 79, 6366-6371.
- 31 X. Shang, L. Xu, W. Yang, J. Zhou, M. Miao and H. Ren, *Eur. J. Org. Chem.*, **2013**, 2013, 5475-5484.
- 32 S. K. Talapatra, N. C. Ganguly, S. Goswami and B. Talapatra, *J. Nat. Prod.*, **1983**, 46, 401-408.
- 33 A. Hafner, C. Hussal and S. Bräse, *Synthesis*, **2014**, 46, 1448-1454.
- 34 V. Capucha, E. Mendes, A. P. Francisco and M. J. Perry, *Bioorg. Med. Chem. Lett.*, **2012**, 22, 6903-6908.
- 35 H. Sun and Y. Huang, *Synlett*, **2015**, 26, 2751-2762.
- 36 A. Khazaei, M. Kazem-Rostami, A. R. Moosavi-Zare, M. Bayat and S. Saednia, *Synlett*, **2012**, 23, 1893-1896.
- 37 Y. Zhang, D. Cao, W. Liu, H. Hu, X. Zhang and C. Liu, *Curr. Org. Chem.*, **2015**, 19, 151-178.
- 38 D. Cao, Y. Zhang, C. Liu, B. Wang, Y. Sun, A. Abdukadera, H. Hu and Q. Liu, *Org. Lett.*, **2016**, 18, 2000-2003.
- 39 Y. Zhang, H. Hu, C.-J. Liu, D. Cao, B. Wang, Y. Sun and A. Abdukader, *Asian J. Org. Chem.*, **2016**, 6, 102-107.
- 40 M. M. Zieger, P. Mueller, A. S. Quick, M. Wegener and C. Barner-Kowollik, *Angew. Chem.*, **2017**, 129, 5717-5721.
- 41 C. Zinelaabidine, O. Souad, J. Zoubir, B. Malika and A. Nour-Eddine, *Int. J. Chem.*, **2012**, 4, 73-79.
- 42 F. M. Akwi, C. Bosma and P. Watts, *Journal of Flow Chemistry*, **2016**, 6, 73-79.
- 43 F. M. Akwi and P. Watts, *Beilstein J Org Chem*, **2016**, 12, 1987.
- 44 © Merck KGaA Darmstadt Germany (Reprint permission obtained on 24/11/2016 from Heike Müller).
- 45 D. L. Goodstein, *States of matter*, Dover Publications-Courier Corporation, New York, USA, **2014**.
- 46 https://en.wikipedia.org/wiki/State_of_matter.
- 47 K. Hiltrop and H. Stegemeyer, *Mol Cryst Liq Cryst*, **1978**, 49, 61-65.
- 48 L.-N. Zou and S. R. Nagel, *Phys. Rev. Lett.*, **2006**, 96, 138301-138304.
- 49 K. Sun, Z. Xiao, S. Lu, W. Zajackowski, W. Pisula, E. Hanssen, J. M. White, R. M. Williamson, J. Subbiah, J. Ouyang, A. B. Holmes, W. W. H. Wong and D. J. Jones, **2015**, 6, 6013-6022.
- 50 S. Singh and D. A. Dunmur, *Liquid crystals: fundamentals*, World Scientific Printers, Singapore, **2002**.
- 51 C. W. R. U. The photo credit goes to Dr Ji-Hoon Lee (Department of Physics, Cleveland, Ohio 44106-7079 USA) <http://liq-xtal.cwru.edu/>.

- 52 G. Vertogen and W. H. de Jeu, *Thermotropic liquid crystals, fundamentals*, Springer Science & Business Media, **2012**.
- 53 P. J. Wojtowicz, P. Sheng and E. Priestley, *Introduction to liquid crystals*, Springer, **1975**.
- 54 T. J. White and D. J. Broer, *Nat Mater*, **2015**, *14*, 1087-1098.
- 55 H. Finkelmann, S. T. Kim, A. Munoz, P. Palffy-Muhoray and B. Taheri, *Adv. Mater.*, **2001**, *13*, 1069-1072.
- 56 M. Warner and E. M. Terentjev, *Liquid crystal elastomers*, OUP Oxford, **2003**.
- 57 D. W. Berreman, *Phys. Rev. Lett.*, **1972**, *28*, 1683-1686.
- 58 <http://www.sigmaaldrich.com/catalog/product/aldrich/338648?lang=en®ion=AU>
- 59 J. V. Badami, C. Bernstein, C. Maldarelli and R. S. Tu, *Soft Matter*, **2015**, *11*, 6604-6612.
- 60 D. Coates and G. W. Gray, *Mol Cryst Liq Cryst*, **1976**, *37*, 249-262.
- 61 M. Schadt, R. Buchecker and K. Müller, *Liq. Cryst.*, **1989**, *5*, 293-312.
- 62 H. Takezoe, *Ferroelectrics*, **2014**, *468*, 1-17.
- 63 X. Li, P. T. Au, P. Xu, A. Muravsky, A. Muravsky, Z. Liu, V. Chigrinov and H. S. Kwok, **2006**, presented in part at the J Soc Inf Disp (Symposium Digest of Technical Papers).
- 64 J. Osterman, C. Adås, L. Madsen, K. Skarp, A. P. Tong, L. Xihua and V. Chigrinov, *J Soc Inf Disp (Symposium Digest of Technical Papers)*, **2005**, *36*, 772-775.
- 65 J. Osterman, A. P. Tong, K. Skarp, V. Chigrinov and H. S. Kwok, *J Soc Inf Disp*, **2005**, *13*, 1003-1009.
- 66 S. Valyukh, J. Osterman, K. Skarp and V. Chigrinov, *J Soc Inf Disp (Symposium Digest of Technical Papers)*, **2005**, *36*, 702-705.
- 67 A. Muravsky, A. Murauski, X. Li and V. Chigrinov, **2006**, presented in part at the Proceedings of the 13th International Display Workshops (IDW'06).
- 68 T. K. Claus, S. Telitel, A. Welle, M. Bastmeyer, A. P. Vogt, G. Delaittre and C. Barner-Kowollik, *Chem. Commun.*, **2017**, *53*, 1599-1602.
- 69 A. Murauski, V. Chigrinov, L. Xihua and H. S. Kwok, IDW/AD'05 - Proceedings of the 12th International Display Workshops in Conjunction with Asia Display 2005, Takamatsu, **2005**, presented in part at the IDW/AD'05 - 12th International Display Workshops in Conjunction with Asia Display 2005, Takamatsu.
- 70 K. Ichimura, Y. Suzuki, T. Seki, A. Hosoki and K. Aoki, *Langmuir*, **1988**, *4*, 1214-1216.
- 71 H. Akiyama, T. Kawara, H. Takada, H. Takatsu, V. Chigrinov, E. Prudnikova, V. Kozenkov and H. Kwok, *Liq. Cryst.*, **2002**, *29*, 1321-1327.
- 72 V. Chigrinov, A. Muravski, H. S. Kwok, H. Takada, H. Akiyama and H. Takatsu, *Physical Review E*, **2003**, *68*, 061702.
- 73 V. Chigrinov, S. Pikin, A. Verevochnikov, V. Kozenkov, M. Khazimullin, J. Ho, D. D. Huang and H.-S. Kwok, *Physical Review E*, **2004**, *69*, 061713.
- 74 K. Ichimura, *Chem. Rev.*, **2000**, *100*, 1847-1874.
- 75 V. G. Chigrinov, V. M. Kozenkov and H.-S. Kwok, *Photoalignment of liquid crystalline materials: physics and applications*, John Wiley & Sons, **2008**.
- 76 M. N. Inscoe, J. H. Gould, M. E. Corning and W. R. Brode, *Journal of Research of the National Bureau of Standards*, **1958**, *60*, 65.

- 77 M. Osawa, R. Alkire, D. Kolb, P. Ross and J. Lipkowski, *Advances in Electrochemical Science and Engineering*, **2006**, 9, 343.
- 78 M. Schadt, *Mol Cryst Liq Cryst*, **2001**, 364, 151-169.
- 79 C. Alejandro Parraga, J. Roca-Vila, D. Karatzas and S. M. Wuerger, *Displays*, **2014**, 35, 227-239.
- 80 C. Nieuwkerk, T. Mol, S. Stallinga, F. Leenhouts, P. van de Witte, J. van Haaren and D. Broer, *J Soc Inf Disp (Symposium Digest of Technical Papers)*, **2000**, 31, 842-845.
- 81 H. J. Syed, R. K. Jack and L. W. John, *Jpn J Appl Phys*, **1995**, 34, 1368-1371.
- 82 H. Takada, H. Akiyama, H. Takatsu, V. Chigrinov, E. Prudnikova, V. Kozenkov and H. S. Kwok, *J Soc Inf Disp (Symposium Digest of Technical Papers)*, **2003**, 34, 620-623.
- 83 T. G. Pedersen, P. S. Ramanujam, P. M. Johansen and S. Hvilsted, *J. Opt. Soc. Am. B*, **1998**, 15, 2721-2730.
- 84 Byoungchoo Park, Youngyi Jung, Hee C. Hyun, Keun H. Ha, Youngkyoo Kim, Sooman Lee, Hum J. Sei, aki K. Masa and Hideo Takezoe, *Jpn J Appl Phys*, **1998**, 37, 5663-5668.
- 85 W. W. H. Wong, J. L. Banal, P. B. Geraghty, Q. Hong, B. Zhang, A. B. Holmes and D. J. Jones, *The Chemical Record*, **2015**, 15, 1006-1020.
- 86 M. Nishikawa, B. Taheri and J. L. West, *Appl. Phys. Lett.*, **1998**, 72, 2403-2405.
- 87 G. Shaoqin, K. Jerzy, M. Lan and Z. Z. Z. John, *Jpn J Appl Phys*, **1999**, 38, 5996-6004.
- 88 S. Martin, S. Klaus, K. Vladimir and C. Vladimir, *Jpn J Appl Phys*, **1992**, 31, 2155-2164.
- 89 M. Nishikawa, B. Taheri, J. L. West and Y. Rennikov, *Jpn J Appl Phys*, **1998**, 37, 1393-1395.
- 90 T. J. White, M. E. McConney and T. J. Bunning, *J. Mater. Chem.*, **2010**, 20, 9832-9847.
- 91 M. Mathews, R. S. Zola, D.-k. Yang and Q. Li, *J. Mater. Chem.*, **2011**, 21, 2098-2103.
- 92 M. Zahangir Alam, T. Yoshioka, T. Ogata, T. Nonaka and S. Kurihara, *Liq. Cryst.*, **2007**, 34, 1215-1219.
- 93 J. G. Finden, E. Yuh, C. Huntley and R. P. Lemieux, *Liq. Cryst.*, **2007**, 34, 1095-1106.
- 94 Q. Cui and R. P. Lemieux, *J. Mater. Chem. C*, **2013**, 1, 1011-1017.
- 95 Q. Cui, C. M. Huntley and R. P. Lemieux, *J. Mater. Chem.*, **2009**, 19, 5188-5192.
- 96 C. J. Boulton, J. J. Sutherland and R. P. Lemieux, *J. Mater. Chem.*, **2003**, 13, 644-646.
- 97 C. J. Boulton, J. G. Finden, E. Yuh, J. J. Sutherland, M. D. Wand, G. Wu and R. P. Lemieux, *J. Am. Chem. Soc.*, **2005**, 127, 13656-13665.
- 98 H.-K. Kwon, K.-T. Lee, K. Hur, S. H. Moon, M. M. Quasim, T. D. Wilkinson, J.-Y. Han, H. Ko, I.-K. Han, B. Park, B. K. Min, B.-K. Ju, S. M. Morris, R. H. Friend and D.-H. Ko, *Adv. Energy Mater.*, **2015**, 5, 1401347-1401353.
- 99 Q. Li, L. Green, N. Venkataraman, I. Shiyonovskaya, A. Khan, A. Urbas and J. W. Doane, *J. Am. Chem. Soc.*, **2007**, 129, 12908-12909.
- 100 O. Jin, D. Fu, Y. Ge, J. Wei and J. Guo, *New J. Chem.*, **2015**, 39, 254-261.
- 101 H. Huang, T. Orlova, B. Matt and N. Katsonis, *Macromol. Rapid Commun.*, **2018**, 39, 1700387-n/a.
- 102 Q. Li, *Nanoscience with Liquid Crystals*, Springer, Ohio, USA, **2014**.
- 103 Y. Zhao and T. Ikeda, *Smart light-responsive materials: azobenzene-containing polymers and liquid crystals*, John Wiley & Sons Inc., New Jersey, USA, **2009**.

- 104 R. Eelkema, *Liq. Cryst.*, **2011**, 38, 1641-1652.
- 105 D.-Y. Kim, S.-A. Lee, Y.-J. Choi, S.-H. Hwang, S.-W. Kuo, C. Nah, M.-H. Lee and K.-U. Jeong, *Chem. - Eur. J.*, **2014**, 20, 5689-5695.
- 106 D. G. Patel, J. B. Benedict, R. A. Kopelman and N. L. Frank, *Chem. Commun.*, **2005**, 1, 2208-2210.
- 107 R. A. Kopelman, S. M. Snyder and N. L. Frank, *J. Am. Chem. Soc.*, **2003**, 125, 13684-13685.
- 108 Y. Hirshberg, E. Bergmann and F. Bergmann, *J. Am. Chem. Soc.*, **1950**, 72, 5120-5123.
- 109 J. Yuan, Y. Yuan, X. Tian, J. Sun and Y. Ge, *J Phys Chem C*, **2016**, 120, 14840-14853.
- 110 D. H. Waldeck, *Chem. Rev.*, **1991**, 91, 415-436.
- 111 S. Herre, W. Steinle and K. Rück-Braun, *Synthesis*, **2005**, 2005, 3297-3300.
- 112 S. Kitzig, M. Thilemann, T. Cordes and K. Rück-Braun, *ChemPhysChem*, **2016**, 17, 1252-1263.
- 113 A. R. Moosavi-Zare, M. A. Zolfigol, E. Noroozizadeh, R. Salehi-Moratab and M. Zarei, *J. Mol. Catal. A: Chem.*, **2016**, 420, 246-253.
- 114 A. R. Moosavi-Zare, M. A. Zolfigol, E. Noroozizadeh, M. Zarei, R. Karamian and M. Asadbegy, *J. Mol. Catal. A: Chem.*, **2016**, 425, 217-228.
- 115 E. Merino and M. Ribagorda, *Beilstein J Org Chem*, **2012**, 8, 1071-1090.
- 116 H. M. D. Bandara and S. C. Burdette, *Chem. Soc. Rev.*, **2012**, 41, 1809-1825.
- 117 B. V. K. J. Schmidt and C. Barner-Kowollik, *Angew. Chem.*, **2017**, 129, 8468-8488.
- 118 D. Wang and X. Wang, *Prog. Polym. Sci.*, **2013**, 38, 271-301.
- 119 T. Yoshioka, T. Ogata, T. Nonaka, M. Moritsugu, S.-N. Kim and S. Kurihara, *Adv. Mater. (Weinheim, Ger.)*, **2005**, 17, 1226-1229.
- 120 S. H. Wilen, J. Z. Qi and P. G. Williard, *J. Org. Chem.*, **1991**, 56, 485-487.
- 121 A. Greenberg, N. Molinaro and M. Lang, *J. Org. Chem.*, **1984**, 49, 1127-1130.
- 122 M. Kazem-Rostami, *Synthesis*, **2017**, 49, 1214-1222.
- 123 U. Kiehne, T. Bruhn, G. Schnakenburg, R. Fröhlich, G. Bringmann and A. Lützen, *Chem. Eur. J.*, **2008**, 14, 4246-4255.
- 124 A. Jarzebski, C. Bannwarth, C. Tenten, C. Benkhäuser, G. Schnakenburg, S. Grimme and A. Lützen, *Synthesis*, **2015**, 47, 3118-3132.
- 125 S. Sergeev and F. Diederich, *Chirality*, **2006**, 18, 707-712.
- 126 S. H. Wilen, J. Z. Qi and P. G. Williard, *J. Org. Chem.*, **1991**, 56, 485-487.
- 127 C. A. Weatherly, Y.-C. Na, Y. S. Nanayakkara, R. M. Woods, A. Sharma, J. Lacour and D. W. Armstrong, *J. Chromatogr. B*, **2014**, 955-956, 72-80.
- 128 C. Benkhäuser-Schunk, B. Wezislä, K. Urbahn, U. Kiehne, J. Daniels, G. Schnakenburg, F. Neese and A. Lützen, *ChemPlusChem*, **2012**, 77, 396-403.
- 129 M. S. Newman and D. Lednicer, *J. Am. Chem. Soc.*, **1956**, 78, 4765-4770.
- 130 www.sigmaaldrich.com
- 131 D. L. Jameson, T. Field, M. R. Schmidt, A. K. DeStefano, C. J. Stiteler, V. J. Venditto, B. Krovic, C. M. Hoffman, M. T. Ondisco and M. E. Belowich, *J. Org. Chem.*, **2013**, 78, 11590-11596.
- 132 V. Prelog and P. Wieland, *Helv. Chim. Acta*, **1944**, 27, 1127-1134.

- 133 S. Sergeyev, *Helv. Chim. Acta*, **2009**, *92*, 415-444.
- 134 M. Valík, B. Dolenský, E. Herdtweck and V. Král, *Tetrahedron Asymmetry*, **2005**, *16*, 1969-1974.
- 135 M. Faroughi, A. C. Try, J. Klepetko and P. Turner, *Tetrahedron Lett.*, **2007**, *48*, 6548-6551.
- 136 S. Sergeyev, D. Didier, V. Boitsov, A. Teshome, I. Asselberghs, K. Clays, C. M. L. Vande Velde, A. Plaquet and B. Champagne, *Chem. Eur. J.*, **2010**, *16*, 8181-8190.
- 137 M. Harmata and M. Kahraman, *Tetrahedron Asymmetry*, **2000**, *11*, 2875-2879.
- 138 Y. Goldberg and H. Alper, *Tetrahedron Lett.*, **1995**, *36*, 369-372.
- 139 E. M. Boyle, S. Comby, J. K. Molloy and T. Gunnlaugsson, *J. Org. Chem.*, **2013**, *78*, 8312-8319.
- 140 M. Bhaskar Reddy, M. Shailaja, A. Manjula, J. R. Premkumar, G. N. Sastry, K. Sirisha and A. V. S. Sarma, *Org. Biomol. Chem.*, **2015**, *13*, 1141-1149.
- 141 C. S. Wilcox and M. D. Cowart, *Tetrahedron Lett.*, **1986**, *27*, 5563-5566.
- 142 A. Tatar, M. Valík, J. Novotná, M. Havlík, B. Dolenský, V. Král and M. Urbanová, *Chirality*, **2014**, *26*, 361-367.
- 143 U. Kiehne, T. Weilandt and A. Lützen, *Org. Lett.*, **2007**, *9*, 1283-1286.
- 144 S. Goswami, K. Ghosh and S. Dasgupta, *J Org Chem*, **2000**, *65*, 1907-1914.
- 145 M. Valík, R. M. Strongin and V. Král, *Supramol. Chem.*, **2005**, *17*, 347-367.
- 146 A. Abdolmaleki, S. Heshmat-Azad and M. Kheradmand-fard, *J. Appl. Polym. Sci.*, **2011**, *122*, 282-288.
- 147 T. V. Shishkanova, M. Havlík, V. Král, D. Kopecký, P. Matějka, M. Dendisová and V. M. Mirsky, *Electrochim. Acta*, **2017**, *224*, 439-445.
- 148 M. Havlik, V. Kral, R. Kaplanek and B. Dolensky, *Org. Lett.*, **2008**, *10*, 4767-4769.
- 149 A. Tatar, J. Cejka, V. Kral and B. Dolensky, *Org. Lett.*, **2010**, *12*, 1872-1875.
- 150 S. Sergeyev and F. Diederich, *Angew. Chem. Int. Ed.*, **2004**, *43*, 1738-1740.
- 151 S. Sergeyev, M. Schär, P. Seiler, O. Lukyanova, L. Echegoyen and F. Diederich, *Chem. Eur. J.*, **2005**, *11*, 2284-2294.
- 152 Y. Sugawara, N. Jasinski, M. Kaupp, A. Welle, N. Zydziak, E. Blasco and C. Barner-Kowollik, *Chem. Commun.*, **2015**, *51*, 13000-13003.
- 153 A. Armin, J. Subbiah, M. Stolterfoht, S. Shoaee, Z. Xiao, S. Lu, D. J. Jones and P. Meredith, *Adv. Energy Mater.*, **2016**, *6*, 1600939.
- 154 J. Subbiah, V. D. Mitchell, N. K. C. Hui, D. J. Jones and W. W. H. Wong, *Angew. Chem.*, **2017**, *129*, 8551-8554.
- 155 B. Zhang, J. M. White, D. J. Jones and W. W. H. Wong, *Org. Biomol. Chem.*, **2015**, *13*, 10505-10510.
- 156 B. Zhang, J. Subbiah, D. J. Jones and W. W. H. Wong, *Beilstein J Org Chem*, **2016**, *12*, 903-911.
- 157 M. Pfaff, P. Müller, P. Bockstaller, E. Müller, J. Subbiah, W. W. H. Wong, M. F. G. Klein, A. Kiersnowski, S. R. Puniredd, W. Pisula, A. Colsmann, D. Gerthsen and D. J. Jones, *ACS Applied Materials & Interfaces*, **2013**, *5*, 11554-11562.

- 158 K. Sun, B. Zhao, V. Murugesan, A. Kumar, K. Zeng, J. Subbiah, W. W. H. Wong, D. J. Jones and J. Ouyang, *J. Mater. Chem.*, **2012**, 22, 24155-24165.
- 159 Z. Wang, D. Wang, F. Zhang and J. Jin, *ACS Macro Lett.*, **2014**, 3, 597-601.
- 160 S. Goswami, S. Dey, A. C. Maity and S. Jana, *Tetrahedron Lett.*, **2005**, 46, 1315-1318.
- 161 S. Goswami and S. Dey, *J. Org. Chem.*, **2006**, 71, 7280-7287.
- 162 S. Goswami and K. Ghosh, *Tetrahedron Lett.*, **1997**, 38, 4503-4506.
- 163 Z. Wang, D. Wang, S. Zhang, L. Hu and J. Jin, *Adv. Mater. (Weinheim, Ger.)*, **2016**, 28, 3399-3405.
- 164 Z. Wang, D. Wang and J. Jin, *Macromolecules (Washington, DC, U. S.)*, **2014**, 47, 7477-7483.
- 165 C. Pardo, E. Sesmilo, E. Gutiérrez-Puebla, A. Monge, J. Elguero and A. Fruchier, *J. Org. Chem.*, **2001**, 66, 1607-1611.
- 166 T. Weilandt, U. Kiehne, J. Bunzen, G. Schnakenburg and A. Lützen, *Chem. - Eur. J.*, **2010**, 16, 2418-2426.
- 167 Q. M. Malik, Thesis (PhD)-Dept. of Chemistry and Biomolecular Sciences, Macquarie University, Australia, **2008**.
- 168 A. B. Mahon, Thesis (PhD)-Dept. of Chemistry and Biomolecular Sciences, Macquarie University, Australia, **2008**.
- 169 S. Ijaz, Thesis (PhD)-Dept. of Chemistry and Biomolecular Sciences, Macquarie University, Australia, **2009**.
- 170 J. Tröger, *J. Prakt. Chem.*, **1887**, 36, 225-245.
- 171 J. Sturala and R. Cibulka, *Eur. J. Org. Chem.*, **2012**, 2012, 7066-7074.
- 172 M. D. H. Bhuiyan, A. B. Mahon, P. Jensen, J. K. Clegg and A. C. Try, *Eur. J. Org. Chem.*, **2009**, 2009, 687-698.
- 173 D. Didier and S. Sergeyev, *Tetrahedron*, **2007**, 63, 3864-3869.
- 174 M. Havlík, V. Král and B. Dolenský, *Org. Lett.*, **2006**, 8, 4867-4870.
- 175 S. Telitel, E. Blasco, L. D. Bangert, F. H. Schacher, A. S. Goldmann and C. Barner-Kowollik, *Polymer Chemistry*, **2017**, 8, 4038-4042.
- 176 M. Camacho-Lopez, H. Finkelmann, P. Palffy-Muhoray and M. Shelley, *Nat Mater*, **2004**, 3, 307-310.
- 177 M. Morimoto and M. Irie, *J. Am. Chem. Soc.*, **2010**, 132, 14172-14178.
- 178 Y. Yu, M. Nakano and T. Ikeda, *Nature*, **2003**, 425, 145-145.
- 179 E. Blasco, M. Wegener and C. Barner-Kowollik, *Adv. Mater.*, **2017**, 29, 1604005-1604034.
- 180 A. M. Schenzel, N. Moszner and C. Barner-Kowollik, *ACS Macro Letters*, **2017**, 6, 16-20.
- 181 M. Yamada, M. Kondo, J.-i. Mamiya, Y. Yu, M. Kinoshita, C. J. Barrett and T. Ikeda, *Angew. Chem. Int. Ed.*, **2008**, 47, 4986-4988.
- 182 M. Yamada, M. Kondo, J.-i. Mamiya, Y. Yu, M. Kinoshita, C. J. Barrett and T. Ikeda, *Angew. Chem. Int. Ed.*, **2008**, 47, 4940-4940.
- 183 V. D. Mitchell, W. W. H. Wong, M. Thelakkat and D. J. Jones, *Polym. J.*, **2017**, 49, 155-161.
- 184 Y. Norikane and N. Tamaoki, *Org. Lett.*, **2004**, 6, 2595-2598.

- 185 M. Banghart, K. Borges, E. Isacoff, D. Trauner and R. H. Kramer, *Nature neuroscience*, **2004**, 7, 1381-1386.
- 186 M. R. Banghart, A. Mourot, D. L. Fortin, J. Z. Yao, R. H. Kramer and D. Trauner, *Angew. Chem. Int. Ed.*, **2009**, 48, 9097-9101.
- 187 M. Volgraf, P. Gorostiza, R. Numano, R. H. Kramer, E. Y. Isacoff and D. Trauner, *Nature chemical biology*, **2006**, 2, 47-52.
- 188 N. R. Krekiehni, M. Müller, U. Jung, S. Ulrich, R. Herges and O. M. Magnussen, *Langmuir*, **2015**, 31, 8362-8370.
- 189 G. Liu, J. Liu, T. P. Davis and J. J. Gooding, *Biosens. Bioelectron.*, **2011**, 26, 3660-3665.
- 190 K. N. R. Wuest, V. Trouillet, R. Koppe, P. W. Roesky, A. S. Goldmann, M. H. Stenzel and C. Barner-Kowollik, *Polymer Chemistry*, **2017**, 8, 838-842.
- 191 A. Rahmouni, Y. Bougdid, S. Moujdi, D. V. Nesterenko and Z. Sekkat, *J Phys Chem B*, **2016**, 120, 11317-11322.
- 192 P. Mueller, M. M. Zieger, B. Richter, A. S. Quick, J. Fischer, J. B. Mueller, L. Zhou, G. U. Nienhaus, M. Bastmeyer, C. Barner-Kowollik and M. Wegener, *ACS Nano*, **2017**, 11, 6396-6403.
- 193 T. Kamiyama, L. Sigrist and J. Cvengroš, *Synthesis*, **2016**, 48, 3957-3964.
- 194 F. Cooper and M. Partridge, *J. Chem. Soc.*, **1957**, 2888-2893.
- 195 A. Lauber, B. Zelenay and J. Cvengroš, *Chem. Commun.*, **2014**, 50, 1195-1197.
- 196 S. Goswami, K. Ghosh and M. Halder, *Tetrahedron Lett.*, **1999**, 40, 1735-1738.
- 197 M. K. Rofouei, A. Sabouri, A. Ahmadalinezhad and H. Ferdowsi, *J. Hazard. Mater.*, **2011**, 192, 1358-1363.
- 198 M. K. Rofouei, M. Payehghadr, M. Shamsipur and A. Ahmadalinezhad, *J. Hazard. Mater.*, **2009**, 168, 1184-1187.
- 199 M. K. Rofouei, M. Mohammadi and M. B. Gholivand, *Materials Science & Engineering C-Materials for Biological Applications*, **2009**, 29, 2154-2159.
- 200 A. H. Durgaryan, N. A. Durgaryan, R. H. Arakelyan and E. E. Matinyan, *Synth. Met.*, **2010**, 160, 180-186.
- 201 J. Steinkoenig, M. M. Zieger, H. Mutlu and C. Barner-Kowollik, *Macromolecules*, **2017**, 50, 5385-5391.
- 202 C. Hörenz, C. Pietsch, A. S. Goldmann, C. Barner-Kowollik and F. H. Schacher, *Advanced Materials Interfaces*, **2015**, 2, 1500042-1500054.
- 203 K. Aich, S. Das, S. Goswami, C. K. Quah, D. Sarkar, T. K. Mondal and H.-K. Fun, *New J. Chem.*, **2016**, 40, 6907-6915.
- 204 S. Goswami, S. Das, K. Aich, B. Pakhira, S. Panja, S. K. Mukherjee and S. Sarkar, *Org. Lett.*, **2013**, 15, 5412-5415.
- 205 A. K. Das and S. Goswami, *Sensors and Actuators B: Chemical*, **2017**, 245, 1062-1125.
- 206 R. Maji, A. K. Mahapatra, K. Maiti, S. Mondal, S. S. Ali, P. Sahoo, S. Mandal, M. R. Uddin, S. Goswami, C. K. Quah and H.-K. Fun, *RSC Adv.*, **2016**, 6, 70855-70862.
- 207 L. A. Evans, M. Petrovic, M. Antonijevic, C. Wiles, P. Watts and J. Wadhawan, *J Phys Chem C*, **2008**, 112, 12928-12935.

- 208 A. R. Forrester and R. H. Thomson, *Nature*, **1964**, *203*, 74-75.
- 209 X. Gao, C. S. Hampton and M. Harmata, *Eur. J. Org. Chem.*, **2012**, *2012*, 7053-7056.
- 210 G. Copley, J. G. Gillmore, J. Crisman, G. Kodis, C. L. Gray, B. R. Cherry, B. D. Sherman, P. A. Liddell, M. M. Paquette, L. Kelbaskas, N. L. Frank, A. L. Moore, T. A. Moore and D. Gust, *J. Am. Chem. Soc.*, **2014**, *136*, 11994-12003.
- 211 M. M. Paquette, B. O. Patrick and N. L. Frank, *J. Am. Chem. Soc.*, **2011**, *133*, 10081-10093.
- 212 W. L. Hubbell and C. Altenbach, *Current Opinion in Structural Biology*, **1994**, *4*, 566-573.
- 213 X. Zhang, C. F. Chamberlayne, A. Kurimoto, N. L. Frank and E. J. Harbron, *Chem. Commun.*, **2016**, *52*, 4144-4147.
- 214 U. A. Hrozhyk, S. V. Serak, N. V. Tabiryan and T. J. Bunning, *Adv. Mater.*, **2007**, *19*, 3244-3247.

Appendices

Appendix 1: The DSC results



«Appendix I»

DSC Results

Table of Contents

Background	247
DSC experimental set up	247
Thermal analysis results and discussion	248
Conclusion	250
DSC thermograms	251
DSC, Compound P1.1	251
DSC, Compound P1.4	255
DSC, Compound P1.7	260
DSC, Compound P1.10	264
DSC, Compound P1.13	266
DSC, Compound P1.17	267
DSC, Compound P1.2	268
DSC, Compound P1.16	270
DSC, Compound P2.1	271
DSC, Compound P2.5	273
DSC, Compound P2.1b	275
DSC Calibrations	278
DSC, Indium	278
DSC, 4'-Heptyl-4-biphenylcarbonitrile	278
DSC, 1,8-Naphthalic anhydride	281
DSC, 2,6-Dimethoxyphenol	282
DSC, (E)-4-(phenyldiazenyl)phenol	282
References	286

Background

Differential Scanning Calorimetry (DSC) is a reliable thermo-analytical method for accurately determining the heat capacity, purity and phase transition onset(s) of solids and liquids.¹ A DSC thermogram is recorded as a function of time and heat-flow and reveals the physical change that a substance undertakes at different stages of heating or cooling. Accordingly, DSC is a useful method for detecting phase transitions expected for thermotropic liquid-crystals,^{2,3} as well as thermal stability of compounds.^{4,5}

An example of a DSC thermogram is shown for 4-heptyl-4'-cyanobiphenyl (7CB),⁶ which is well known for its liquid-crystal properties. As can be seen, endothermic peaks are observed on its DSC thermogram, indicating the phase transitions. In contrast, the thermolysis (thermal decomposition) of compounds appear as exothermic peak(s) on the DSC thermogram. DSC was used in this project to evaluate the thermal stability and potential liquid-crystalline properties of the Tröger's base analogues listed in the table of contents of this section.

DSC experimental set up

The DSC analyser usually has a chamber kept under constant flow of an inert gas and its temperature is fully controlled by the DSC operator. The DSC instrument is often equipped with two ultra-sensitive heat sensors which record the differences between the amount of heat absorbed by a pair of cans in which one of them is loaded with a chemical sample and the other one is left empty. This measurement is proportional to the sample's mass and is recorded as a function of time and heat-flow.

An aluminium can loaded with the sample was heated under a constant flow of nitrogen gas in the chamber of a Differential Scanning Calorimeter DSC2010TA (TA Instruments, New Castle, DE). An identical but empty can was used as the reference. An indium block was used for calibrating⁷ the DSC instrument and to ensure its accuracy, pure commercial (Sigma-Aldrich) samples of 1,8-naphthalic anhydride (melting point: 270-276°C),⁸ 2,6-dimethoxyphenol (melting point: 52-57°C),⁹ and (*E*)-4-(phenyldiazenyl)phenol (melting point: 150-157°C) were tested. The results were found to be in agreement with the literature.^{6,8,9}

Thermal analysis results and discussion

As described in the introduction, azo carrying Tröger's base analogues were chosen for this study due to their potential LCD related applications. Azo materials, however, are well documented to be unstable upon heating, releasing a nitrogen molecule and carbon centred radicals (Figure 1).¹⁰

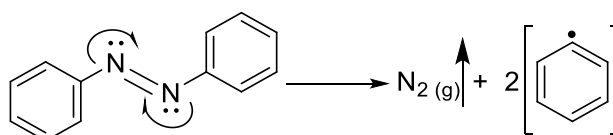


Figure 1. Thermolysis of typical azo compounds

The stability of azo analogues of TB was unknown before this project. To determine the stability of the azo carrying TBAs introduced in this thesis, selected compounds (listed in Table 1) were heated in the DSC to the point of observing a large exothermic peak on their DSC thermogram, at which stage the sample colour turned black. Compound **P1.1** (the first compound from Paper I) was the least stable thermally, decomposing at 254°C, while compound **P1.7** and **P1.10** were the most stable, decomposing at around 295°C.

Figure 2 is a representation of how compound **P1.4** turned from a shiny orange powder (**a**, at r.t.) to a glassy orange solid (**b**, heated up to 180°C) and finally turned to black at the end of the pyrolysis (**c**, heated up to 400°C).

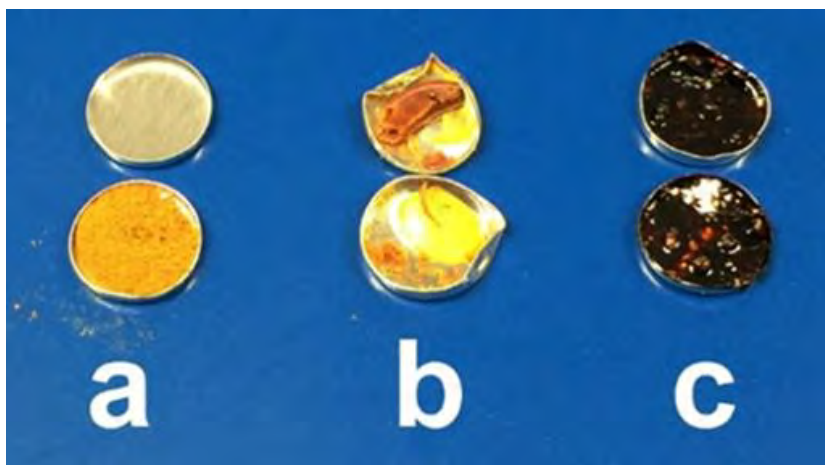
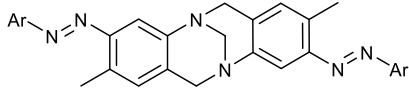
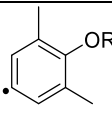
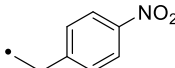
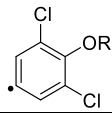
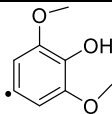
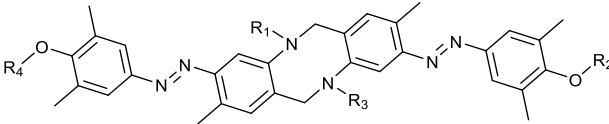


Figure 2. Stepwise pyrolysis of **P1.4**

Following confirmation of the high temperature stability of the azo compounds, they were then investigated for their liquid-crystal properties by heating them below their decomposition temperature, then cooling and reheating. As a positive control, this experiment was also done for the known liquid-crystal compound 7CB. The thermograms for each compound were collected, showing each heating and cooling cycle. This appendix also reports the endothermic transitions of the compounds with reproducible repeatable solid-liquid transitions below their decomposition. As can be seen from compound 7CB, with known liquid crystalline properties, a liquid-crystal will show repeatable phase transitions.

Table 1 Summary of the DSC results

						
Compd Ref.	Ar	R	Transition(s)°C		Decomposition°C	
P1.1 ¹¹		H	153–158 ^{Rep.} and 187–198		254–259	
P1.4 ¹¹		hexyl	66–78, 105–124, 149–159 ^{MP}		293–313	
P1.7 ¹¹		dodecyl	59–75, 81–89 ^{MP}		296–351	
P1.10 ¹¹		octadecyl	33–38, 44–51 ^{MP}		295–348	
P1.13 ¹¹		2-bromoethyl	N/E		252–258	
P1.17 ¹¹		N/A	N/E		238–265	
P2.1 ¹²		H	32–58		243–265	
P2.1b ¹²		hexyl	62–92, 141–150		288–300	
P2.5 ¹²		N/A	N/E		298–301	
						
Compd Ref.	R ₁	R ₂	R ₃	R ₄	Transition(s)°C	Dec.°C
P1.2 ¹¹	methyl	methyl	methyl	methyl	250–262 ^{MP (Rep.)}	301–316
P1.16 ¹¹	H	benzyl	benzyl	H	N/E	247–258

Compd: compound; Ref.: reference; Rep.: reproducible peak upon cooling and reheating; MP: melting point; N/A: not applicable; N/E: non-existing.

Degradation of **P2.1**, **P1.16** and **P1.13** occurred around 250°C, but occurs at a slightly different temperature for **P2.5** (300°C) and **P1.17** (238°C). **P1.2**, which lacks the rigidity of the TB scaffold due to the methylated bridge-head nitrogen atoms, melts around 250°C with no sign of degradation until reaching 300°C, where it totally decomposes and leaves a charcoal-like black residues (Figure 2). Fortunately, all compounds showed an acceptable thermal stability and their stability also confirmed that they should be able to be heated for further modification reactions, such as alkylation reactions or removal of solvents by evaporation, at 65–110 and 45°C, respectively, making them useful precursors for other reactions.

Compound **P1.1** showed a repeatable transition step at 154°C. The endothermic heat exchange peaks of **P1.4** (at 67, 105 and 151°C), **P1.7** (at 59, 82°C) and **P1.10** (37 and 45°C) were not reproducible. In the case of compounds **P1.4**, **P1.7** and **P1.10**, after the first heating the samples turned into a glassy orange form and had identical ¹HNMR spectra with the non-heated samples; however, following reheating the peaks on the DSC thermograms disappeared. It is assumed that the loss of the peaks may be due to rearrangements in the crystalline phase(s). Similarly **P2.1b** and **P1.4** showed multiple but not reproducible transitions at slightly different temperatures (62 and 141°C) and degraded by 288°C.

Further investigation requires more advanced techniques which is beyond the scope of this study. This could include combined power-compensation with heat-flux DSCs,² and simultaneous DSC/X-Ray studies.³

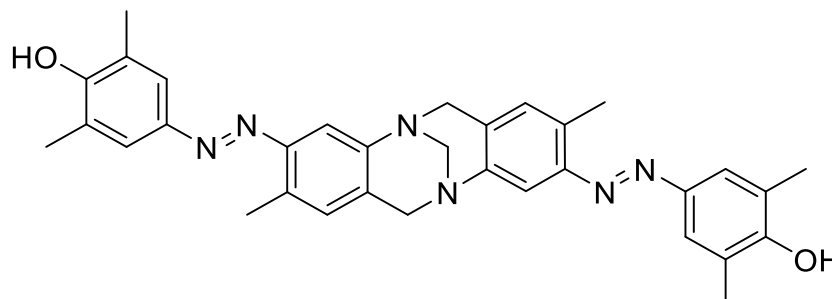
Conclusion

The melting point and the DSC data of the selected azo products suggest that the longer the alkyl chain, the lower the phase transition onsets. Also, it can be concluded that shorter alkyl groups show more distinguishable phase transitions. Furthermore, it was found that due to the rigidity of the structures of none-alkylated or benzylated derivatives, they had no distinct melting point and instead decomposed at high temperature. The thermal analysis results also assured that these products were all stable up to 200°C. This eliminated all reservations about their decomposition during the synthesis and purification steps and the future modifications.

DSC thermograms

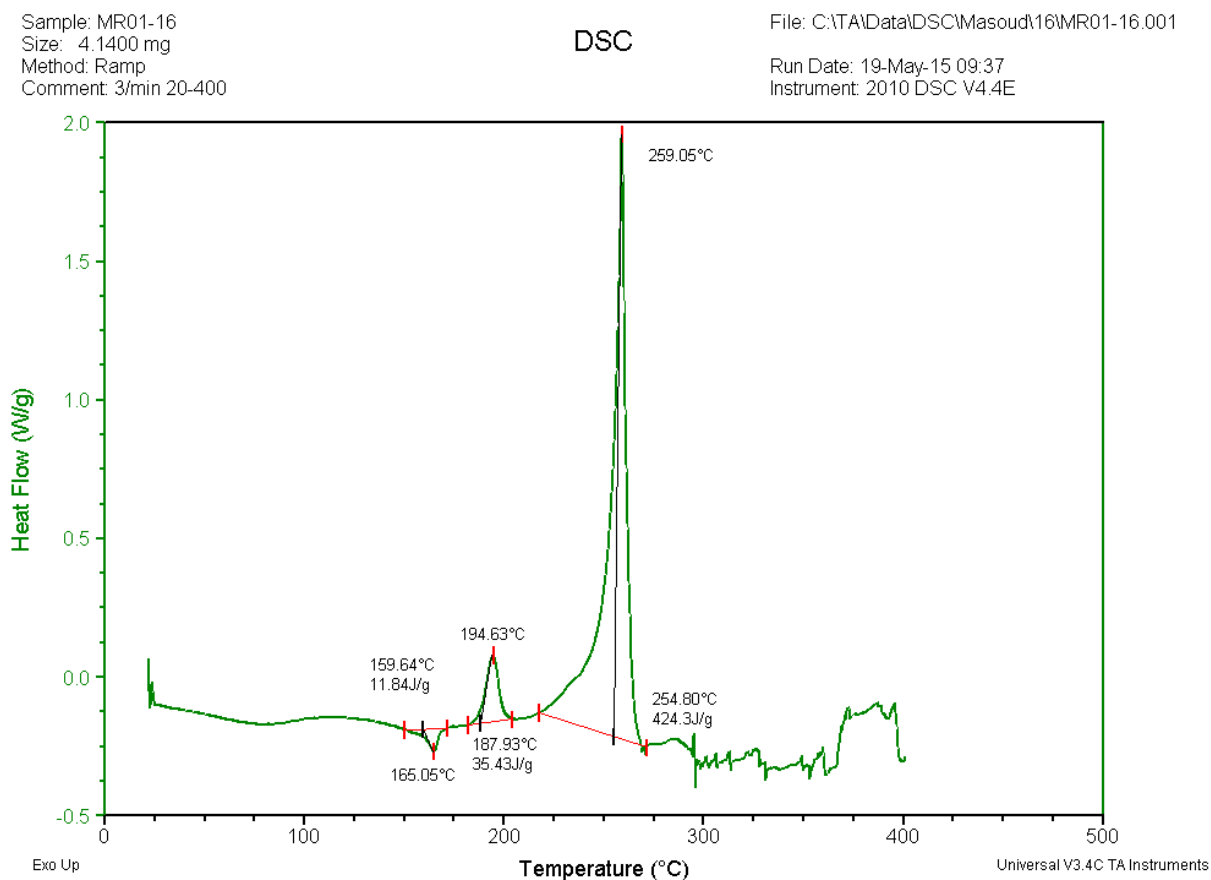
DSC, Compound P1.1

4,4'-((2,8-dimethyl-6H,12H-5,11-methanodibenzo[b,f][1,5]diazocine-3,9-diyl)bis(diazeno-2,1-diyl)) bis(2,6-dimethylphenol)



Compound P1.1

The residue of this orange sample, after this heating experiment, looked like charcoal and the decomposition occurred beyond 220°C under nitrogen gas. During the melting point tests, the sample remained as a solid in the capillary tube and slowly turned from orange to brownish orange and then to black between 176-184°C).



Compound P1.1, Sample 1, Ramp 20-400°C, Heating Rate 3°C/min

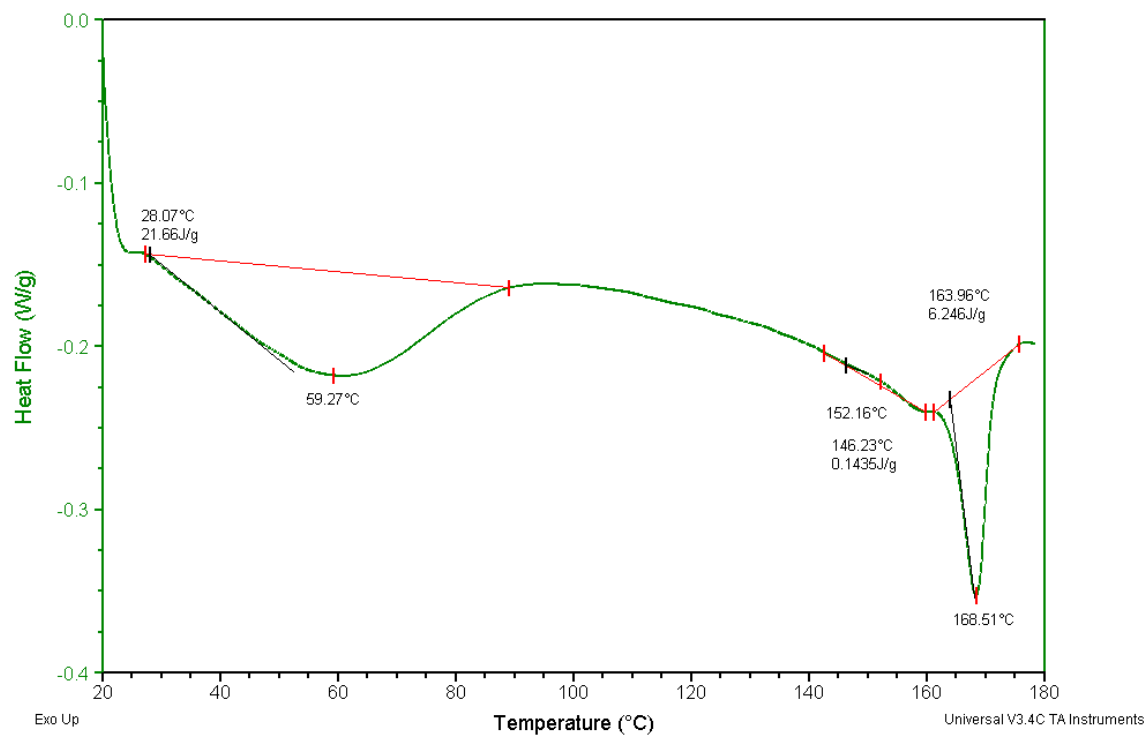
Sample: MR01-32 new
Size: 9.0100 mg

DSC

File: C:\DSC\Masoud\16\MR01-32 new 1run.001

Run Date: 15-Jul-15 09:03
Instrument: 2010 DSC V4.4E

Comment: 6c/min-180c- 1st run



Compound P1.1, Sample 2, Ramp 20-180°C

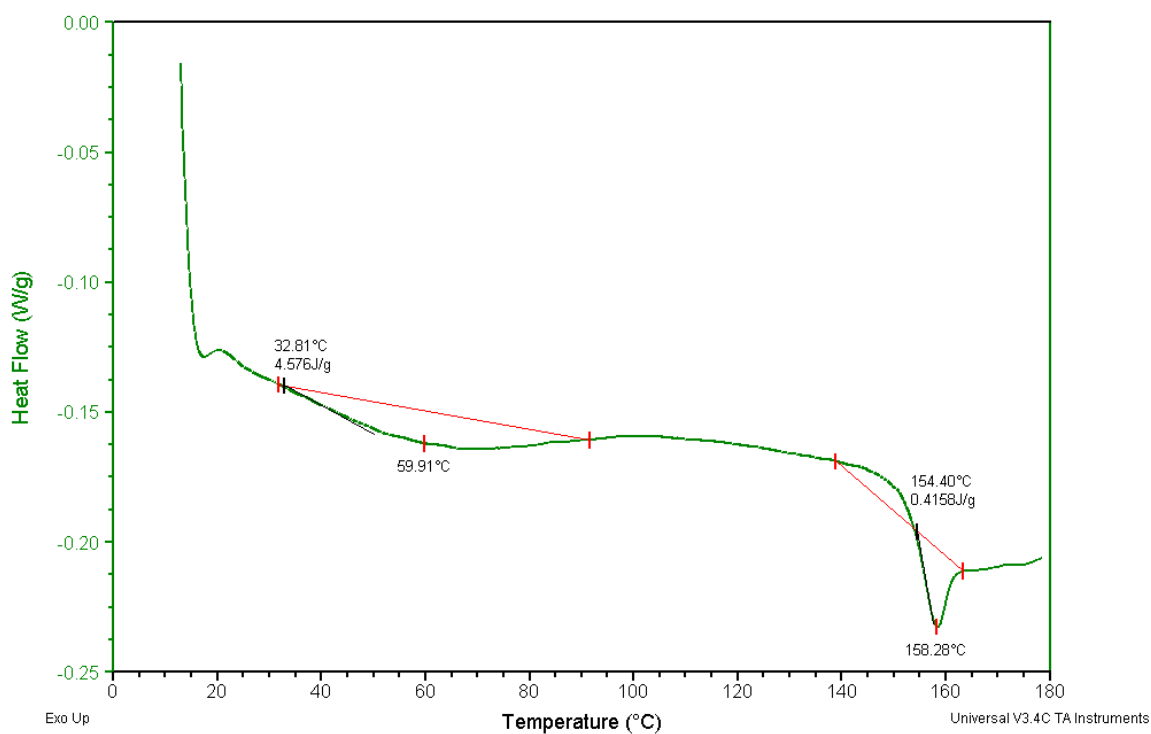
Sample: MR01-32 new 2run
Size: 9.0100 mg

DSC

File: C:\DSC\Masoud\16\MR01-32 new 2run.001

Run Date: 15-Jul-15 10:51
Instrument: 2010 DSC V4.4E

Comment: 6c/min-180c- 2run



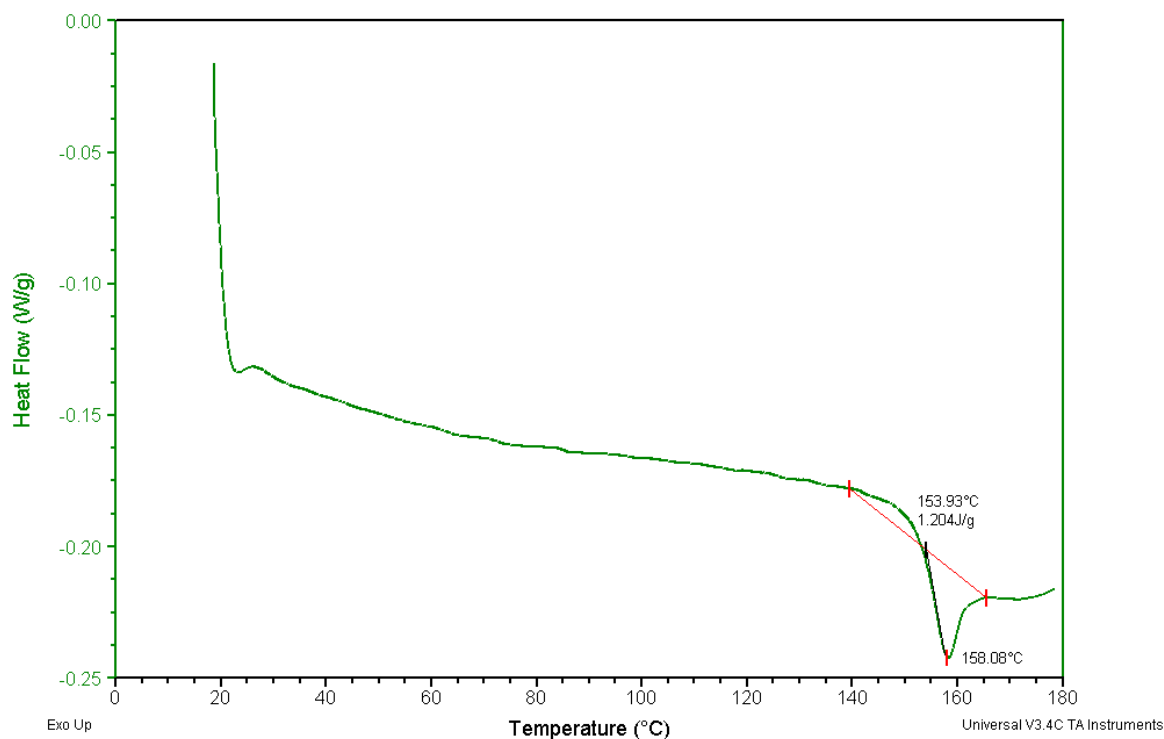
Compound P1.1, Sample 2, Ramp 20-180°C (first reheat)

Sample: MR01-32 new 3run
Size: 9.0100 mg
Comment: 6c/min-180c- 3run

DSC

File: C:\DSC\Masoud\16\MR01-32 new 3run.001

Run Date: 15-Jul-15 12:19
Instrument: 2010 DSC V4.4E



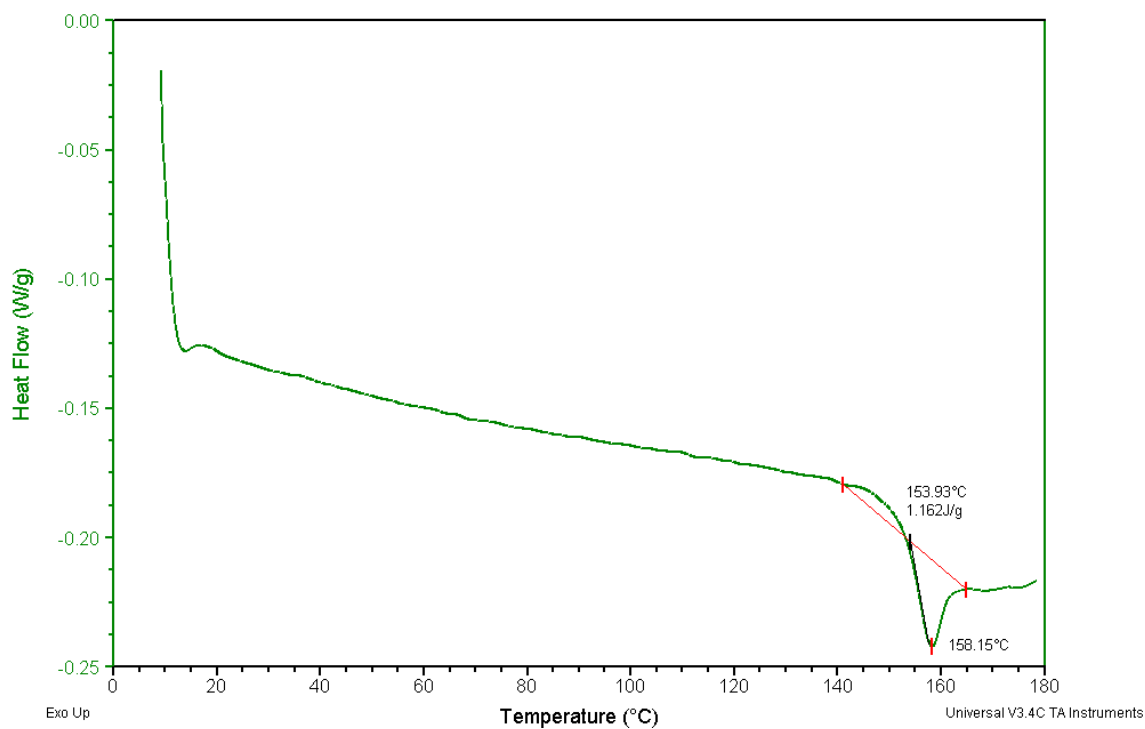
Compound P1.1, Sample 2, Ramp 20-180°C (second reheat)

Sample: MR01-32 new 4run
Size: 9.0100 mg
Comment: 6c/min-180c- 4run

DSC

File: C:\DSC\Masoud\16\MR01-32 new 4run.001

Run Date: 15-Jul-15 13:16
Instrument: 2010 DSC V4.4E

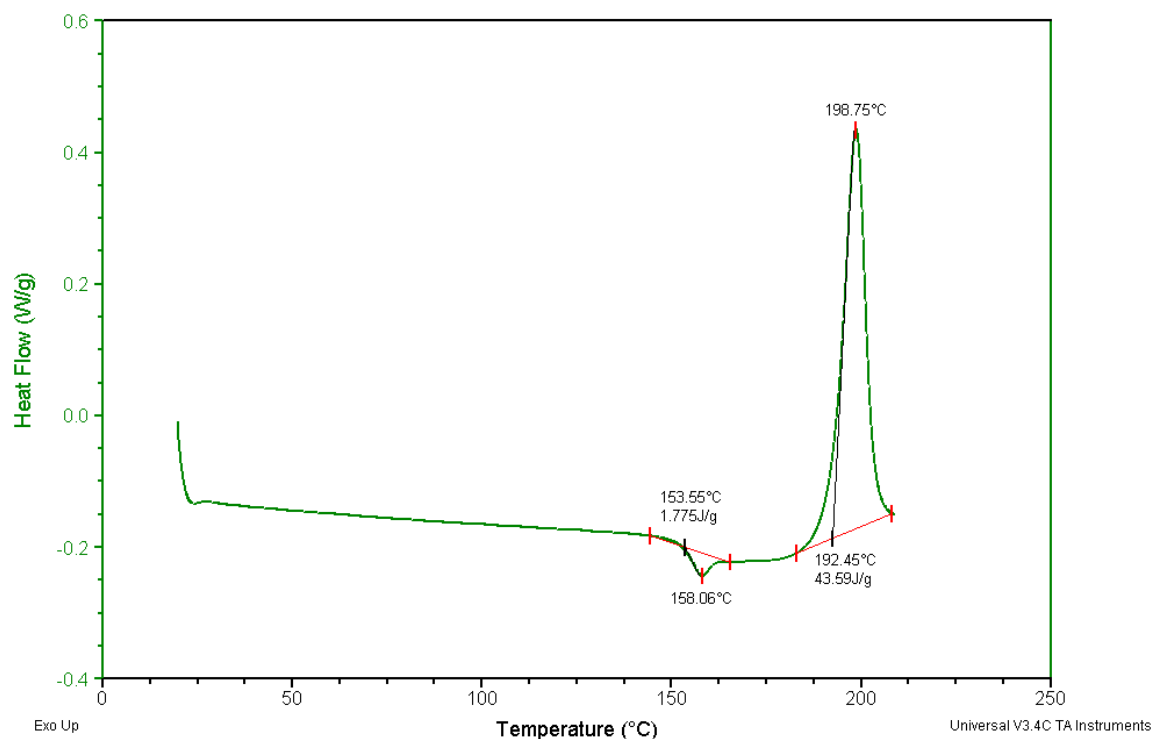


Compound P1.1, Sample 2, Ramp 20-180°C (third reheat)

Sample: MR01-32 new 5run
Size: 9.0100 mg
Comment: 6c/min-210c- 5run

DSC

File: C:\DSC\Masoud\16\MR01-32 new 5run.001
Run Date: 15-Jul-15 14:07
Instrument: 2010 DSC V4.4E

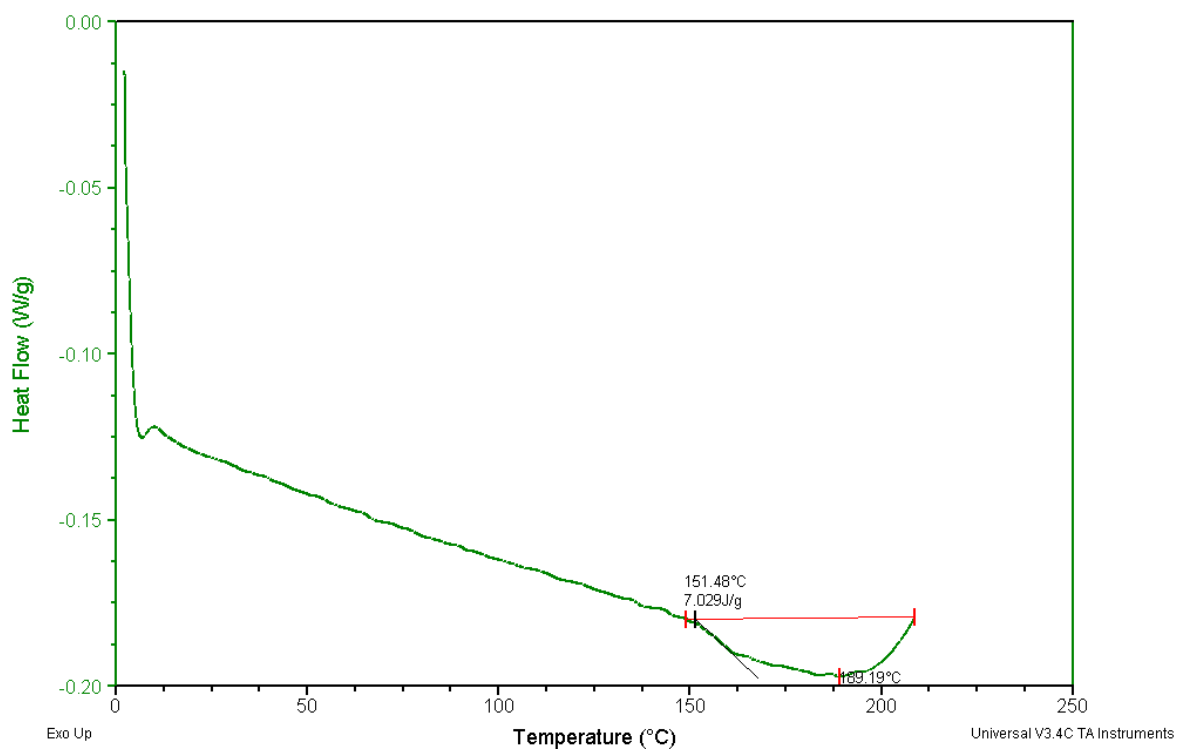


Compound P1.1, Sample 2, Ramp 20-220°C (forth reheat)

Sample: MR01-32 new 6run
Size: 9.0100 mg
Comment: 6c/min-210c- 6run

DSC

File: C:\DSC\Masoud\16\MR01-32 new 6run.001
Run Date: 15-Jul-15 15:03
Instrument: 2010 DSC V4.4E

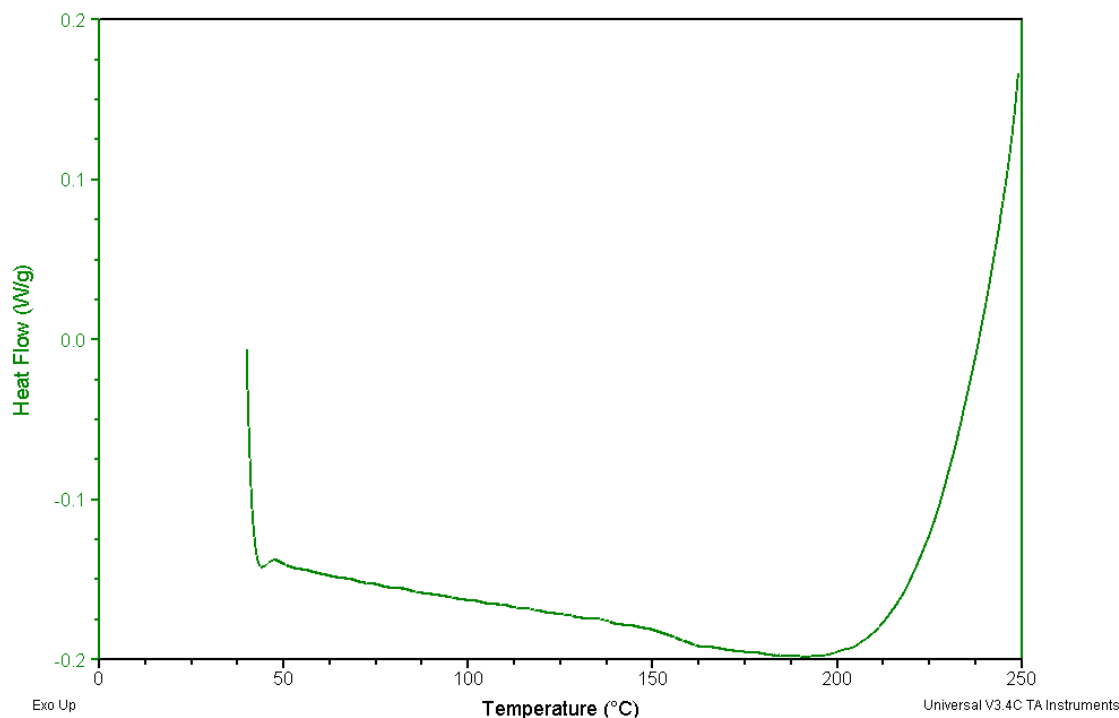


Compound P1.1, Sample 2, Ramp 20-220°C (fifth reheat)

Sample: MR01-32 new 7run
 Size: 9.0100 mg
 Comment: 6c/min-210c- 7run

DSC

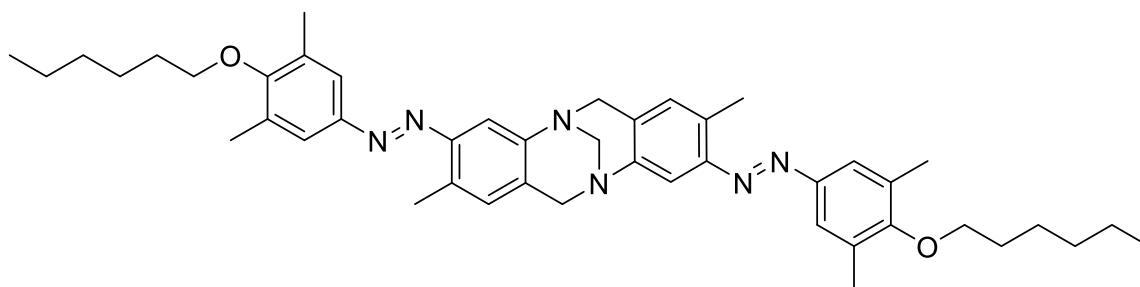
File: C:\...DSC\Masoud\16\MR01-32 new 7run.001
 Run Date: 15-Jul-15 16:57
 Instrument: 2010 DSC V4.4E



Compound P1.1, Sample 2, Ramp 20-250°C (sixth reheat)

DSC, Compound P1.4

3,9-bis((*E*)-(4-(hexyloxy)-3,5-dimethylphenyl)diazenyl)-2,8-dimethyl-6H,12H-5,11-methanodibenzo [b,f][1,5]diazocine



Compound P1.4

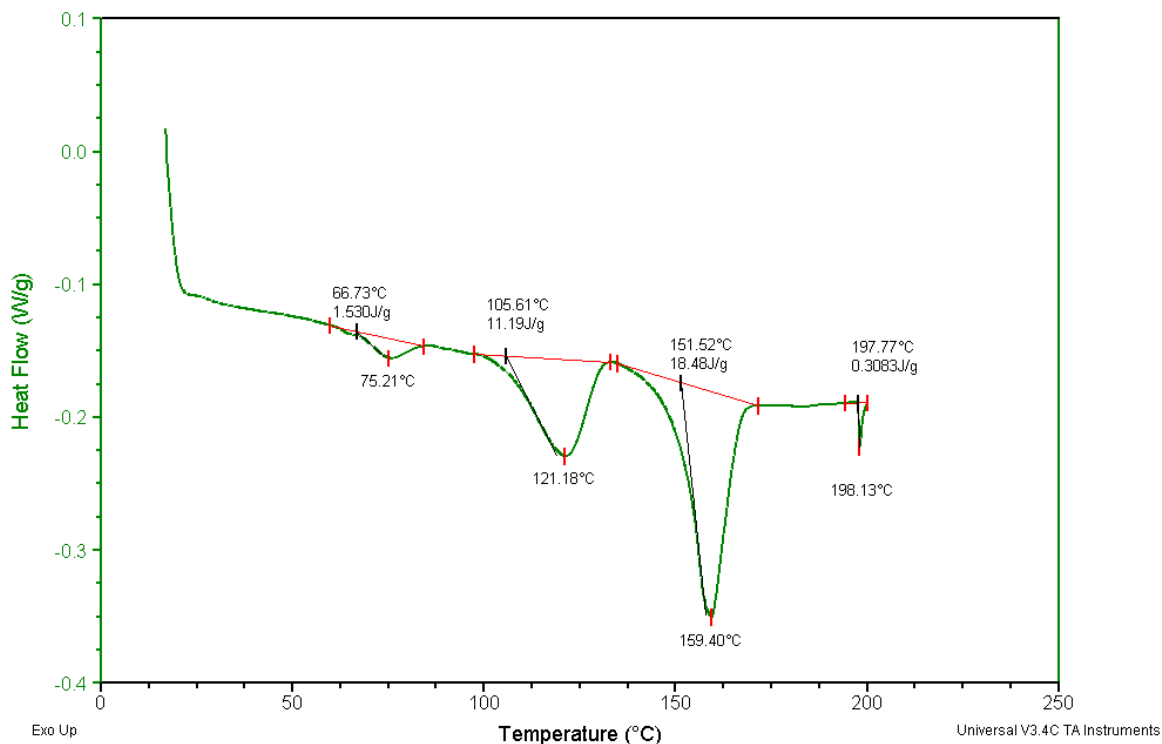
Heating the sample turned it from a powder into a glassy orange substance, which looked very transparent even at room temperature and remained so for several weeks. The sample that was heated up to 200°C was retrieved from the DSC can and its ¹H NMR spectra was identical to the original compound. Upon melting, the compound changed from an orange powder to a sticky orange substance (100-115°C) and it turned to semi-molten (118-127°C) and then liquefied (152-159°C). Upon reheating, none of the peaks were reproducible e.g. the sample which was heated up to 90°C twice, only showed the first peak once. Similarly, when it was heated to 130°C, it only showed the second peak once. Again, when it was heated to 175°C, it showed the third peak once.

Sample: MR01-18 LargeSample
 Size: 28.3600 mg
 Method: Ramp
 Comment: 6c/min-200c

DSC

File: C:\...Masoud\18\MR01-18 LargeSample.001

Run Date: 4-Jun-15 10:05
 Instrument: 2010 DSC V4.4E



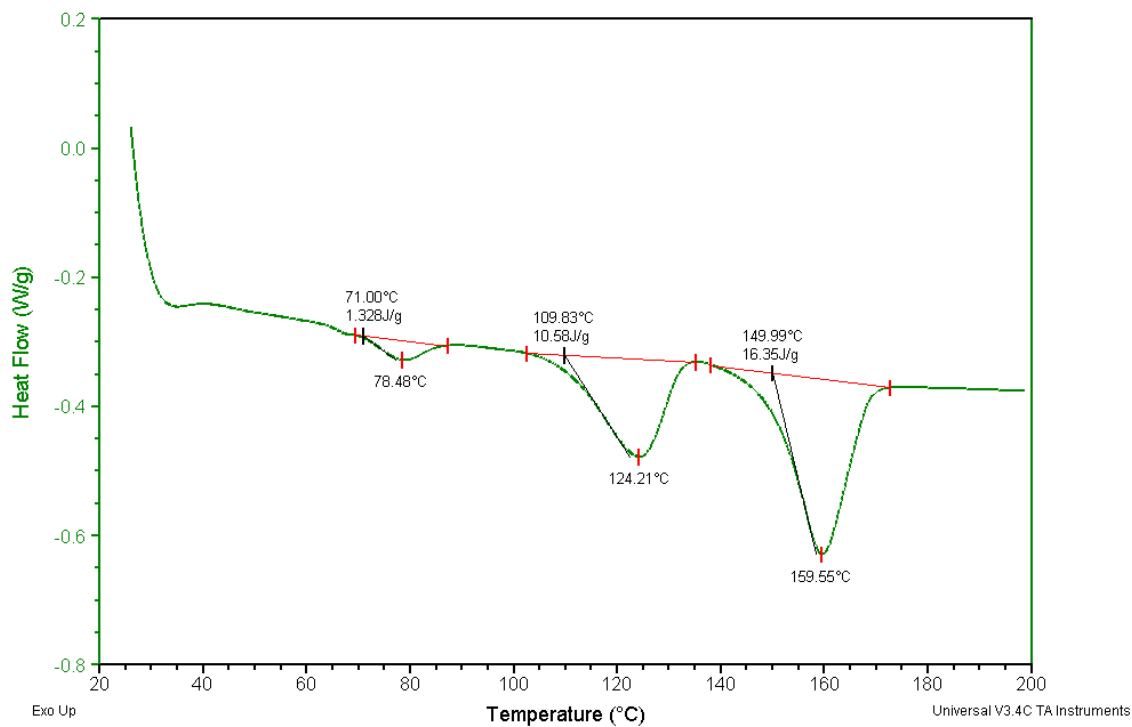
Compound P1.4, Sample 1, Ramp 20-200°C

Sample: MR01-18 LargeSample2
 Size: 15.7000 mg
 Method: Ramp
 Comment: 12c/min-200c

DSC

File: C:\...18\MR01-18 LargeSample2.001

Run Date: 4-Jun-15 11:41
 Instrument: 2010 DSC V4.4E



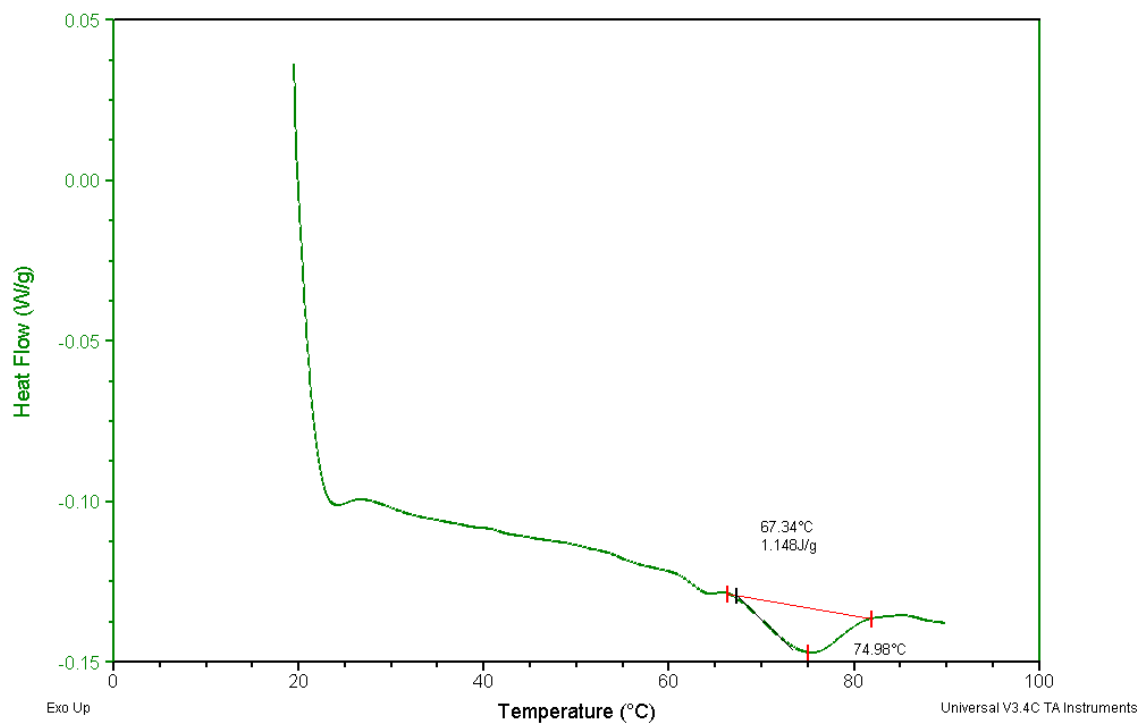
Compound P1.4, Sample 2, Ramp 20-200°C

Sample: MR01-18 fraction heating
Size: 11.8300 mg
Method: Ramp
Comment: 6c/min-90c

DSC

File: C:\TA\Data\DSC\Masoud\LC7.004

Run Date: 5-Jun-15 13:20
Instrument: 2010 DSC V4.4E



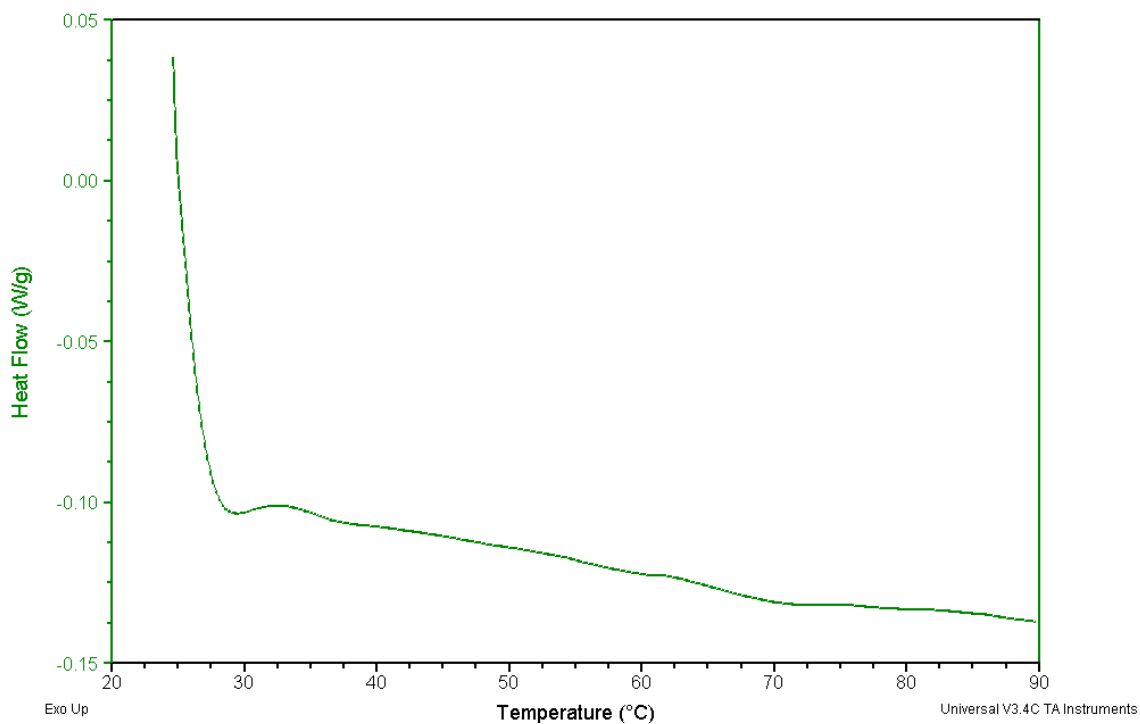
Compound P1.4, Sample 3, Ramp 20-90°C

Sample: MR01-18 fraction heating
Size: 11.8300 mg
Method: Ramp
Comment: 6c/min-90c

DSC

File: C:\TA\Data\DSC\Masoud\LC7.005

Run Date: 5-Jun-15 15:11
Instrument: 2010 DSC V4.4E



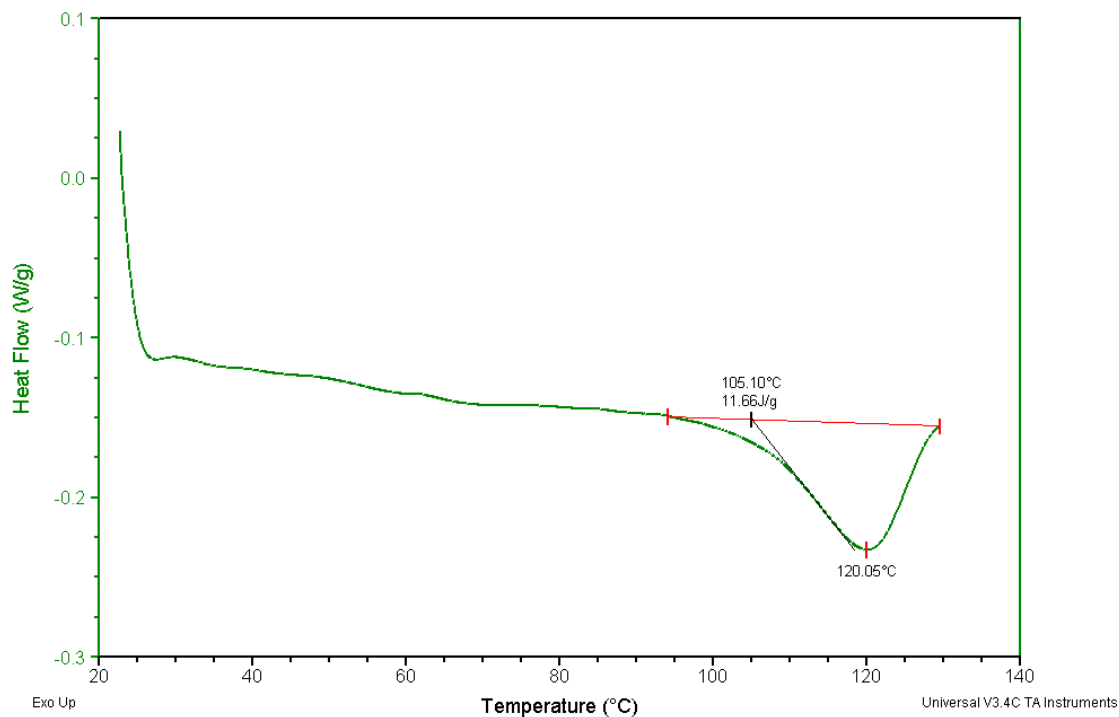
Compound P1.4, Sample 3, Ramp 20-90°C

Sample: MR01-18 fraction heating
Size: 11.8300 mg
Method: Ramp
Comment: 6c/min-130c

DSC

File: C:\TA\Data\DSC\Masoud\LC7.006

Run Date: 9-Jun-15 12:36
Instrument: 2010 DSC V4.4E



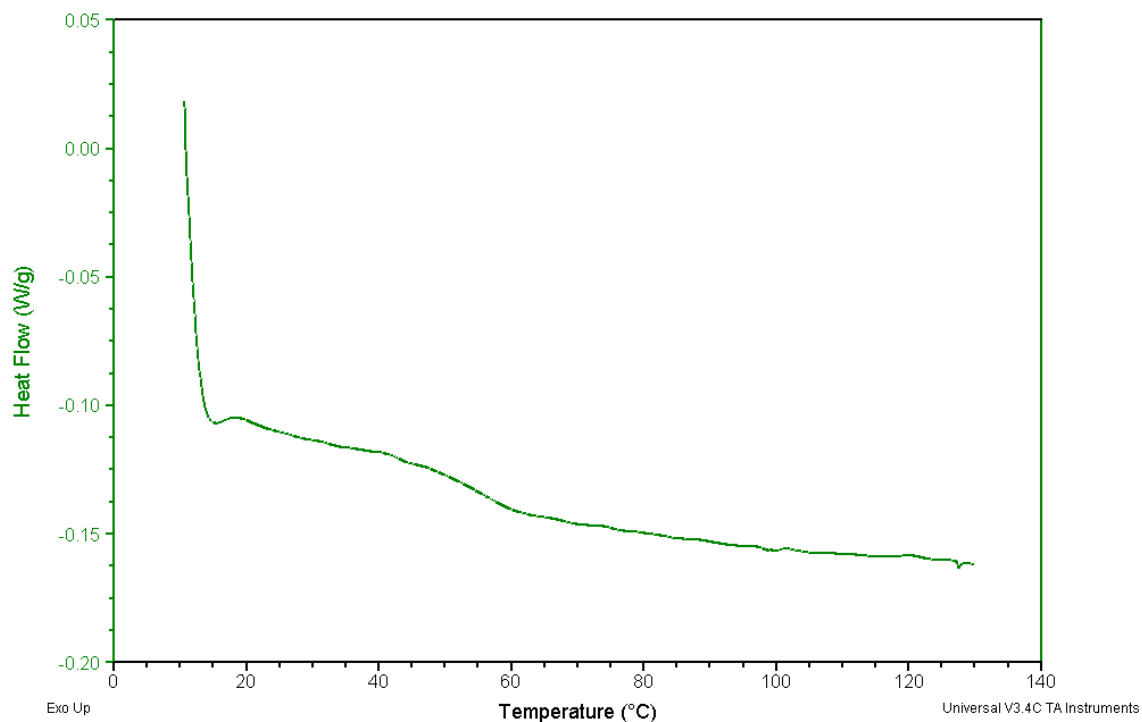
Compound P1.4, Sample 3, Ramp 20-130°C

Sample: MR01-18 fraction heating
Size: 11.8300 mg
Method: Ramp
Comment: 6c/min-130c

DSC

File: C:\TA\Data\DSC\Masoud\LC7.007

Run Date: 9-Jun-15 13:42
Instrument: 2010 DSC V4.4E



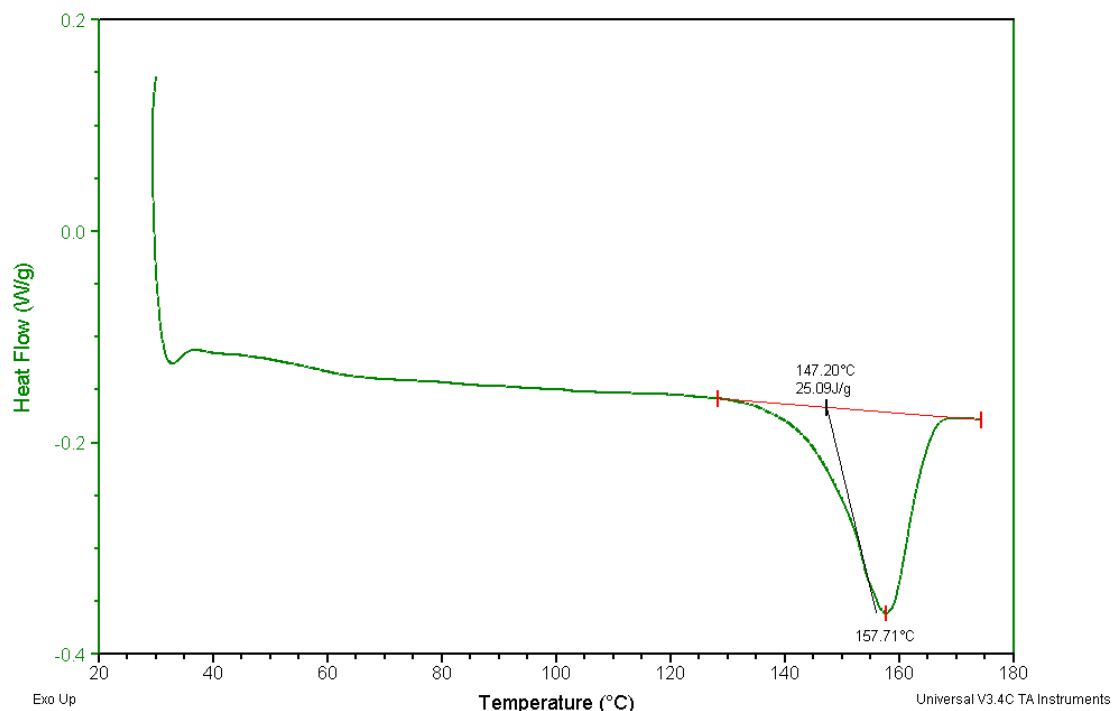
Compound P1.4, Sample 3, Ramp 20-130°C

Sample: MR01-18 fraction heating
Size: 11.8300 mg
Method: Ramp
Comment: 6c/min-175c

DSC

File: C:\TA\Data\DSC\Masoud\LC7.008

Run Date: 9-Jun-15 14:21
Instrument: 2010 DSC V4.4E



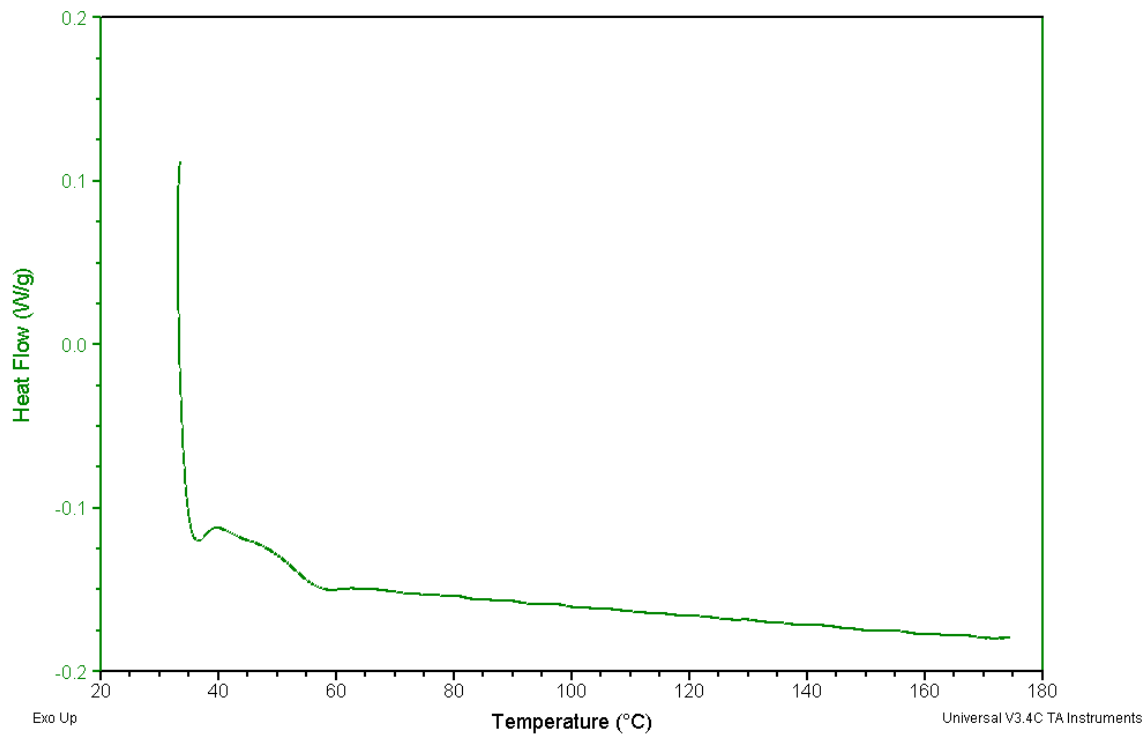
Compound P1.4, Sample 3, Ramp 20-175°C

Sample: MR01-18 fraction heating
Size: 11.8300 mg
Method: Ramp
Comment: 6c/min-175c

DSC

File: C:\TA\Data\DSC\Masoud\LC7.009

Run Date: 9-Jun-15 15:20
Instrument: 2010 DSC V4.4E



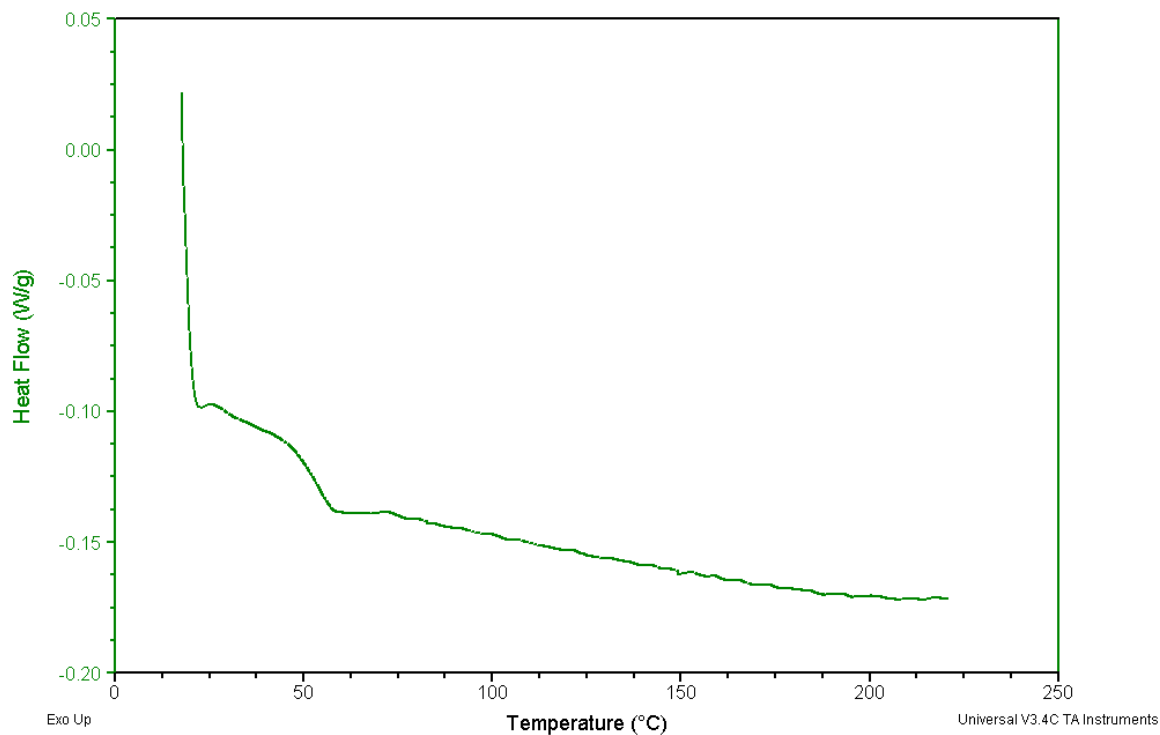
Compound P1.4, Sample 3, Ramp 20-175°C

Sample: MR01-18 fraction heating
 Size: 11.8300 mg
 Method: Ramp
 Comment: 6c/min-220c

DSC

File: C:\TA\DATA\DSC\Masoud\LC7.010

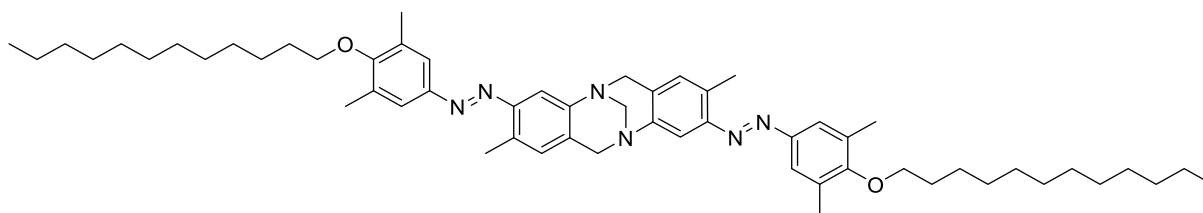
Run Date: 9-Jun-15 16:01
 Instrument: 2010 DSC V4.4E



Compound P1.4, Sample 3, Ramp 20-220°C

DSC, Compound P1.7

3,9-bis((*E*)-(4-(dodecyloxy)-3,5-dimethylphenyl)diazenyl)-2,8-dimethyl-6H,12H-5,11-methanodibenzo [b,f][1,5] diazocine



Compound P1.7

The melting point tests showed that this orange product became more transparent and stickier from 71 to 92°C; afterwards, it became totally molten and turned to an orange liquid between 92-95°C.

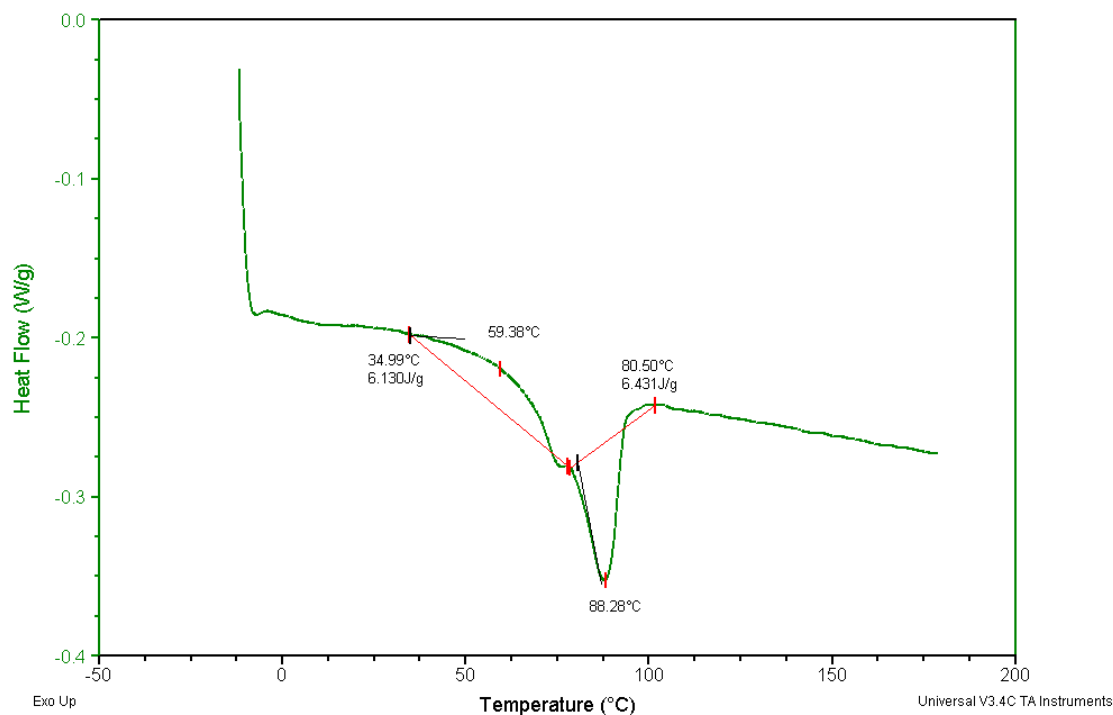
Sample: MR01-54 R1
Size: 3.3000 mg

DSC

File: C:\TA\Data\DSC\Masoud\54\MR01-54 R1.001

Run Date: 16-Jul-15 10:13
Instrument: 2010 DSC V4.4E

Comment: 6c/min-180c- R1



Compound P1.7, Sample 1, Ramp 20-180°C

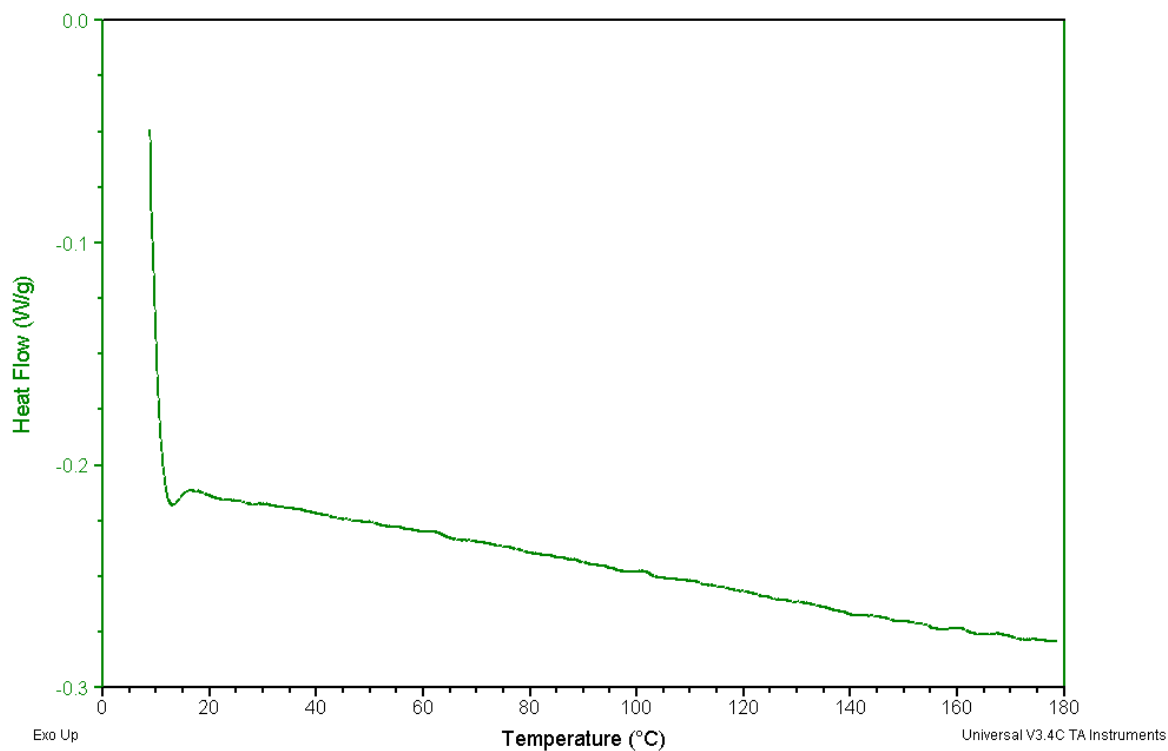
Sample: MR01-54 R2
Size: 3.3000 mg

DSC

File: C:\TA\Data\DSC\Masoud\54\MR01-54 R2.001

Run Date: 16-Jul-15 11:25
Instrument: 2010 DSC V4.4E

Comment: 6c/min-180c- R2



Compound P1.7, Sample 1, Ramp 20-180°C, reheat

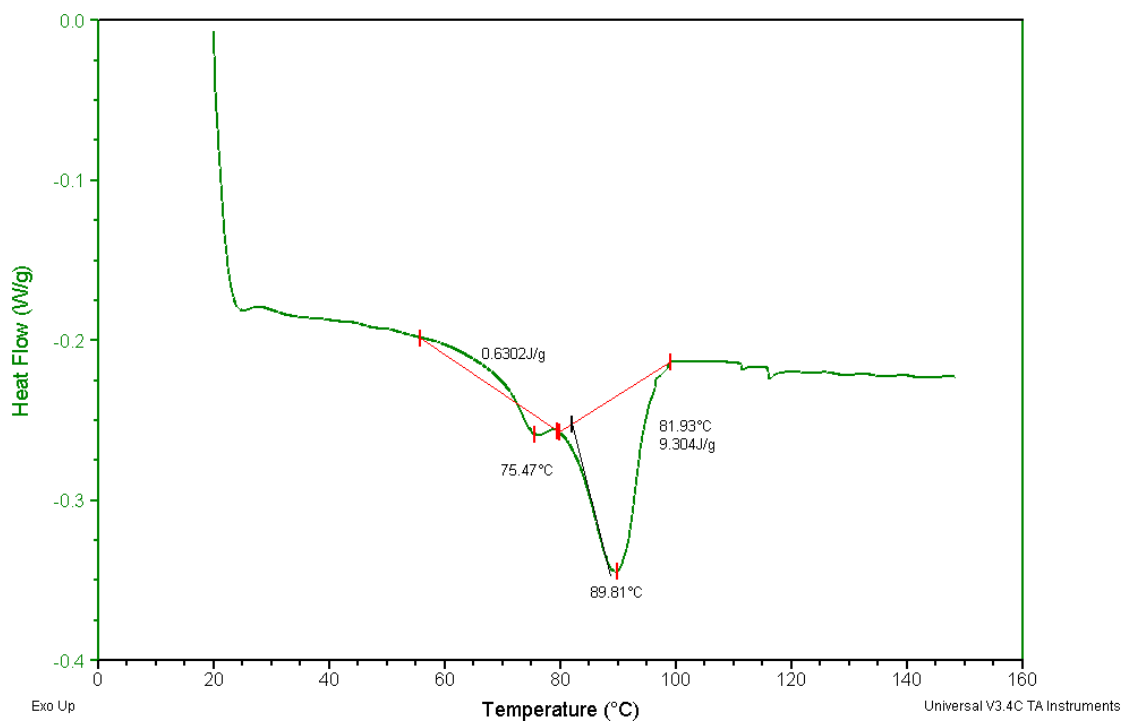
Sample: MR01-54 Large Sample R 1
Size: 14.4100 mg

DSC

File: C:\...154\MR01-54 Large Sample R 1.001

Run Date: 5-Aug-15 10:30
Instrument: 2010 DSC V4.4E

Comment: 6c/min-150c



Compound P1.7, Sample 2, Ramp 20-150°C

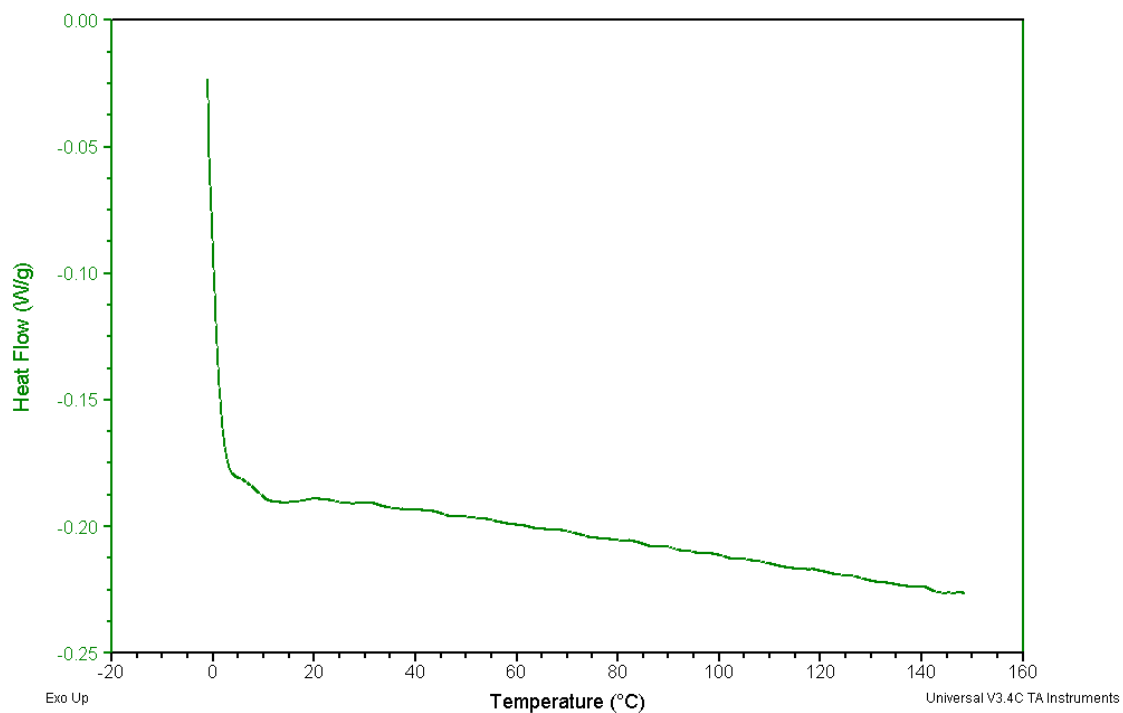
Sample: MR01-54 Large Sample R 2
Size: 14.4100 mg

DSC

File: C:\...154\MR01-54 Large Sample R 2.001

Run Date: 5-Aug-15 11:22
Instrument: 2010 DSC V4.4E

Comment: 6c/min-150c



Compound P1.7, Sample 2, Ramp 20-150°C, reheat

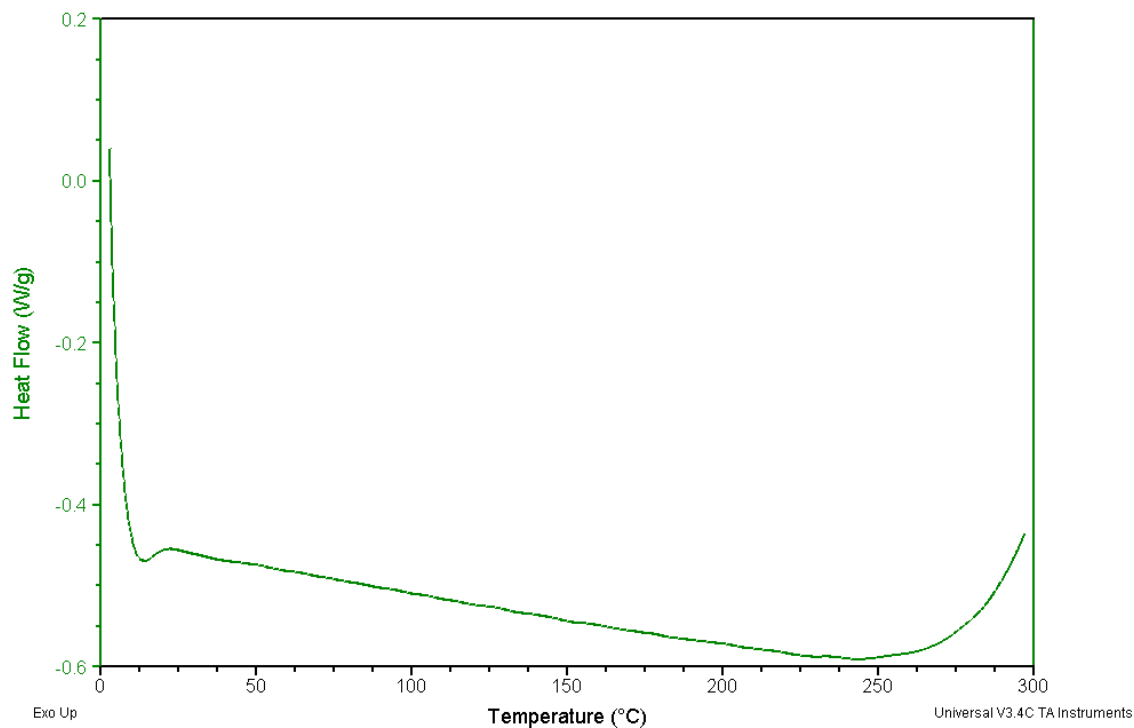
Sample: MR01-54 Large Sample R 3
Size: 14.4100 mg

DSC

File: C:\...54\MR01-54 Large Sample R 3.001

Run Date: 5-Aug-15 11:55
Instrument: 2010 DSC V4.4E

Comment: 15c/min-300c



Compound P1.7, Sample 2, Ramp 20-300°C

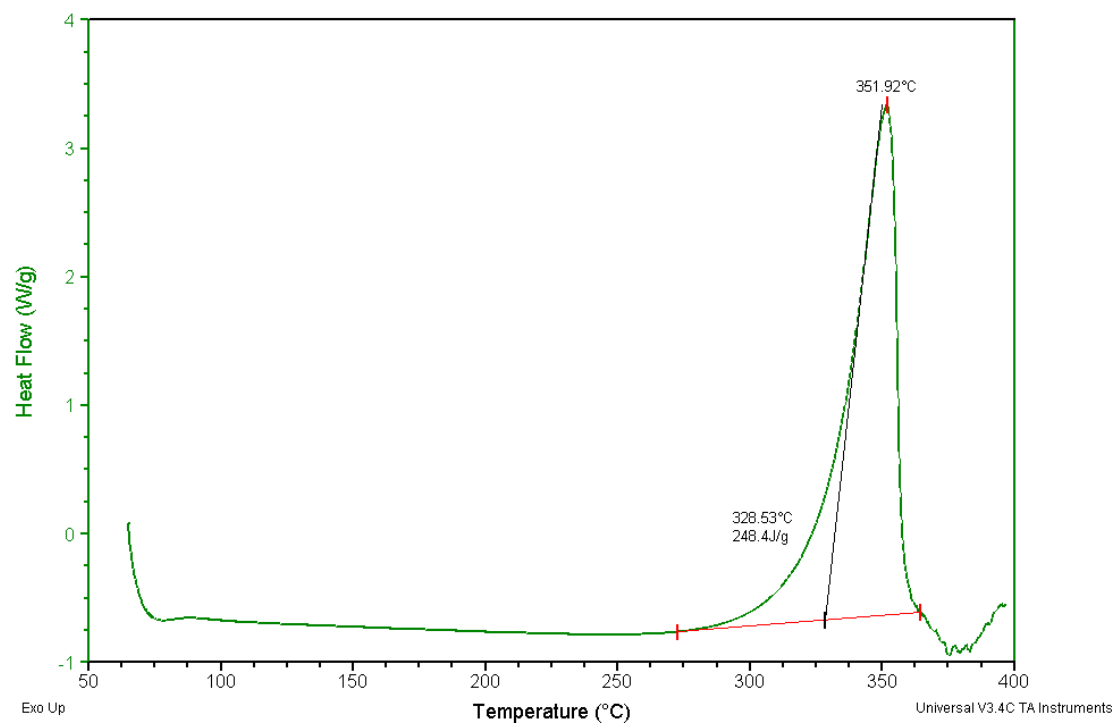
Sample: MR01-54 Large Sample R 4
Size: 14.4100 mg

DSC

File: C:\...54\MR01-54 Large Sample R 4.001

Run Date: 5-Aug-15 12:24
Instrument: 2010 DSC V4.4E

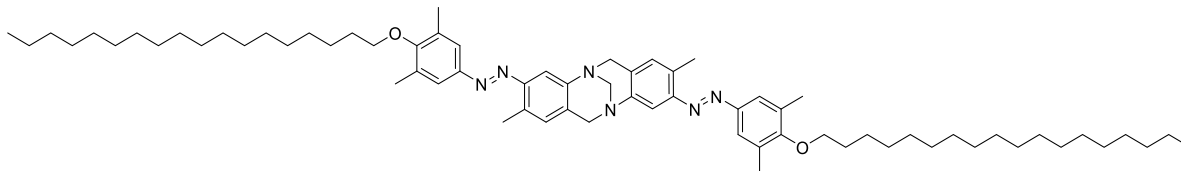
Comment: 20c/min-400c



Compound P1.7, Sample 2, Ramp 20-400°C

DSC, Compound P1.10

3,9-bis((*E*)-(3,5-dimethyl-4-(octadecyloxy)phenyl)diazenyl)-2,8-dimethyl-6H,12H-5,11-methanodibenzo [b,f][1,5] diazocine



Compound P1.10

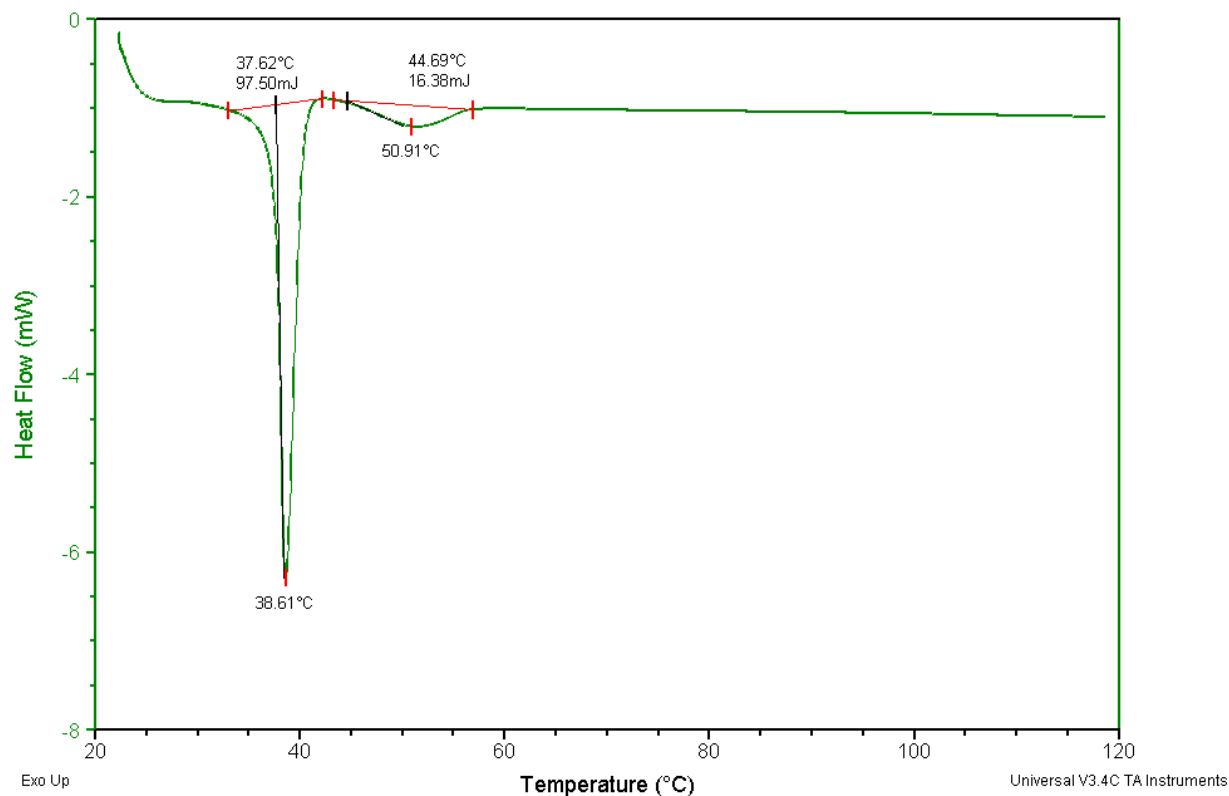
The heated can (400°C) only contained a burnt residue, which looked like charcoal. The melting point tests showed that the compound softens and becomes stickier from 38 to 50°C and then gradually starts melting from 51°C and becomes an orange liquid at 53°C.

Sample: MR01-58
Size: 0.0000 mg
Comment: 6c/min-120c

DSC

File: C:\TA\Data\DSC\Masoud\58\MR01-58.001

Run Date: 7-Aug-15 17:44
Instrument: 2010 DSC V4.4E



Compound P1.10, Sample 1, Ramp 20-120°C, 3.2 mg

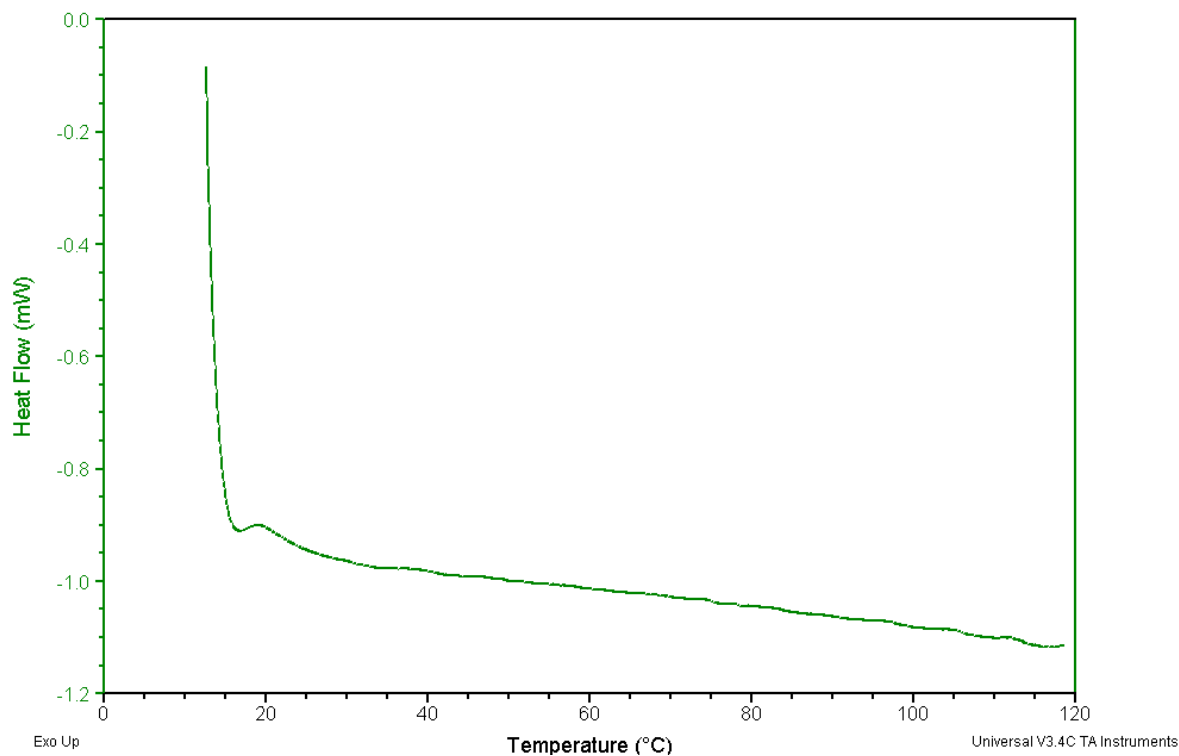
Sample: MR01-58 R2
Size: 0.0000 mg

DSC

File: C:\TA\Data\DSC\Masoud\58\MR01-58 R2.001

Run Date: 7-Aug-15 18:20
Instrument: 2010 DSC V4.4E

Comment: 6c/min-120c



Compound P1.10, Sample 1, Ramp 20-120°C, 3.2 mg, reheat

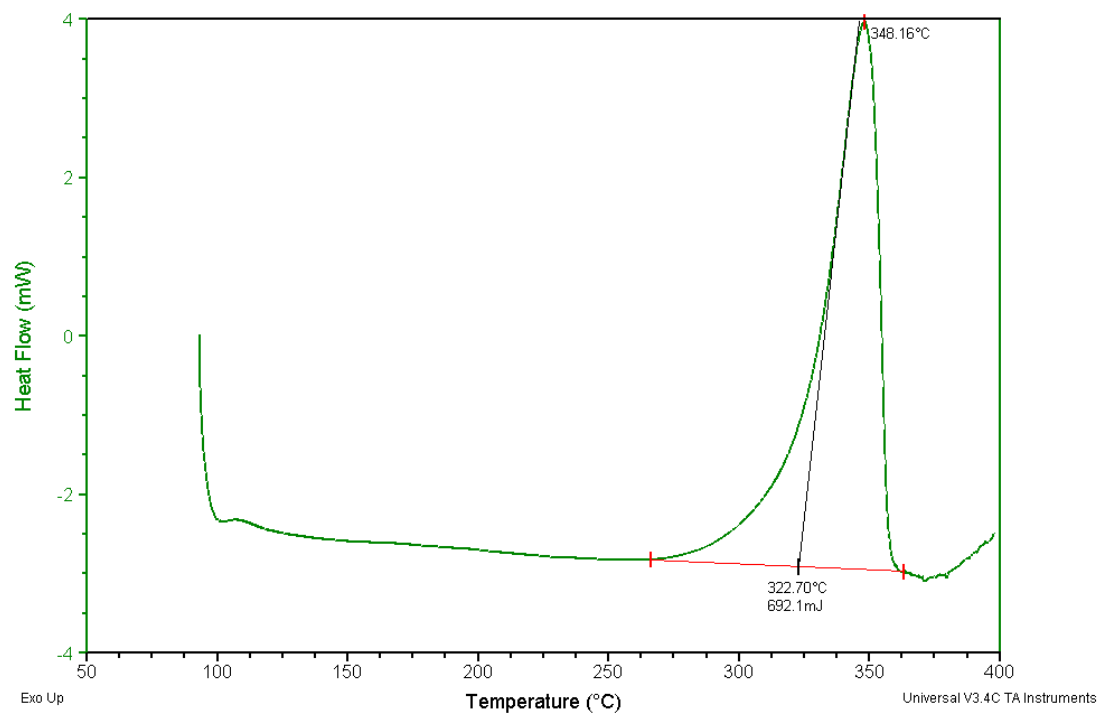
Sample: MR01-58 R2
Size: 0.0000 mg

DSC

File: C:\TA\Data\DSC\Masoud\58\MR01-58 R2.002

Run Date: 7-Aug-15 18:46
Instrument: 2010 DSC V4.4E

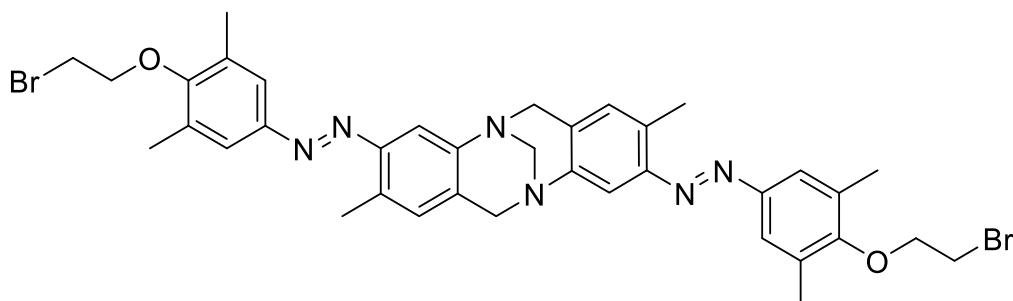
Comment: 15c/min-400c



Compound P1.10, Sample 1, Ramp 20-400°C, 3.2 mg, reheat

DSC, Compound P1.13

3,9-bis((*E*)-(4-(2-bromoethoxy)-3,5-dimethylphenyl)diazenyl)-2,8-dimethyl-6H,12H-5,11-methanodibenzo [b,f][1,5] diazocine



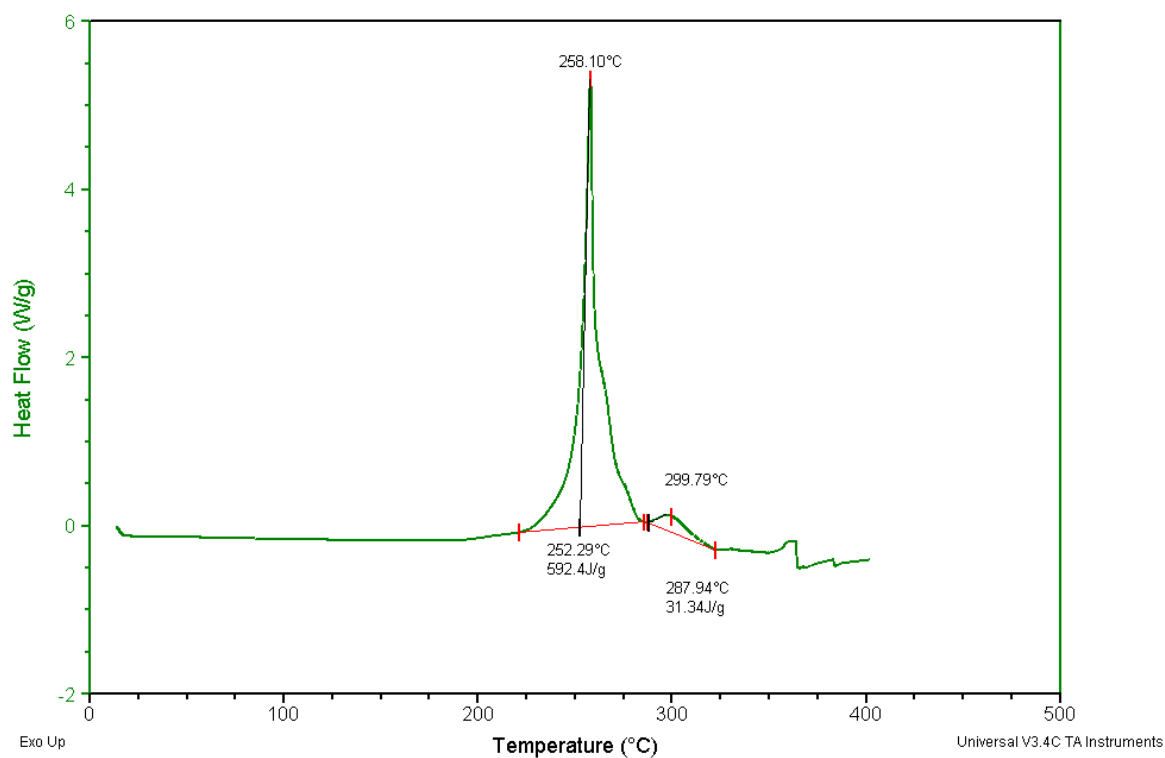
Compound P1.13

Sample: MR01-98
Size: 5.8800 mg
Method: Ramp
Comment: 6c/min 20-400 c

DSC

File: C:\TA\Data\DSC\Masoud\98\MR01-98.001

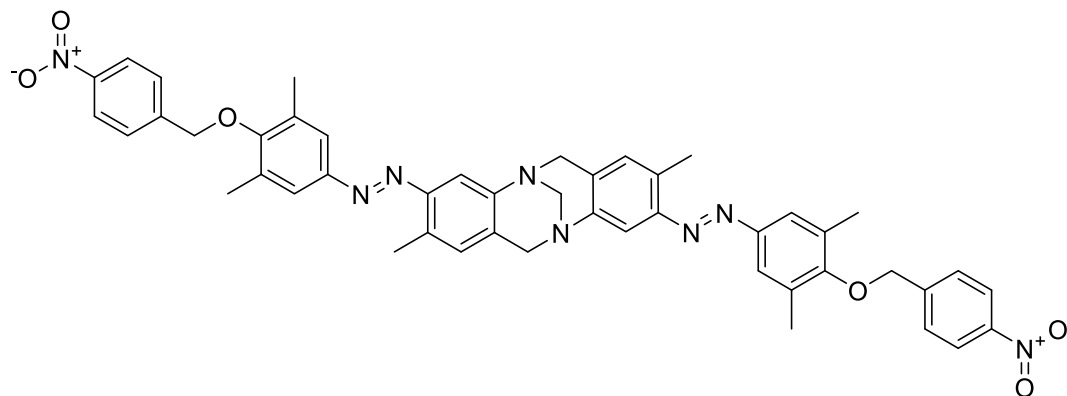
Run Date: 20-Oct-15 15:20
Instrument: 2010 DSC V4.4E



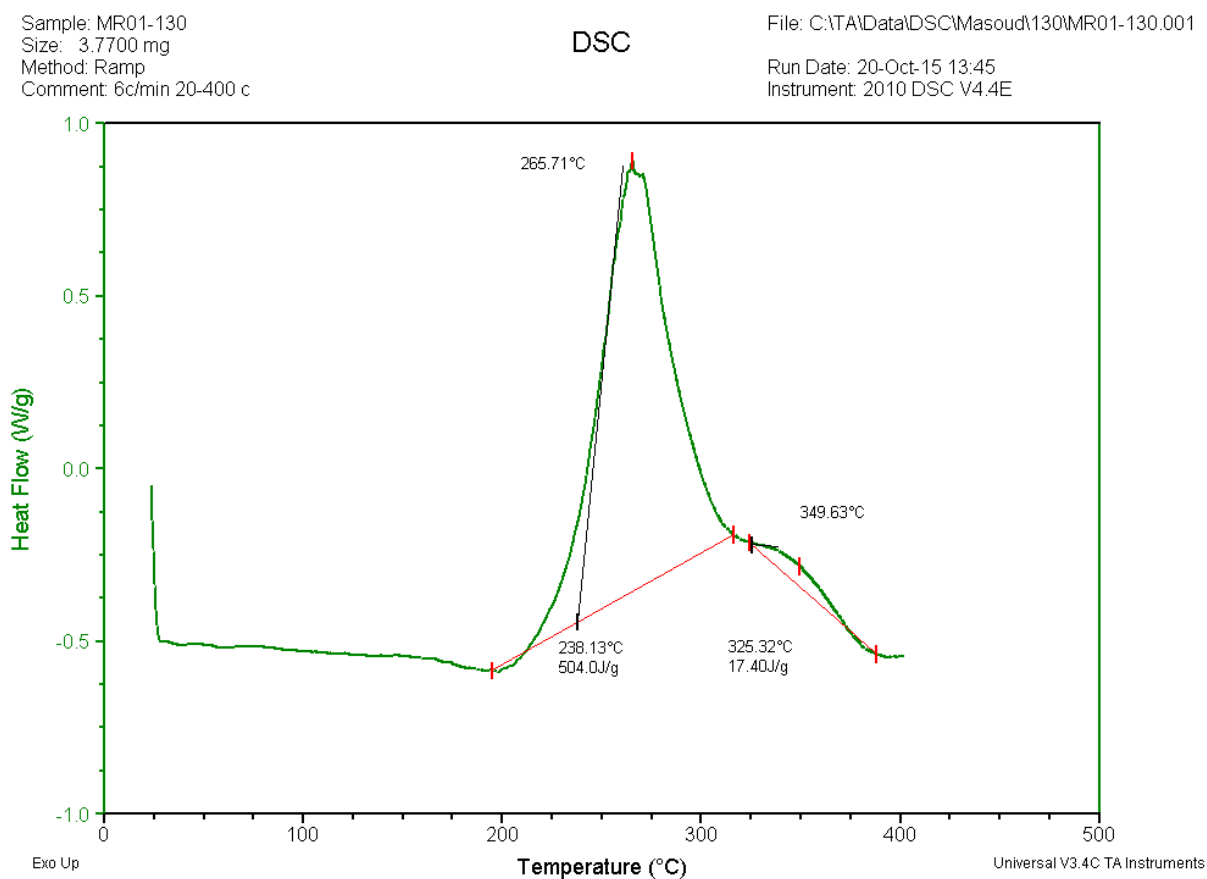
Compound P1.13, Sample 1, Ramp 20-400°C

DSC, Compound P1.17

3,9-bis((*E*)-(3,5-dimethyl-4-((4-nitrobenzyl)oxy)phenyl)diazenyl)-2,8-dimethyl-6H,12H-5,11-methanodibenzo [b,f][1,5] diazocine



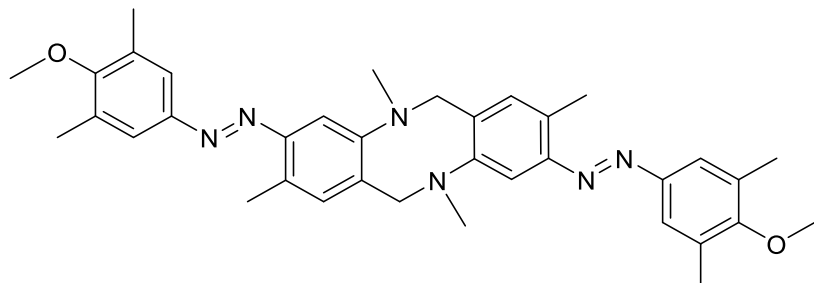
Compound P1.17



Compound P1.17, Sample 1, Ramp 20-400°C

DSC, Compound P1.2

3,9-bis((*E*)-(4-methoxy-3,5-dimethylphenyl)diazenyl)-2,5,8,11-tetramethyl-5,6,11,12-tetrahydrodibenzo [b,f][1,5] diazocine



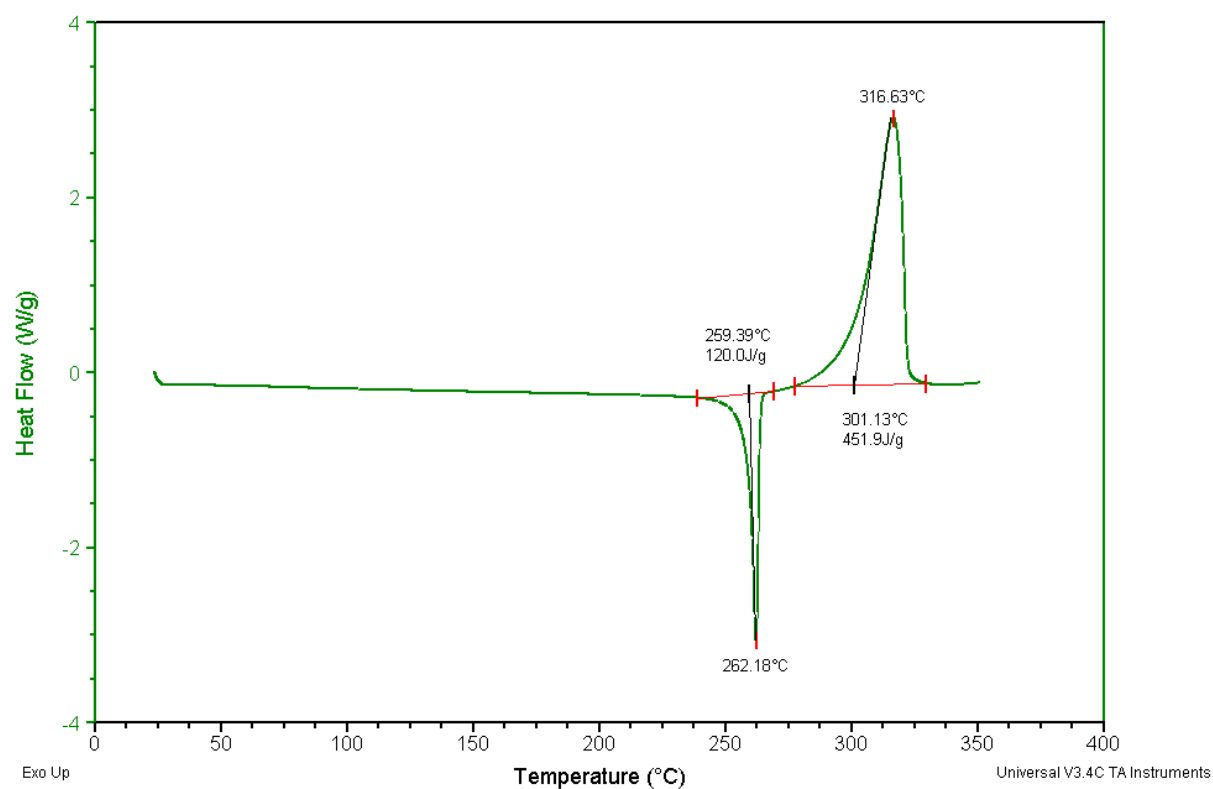
Compound P1.2

Sample: MR01-116
Size: 3.8000 mg
Method: Ramp
Comment: 6c/min 20-400

DSC

File: C:\TA\Data\DSC\Masoud\116\MR01-116.001

Run Date: 19-Oct-15 16:33
Instrument: 2010 DSC V4.4E



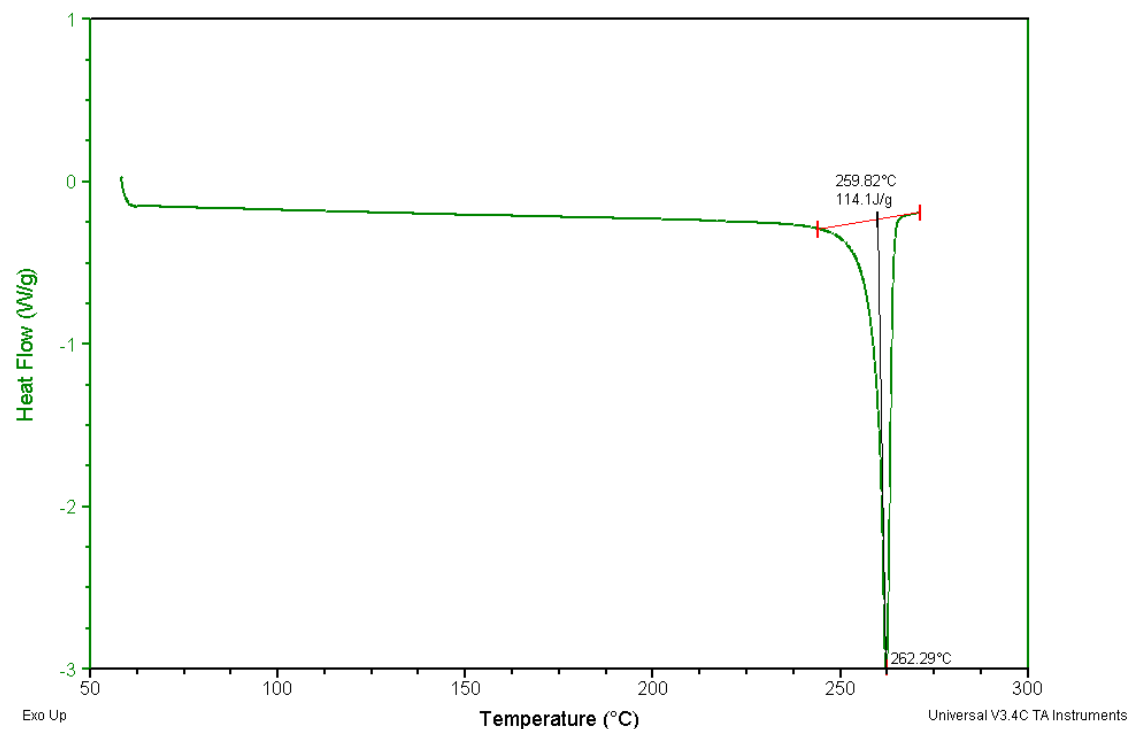
Compound P1.2, Sample 1, Ramp 20-350°C

Sample: MR01-116 2th sample,run1
Size: 4.3500 mg
Method: Ramp
Comment: 6c/min 20-272 c,2th sample,run1

DSC

File: C:\116\MR01-116 2th sample,run1.001

Run Date: 19-Oct-15 17:42
Instrument: 2010 DSC V4.4E



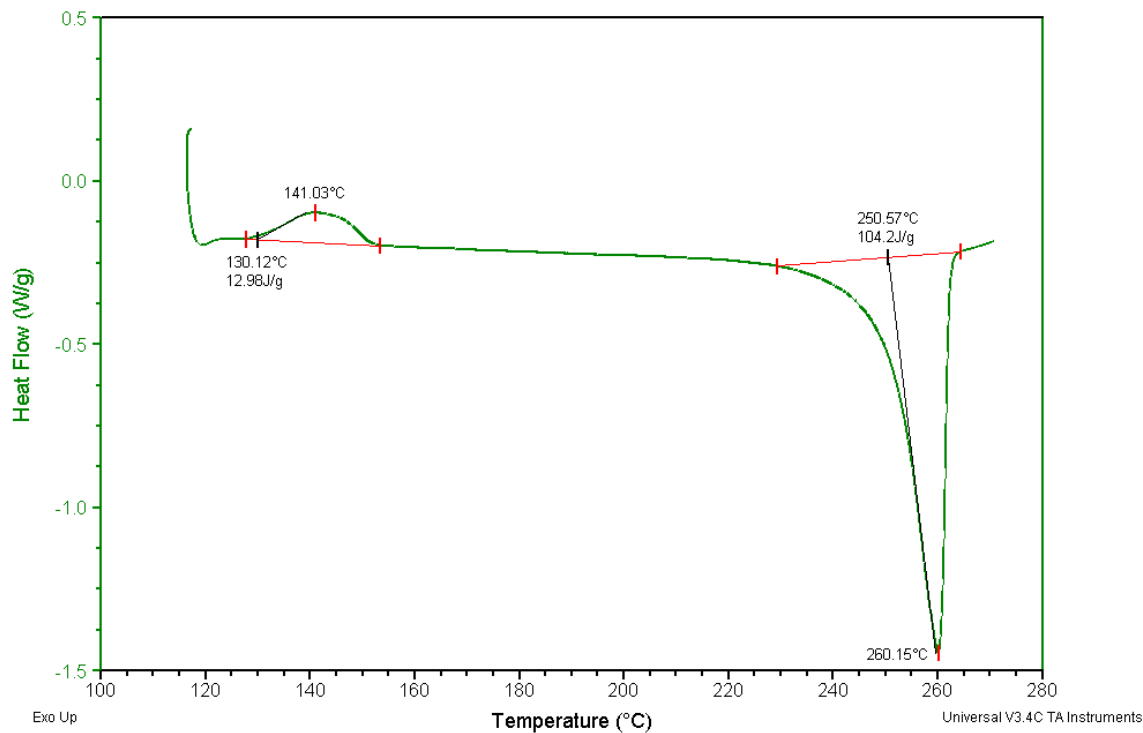
Compound P1.2, Sample 2, Ramp 20-270°C

Sample: MR01-116 2th sample,run2
Size: 4.3500 mg
Method: Ramp
Comment: 6c/min 20-272 c,2th sample,run2

DSC

File: C:\116\MR01-116 2th sample,run2.001

Run Date: 19-Oct-15 18:23
Instrument: 2010 DSC V4.4E



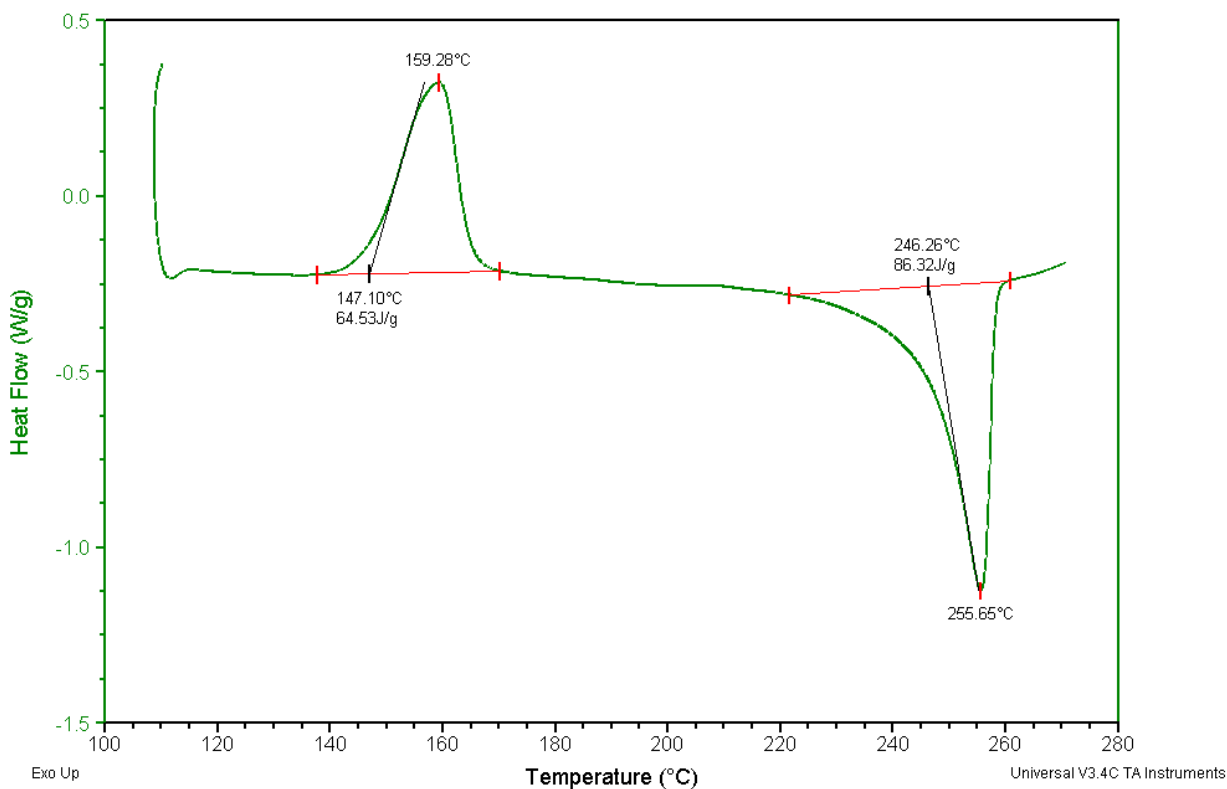
Compound P1.2, Sample 2, Ramp 20-270°C, first reheat

Sample: MR01-116 2th sample,run3
 Size: 4.3500 mg
 Method: Ramp
 Comment: 6c/min 20-272 c,2th sample,run3

DSC

File: C:\...116\MR01-116 2th sample,run3.001

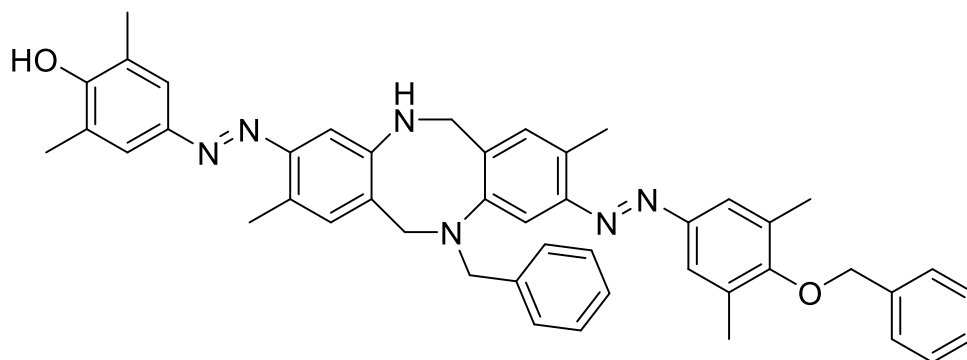
Run Date: 19-Oct-15 18:54
 Instrument: 2010 DSC V4.4E



Compound P1.2, Sample 2, Ramp 20-270°C, second reheat

DSC, Compound P1.16

4-((*E*)-(11-benzyl-9-((*E*)-(4-(benzyloxy)-3,5-dimethylphenyl)diazenyl)-2,8-dimethyl-5,6,11,12-tetrahydrodibenzo [b,f][1,5]diazocin-3-yl)diazenyl)-2,6-dimethylphenol



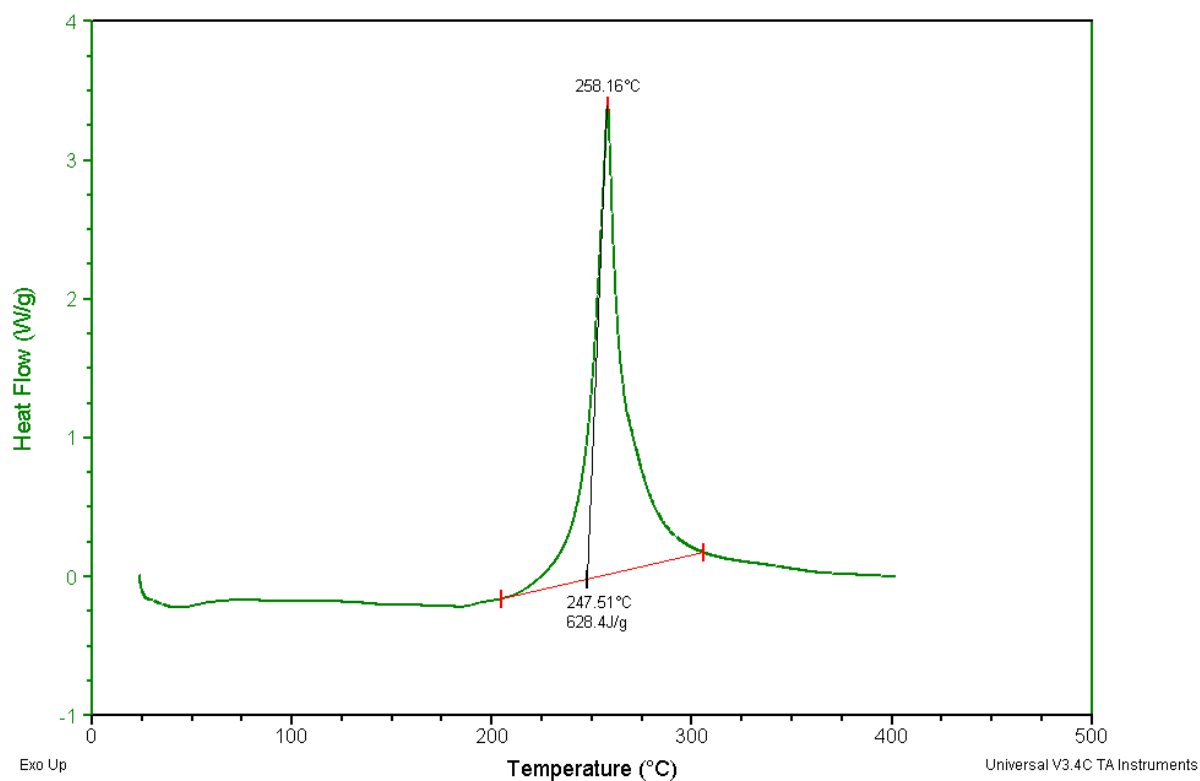
Compound P1.16

Sample: MR01-118
 Size: 4.7200 mg
 Method: Ramp
 Comment: 6c/min 20-400

DSC

File: C:\TA\Data\DSC\Masoud\118\MR01-118.001

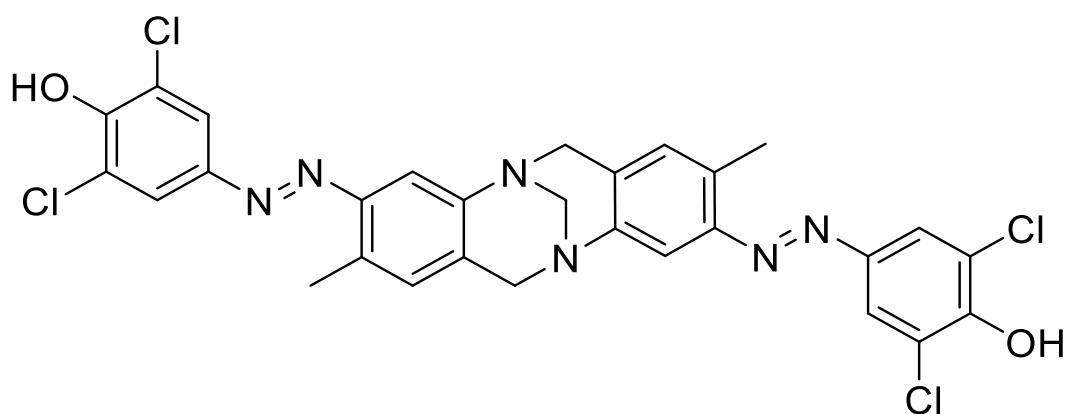
Run Date: 19-Oct-15 14:57
 Instrument: 2010 DSC V4.4E



Compound P1.16, Sample 1, Ramp 20-400°C

DSC, Compound P2.1

4,4'-((1*E*,1'*E*)-(2,8-dimethyl-6H,12H-5,11-methanodibenzo[b,f][1,5]diazocine-3,9-diyl)bis(diazene-2,1-diyl)) bis(2,6-dichlorophenol)



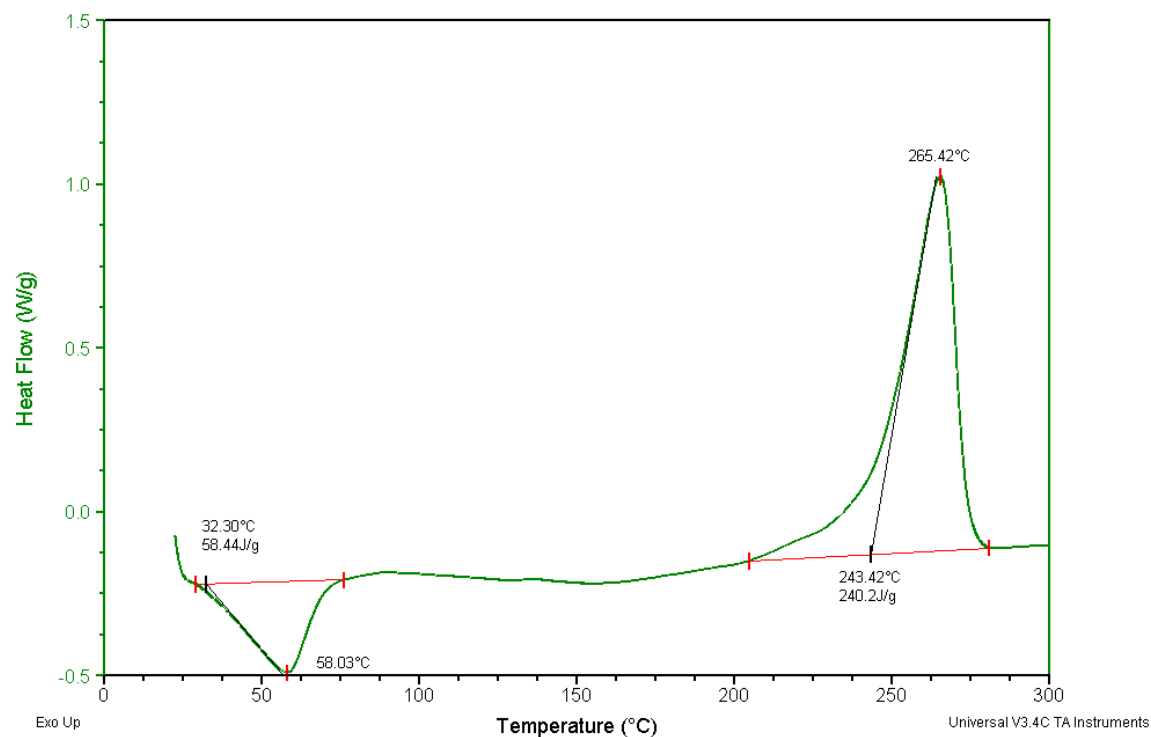
Compound P2.1

Sample: MR01-34
Size: 4.5700 mg
Comment: 6c/min-300c

DSC

File: C:\TA\Data\DSC\Masoud\34\MR01-34.001

Run Date: 28-Jul-15 14:25
Instrument: 2010 DSC V4.4E



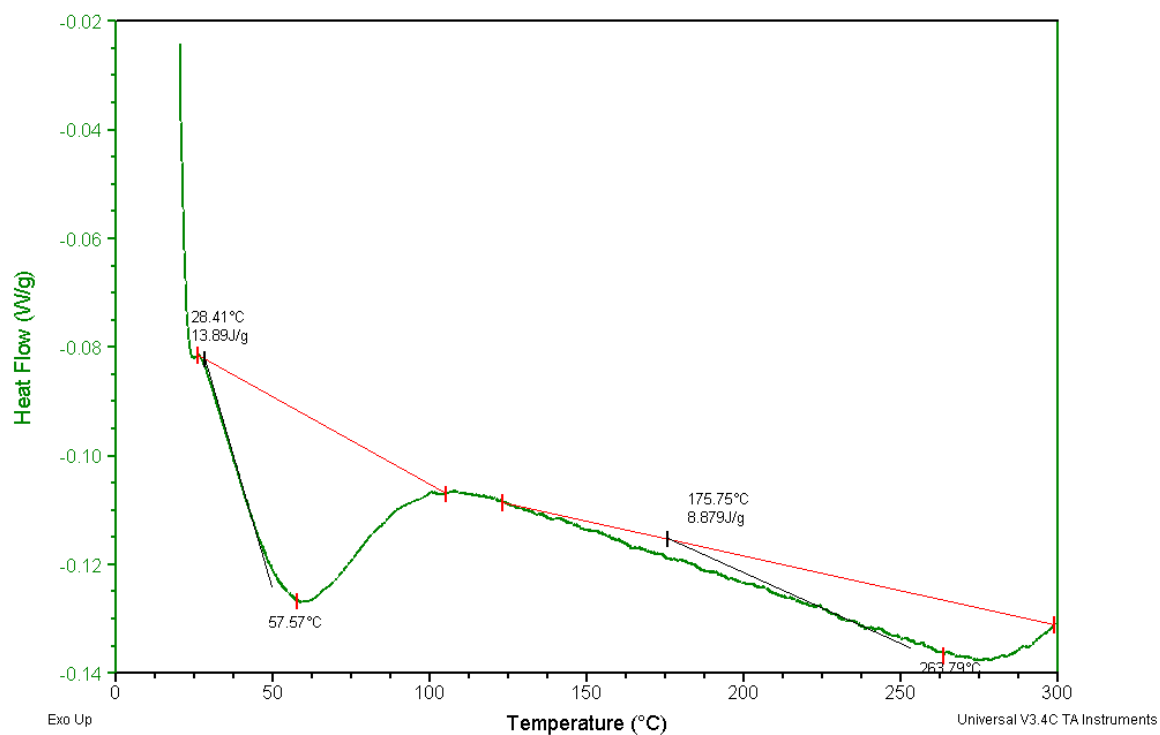
Compound P2.1, Sample 1, Ramp 20-300°C

Sample: MR01-34 run2
Size: 4.5700 mg
Comment: 6c/min-300c run2

DSC

File: C:\TA\Data\DSC\Masoud\34\MR01-34 run2.001

Run Date: 28-Jul-15 16:00
Instrument: 2010 DSC V4.4E



Compound P2.1, Sample 1, Ramp 20-300°C, reheat

Sample: MR01-34 run3

Size: 4.5700 mg

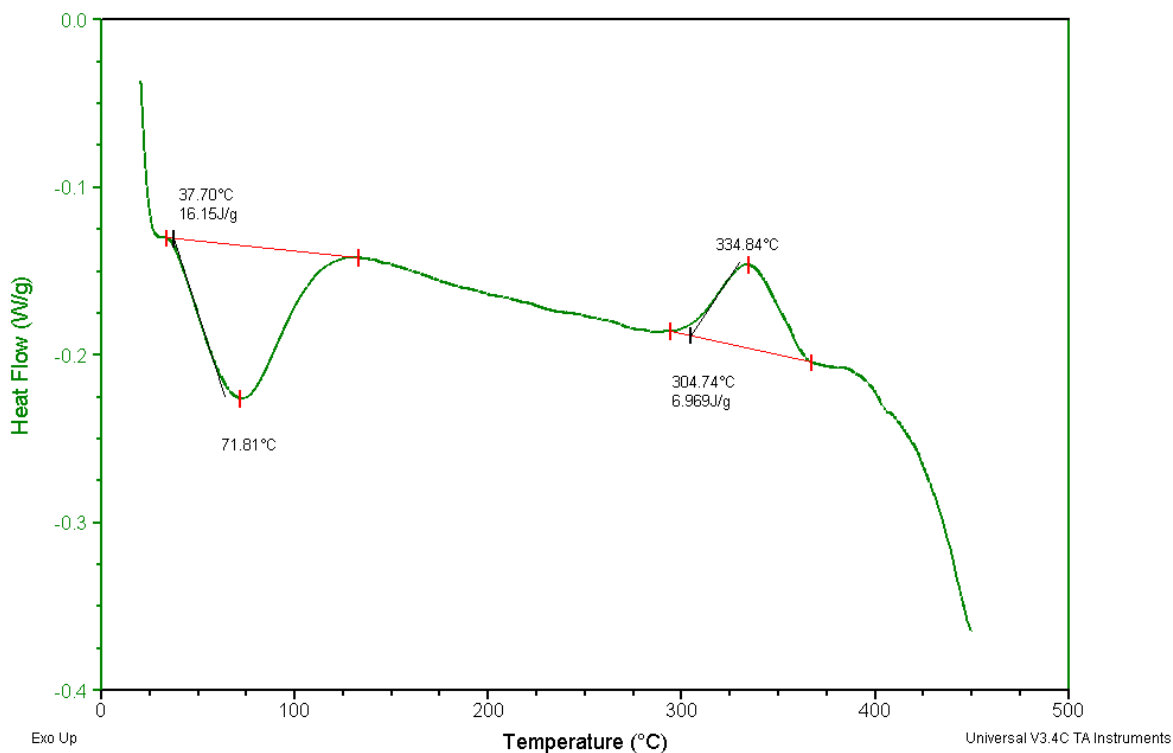
Comment: 6c/min-450c run3

DSC

File: C:\...\DSC\Masoud\34\MR01-34 run3.001

Run Date: 28-Jul-15 18:31

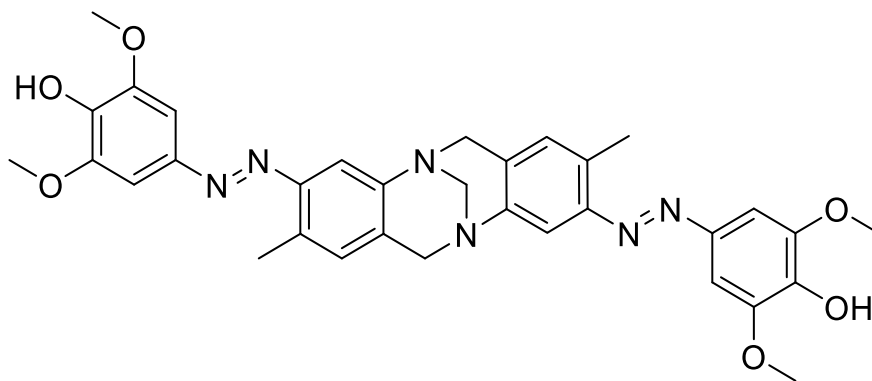
Instrument: 2010 DSC V4.4E



Compound P2.1, Sample 1, Ramp 20-450°C, reheat

DSC, Compound P2.5

4,4'-((1*E*,1'*E*)-(2,8-dimethyl-6H,12H-5,11-methanodibenzo[b,f][1,5]diazocine-3,9-diyl)bis(diazene-2,1-diyl)) bis(2,6-dimethoxyphenol)



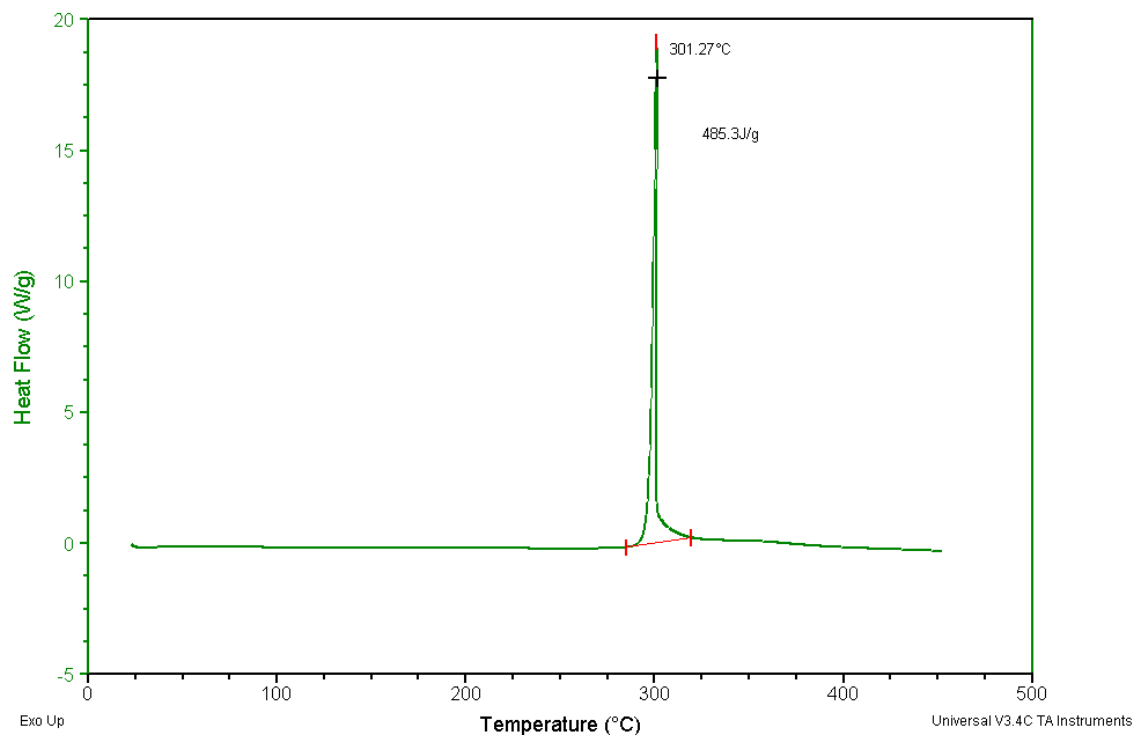
Compound P2.5

This sample during the melting point test showed no change up to 180°C. Afterwards, a gradual change of the yellow colour was observed about 255°C then to a darker spectrum of orange colour and at 275°C to brown and finally 288°C to black. No liquid form was observed.

Sample: MR01-38
Size: 2.6900 mg
Comment: 6c/min-450c

DSC

File: C:\MR01-38\MR01-38 another sample.001
Run Date: 31-Jul-15 13:48
Instrument: 2010 DSC V4.4E

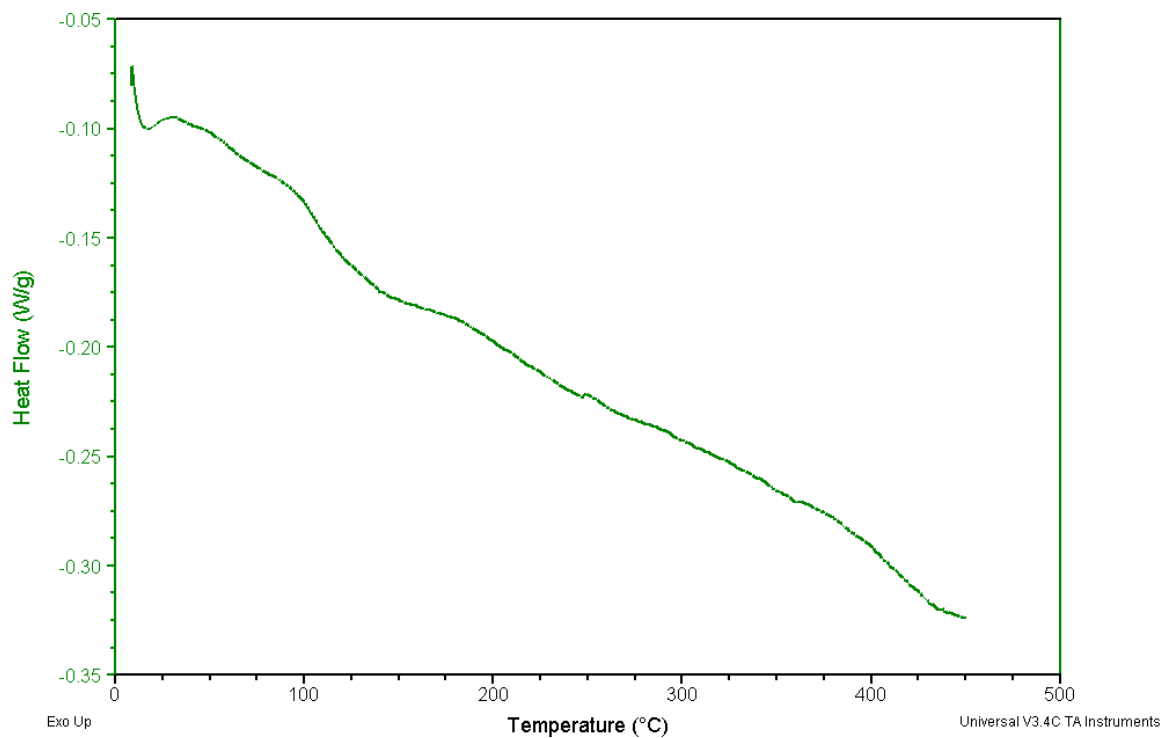


Compound P2.5, Sample 1, Ramp 20-450°C

Sample: MR01-38 R2
Size: 2.6900 mg
Comment: 15c/min-450c

DSC

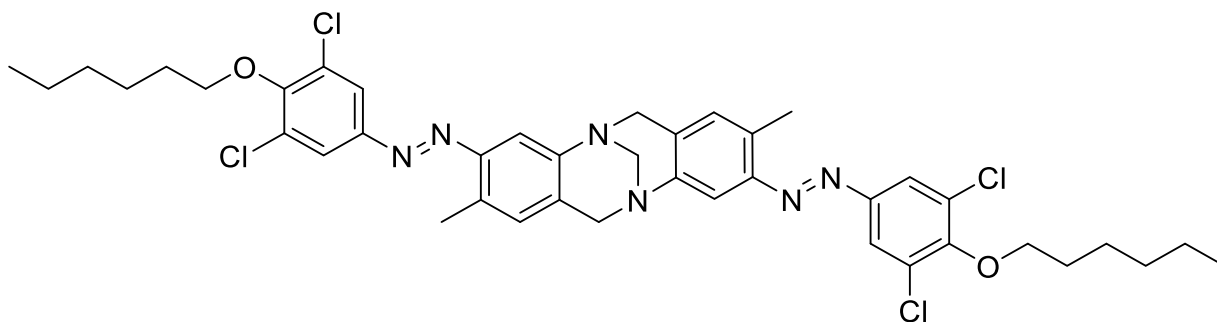
File: C:\MR01-38 another sample R2.001
Run Date: 31-Jul-15 15:10
Instrument: 2010 DSC V4.4E



Compound P2.5, Sample 1, Repeating Ramp 20-450°C

DSC, Compound P2.1b

3,9-bis((*E*)-(3,5-dichloro-4-(hexyloxy)phenyl)diazenyl)-2,8-dimethyl-6H,12H-5,11-methanodibenzo[b,f][1,5]diazocine



Compound P2.1b

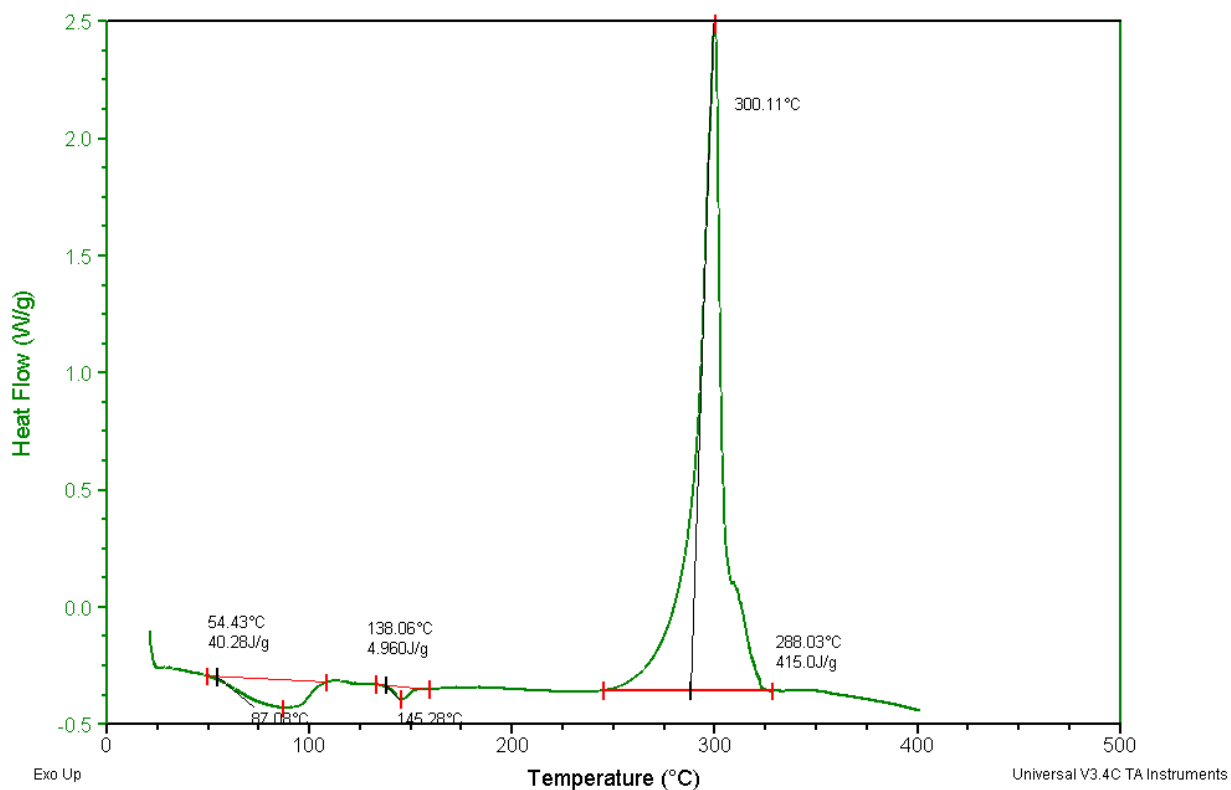
Sample: MR01-114 RAMP
Size: 2.1500 mg

DSC

File: C:\TA\Data\DSC\Masoud\114\MR01-114.001

Run Date: 10-Aug-15 12:18
Instrument: 2010 DSC V4.4E

Comment: 6c/min-400c

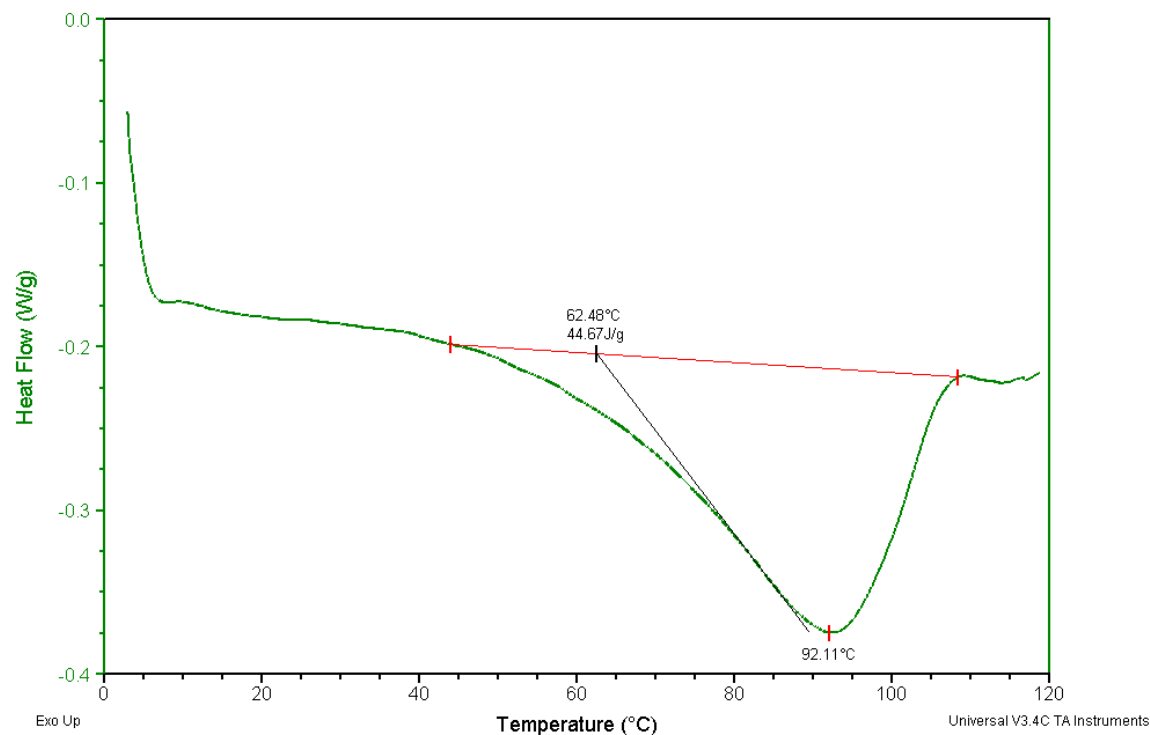


Compound P2.1b, Sample 1, Ramp 20-400°C

Sample: MR01-114 R1
Size: 5.5800 mg
Comment: 6c/min-120c

DSC

File: C:\...\Masoud\114\MR01-114 R1 20-120.001
Run Date: 10-Aug-15 14:41
Instrument: 2010 DSC V4.4E

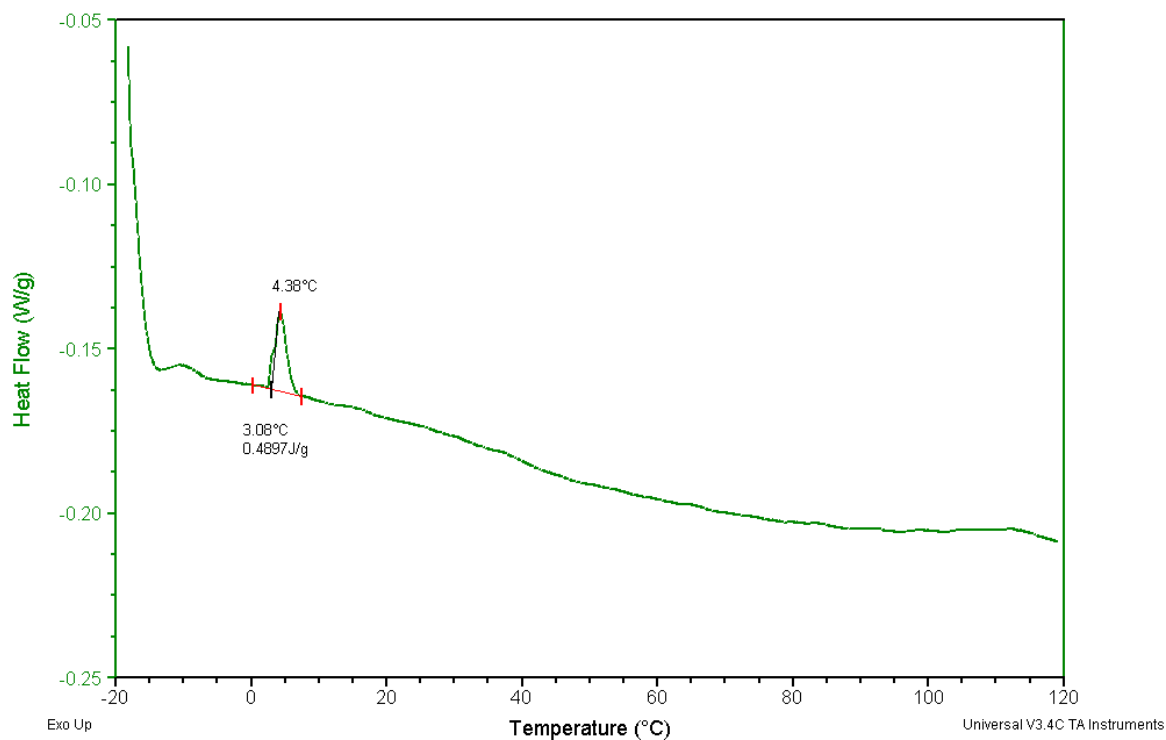


Compound P2.1b, Sample 2, Ramp 20-120°C

Sample: MR01-114 R2
Size: 5.5800 mg
Comment: 6c/min-120c

DSC

File: C:\...\DSC\Masoud\114\MR01-114 R2.001
Run Date: 10-Aug-15 15:15
Instrument: 2010 DSC V4.4E

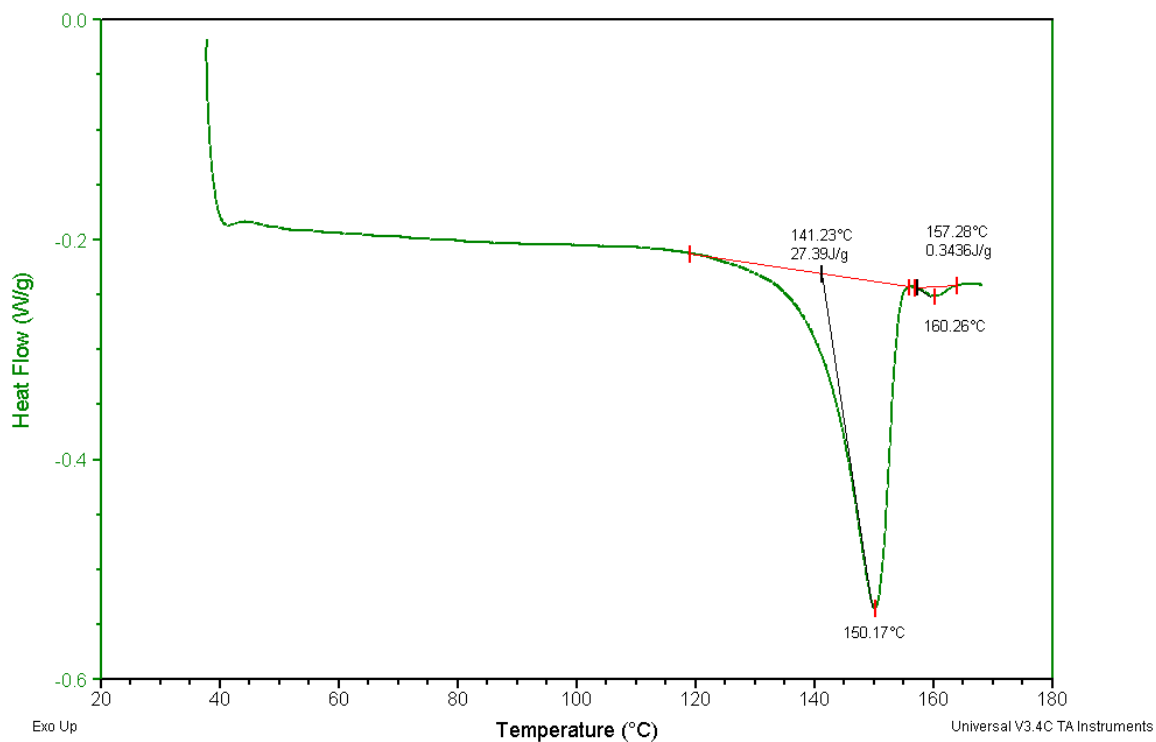


Compound P2.1b, Sample 2, Ramp 20-120°C, 1st reheat

Sample: MR01-114 R3
Size: 5.5800 mg
Comment: 6c/min-170c

DSC

File: C:\DSC\Masoud\114\MR01-114 R3.001
Run Date: 10-Aug-15 15:50
Instrument: 2010 DSC V4.4E

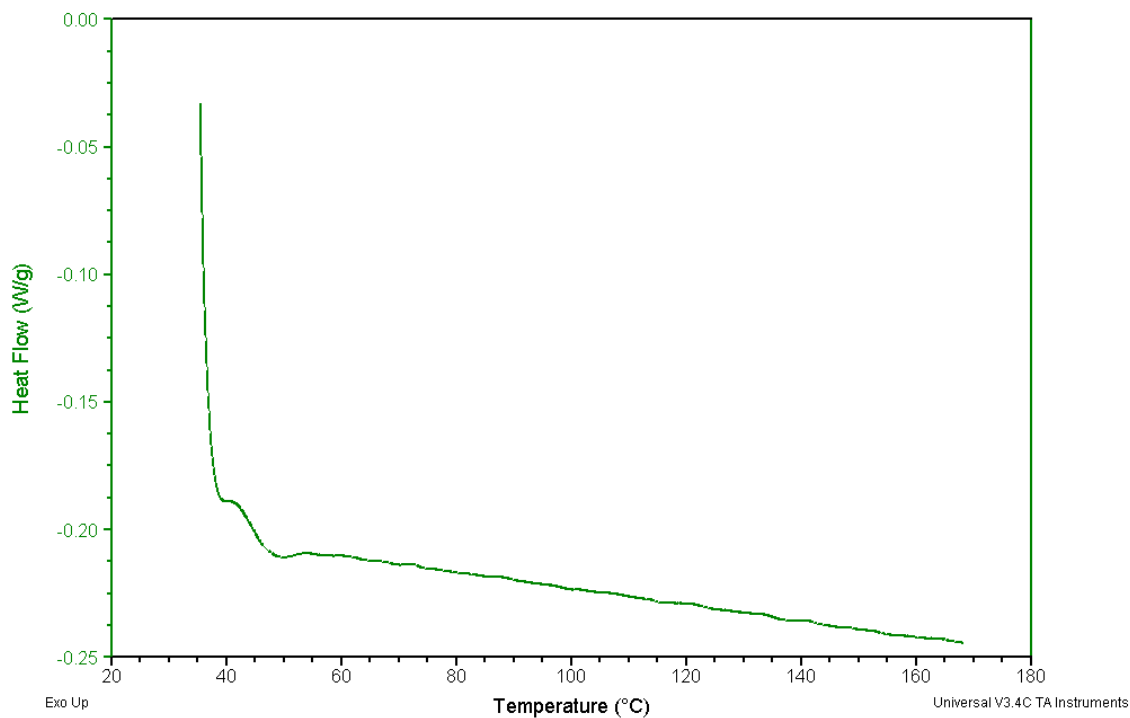


Compound P2.1b, Sample 2, Ramp 20-180°C, 2nd reheat

Sample: MR01-114 R4
Size: 5.5800 mg
Comment: 6c/min-170c

DSC

File: C:\DSC\Masoud\114\MR01-114 R4.001
Run Date: 10-Aug-15 16:30
Instrument: 2010 DSC V4.4E

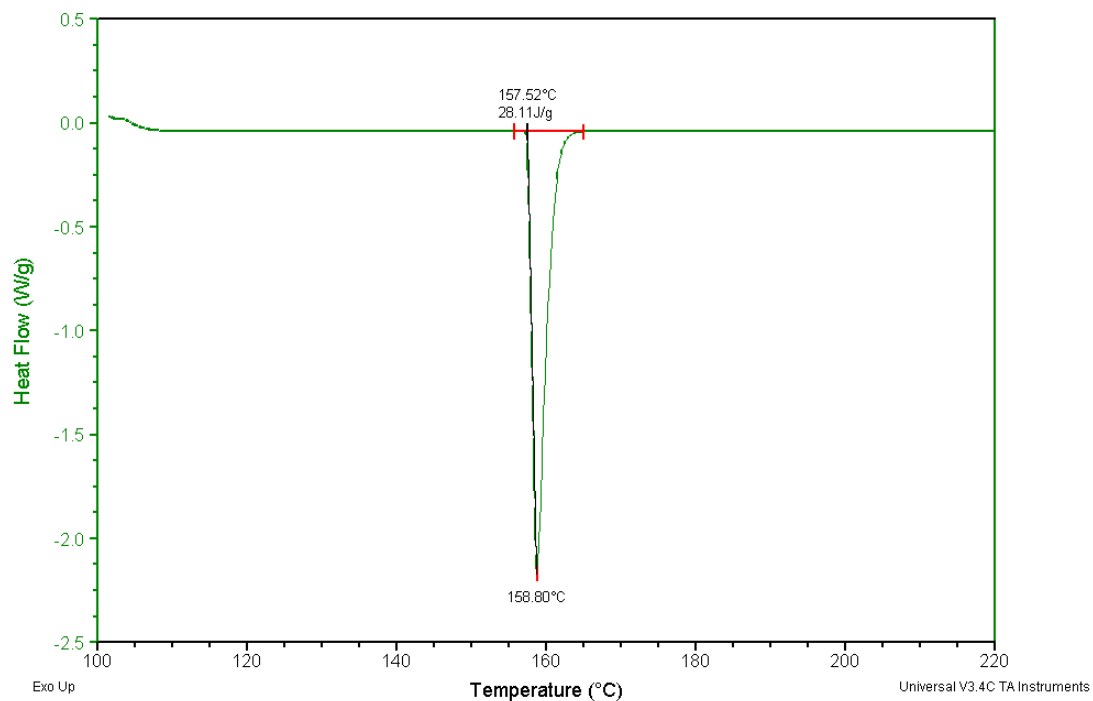


Compound P2.1b, Sample 2, Ramp 20-180°C, 3rd reheat

DSC Calibrations

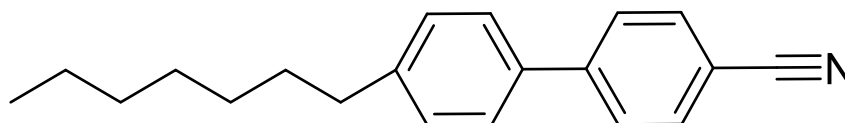
DSC, Indium

Indium (DSC)



Melting point (MSDS): 156.6°C

DSC, 4'-Heptyl-4-biphenylcarbonitrile



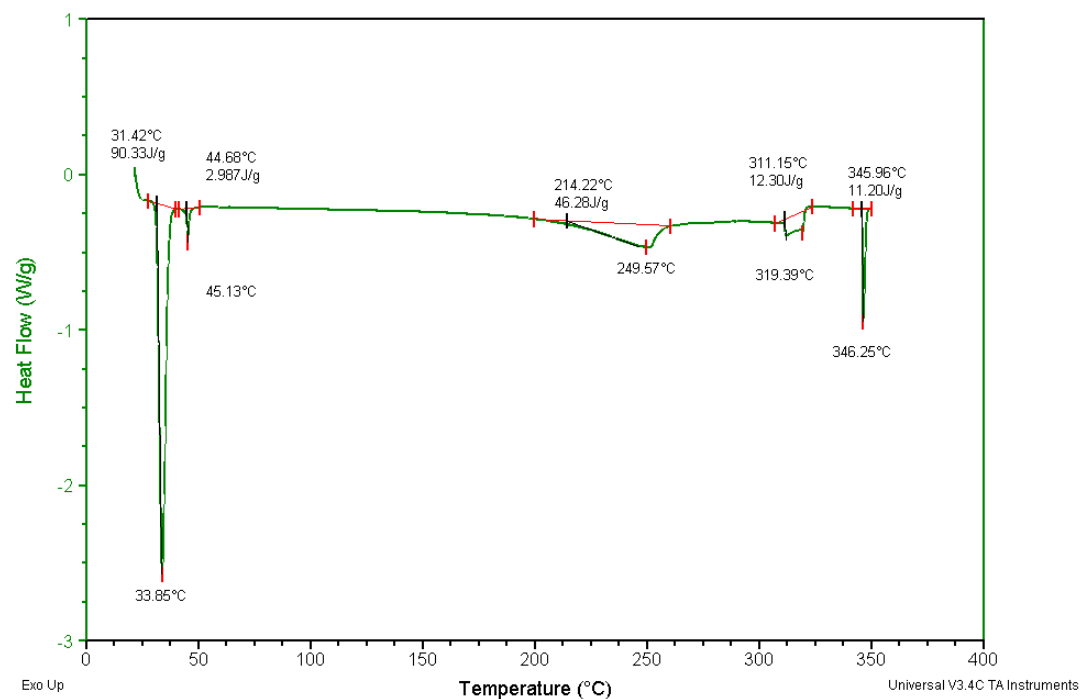
Melting Point (Exp. SciFinder): 30-44°C

Boiling point (Exp. SciFinder): 196-199°C (2 Torr)

Sample: MR LC 7
Size: 7.1000 mg
Method: Ramp
Comment: MR LC 7

DSC

File: C:\...MR LC 7.001
Run Date: 7-May-15 10:26
Instrument: 2010 DSC V4.4E

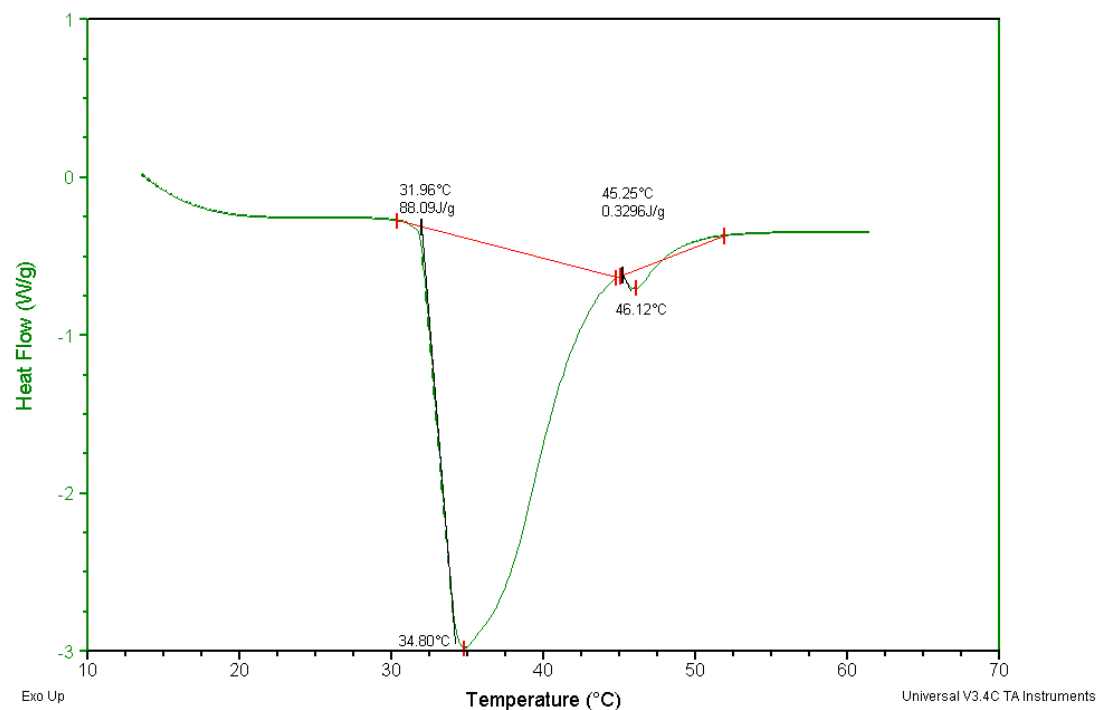


4'-Heptyl-4-biphenylcarbonitrile, Sample 1, Ramp 20-350°C

Sample: LC7
Size: 17.0900 mg
Method: Ramp
Comment: 12c/min-200c

DSC

File: C:\...LC7.001
Run Date: 4-Jun-15 15:27
Instrument: 2010 DSC V4.4E



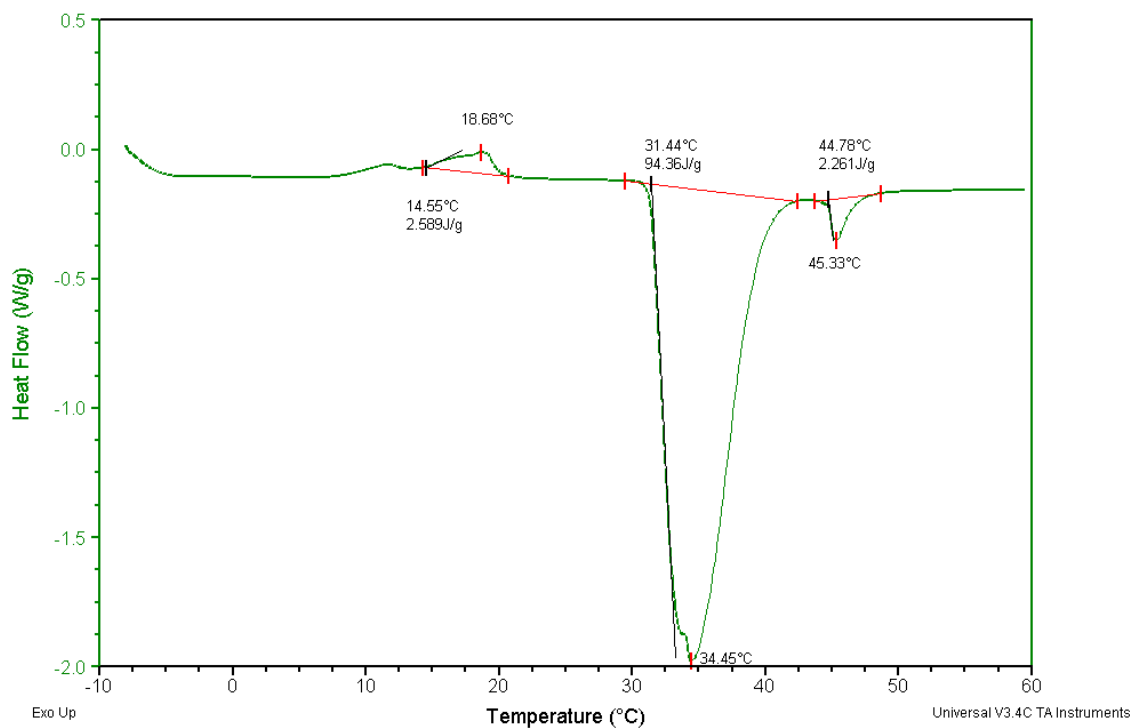
4'-Heptyl-4-biphenylcarbonitrile, Sample 2, Ramp 20-60°C, Heating Rate 12°C/min

Sample: LC7 2nd
Size: 17.0900 mg
Method: Ramp
Comment: 6c/min-60c

DSC

File: C:\...LC7.002

Run Date: 4-Jun-15 15:41
Instrument: 2010 DSC V4.4E



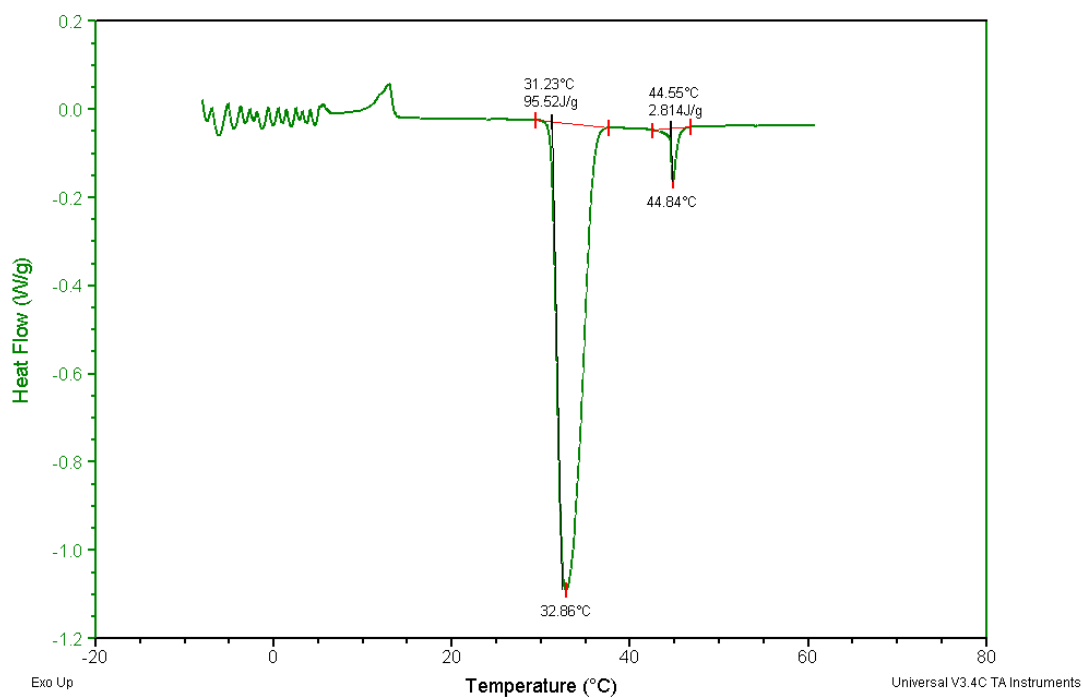
4'-Heptyl-4-biphenylcarbonitrile, Sample 2, Ramp 20-60°C, 1st Reheating Rate 6°C/min

Sample: LC7 3rd
Size: 17.0900 mg
Method: Ramp
Comment: 2c/min-60c

DSC

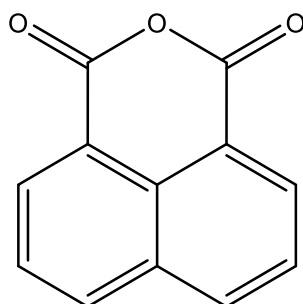
File: C:\TA\Data\DSC\Masoud\LC7.003

Run Date: 4-Jun-15 16:00
Instrument: 2010 DSC V4.4E



4'-Heptyl-4-biphenylcarbonitrile, Sample 2, Ramp 20-60°C, 2nd Reheating Rate 2°C/min

DSC, 1,8-Naphthalic anhydride



Melting Point (Exp. Scifinder): 270-276°C

Melting Point (MSDS): 267-269°C

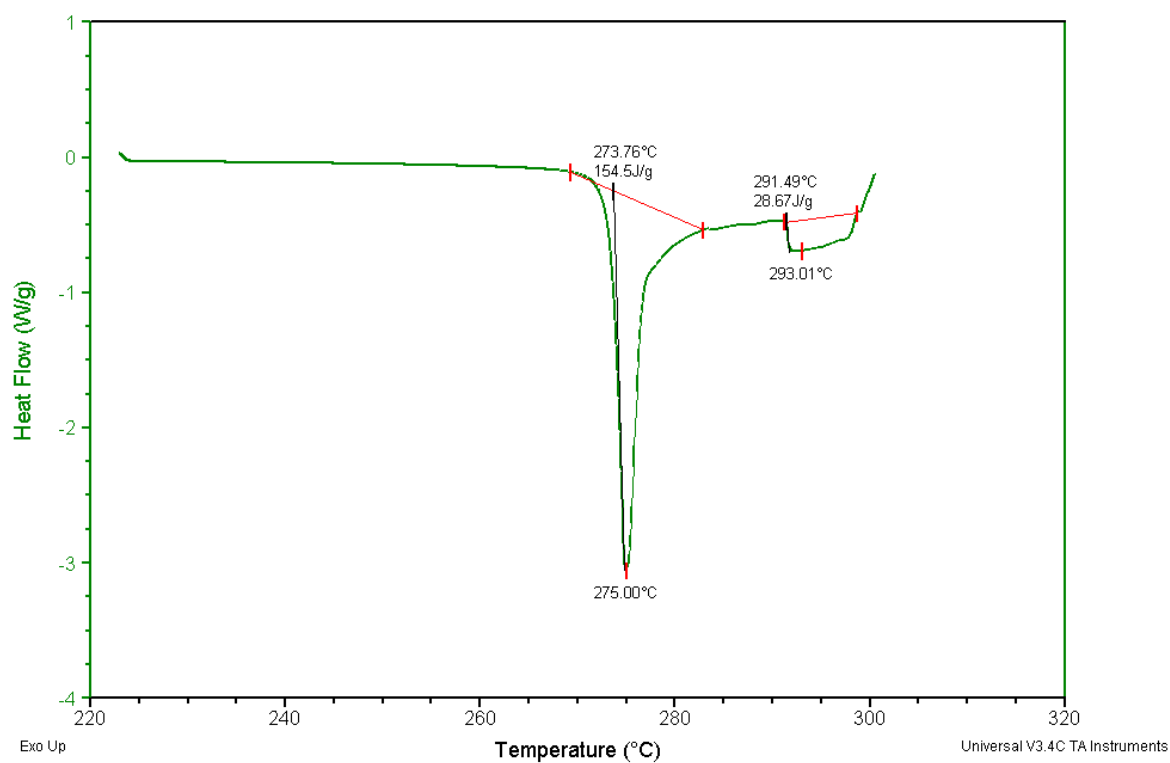
Sample: 1,8 Naphthalic anhydride
Size: 8.1800 mg
Method: Ramp
Comment: 1,8 Naphthalic anhydride

DSC

File: C:\...1,8 Naphthalic anhydride.001

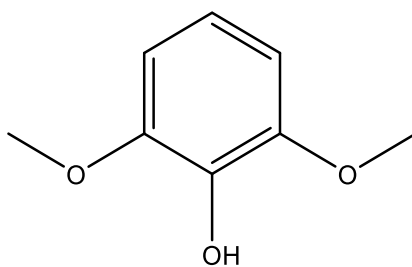
Run Date: 3-Jun-15 16:09

Instrument: 2010 DSC V4.4E



1,8-Naphthalic anhydride, Sample 1, Ramp 20-300°C

DSC, 2,6-Dimethoxyphenol



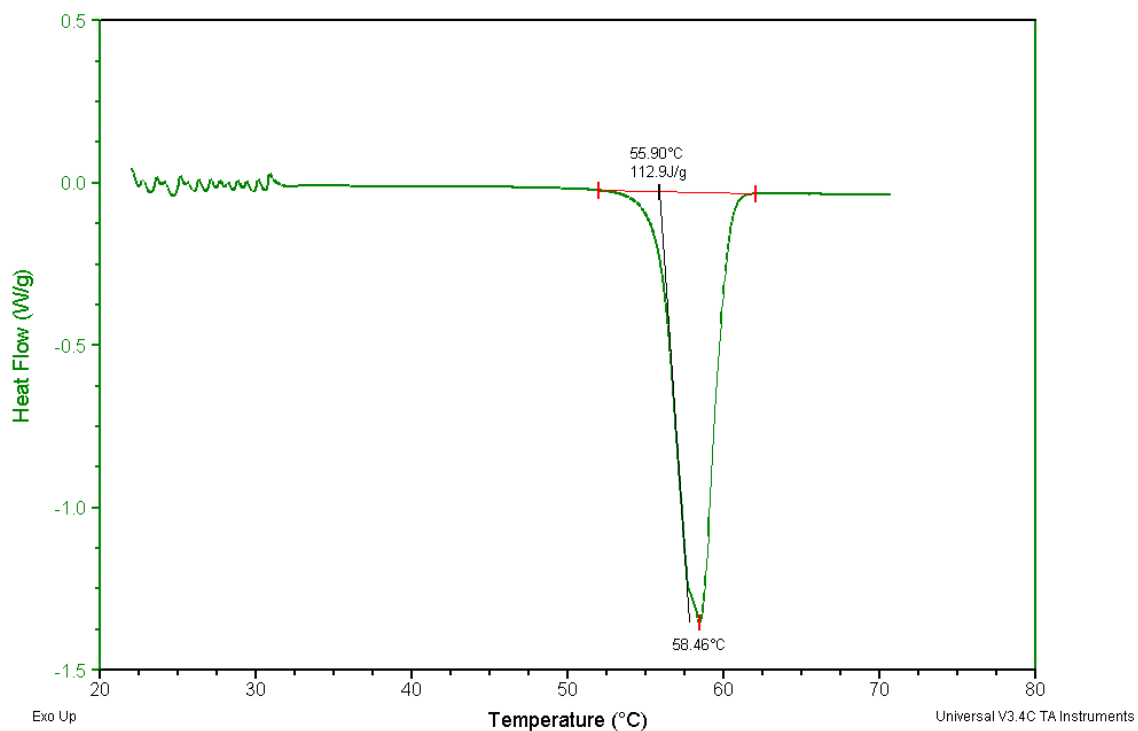
Melting Point (Exp. Scifinder): 52-57°C

Sample: 2,6 DimethoxyPhenol
Size: 11.4400 mg
Method: Ramp
Comment: 2,6 DimethoxyPhenol

DSC

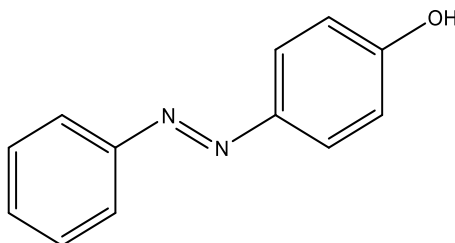
File: C:\...\2,6 DimethoxyPhenol.001

Run Date: 3-Jun-15 15:20
Instrument: 2010 DSC V4.4E



2,6-DimethoxyPhenol, Sample 1, Ramp 20-75°C

DSC, (E)-4-(phenyldiazenyl)phenol



Melting Point (Exp. Scifinder): 150-157°C

Melting Point (on package and MSDS): 150-152°C

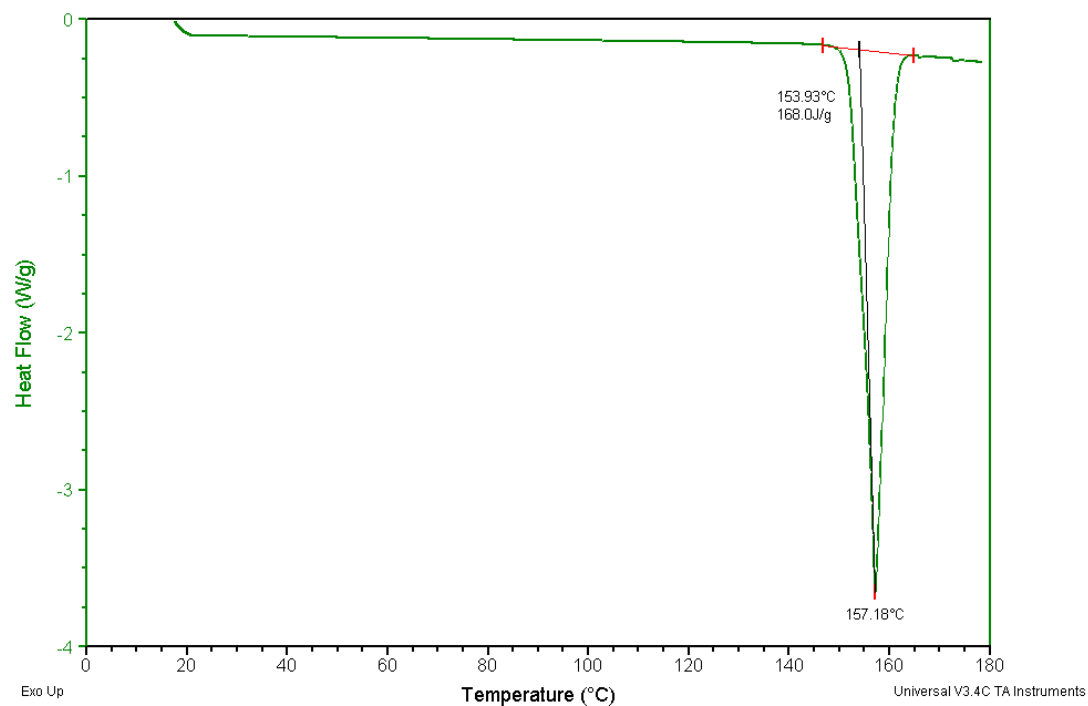
Sample: Calibration 9.58mg
Size: 9.5800 mg

DSC

File: C:\DSC\Masoud\198\Calibration 9.58mg

Run Date: 15-Jul-15 10:08
Instrument: 2010 DSC V4.4E

Comment: 6c/min-180c- Calibration



(E)-4-(phenyldiazenyl)phenol, Sample 1, Ramp 20-180°C

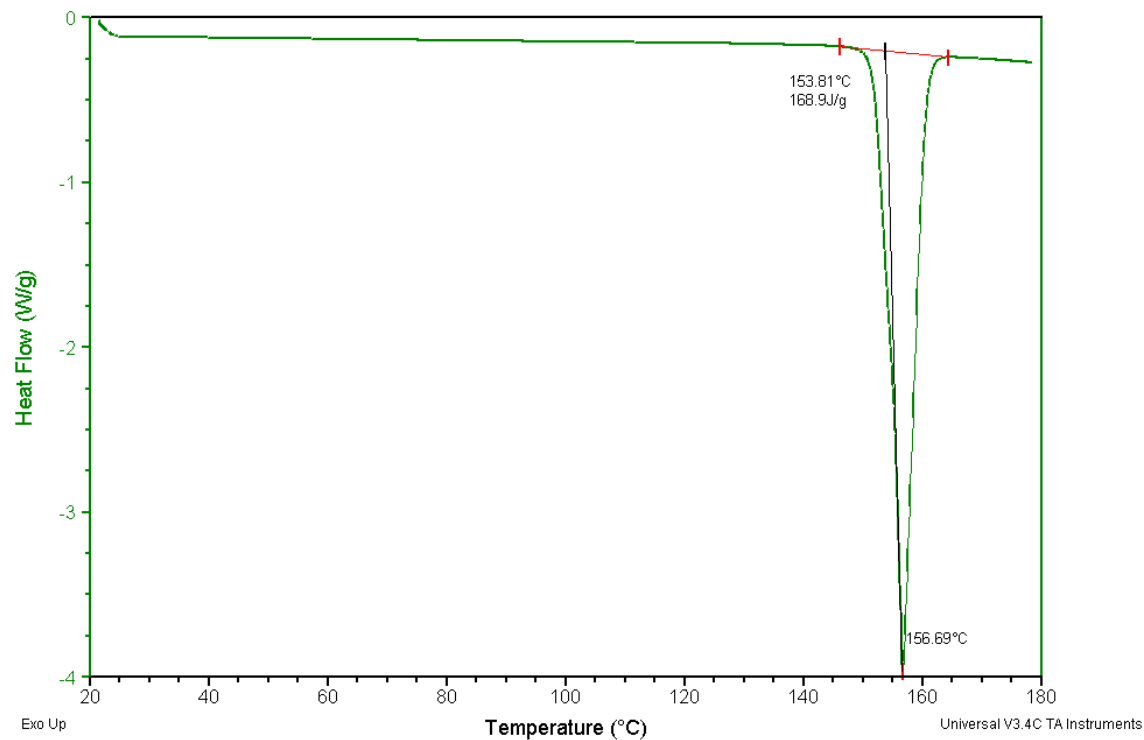
Sample: MR01-198 new
Size: 9.5900 mg

DSC

File: C:\DSC\Masoud\198\MR01-198 new1.001

Run Date: 14-Jul-15 10:09
Instrument: 2010 DSC V4.4E

Comment: 6c/min



(E)-4-(phenyldiazenyl)phenol, Sample 2, Reheat 20-180°C

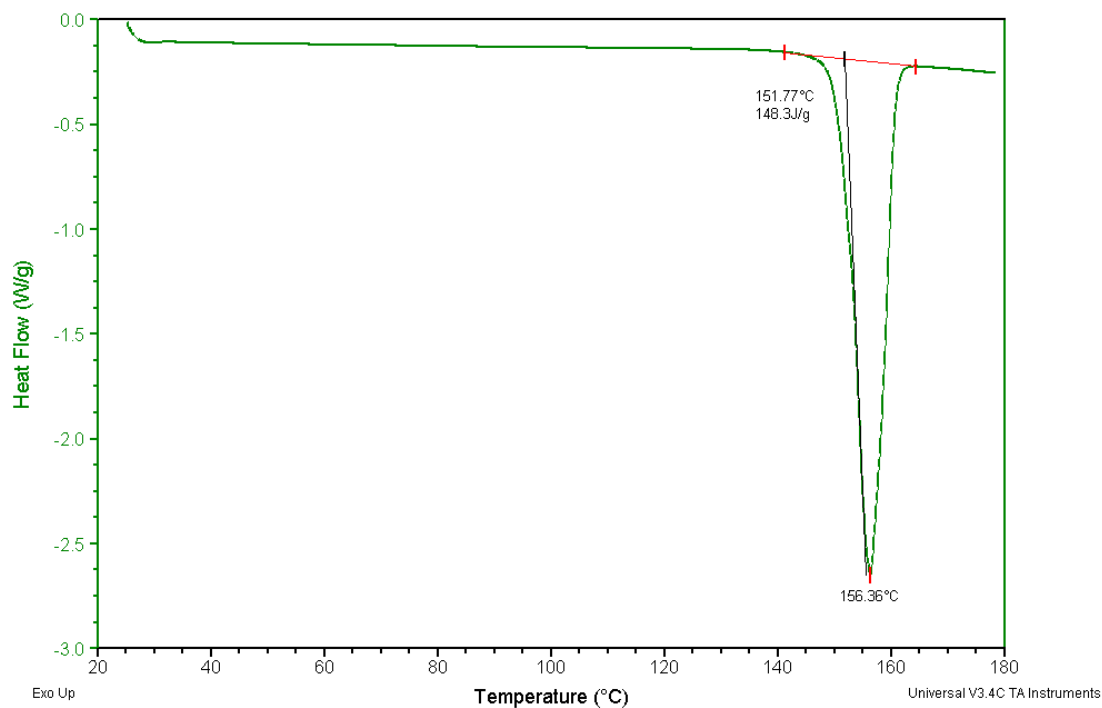
Sample: MR01-198 new
Size: 9.5900 mg

DSC

File: C:\...Masoud\198\MR01-198 new1redo 1.001

Run Date: 14-Jul-15 12:11
Instrument: 2010 DSC V4.4E

Comment: 6c/min



(E)-4-(phenyldiazenyl)phenol, Sample 2, Reheat 20-180°C

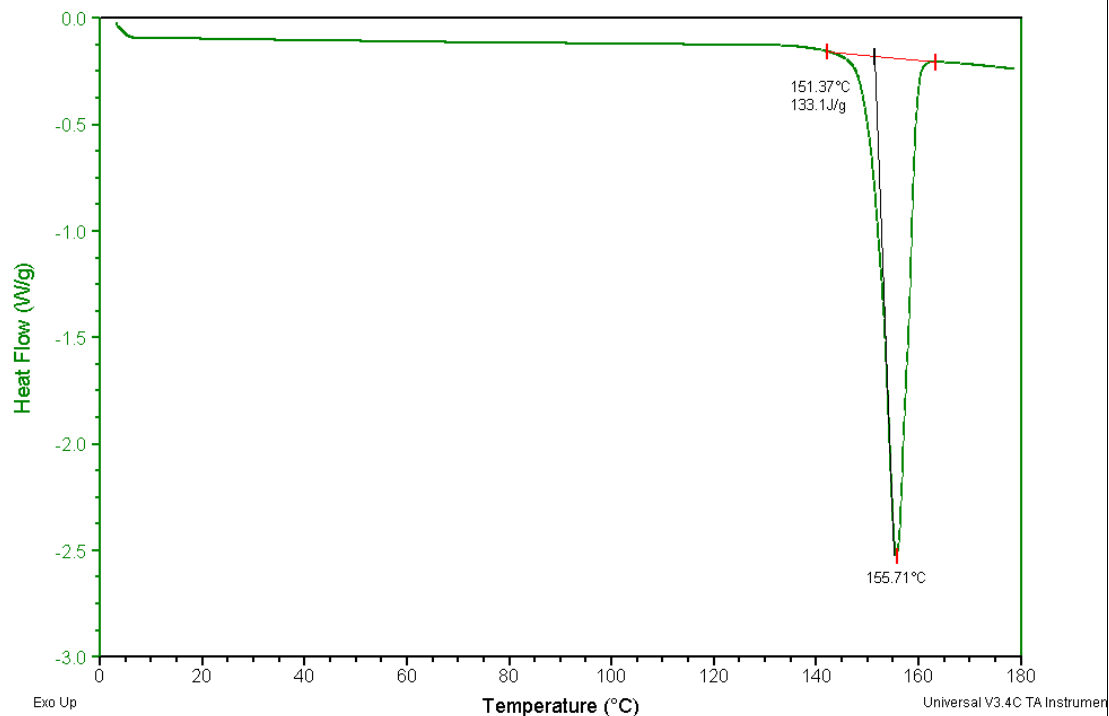
Sample: MR01-198 new
Size: 9.5900 mg

DSC

File: C:\...Masoud\198\MR01-198 new1redo 2.001

Run Date: 14-Jul-15 13:03
Instrument: 2010 DSC V4.4E

Comment: 6c/min



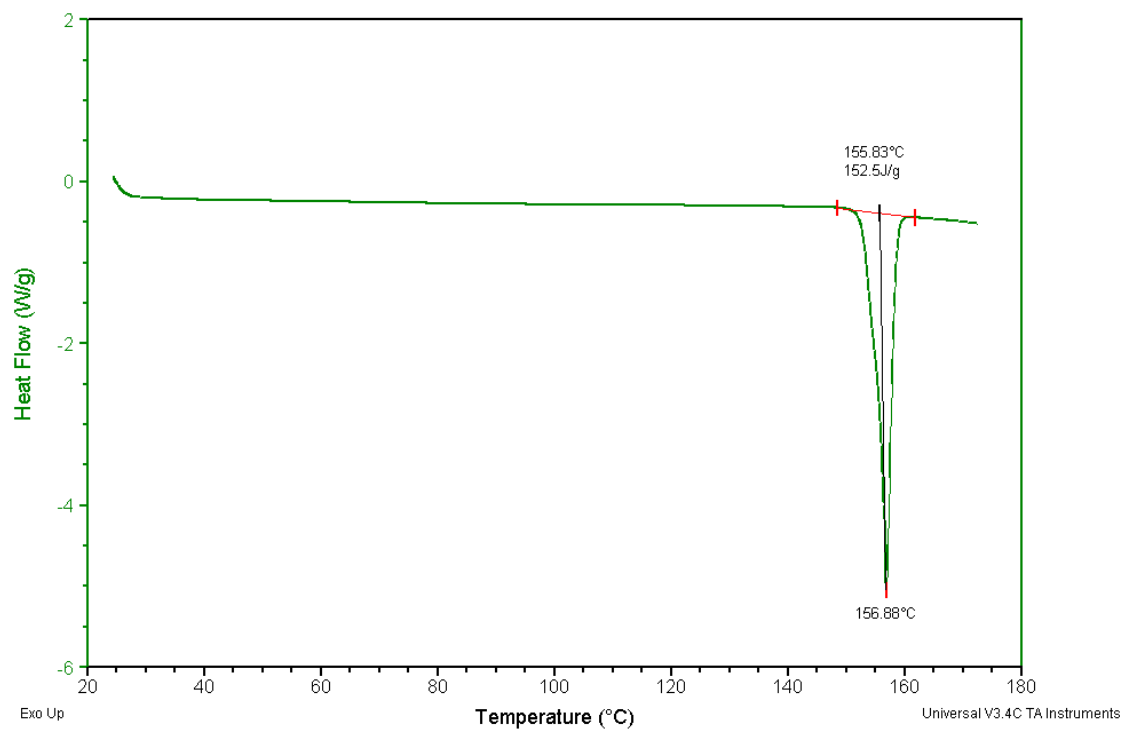
(E)-4-(phenyldiazenyl)phenol, Sample 2, Reheat 20-180°C

Sample: MR01-198
Size: 3.5000 mg
Method: Ramp

DSC

File: C:\TA\Data\DSC\Masoud\198\MR01-198.001

Run Date: 5-May-15 12:49
Instrument: 2010 DSC V4.4E



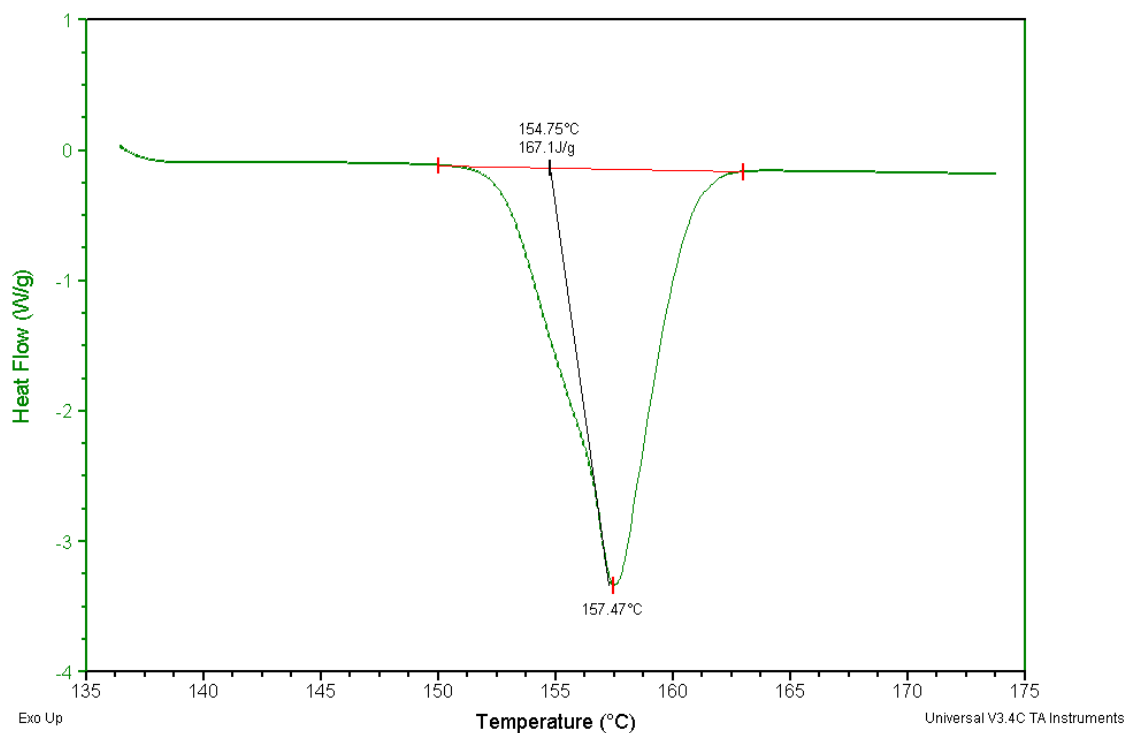
(E)-4-(phenyldiazenyl)phenol, Sample 3, Ramp 20-180°C

Sample: MR01-198 RED01
Size: 10.2000 mg
Method: Ramp
Comment: MR01-198 RED01

DSC

File: C:\DSC\Masoud\198\MR01-198 RED01.001

Run Date: 29-May-15 15:08
Instrument: 2010 DSC V4.4E



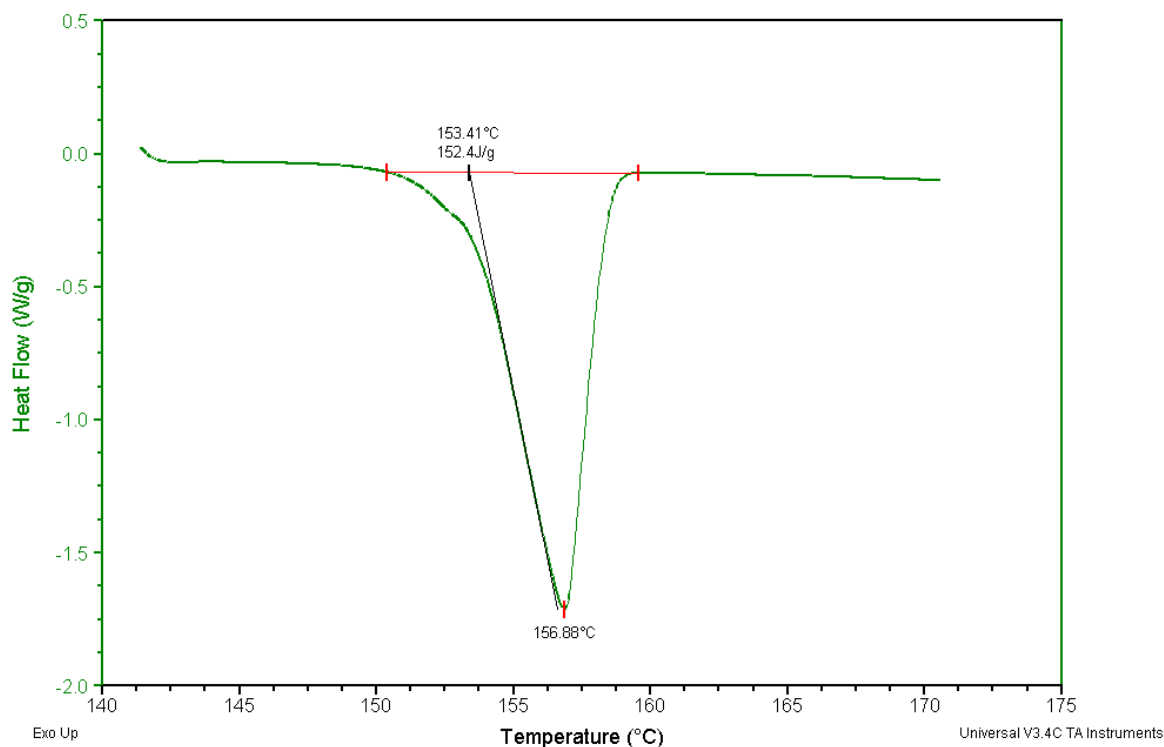
(E)-4-(phenyldiazenyl)phenol, Sample 4, Ramp 20-180°C

Sample: MR01-198 REDO2
Size: 10.2000 mg
Method: Ramp
Comment: MR01-198 REDO2

DSC

File: C:\DSC\Masoud\198\MR01-198 REDO2.001

Run Date: 29-May-15 15:33
Instrument: 2010 DSC V4.4E

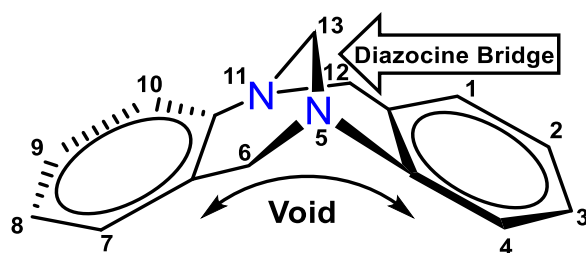


(E)-4-(phenyldiazenyl)phenol, Sample 4, Ramp 20-180°C

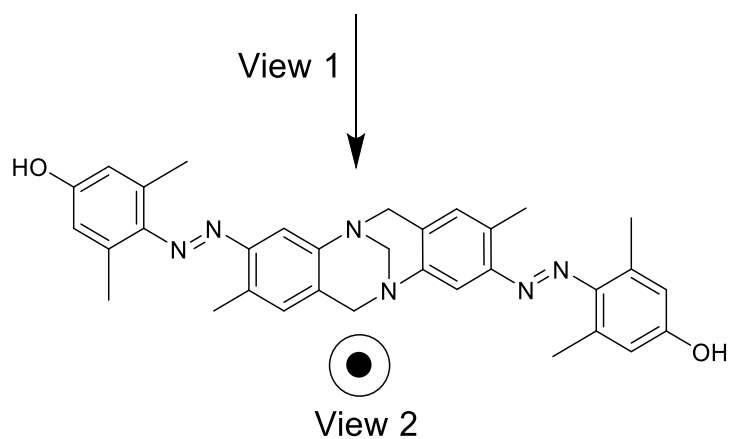
References

- 1 A. A. van Dooren and B. W. Müller, *Int. J. Pharm.*, **1984**, 20, 217-233.
- 2 Z. Bashir, N. Khan and D. M. Price, *Thermochim. Acta*, **1998**, 319, 47-53.
- 3 G. Ungar and J. Feijoo, *Mol Cryst Liq Cryst*, **1990**, 180, 281-291.
- 4 B. Kowalski, *Thermochim. Acta*, **1991**, 184, 49-57.
- 5 L. Stradella and M. Argentero, *Thermochim. Acta*, **1993**, 219, 315-323.
- 6 M. Kuribayashi and K. Hori, *Liq. Cryst.*, **1999**, 26, 809-815.
- 7 C. J. Coombes, *Journal of Physics F: Metal Physics*, **1972**, 2, 441.
- 8 S. Ranganathan, D. Ranganathan and P. V. Ramachandran, *Tetrahedron*, **1984**, 40, 3145-3151.
- 9 A. Sharma, R. Kumar, N. Sharma, V. Kumar and A. K. Sinha, *Adv. Synth. Catal.*, **2008**, 350, 2910-2920.
- 10 C.-H. S. Wu, G. S. Hammond and J. M. Wright, *J. Am. Chem. Soc.*, **1960**, 82, 5386-5394.
- 11 M. Kazem-Rostami, *Synthesis*, **2017**, 49, 1214-1222.
- 12 M. Kazem-Rostami and A. Moghanian, *Org Chem Front*, **2017**, 4, 224-228.

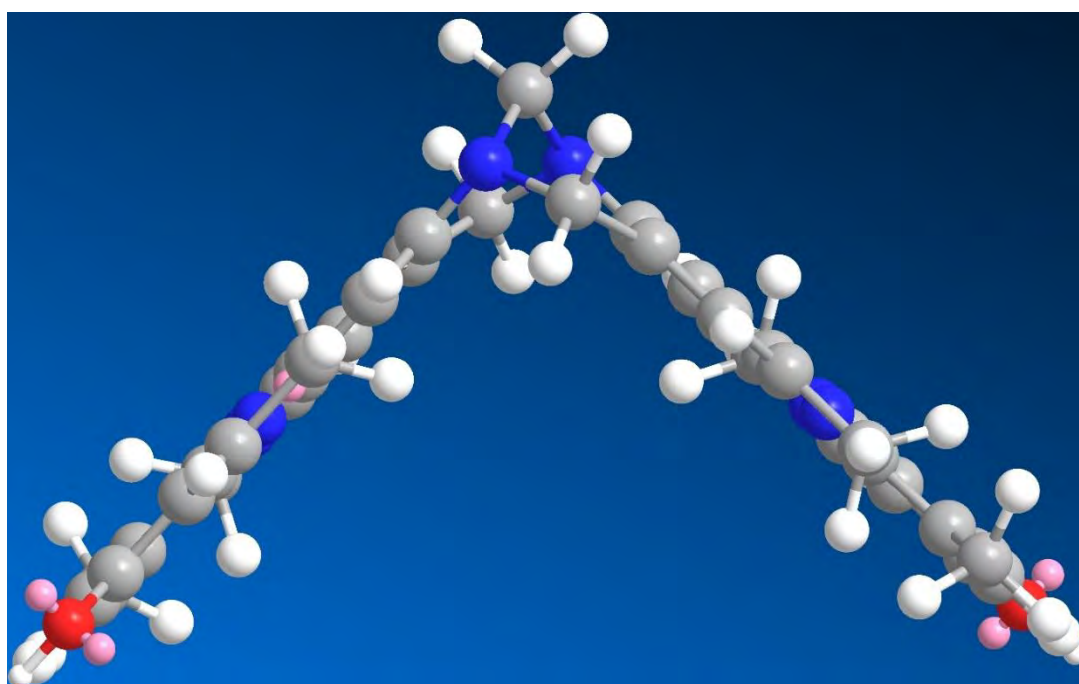
Appendix 2: 3D presentation of the Λ -shaped void of the selected products



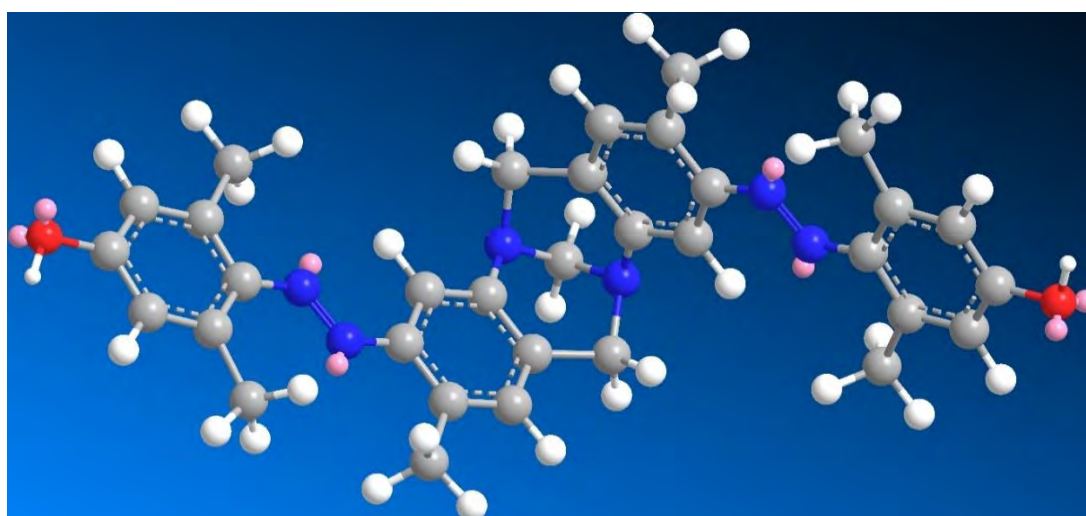
This appendix presents the 3-dimensional views of the selected products of this thesis. The presented figures in this appendix are produced by 3D ChemBioDraw professional V.15. The molecular structures were optimised by molecular mechanics using the force field.



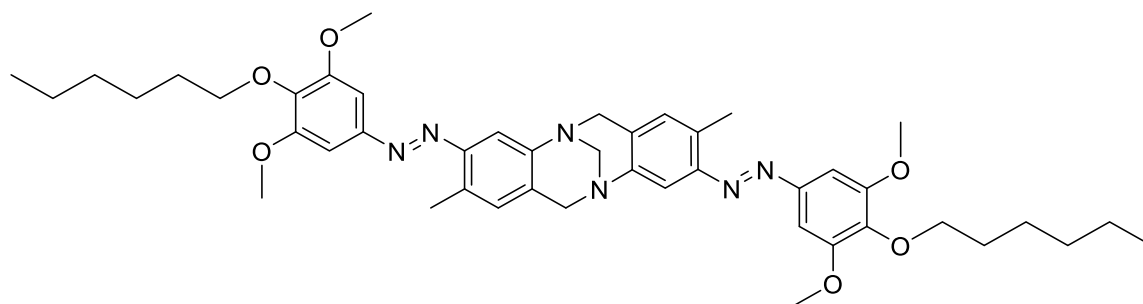
2D structure of compound 2-P11



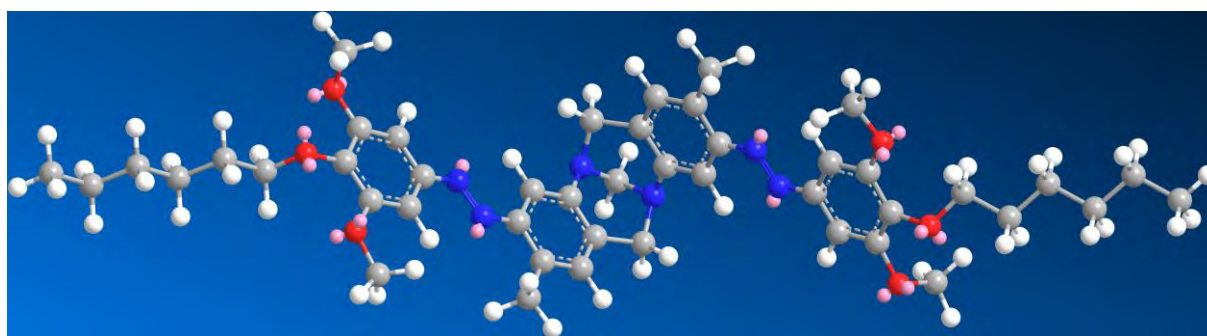
3D structure of compound 2-P11



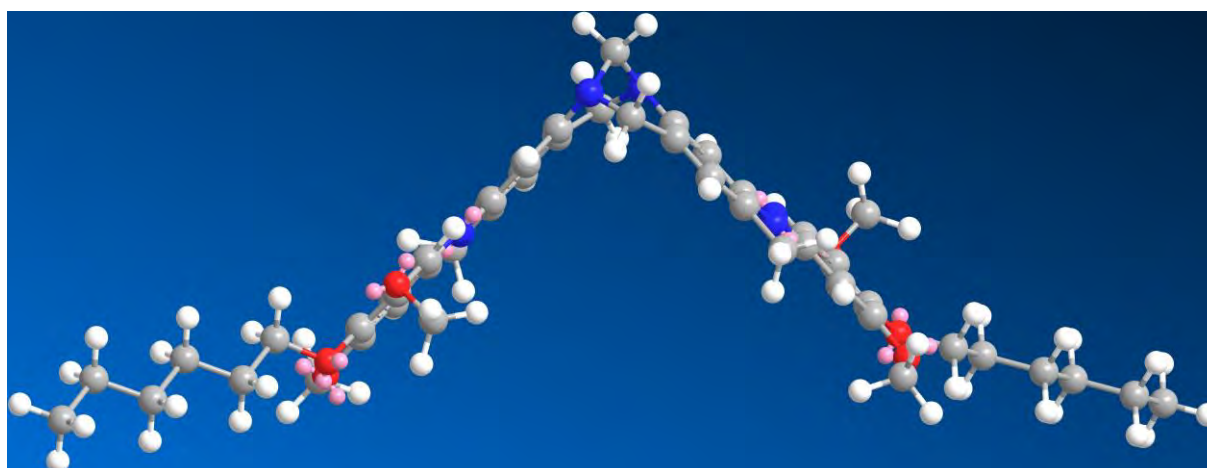
3D structure of compound 2-P11



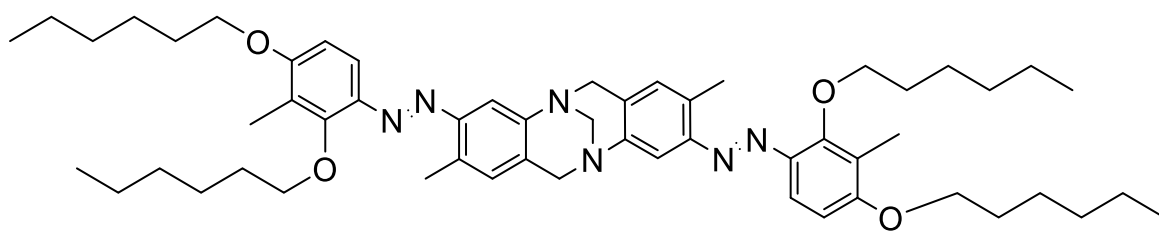
2D structure of compound 5a-P11



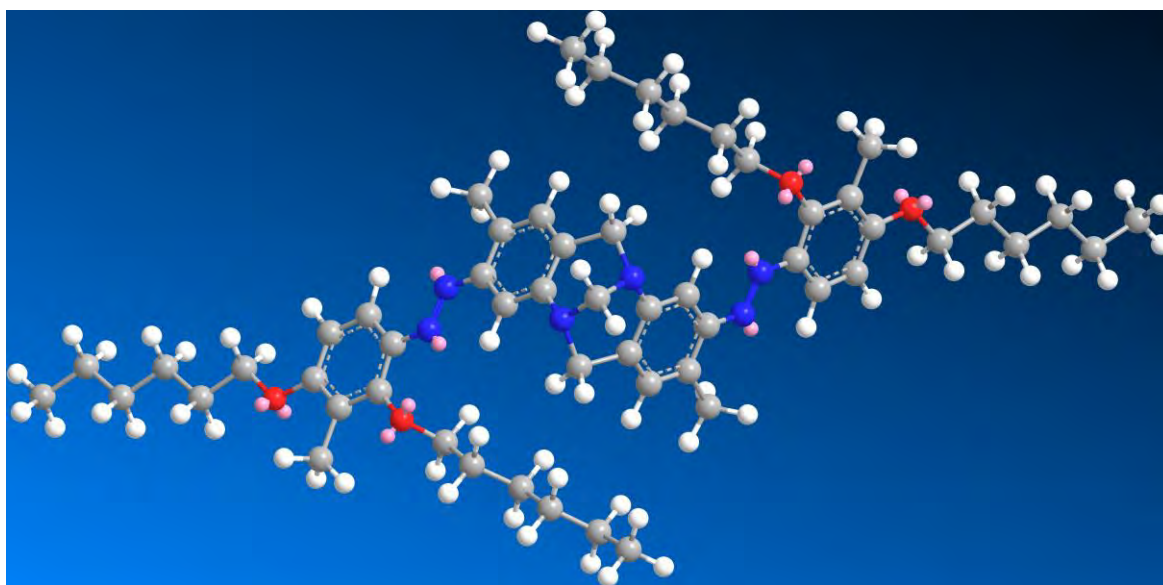
3D structure of compound 5a-P11



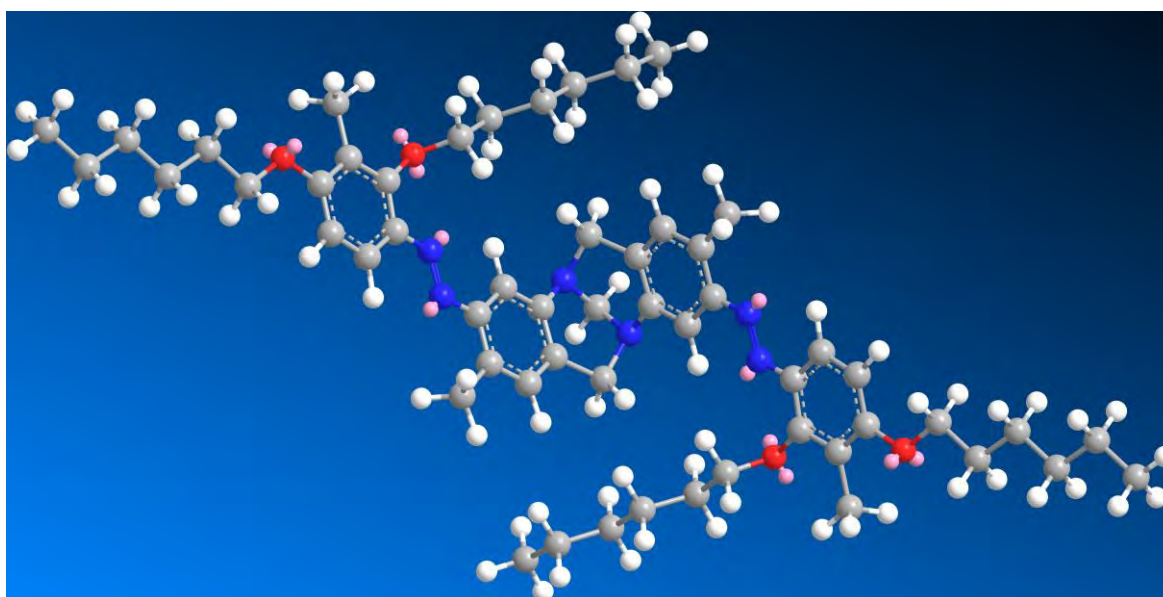
3D structure of compound 5a-P11



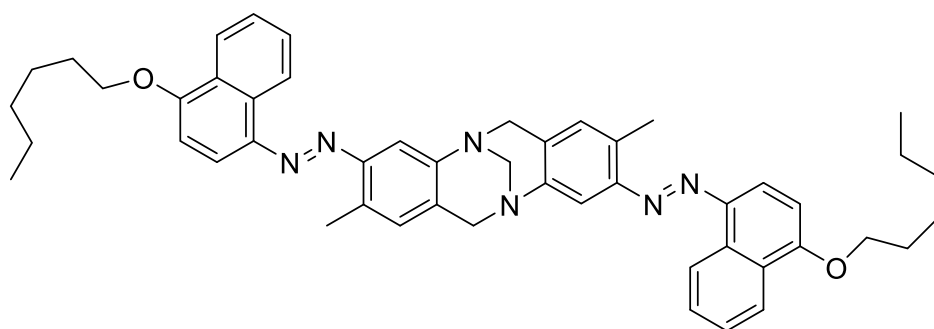
2D structure of compound 6a-P11



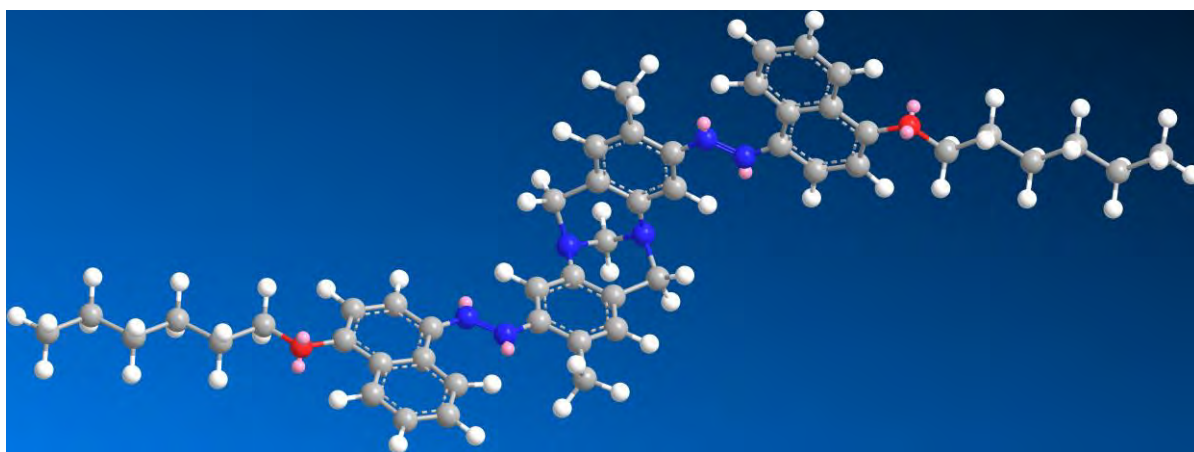
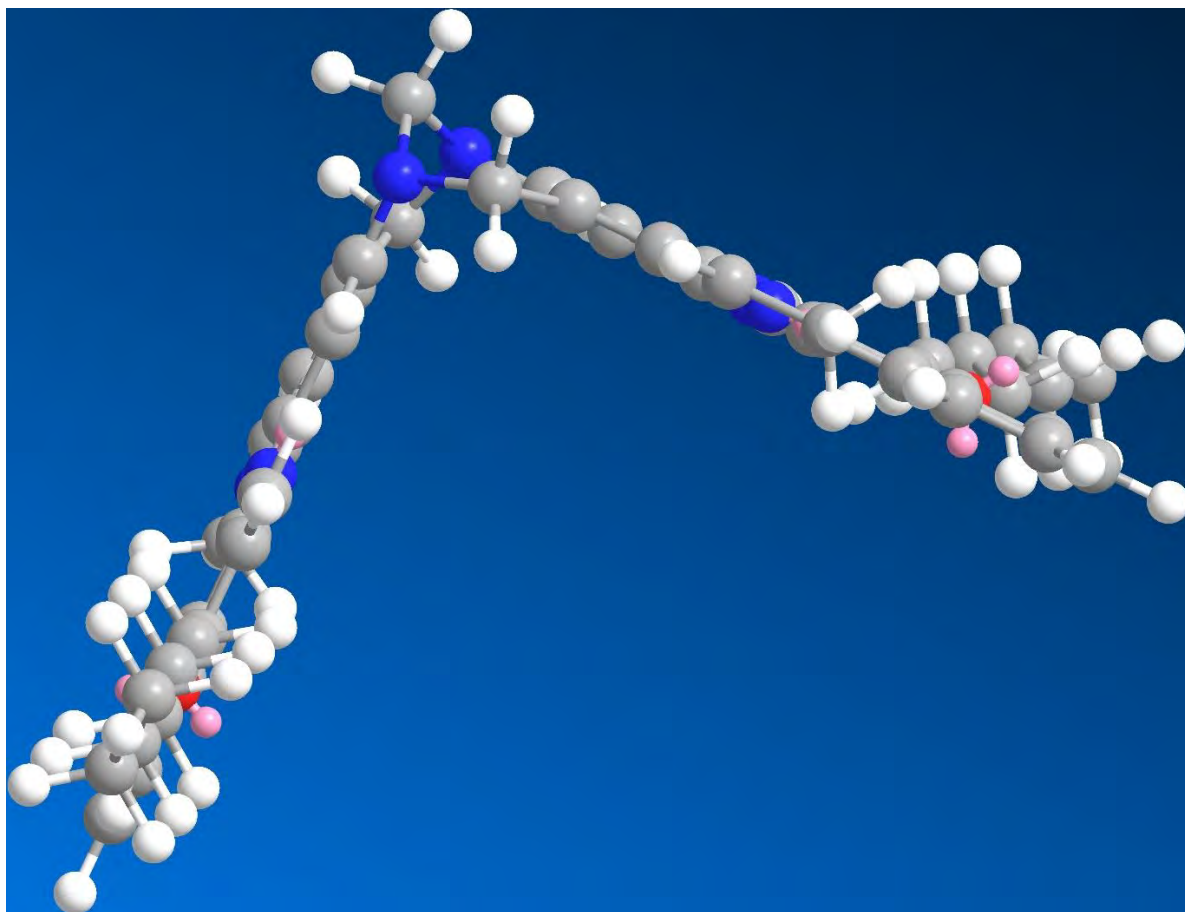
3D structure of compound 6a-P11



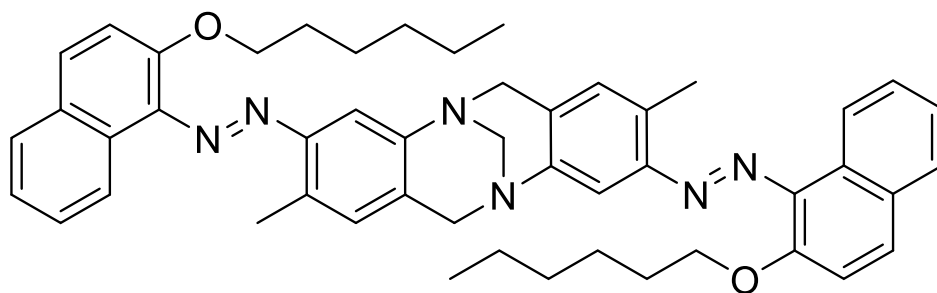
3D structure of compound 6a-P11



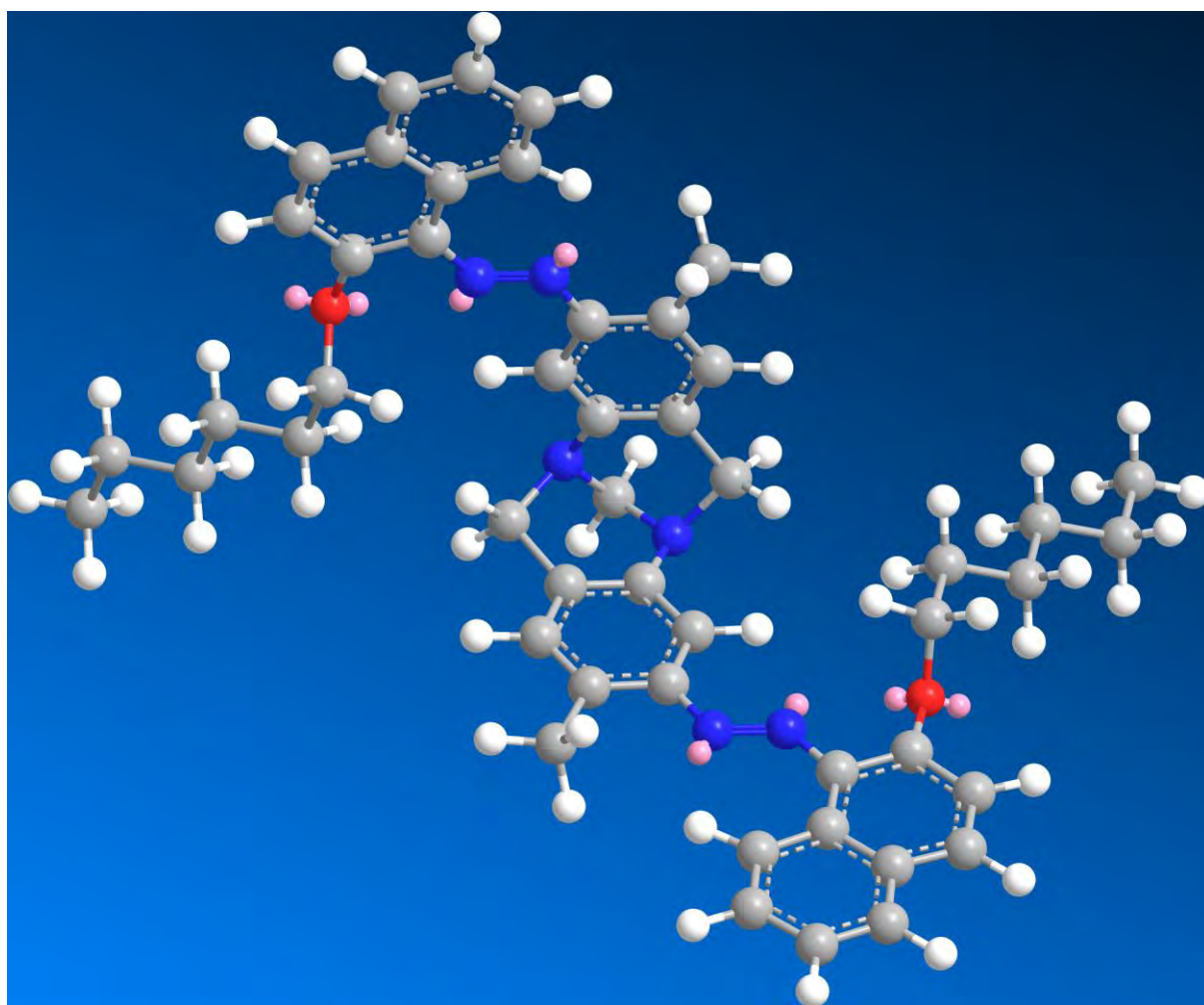
2D structure of compound 8a-P11



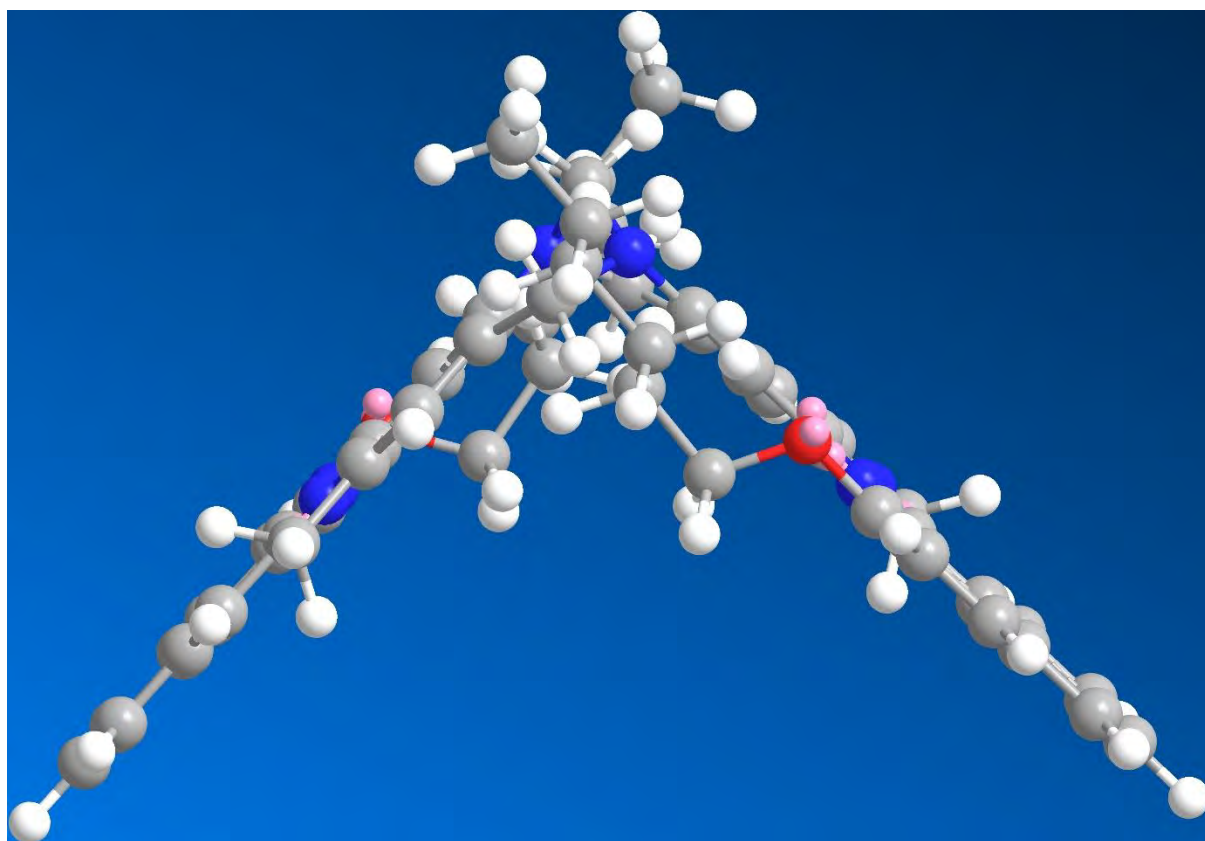
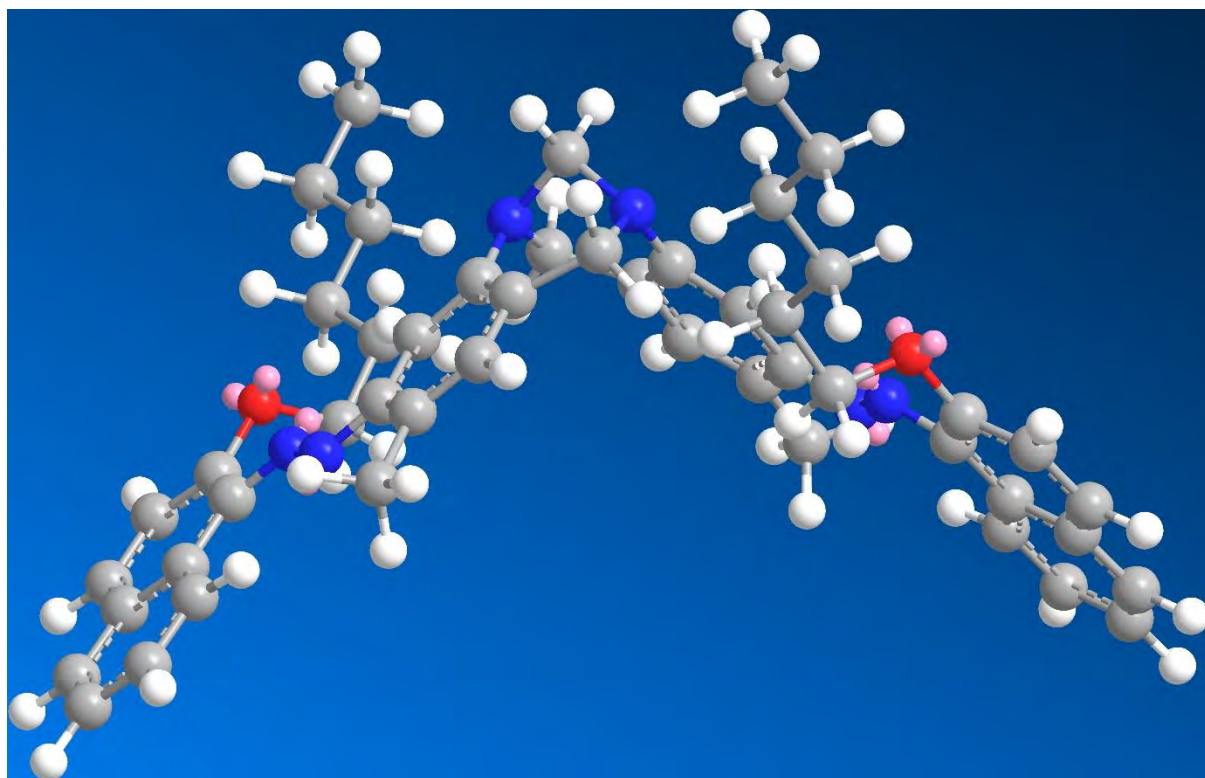
3D structure of compound 8a-P11



2D structure of compound 9a-P11



3D structure of compound 9a-P11



3D structure of compound 9a-P1I

Appendix 3: The X-ray crystallography results



3,9-Bis((*E*)-(4-(hexyloxy)-3,5-dimethylphenyl)diazenyl)-2,8-dimethyl-6H,12H-5,11-methanodibenzo[*b,f*][1,5]diazocine

Masoud Kazem-Rostami,^a Jason R Smith,^b Peter Turner,^{c*} Suzanne Lindsay,^d Andrew Try, and Joanne Jamie^a

^a Department of Chemistry and Biomolecular Sciences, Faculty of Science and Engineering, Macquarie University, NSW 2109, Australia; ^b Department of Chemistry, Simon Fraser University, V5A-1S6 Burnaby, BC, Canada; ^c Crystal Structure Analysis Facility, School of Chemistry, The University of Sydney, NSW 2006, Australia; ^d Microscopy Unit, Faculty of Science and Engineering, Macquarie University, NSW 2109, Australia.

*Correspondence e-mail: p.turner@chem.usyd.edu.au

Key indicators: single-crystal X-ray study; $T = 150$ K; mean $\sigma(\text{C}-\text{C}) = 0.002$ Å; disorder in main residue; R factor = 0.0779; wR factor = 0.2078; data-to-parameter ratio = 17.2.

A red rectangular prismatic crystal of the title compound, displayed in Figure 1, was attached with Exxon Paratone N to a nylon loop and quenched in a cold nitrogen gas stream from an Oxford Cryosystems Cryostream. A SuperNova Dual equipped with an Atlas detector and employing mirror monochromated Cu ($K\alpha$) radiation from a micro-source was used for the data collection. Cell constants were obtained from a least squares refinement against 12879 reflections located between 7 and $148^\circ 2\theta$. Data were collected at 150(1) Kelvin with ω scans to $152^\circ 2\theta$. The data processing was undertaken with CrysAlis Pro¹ and subsequent computations were carried out with WinGX² and ShelXle.³ A multi-scan absorption correction was applied¹ to the data. The structure was solved in the space group $P\bar{1}(\#2)$ by direct methods with SHELXT⁴ and extended and refined with SHELXL-2014/7.⁵ The asymmetric unit contains two crystallographically independent molecules, one of which has site disorder in one of its pendant residues. Occupancies for these sites were refined and then fixed at the first decimal place. In general the non-hydrogen atoms in the asymmetric unit were modelled with anisotropic displacement parameters and a riding atom model with isotropic displacement parameters was used for the hydrogen atoms. Isotropic displacement parameters were used for the disordered carbon sites. An ORTEP⁶ depiction of one of the molecules with 50% displacement ellipsoids is provided in Figure 2. The molecules pack in columns in a complementary manner, as shown in Figure 3, which was generated using Mercury.⁷

The angles between the least squares planes defined the two aryl rings joined to the two diazocine rings is $84.7(1)^\circ$, which is within the literature⁸ range of 82° ⁹ to 104° .¹⁰ The torsion angles across the diazo bridges are $177.8(2)^\circ$ and $-178.3(2)^\circ$ for one molecule and $-177.4(2)^\circ$ and $-177.0(2)^\circ$ for the second molecule. The angles between the aryl groups linked by the diazo bridges are $12.0(1)^\circ$ and $7.3(1)^\circ$ for one molecules and $13.2(1)^\circ$ and $9.9(1)^\circ$ for the second.

The title compound was prepared according to the literature.¹¹ The crystals (Fig. 2) were obtained by decreasing the temperature of a solution (in *i*-PrOH–acetone 9:1) of the title compound from 325 to 273K.

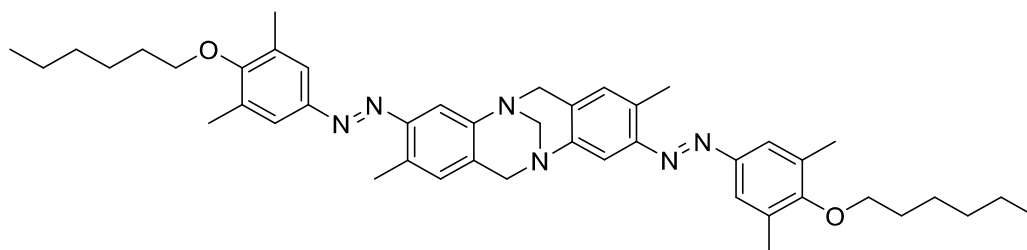


Figure 1. Chemical structure of the title compound

Experimental

Crystal data

$C_{45}H_{58}N_6O_2$

$M_r = 714.97$

Triclinic, $P \bar{1}(\#2)$

Space Group

$a = 6.3862(2) \text{ \AA}$

$b = 23.0353(7) \text{ \AA}$

$c = 27.8710(7) \text{ \AA}$

$\alpha = 82.153(2)^\circ$

$\beta = 86.169(2)^\circ$

$\gamma = 87.677(3)^\circ$

$V = 4050.5(2) \text{ \AA}^3$

$Z = 4$

Cu $K\alpha$ radiation

$\mu = 0.566 \text{ mm}^{-1}$

$T = 150(1) \text{ K}$

0.120 x 0.088 x 0.040 mm

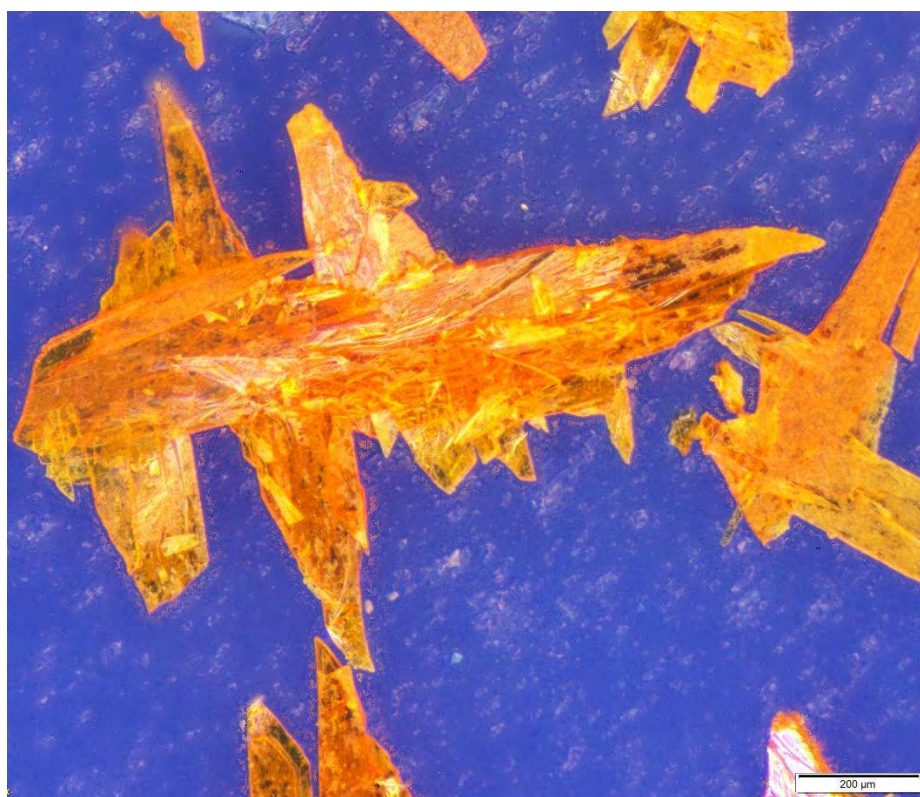


Figure 2. Microscopic image of the title compound crystals taken by Olympus® SZX16

Acknowledgment

MKR appreciates the Australian Government for awarding him with a Research Training Program Scholarship IPRS-2014004, and Macquarie University for HDR-43010477 and PGRF-2016R2-1672525 funds.

References

1. CrysAlisPro Version 1.171.37.35. Agilent Technologies, 2015.
2. WinGX, Farrugia, L. J. (1999) *J. Appl. Cryst.*, 32, 837-838.
3. ShelXle: a Qt graphical user interface for SHELXL; C. B. Hübschle, G. M. Sheldrick and B. Dittrich. *J. Appl. Cryst.* (2011). 44, 1281-1284.
4. Sheldrick, G.M. (2015), *Acta Cryst. A* 71 3-85.
5. (a) Sheldrick, G. M. (2015), *Acta Cryst. C* 71, 3-8. (b) G. M. Sheldrick, *Acta Crystallogr., Sect. A: Found. Crystallogr.*, 2008, 64, 112-122.
6. ORTEP for Windows; L. J. Farrugia, *J. Appl. Crystallogr.*, 1997, 30, 565. (b) ORTEP III; M. N. Burnett and C. K. Johnson, ORTEP-III Report ORNL-6895. Oak Ridge National Laboratory, Tennessee, USA, 1996.
7. Mercury CSD 2.0 - New Features for the Visualization and Investigation of Crystal Structures C. F. Macrae, I. J. Bruno, J. A. Chisholm, P. R. Edgington, P. McCabe, E. Pidcock, L. Rodriguez-Monge, R. Taylor, J. van de Streek and P. A. Wood, *J. Appl. Cryst.*, 41, 466-470, 2008. [DOI: 10.1107/S0021889807067908]
8. M. Faroughi, A. C. Try, P. Turner (2006), *Acta Cryst. E* 62: o3893-o3894.
9. Solano, C., Svensson, D., Olomi, Z., Jensen, J., Wendt, O. F. & Wärnmark, K. (2005). *Eur. J. Org. Chem.* pp. 3510–3517.
10. Wilcox, C. S., Greer, L. M. & Lynch, V. (1987). *J. Am. Chem. Soc.* 109, 1865–1867.
11. Kazem-Rostami, M. (2017) *Synthesis* 49, 1214–1222.

Supplementary Materials

Crystallographic details for Compound: 3,9-bis((*E*)-(4-(hexyloxy)-3,5-dimethylphenyl)diazenyl)-2,8-dimethyl-6H,12H-5,11-methanodibenzo[b,f][1,5]diazocine

Table 1. Crystallographic data for the title compound

Formula of the Refinement Model	C ₄₅ H ₅₈ N ₆ O ₂
Model Molecular Weight	714.97
Crystal System	triclinic
Space Group	<i>P</i> $\bar{1}$ (#2)
<i>a</i>	6.3862(2) Å
<i>b</i>	23.0353(7) Å
<i>c</i>	27.8710(7) Å
α	82.153(2)°
β	86.169(2)°
γ	87.677(3)°
<i>V</i>	4050.5(2) Å ³
<i>D</i> _c	1.172 g cm ⁻³
<i>Z</i>	4
Crystal Size	0.120x0.088x0.040 mm
Crystal Colour	red
Crystal Habit	rectangular prismatic
Temperature	150(1) Kelvin
λ (Cu K α)	1.5418 Å
μ (Cu K α)	0.566 mm ⁻¹
<i>T</i> _{min,max}	0.991, 1.00
2 θ _{max}	152.42°
<i>hkl</i> range	-8 8, -28 28, -34 34
<i>N</i>	83956
<i>N</i> _{ind}	16495(<i>R</i> _{merge} 0.0648)
<i>N</i> _{obs}	10871(<i>I</i> > 2 σ (<i>I</i>))
<i>N</i> _{var}	963
Residuals* <i>R</i> 1(<i>F</i>), <i>wR</i> 2(<i>F</i> ²)	0.0779, 0.2078
GoF(all)	1.047
Residual Extrema	-0.447, 1.021 e ⁻ Å ⁻³

* $R1 = \Sigma ||F_o| - |F_c|| / \Sigma |F_o|$ for $F_o > 2\sigma(F_o)$; $wR2 = (\Sigma w(F_o^2 - F_c^2)^2 / \Sigma (wF_c^2)^2)^{1/2}$ all reflections
 $w = 1 / [\sigma^2(F_o^2) + (0.07P)^2 + 4.0P]$ where $P = (F_o^2 + 2F_c^2) / 3$

Table 2. Non-Hydrogen Atom Coordinates, Isotropic Thermal Parameters and Occupancies

atom	x	y	z	$U_{eq}(\text{\AA}^2)$	Occ
O(1_1)	0.2341(3)	0.71379(9)	0.57238(7)	0.0437(5)	1
O(2_1)	-1.2956(3)	0.61703(12)	0.00649(8)	0.0590(6)	1
N(1_1)	0.1762(3)	0.49099(12)	0.27434(8)	0.0400(5)	1
N(2_1)	-0.0847(4)	0.45854(11)	0.22503(8)	0.0386(5)	1
N(3_1)	-0.0596(3)	0.54632(10)	0.43378(8)	0.0336(5)	1
N(4_1)	0.1034(3)	0.57518(10)	0.42991(8)	0.0349(5)	1
N(5_1)	-0.4985(4)	0.60594(12)	0.12437(8)	0.0422(6)	1
N(6_1)	-0.6106(4)	0.56432(12)	0.11878(8)	0.0408(6)	1
C(1_1)	0.0171(4)	0.49156(13)	0.31343(9)	0.0348(6)	1
C(2_1)	-0.1790(4)	0.46636(12)	0.31158(9)	0.0334(6)	1
C(3_1)	-0.3241(4)	0.46664(12)	0.35101(9)	0.0324(5)	1
C(4_1)	-0.2842(4)	0.49109(11)	0.39215(9)	0.0308(5)	1
C(5_1)	-0.0913(4)	0.51849(12)	0.39224(9)	0.0326(5)	1
C(6_1)	0.0573(4)	0.51794(12)	0.35340(9)	0.0338(6)	1
C(7_1)	-0.2326(4)	0.44069(13)	0.26693(9)	0.0387(6)	1
C(8_1)	-0.4439(4)	0.48876(13)	0.43460(9)	0.0363(6)	1
C(9_1)	0.1280(4)	0.44949(15)	0.24186(10)	0.0441(7)	1
C(10_1)	0.1344(4)	0.60509(12)	0.47018(9)	0.0322(5)	1
C(11_1)	-0.0007(4)	0.60357(12)	0.51168(9)	0.0321(5)	1
C(12_1)	0.0364(4)	0.63728(12)	0.54739(9)	0.0329(5)	1
C(13_1)	0.2105(4)	0.67343(12)	0.54072(10)	0.0352(6)	1
C(14_1)	0.3521(4)	0.67399(12)	0.50023(10)	0.0346(6)	1
C(15_1)	0.3098(4)	0.63964(12)	0.46528(9)	0.0336(6)	1
C(16_1)	-0.1107(4)	0.63745(14)	0.59195(10)	0.0408(6)	1
C(17_1)	0.5391(4)	0.71273(13)	0.49448(11)	0.0420(7)	1
C(18_1)	0.3344(5)	0.69296(14)	0.61557(10)	0.0425(7)	1
C(19_1)	0.4475(5)	0.74359(14)	0.63119(11)	0.0448(7)	1
C(20_1)	0.5488(5)	0.72623(16)	0.67909(11)	0.0525(8)	1
C(21_1)	0.6579(6)	0.77639(17)	0.69681(13)	0.0584(9)	1
C(22_1)	0.8446(6)	0.79867(18)	0.66562(15)	0.0639(10)	1
C(23_1)	0.9634(6)	0.84333(17)	0.68868(17)	0.0694(11)	1
C(24_1)	-0.1211(4)	0.51846(13)	0.20509(9)	0.0350(6)	1
C(25_1)	0.0105(4)	0.56299(14)	0.21294(9)	0.0381(6)	1
C(26_1)	-0.0303(5)	0.61977(14)	0.19105(10)	0.0433(7)	1
C(27_1)	-0.1982(5)	0.63469(14)	0.16220(10)	0.0434(7)	1
C(28_1)	-0.3299(4)	0.58951(14)	0.15543(9)	0.0384(6)	1
C(29_1)	-0.2906(4)	0.53243(13)	0.17644(9)	0.0364(6)	1
C(30_1)	0.1928(4)	0.54907(15)	0.24504(10)	0.0425(7)	1
C(31_1)	-0.2365(6)	0.69697(16)	0.13934(14)	0.0608(9)	1

C(32_1)	-0.7751(4)	0.58008(14)	0.08680(10)	0.0408(7)	1
C(33_1)	-0.8001(5)	0.63493(15)	0.05992(11)	0.0468(7)	1
C(34_1)	-0.9702(5)	0.64711(16)	0.03152(11)	0.0502(8)	1
C(35_1)	-1.1131(4)	0.60300(16)	0.03044(11)	0.0475(7)	1
C(36_1)	-1.0863(4)	0.54683(15)	0.05502(10)	0.0441(7)	1
C(37_1)	-0.9151(4)	0.53649(15)	0.08374(10)	0.0422(7)	1
C(38_1)	-1.0010(6)	0.70707(18)	0.00274(15)	0.0696(11)	1
C(39_1)	-1.2375(5)	0.49944(17)	0.05200(12)	0.0537(8)	1
C(40_1)	-1.2841(5)	0.60969(18)	-0.04325(12)	0.0589(9)	1
C(41_1)	-1.4801(6)	0.63861(17)	-0.06428(13)	0.0604(9)	1
C(42_1)	-1.4886(6)	0.63610(19)	-0.11764(13)	0.0672(11)	1
C(43_1)	-1.6911(6)	0.6698(2)	-0.13727(13)	0.0675(10)	1
C(44_1)	-1.6921(7)	0.6747(2)	-0.19040(15)	0.0768(12)	1
C(45_1)	-1.8920(7)	0.7037(2)	-0.20887(15)	0.0797(13)	1
O(1_2)	-0.7964(4)	0.12054(13)	-0.01836(9)	0.0621(7)	1
O(2_2)	0.8300(4)	0.16415(11)	0.60097(9)	0.0600(6)	1
N(1_2)	0.3726(4)	-0.01413(11)	0.22085(8)	0.0393(5)	1
N(2_2)	0.6274(3)	0.02395(11)	0.26867(8)	0.0390(5)	1
N(3_2)	-0.0348(4)	0.12219(12)	0.10989(8)	0.0409(5)	1
N(4_2)	-0.1549(4)	0.08062(12)	0.10923(8)	0.0407(5)	1
N(5_2)	0.4132(3)	0.06418(10)	0.43400(8)	0.0362(5)	1
N(6_2)	0.5727(4)	0.09417(11)	0.43139(8)	0.0378(5)	1
C(1_2)	0.3309(4)	0.04471(13)	0.19835(9)	0.0348(6)	1
C(2_2)	0.4589(4)	0.09095(13)	0.20398(9)	0.0358(6)	1
C(3_2)	0.4213(4)	0.14555(13)	0.17736(10)	0.0397(6)	1
C(4_2)	0.2594(5)	0.15620(14)	0.14618(10)	0.0407(6)	1
C(5_2)	0.1271(4)	0.10986(13)	0.14305(9)	0.0365(6)	1
C(6_2)	0.1639(4)	0.05492(13)	0.16870(9)	0.0363(6)	1
C(7_2)	0.6364(4)	0.08123(14)	0.23802(10)	0.0395(6)	1
C(8_2)	0.2324(6)	0.21504(15)	0.11579(12)	0.0528(8)	1
C(9_2)	0.5857(5)	-0.01984(14)	0.23771(11)	0.0443(7)	1
C(10_2)	-0.3105(4)	0.09273(14)	0.07431(10)	0.0410(6)	1
C(11_2)	-0.3157(5)	0.14259(15)	0.04006(12)	0.0484(7)	1
C(12_2)	-0.4744(5)	0.15138(16)	0.00795(12)	0.0516(8)	1
C(13_2)	-0.6271(5)	0.10879(17)	0.01090(12)	0.0508(8)	1
C(14_2)	-0.6198(5)	0.05747(16)	0.04365(11)	0.0476(7)	1
C(15_2)	-0.4594(4)	0.05068(15)	0.07556(10)	0.0426(7)	1
C(16_2)	-0.7799(5)	0.01076(18)	0.04504(12)	0.0570(9)	1
C(17_2)	-0.4817(7)	0.20602(18)	-0.02925(15)	0.0711(11)	1
C(18_2)	-0.7687(6)	0.09996(18)	-0.06403(12)	0.0578(9)	1
C(19_2)	-0.9294(6)	0.13107(17)	-0.09675(13)	0.0599(9)	1
C(20_2)	-0.9153(7)	0.11039(19)	-0.14629(14)	0.0665(10)	1
C(21_2)	-1.0404(8)	0.1493(2)	-0.18491(16)	0.0849(14)	1
C(22_2)	-1.2649(8)	0.1541(3)	-0.17305(19)	0.0916(15)	1

C(23_2)	-1.3873(8)	0.1926(2)	-0.21301(18)	0.0925(15)	1
C(24_2)	0.4700(4)	0.02282(13)	0.30844(9)	0.0355(6)	1
C(25_2)	0.2787(4)	-0.00493(12)	0.30742(9)	0.0343(6)	1
C(26_2)	0.1408(4)	-0.00903(12)	0.34840(9)	0.0347(6)	1
C(27_2)	0.1829(4)	0.01316(12)	0.39017(9)	0.0339(6)	1
C(28_2)	0.3714(4)	0.04290(12)	0.38984(9)	0.0343(6)	1
C(29_2)	0.5132(4)	0.04737(12)	0.34928(9)	0.0356(6)	1
C(30_2)	0.2254(5)	-0.03122(13)	0.26305(10)	0.0398(6)	1
C(31_2)	0.0343(4)	0.00484(14)	0.43464(10)	0.0407(6)	1
C(32_2)	0.6201(4)	0.11292(12)	0.47616(10)	0.0342(6)	1
C(33_2)	0.5011(4)	0.10042(12)	0.51978(10)	0.0347(6)	1
C(34_2)	0.5627(4)	0.11993(12)	0.56156(10)	0.0373(6)	1
C(35_2)	0.7485(5)	0.15092(13)	0.55870(10)	0.0408(6)	1
C(36_2)	0.8671(4)	0.16444(12)	0.51510(11)	0.0388(6)	1
C(37_2)	0.8000(4)	0.14519(12)	0.47393(10)	0.0380(6)	1
C(38_2)	0.4312(5)	0.10815(15)	0.60859(11)	0.0497(8)	1
C(39_2)	1.0608(5)	0.20000(15)	0.51246(12)	0.0498(8)	1
C(40A_2)	0.7190(12)	0.2141(3)	0.6175(3)	0.0681(18)	0.6
C(41A_2)	0.8389(13)	0.2352(4)	0.6582(3)	0.082(2)	0.6
C(42A_2)	1.0366(10)	0.2663(3)	0.6394(2)	0.0568(14)	0.6
C(40B_2)	0.8079(18)	0.2197(4)	0.6099(4)	0.064(3)	0.4
C(41B_2)	0.9784(14)	0.2314(4)	0.6434(3)	0.0523(19)	0.4
C(42B_2)	0.9217(14)	0.2909(4)	0.6618(3)	0.058(2)	0.4
C(43_2)	1.1226(8)	0.3019(2)	0.68152(19)	0.0921(14)	1
C(44_2)	1.3052(6)	0.33172(18)	0.65869(15)	0.0669(10)	1
C(45_2)	1.4171(7)	0.3647(2)	0.69269(18)	0.0815(13)	1

Table 3. Anisotropic Thermal Parameters (\AA^2)

atom	U(1,1)	U(2,2)	U(3,3)	U(1,2)	U(1,3)	U(2,3)
O(1_1) 0.0099(9)	0.0494(11)	0.0387(11)	0.0458(11)	-0.0008(9)	-0.0154(9)	-
O(2_1) 0.0143(12)	0.0396(11)	0.0910(19)	0.0483(13)	0.0030(11)	-0.0095(10)	-
N(1_1) 0.0099(11)	0.0323(11)	0.0610(16)	0.0281(11)	-0.0048(10)	-0.0014(9)	-
N(2_1) 0.0096(10)	0.0380(12)	0.0511(14)	0.0283(11)	-0.0018(10)	-0.0039(9)	-
N(3_1) 0.0042(9)	0.0327(11)	0.0408(12)	0.0279(10)	-0.0065(9)	-0.0048(8)	-
N(4_1) 0.0056(10)	0.0329(11)	0.0426(13)	0.0300(11)	-0.0069(9)	-0.0045(9)	-
N(5_1) 0.0047(11)	0.0392(12)	0.0564(16)	0.0309(11)	-0.0031(11)	-0.0029(9)	-
N(6_1) 0.0051(11)	0.0366(12)	0.0583(16)	0.0275(11)	-0.0040(11)	-0.0014(9)	-

C(1_1) 0.0038(11)	0.0326(13)	0.0459(15)	0.0258(12)	-0.0034(11)	-0.0031(10)	-
C(2_1) 0.0044(11)	0.0351(13)	0.0398(14)	0.0263(12)	-0.0056(11)	-0.0069(10)	-
C(3_1) 0.0031(11)	0.0293(12)	0.0402(14)	0.0283(12)	-0.0068(10)	-0.0054(9)	-
C(4_1) 0.0010(10)	0.0306(12)	0.0350(13)	0.0263(12)	-0.0019(10)	-0.0030(9)	-
C(5_1) 0.0027(11)	0.0322(12)	0.0409(14)	0.0248(11)	-0.0036(10)	-0.0048(9)	-
C(6_1) 0.0049(11)	0.0279(12)	0.0449(15)	0.0294(12)	-0.0068(10)	-0.0050(10)	-
C(7_1) 0.0061(12)	0.0395(14)	0.0483(16)	0.0297(13)	-0.0089(12)	-0.0055(11)	-
C(8_1) 0.0059(12)	0.0315(13)	0.0478(16)	0.0301(13)	-0.0065(11)	-0.0014(10)	-
C(9_1) 0.0136(14)	0.0373(14)	0.064(2)	0.0333(14)	0.0039(13)	-0.0051(11)	-
C(10_1) 0.0027(11)	0.0307(12)	0.0374(14)	0.0287(12)	-0.0025(10)	-0.0064(10)	-
C(11_1) 0.0031(11)	0.0281(12)	0.0351(13)	0.0332(13)	-0.0040(10)	-0.0050(10)	-
C(12_1) 0.0056(11)	0.0331(13)	0.0351(14)	0.0309(13)	0.0005(10)	-0.0036(10)	-
C(13_1) 0.0070(11)	0.0379(14)	0.0332(14)	0.0362(14)	-0.0011(11)	-0.0092(11)	-
C(14_1) 0.0025(11)	0.0308(12)	0.0349(14)	0.0384(14)	-0.0040(10)	-0.0071(10)	-
C(15_1) 0.0033(11)	0.0315(12)	0.0386(14)	0.0305(12)	-0.0024(10)	-0.0024(10)	-
C(16_1) 0.0104(13)	0.0386(14)	0.0496(17)	0.0358(14)	-0.0035(12)	-0.0022(11)	-
C(17_1) 0.0045(13)	0.0379(14)	0.0440(16)	0.0451(16)	-0.0113(12)	-0.0077(12)	-
C(18_1) 0.0021(13)	0.0402(15)	0.0478(17)	0.0393(15)	-0.0041(12)	-0.0058(12)	-
C(19_1) 0.0116(13)	0.0469(16)	0.0462(17)	0.0435(16)	-0.0021(13)	-0.0082(13)	-
C(20_1) 0.0092(15)	0.0519(18)	0.067(2)	0.0402(16)	-0.0153(16)	-0.0038(13)	-
C(21_1) 0.0208(18)	0.0535(19)	0.072(2)	0.055(2)	-0.0080(17)	-0.0098(15)	-
C(22_1) 0.024(2)	0.054(2)	0.069(2)	0.074(2)	-0.0136(17)	-0.0068(18)	-
C(23_1)	0.060(2)	0.053(2)	0.098(3)	-0.0112(17)	-0.027(2)	-0.010(2)
C(24_1) 0.0110(11)	0.0340(13)	0.0513(16)	0.0213(11)	-0.0056(11)	0.0025(9)	-
C(25_1) 0.0073(12)	0.0355(14)	0.0548(17)	0.0243(12)	-0.0083(12)	0.0036(10)	-

C(26_1)	0.0447(15)	0.0550(18)	0.0324(14)	-0.0154(13)	0.0002(12)	-
0.0111(13)						
C(27_1)	0.0492(16)	0.0486(17)	0.0328(14)	-0.0065(13)	0.0009(12)	-
0.0073(13)						
C(28_1)	0.0360(14)	0.0541(17)	0.0262(12)	-0.0046(12)	0.0007(10)	-
0.0090(12)						
C(29_1)	0.0359(13)	0.0503(16)	0.0244(12)	-0.0081(12)	0.0000(10)	-
0.0088(11)						
C(30_1)	0.0327(13)	0.066(2)	0.0300(13)	-0.0120(13)	0.0014(10)	-
0.0096(13)						
C(31_1)	0.073(2)	0.052(2)	0.058(2)	-0.0076(17)	-0.0107(18)	-
0.0065(17)						
C(32_1)	0.0354(14)	0.0600(19)	0.0269(13)	-0.0021(12)	0.0007(10)	-
0.0062(13)						
C(33_1)	0.0396(15)	0.0589(19)	0.0409(15)	-0.0075(13)	-0.0045(12)	
0.0003(14)						
C(34_1)	0.0429(16)	0.062(2)	0.0431(16)	-0.0005(14)	-0.0054(13)	
0.0022(15)						
C(35_1)	0.0331(14)	0.073(2)	0.0365(15)	0.0019(14)	-0.0032(11)	-
0.0089(15)						
C(36_1)	0.0364(14)	0.064(2)	0.0333(14)	-0.0065(13)	0.0038(11)	-
0.0108(14)						
C(37_1)	0.0419(15)	0.0577(19)	0.0268(13)	-0.0031(13)	0.0013(11)	-
0.0058(13)						
C(38_1)	0.059(2)	0.075(3)	0.071(2)	-0.0019(19)	-0.0205(19)	
0.012(2)						
C(39_1)	0.0475(17)	0.072(2)	0.0450(17)	-0.0127(16)	-0.0012(14)	-
0.0165(16)						
C(40_1)	0.0506(19)	0.079(3)	0.0463(18)	-0.0032(17)	-0.0102(14)	-
0.0025(17)						
C(41_1)	0.0531(19)	0.063(2)	0.064(2)	-0.0122(16)	-0.0209(16)	
0.0071(18)						
C(42_1)	0.062(2)	0.080(3)	0.056(2)	-0.0248(19)	-0.0186(17)	
0.0145(19)						
C(43_1)	0.062(2)	0.084(3)	0.054(2)	-0.007(2)	-0.0063(17)	
0.0052(19)						
C(44_1)	0.079(3)	0.092(3)	0.059(2)	-0.001(2)	-0.015(2)	-0.004(2)
C(45_1)	0.074(3)	0.102(3)	0.063(2)	0.015(2)	-0.015(2)	-0.009(2)
O(1_2)	0.0447(12)	0.0909(19)	0.0557(14)	0.0049(12)	-0.0140(10)	-
0.0243(13)						
O(2_2)	0.0664(15)	0.0639(15)	0.0530(13)	-0.0142(12)	-0.0159(11)	-
0.0102(12)						
N(1_2)	0.0393(12)	0.0467(14)	0.0340(12)	-0.0045(10)	-0.0048(9)	-
0.0103(10)						
N(2_2)	0.0325(11)	0.0524(14)	0.0336(11)	-0.0039(10)	-0.0021(9)	-
0.0105(11)						
N(3_2)	0.0378(12)	0.0537(15)	0.0325(12)	-0.0052(11)	-0.0026(9)	-
0.0091(11)						
N(4_2)	0.0351(12)	0.0550(15)	0.0332(12)	-0.0063(11)	-0.0017(9)	-
0.0093(11)						

C(26_2)	0.0310(12)	0.0379(14)	0.0348(13)	-0.0075(10)	-0.0049(10)	
0.0002(11)						
C(27_2)	0.0321(13)	0.0378(14)	0.0309(13)	-0.0039(10)	-0.0024(10)	-
0.0007(11)						
C(28_2)	0.0341(13)	0.0388(14)	0.0302(13)	-0.0049(11)	-0.0058(10)	-
0.0025(11)						
C(29_2)	0.0312(13)	0.0448(15)	0.0308(13)	-0.0079(11)	-0.0052(10)	-
0.0010(11)						
C(30_2)	0.0440(15)	0.0416(15)	0.0349(14)	-0.0096(12)	-0.0072(11)	-
0.0039(12)						
C(31_2)	0.0360(14)	0.0489(17)	0.0365(14)	-0.0084(12)	0.0024(11)	-
0.0032(13)						
C(32_2)	0.0320(13)	0.0371(14)	0.0336(13)	-0.0020(10)	-0.0045(10)	-
0.0039(11)						
C(33_2)	0.0315(13)	0.0369(14)	0.0357(13)	-0.0054(10)	-0.0057(10)	-
0.0022(11)						
C(34_2)	0.0393(14)	0.0392(15)	0.0331(13)	-0.0027(11)	-0.0050(11)	-
0.0025(12)						
C(35_2)	0.0447(15)	0.0429(16)	0.0373(14)	-0.0085(12)	-0.0125(12)	-
0.0070(12)						
C(36_2)	0.0353(14)	0.0348(14)	0.0466(15)	-0.0058(11)	-0.0110(11)	-
0.0013(12)						
C(37_2)	0.0347(13)	0.0409(15)	0.0375(14)	-0.0034(11)	-0.0021(11)	-
0.0017(12)						
C(38_2)	0.0547(18)	0.060(2)	0.0355(15)	-0.0116(15)	-0.0022(13)	-
0.0075(14)						
C(39_2)	0.0415(16)	0.0520(18)	0.0572(19)	-0.0139(14)	-0.0152(14)	-
0.0020(15)						
C(44_2)	0.067(2)	0.068(2)	0.068(2)	-0.0073(19)	-0.0217(19)	-
0.008(2)						
C(45_2)	0.076(3)	0.079(3)	0.096(3)	-0.028(2)	-0.022(2)	-0.020(3)

Table 4. Non-Hydrogen Bond Lengths (Å)

atom	atom	Distance	atom	atom	Distance
O(1_1)	C(13_1)	1.385(3)	O(1_1)	C(18_1)	1.418(3)
O(2_1)	C(35_1)	1.386(4)	O(2_1)	C(40_1)	1.416(4)
N(1_1)	C(1_1)	1.440(3)	N(1_1)	C(9_1)	1.458(4)
N(1_1)	C(30_1)	1.473(4)	N(2_1)	C(24_1)	1.432(4)
N(2_1)	C(9_1)	1.464(3)	N(2_1)	C(7_1)	1.476(3)
N(3_1)	N(4_1)	1.249(3)	N(3_1)	C(5_1)	1.427(3)
N(4_1)	C(10_1)	1.423(3)	N(5_1)	N(6_1)	1.252(3)
N(5_1)	C(28_1)	1.433(4)	N(6_1)	C(32_1)	1.427(4)
C(1_1)	C(6_1)	1.383(4)	C(1_1)	C(2_1)	1.408(4)
C(2_1)	C(3_1)	1.390(4)	C(2_1)	C(7_1)	1.513(4)
C(3_1)	C(4_1)	1.387(4)	C(4_1)	C(5_1)	1.407(4)

C(4_1)	C(8_1)	1.506(3)	C(5_1)	C(6_1)	1.392(4)
C(10_1)	C(15_1)	1.389(4)	C(10_1)	C(11_1)	1.393(4)
C(11_1)	C(12_1)	1.381(4)	C(12_1)	C(13_1)	1.403(4)
C(12_1)	C(16_1)	1.507(4)	C(13_1)	C(14_1)	1.397(4)
C(14_1)	C(15_1)	1.383(4)	C(14_1)	C(17_1)	1.507(4)
C(18_1)	C(19_1)	1.523(4)	C(19_1)	C(20_1)	1.519(4)
C(20_1)	C(21_1)	1.527(5)	C(21_1)	C(22_1)	1.494(5)
C(22_1)	C(23_1)	1.535(5)	C(24_1)	C(29_1)	1.390(4)
C(24_1)	C(25_1)	1.401(4)	C(25_1)	C(26_1)	1.388(4)
C(25_1)	C(30_1)	1.513(4)	C(26_1)	C(27_1)	1.387(4)
C(27_1)	C(28_1)	1.404(4)	C(27_1)	C(31_1)	1.506(5)
C(28_1)	C(29_1)	1.385(4)	C(32_1)	C(37_1)	1.386(4)
C(32_1)	C(33_1)	1.387(4)	C(33_1)	C(34_1)	1.384(4)
C(34_1)	C(35_1)	1.398(5)	C(34_1)	C(38_1)	1.512(5)
C(35_1)	C(36_1)	1.389(5)	C(36_1)	C(37_1)	1.392(4)
C(36_1)	C(39_1)	1.501(4)	C(40_1)	C(41_1)	1.509(5)
C(41_1)	C(42_1)	1.501(5)	C(42_1)	C(43_1)	1.573(5)
C(43_1)	C(44_1)	1.470(5)	C(44_1)	C(45_1)	1.506(6)
O(1_2)	C(13_2)	1.393(4)	O(1_2)	C(18_2)	1.416(4)
O(2_2)	C(40B_2)	1.336(8)	O(2_2)	C(35_2)	1.395(4)
O(2_2)	C(40A_2)	1.438(6)	N(1_2)	C(1_2)	1.436(4)
N(1_2)	C(9_2)	1.465(4)	N(1_2)	C(30_2)	1.476(4)
N(2_2)	C(24_2)	1.444(3)	N(2_2)	C(9_2)	1.457(4)
N(2_2)	C(7_2)	1.472(4)	N(3_2)	N(4_2)	1.254(3)
N(3_2)	C(5_2)	1.427(3)	N(4_2)	C(10_2)	1.430(4)
N(5_2)	N(6_2)	1.246(3)	N(5_2)	C(28_2)	1.430(3)
N(6_2)	C(32_2)	1.430(4)	C(1_2)	C(6_2)	1.385(4)
C(1_2)	C(2_2)	1.400(4)	C(2_2)	C(3_2)	1.391(4)
C(2_2)	C(7_2)	1.516(4)	C(3_2)	C(4_2)	1.387(4)
C(4_2)	C(5_2)	1.403(4)	C(4_2)	C(8_2)	1.507(4)
C(5_2)	C(6_2)	1.385(4)	C(10_2)	C(15_2)	1.380(4)
C(10_2)	C(11_2)	1.390(4)	C(11_2)	C(12_2)	1.387(4)
C(12_2)	C(13_2)	1.402(5)	C(12_2)	C(17_2)	1.519(5)
C(13_2)	C(14_2)	1.392(5)	C(14_2)	C(15_2)	1.391(4)
C(14_2)	C(16_2)	1.509(4)	C(18_2)	C(19_2)	1.512(5)
C(19_2)	C(20_2)	1.517(5)	C(20_2)	C(21_2)	1.547(6)
C(21_2)	C(22_2)	1.453(6)	C(22_2)	C(23_2)	1.558(7)
C(24_2)	C(29_2)	1.386(4)	C(24_2)	C(25_2)	1.405(4)
C(25_2)	C(26_2)	1.390(4)	C(25_2)	C(30_2)	1.513(4)
C(26_2)	C(27_2)	1.380(4)	C(27_2)	C(28_2)	1.408(4)
C(27_2)	C(31_2)	1.505(4)	C(28_2)	C(29_2)	1.396(4)
C(32_2)	C(37_2)	1.387(4)	C(32_2)	C(33_2)	1.392(4)
C(33_2)	C(34_2)	1.389(4)	C(34_2)	C(35_2)	1.402(4)
C(34_2)	C(38_2)	1.507(4)	C(35_2)	C(36_2)	1.393(4)

C(36_2)	C(37_2)	1.385(4)	C(36_2)	C(39_2)	1.503(4)
C(40A_2)	C(41A_2)	1.552(11)	C(41A_2)	C(42A_2)	
1.505(10)					
C(42A_2)	C(43_2)	1.655(8)	C(40B_2)	C(41B_2)	
1.535(13)					
C(41B_2)	C(42B_2)	1.549(13)	C(42B_2)	C(43_2)	
1.474(10)					
C(43_2)	C(44_2)	1.443(6)	C(44_2)	C(45_2)	
1.522(5)					

Table 5. Non-Hydrogen Bond Angles (°)

atom	atom	atom	angle
C(13_1)	O(1_1)	C(18_1)	116.6(2)
C(35_1)	O(2_1)	C(40_1)	115.7(3)
C(1_1)	N(1_1)	C(9_1)	111.0(2)
C(1_1)	N(1_1)	C(30_1)	111.4(2)
C(9_1)	N(1_1)	C(30_1)	107.4(2)
C(24_1)	N(2_1)	C(9_1)	110.7(2)
C(24_1)	N(2_1)	C(7_1)	111.6(2)
C(9_1)	N(2_1)	C(7_1)	107.4(2)
N(4_1)	N(3_1)	C(5_1)	113.8(2)
N(3_1)	N(4_1)	C(10_1)	114.8(2)
N(6_1)	N(5_1)	C(28_1)	114.1(2)
N(5_1)	N(6_1)	C(32_1)	114.3(3)
C(6_1)	C(1_1)	C(2_1)	119.4(2)
C(6_1)	C(1_1)	N(1_1)	119.2(2)
C(2_1)	C(1_1)	N(1_1)	121.4(2)
C(3_1)	C(2_1)	C(1_1)	118.9(2)
C(3_1)	C(2_1)	C(7_1)	120.6(2)
C(1_1)	C(2_1)	C(7_1)	120.5(2)
C(4_1)	C(3_1)	C(2_1)	122.6(2)
C(3_1)	C(4_1)	C(5_1)	117.5(2)
C(3_1)	C(4_1)	C(8_1)	120.7(2)
C(5_1)	C(4_1)	C(8_1)	121.8(2)
C(6_1)	C(5_1)	C(4_1)	120.7(2)
C(6_1)	C(5_1)	N(3_1)	123.0(2)
C(4_1)	C(5_1)	N(3_1)	116.3(2)
C(1_1)	C(6_1)	C(5_1)	120.8(2)
N(2_1)	C(7_1)	C(2_1)	111.9(2)
N(1_1)	C(9_1)	N(2_1)	112.6(2)
C(15_1)	C(10_1)	C(11_1)	119.8(2)
C(15_1)	C(10_1)	N(4_1)	115.3(2)

C(11_1)	C(10_1)	N(4_1)	124.9(2)
C(12_1)	C(11_1)	C(10_1)	120.3(2)
C(11_1)	C(12_1)	C(13_1)	118.8(2)
C(11_1)	C(12_1)	C(16_1)	121.2(2)
C(13_1)	C(12_1)	C(16_1)	120.0(2)
O(1_1)	C(13_1)	C(14_1)	118.1(2)
O(1_1)	C(13_1)	C(12_1)	119.8(3)
C(14_1)	C(13_1)	C(12_1)	121.8(3)
C(15_1)	C(14_1)	C(13_1)	117.7(2)
C(15_1)	C(14_1)	C(17_1)	121.8(3)
C(13_1)	C(14_1)	C(17_1)	120.5(3)
C(14_1)	C(15_1)	C(10_1)	121.6(2)
O(1_1)	C(18_1)	C(19_1)	108.4(2)
C(20_1)	C(19_1)	C(18_1)	112.2(3)
C(19_1)	C(20_1)	C(21_1)	113.7(3)
C(22_1)	C(21_1)	C(20_1)	114.9(3)
C(21_1)	C(22_1)	C(23_1)	112.3(3)
C(29_1)	C(24_1)	C(25_1)	119.3(3)
C(29_1)	C(24_1)	N(2_1)	118.6(2)
C(25_1)	C(24_1)	N(2_1)	122.1(2)
C(26_1)	C(25_1)	C(24_1)	118.9(3)
C(26_1)	C(25_1)	C(30_1)	121.0(3)
C(24_1)	C(25_1)	C(30_1)	120.2(3)
C(27_1)	C(26_1)	C(25_1)	122.9(3)
C(26_1)	C(27_1)	C(28_1)	117.3(3)
C(26_1)	C(27_1)	C(31_1)	120.9(3)
C(28_1)	C(27_1)	C(31_1)	121.8(3)
C(29_1)	C(28_1)	C(27_1)	120.8(3)
C(29_1)	C(28_1)	N(5_1)	123.1(3)
C(27_1)	C(28_1)	N(5_1)	116.0(3)
C(28_1)	C(29_1)	C(24_1)	120.9(3)
N(1_1)	C(30_1)	C(25_1)	111.9(2)
C(37_1)	C(32_1)	C(33_1)	120.2(3)
C(37_1)	C(32_1)	N(6_1)	115.7(3)
C(33_1)	C(32_1)	N(6_1)	124.1(3)
C(34_1)	C(33_1)	C(32_1)	120.0(3)
C(33_1)	C(34_1)	C(35_1)	118.5(3)
C(33_1)	C(34_1)	C(38_1)	120.5(3)
C(35_1)	C(34_1)	C(38_1)	121.0(3)
O(2_1)	C(35_1)	C(36_1)	118.7(3)
O(2_1)	C(35_1)	C(34_1)	118.5(3)
C(36_1)	C(35_1)	C(34_1)	122.6(3)
C(35_1)	C(36_1)	C(37_1)	117.1(3)
C(35_1)	C(36_1)	C(39_1)	121.8(3)

C(37_1)	C(36_1)	C(39_1)	121.0(3)
C(32_1)	C(37_1)	C(36_1)	121.3(3)
O(2_1)	C(40_1)	C(41_1)	106.8(3)
C(42_1)	C(41_1)	C(40_1)	113.4(3)
C(41_1)	C(42_1)	C(43_1)	110.3(4)
C(44_1)	C(43_1)	C(42_1)	111.9(4)
C(43_1)	C(44_1)	C(45_1)	111.8(4)
C(13_2)	O(1_2)	C(18_2)	114.8(3)
C(40B_2)	O(2_2)	C(35_2)	117.1(5)
C(35_2)	O(2_2)	C(40A_2)	110.5(4)
C(1_2)	N(1_2)	C(9_2)	110.2(2)
C(1_2)	N(1_2)	C(30_2)	112.1(2)
C(9_2)	N(1_2)	C(30_2)	107.8(2)
C(24_2)	N(2_2)	C(9_2)	110.4(2)
C(24_2)	N(2_2)	C(7_2)	112.9(2)
C(9_2)	N(2_2)	C(7_2)	107.7(2)
N(4_2)	N(3_2)	C(5_2)	114.4(2)
N(3_2)	N(4_2)	C(10_2)	113.7(2)
N(6_2)	N(5_2)	C(28_2)	114.6(2)
N(5_2)	N(6_2)	C(32_2)	114.5(2)
C(6_2)	C(1_2)	C(2_2)	119.7(3)
C(6_2)	C(1_2)	N(1_2)	118.4(2)
C(2_2)	C(1_2)	N(1_2)	121.9(2)
C(3_2)	C(2_2)	C(1_2)	118.6(2)
C(3_2)	C(2_2)	C(7_2)	120.9(2)
C(1_2)	C(2_2)	C(7_2)	120.4(3)
C(4_2)	C(3_2)	C(2_2)	122.5(3)
C(3_2)	C(4_2)	C(5_2)	117.6(3)
C(3_2)	C(4_2)	C(8_2)	120.7(3)
C(5_2)	C(4_2)	C(8_2)	121.6(3)
C(6_2)	C(5_2)	C(4_2)	120.7(3)
C(6_2)	C(5_2)	N(3_2)	123.3(3)
C(4_2)	C(5_2)	N(3_2)	115.9(3)
C(5_2)	C(6_2)	C(1_2)	120.7(3)
N(2_2)	C(7_2)	C(2_2)	112.3(2)
N(2_2)	C(9_2)	N(1_2)	112.8(2)
C(15_2)	C(10_2)	C(11_2)	120.2(3)
C(15_2)	C(10_2)	N(4_2)	115.8(3)
C(11_2)	C(10_2)	N(4_2)	124.0(3)
C(12_2)	C(11_2)	C(10_2)	120.3(3)
C(11_2)	C(12_2)	C(13_2)	118.3(3)
C(11_2)	C(12_2)	C(17_2)	120.5(3)
C(13_2)	C(12_2)	C(17_2)	121.2(3)
C(14_2)	C(13_2)	O(1_2)	119.8(3)

C(14_2)	C(13_2)	C(12_2)	122.2(3)
O(1_2)	C(13_2)	C(12_2)	117.9(3)
C(15_2)	C(14_2)	C(13_2)	117.6(3)
C(15_2)	C(14_2)	C(16_2)	120.7(3)
C(13_2)	C(14_2)	C(16_2)	121.7(3)
C(10_2)	C(15_2)	C(14_2)	121.3(3)
O(1_2)	C(18_2)	C(19_2)	108.4(3)
C(18_2)	C(19_2)	C(20_2)	112.1(3)
C(19_2)	C(20_2)	C(21_2)	114.5(4)
C(22_2)	C(21_2)	C(20_2)	114.8(4)
C(21_2)	C(22_2)	C(23_2)	113.7(4)
C(29_2)	C(24_2)	C(25_2)	119.6(2)
C(29_2)	C(24_2)	N(2_2)	119.0(2)
C(25_2)	C(24_2)	N(2_2)	121.3(2)
C(26_2)	C(25_2)	C(24_2)	118.8(2)
C(26_2)	C(25_2)	C(30_2)	120.4(2)
C(24_2)	C(25_2)	C(30_2)	120.8(2)
C(27_2)	C(26_2)	C(25_2)	122.9(2)
C(26_2)	C(27_2)	C(28_2)	117.5(2)
C(26_2)	C(27_2)	C(31_2)	121.1(2)
C(28_2)	C(27_2)	C(31_2)	121.4(2)
C(29_2)	C(28_2)	C(27_2)	120.7(3)
C(29_2)	C(28_2)	N(5_2)	122.9(2)
C(27_2)	C(28_2)	N(5_2)	116.3(2)
C(24_2)	C(29_2)	C(28_2)	120.4(2)
N(1_2)	C(30_2)	C(25_2)	112.3(2)
C(37_2)	C(32_2)	C(33_2)	120.4(3)
C(37_2)	C(32_2)	N(6_2)	115.0(2)
C(33_2)	C(32_2)	N(6_2)	124.6(2)
C(34_2)	C(33_2)	C(32_2)	120.1(2)
C(33_2)	C(34_2)	C(35_2)	118.4(3)
C(33_2)	C(34_2)	C(38_2)	120.4(3)
C(35_2)	C(34_2)	C(38_2)	121.1(3)
C(36_2)	C(35_2)	O(2_2)	117.9(3)
C(36_2)	C(35_2)	C(34_2)	121.9(3)
O(2_2)	C(35_2)	C(34_2)	119.9(3)
C(37_2)	C(36_2)	C(35_2)	118.3(2)
C(37_2)	C(36_2)	C(39_2)	120.7(3)
C(35_2)	C(36_2)	C(39_2)	121.0(3)
C(36_2)	C(37_2)	C(32_2)	120.8(3)
O(2_2)	C(40A_2)	C(41A_2)	109.3(6)
C(42A_2)	C(41A_2)	C(40A_2)	113.1(7)
C(41A_2)	C(42A_2)	C(43_2)	110.2(5)
O(2_2)	C(40B_2)	C(41B_2)	108.8(8)

C(40B_2)	C(41B_2)	C(42B_2)	107.6(7)
C(43_2)	C(42B_2)	C(41B_2)	99.7(7)
C(44_2)	C(43_2)	C(42B_2)	130.7(6)
C(44_2)	C(43_2)	C(42A_2)	105.0(4)
C(43_2)	C(44_2)	C(45_2)	113.5(4)

Table 6. Torsion Angles (°)

atom	atom	atom	atom	angle
C(5_1)	N(3_1)	N(4_1)	C(10_1)	177.8(2)
C(28_1)	N(5_1)	N(6_1)	C(32_1)	-178.3(2)
C(9_1)	N(1_1)	C(1_1)	C(6_1)	165.8(3)
C(30_1)	N(1_1)	C(1_1)	C(6_1)	-74.6(3)
C(9_1)	N(1_1)	C(1_1)	C(2_1)	-14.8(4)
C(30_1)	N(1_1)	C(1_1)	C(2_1)	104.8(3)
C(6_1)	C(1_1)	C(2_1)	C(3_1)	-2.5(4)
N(1_1)	C(1_1)	C(2_1)	C(3_1)	178.1(2)
C(6_1)	C(1_1)	C(2_1)	C(7_1)	176.0(3)
N(1_1)	C(1_1)	C(2_1)	C(7_1)	-3.4(4)
C(1_1)	C(2_1)	C(3_1)	C(4_1)	0.4(4)
C(7_1)	C(2_1)	C(3_1)	C(4_1)	-178.2(3)
C(2_1)	C(3_1)	C(4_1)	C(5_1)	2.6(4)
C(2_1)	C(3_1)	C(4_1)	C(8_1)	-178.2(2)
C(3_1)	C(4_1)	C(5_1)	C(6_1)	-3.5(4)
C(8_1)	C(4_1)	C(5_1)	C(6_1)	177.3(2)
C(3_1)	C(4_1)	C(5_1)	N(3_1)	176.4(2)
C(8_1)	C(4_1)	C(5_1)	N(3_1)	-2.8(4)
N(4_1)	N(3_1)	C(5_1)	C(6_1)	7.0(4)
N(4_1)	N(3_1)	C(5_1)	C(4_1)	-172.8(2)
C(2_1)	C(1_1)	C(6_1)	C(5_1)	1.7(4)
N(1_1)	C(1_1)	C(6_1)	C(5_1)	-178.9(2)
C(4_1)	C(5_1)	C(6_1)	C(1_1)	1.4(4)
N(3_1)	C(5_1)	C(6_1)	C(1_1)	-178.5(2)
C(24_1)	N(2_1)	C(7_1)	C(2_1)	-74.1(3)
C(9_1)	N(2_1)	C(7_1)	C(2_1)	47.4(3)
C(3_1)	C(2_1)	C(7_1)	N(2_1)	164.6(2)
C(1_1)	C(2_1)	C(7_1)	N(2_1)	-13.9(4)
C(1_1)	N(1_1)	C(9_1)	N(2_1)	52.1(3)
C(30_1)	N(1_1)	C(9_1)	N(2_1)	-69.8(3)
C(24_1)	N(2_1)	C(9_1)	N(1_1)	52.0(3)
C(7_1)	N(2_1)	C(9_1)	N(1_1)	-70.0(3)
N(3_1)	N(4_1)	C(10_1)	C(15_1)	-177.0(2)
N(3_1)	N(4_1)	C(10_1)	C(11_1)	0.4(4)

C(15_1)	C(10_1)	C(11_1)	C(12_1)	1.5(4)
N(4_1)	C(10_1)	C(11_1)	C(12_1)	-175.7(2)
C(10_1)	C(11_1)	C(12_1)	C(13_1)	0.8(4)
C(10_1)	C(11_1)	C(12_1)	C(16_1)	178.4(2)
C(18_1)	O(1_1)	C(13_1)	C(14_1)	-100.5(3)
C(18_1)	O(1_1)	C(13_1)	C(12_1)	85.5(3)
C(11_1)	C(12_1)	C(13_1)	O(1_1)	170.7(2)
C(16_1)	C(12_1)	C(13_1)	O(1_1)	-7.0(4)
C(11_1)	C(12_1)	C(13_1)	C(14_1)	-3.2(4)
C(16_1)	C(12_1)	C(13_1)	C(14_1)	179.2(2)
O(1_1)	C(13_1)	C(14_1)	C(15_1)	-170.8(2)
C(12_1)	C(13_1)	C(14_1)	C(15_1)	3.2(4)
O(1_1)	C(13_1)	C(14_1)	C(17_1)	6.9(4)
C(12_1)	C(13_1)	C(14_1)	C(17_1)	-179.2(2)
C(13_1)	C(14_1)	C(15_1)	C(10_1)	-0.8(4)
C(17_1)	C(14_1)	C(15_1)	C(10_1)	-178.4(2)
C(11_1)	C(10_1)	C(15_1)	C(14_1)	-1.5(4)
N(4_1)	C(10_1)	C(15_1)	C(14_1)	176.0(2)
C(13_1)	O(1_1)	C(18_1)	C(19_1)	150.3(2)
O(1_1)	C(18_1)	C(19_1)	C(20_1)	176.4(3)
C(18_1)	C(19_1)	C(20_1)	C(21_1)	-178.2(3)
C(19_1)	C(20_1)	C(21_1)	C(22_1)	-65.7(4)
C(20_1)	C(21_1)	C(22_1)	C(23_1)	-172.6(3)
C(9_1)	N(2_1)	C(24_1)	C(29_1)	163.8(2)
C(7_1)	N(2_1)	C(24_1)	C(29_1)	-76.6(3)
C(9_1)	N(2_1)	C(24_1)	C(25_1)	-15.1(3)
C(7_1)	N(2_1)	C(24_1)	C(25_1)	104.4(3)
C(29_1)	C(24_1)	C(25_1)	C(26_1)	-1.2(4)
N(2_1)	C(24_1)	C(25_1)	C(26_1)	177.8(2)
C(29_1)	C(24_1)	C(25_1)	C(30_1)	178.4(2)
N(2_1)	C(24_1)	C(25_1)	C(30_1)	-2.6(4)
C(24_1)	C(25_1)	C(26_1)	C(27_1)	1.0(4)
C(30_1)	C(25_1)	C(26_1)	C(27_1)	-178.6(3)
C(25_1)	C(26_1)	C(27_1)	C(28_1)	-0.1(4)
C(25_1)	C(26_1)	C(27_1)	C(31_1)	179.8(3)
C(26_1)	C(27_1)	C(28_1)	C(29_1)	-0.7(4)
C(31_1)	C(27_1)	C(28_1)	C(29_1)	179.4(3)
C(26_1)	C(27_1)	C(28_1)	N(5_1)	-178.3(3)
C(31_1)	C(27_1)	C(28_1)	N(5_1)	1.8(4)
N(6_1)	N(5_1)	C(28_1)	C(29_1)	1.6(4)
N(6_1)	N(5_1)	C(28_1)	C(27_1)	179.2(2)
C(27_1)	C(28_1)	C(29_1)	C(24_1)	0.5(4)
N(5_1)	C(28_1)	C(29_1)	C(24_1)	178.0(2)
C(25_1)	C(24_1)	C(29_1)	C(28_1)	0.4(4)

N(2_1)	C(24_1)	C(29_1)	C(28_1)	-178.6(2)
C(1_1)	N(1_1)	C(30_1)	C(25_1)	-74.1(3)
C(9_1)	N(1_1)	C(30_1)	C(25_1)	47.7(3)
C(26_1)	C(25_1)	C(30_1)	N(1_1)	165.1(2)
C(24_1)	C(25_1)	C(30_1)	N(1_1)	-14.5(4)
N(5_1)	N(6_1)	C(32_1)	C(37_1)	-173.6(2)
N(5_1)	N(6_1)	C(32_1)	C(33_1)	6.2(4)
C(37_1)	C(32_1)	C(33_1)	C(34_1)	2.8(5)
N(6_1)	C(32_1)	C(33_1)	C(34_1)	-177.0(3)
C(32_1)	C(33_1)	C(34_1)	C(35_1)	-0.5(5)
C(32_1)	C(33_1)	C(34_1)	C(38_1)	178.9(3)
C(40_1)	O(2_1)	C(35_1)	C(36_1)	-93.6(4)
C(40_1)	O(2_1)	C(35_1)	C(34_1)	90.6(4)
C(33_1)	C(34_1)	C(35_1)	O(2_1)	172.8(3)
C(38_1)	C(34_1)	C(35_1)	O(2_1)	-6.6(5)
C(33_1)	C(34_1)	C(35_1)	C(36_1)	-2.8(5)
C(38_1)	C(34_1)	C(35_1)	C(36_1)	177.7(3)
O(2_1)	C(35_1)	C(36_1)	C(37_1)	-171.9(3)
C(34_1)	C(35_1)	C(36_1)	C(37_1)	3.7(5)
O(2_1)	C(35_1)	C(36_1)	C(39_1)	6.5(4)
C(34_1)	C(35_1)	C(36_1)	C(39_1)	-177.8(3)
C(33_1)	C(32_1)	C(37_1)	C(36_1)	-1.8(4)
N(6_1)	C(32_1)	C(37_1)	C(36_1)	178.0(3)
C(35_1)	C(36_1)	C(37_1)	C(32_1)	-1.4(4)
C(39_1)	C(36_1)	C(37_1)	C(32_1)	-179.8(3)
C(35_1)	O(2_1)	C(40_1)	C(41_1)	-168.7(3)
O(2_1)	C(40_1)	C(41_1)	C(42_1)	178.3(3)
C(40_1)	C(41_1)	C(42_1)	C(43_1)	-177.1(3)
C(41_1)	C(42_1)	C(43_1)	C(44_1)	172.9(4)
C(42_1)	C(43_1)	C(44_1)	C(45_1)	176.5(4)
C(5_2)	N(3_2)	N(4_2)	C(10_2)	-177.4(2)
C(28_2)	N(5_2)	N(6_2)	C(32_2)	-177.0(2)
C(9_2)	N(1_2)	C(1_2)	C(6_2)	162.5(2)
C(30_2)	N(1_2)	C(1_2)	C(6_2)	-77.4(3)
C(9_2)	N(1_2)	C(1_2)	C(2_2)	-14.8(3)
C(30_2)	N(1_2)	C(1_2)	C(2_2)	105.3(3)
C(6_2)	C(1_2)	C(2_2)	C(3_2)	-3.5(4)
N(1_2)	C(1_2)	C(2_2)	C(3_2)	173.8(2)
C(6_2)	C(1_2)	C(2_2)	C(7_2)	177.2(2)
N(1_2)	C(1_2)	C(2_2)	C(7_2)	-5.5(4)
C(1_2)	C(2_2)	C(3_2)	C(4_2)	1.3(4)
C(7_2)	C(2_2)	C(3_2)	C(4_2)	-179.4(3)
C(2_2)	C(3_2)	C(4_2)	C(5_2)	1.8(4)
C(2_2)	C(3_2)	C(4_2)	C(8_2)	-176.3(3)

C(3_2)	C(4_2)	C(5_2)	C(6_2)	-2.8(4)
C(8_2)	C(4_2)	C(5_2)	C(6_2)	175.3(3)
C(3_2)	C(4_2)	C(5_2)	N(3_2)	-178.8(3)
C(8_2)	C(4_2)	C(5_2)	N(3_2)	-0.7(4)
N(4_2)	N(3_2)	C(5_2)	C(6_2)	6.6(4)
N(4_2)	N(3_2)	C(5_2)	C(4_2)	-177.5(2)
C(4_2)	C(5_2)	C(6_2)	C(1_2)	0.6(4)
N(3_2)	C(5_2)	C(6_2)	C(1_2)	176.3(2)
C(2_2)	C(1_2)	C(6_2)	C(5_2)	2.6(4)
N(1_2)	C(1_2)	C(6_2)	C(5_2)	-174.8(2)
C(24_2)	N(2_2)	C(7_2)	C(2_2)	-77.2(3)
C(9_2)	N(2_2)	C(7_2)	C(2_2)	44.9(3)
C(3_2)	C(2_2)	C(7_2)	N(2_2)	170.3(2)
C(1_2)	C(2_2)	C(7_2)	N(2_2)	-10.4(4)
C(24_2)	N(2_2)	C(9_2)	N(1_2)	53.9(3)
C(7_2)	N(2_2)	C(9_2)	N(1_2)	-69.8(3)
C(1_2)	N(1_2)	C(9_2)	N(2_2)	53.2(3)
C(30_2)	N(1_2)	C(9_2)	N(2_2)	-69.5(3)
N(3_2)	N(4_2)	C(10_2)	C(15_2)	-173.7(3)
N(3_2)	N(4_2)	C(10_2)	C(11_2)	7.3(4)
C(15_2)	C(10_2)	C(11_2)	C(12_2)	2.1(5)
N(4_2)	C(10_2)	C(11_2)	C(12_2)	-179.0(3)
C(10_2)	C(11_2)	C(12_2)	C(13_2)	-0.3(5)
C(10_2)	C(11_2)	C(12_2)	C(17_2)	179.5(3)
C(18_2)	O(1_2)	C(13_2)	C(14_2)	-91.4(4)
C(18_2)	O(1_2)	C(13_2)	C(12_2)	92.1(4)
C(11_2)	C(12_2)	C(13_2)	C(14_2)	-2.3(5)
C(17_2)	C(12_2)	C(13_2)	C(14_2)	177.9(3)
C(11_2)	C(12_2)	C(13_2)	O(1_2)	174.1(3)
C(17_2)	C(12_2)	C(13_2)	O(1_2)	-5.7(5)
O(1_2)	C(13_2)	C(14_2)	C(15_2)	-173.4(3)
C(12_2)	C(13_2)	C(14_2)	C(15_2)	3.0(5)
O(1_2)	C(13_2)	C(14_2)	C(16_2)	6.3(5)
C(12_2)	C(13_2)	C(14_2)	C(16_2)	-177.4(3)
C(11_2)	C(10_2)	C(15_2)	C(14_2)	-1.4(5)
N(4_2)	C(10_2)	C(15_2)	C(14_2)	179.6(3)
C(13_2)	C(14_2)	C(15_2)	C(10_2)	-1.1(4)
C(16_2)	C(14_2)	C(15_2)	C(10_2)	179.2(3)
C(13_2)	O(1_2)	C(18_2)	C(19_2)	-162.9(3)
O(1_2)	C(18_2)	C(19_2)	C(20_2)	-178.4(3)
C(18_2)	C(19_2)	C(20_2)	C(21_2)	-167.3(3)
C(19_2)	C(20_2)	C(21_2)	C(22_2)	-60.3(6)
C(20_2)	C(21_2)	C(22_2)	C(23_2)	-178.9(4)
C(9_2)	N(2_2)	C(24_2)	C(29_2)	160.6(3)

C(7_2)	N(2_2)	C(24_2)	C(29_2)	-78.8(3)
C(9_2)	N(2_2)	C(24_2)	C(25_2)	-16.5(4)
C(7_2)	N(2_2)	C(24_2)	C(25_2)	104.1(3)
C(29_2)	C(24_2)	C(25_2)	C(26_2)	-2.5(4)
N(2_2)	C(24_2)	C(25_2)	C(26_2)	174.5(2)
C(29_2)	C(24_2)	C(25_2)	C(30_2)	178.9(3)
N(2_2)	C(24_2)	C(25_2)	C(30_2)	-4.0(4)
C(24_2)	C(25_2)	C(26_2)	C(27_2)	0.2(4)
C(30_2)	C(25_2)	C(26_2)	C(27_2)	178.8(3)
C(25_2)	C(26_2)	C(27_2)	C(28_2)	2.3(4)
C(25_2)	C(26_2)	C(27_2)	C(31_2)	-176.6(3)
C(26_2)	C(27_2)	C(28_2)	C(29_2)	-2.6(4)
C(31_2)	C(27_2)	C(28_2)	C(29_2)	176.3(3)
C(26_2)	C(27_2)	C(28_2)	N(5_2)	-178.5(2)
C(31_2)	C(27_2)	C(28_2)	N(5_2)	0.4(4)
N(6_2)	N(5_2)	C(28_2)	C(29_2)	9.5(4)
N(6_2)	N(5_2)	C(28_2)	C(27_2)	-174.7(2)
C(25_2)	C(24_2)	C(29_2)	C(28_2)	2.2(4)
N(2_2)	C(24_2)	C(29_2)	C(28_2)	-174.9(2)
C(27_2)	C(28_2)	C(29_2)	C(24_2)	0.4(4)
N(5_2)	C(28_2)	C(29_2)	C(24_2)	176.1(3)
C(1_2)	N(1_2)	C(30_2)	C(25_2)	-77.0(3)
C(9_2)	N(1_2)	C(30_2)	C(25_2)	44.5(3)
C(26_2)	C(25_2)	C(30_2)	N(1_2)	170.6(2)
C(24_2)	C(25_2)	C(30_2)	N(1_2)	-10.9(4)
N(5_2)	N(6_2)	C(32_2)	C(37_2)	178.6(2)
N(5_2)	N(6_2)	C(32_2)	C(33_2)	-0.8(4)
C(37_2)	C(32_2)	C(33_2)	C(34_2)	-0.4(4)
N(6_2)	C(32_2)	C(33_2)	C(34_2)	179.0(3)
C(32_2)	C(33_2)	C(34_2)	C(35_2)	-1.5(4)
C(32_2)	C(33_2)	C(34_2)	C(38_2)	178.1(3)
C(40B_2)	O(2_2)	C(35_2)	C(36_2)	80.3(7)
C(40A_2)	O(2_2)	C(35_2)	C(36_2)	106.6(5)
C(40B_2)	O(2_2)	C(35_2)	C(34_2)	-105.6(6)
C(40A_2)	O(2_2)	C(35_2)	C(34_2)	-79.4(5)
C(33_2)	C(34_2)	C(35_2)	C(36_2)	2.5(4)
C(38_2)	C(34_2)	C(35_2)	C(36_2)	-177.1(3)
C(33_2)	C(34_2)	C(35_2)	O(2_2)	-171.3(3)
C(38_2)	C(34_2)	C(35_2)	O(2_2)	9.1(4)
O(2_2)	C(35_2)	C(36_2)	C(37_2)	172.4(3)
C(34_2)	C(35_2)	C(36_2)	C(37_2)	-1.5(4)
O(2_2)	C(35_2)	C(36_2)	C(39_2)	-8.8(4)
C(34_2)	C(35_2)	C(36_2)	C(39_2)	177.3(3)
C(35_2)	C(36_2)	C(37_2)	C(32_2)	-0.5(4)

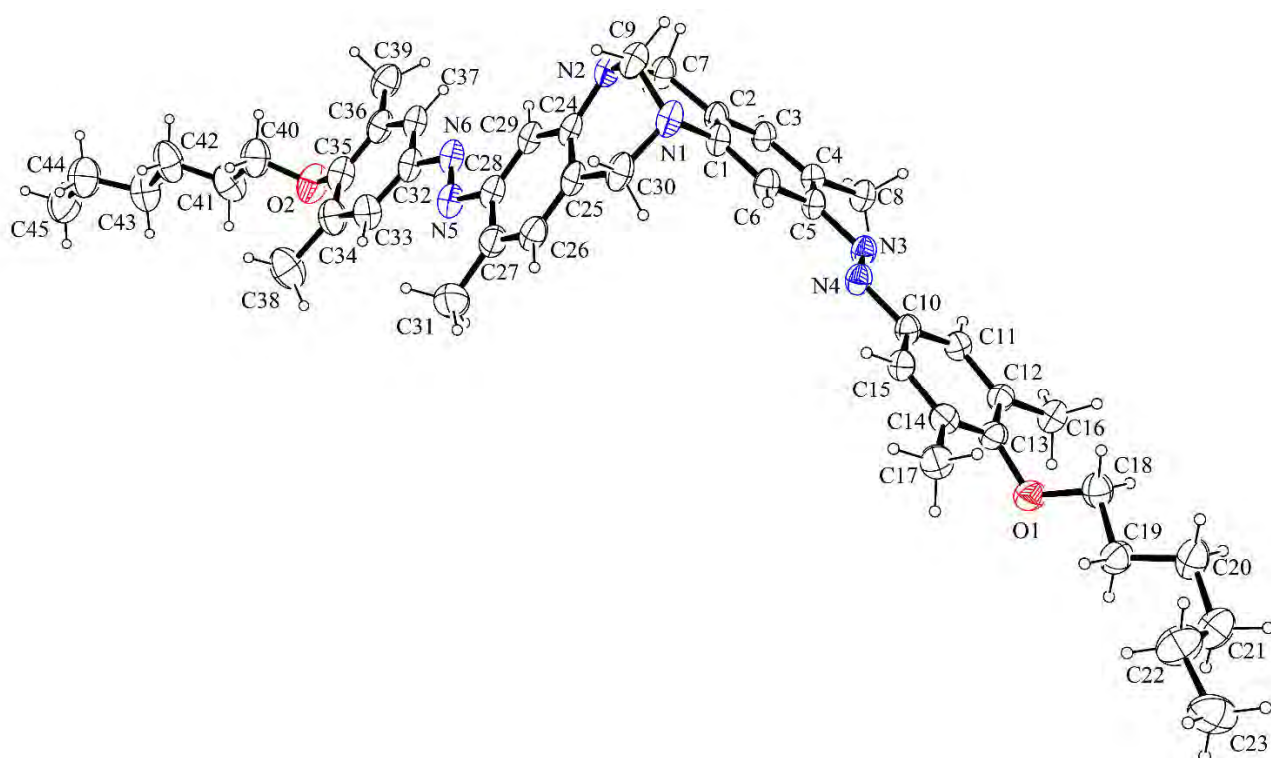


Figure 2. ORTEP⁶ depiction, with 50% ellipsoids, of one of the two crystallographically independent molecules in the crystal structure of the title compound.

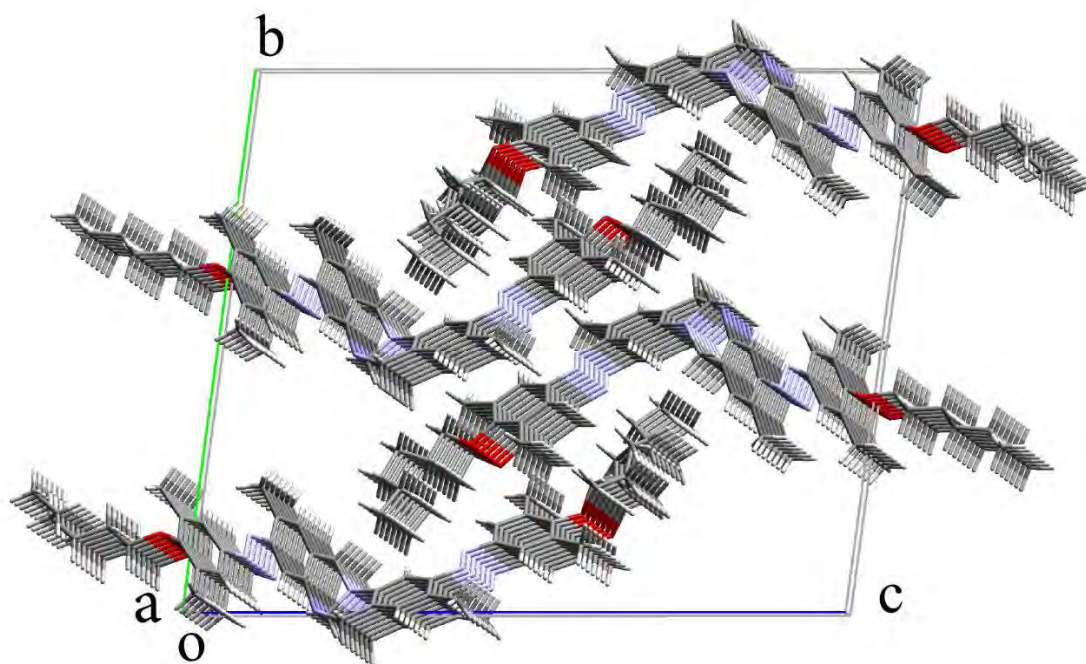


Figure 3. Mercury representation of the crystal packing of the title compound, viewed along the *a* axis of the unit cell.

Structure prediction by semi-empirical and quantum methods

We took a brief look at predicting the main conformers present after excitation from the *trans-trans* to the *cis-cis* state (*cis*[*exo*]-*cis*[*exo*], *cis*[*endo*]-*cis*[*exo*], and *cis*[*endo*]-*cis*[*endo*]) using semi-empirical, restricted Hartree-Fock (RHF) and density-functional theory (DFT) quantum mechanical methods. These methods have been used previously to simulate the structures and properties of azobenzene compounds (*e.g.* [1-4]). In this work, a systematic search for conformers in both *trans-trans* and *cis-cis* forms was conducted using the Amber12 forcefield with extended Huckel theory treatment. These conformers were then optimised using the PM7 semi-empirical method. Representative conformations from both the Amber and PM7 results were also optimised at the RHF 3-21G and B3LYP 6-31G* levels.

We noticed sizeable discrepancies between the semi-empirical and RHF or DFT structures. Notably, in the *trans-trans* form, the planarity of the aryl rings across the azide bond depended heavily on the method employed; with the greatest deviation (from the crystal structure) arising from the semi-empirical method, followed by HF 3-21G, and then B3LYP 6-31G* (Figure 1 A-C). When the methyl groups adjacent to the azides were removed, the rings assume a more linear conformation in both AM1 and PM7, suggesting they are at least partially responsible for the error (Figure 1 F). In considering the *cis-cis* forms, the PM7 method gave an *endo-endo* conformation that was not found in any other quantum method. When this PM7 structure was used as the input for a B3LYP calculation, it repeatedly assumed the conformation shown in Figure 1 E. The *cis*[*exo*]-*cis*[*exo*] structures were essentially identical in both PM7 and B3LYP results (Figure 1 D).

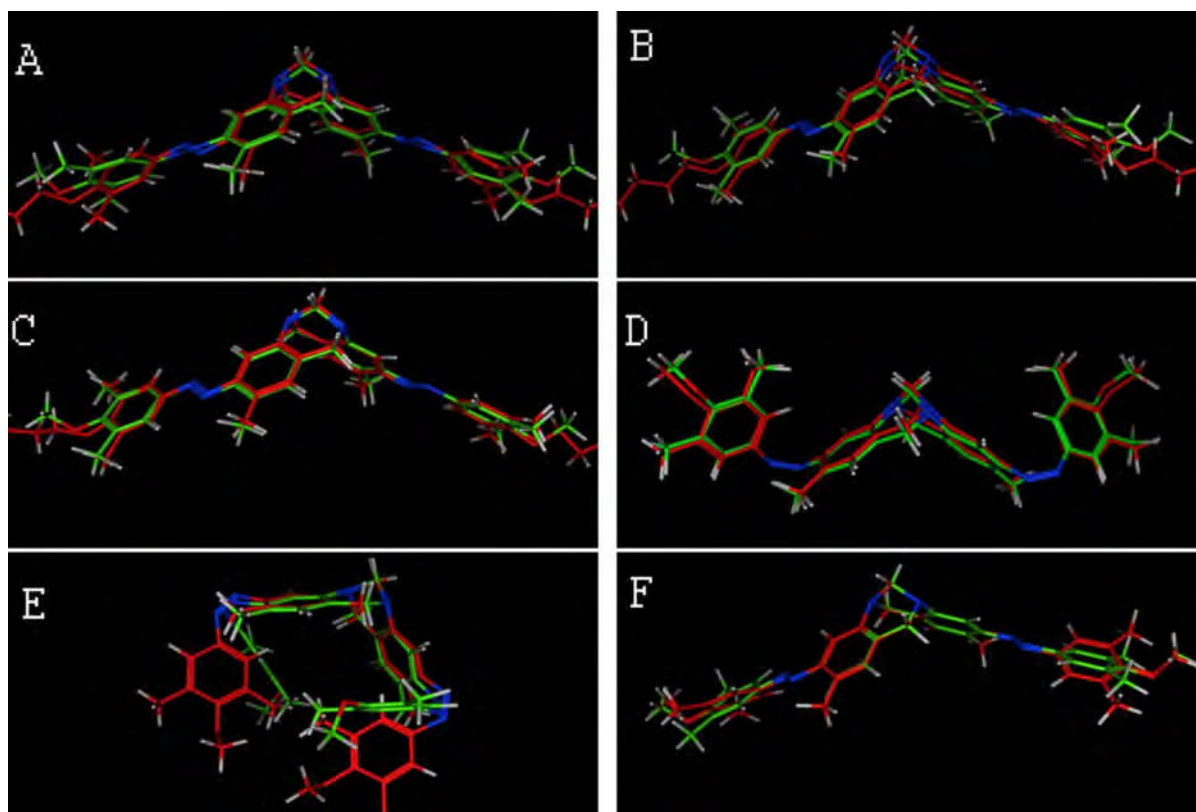


Figure 1. A) Crystal structure (red carbons) of *trans-trans* compared to PM7 results (green carbons). B) Crystal structure (red carbons) of *trans-trans* compared to RHF 3-21G results (green carbons). C) Crystal structure (red carbons) of *trans-trans* compared to B3LYP 6-31G* results (green carbons). D) Predicted lowest energy structure of the *cis*[*exo*]-*cis*[*exo*] form calculated at PM7 (red carbons) and B3LYP 6-31G* (green carbons) levels. E) Predicted lowest energy structure of the *cis*[*endo*]-*cis*[*endo*] form calculated at PM7 (red carbons) and B3LYP 6-31G* (green carbons) levels. F) *Trans-trans* conformation with (red) and without (green) methyl groups.

Calculation of relative energies of the conformations likewise gave disagreeing results between semi-empirical and other methods (Table 1). The PM7 method actually predicted both *cis-cis* forms as being lower in energy than the *trans-trans*. Conversely, both RHF and B3LYP methods have the *trans-trans* structure as being lower in energy than the *cis-cis* forms. Therefore, despite semi-empirical methods being used successfully in previous work (e.g. [1-4]), they were not applicable to these examples of Troger's base azobenzenes, being outperformed by both Amber12 and very low level Hartree-Fock, as well as B3LYP. In all cases, the *trans-cis* conformers had intermediate energies between their respective *trans-trans* and *cis-cis* counterparts. The complete potential energy surface between these conformations was not calculated, but the small differences between *cis*[*endo*]-*cis*[*endo*] and *cis*[*exo*]-*cis*[*exo*] suggests that there is no large preference between the forms in the gas phase.

Table 1. relative energies of *trans-trans* and *cis-cis* conformers from quantum calculations.

Method	<i>Trans-Trans</i>	<i>Cis-Cis</i>
PM7 (ΔH , kcal/mol)	78.77928	59.73188 (endo-endo) 64.32351 (exo-exo)
RHF 3-21G (SCF energy, Hartrees)	-1813.661928	-1813.603472 (endo-endo) -1813.596602 (exo-exo)
B3LYP 6-31G* (SCF energy, Hartrees)	-1835.4873681	-1835.440585 (endo-endo) -1835.435236 (exo-exo)

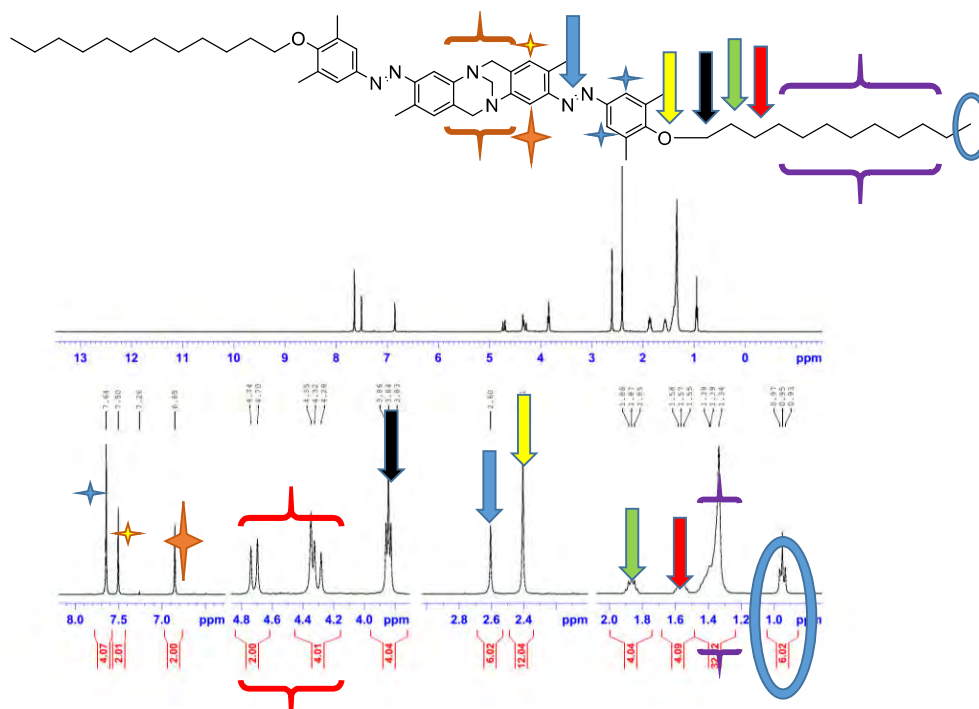
Methods

A systematic search of conformations was performed in the Molecular Operating Environment version 2015 (MOE, Chemical Computing Group, Montreal, Ca.) using the Amber12:EHT forcefield with duplicate conformations being discarded, as were those > 20 kcal/mol higher in energy than the minimum found. These structures were then optimised using PM7 in MOPAC 2016 (Stewart Computational Chemistry, Colorado Springs, USA) using the keywords: Let gnorn=0.0001 precise ddmin=0.00001. MOPAC output was visualised with Avogadro version 1.2.0 [5] which also handled file conversion from MOPAC to PDB. Selected structures, representing a diverse and distinct subset of rotamers were taken from the Amber and PM7 results and optimised using both restricted Hartree-Fock (RHF 3-21G) and density-functional theory (DFT, B3LYP 6-31G*) in Spartan'08 version 1.2.0 (Wavefunction Inc., Irvine, USA), with the increased convergence criteria option selected. All PM7, RHF and B3LYP structures were subjected to a force analysis to ensure that a true minima had been found. All calculations were performed in the gas phase. Alignment of the minimised structures was performed in MOE.

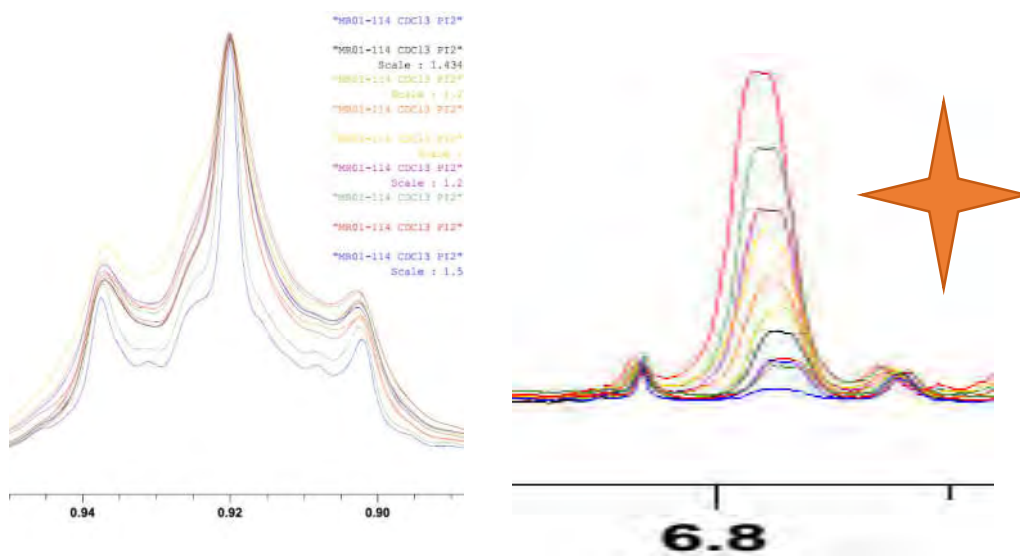
1. Floß, G. and P. Saalfrank, *The Photo-induced E \rightarrow Z Isomerization of Bisazobenzenes: A Surface Hopping Molecular Dynamics Study*. The Journal of Physical Chemistry A, 2015. **119**(20): p. 5026-5037.
2. Wegermann, C.A., et al., *Semi-empirical ZINDO/S description of the electronic structure and the spectral features of methyl orange and its products of oxidation. A study of relationship between molecular geometry and spectroscopic properties*. Dyes and Pigments, 2013. **99**(3): p. 839-849.
3. Cojocaru, C., A. Airinei, and N. Fifere, *Molecular structure and modeling studies of azobenzene derivatives containing maleimide groups*. SpringerPlus, 2013. **2**(1): p. 586-604.
4. Sıdır, İ. and Y. Gülseven Sıdır, *Estimation of ground and excited state dipole moments of Oil Red O by solvatochromic shift methods*. Spectrochimica Acta Part A: Molecular and Biomolecular Spectroscopy, 2015. **135**(Epub 2014 Jul 29): p. 560-567.
5. Hanwell, M.D., et al., *Avogadro: an advanced semantic chemical editor, visualization, and analysis platform*. Journal of Cheminformatics, 2012. **4**(1): p. 17.

Appendix 4: Photo-isomerisation studies by NMR

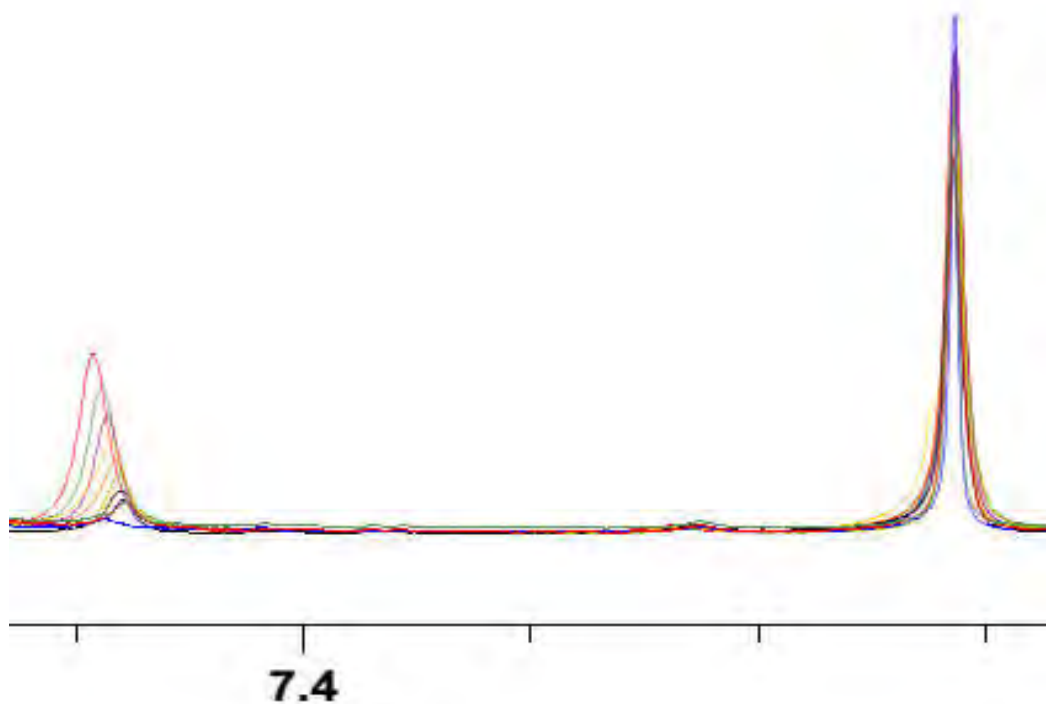
The photo-isomerisation of a UV-active product introduced as compound **7** in Paper I was tracked by NMR and the obtained spectra are shown in this appendix. This product has distinguishable peaks appearing in different regions of the NMR spectra. The functional groups located far from the photo-switchable units can be used as references owing to the fact that they are not influenced by the photo-isomerisation; for instance, those circled in blue in the following figure. The photo-excitation led to a new series of peaks (belonging to the *cis* isomer), which disappear over a few days due to the thermal relaxation. This process was found to be absolutely repeatable and reversible. Recollection of the ^1H NMR spectra after illuminating the sample with 3 naked UV lamps (365 nm, 30 minutes) showed no sign of photo-degradation. As shown in the following figures, the initial assessments were promising and proved the concept. Therefore a series of different 1D and 2D NMR experiments can be done in the future to obtain further detail on the isomerisation kinetics, and detect the changes in the molecule geometry. Afterwards, host-guest chemistry and molecule recognition tests will be performed.



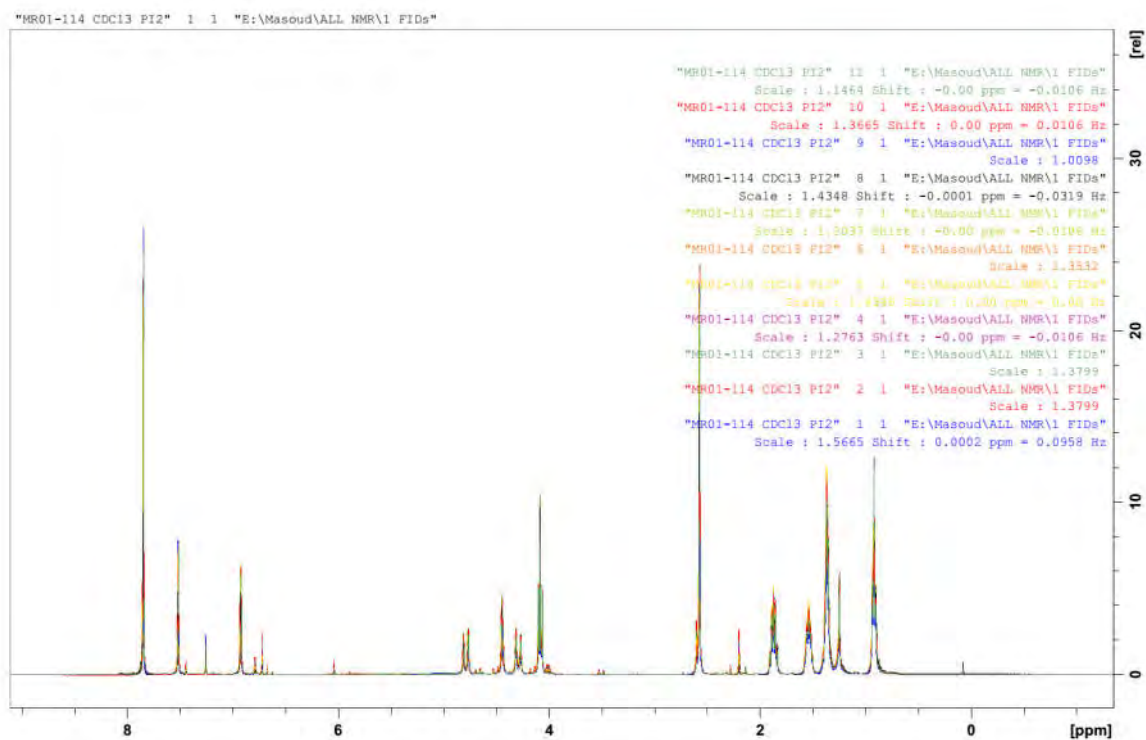
Chemical structure and ^1H NMR spectra of **7** before illumination, (CDCl_3 , 400MHz)



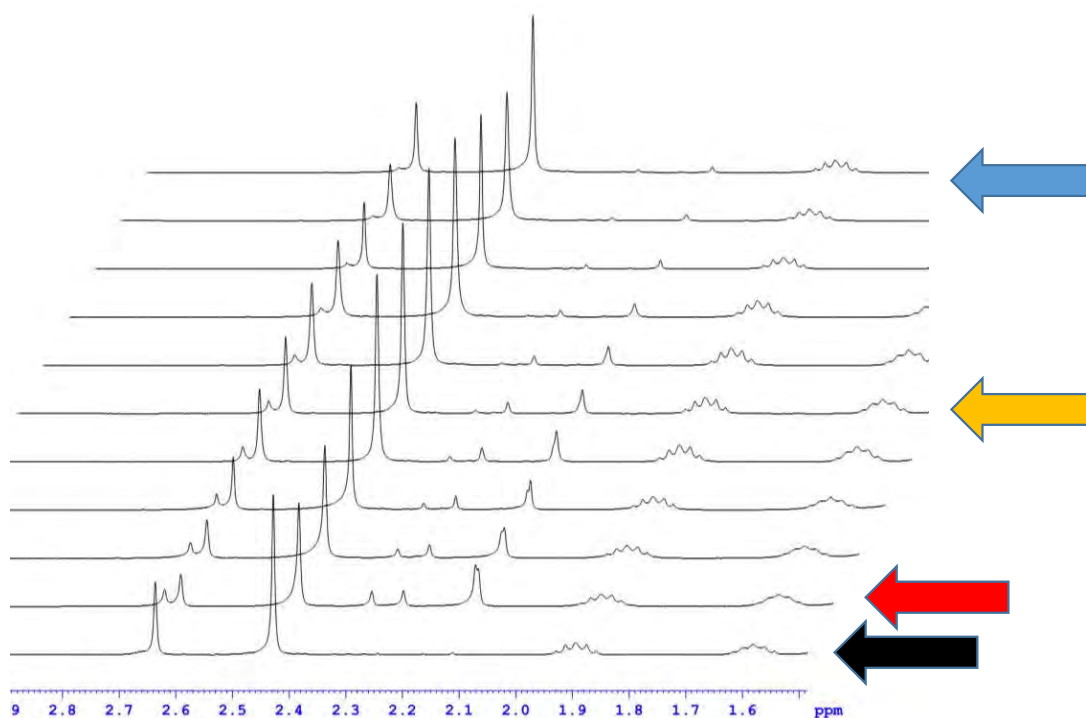
A reference peak (left) and a changing peak (right)



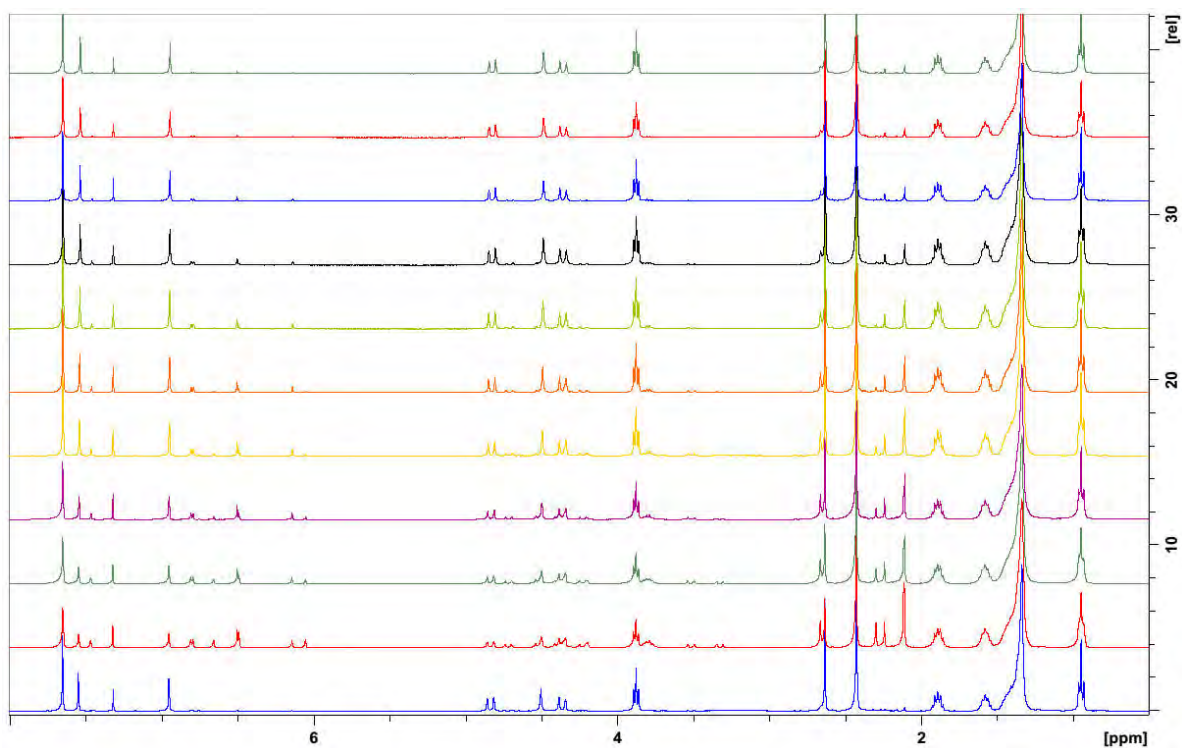
A reference peak (right) and a changing peak (left)



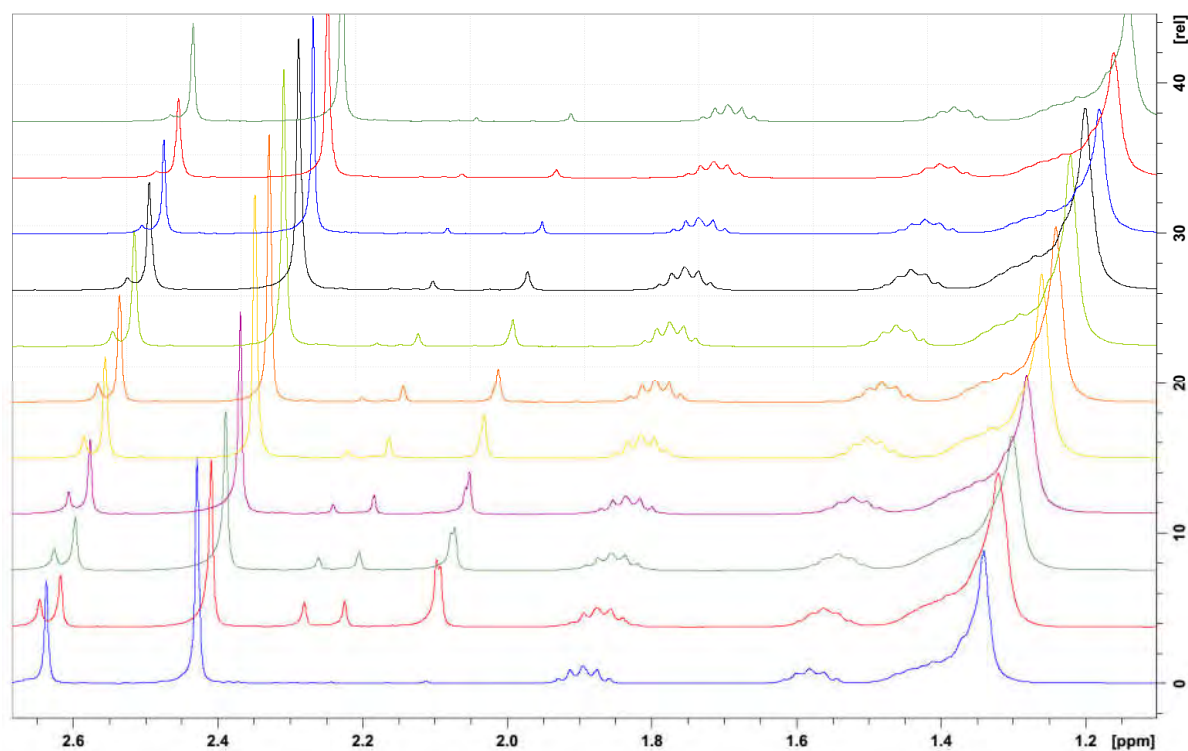
Overlaid ^1H NMR spectra before and after illumination with 365 nm



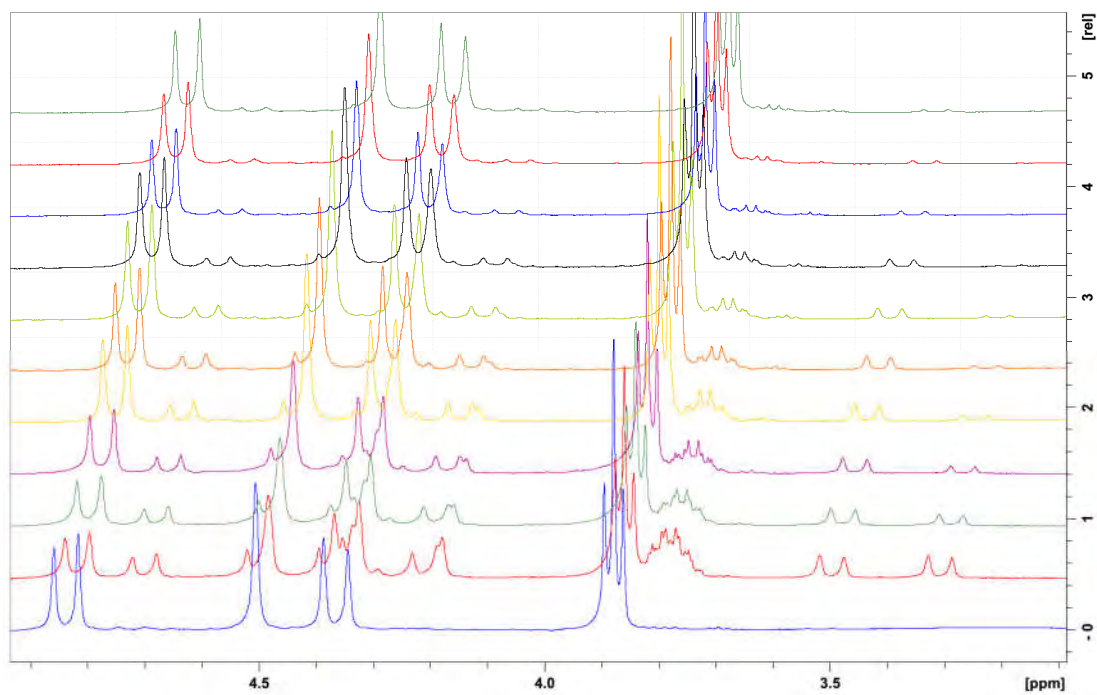
Dark incubated (black), just illuminated (red), half way relaxed (orange) and almost back to the initial state (blue).



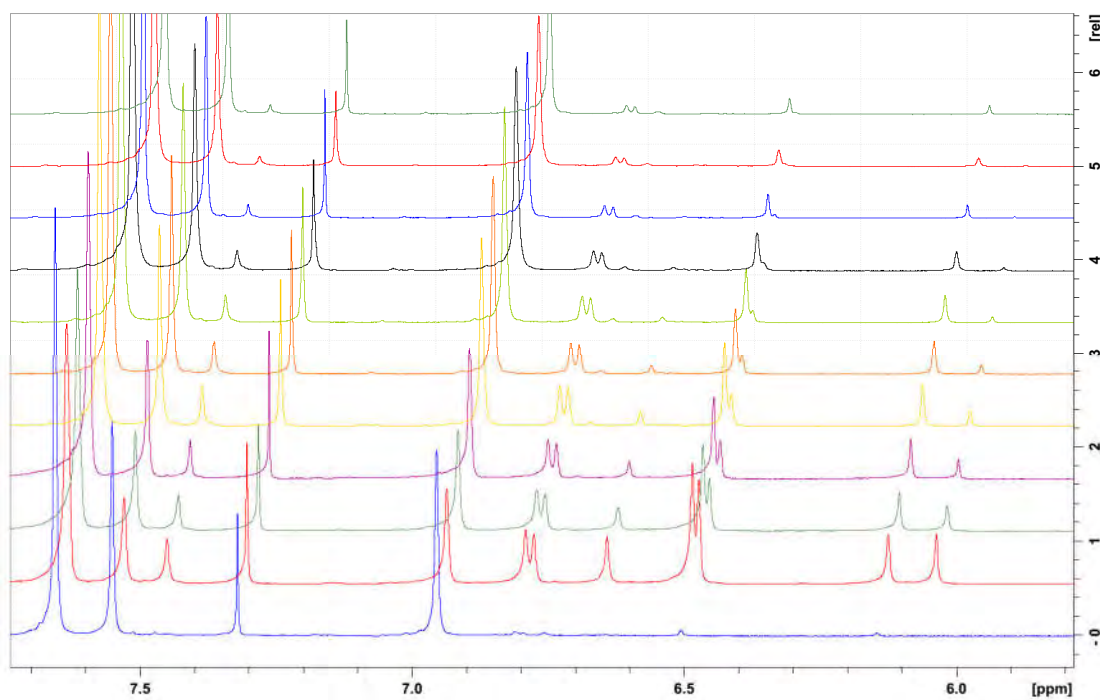
Tracking the photo-isomerisation of **7**, stacked view ^1H NMR spectra (400MHz, CDCl_3)



Tracking the photo-isomerisation of **7** by ^1H NMR spectra, stacked view (expansion)



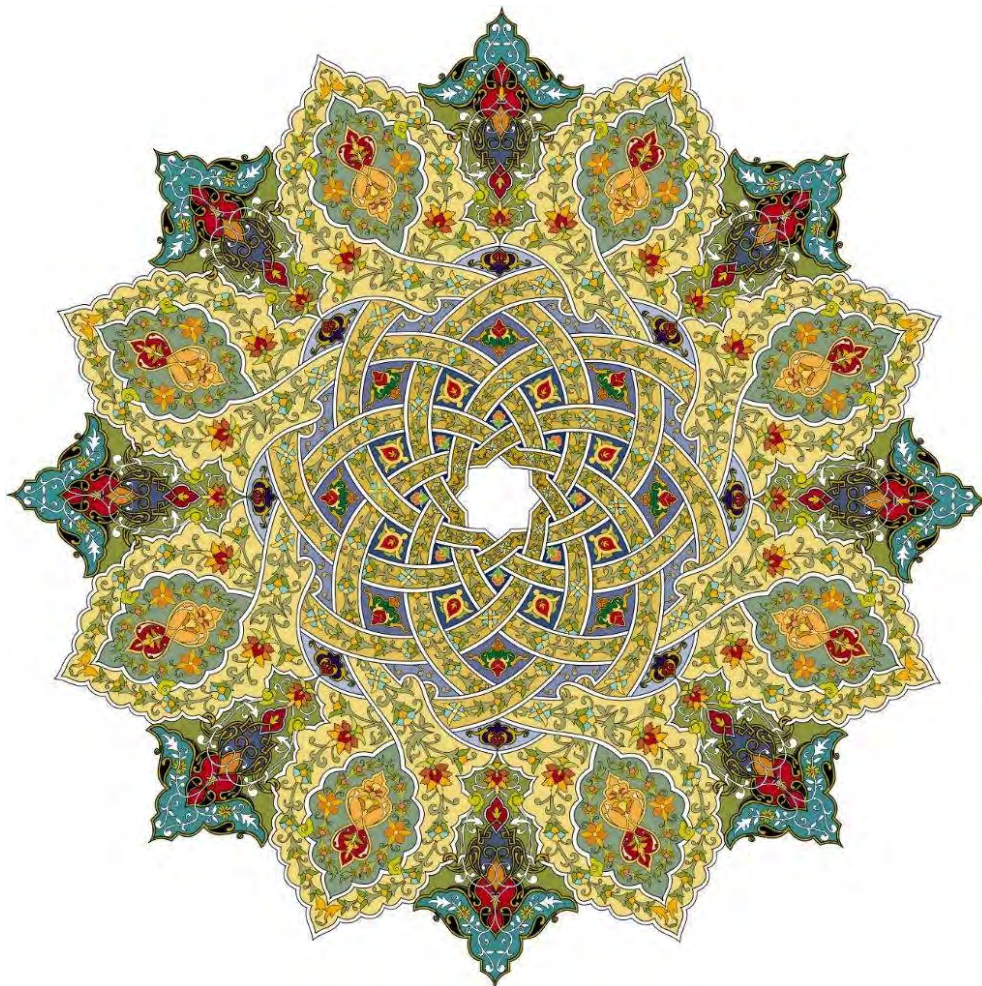
Tracking the photo-isomerisation of **7** by ^1H NMR spectra, stacked view (expansion)



Tracking the photo-isomerisation of **7** by ^1H NMR spectra, stacked view (expansion)

Appendix 5: The author's biography

Avicenna (Bu-Ali Sina پورسینا), a Persian polymath born in August 980 AD and authored 450 works, passed away 980 years ago in Hamedan city of Iran. To pay tribute to his contribution in sciences, the state university of Hamedan province was named after him as “Bu-Ali Sina University” in 1973.



Masoud Kazem-Rostami was born in 1986 in Qazvin province of Iran, where he spent almost three years of his early life under the imposed war of Iraq's invasion until August 1988. He was fortunate to be born alive and survive, despite the severe medical condition of his mother at the time, and inherit the nick-name of his grandfather — Masoud (means fortunate) — who passed away as an honourable man just before Masoud's birth.

Masoud's thirst for learning and tremendous curiosity encouraged his family to provide him with a miniature laboratory at home in 1997. Two years later he was ranked 1st among 450 participants in the empirical science-olympiad (ERAM) in Qazvin province, Iran.



Methyl orange preparation, Masoud's mini-lab in 2001 at home

In 2004, he was ranked at the top 2% of participants in Iran's nationwide university admission exam and became admitted to the Bachelor's degree in Pure Chemistry in Qazvin State University known as "Imam Khomeini International University", and later became a coach in swimming and kung-fu.

In 2009, he qualified in the top 3% in Iran's nationwide post-graduates qualification exams to commence his Master's Program in Organic Chemistry in Bu-Ali Sina University under the supervision of Professor Ardeshtir Khazaei in Hamedan, Iran. After graduation in 2012, he became an active member of Iran's Young Researchers and Elites Club. His contributions as an independent researcher resulted in the accomplishment of 5 academic projects until 2014.

In 2014, Masoud joined the Department of Chemistry and Biomolecular Sciences at Macquarie University. He submitted the presented thesis in August 2017, following 980 days of hard work and passing numerous challenges.

He has always been inspired by Avicenna's words:

*"There are no incurable diseases,
only, the lack of will..."*



Avicenna (Bu Ali-Sina پورسینا)
980–1037 AD